TÉCNICO LISBOA

UNIVERSIDADE DE LISBOA

INSTITUTO SUPERIOR TÉCNICO

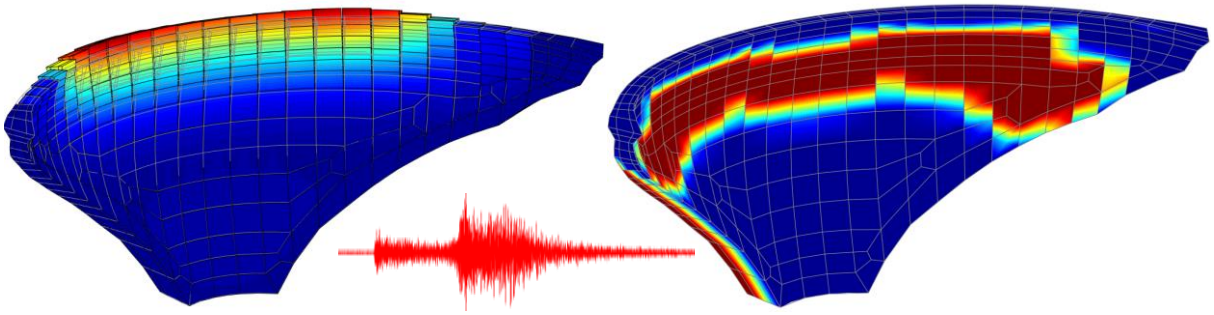

Modelling and monitoring the dynamic behaviour of concrete dams. Modal analysis and seismic response

André Filipe Moreira Alegre

Supervisor: Doctor Sérgio Bruno Martins de Oliveira

Co-Supervisors: Doctor Jorge Miguel Silveira Filipe Mascarenhas Proença
Doctor Paulo Jorge Henriques Mendes

Thesis approved in public session to obtain the PhD Degree in Civil Engineering

Jury final classification: Pass with distinction

2021

TÉCNICO LISBOA

UNIVERSIDADE DE LISBOA

INSTITUTO SUPERIOR TÉCNICO

Modelling and monitoring the dynamic behaviour of concrete dams. Modal analysis and seismic response

André Filipe Moreira Alegre

Supervisor: Doctor Sérgio Bruno Martins de Oliveira

Co-Supervisors: Doctor Jorge Miguel Silveira Filipe Mascarenhas Proença
Doctor Paulo Jorge Henriques Mendes

Thesis approved in public session to obtain the PhD Degree in Civil Engineering

Jury final classification: Pass with distinction

Jury

Chairperson: Doctor Eduardo Nuno Brito Santos Júlio, Instituto Superior Técnico, Universidade de Lisboa

Members of the Committee:

Doctor Nuno Manuel Mendes Maia, Instituto Superior Técnico, Universidade de Lisboa

Doctor Luís Manuel Coelho Guerreiro, Instituto Superior Técnico, Universidade de Lisboa

Doctor Tiago Alexandre Narciso da Silva, Faculdade de Ciências e Tecnologia, Universidade Nova de Lisboa

Doctor Carlos Manuel Tiago Tavares Fernandes, Instituto Superior Técnico, Universidade de Lisboa

Doctor Sérgio Bruno Martins de Oliveira, Laboratório Nacional de Engenharia Civil

Doctor Nuno Miguel Monteiro Azevedo, Laboratório Nacional de Engenharia Civil

INSTITUIÇÃO FINANCIADORA
FCT – Fundação para a Ciência e Tecnologia

2021

ABSTRACT

Large concrete dams, essential infrastructures in the management of water resources, are generally structures of high potential risk. Therefore, it is fundamental to assess their safety for current and failure scenarios, under both static and dynamic loads. With that goal, the dynamic behaviour of large concrete dams must be continuously evaluated, in order to detect possible evolutive deterioration processes, using methodologies based on the analysis of measured vibrations under ambient/operational excitations, and to monitor the response under seismic loads, during low, medium, or high intensity seismic events. Additionally, the structural performance of dams under strong earthquakes must be evaluated for seismic safety assessment, considering appropriate methods of analysis and performance criteria. In this context, it is emphasized the need to: (i) develop advanced numerical models for simulating the dynamic behaviour of dam-reservoir-foundation systems for various scenarios that can occur over time, involving the variation of static and dynamic loads and possible structural changes due to deterioration; and (ii) to develop and install systems to continuously measure vibrations, for Seismic and Structural Health Monitoring (SSHM), and to implement methodologies that allow a simple comparison between the measured response and the response predicted using numerical models.

The present work begins with the development of a new finite element model for dynamic analysis of arch dam-reservoir-foundation systems. A formulation in displacements and hydrodynamic pressures is adopted, considering the dam-water dynamic interaction and the propagation of pressure waves in the reservoir. The proposed model is implemented into a finite element program and, besides pre- and post- processing tools, it includes three modules, namely for: (i) complex modal analysis, based a new state-space approach that allows to consider generalized damping; (ii) linear seismic analysis, using a coupled time-stepping formulation based on the Newmark method; and (iii) non-linear seismic analysis, by combining the time-stepping method with a stress-transfer method, considering a) the non-linear behaviour of concrete up to failure, using on a strain-softening constitutive damage model with two independent damage variables (d^+ and d^-), and b) the opening/closing and sliding movements of joints, using a constitutive model based on the Mohr-Coulomb failure criterion and on appropriate relative displacement-stress laws.

After that, the work dedicates to the development of computational tools to integrate and complement the software component of SSHM systems installed in large concrete dams, in particular for: (i) automatic analysis and management of dynamic monitoring data, in order to assess data quality, automatically detect vibrations induced by seismic events, and perform the maintenance of the database; and (ii) automatic modal identification, based on the classic frequency domain decomposition method, and using new techniques proposed to automate peak selection and to enhance the modal parameter identification for dams over time.

Application examples are presented for two case studies, namely Cabril dam (132 m high), in Portugal, and Cahora Bassa dam (170 m high), in Mozambique, two double curvature arch dams which have been under continuous dynamic monitoring since 2008 and 2010, respectively. The provided results are mainly focused on: (i) the analysis of the evolution of identified natural frequencies over time and the comparison with numerical values, in order to evaluate the influence of reservoir level variations and to perform evolutive damage detection; (ii) the study of the response during real seismic events, based on the comparison between measured and computed accelerations in the dam body, aiming to investigate the influence of the seismic input and damping ratios used in the models; (iii) the simulation of the non-linear seismic behaviour under a strong earthquake, with a view to evaluate influence of joint movements in the structural dam response (displacements and stresses), and (iv) the seismic safety assessment of large concrete dams based on the Endurance Time method, by analysing the progression of tensile and compressive concrete damage under intensifying seismic accelerations.

RESUMO

As grandes barragens de betão, infraestruturas essenciais na gestão dos recursos hídricos, são, geralmente, obras de elevado risco potencial. Assim, é fundamental avaliar a sua segurança para cenários correntes e excecionais, sob ações estáticas e dinâmicas. Com esse objetivo, o comportamento dinâmico das grandes barragens de betão deve ser avaliado de forma contínua, com vista a detetar eventuais processos de deterioração evolutiva, recorrendo a metodologias baseadas na análise de vibrações medidas sob excitação ambiente/operacional, e a controlar a resposta sob ações sísmicas, para eventos de pequena, média, ou grande intensidade. Além disso, o comportamento estrutural das barragens sob sismos de grande intensidade deve ser analisado para verificação da segurança sísmica, com base métodos de análise e em critérios de desempenho adequados. Neste contexto, destaca-se a necessidade de: (i) desenvolver avançados modelos numéricos que permitam simular o comportamento dinâmico dos sistemas barragem-fundação-albufeira para várias situações que podem ocorrer ao longo da vida das barragens, envolvendo a variação das ações estáticas e dinâmicas e possíveis alterações estruturais devido a processos de deterioração; e (ii) desenvolver e instalar sistemas para medição de vibrações em contínuo, para Monitorização Sísmica e da Integridade Estrutural (SSHM), e implementar metodologias para comparar de forma simples a resposta observada e a resposta prevista com os modelos numéricos.

Este trabalho inicia-se com o desenvolvimento de um novo modelo de elementos finitos para análise dinâmica de sistemas barragem-fundação-albufeira. Adotou-se uma formulação acoplada em deslocamento e pressões, considerando a interação dinâmica barragem-albufeira e a propagação de ondas de pressão na água. O modelo proposto é implementado num programa de elementos finitos, e, para além de ferramentas de pré- e pós-processamento, inclui três módulos, nomeadamente para: (i) análise modal complexa, com base numa nova abordagem de estado que permite considerar amortecimento generalizado; (ii) análise sísmica em regime linear, utilizando uma formulação para integração numérica no tempo baseada no método de Newmark; e (iii) análise sísmica não-linear, combinando a formulação de integração no tempo com o método de *stress-transfer*, tendo em conta a) o comportamento não-linear do betão até à rotura, usando um modelo de dano com enfraquecimento e duas variáveis escalares independentes (d^+ e d^-), e b) os movimentos de abertura/fecho e deslizamento de juntas, usando um modelo constitutivo baseado no critério de Mohr-Coulomb e em leis deslocamento-tensão adequadas.

Na fase seguinte, o trabalho dedica-se ao desenvolvimento de ferramentas computacionais para integrar e complementar a componente de software dos sistemas SSHM instalados em grandes barragens de betão, em particular para: (i) análise e gestão automática dos dados de monitorização em contínuo, tendo em vista a avaliação da sua qualidade, a deteção automática de vibrações medidas durante eventos sísmicos, e a manutenção das bases de dados; e (ii) identificação modal automática, com base no método clássico de decomposição no domínio da frequência, e usando nova metodologias propostas para automatizar a seleção de picos e melhorar a identificação de parâmetros modais em barragens ao longo do tempo.

Apresentam-se exemplos de aplicação para dois casos de estudo, a barragem do Cabril (132 m de altura), em Portugal, e a barragem de Cahora Bassa (170 m), em Moçambique, duas grandes barragens abóbada que estão sob monitorização dinâmica em contínuo desde 2008 e 2010, respetivamente. Os resultados apresentados focam-se essencialmente: (i) na análise da evolução das frequências naturais identificadas ao longo do tempo e na comparação com valores numéricos, tendo em vista a avaliação da influência das variações do nível da água e a deteção de eventuais processos de dano evolutivo; (ii) no estudo da resposta durante eventos sísmicos reais, com base na comparação de acelerações medidas e calculadas em diversos pontos na barragem, para avaliar a influência do input sísmico e do amortecimento usados nos modelos; (iii) na previsão da resposta sísmica não-linear sob sismos de grande intensidade, com vista a avaliar a influência dos movimentos de juntas na resposta estrutural das obras (deslocamentos e tensões), e (iv) na verificação da segurança sísmica de grandes barragens de betão com base no *Endurance Time Method*, analisando as roturas no betão à tração e à compressão sob acelerações sísmicas de amplitude crescente.

KEYWORDS

Dynamic behaviour of concrete dams

Coupled finite element modelling of dam-reservoir-foundation systems

Seismic and Structural Health Monitoring

State-space complex modal analysis

Linear and non-linear seismic response (joint movements and concrete damage)

PALAVRAS-CHAVE

Comportamento dinâmico de barragens de betão

Modelação acoplada com elementos finitos de sistemas barragem-fundação-albufeira

Monitorização sísmica e da integridade estrutural

Análise modal complexa no espaço de estados

Resposta sísmica linear e não-linear (movimentos de juntas e roturas no betão)

ACKNOWLEDGMENTS

This document, along with all the work carried out over the past four years, is the result of great commitment, hard work and dedication, and represents the successful culmination of the most important and challenging phase of my academic career. However, I would have never been able to do it alone, and thus there are several professional and personal acknowledgments to be addressed.

Professional acknowledgements

First and foremost, I am deeply grateful to my esteemed supervisors, Doctor Sérgio Oliveira (National Laboratory for Civil Engineering), Doctor Jorge Proença (Instituto Superior Técnico), and Doctor Paulo Mendes (Instituto Superior de Engenharia de Lisboa), for accepting this challenge and for their invaluable advice and continuous support during this entire time.

Then, I would like to express my sincere thanks to the Portuguese Foundation for Science and Technology (FCT), for funding this work with the doctoral scholarship SFRH/BD/116417/2016, thus granting me the means to continue working on this subject.

Furthermore, I would also like to extend my gratitude to the National Laboratory for Civil Engineering (LNEC), an institution of recognized reputation and value, for giving me the opportunity to conduct my research at the Concrete Dams Department (DBB). In LNEC, I would also like to offer my special thanks to Renato Pereira, Nuno Azevedo, Luísa Braga, João Silva and Margarida Espada, for welcoming me, for their feedback and for contributing to such a pleasant working environment since my first day at the DBB, as well as to Eng. Carlos Santos, from the Scientific Instrumentation Centre (CIC), for helping in the repair and maintenance of the monitoring system of Cabril dam, which was of vital importance for this work.

My appreciation also goes to Energias de Portugal (EDP), for allowing the use of the monitoring data from the system installed in Cabril dam. Special thanks are due to Eng. Ilídio Ferreira, for supporting the conducted studies about Cabril dam, and to Mr. Jorge Fernandes, for his availability, support and interest shown during all our visits to Cabril dam, as well as to all other EDP technicians

Additionally, I am grateful to Hidroelétrica de Cahora Bassa (HCB), for allowing the use of the monitoring data of Cahora Bassa dam, and in particular to Eng. Ezequiel Carvalho and Eng. Bruno Matsinhe, for their prompt collaboration in several studies.

Finally, I would like to thank Eng. Emmannuel Robbe, from Électricité de France (EDF), for his collaboration in studying the seismic response of Cabril dam and for his important and assertive feedback.

Personal acknowledgements

First, I would like to thank myself for all my hard-work, relentless dedication and for never giving up until all my goals were completed.

I would like to express my thanks to all the colleagues that I have met since my first time in LNEC, during an internship for developing the master's thesis back in 2015. From master to doctoral students, including Alexandre, Emanuel, Miguel, Rodrigo, Rafael, Mariana, Cláudia, Patricia, Igor, Magda, Manuel, and Gonçalo, thank you for your companionship and the always fun lunch times.

I would also like to sincerely thank my good old friends from my hometown of Entroncamento, in particular to Pedro and Sofia, for their friendship since the beginning of times.

Por fim, gostaria de agradecer à minha família. Por tudo o que me deram ao longo da minha vida e por me terem ajudado a ser a pessoa que sou hoje. Um agradecimento especial vai para a minha mãe, Rosa, pelo amor e pelo apoio infindável ao longo de todos estes anos, e por ter estado sempre lá para mim, em todos os momentos. Um obrigado ao meu irmão, João, aos meus avós, Maria e Cândido, e ao meu pai, Emílio. Espero ter-vos deixado orgulhosos.

CONTENTS

CHAPTER 1

INTRODUCTION

1. INTRODUCTION

1.1 RESEARCH CONTEXT

Large concrete dams (Fig. 1.1) are civil engineering structures that play a fundamental role in the management of water resources, namely for energy production, water supply, flood control, soil irrigation, and navigation. Furthermore, large dams have become increasingly important over time (ICOLD, 2016b, 2019a), not only due to the rapid growth of world population and the economic development that occurred over the last decades (UN, 2019b, 2019a) leading to a global increase in water needs (UNESCO UN-Water, 2020), but also because of the effects of climate change (IPCC, 2018), since dams allow to attenuate the difficulties faced in the management of water reserves following periods of prolonged drought succeeded by heavy rains, which has become more often.

Jinping-I Dam (2013), China, 305 m high

Kurobe dam (1963), Japan, 186 m high

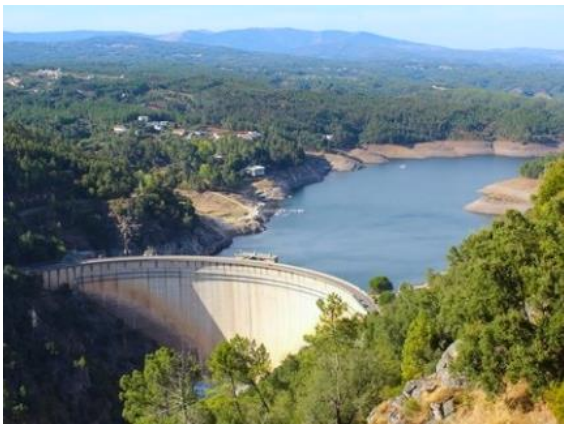

Cabril dam (1954), Portugal, 132 m high

Luzzone dam (1963), Switzerland, 225 m high

Fig. 1.1 Examples of large concrete dams: Jinping-I dam (China), Kurobe dam (USA), Cabril dam (Portugal), and Luzzone dam (Switzerland).

As high potential risk structures, it is essential to ensure the best safety conditions of large concrete dams from the construction phase to the end of their useful life, for any scenarios involving static and dynamic

actions, namely seismic loads, and considering relevant concrete deterioration processes. With that goal, the performance of new and older dams must be evaluated in normal operating conditions and during seismic events (ICOLD, 2019b), in order to control structural integrity over time, in particular for dams with deterioration problems (e.g. cracks, concrete internal swelling, etc.) and/or dams located in regions of high seismicity (Fig. 1.2). Moreover, the structural behaviour of large concrete dams under strong earthquakes must be analysed for seismic safety assessment, according to modern seismic design and performance criteria (ICOLD, 2016a). To this day, dam safety remains one of the main concerns and challenges in dam engineering, not only for owners, but also for researchers and entities responsible for safety control.

Nowadays, there are about 60 000 large dams in operation all over the world, of which around 11 000 are large concrete dams (ICOLD, 2020). Also, according to recent data (IJHD, 2020), about 250 large dams over 60 m high are currently under construction or in the planning phase (Fig. 1.2), namely in regions such as Asia, Africa, South America, the Balkans, and the Caucasus, many of them in zones of high seismicity.

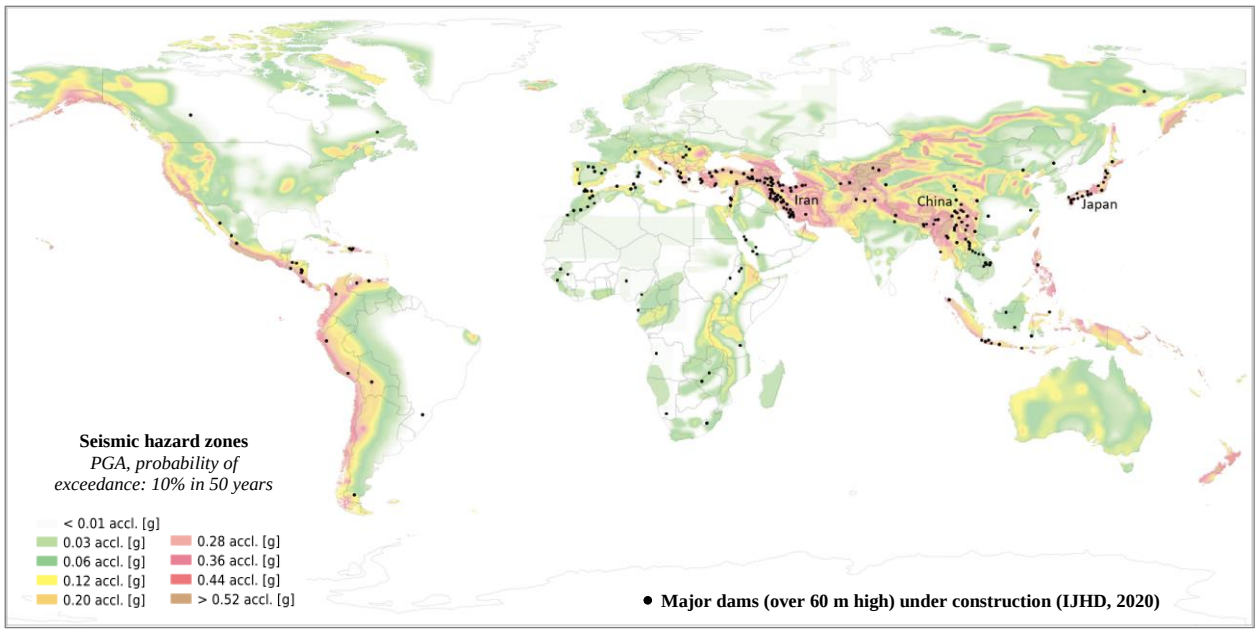

Fig. 1.2 World map with seismic hazard zones (Swiss Seismological Service; www.seismo.ethz.ch]) and major dams (over 60 m high) under construction worldwide in 2019 (IJHD, 2020).

The study of the dynamic behaviour of concrete dams, subject of this thesis, has been for several decades one the greatest challenges for structural engineers, since dams are special structures with very specific features. In addition to the large dimensions and the complex geometry of most concrete dams, particularly for the case of arch dams, their behaviour can be influenced by movements of the vertical construction joints (Clough, 1980; Fenves et al., 1992) or of other discontinuities in the dam body, and structural changes may occur due to concrete failure or eventual processes of evolutive damage over time (S. Oliveira, 2000). Furthermore, dams vibrate together with the foundation and the reservoir (Câmara, 1989). Therefore, their dynamic response under ambient/operational vibrations or under seismic actions is strongly conditioned by

the dynamic water-structure interaction (Westergaard, 1933; Zienkiewicz & Bettess, 1978) and the reservoir water level variations (Alegre, Carvalho, et al, 2019; Darbre & Proulx, 2002; Sevim et al., 2012), as well as by the interaction with the surrounding foundation (Chopra & Tan, 1992; Fok & Chopra, 1986a; C. Zhang et al., 2009). Thus, the dynamic behaviour of dams must be analysed considering a global, complex dam-reservoir-foundation system and the interaction between all parts. As a result, this is a research field where important questions and challenges still arise in terms of numerical modelling and continuous dynamic monitoring.

In this context, aiming to ensure the best operating conditions and the safety of large concrete dams, and to increase knowledge on their dynamic behaviour, it is worth emphasizing the need to continue working on: (i) numerical modelling of the dynamic response of dam-reservoir-foundation systems, by developing advanced finite element models for modal analysis, to obtain natural frequencies, mode shapes, and damping ratios, and for simulation of the seismic response, considering linear and non-linear behaviour; and (ii) continuous dynamic monitoring, through the implementation of Seismic and Structural Health Monitoring (SSHM) systems, for measuring vibrations on large dams, and the development of computational tools for automatic management and analysis of monitoring data, to enable the detection of vibrations during seismic events and the experimental identification of the main modal parameters (see Fig. 1.3).

A serious investment in both advanced finite element models and in sophisticated SSHM systems should enable the combined use of reliable numerical and experimental results and, consequently, provide valuable information to owners, technicians and engineers responsible for dam safety, and researchers (Fig. 1.4). As intended to demonstrate in this work, this data can be used: (i) to analyse the evolution of modal parameters over time, based on vibrations measured in normal operating conditions, enabling a) to investigate the influence of water level and/or thermal variations on the dynamic properties of the dam-reservoir foundation system, and b) to evaluate the effects of ageing, possibly to detect evolutive damage processes, or assess possible structural changes caused by strong earthquakes, by comparing recently observed behaviour with a reference state or with numerical results; and (ii) to characterize the seismic actions at the dam site, as well as to study the seismic response based on measured and computed acceleration records in the dam body, allow for an evaluation of the base-to-top acceleration amplification factors and the investigation of damping values required in the numerical models.

This type of approach can also be extremely useful to provide additional insight on the dynamic behaviour of dam-reservoir-foundation systems and gather valuable data on the performance of large concrete dams. Additionally, the use of reliable experimental information should enable to support the calibration and validation of existing numerical models and help in the development of new ones, which will then be used to in behaviour prediction studies. In this way, it will be possible to properly simulate and analyse various scenarios, for both modal analysis and seismic analysis, involving the variation of static and dynamic loads and structural changes due to deterioration processes, aiming to support structural health monitoring and safety verifications of existing dams, help in the design of new dams, and even contribute for re-evaluating regulation aspects.

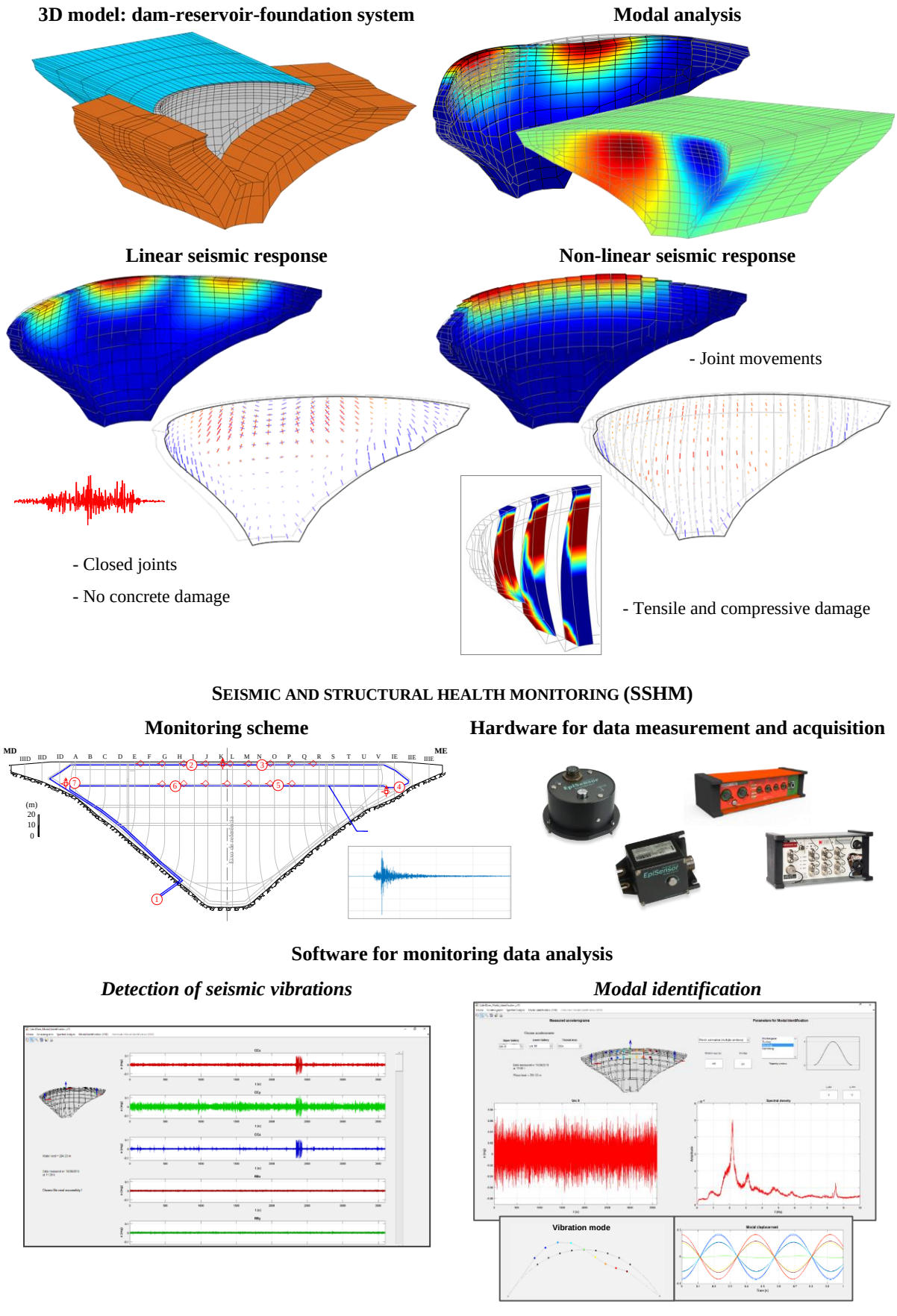

Fig. 1.3 Modelling and monitoring the dynamic behaviour of large concrete dams.

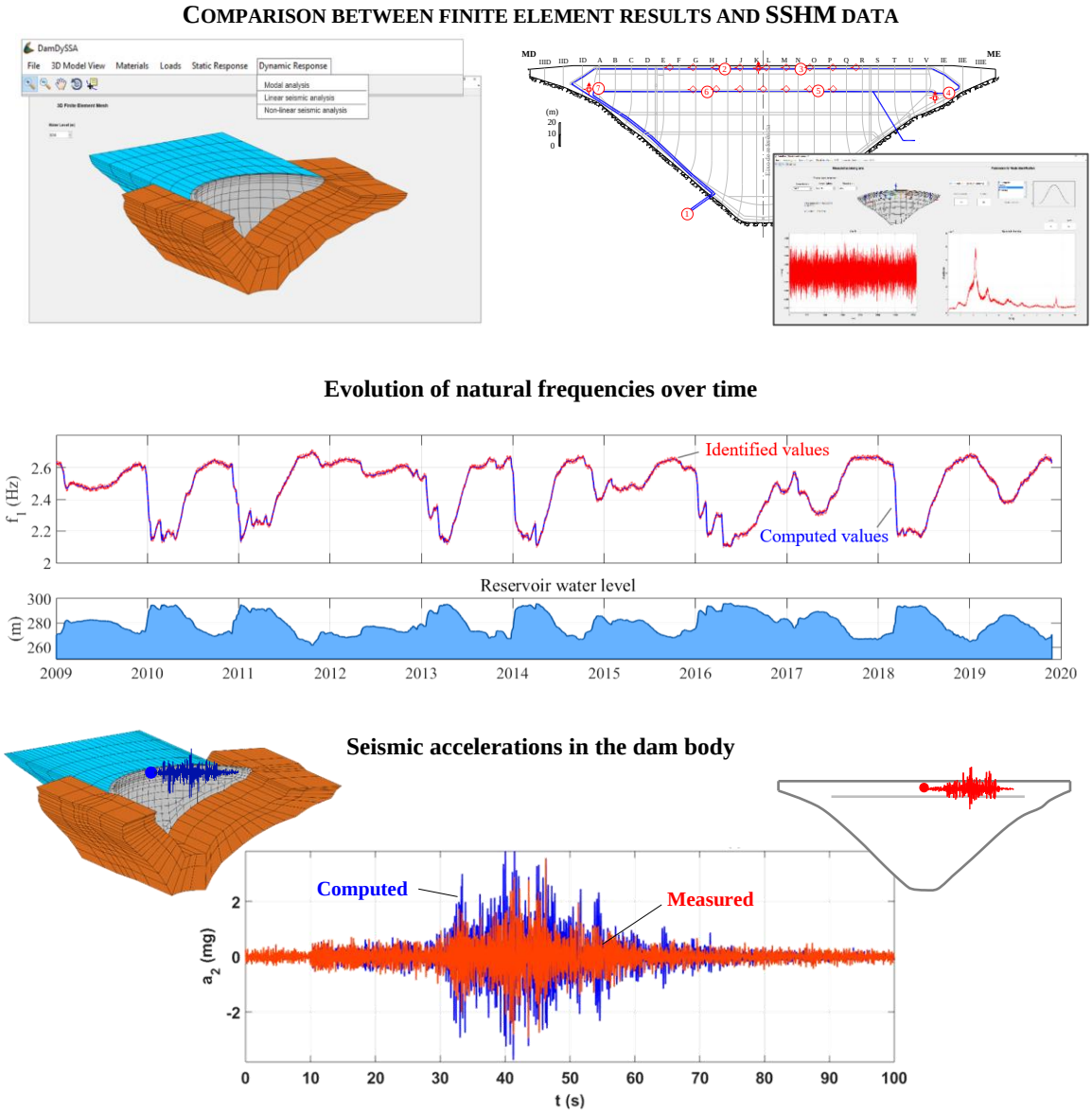

Fig. 1.4 Combined use of results from finite element analysis and results from continuous dynamic monitoring: evolution of natural frequencies over time and seismic accelerations.

INTEGRATION IN THE LNEC CONCRETE DAMS DEPARTMENT RESEARCH PROGRAM

Considering that the research work of this thesis was carried out at the Concrete Dams Department (DBB) of the National Laboratory for Civil Engineering (LNEC), it should be noted that the chosen subject fits perfectly into the activities conducted at the DBB since the 1960s, particularly with regard to the dynamic behaviour analysis, structural health monitoring, and seismic safety control.

Some of the main projects developed over the years included studies of current and failure scenarios using reduced-scale physical models (Borges et al., 1963; Gomes, 2006, 2010; Pedro & Pereira, 1979; J. Pereira & Ravara, 1973), forced vibration tests (Gomes & Carvalho, 2014; Gomes & Lemos, 2016; Gomes & Oliveira, 1994; Pina & Gomes, 1996; Portugal, 1990) and ambient vibration tests (S. Oliveira, Rodrigues, Mendes, et al., 2003; Portugal & Caetano, 1992) for characterizing the dynamic properties of several dams,

and the development of finite element numerical models (Câmara, 1989; S. Oliveira, 2000; Pedro, 1977; Pedro et al., 1996; Pina, 1988) for simulating different scenarios under static and/or dynamic loads.

Based on the knowledge obtained over several decades on both modelling and monitoring, the advantages of using reliable experimental data for dynamic behaviour analysis and safety control of dams, as well as for calibrating and validating numerical models, was recognised. Therefore, a pioneer project was initiated in 2002 (S. Oliveira, 2002), with funding from the Portuguese Foundation for Science and Technology (FCT) and the support of Energias de Portugal (EDP), aiming at the development and installation of the first automated continuous dynamic monitoring system in Portugal and in the World, namely in Cabril dam (Mendes, 2010), which is in operation since 2008. Later, on the scope of another project funded by FCT (S. Oliveira & Lima, 2012), the displacement monitoring was improved by installing a new automatic monitoring component based on Global Navigation Satellite System (GNSS), in order to complement traditional observation methods (e.g. using plumb lines or geodetic methods).

In view of the success achieved on the dynamic monitoring of Cabril dam and the results of great interest obtained in several studies (S. Oliveira et al., 2010, 2011, 2012; S. Oliveira, Silvestre, Espada, et al., 2014; S. Oliveira & Alegre, 2018), EDP decided, with support from LNEC, to invest in the installation of similar system for continuous dynamic monitoring at the Baixo Sabor dam (Gomes et al., 2018; S. Pereira et al., 2017) and Foz Tua dam (Silva Matos et al. 2019a; Silva Matos et al. 2019b), as well as in the implementation of trigger-event type systems for measuring seismic vibrations at several other dams, such as Alqueva, Alto-Ceira II and Ribeiradio dams.

All the accumulated knowledge and the developments resulting from the studies and projects carried out at the DBB made a significant contribution to the dam engineering community about the dynamic behaviour of large concrete dams and the safety control of dams, and, at the same time, laid the foundations for more recent research works, including those carried out within the framework of the present thesis.

1.2 OBJECTIVES AND MAIN CONTRIBUTIONS

1.2.1 OBJECTIVES

Considering the research context presented above, as well as the identified needs and opportunities for contribution, the main goals of this thesis are:

i. The development of a complete finite element model for dynamic analysis of dam-reservoir-foundation systems, to be implemented in the 3D finite element program *DamDySSA*, including proposed calculation methods based on a new approach for a) complex modal analysis, b) linear seismic response analysis, and c) non-linear seismic response analysis; and

ii. The development of computational tools to integrate and complement the software component of SSHM systems installed in large concrete dams, namely a) *DamSSHM*, a program for automatic analysis and management of dynamic monitoring data, to be tested in the monitoring system of

Cabril dam, and b) *DamModalID*, a program for automatic modal identification of dams, to enable the estimation of natural frequencies and modal configurations.

Essentially, the aim is to contribute to the field of dam engineering with an advanced finite element program for dynamic analysis of concrete dams and with software for complementing the SSHM systems installed in large concrete dams, which can be used in the future to study the dynamic behaviour, to support seismic monitoring and structural health monitoring, and to perform seismic safety assessment.

Following the development of a numerical model for simulating the dynamic behaviour of dam-reservoir-foundation systems and of the programs to support the continuous dynamic monitoring of large concrete dams, another fundamental goal of this thesis is to provide the main results from application studies conducted for two large arch dams, namely Cabril dam (132 m high), in Portugal, and Cahora Bassa dam (170 m high), in Mozambique. Experimental results, obtained from monitoring data, are compared with numerical results, including: (i) the analysis of the evolution of the identified natural frequencies (and corresponding mode shapes) over time and the comparison with finite element results, in order to investigate the influence of water level variations in the dynamic properties and to evaluate the occurrence of possible deterioration problems; and (ii) the study of the measured seismic response during low to medium intensity seismic events, based on the comparison between recorded and computed accelerations in the dam body, aiming to study the importance of the used seismic input and modal damping ratios in the models. After that, non-linear seismic analyses under strong earthquakes are conducted, in order to: (i) analyse the influence of the opening/closing and sliding joint movements in the seismic behaviour of the dams; and (ii) to assess seismic safety based on the Endurance Time method, by evaluating the evolution of tensile and compressive damage under intensifying seismic accelerations.

1.2.2 CONTRIBUTIONS AND INNOVATIONS

In addition to the main goals of this thesis, it is also important to highlight more clearly the main contributions and innovations intended with this work.

Regarding the numerical modelling of the dynamic behaviour of dam-reservoir-foundation systems, the emphasis is on the finite element-based mathematical formulations implemented in the program *DamDySSA*. First, a new coupled state space formulation is proposed for complex modal analysis of dam-reservoir-foundation systems, which enables the consideration of generalized (or non-proportional) damping and the calculation of non-stationary vibration modes. Second, the implementation of a time-stepping procedure based on the Newmark method for linear seismic analysis, to solve coupled dynamic equation of the solid-fluid system and calculate the forced response in time domain. And third, the development of an enhanced formulation for calculating the non-linear seismic response of the dam, by combining the time-stepping procedure with an iterative stress-transfer method, to account for the redistribution of unbalanced stresses in the dam, considering a) the non-linear behaviour of concrete up to failure, based on a strain-softening damage model with two independent scalar damage variables (d^+ for tension and d^- for compression), and b) the opening/closing and sliding movements of joints and cracks,

using a constitutive model based on the Mohr-Coulomb failure criterion and on appropriate relative displacement-stress laws.

In what concerns the continuous dynamic monitoring of large concrete dams, the focus is on the computational tools developed for complementing the SSHM systems. First, the new program *DamSSHM* is specifically optimized to complement the SSHM system installed in Cabril dam, in order to carry out the automatic analysis and management of continuous dynamic monitoring data, including daily tasks such as a) assessment of data quality, b) automatic detection of vibrations during seismic events, c) perform maintenance of the database, and d) send emails with relevant information. Second, the development of *DamModalID*, a modal identification program, which is based on the Frequency Domain Decomposition method, with Singular Value Decomposition, and uses innovative techniques to automate the selection of spectral peaks and to enhance modal identification of dams over time based on previous dynamic monitoring data, considering the reservoir level variations.

In this work, a considerable effort is also made in terms of the graphical interfaces and to enhance the presentation of both experimental and numerical results. On the one hand, to facilitate the use of the programs, graphical user interfaces are developed for the 3D finite element program *DamDySSA*, in order to simplify the simulation and evaluation of different scenarios, and for the modal identification program *DamModalID*, with a view to estimate the modal parameters from acceleration records measured in specific dates. On the other hand, aiming at the combined use of experimental and numerical results for seismic monitoring and structural health monitoring, new graphical tools are developed, namely: (i) to compare the identified frequencies over time with computed frequency values, in order to a) evaluate the relation between frequency values and reservoir level variations, and b) perform damage detection, by comparing vibration-based results and numerical results obtained using reference models without damage and models considering evolutive damage; and (ii) to compare accelerations measured during seismic events with the acceleration calculated in various positions of the dam body, to investigate the peak acceleration amplification factors and the damping required in the models. Furthermore, in the case of *DamDySSA*, the outputs of the non-linear seismic calculations are enhanced, including high-quality 3D graphic representations of modal configurations, deformed shapes with joint movements, stress fields at both upstream and downstream faces, arch and cantilever stress envelopes, and tensile and compressive damage distributions.

Finally, with respect to the application studies to be carried out, the intent is to contribute by presenting results of great interest on the dynamic behaviour of two large arch dams, in particular to the scientific community of dam engineering. For example, this work presents, for the first time, the main results and conclusions from over 10 years of continuous dynamic monitoring of two large concrete dams, which involve evaluations of the evolution of natural frequencies over time, analyses for vibration-based damage detection, and studies based on acceleration time histories recorded during seismic events. Also, this thesis provides a series of numerical results on the non-linear seismic response of large arch dams considering both joint movements and concrete damage, something that has never been done in LNEC, and a seismic safety evaluation of two large arch dams, based on a new methodology.

1.3 THESIS ORGANIZATION

This thesis is divided into 6 chapters. The content of each one is summarised next.

Chapter 1 introduces the thesis, starting with a contextualization of the theme and of the conducted work, followed by the presentation of the main goals and important contributions, finishing with the present description of the organization of the text.

Chapter 2 is dedicated to large concrete dams, particularly in what concerns their dynamic behaviour and safety. It starts with general considerations about large concrete dams, including the different structural types, the main loads, and fundamental aspects regarding the dynamic behaviour of dam-reservoir-foundation systems, with emphasis on arch dams. Then, Chapter 2 chapter addresses the subject of dam safety, first regarding structural safety control, with reference to observation systems and dynamic behaviour monitoring and to the types of models used for interpretation, analysis, and simulation of dam behaviour, and then concerning seismic safety, including seismic hazard, seismic design and performance criteria, and models and methods of analysis. The chapter ends with a detailed overview of the work conducted over time in the field of modelling and monitoring the dynamic behaviour of concrete dams. In the first part, the main developments on finite element models of dam-reservoir-foundation systems and on the use of physical models are addressed, with reference to several studies of interest, namely in what concerns the study of modal parameters and seismic response analysis. The second part is dedicated to monitoring vibrations on large concrete dams, by making reference to large concrete dams instrumented for seismic monitoring, to forced and ambient vibration tests performed on dams, and to cases of large concrete dams in which continuous dynamic monitoring systems have been installed.

Chapter 3 is focused on the numerical modelling of the dynamic behaviour of dam-reservoir-foundation systems, and its main goal is to present the developed finite element mathematical formulations and the program *DamDySSA*. The chapter starts with the state-of-the-art, where the types of models used in current practice for simulating the dynamic water-structure interaction and the foundation behaviour, as well as the formulations most commonly used for modal analysis and seismic response analysis, are referred. Then, in order to present the mathematical notation and the bases for the mathematical formulations used in the rest of the chapter, the fundamental equations of Solid Mechanics, namely when applied for dynamic analysis, and the essential concepts and properties used in constitutive joint models, are addressed. After that, on a first phase, the implemented model for simulating the dynamic behaviour of the dam-reservoir-foundation system is described in detail, and the proposed formulations for complex modal analysis, linear seismic analysis, and non-linear seismic analysis, are presented. On a second phase, the program *DamDySSA* is described, its graphical user interface is shown, and tests for validation of the developed mathematical formulations are performed. Finally, it is described the new module for the program *DamMesh*, used in LNEC for automatic generation of 3D finite element meshes of dam-reservoir-foundation systems, which was developed to automatically introduce joints in the dam mesh.

Chapter 4 deals with the seismic and structural health monitoring of large concrete dams, and it aims at describing the programs *DamSSHM* and *DamModalID*, specifically developed to integrate and complement

SSHM systems installed in large concrete dams. Therefore, this chapter starts with a state-of-the-art on SSHM systems for large concrete dams, with reference to the main goals of SSHM and to their advantages for safety control, to the monitoring schemes and their main components, and also to their installation and operation. After that, the computational tools developed for integrating the SSHM systems installed in large concrete dams are presented. First, the program *DamSSHM*, implemented for testing in the SSHM system of Cabril dam, is described in detail, including the main tasks it performs for automatic analysis and management of continuous dynamic monitoring data. Second, an overview is given on Operational Modal Analysis, on signal processing, and on frequency domain modal identification, followed by detailed descriptions of the implemented frequency domain method and of the new techniques developed for automatic and enhanced selection of spectral peaks for large dams, finishing with the presentation of the program *DamModalID*, developed for automatic modal identification of large dams, and of its graphical user interface.

Following the developed work described in Chapters 3 and 4, Chapter 5 aims to present the application studies carried out for analysing the dynamic behaviour of two large arch dams, namely Cabril dam (Portugal) and Cahora Bassa dam (Mozambique). The chapter is divided into two subchapters, one dedicated to each dam. Each subchapter starts with a detailed description of the dam and of the installed continuous dynamic monitoring systems, and addresses the seismic action considered for the dam site. Then, the main results from the performed application studies are presented. On a first phase, experimental results obtained from continuous dynamic monitoring over the last decade are compared with numerical results from finite element calculations, aiming a) to analyse the evolution of the identified natural frequencies over time, and b) to investigate the measured response during seismic events. On a second phase, numerical simulations for non-linear seismic analysis under strong earthquakes are performed, in order to a) investigate the influence of joint opening/closing and sliding movements on the structural response, b) to evaluate the seismic dam safety based on the Endurance time method, by examining tensile and compressive damage in the dam body.

Finally, Chapter 6 describes the main conclusions of this thesis and presents future perspectives.

CHAPTER 2

LARGE CONCRETE DAMS.
DYNAMIC BEHAVIOUR AND SAFETY

2. LARGE CONCRETE DAMS. DYNAMIC BEHAVIOUR AND SAFETY

2.1 INTRODUCTION

Large concrete dams have a key role in the proper management of water resources, by making a decisive contribution to water supply, flood control, irrigation, and electrical energy production. Usually, these are structures of high potential risk, since incidents or accidents involving this type of dams can result in significant losses for populations and the environment (Wieland, 2016). Furthermore, according to the International Commission on Large Dams (ICOLD) it is fundamental to evaluate their performance in normal operating conditions and under seismic events (ICOLD, 2018, 2019b), particularly in the case of dams subject to concrete deterioration phenomena and/or those located in areas of medium-high seismicity. Aiming to ensure the best operating conditions for large concrete dams and to ensure the safety during their lifetime, the structural safety must be evaluated for current and failure scenarios, under static and dynamic loads.

Therefore, the study of the dynamic behaviour of large concrete dams, focusing on the evaluation of the main modal parameters and on the analysis of the seismic response, is not only important to increase knowledge on the behaviour of the dam-reservoir-foundation system, but it is also fundamental to support structural health monitoring over time and the safety assessment under seismic loads, aiming to ensure the best operating and safety conditions. Nevertheless, despite the conducted work and the developments achieved in dam engineering over decades, this is a field where significant questions and challenges continue to arise in terms of numerical modelling and continuous dynamic monitoring.

In this context, the present chapter presents important considerations on large concrete dams and their dynamic behaviour, namely in what concerns structural safety control and seismic safety assessment. The aim is to give a state-of-the-art overview on the addressed subjects and properly frame the work developed in this thesis on numerical modelling of the dynamic behaviour of dam-reservoir-foundation systems (Chapter 3) and on continuous dynamic monitoring of large dams (Chapter 4), as well as the performed application studies (Chapter 5).

Subchapter 2.2 starts with general remarks on large concrete dams, followed by sections addressing the different types of concrete dams, the main loads on dams, and fundamental aspects on the dynamic behaviour of the complex dam-reservoir-foundation systems, with emphasis on arch dans. After that, subchapter 2.3 regards dam safety, with focus on structural health control, and it addresses important aspects regarding visual inspections, dam observation systems and dynamic behaviour modelling, and models used for interpretation, analysis, and prediction of dam behaviour. Then, subchapter 2.4 is about seismic safety, and it covers topics such as seismic hazard, seismic design and performance criteria, models and methods for seismic analysis, and the relevance of seismic records. Finally, subchapter 2.5 presents a general review concerning both modelling and monitoring the dynamic behaviour of large concrete dams with one section for each. The first section addresses the main developments on the use of physical models and of finite element models for simulating the dynamic behaviour of dam-reservoir-foundation systems, from the first half of 20th century to the present day, and reference is made to several studies of interest.

The remaining three sections provide an extensive overview on monitoring vibrations in large dams, with references about dams instrumented for seismic monitoring, forced and ambient vibration testes performed on dams, and cases of large concrete dams, over the world and in Portugal, where continuous dynamic monitoring systems have been installed.

2.2 LARGE CONCRETE DAMS

Large dams are civil engineering structures of considerable dimensions and complex geometry, built for storage of a significant water mass (Fig. 2.1). According to ICOLD, a large dam is a dam with a height of 15 m or greater, from the lowest point at the base to the crest level, or a dam which is between 5 and 15 m high and impounds more than 3 million m^3 of water (ICOLD, 2020).

As regards their role, dams can be designed and built as single- or multi-purpose dams. Most dams have a single purpose, although the number of multipurpose dams is growing (ICOLD, 2020). The main purposes of dams are production of hydroelectric energy, water supply for domestic and industrial use, irrigation of land for cultivation, flood control and river level regulation, inland navigation, and recreation, among others. The most common purpose is, by far, irrigation, followed by hydropower.

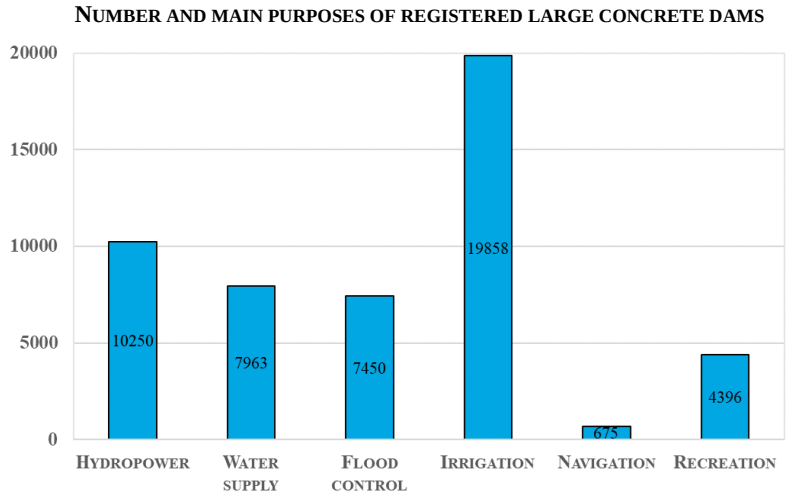

Alqueva multipurpose dam (2003), 96 m high, Portugal

Baihetan hydropower dam (2021), 289 m high, China

Fig. 2.1 Number and main purposes of registered large dams (ICOLD, 2020) and example of two large dams: Alqueva multipurpose dam (2003), Portugal, and Baihetan hydropower dam (2021), China.

Nowadays, the key role of large concrete dams in the proper management and control of available water resources is widely recognised (ICOLD, 2014, 2021), especially considering that water resources are subject to seasonal variations and unevenly distributed worldwide. This makes dams essential for populations, by providing a range of economic, environmental, and social benefits, as well as for a sustainable development. However, large dams are projects that require significant investments, both economically and in labour (ICOLD, 2007), from the design phase to the end of their service life, including the maintenance and the observation and analysis of long-term behaviour during the operating phase (ICOLD, 2018). Therefore, it is vital to ensure the economic and technical feasibility of large dams and to guarantee the best operating and safety conditions (DSR, 2018), aiming to optimise their exploitation and extend their useful life, and to avoid incidents and accidents that may cause significant damage to populations and the environment. Furthermore, it is fundamental to define clear, well-planned strategies for an adequate integration of dams in social, environmental and economic terms (ICOLD, 1997, 2007, 2014).

2.2.1 TYPES OF CONCRETE DAMS

Large dams can be constructed using different types of materials and present different structural characteristics (ICOLD, 2020). In terms of the used material, dams are classified as concrete, masonry, earth fill or rock fill dams. As for the type of structure, dams built of concrete or masonry can be gravity dams, arch dams, or buttress dams, while dams built of earth and/or rock fill are commonly known as embankment dams. Regarding concrete dams, they represent about 20% of the large dams currently in operation worldwide (ICOLD, 2020). The different types of concrete dams are described next.

Gravity dams are designed as massive concrete structures, which essentially resist the water pressures from the reservoir through their self-weight, thus transmitting the resulting forces to the foundation. These dams typically have an approximately triangular cross section to ensure greater structural stability and to avoid overstressing of the dam and foundation. The dam body can be solid or hollow in case there are voids in its cross section. In what concerns the plan (or top) view, the dam can be rectilinear or present a certain curvature, depending on the soil conditions, the topographic conditions, and/or the construction system to be used. Gravity dams constructed using regular concrete are formed by sets of monolithic blocks, separated by transversal contraction joints. Good examples are Grande Dixence dam, 285 m high and 700 m long, in Switzerland (Fig. 2.2), Three-Gorges Dam, 181 m high and 2335 m long, in China, or Itaipu Dam, 196 m high and 7919 m long, in the Brazil/Paraguay border.

Alternatively, gravity dams can be built in roller-compacted concrete, in which case the compaction of each block is achieved through the passing of vibrating rollers over successively placed concrete layers, a technique used in Gilgel Gibe III dam, 250 m high, in Ethiopia, (Fig. 2.3), and in Longtan dam, 216.2 m high, in China. Gravity dams are best suited for regions with smoother topography, wider valleys, and compact rock foundations.

Fig. 2.2 Gravity dam: Grande Dixence dam (1961), Switzerland, 285 m high.

Fig. 2.3 Roller-compacted gravity dam: Gilgel Gibe III dam (2015), Ethiopia, 250 m high.

Buttress dams are built as a continuous, water-tight structure, with a vertical or sloped upstream face, which is supported by a series of vertical supports that run along the downstream face. These vertical supports, usually parallel and equidistant, are called buttresses. In addition to their self-weight, buttress dams resist to the water pressures by making use of strength of the buttresses, which increase structural stability and convey the forces to the foundation. The dam body, which is the water-tight part of the structure, can be a plain deck slab, a series of arch slabs, or a direct continuation of the buttresses, forming a massive round or diamond-shaped head. Compared to gravity dams, buttress dams enable to save in terms of the used concrete, however they require more formwork and reinforcement steel for concrete. Buttress dams are good solutions for areas with flat topography and wide valleys, and they need high strength foundations to

properly support the buttresses. Well-known examples are Roselend dam, 150 m high, in France (Fig. 2.4), and Daniel-Johnson dam, 214 m high, in Canada.

Fig. 2.4 Buttress dam: Roselend dam (1962), France, 150 m high.

Arch dams are those that present a horizontal curvature, oriented towards upstream. When they also have curvature in the vertical direction, they are called double curvature arch dams. This type of dam is designed to resist the water forces essentially by transmitting the forces to the abutments, in order to take advantage of the high compressive strength of concrete. Arch dams are usually thin structures, especially those with double curvature, with reduced thickness at the top. Regarding the construction process, arch dams are built sequentially by vertical blocks, which are separated by contraction joints that are later injected with cement grout. Moreover, in some cases the dam body is constructed on the pulvino, a type of concrete saddle structure that supports the dam weight and transmits it to the ground.

In general, arch dams are designed with a small volume in comparison with other dams, particularly with gravity dams, thus enabling to exploit the concrete strength more efficiently. Furthermore, these are very durable and reliable structures, particularly to resist exceptional events such as strong earthquakes or overtopping cases. However, they will lead to higher costs as they require concrete of superior quality, rigorous construction planning and execution, more sophisticated design and analysis methods, and more rigorous performance monitoring. Moreover, as an alternative to regular concrete, the technique of roller-compacted concrete can also be used. Arch dams are particularly good solutions for regions with irregular topography, narrow valleys, and highly resistant rock mass foundations. Well-known cases of large arch dams are the tallest dam in the world, Jinping-I dam, 305 m high, in China (Fig. 2.5), Enguri dam, 271.5 m high, in Georgia, Mauvoisin dam, 250 m high, in Switzerland, Pacoima dam, 113 m high, in the United States, and, of course, Cabril dam, 132 m high, in Portugal.

Fig. 2.5 Arch dam: Xiaowan dam (2010), China, 292 m high.

For the application studies to be conducted in this work, two double curvature large arch dams were chosen as case studies, namely Cabril dam, 132 m high, in Portugal, and Cahora Bassa dam, 170 m high, in Mozambique (described in detail in Chapter 5). Their cross section is compared to the those of other large dams over the world and in Portugal in Fig. 2.6.

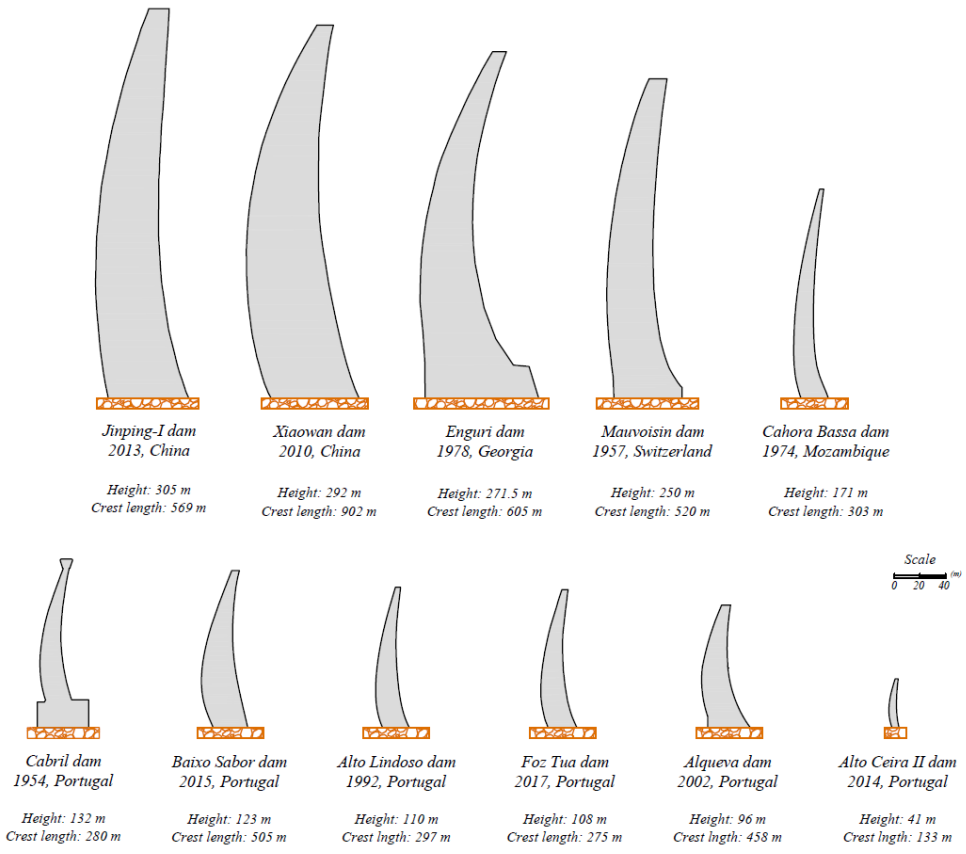

Fig. 2.6 Examples of double curvature arch dams. Central cantilever cross sections.

There are also other types of concrete dams that combine structural characteristics of the dams described above. For example, there are arch-gravity dams (Fig. 2.7), which have curvature in plan and present a greater cross section thickness that conventional arch dams, and multiple arch-dams (Fig. 2.8), which usually present a long-span crest and are composed by multiple arches, supported by concrete buttress on the downstream side.

Fig. 2.7 Arch-gravity dam: Hoover dam (1936), Unite States of America, 225 m high.

Fig. 2.8 Multiple-arch dam: Aguieira dam (1972), Portugal, 89 m high.

2.2.2 MAIN LOADS ON CONCRETE DAMS

Large concrete dams are unique three-dimensional structures, founded on a rock mass foundation, which support a considerable water mass to form a reservoir. Over their lifetime– construction, first reservoir filling, operation, and abandonment -, dams are subject to different types of actions and interactions (Fig. 2.9), which may be always present, remaining constant or varying over time, occur sporadically, or arise only in exceptional occurrences (Pedro, 1999). Therefore, these actions and the resulting structural effects should be adequately considered, both in behaviour monitoring and in the numerical models, for analysis and interpretation of the dynamic behaviour of dams in normal operating conditions or in exceptional situations. Furthermore, is important to properly define the scenarios to be evaluated and the corresponding load combinations in the different phases of the lifetime of the dam, for studies supporting the design and structural safety evaluations of dams.

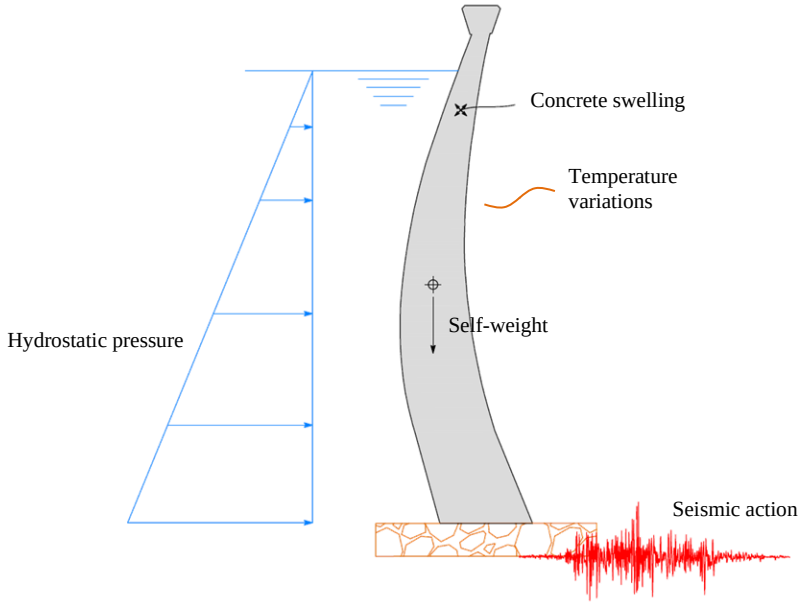

Fig. 2.9 Schematic representation of loads on an arch dam.

The loads that act on dams can be classified and grouped according to different criteria (S. Oliveira, 2000). On the one hand, loads can be (i) static, like the self-weight, the hydrostatic pressure, and thermal variations or (ii) dynamic, including small, medium, or high intensity earthquakes, the wind, vibrations induced by the operation of the power production groups or the operation of spillways, and vibrations due to other occurrences in or close to the dam site (e.g., human activity, traffic, or explosions nearby). On the other hand, the loads that act on dams can be defined as (i) external, including the water pressure, thermal variations, earthquakes, the wind, etc., or (ii) internal, such as concrete swelling reactions or thermo-hygrometric variations.

There are also other possibilities to classify loads on dams, for instance considering their importance and occurrence probability (Novak et al., 2007). According to this criterion, there are: (i) primary loads, which

are present on all dams, being of prime importance, like the self-weight or water related loads; (ii) secondary loads, which include a) more common loads but of lower importance, e.g. vibrations induced by operational sources as power groups or spillway or by small/medium intensity seismic events, and b) loads of major importance, but only to certain types of dams, such as concrete swelling reactions, significant thermal variations, or ice related loads; and (iii) exceptional loads, with low probability of occurrence but of high impact, including strong earthquakes and overtopping.

In what concerns the different phases of the dam lifetime, there are loads that assume particular importance or that arise only in certain periods (S. Oliveira, 2000; Pedro, 1999). For example, during the construction process (Fig. 2.10), taking into account the different stages, it is important to consider the self-weight of the different blocks, the pressure of the cement grout injection in the vertical contraction joints and at the base, or the cooling of the blocks due to the dissipation of the heat of hydration in each concreting layer. During the first filling of the reservoir, it should be considered the increasing hydrostatic pressure on the upstream face, the temperature variations on both upstream and downstream sides due to the rising water level, or, in an exceptional scenario, induced seismicity phenomena and foundation movements. As for the normal operating period, relevant loads are the dam self-weigh, the hydrostatic pressure, which depends on the reservoir water level, actions due to thermal variations, vibrations induced by the power production machinery or discharge elements, wind, or earthquakes of different magnitudes.

a) **b)**

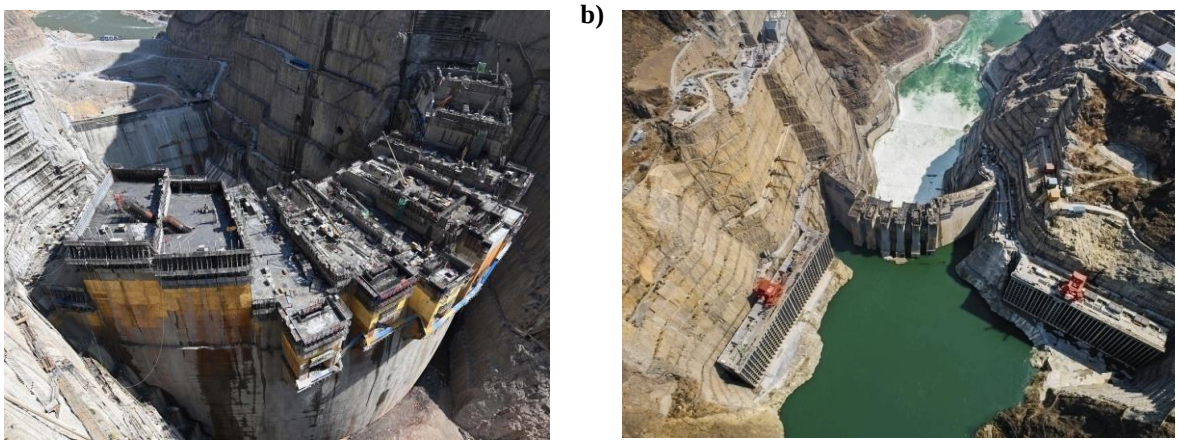

Fig. 2.10 Wudongde dam (2020), China, 240 m high. a) During construction and b) in operation.

STATIC LOADS

Regarding the self-weight load, there are basically two methodologies to simulate the self-weight of the dam. In case the aim is to analyse the response during the construction process, it is necessary to simulate the growth of the various blocks, by considering a sequential application of the weight of each block and the corresponding stress states (Batista, 1998). However, if the aim is to evaluate the structural response for current or failure scenarios under static and/or dynamic loads, it is usual to simply assume that the stress field due to the self-weight load corresponds to the one resulting from the instantaneous application of the self-weight of the whole dam at once.

The water load is one of the most important to take into account for analysing the structural behaviour and safety of a dam, representing one of the factors that makes dams such unique structures. On dams, after the first filling of the reservoir, the water level can suffer significant variations during the normal operation phase, depending on the weather conditions and on established reservoir exploitation management. In addition to the hydrostatic pressures on upstream side, water-related loads can also manifest by hydrostatic pressures on the bottom of the downstream side, internal pressures inside cracks or other discontinuities in the dam body (and also in the foundation), and uplift pressures at the dam base, along the dam-foundation interface (S. Oliveira, 2000; Pedro, 1999). Other actions or effects on dams associated with water include the chemical alteration and erosion of the foundation materials or even of the concrete itself due to water seepage, as well as the erosion of the spillways. Furthermore, as mentioned later, the dynamic properties of the dam-reservoir-foundation system and thus its dynamic behaviour can be significantly influenced by variations in the reservoir water level (Alegre, Carvalho, et al., 2019; Darbre & Proulx, 2002; Fanelli, 1999; Okuma et al., 2008; Sevim, Altunışık, et al., 2011).

Thermals loads, generated by temperature variations associated with changes in ambient conditions and with cement cooling and hydration, can have important effects and thus must be properly considered for dam behaviour analysis in the different phases of the lifetime of dams. During the construction process, as well as in the first few years of operation, thermal variations will occur due to the generation and dissipation of cement hydration heat, particularly in the connection between a recently concreted layer and the layer below that one, which is in a more advanced cooling state. Furthermore, during the operation phase, important thermal loads can arise due to the air and water temperature variations, which can be especially significant for dams located in zones with high daily or annual thermal variations. In such cases, thermal variations can not only have a strong influence on the structural response of dams (Malm et al., 2014; Malm & Ansell, 2011), but also alter the dynamic characteristics of the dam-reservoir-foundation system (Okuma et al., 2012; Ueshima et al., 2017).

With respect to processes that lead to concrete deterioration over time, swelling phenomena caused by chemical reactions between the concrete elements, namely alkali-aggregate (Piteira Gomes, 2007) or by sulphates (Silva, 1993), have been detected more often in large concrete dams. For example, alkali-aggregate chemical reactions originate the formation of an expansive gel inside the concrete that generally leads to an increase of volume and possibly cause concrete cracking (decrease of its mechanical properties). This type of phenomena can occur in an initial stage of the lifetime of dams and are characterized by a slow, steady development over time, and therefore its structural consequences are only observed in later stages. Typical effects include upward displacement at the crest, with concrete cracking in a typical pattern, radial displacements towards upstream, and tangential displacements towards the abutments.

DYNAMIC LOADS

During the operation phase, concrete dams can be subject to various types of dynamic excitations of ambient or operational source, such as the wind, vibrations induced by the operation of the power groups or spillways, traffic, etc., all of which normally induce vibrations of low amplitude (of the order of magnitude

of milli-g) in the dam body. Thus, these dynamic loads are not significant from a structural response analysis point of view. However, in these ambient/operational dynamic loading conditions it is possible to study the dynamic behaviour of the dam-reservoir-foundation system and the performance of the dam itself by analysing the vibrations measured in ambient vibration tests or with SSHM systems, using high precision sensors. This can be achieved based on frequency or time domain methods for Operational Modal Analysis (OMA) (Brincker & Ventura, 2015; Peeters, 2000), which are used to estimate the main modal parameters from the measured data and thus analyse their evolution over time. The extracted results can be of great use to evaluate the dynamic performance of dams in normal operating conditions, particularly to study the influence of water level and/or thermal variations (Calcina et al., 2014; S. Oliveira et al., 2012; Proulx et al., 2001; Ueshima et al., 2017), and to perform structural health assessments, namely using vibration-based methodologies for damage detection (Alegre, Oliveira, et al., 2020), as shown in this thesis.

Furthermore, it is worth mentioning that dams may be subject to several seismic actions during their operating period, which will naturally cause different structural responses. Therefore, earthquakes that hit the dam site with different intensities[1] may induce vibrations (and thus inertia forces) of lower or higher amplitude in the structure, resulting in a linear structural response or in non-linear behaviour, involving concrete damage and joint movements. In what concerns seismic monitoring, the measurement of acceleration time histories at the foundation and in the dam body can be of great value to characterize the ground motion and its spatial variation (Chopra & Wang, 2010), as well as to analyse the seismic performance of the dam based on recorded accelerations, e.g. to study acceleration amplification factors and the damping to be used in numerical models of the dam-reservoir-foundation system (Chopra & Wang, 2012; Proulx et al., 2004; Proulx & Darbre, 2008; Robbe, 2017; Robbe et al., 2017). Regarding the structural safety assessment under strong earthquakes, appropriate seismic actions must be considered to conduct seismic safety verifications of both current and failure scenarios (ICOLD, 2016a; Wieland, 2014). To that end, first, specific studies must be carried out, considering the characteristics and seismicity of the dam site, in order to estimate adequate ground motion parameters based on deterministic or probabilistic methods (H. Chen, 2014; Wieland, 2016). Then, the required scenarios are evaluated based on seismic performance evaluation methods, such as Incremental Dynamic Analysis (Vamvatsikos & Cornell, 2002) or Endurance Time Analysis (Estekanchi et al., 2004), considering specific performance criteria, and using advanced finite element models or physical models on shaking tables to simulate the non-linear seismic response. Finally, it is worth emphasizing that seismic hazard is actually multi-hazard (Wieland, 2016), given that strong earthquakes can originate not only significant ground motion, but also movements along faults or discontinuities in the foundation or mass movements into the reservoir that induce impulse waves.

[1] The strength of an earthquake is defined by its magnitude, which measures the energy released at its source, based on measurements from seismographs, while intensity indicates the amplitude of shaking at a certain location, based on the effects on people, structures, and environment.

2.2.3 THE DAM-RESERVOIR-FOUNDATION SYSTEM. STATIC AND DYNAMIC BEHAVIOUR

Large concrete dams are structures of considerable dimensions, usually with unique geometry and built from a material with complex physical properties. Additionally, their behaviour under static and dynamic loads is strongly influenced by the interaction with both the reservoir and the foundation (Câmara, 1989; Pedro & Câmara, 1986). Therefore, for analysing the observed behaviour and for numerical modelling, it must be taken into account that these structures are part of a complex dam-reservoir-foundation system (Fig. 2.11), whose global response depends on the dam-water interaction (Westergaard, 1933; Zienkiewicz & Bettess, 1978) and on the foundation behaviour (Chopra & Tan, 1992; Fok & Chopra, 1986a).

Furthermore, the properties of the dam-reservoir-foundation system and thus its global behaviour change significantly over time, namely due to reservoir water level and thermal variations (Alegre, Carvalho, et al., 2019; Darbre & Proulx, 2002; Sevim et al., 2012), and to structural changes in the dam body, including processes of concrete deterioration over time (S. Oliveira, 2000) and movements of vertical contraction joints or other discontinuities (Clough, 1980; Fenves et al., 1992).

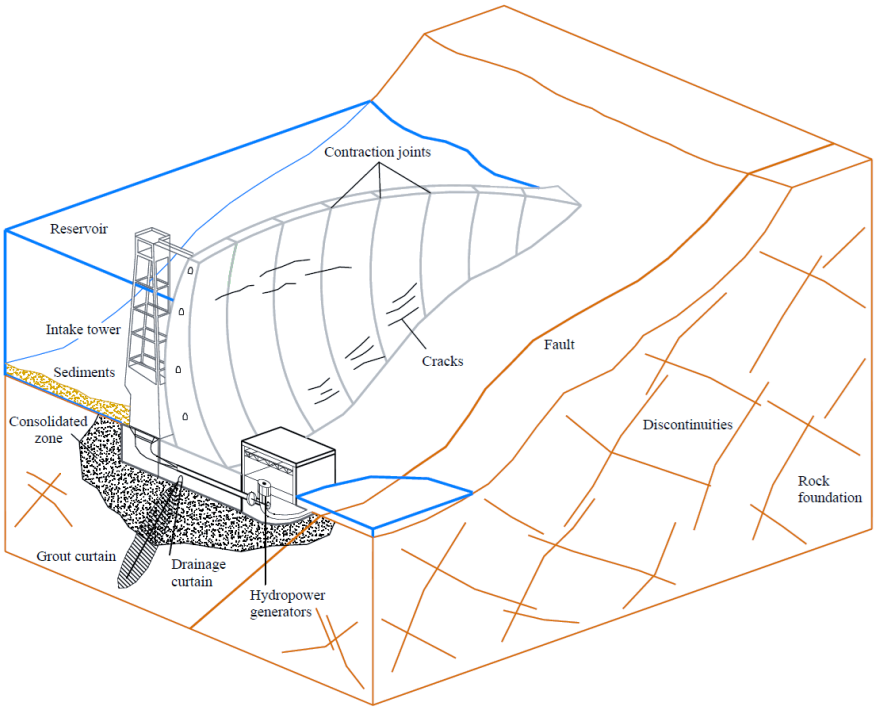

Fig. 2.11 Arch dam-reservoir-foundation system [adapted from (Mendes, 2010)].

In terms of structural integrity, it is usual in these dams the development of cracks in concrete, namely due to high tensile stresses (Wieland, 2005) cause by the water loads, significant thermal variations, or strong earthquakes, as well as the occurrence of deterioration phenomena over the lifetime of dams (S. Oliveira, 2000). An example of that is Cahora Bassa dam, in operation since 1974 in Mozambique, which has small horizontal cracks at the downstream face and a pattern visible at the crest that is typically associated to swelling phenomena (Fig. 2.12).

The ageing and deterioration of concrete over time, e.g. due to time-dependent effects (S. Oliveira, 2000) or to swelling reactions (Piteira Gomes, 2007), will naturally reduce the material strength and thus lead to a decrease in the global resistant capacity of the dam, as exemplified in numerical and experimental studies for simulating the so-called concrete strength decrease scenario (S. Oliveira & Faria, 2006; Rocha & Serafim, 1958). Furthermore, the significant deterioration of the structural integrity of the dam can alter the dynamic properties and thus the global response of the dam-reservoir-foundation system, a phenomenon that can possibly be detected by analysing the modal parameters estimated from continuous vibrations monitoring data and comparing with numerical results obtained using advanced finite element models (Alegre, Oliveira, et al., 2020; S. Oliveira & Alegre, 2020).

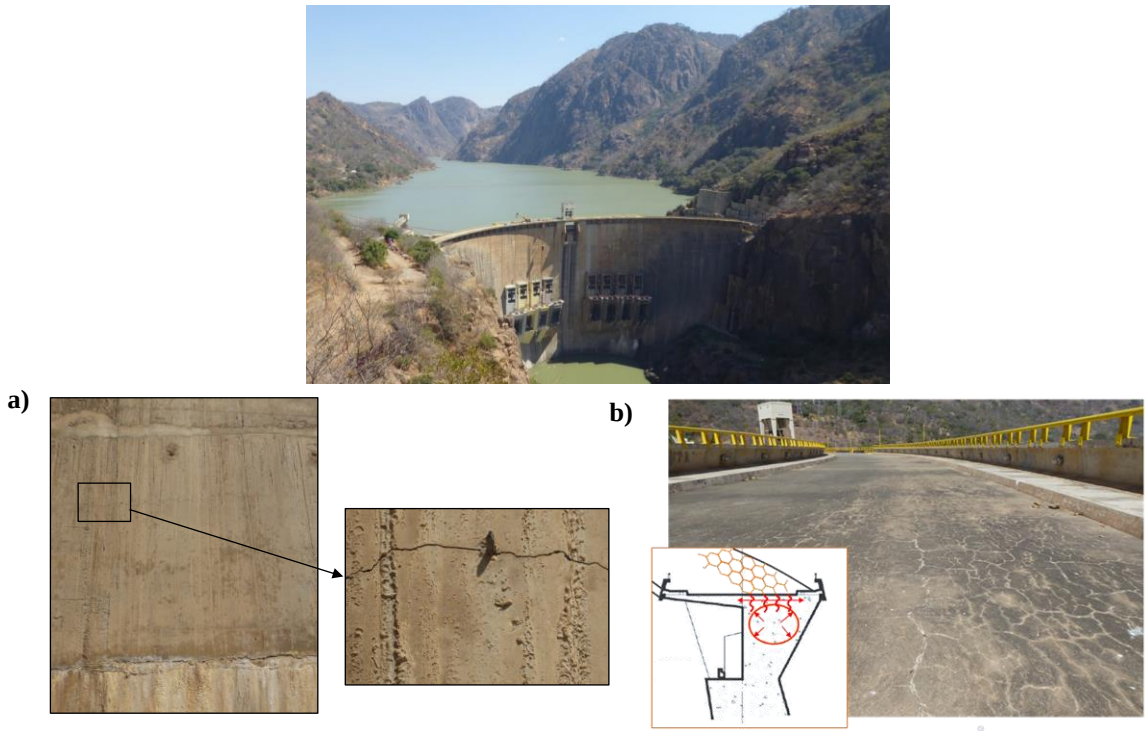

Fig. 2.12 Cahora Bassa dam (1974), Mozambique, 170 m high. a) Small horizontal crack at the downstream face and b) visible pattern at the crest due to concrete swelling.

With respect to the behaviour of the dam-reservoir-foundation system, the water load and the dam-reservoir interaction are of paramount importance. Naturally, this will depend on the reservoir water level: as mentioned, after the first reservoir filling the water level will vary during the normal operation phase, depending on the weather conditions and on the established reservoir exploitation management.

Regarding the water-related loads, higher reservoir levels will result in significant hydrostatic pressures at the upstream face of the dam, which will originate high tensile stresses at the base. In the case of arch dams, it is common for significant tensions to appear along the upstream base due to the water pressures, which may cause the appearance of cracks there – in this scenario, a possible solution is the construction of a perimetral curved joint to release these tensions and hence avoid concrete damage (Fanelli, 1999). On the other hand, the uplift pressures at the dam-rock interface reduce the normal force at the base of dam, thus

reducing cohesion and the resistance to sliding. The uplift pressure is a very important load to consider in the evaluation of the stability of gravity dams, but is usually neglected for analysing the behaviour of arch dams (Ghanaat, 1993). For dams in which such phenomenon has a considerable influence, drainage curtains and/or grout curtains can be implemented.

In terms of global dynamic behaviour, for higher water levels there is an increase of the reservoir mass and hence of the mass of the global dam-reservoir-foundation system, which leads to a decrease in the values of the natural frequencies. Additionally, the energy dissipation associated with the propagation of pressure waves along the reservoir becomes more significant, which has influence on the damping of the global dam-reservoir-foundation system (Zienkiewicz & Bettess, 1978). Furthermore, under high intensity earthquakes, important hydrodynamic pressures develop in the reservoir, particularly on the upstream face of the dam (Chopra, 1967; Westergaard, 1933; Zienkiewicz & Nath, 1963), which naturally affects the structural response. In the particular case of arch dams, greater water pressures due to higher water levels will push the dam towards downstream and the vertical contraction joints tend to close, thus increasing the global stiffness of the dam body and changing the dynamic behaviour of the whole system. In summary, reservoir water level variations can have a considerable influence on the mass, stiffness, and damping of the dam-reservoir-foundation system, and therefore on the evolution of the modal parameters over time. This behaviour has been evidenced in studies carried out for large concrete dams, as seen for the cases of Emosson dam (Proulx et al., 2001) and Mauvoisin dam (Darbre et al., 2000), in Switzerland, of Cabril dam (S. Oliveira & Alegre, 2019a, 2018), in Portugal, and of Hitotsuse dam (Fig. 2.13) (Okuma et al., 2008, 2012), in Japan.

Also, with regard to reservoir level variations, it is worth noting that a rapid rise of the reservoir water level, e.g., in the first filling phase, can lead to reservoir-triggered seismicity (H. Chen, 2014; Severn, 1999; Wieland, 2016), which must be properly accounted for in specific seismic hazard analysis for the dam site. Another phenomenon to be considered is the eventual accumulation of sediments at the bottom of the reservoir, which can have an additional effect of mass and affect the radiation and reflection of pressure waves at the reservoir-foundation interface (Bouaanani & Lu, 2009; Clough, 1980).

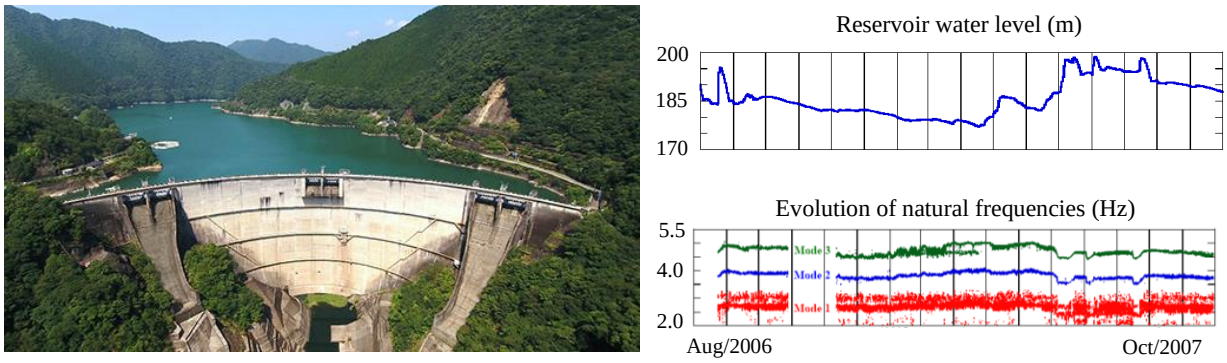

Fig. 2.13 Hitotsuse dam, Japan. Results from long-term ambient vibration testing (August 2006 to October 2007): water level variations and evolution of the first three vibration modes (Okuma et al., 2008, 2012).

For dams located in regions where significant thermal variations occur, winter/summer temperature distributions can considerably influence the structural response of a dam in terms of both displacements and stresses (Malm et al., 2014; Malm & Ansell, 2011), and potentially lead to higher deformations that cause the appearance of cracks in concrete (Fig. 2.14a) (Nordström et al., 2019). Furthermore, the dynamic behaviour of the dam-reservoir-foundation system can be altered due to seasonal thermal variations. In the summer, the temperature rises, and the dam volume increases as the concrete expands, leading to the closing of the vertical contraction joints, which increases the global stiffness and thus the values of the natural frequencies. On the other hand, during the winter the temperatures falls and thus there is a volume decrease that originates the opening of the joints, resulting in a decrease of global stiffness and hence of the frequency values. As mentioned in relation to the reservoir level variations, the influence of thermal variations on the dynamic behaviour of the dam-reservoir-foundation system can also be detected based on the evolution of the identified natural frequencies over time. One such case is Okhura Dam (Fig. 2.14b), in Japan, with dam surface temperatures ranging from a maximum of about 30º C in the summer to approximately – 5º C in the winter (Ueshima et al., 2017).

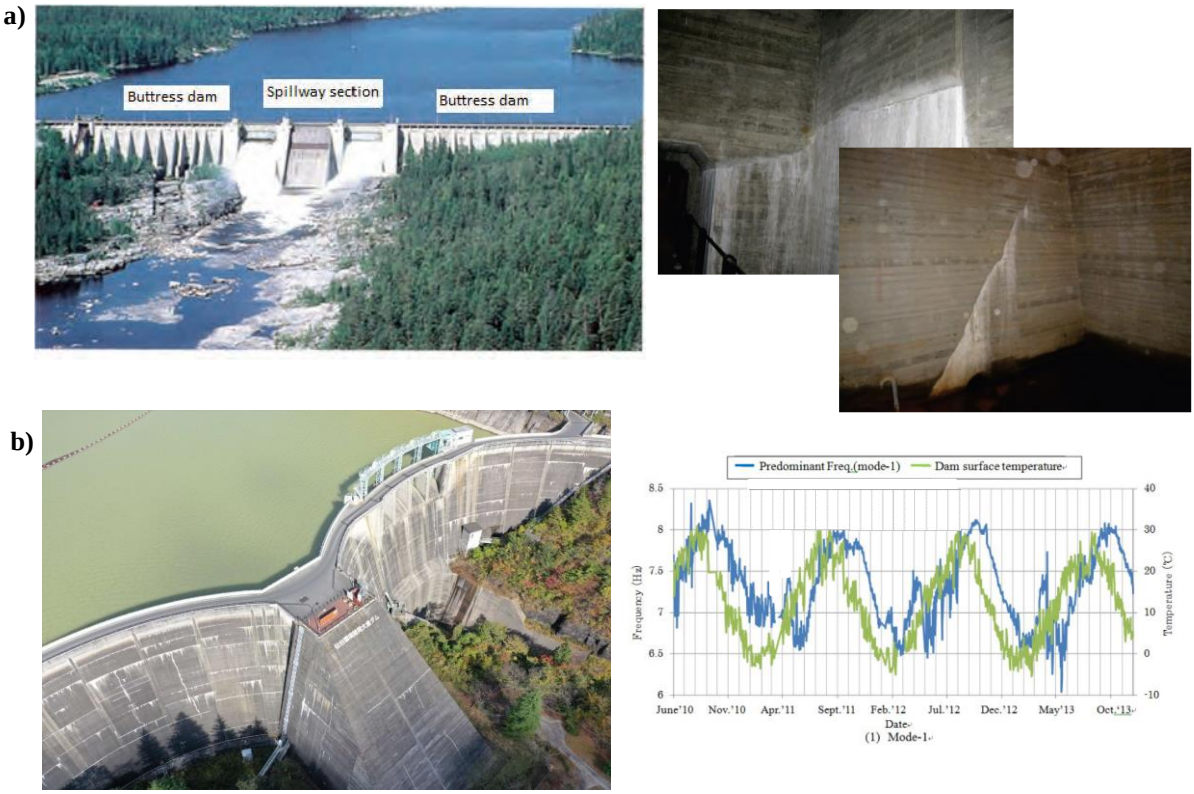

Fig. 2.14 a) Power plant (1958) in Lapland, Sweden, consisting of two buttress sections and a central spillway: cracks in front slab and buttress before repairs (Nordström et al., 2019); b) Ohkura double-arch dam (1961) in Japan: time evolution of natural frequencies and dam surface temperature for three and a half years (Ueshima et al., 2017).

Regarding the structural response of the dam, high-intensity earthquakes can result in considerable seismic loads that cause high tensile and compressive stresses in the dam body, and, consequently, concrete damage. For example, in the case of gravity dams, concrete failure is expected at the upper part of the dam, more

specifically around the zone that connects the dam body to the crest, in both upstream and downstream faces and along the thickness, as well as along the upstream base, which tends to propagate in the normal direction to the dam surface, as shown in studies about Koyna dam (Cervera et al., 1995; Chopra & Chakrabarti, 1972; Niwa & Clough, 1982). As for arch dams, when the seismic load pushes the dam towards upstream, the vertical contraction joints tend to open (H. Chen, 1994; Clough, 1980; Niwa & Clough, 1982), resulting in stress redistribution processes that lead to the release of arch stresses at the upper part of the structure and the consequent increase of vertical tensile and compressive stresses along the height of the cantilevers (Fenves et al., 1992). When the dam moves towards downstream, the joints close, arch compressions increase, and high tensions usually arise at the downstream base, normally oriented to the insertion. Thus, for greater excitation levels, the occurrence of concrete damage is expected, resulting in cracking under tensions or ultimately in crushing under compressions (Espandar & Lotfi, 2003; Faria et al., 1998; Valliappan et al., 1999). This behaviour was observed in many studies conducted for large arch dams and several citations are provided in this work.

In order to avoid unacceptable joint opening and the occurrence of high stresses in unwanted zones, it can be beneficial to consider the use of shear-keys in the contact surfaces between adjacent blocks or joint reinforcements, of steel belts at the upper part of the dam in the arch direction, and the installation of reinforcement steel nets in the zones where higher tensions are expected, e.g., at the upstream base (Fig. 2.15), as proposed for several large arch dams in China (Lau et al., 1998; R. Wang, 2016; R. Wang et al., 2018; C. Zhang et al., 2000, 2004). Other examples of dams with seismic steel belts include Rapel dam, 112 m high, Chile, Sir dam, 116 m high, Turkey, Katse dam, 185 m high, Lesotho and Enguri dam, 271.5 m high, Georgia (Wieland, 2003).

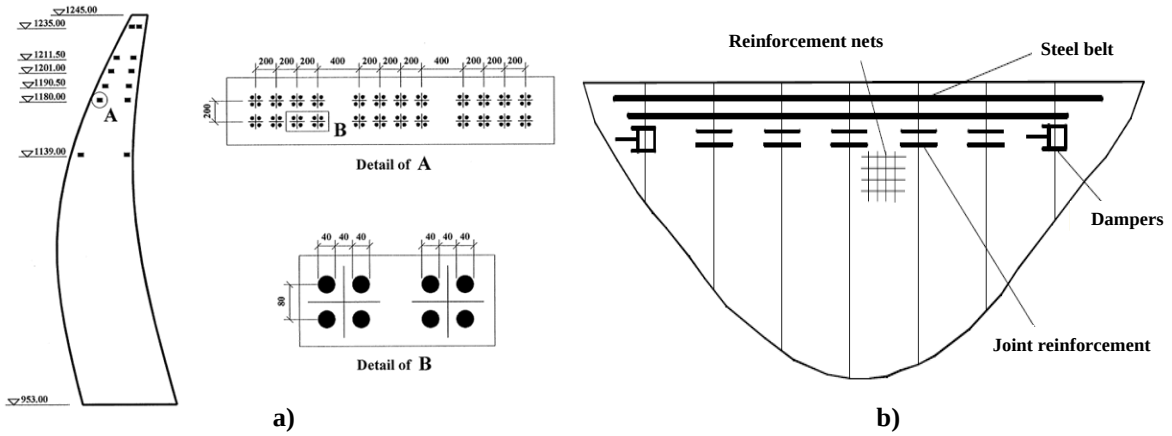

Fig. 2.15 Seismic reinforcements for large concrete dams. a) Scheme of seismic strengthening measures (C. Zhang et al., 2004); b) Layout of possible seismic reinforcements proposed for Xiaowan arch dam (C. Zhang et al., 2000).

The foundation rock mass (Fig. 2.16) is a crucial element of the dam-reservoir-foundation system because of their contribution for the structural stability and safety of dams, namely by supporting the loads transmitted by the structure along the dam-rock interface. Rock masses are discontinuous and in most cases heterogeneous and anisotropic, and their behaviour can be conditioned by existing discontinuities such as

joints and geological faults, which in turn are filled with deformable materials with reduced strength (Braga Farinha, 2010). In terms of the dynamic behaviour of the dam-reservoir-foundation system, particularly under seismic loads, the dam-foundation interaction (Chopra & Tan, 1992) must be properly considered in the numerical models, as it will influence the dam structural response in terms of displacements and stresses (Tan & Chopra, 1996), while the energy dissipation due to the propagation of pressure waves in the rock mass can change the damping of the global system (Chuhan et al., 2009). Moreover, it should be noted that, due to strong earthquakes, or caused by other alterations in the surrounding rock mass, there a risk of block sliding on the upstream or downstream slopes, and new cracks can occur in the foundation, leading to an increase of seepage and consequently of the uplift pressures inside the discontinuities.

Fig. 2.16 Aerial view of the foundation of Baihetan dam (China) in 2017, before construction. Insertion surface.

To summarise, based on the considerations addressed above, it is worth stressing the importance of considering the global behaviour of the dam-reservoir-foundation system and the effects due to the interaction between all parts when intending to study behaviour of large concrete dams under static dynamic loads. This is fundamental for the interpretation and analysis of the observed behaviour, as well as for the development of numerical models to be used in behaviour prediction studies.

2.3 DAM SAFETY. STRUCTURAL SAFETY CONTROL

Large concrete dams are civil engineering structures with a significant social, environmental and economic impact (ICOLD, 2019b), considering that they require a considerable investment, provide a fundamental contribution for the proper and efficient management of freshwater resources, and are structures of high potential risk. Therefore, it is vital that all entities involved in the safety control of large dams take the necessary measures from the design phase to the end of their lifetime, with the goal of ensuring the best behaviour and safety conditions during constructing, first filling of the reservoir, the operation phase, and

abandonment (Pedro, 1999), for any hazards of anthropogenic or natural origin. Examples of hazards for dam projects or hydropower plants can be (Wieland, 2014, 2016): (i) natural environment hazards, including floods, earthquakes, mass movements, and extreme weather conditions; (ii) structural hazards, such as blockage of spillway gates, differential structural movements on joints or interfaces, foundation seepage, ageing or alkali-aggregate reactions, failure of equipment used for operational purposes, etc.; and (iii) man-made hazards, involving design errors, inadequate construction, faulty equipment operation, etc.

The safety of dams is one of the main concerns in dam engineering and continues to be one of the main challenges for researchers and for all entities involved in safety control, from technicians to engineers, being a subject of particular interest for owners and stakeholders. This subject has become increasingly important over time, given the advances in safety requirements and considering the increase in specific knowledge about large concrete dams, which has resulted from several decades of work and experience in this area (ICOLD, 2019a, 2019b). In this scope, ICOLD and the National Commissions on Large Dams of its various member countries have been playing a crucial role in the discussion about dam safety and on the need to properly monitor and analyse the static and dynamic behaviour of dams (ICOLD, 2016a, 2017a, 2017b, 2018), not only for new dams, but also for older dams (Fig. 2.17), most of them built decades ago and with possible deterioration problems, particularly for those located in high seismic risk zones.

Mauvoisin dam (1957), Switzerland, 250 m high

Enguri dam (1987), Georgia, 271.5 m high

Xiluodu dam (2013), China, 285.5 m high

Foz Tua dam (2017), Portugal, 108 m high

Fig. 2.17 Examples of large concrete dams constructed several decades ago and recently constructed.

The structural safety control of concrete dams is essentially based on modelling and monitoring dam behaviour, and on analysing and interpreting the measured response and predict results from behaviour models. The structural safety control encompasses a set of measures to be taken in the design phase, during the construction, the first filling of the reservoir, and the operating phase, with the goal of achieving the best operating and safety conditions in the long-term. Furthermore, during the first filling of the reservoir and the operating phase, such measures must also allow a deep and continuously updated knowledge on the performance and structural integrity, as well as the timely detection of possible issues and behavioural anomalies, thus enabling an effective decision making in face of regular maintenance situations or of eventual emergencies (DSR, 2018; ICOLD, 2018).

Therefore, in addition to ensuring the suitability of dam design and the quality of the construction process, it is essential to develop appropriate strategies and to implement an observation plan, aiming to control structural safety during the construction, the first filling of the reservoir, the first few years of operation, and the subsequent normal operating period. The implementation of an adequate observation plan can also make an important contribution to increase knowledge on the performance of dams in normal operating conditions, which can be useful to improve the safety control measures for existing dams and the design of dams to be built in the future, as well as to provide valuable information to support the calibration and validation of existing numerical models and the development of new ones, which are used to simulate the behaviour dam-reservoir-foundation systems. The observation plan, which must be prepared according to the unique features of each dam, should include specific measures and requirements for an effective structural safety control of the dam and appurtenant works, namely regarding visual inspection campaigns, the installation and operation of monitoring systems, and the analysis of dam behaviour and evaluation of the structural safety. Additionally, the main incident and accident scenarios, as well as other exceptional events must be taken into consideration, including floods and strong earthquakes.

2.3.1 VISUAL INSPECTIONS

The carrying out of periodic visual inspections aims at the detection of deterioration or ageing signs in certain zones of the dams and appurtenant works. According to the Portuguese Regulation on Dam Safety (RSB, 2018), the observation plan should indicate the type of inspections to be carried out on dams, the regularity with which they will be performed in the different phases of their lifetime, the main aspects to be evaluated, and the form of presentation of the results. Based on the gathered information, these inspections should enable to analyse the evolution of existing pathologies or anomalies or help in the identification of new ones. For example, visual inspections can be useful to detect structural changes caused by high-intensity earthquake events or other relevant dynamic loads.

The main pathologies or anomalies usually detected in concrete dams are essentially related to the existence of cracks in concrete, the opening of joints due to differential movements between blocks, the occurrence of swelling reactions, or the unwanted percolation of water along the discontinuities of the dam or the foundation – as seen, e.g., in the old Alto Ceira dam (Fig. 2.18). In addition, in elements like spillways or

bottom outlets it is common to notice deterioration due to hydraulic-operational reasons or to the exposure to atmospheric agents.

In general, visual inspections allow for a qualitative assessment of the occurrence and evolution of pathologies and of the state of structural integrity of dams. Therefore, the information gathered during these inspections serves as complement to the quantitative data obtained with the observation systems and behaviour models, in order to support structural safety control.

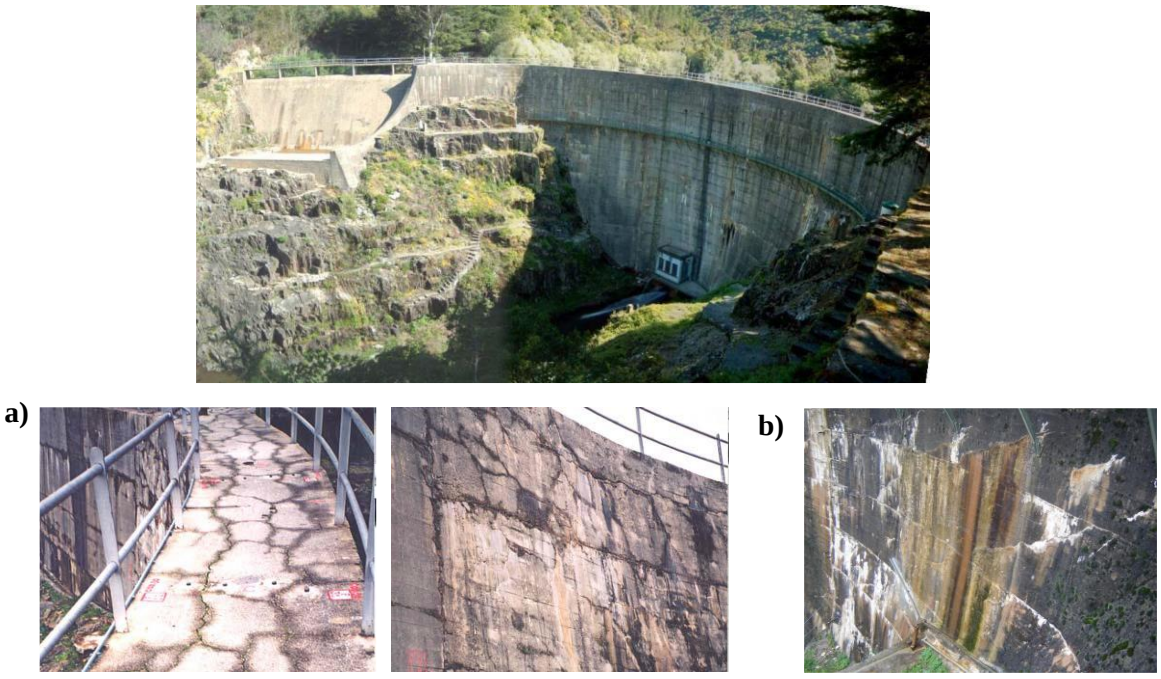

Fig. 2.18 Old Alto Ceira I dam (1949), Portugal, 34 m high. a) Cracking at the crest and on the downstream face; b) Signs of water percolation through joints/cracks and products of swelling reactions (Batista & Piteira Gomes, 2014).

2.3.2 OBSERVATION SYSTEMS AND DYNAMIC BEHAVIOUR MONITORING

An observation system consists of a set of devices installed for measuring the main quantities that allow for a characterization of the static and dynamic behaviour of a dam, which will then gathered and properly presented for analysis and interpretation. Therefore, the implementation of an observation system should enable to obtain reliable experimental information aiming at dam behaviour analysis and safety control, by comparing the measured response with the predicted response based on reference models, in order to (re)assess structural health, and by issuing warnings about structural changes that can endanger structural safety.

Regarding the installation and operation of the observation system, as mentioned in the Portuguese Dam Safety Regulation (RSB, 2018), the observation plan should indicate: (i) the quantities to be measured for evaluation of a) the actions, namely water level, temperatures, and seismic accelerations, b) the structural properties, e.g., concrete Young's modulus, vibrations in normal operating conditions, etc., and c) the structural response, including displacements (Fig. 2.19), stresses, strains, joint movements, temperatures,

accelerations, etc.; (ii) the measurement devices to be used, such as piezometers, thermometers, plumb-lines, extensometers, stress meters, joint meters, accelerometers, GNSS antennas, etc., as well as their number and locations, and (iii) the frequency of the measuring campaigns during the various phases of the dam lifetime, and the criteria for their adaptation in case the necessity arises. In addition, the observation plan must also give indications in terms of the data acquisition, reading, and processing, as well as on the technical qualifications on the agents in charge of the installation and operation of the observation system on the dam site. Furthermore, during the first exploration phase, dam behaviour reports must be prepared, including analyses on the observed quantities, the definition of parameters for what is considered as normal behaviour, to be taken as reference over the subsequent operation period, and, if necessary, eventual proposals to update the observation plan and the models used for simulating dam behaviour.

Over time, there has been a tendency towards the development and implementation of observation systems with automatic data acquisition features (ICOLD, 1999, 2018), usually referred as Automatic Data Acquisition Systems (ADAS), for the characterization of both static behaviour (Braga Farinha et al., 2004; Fanelli, 1980) and dynamic behaviour (Mendes, 2010; S. Oliveira, 2002), something that was made possible due to the evolution in the technology available for data measurement, acquisition, transmission, and storage. However, it is important to note that new difficulties may arise when this type of solution is adopted, particularly concerning equipment maintenance, which require periodical inspection, and of data storage, management, and analysis, given the large amount of gathered information.

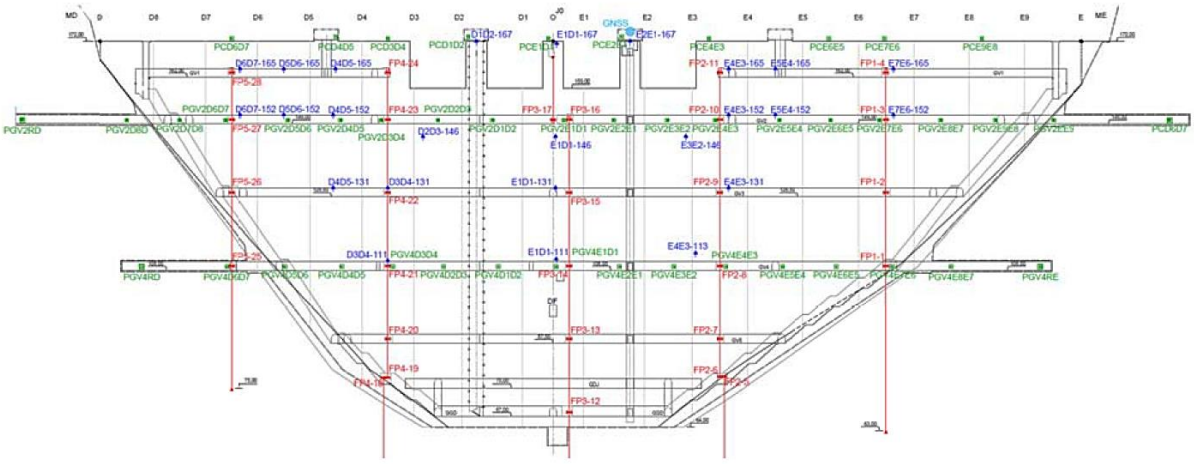

Fig. 2.19 Static observation system of Foz Tua dam. Horizontal displacements measuring instruments, including plumb lines (red), precise traverse in the crest and in two galleries (gree), 3D continuous geodetic monitoring system (dark blue), and GNSS (light blue) (Silva Matos, Tavares de Castro, Gomes, Faria, et al., 2019).

Regarding dynamic behaviour monitoring, the evaluation of the response of the dam can be carried out based on vibrations measured in the dam body. The dynamic properties, or modal parameters, of the dam-reservoir-foundation system, which include natural frequencies, mode shapes and damping ratios, can be estimated from recorded vibrations using modal analysis techniques (Brincker & Ventura, 2015; Maia &

Silva, 1997). There are two classical testing methods available for the observation of dynamic behaviour: forced vibration testing and ambient vibration testing.

FORCED VIBRATION TESTS

Forced vibration tests are performed by applying known and controlled excitations, using special devices like eccentric mass vibrations or hydraulic shakers, and by measuring the dynamic response in various positions of the structure. This is referred to in common practice as input-output testing, and it has been widely used with success for studying the dynamic behaviour of civil engineering structures, such as bridges, buildings, and dams (Cunha & Caetano, 2006; Severn, 2010). For example, since the 1960s several forced vibration tests were performed in the scope of LNEC's studies for various Portuguese dams (Portugal, 1990), namely in Alto Lindoso dam (Gomes & Oliveira, 1994) and Cabril dam (Pina & Gomes, 1996), and, more recently on the Alto Ceira II (Fig. 2.20) (Gomes et al., 2016) and Baixo Sabor (Gomes & Lemos, 2016) dams. Nevertheless, despite enabling to achieve results of great interest for characterising the dynamic behaviour of dams, forced vibration tests are somewhat expensive, given that transportation to the dam site and logistics to install the excitation devices are difficult, considering that heavy and large equipment is required.

Fig. 2.20 Alto Ceira II arch dam (41 m high), Portugal. Eccentric mass shaker used in forced vibration test.

AMBIENT VIBRATION TESTS

As the name indicates, ambient vibration tests are carried out by measuring vibrations at various locations of the dam body in normal operating conditions, under dynamic excitations of ambient and/or operational sources like the wind, power groups operation, traffic, etc. This methodology is known as output-only, as the dynamic response (output) is measured without knowing the excitation, which is assumed to be random (more details on this are given on Chapter 4). It is worth mentioning that the vibrations measured under these conditions are generally of very low amplitude, thus requiring the use of high precision sensors with

very low noise levels – the technological advances that occurred at this level clearly contributed to the development and growth of this methodology. Ambient vibration testing has the important advantage of enabling the dynamic of dams under ambient/operational vibrations without disturbing its normal operating conditions, since there is no need to apply an external excitation. Furthermore, ambient vibration tests are also more economical and simpler to perform. There are many examples of ambient vibration tests conducted for characterizing the dynamic behaviour of large concrete dams since the 1980s, namely on Contra dam (Brownjohn et al., 1986) and on Mauvoisin dam (Darbre et al., 2000), both in Switzerland. In Portugal, within the scope of LNEC's research activities, several ambient vibration tests were performed in Cabril dam (Fig. 2.21) (Mendes et al., 2004; Mendes & Oliveira, 2009; S. Oliveira et al., 2004).

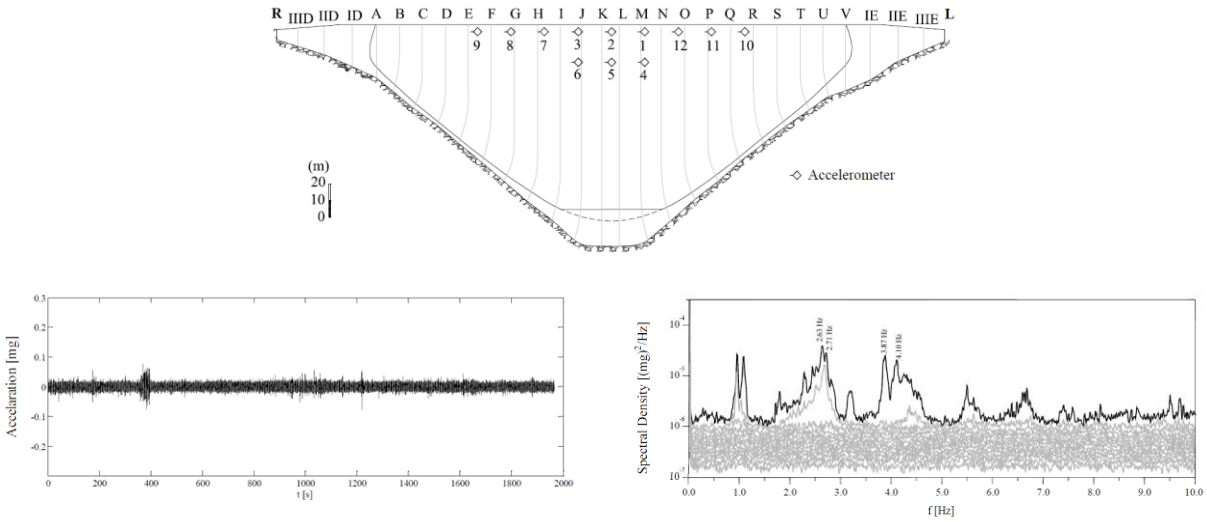

Fig. 2.21 Ambient vibrations test carried out in Cabril dam in 2002. Positions of the accelerometers, recorded acceleration time history (crest of central cantilever) and singular value spectrum (Mendes & Oliveira, 2009).

CONTINUOUS DYNAMIC MONITORING

The experimental information obtained in forced vibration or ambient vibration tests is of great value for characterizing the dynamic properties and the dynamic behaviour of dams, and to help in the development, calibration, and validation of numerical models. However, this type of testing can only be carried out sporadically, which is naturally not enough to provide data for supporting an effective and continuous structural safety control of dams under dynamic loads, as required.

In this context, the importance of continuously monitoring the dynamic performance of dams and the need to automatically obtain reliable experimental data was comprehended and reinforced over the years, due to its obvious advantages and to meet the increasingly demanding safety requirements for large concrete dams. Therefore, aiming to complement the classic observation systems required in current regulation and to meet the ICOLD recommendations on monitoring the performance of dams (ICOLD, 2018, 2019b), continuous dynamic monitoring systems began to be developed for large concrete dams for behaviour control in normal operating conditions and during seismic events. This type of systems, used in current practice for structural

health monitoring and seismic monitoring, have been installed in several large concrete dams over the world. Examples include Cabril dam, Baixo Sabor dam, and Foz Tua dam, in Portugal, as well as Cahora Bassa dam and Roode Elsberg dam, in Africa (more details are given in section 2.5.4).

2.3.3 MODELS FOR INTERPRETATION, ANALYSIS AND PREDICTION OF DAM BEHAVIOUR

The structural behaviour analysis and safety assessment of dams is carried out based on the interpretation and evaluation of experimental data and the comparison with reference values obtained with behaviour prediction models (ICOLD, 2018). In case the measurements are in agreement with the reference values, then dam performance is assumed to be normal, and regular operating conditions can continue. Otherwise, if the observed behaviour is not compatible with the predictions of models, additional studies should be conducted to provide further insight into the verified anomalies, or, alternatively, actions should be taken in order to prevent incidents or accidents or to minimize their consequences. Therefore, it is fundamental the development of reliable models for interpretation and analysis of the observed behaviour, as well as of behaviour prediction models that enable an accurate simulation of dam behaviour for current and failure scenarios that can occur over their lifetime, involving the variation of static and dynamic loads and eventual structural changes.

In this regard, the current Portuguese regulation (RSB, 2018) states that the observation plan should define the measured quantities (displacements, joint openings, strains, natural frequencies, etc.) that enable the identification and characterization of unexpected or anomalous behaviour, particularly those associated with the accident or incident scenarios established in the design phase. It should also give indications on the interpretation and behaviour prediction models to be used for structural safety control, which can be numerical models, physical models, modal identification models, and data-based models.

NUMERICAL MODELS

Numerical models are essentially a combination of mathematical equations, based on physical laws that describe the phenomena involved in the static or dynamic problem to be simulated, which are solved in order to compute an approximate solution for that problem. Their application for simulating the behaviour of dams enables to calculate displacements, strains, stresses, and damages, for structural analysis under static or seismic loads, or natural frequencies, mode shapes, and damping ratios, for modal analysis.

Numerical models can entail several degrees of complexity. In many cases it is common to consider linear behaviour, by assuming simplifying hypothesis such as monolithic dam behaviour (no joints nor cracks), linear constitutive model for concrete (no damage), and continuous foundation without discontinuities. This is a valid approach, e.g. to calculate the seismic response under low intensity earthquakes (Chopra & Wang, 2010; Proulx & Darbre, 2008) or to evaluate the free vibration response for modal analysis (Alegre, Carvalho, et al., 2019; Calcina et al., 2014; S. Oliveira et al., 2012). However, the simulation of certain scenarios requires more complex models, considering joint movements, damage in concrete, or the effects of non-linearities in the foundation. This can be the case for analysing non-linear behaviour under strong

earthquakes (Cervera et al., 1995; Clough, 1980; Espandar & Lotfi, 2003; Faria et al., 1998; Fenves et al., 1992; J.-T. Wang et al., 2013) and for simulation of evolutive concrete deterioration over time for modal analysis (Alegre, Oliveira, et al., 2020; S. Oliveira & Alegre, 2020).

Regarding their advantages, numerical models use parameters with clear physical meaning and can be calibrated and validated based on experimental data. Moreover, their use is quite practical and economical. Therefore, advanced and properly calibrated numerical models are the most effective tools for simulating the behaviour of dams for various scenarios and for analysing the required quantities.

The development of numerical models evolved significantly over the years, particularly from the 1960s and 1970s, alongside the advances in computational capabilities, leading to the development of various calculation programs and to many studies of interest (this is addressed with greater detail in section 2.5.1). Regarding available numerical methods, it is worth mentioning the Finite Element Method (FEM) (Zienkiewicz et al., 2013; Zienkiewicz & Cheung, 1967) and the Discrete Element Method (DEM) (Cundall, 1971; Lemos, 1999), widely used in current practice (Fig. 2.22) for dynamic analysis of dam-reservoir-foundation systems, particularly for linear/non-linear seismic analysis of concrete dams.

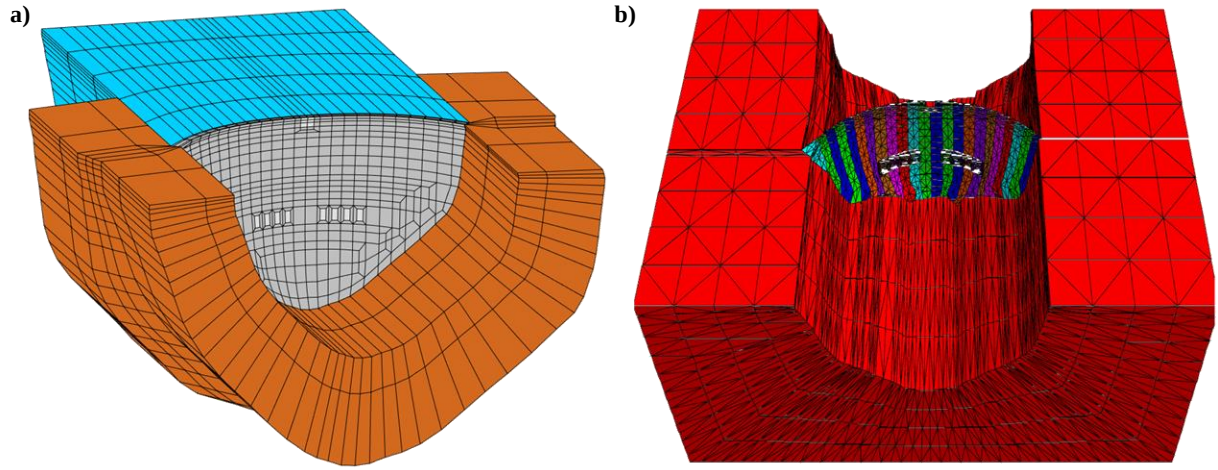

Fig. 2.22 Numerical models for dynamic analysis of Cahora Bassa dam: a) finite element mesh with discretized reservoir (used in this thesis); b) discrete element mesh using blocks and added water masses (LNEC, 2009).

PHYSICAL MODELS

Physical models are reduced scale versions of real prototypes developed based on the Similitude Theory, which states that it is possible to know the behaviour of a prototype if the behaviour of the physically similar model is also known. Experimental studies on physical models can be performed to simulate the behaviour of dams under static and dynamic loads, namely for: (i) current scenarios, to analyse the static response, e.g. under the self-weight (Fialho, 1955) and hydrostatic pressure (Serafim & Costa, 1961), or the free vibration response, under dynamic excitations from ambient/operational type sources (Sevim et al., 2012).; and (ii) failure scenarios, to evaluate the concrete strength decrease scenario (Rocha & Serafim, 1958) or the seismic behaviour up to failure under strong earthquakes (Rosça, 2008; Zhou et al., 2000).

Reduced scale models can be built using different materials (Gomes, 2006; Pina, 1999). The "weightless" models are constructed using gypsum-diatomite or cement mortar mixtures, and they are designated as such because their weight is negligible. This type of model is suitable for analysing the behaviour of the dam in failure scenarios under static loads. The loads, including self-weight, are simulated by applying external forces on the upstream face, using hydraulic jacks (Rocha & Serafim, 1958; Serafim & Costa, 1961). On the other hand, "heavy" models consider the weight of the material in order to correctly reproduce the stresses in the dam due to the self-weight, and they can be constructed from ilmenite sand, red lead, and gypsum, or ilmenite sand, cement, hydraulic lime, limestone powder, and diatomite. These models should be employed for simulating dynamic behaviour, in which it is fundamental to consider the mass of the dam. Seismic behaviour studies are carried out on shaking tables (Rosça, 2008; Zhou et al., 2000).

Physical models were widely used for several decades after the 1920s and 1930s to evaluate current and failure scenarios for concrete dams, namely in experimental tests carried out in LNEC. However, the construction and testing of these models is not practical, let alone economical, and with the advances in computational capabilities and the development of more advanced numerical models, physical models have become less and less used in detriment of numerical models. Still, physical models can be useful in the design phase for studying the dynamic behaviour of dams, in order to provide valuable experimental data to help calibrate and validate numerical models. So, they continued to be employed (Fig. 2.23) in shaking table tests for seismic response analysis (Jorge P. Gomes, 2010; R. Wang, 2016; R. Wang et al., 2018), and for dynamic analysis of dam-reservoir-foundation systems (Mendes & Oliveira, 2007; Sevim et al., 2012).

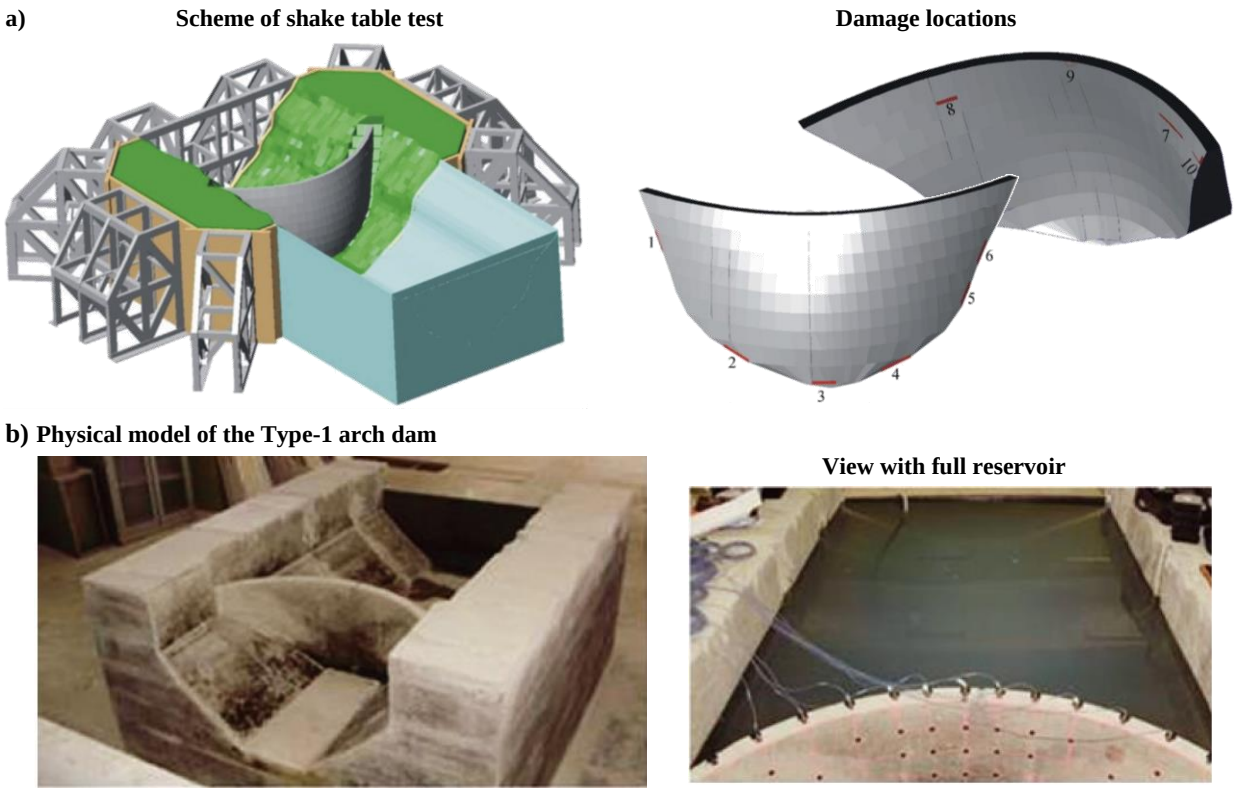

Fig. 2.23 Physical models used for dynamic analysis of concrete dams: a) Scheme of shaking table test and location of damage after the seismic test for Xiluodu dam, 285.5 m high, China (R. Wang et al., 2018); and b) Model of the Type-1 arch dam used for analysing the influence of the reservoir level variations (Sevim et al., 2012).

MODAL IDENTIFICATION MODELS

There are other types of models, to be used only during the operation phase for supporting the interpretation of data from dynamic monitoring, including the so-called modal identification models. These models are used to estimate the main modal parameters of dams (Fig. 2.24), namely natural frequencies, mode shapes and damping ratios.

Essentially, modal parameter identification is carried out based on idealized mathematical models, with the physical properties of the structural system under analysis, which are fitted to or estimated from the measured dynamic response. Extensive work has been conducted in this field, leading to the development of several well-established methods, which can be classified as frequency-domain, time-domain, or joint frequency-time domain methods (Brincker & Ventura, 2015; Peeters, 2000; J. Rodrigues, 2004).

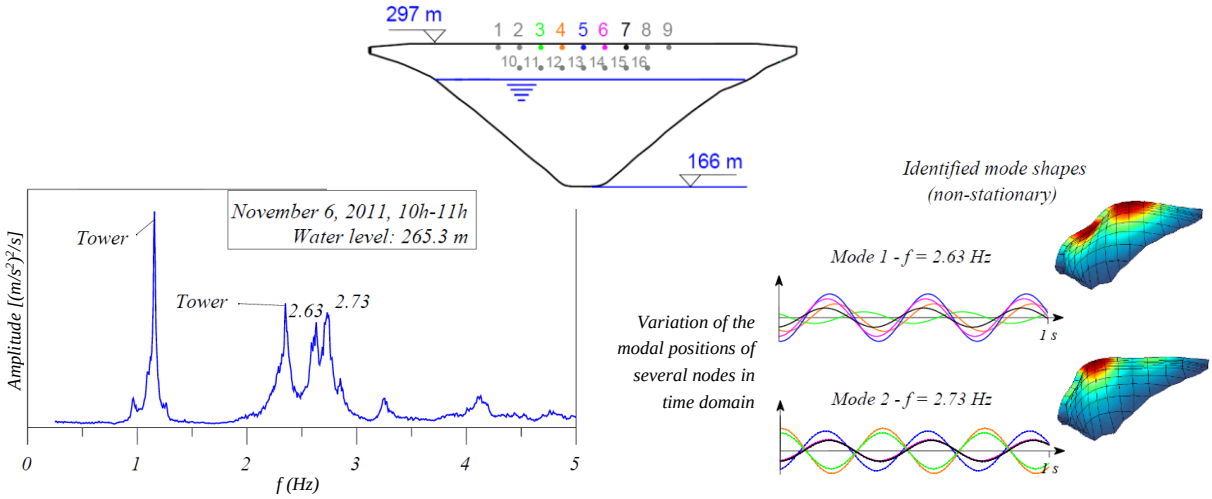

Fig. 2.24 Modal identification results for Cabril dam, using data recorded on November 6, 2011. Identified natural frequencies and mode shapes [adapted from (S. Oliveira et al., 2012)].

In current practice, there are two types of approaches for experimental modal identification, which differ in terms of the origin of the dynamic excitations. The first is Experimental Modal Analysis (EMA), also known as input-output modal analysis (Maia & Silva, 1997), based on deterministic modal identification methods. The modal parameters are obtained based on the relation between the dynamic load (input), which is known and controlled, and the measured response (output), using deterministic modal identification methods. This approach can be employed for modal identification in laboratory tests on physical models or in forced vibration tests carried out on site (Cunha & Caetano, 2006; Severn, 2010). The second is Operational Modal Analysis (OMA), or output-only modal analysis (Brincker & Ventura, 2015; Peeters, 2000; J. Rodrigues, 2004). The modal parameters are identified from the measured dynamic response (output) in operating conditions, assuming the excitation is an unknown random white noise, using stochastic modal identification methods. This methodology is used to analyse the measured vibrations during ambient vibration tests or from continuous dynamic monitoring systems (Li et al., 2016; Limongelli & Çelebi, 2019). Both approaches can be valuable for characterizing the dynamic properties and dynamic

behaviour of dams. However, as mentioned earlier, OMA is the best approach when intending to continuously evaluate the dynamic performance of dams under ambient/operational excitations.

Following the advances in this field and the large number of studies carried out for large concrete dams (see section 2.5.3), it has been recognised that the interpretation and analysis of modal identification outputs can provide valuable information for evaluating the dynamic performance of dams in normal operating conditions, and for validating and calibrating numerical models (S. Oliveira & Alegre, 2020).

DATA-BASED MODELS

The first data-based models were developed by (Rocha et al., 1958) in order to help the interpretation of data from static monitoring of dams. More recently, these models were also used for analysing data from dynamic monitoring, namely to interpret the evolution of natural frequencies over time (Mendes, 2010).

Monitoring dam behaviour leads to the acquisition of data sets which are often difficult to interpret, since they characterize the evolution of the response of dams due to the joint effect of several loads and processes, some of which are known (e.g. self-weight and hydrostatic pressure), while others are possibly unknown (S. Oliveira, 2000). For example, the dynamic behaviour of dams can change considerably due to reservoir level variations, annual or daily thermal variations, and the evolution of concrete deterioration processes. Therefore, data-based models were developed to facilitate interpretation and analysis of observed dam behaviour, as a complement to visual inspections and numerical models.

Data-based or data-driven models aim to predict the values of specific quantities, e.g., displacements or natural frequencies, etc., based on the analysis of temporal series from dam behaviour monitoring, including external variables (reservoir level, air temperature, etc.) or internal variables (temperature in the dam body, displacements, stresses, etc.). These models have the advantage of not being based on physical laws or calculation hypotheses, which can be beneficial for interpreting dam behaviour and for analysing certain phenomena that are not so easily incorporated in numerical models (ICOLD, 2018). Nevertheless, their use requires a great amount of data to be available, and, in general, cannot be applied to non-stationary data. The main limitation of these methods is their inability to generate accurate predictions beyond the variation range of available data (Salazar et al., 2017). Data-based models used for analysing dam monitoring data can be statistical models and machine learning models.

The most popular statistical data-based approach is based on the hydrostatic-seasonal-time (HST) models, developed to interpret and predict displacements from static monitoring of concrete dams. These models consider that the dam response is a linear combination of the reversible effects of the hydrostatic pressure and of air temperature and of the irreversible effects due to the evolution of the dam response over time. The earlier versions of the HST models were presented by (Rocha et al., 1958) in LNEC, where it is also known as quantitative interpretation or effects separation model, and by (Willm & Beaujoint, 1967), which differed in the way of simulating the temperature effect. Over time, several variations were developed, considering new formulas for the effects of time, water level, and temperature (Chouinard & Roy, 2006; Mata et al., 2013, 2014). The HST models can also be applied to analyse strains, in order to determine

stresses (S. Oliveira, 2000), water flow and uplift pressures (Simon et al., 2013), joint/crack openings (Yu et al., 2010). Recently, hybrid HSCT-FEM models, including the separation of the creep structural effects, have also been used to analyse displacement histories (M. Rodrigues et al., 2019, 2020). For dynamic behaviour analysis, HST models can even be applied to investigate the evolution of natural frequencies over time, extracted from continuous vibrations monitoring data (Mendes, 2010).

In recent years, there has been a tendency to invest in machine learning models for interpretation and analysis of dam behaviour, since they are more appropriate for modelling more complex and non-linear phenomena, thus being a possible future alternative to classic models (ICOLD, 2018). The aim is to build data-based predictive models that rely exclusively on data and on their ability to match patterns (Salazar et al., 2017). Machine learning models have been used in several applications for dam monitoring (Kao & Loh, 2013; Mata et al., 2013; Simon et al., 2013), and the vast majority is based on Neural Networks (Bishop, 1995; Mitchell, 1997).

ABOUT THE USE OF MODELS FOR DAM SAFETY

Regarding the structural safety control, the types of models described in this section can be used, as referred, with different purposes in different phases of the lifetime of dams.

In the design phase, only numerical models and physical models can be applied, namely to analyse current scenarios, for safety assessment under load combinations involving static loads and lower-intensity earthquakes, and to evaluate failure scenarios, including the concrete strength decrease scenario, seismic response analysis under strong earthquakes, and dam foundation failure. Additionally, numerical models can also be employed in special studies for predicting the response of dams during the construction phase and during the first filling of the reservoir.

During the operation phase, numerical models are of great value: (i) to control structural integrity by providing reference values or by simulating processes of dam ageing and evolutive deterioration, to be compared with experimental data and/or results obtained using modal identification models (used to estimate the main modal parameters) or data-based models (e.g. effects separation models); and (ii) for monitoring seismic response, by comparing computed accelerations with reference models and recorded accelerations. Furthermore, additional studies might be necessary for re-assessment of structural safety conditions for both current and failure scenarios of dams, using more advanced numerical models and possibly physical models.

In this thesis, the main concerns are the structural safety control of large concrete dams during their operation phase, in normal operating conditions and under seismic events, and the seismic safety assessment under strong earthquakes. Consequently, aiming to ensure the best safety conditions for both new and older large concrete dams in operation, it is important to continue investing in the development of new methodologies and suitable computational tools for analysing their dynamic behaviour, with emphasis on the development of advanced finite element numerical models for simulating the response of dam-reservoir-foundation systems and of software to complement the SSHM systems installed in large concrete dams.

2.4 SEISMIC SAFETY

Currently, the long-term safety of dams is associated with an integral safety concept, which comprises structural safety, monitoring, operational safety and maintenance, and emergency planning (Wieland, 2016). As such, in addition to the structural safety control in normal operating conditions, the seismic safety of large concrete dams must be ensured, namely by monitoring their seismic response under low, medium, or high intensity earthquakes, using suitable measuring devices, and by evaluating their seismic performance for current or failure scenarios, using appropriate ground motion parameters obtained in seismic hazard studies, reliable methods for seismic analysis, and advanced numerical models. The assessment of the seismic safety of dams must be carried out multiple times during their long lifetime.

Large concrete dams were among the first structures to be designed against earthquakes considering specific seismic design criteria (Wieland, 2008). This practice began in the 1930s with the seismic analysis method developed by Westergaard (1933) for studying the behaviour of Hoover arch-gravity dam: this was a simple pseudo-static analysis method, considering both the inertia forces of the dam body in the upstream-downstream direction and the hydrodynamic pressures in the reservoir acting on the upstream face of the dam, but ignoring the dynamic properties of the dam-reservoir system. This method found worldwide acceptance among engineers and designers of concrete dams, and it was widely used for many decades. In addition, it was common practice to consider a seismic coefficient of 0.1 (equivalent to a horizontal ground acceleration of 0.1 g) for seismic response analysis, almost irrespective of the seismic hazard at the dam site (in most cases this was unknown; slightly higher values were considered in exceptional cases, e.g., for dams in Japan or Iran).

However, the turning point in the seismic analysis of dams was the 1971 San Fernando earthquake (6.5 magnitude), in California, which caused damages in the San Fernando embankment dams and also in the Pacoima arch dam (Fig. 2.25), where a section of the upper left abutment (thrust block) slightly moved away from the dam, resulting in an opening of almost 1 cm in the contraction joint and in the formation of a crack in that block. The epicentre of the San Fernando earthquake was at about 8 km to the north of Pacoima dam. Peak ground accelerations of 1.25g (horizontal) and of 0.7g (vertical) were recorded with an accelerometer located at the top of the left bank, about 15 m above the crest level (Alves, 2004; Hall, 1998).

After that, it was recognised that the methods used until then were not reliable for seismic safety assessment of large dams and that ground motions larger than the values commonly applied for design could occur, as mentioned in (Wieland, 2019b). Consequently, along with the advances in computational capacity and the evolution of available numerical methods, the seismic behaviour of large concrete dams started to be analysed using more appropriate methods, in particular based on linear-elastic dynamic analyses of dam-reservoir-foundation system models and considering more rational seismic design and performance criteria (Chopra, 1976; Fenves & Chopra, 1986).

For example, during the 1970s and 1980s several seismic studies were carried out in LNEC, Portugal, using not only physical models but also numerical models for several large dams (Câmara, 1989; Pedro, 1977;

Pedro & Câmara, 1986; Pedro & Pereira, 1979), including for Cabril dam (Fig. 2.26), which showed the good performance of arch dams under earthquakes.

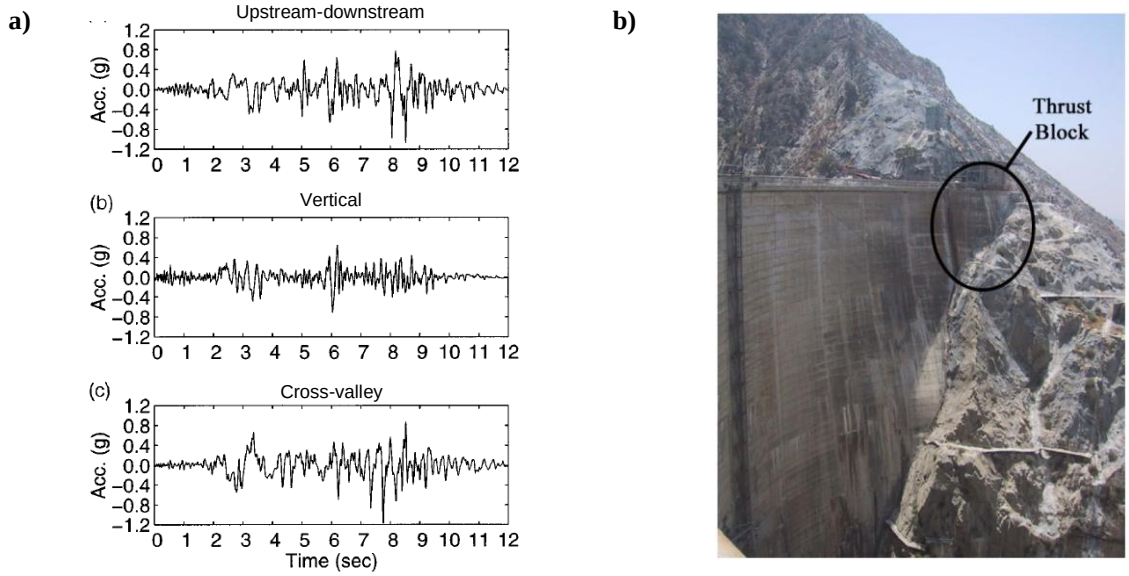

Fig. 2.25 Pacoima dam: a) Ground motions recorded above the left abutment during the 1971 San Fernando earthquake (Hall, 1998) and b) view of the left abutment; thrust block that moved away from the dam (Alves, 2004).

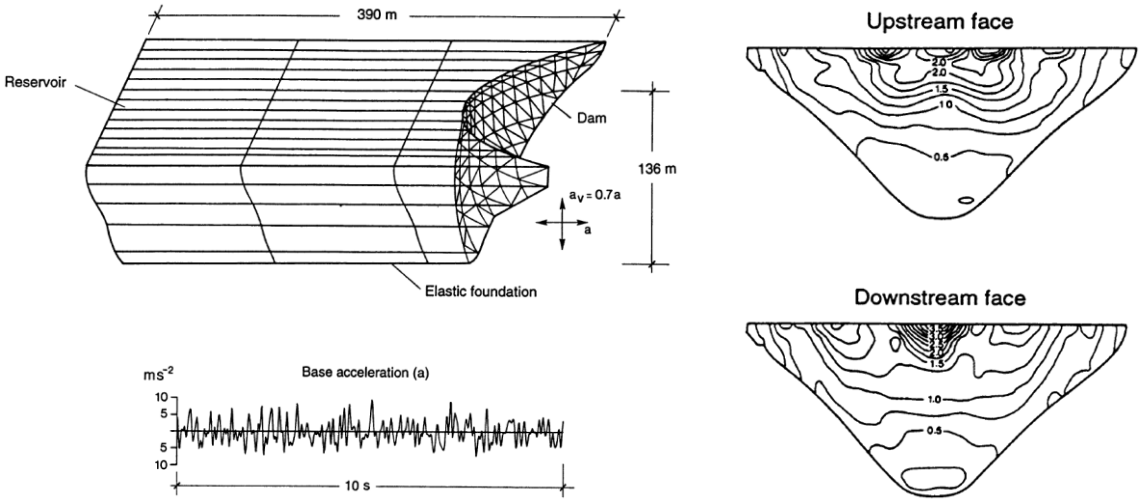

Fig. 2.26 Finite element analysis of Cabril dam for a strong earthquake. Model of dam-reservoir-foundation system, seismic input, and peak compressive stresses at the upstream and downstream faces (Pedro, 1999).

The developments in this field led to the publication of ICOLD guidelines on procedures of earthquake analysis for dams (ICOLD, 1986), comprising linear-elastic dynamic analysis methods that are still used today, and ICOLD guidelines on the selection of seismic designed criteria for large dams (ICOLD, 1989), in which different earthquake levels for seismic design and safety assessment were defined, including the operating basis earthquake (OBE), the maximum design earthquake (MDE), and the maximum credible

earthquake (MCE). The simplest method was the response spectrum or modal superposition method, considering an acceleration response spectrum as seismic input. Although efficient, this method only worked for linear behaviour and proportional damping (Clough & Penzien, 2003; Zienkiewicz et al., 2013). Due to these limitations and to the evolution in available computational resources, the use of direct time integration methods (Clough & Penzien, 2003; Zienkiewicz et al., 2013), in which the seismic input is given in terms of acceleration time histories, was recommended. These methods enable the use of more realistic damping hypothesis and can solve problems considering either linear or non-linear behaviour.

Nowadays, the guidelines for seismic analysis, safety assessment and design of dams are documented in the bulletins from the Committee on Seismic Aspects of Dam Design of ICOLD, which address several topics such as dams on faults and reservoir-triggered seismicity, seismic design concepts and special features, and seismic criteria and analysis methods (ICOLD, 1998, 2001, 2002, 2011, 2016a). In current practice, the methods of analysis for seismic safety assessment require seismic inputs in the form of acceleration time histories, which are essentially models of earthquake ground motion, whose ground motion parameters must be obtained based on site-specific seismic hazard studies (Wieland, 2019a). Furthermore, given that structural non-linearities are acceptable to a certain extent according to modern criteria, time integration methods and advanced models for non-linear response simulations are needed.

Following the conducted work and the advances achieved over time in this field, and aiming to meet the increasing demands from owners and entities responsible for dam safety, the seismic safety assessment became a fundamental requirement to ensure the global structural safety of large concrete dams (H. Chen, 2014; Wieland, 2016), and thus the seismic load became one of the most important for the design of some of the large concrete dams built recently. However, this was not the case for most of the older dams, built decades ago, since the seismic design criteria were outdated, and the methods of analysis used at the time were unreliable. Therefore, the need to reassess the seismic safety of existing dams based on current practices became clear, particularly for those located in high seismicity zones.

For example, a major program started in 1996 in the United States to evaluate the seismic safety of dams, including Deadwood dam, Hoover dam, Monticello dam and Morrow Point dam (USBR, 1998a, 1998b, 1999, 2002), while in Switzerland, in the early 2000s, the seismic safety reassessment of all 208 large dams in the country was required based on modern standards, an endeavour that was completed recently (Darbre et al., 2019). On the other hand, many studies using physical models and advanced numerical models were conducted over the past two decades in China, one of the regions with the highest seismic activity in the world, fostered by the design and construction of many ultra-high concrete dams. From these studies resulted some proposals of seismic reinforcement, in order to prevent or mitigate phenomena like unacceptable joint opening and/or high tensions in unwanted zones, including the use of shear-keys in the contact between adjacent blocks, joint reinforcements, and steel belts or nets (recall Fig. 2.15) where higher tensions are expected (Lau et al., 1998; R. Wang, 2016; R. Wang et al., 2018; C. Zhang et al., 2000, 2004).

2.4.1 SEISMIC HAZARD

It has been recognized that the seismic hazard is a multi-hazard, since it may affect large concrete dams in multiple ways (Wieland, 2010, 2014, 2016). The main hazards are: (i) ground motion, resulting in high amplitude vibrations in the dam, appurtenant structures or other equipment, and in the rock mass, which can cause structural damage; (ii) movements in the foundation along major faults or discontinuities in the footprint of the dam, leading to structural distortions, and in the footprint of the reservoir, inducing water waves; (iii) mass movements with rock falls in the surrounding area, causing damages to appurtenant structures such as spillways, bottom outlets, power plants, intake towers, etc. and blocking access roads and rivers; (iv) mass movements into the reservoir, triggering impulse waves and reservoir level increase which may result in dam overtopping; (v) site-specific hazards, including ground deformations, settlements due to liquefaction and densification of soil, seepage, etc.

Besides the 1971 San Fernando earthquake mentioned above, historic examples of important multi-hazard seismic events are the 7.5 magnitude earthquake that occurred in 1990 in Manjil, Iran, which caused significant damages on the Sefid Rud dam and rockfalls that blocked access roads (Fig. 2.27), and the 7.6 magnitude Chi-Chi earthquake that happened in 1999 in Taiwan, resulting in the failure of two openings of the Shih-Kang weir, close to the right bank due to foundation movements along a fault (Fig. 2.28).

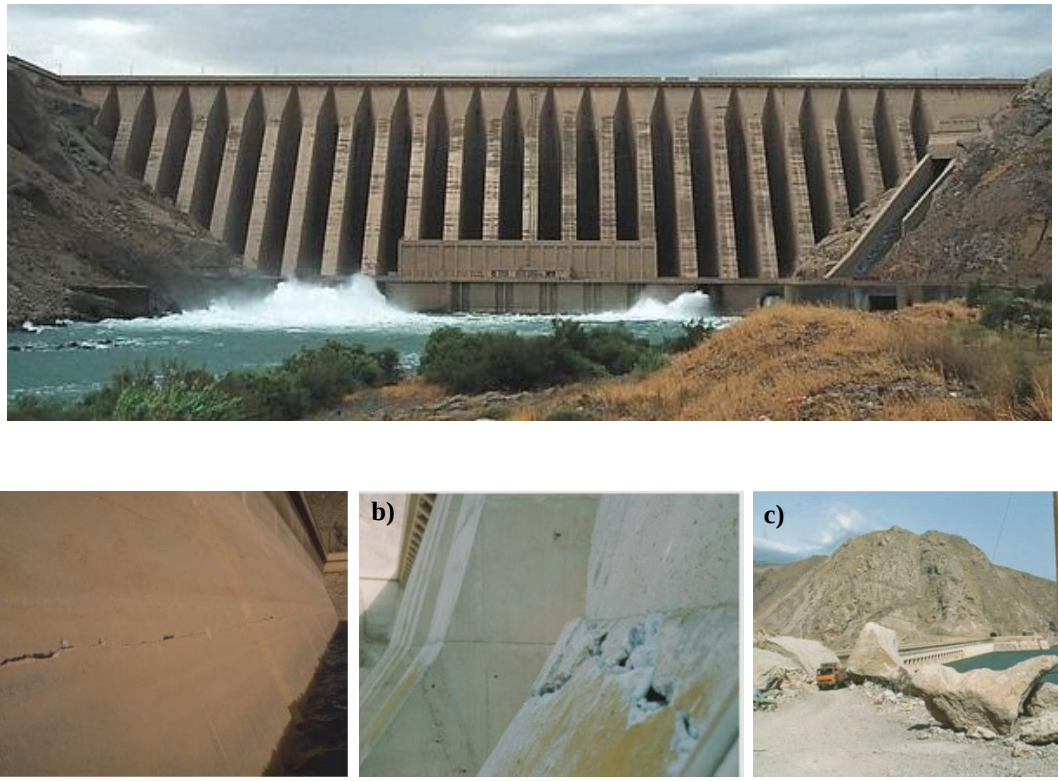

Fig. 2.27 Sefid Rud buttress dam, 106 m high, Iran. Damages during the 1990 Manjil Earthquake: a) crack at the top of the upstream face; b) crack at the kink of a buttress (downstream face); and c) access roads blocked by rockfalls.

Fig. 2.28 Shih-Kang weir, 25 m high and 352 m long, Taiwan. Failure of two openings, close to the right bank due to fault movements during the 1999 Chi-Chi earthquake.

Other example of a multi-hazard earthquake is the May 12, 2008, Wenchuan earthquake. This was a magnitude 8 earthquake that occurred in the Sichuan province in China, the one with the largest hydropower potential in the country. This was perhaps the most important seismic event in decades and affected more dams than any other: there were reports of damages in hundreds of dams (Fig. 2.29), power plants (Fig. 2.30), and reservoirs (Wieland, 2010; Wieland & Chen, 2009). Effects of the earthquake included high intensity and long duration ground shaking, a large number of rockfalls and landslides, overtopping of run-of-river power plants, and failure of hydromechanical equipment. The duration of strong ground shaking was between 90 to 120 seconds, and the maximum recorded peak ground accelerations were of 9.58 m/s^2 in the horizontal direction and of 9.48 m/s^2 in the vertical direction.

The main seismic hazard usually addressed in codes and regulations for seismic design and structural safety assessment of large concrete dams is the earthquake ground motion, given that strong ground motions can induce high amplitude vibrations in the dam body and thus cause important structural effects such as deformations, joint movements, high tensile and compressive stresses that result in concrete damage, etc. Therefore, the ground motion must be properly considered in the assessment of the structural safety of dams for both current and failure scenarios, along with general performance criteria for the dam body, appurtenant structures, and safety-relevant equipment. However, it is worth reminding that the remaining hazards must not be overlooked since they might be critical for the safety of dams and appurtenant works, which must be able to resist the multiple effects of high intensity earthquakes. As such, essential information is required by dam engineers from seismologists and geologists on ground motion, movements in the footprint of a dam, and critical slopes in the dam and reservoir region.

Fig. 2.29 Zipingpu concrete face rockfill dam, 156 m high, China. Consequences of the 2008 Wenchuan earthquake: a) damaged structure on top of the intake tower; b) damage along vertical joints on the concrete upstream face; c) damage on the downstream face and gap between the stone masonry and the crest; and d) crack at the crest.

Fig. 2.30 Shapai RCC arch dam, 132 m high, China. Consequences of the 2008 Wenchuan earthquake: effects of rockfalls on the powerplant and damage equipment inside the powerhouse.

The ground motion parameters can be determined in seismic hazard analysis on the dam site based on deterministic and/or probabilistic methods (ICOLD, 2016a; Wieland, 2019a). In the deterministic approach, the ground motion is estimated for earthquakes corresponding to the worst-case scenarios based on attenuation models, taking into account existing critical faults in the dam and reservoir region, the definition of the maximum magnitude and distance, and the corresponding earthquake mechanism. The scenario resulting in the most severe ground motion at the dam site is selected. As for the probabilistic analysis, the ground motion parameters are defined in terms of return periods, which are associated with specific probabilities of occurrence. Thus, the ground motion parameters can be obtained for various design earthquakes characterized by different return periods.

2.4.2 SEISMIC DESIGN AND PERFORMANCE CRITERIA

According to the ICOLD guidelines on the selection of seismic parameters for large dams (ICOLD, 2016a), there are two main levels to be considered for the seismic design and safety assessment of a large dam project: the Operating Basis Earthquake (OBE) and the Safety Evaluation Earthquake (SEE).

The OBE is the earthquake that may be expected to occur during the dam lifetime, under which significant damage or loss of service must not occur. The OBE is associated with a minimum return period of 145 years, and it has a probability of occurrence of about 50% during a service life of 100 years. The ground motion parameters are estimated based on probabilistic methods and the mean values must be taken.

The SEE corresponds to the earthquake a dam must be able to resist without uncontrolled release of the reservoir, although damage can occur. This is the governing earthquake event for seismic design and safety assessment of the dam and safety-relevant components, which must be functioning after the SEE. The ground motion parameters of the SEE can be estimated based on deterministic or probabilistic seismic hazard analysis: therefore, the SEE can be taken as the Maximum Credible Earthquake (MCE) or the Maximum Design Earthquake (MDE). The MCE is the seismic event that causes the largest ground motion expected at the dam site, considering seismic history and the seismotectonic setup in the dam region (deterministic analysis), while the MDE is the earthquake associated with the return period of 10 000 years for large dams (although shorter return periods can be prescribed for damages with less damage potential), using the mean values of the ground motion parameters (probabilistic analysis). In case both analyses are available, the most unfavourable ground motion parameters must be taken; however, if a realistic assessment of the MCE cannot be made, then the SEE should be at least assumed as the MDE.

In this scope, it is also worth mentioning the Design Basis Earthquake (DBE), which is used in many countries as a design earthquake for the appurtenant structures (return period of 475 years), and the Construction Earthquake (CE), to be used for the design of temporary structures such as coffer dams, considering the duration of their service life. For some dams, another earthquake load can be defined the scenario of reservoir-triggered seismicity (RTS), which has been observed[2] in over 100 reservoirs with

[2] The first and most important case of reservoir-triggered seismicity was the 6.1 magnitude earthquake that occurred after the reservoir filling of the Xinfengjiang dam, in China (L. Chen & Talwani, 1998).

water depths of over 100 m (ICOLD, 2011): the Reservoir-Triggered Earthquake (RTE) represents the maximum ground motion capable of being triggered at the dam site by the filling, drawdown, or the presence of the reservoir. If this phenomenon is possible or expected for a large dam, then the OBE and DBE ground motion parameters ought to cover those from RTS scenarios.

The different design earthquakes, obtained based on either deterministic or probabilistic methods as described above, are characterized by the ground motion parameters, which include the peak ground acceleration and the acceleration response spectra of horizontal and vertical earthquake components, as well as the corresponding spectrum-matched artificially generated acceleration time histories.

With respect to the seismic performance of dams, general performance criteria for the dam body and safety-relevant components and equipment, which include bottom outlets, spillways, gates, hydraulic systems, control panels, power supply, etc., are provided in the ICOLD guidelines (ICOLD, 2016a) and duly explained in (Wieland, 2014, 2016, 2019b).

Regarding the OBE, no structural damage that affects the operation of the dam is acceptable, including cracks, deformations, leakage, etc. Thus, only minor repairable damage that does not cause loss of service is permitted. Furthermore, safety-relevant components and equipment must remain undamaged and be fully operable during and after the earthquake.

As for the SEE, structural damage is considered acceptable, provided that the stability of the dam is ensured and its structural integrity is not compromised, and that the uncontrolled release of water from the reservoir does not occur, in order to avoid flooding in the downstream region. Moreover, minor damage is acceptable in the safety-relevant components and equipment, as long as they can continue functioning properly during and after the earthquake. After the SEE, the reservoir level must be controlled, and it must be possible to lower the reservoir for repairing eventual damages and/or to increase dam safety.

The seismic performance criteria for the OBE can be verified based on linear-elastic dynamic analysis, by analysing stresses and deformations, and on rigid body sliding and overturning stability analysis, by evaluating stability safety factors.

The assessment of the performance criteria under the SEE for the dam body require non-linear dynamic analyses to be carried out, using time domain methods and seismic inputs in the form of accelerations time histories, as already mentioned. For concrete gravity dams and buttress dams, the main seismic failure modes due to earthquake ground motion include global sliding of dam or of blocks along discontinuities in the foundation or along the dam-foundation surface (downstream direction), and local sliding stability of concrete blocks near the dam crest along lift joints (downstream direction). For concrete arch dams, the main failure modes under seismic ground motion are the crushing of concrete in key areas under high compressive arch stresses, leading to the loss of bearing capacity in the arch direction, and the local sliding or overturning stability of blocks at the crest, due to movements in the upstream direction (larger movements occur for lower reservoir levels than for full reservoirs). Therefore, the main results needed may include inelastic deformations, stresses, and tensile and compressive damage after the earthquake.

2.4.3 MODELS AND METHODS FOR SEISMIC ANALYSIS OF DAMS

The study of the seismic behaviour of large concrete dams and the evaluation of their seismic capacity continue to represent some of the most significant challenges in dam engineering, aiming at reliable seismic design and safety assessment. Extensive scientific research activities have been conducted in this field, and nowadays it is recognised the importance of the definition of the seismic input for time history analyses (Houqun, 2020; Wieland, 2019a), of developing advanced numerical models for simulating the dynamic behaviour of dam-reservoir-foundation systems (H. Chen, 2014; Chopra, 2012), and of using suitable methods for seismic performance evaluation (Furgani et al., 2019). Nevertheless, it is relevant to note that uncertainties are inherent to all steps of this process, thus requiring sensitive engineering judgement and results analysis.

The best way to define the earthquake ground motion for seismic design and safety assessment is by means of acceleration time histories (Fig. 2.31), particularly since these are required as seismic input for non-linear dynamic analyses. The earthquake ground motion should preferably be represented by real accelerograms, recorded for site conditions similar to those of the dam to be analysed (Bommer & Acevedo, 2004). However, currently available records of strong earthquakes are not enough to cover the range of possible conditions, and thus artificial accelerations time histories have to be supplemented (ICOLD, 2016a).

Proper acceleration time histories can be generated from response spectra (Clough & Penzien, 2003), taking into account specific features regarding their horizontal and vertical components and duration. Several methods have been developed for generating seismic acceleration time histories, including the classic stochastic stationary procedure implemented in the computer program SIMQKE (Gasparini & Vanmarcke, 1976b, 1976a), widely used by engineers, or the so-called stochastic method developed by (Boore, 2003). In this scope, it is also worth highlighting the stochastic fault rupture and seismic wave propagation model developed by (A. Carvalho, 2007) in LNEC, which generates non-stationary accelerograms, as well as the endurance time excitation functions, corresponding to intensifying acceleration time histories, first developed by (Estekanchi et al., 2004) for Endurance Time Analysis (ETA).

Naturally, the generated accelerograms used in seismic design and safety assessment may be quite different from the acceleration records of real earthquakes since they are simplified models of the seismic load. However, considering appropriate methods of analysis, the use of these artificial acceleration time histories as seismic input in advanced numerical models of dam-reservoir-foundation systems will lead to a safe design or to a proper safety assessment, which is essentially the main goal (Wieland, 2014, 2019a).

a)

b)

c)

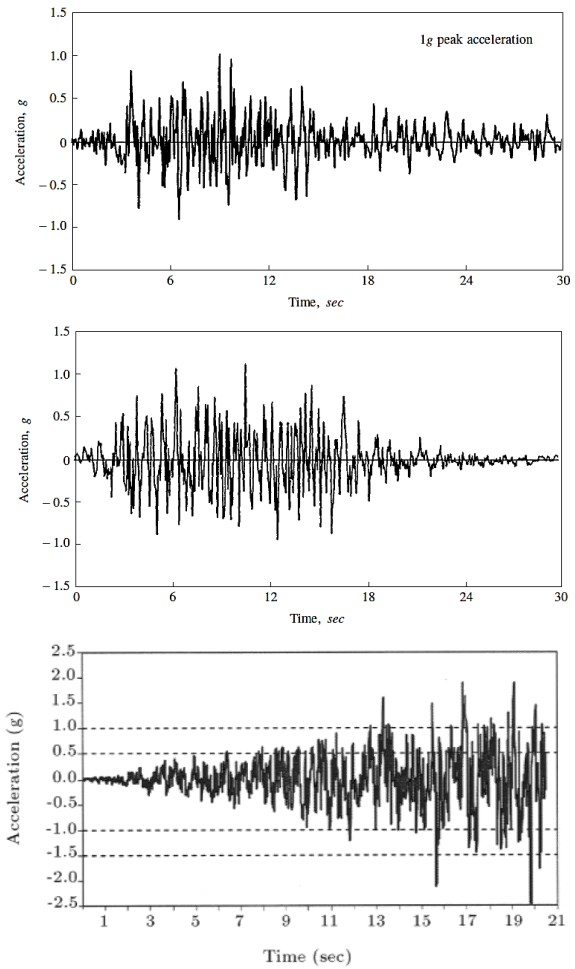

Fig. 2.31 Seismic acceleration time histories: a) real accelerogram (N21ºE component) recorded in 1952 during the magnitude 7.3 Taft earthquake, in California (Clough & Penzien, 2003); b) design spectrum compatible generated acceleration time history (Clough & Penzien, 2003); c) intensifying dynamic excitation produced based on an endurance time excitation function (Estekanchi et al., 2004).

The evaluation of the seismic performance of dams for seismic design and safety assessment requires the use of advanced models for dynamic analysis of three-dimensional dam-reservoir-foundation systems, since large concrete dams are complex structures, whose dynamic behaviour is strongly influenced by the interaction between all parts of the dam-reservoir-foundation system (Câmara, 1989; Pedro & Câmara, 1986). Therefore, critical factors to be considered include dam-water interaction, the pressure waves propagation in the reservoir domain, the dam-foundation interaction, the behaviour of the rock mass, and the damping mechanisms, including viscous damping in the dam and radiation damping in the reservoir and foundation. These factors can have a significant influence in the overall seismic behaviour of the dam-reservoir-foundation system, and thus in the structural response of the dam (H. Chen, 2014; Chopra, 2012).

Additionally, for non-linear dynamic analysis under strong earthquake ground motion, it is fundamental to properly account for the non-linearities associated with opening/closing and sliding movements of contraction joints or other discontinuities, as well as the behaviour of concrete up to failure under tension and compression, which can lead to concrete cracking or crushing, using appropriate constitutive models and accurate material properties.

Significant research in this field led to the development of various formulations and models for seismic analysis of dam-reservoir-foundation systems (see the state-of-the-art review of Chapter 3). In current practice, there are several programs based on the FEM used for linear and non-linear seismic analysis of concrete dams (Fig. 2.32), namely EACD-3D (J.-T. Wang & Chopra, 2008), ANSYS (ANSYS Inc., 2020), ABAQUS (Dassault Systèmes Simulia Corp., 2020), ADINA (ADINA R & D Inc., 2020), DIANA (DIANA FEA BV., 2020), and the open-source software Code_Aster (http://www.code-aster.org). In LNEC, the DEM-based program 3DEC (Itasca Consulting Group Inc., 2020) is commonly used. In this work, new mathematical formulations are developed for linear and non-linear seismic analysis, considering joint movements and concrete damage under tension and compression (see Chapter 3).

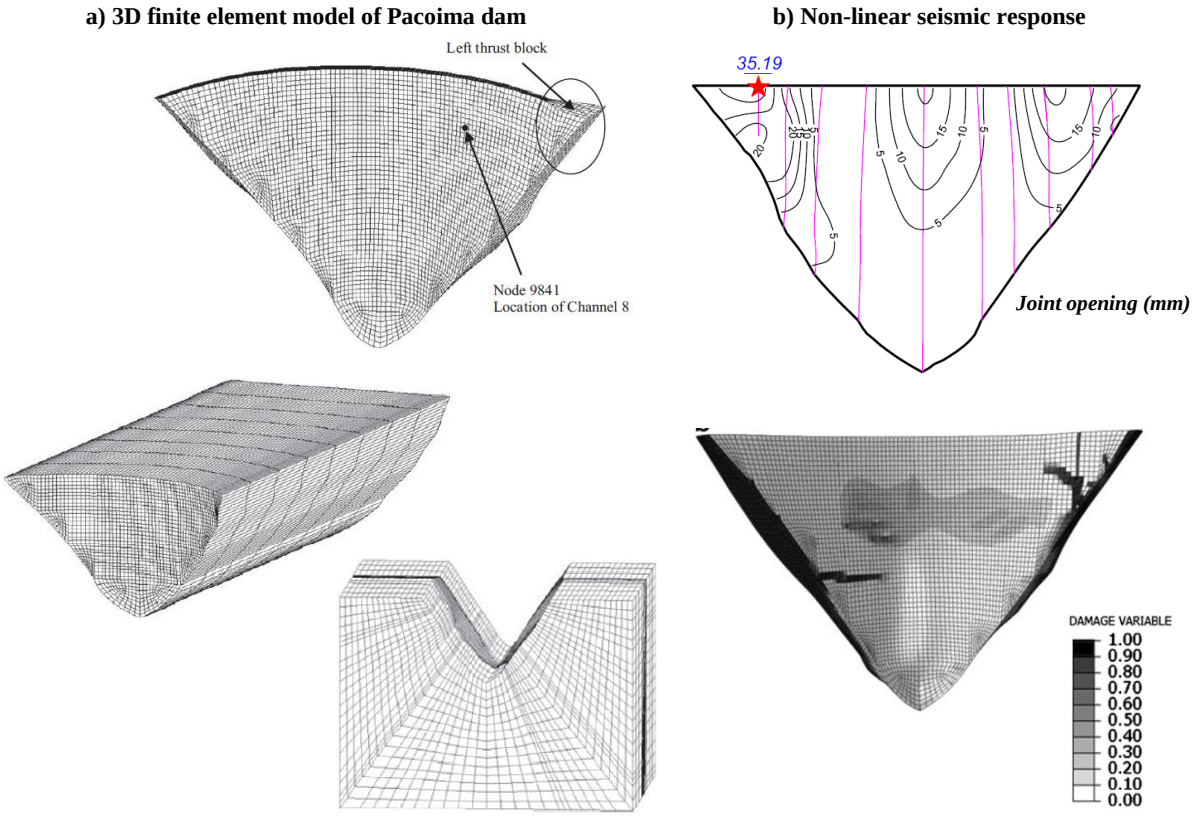

Fig. 2.32 Non-linear seismic analysis of Pacoima dam (J.-T. Wang et al., 2013): a) finite element model of the dam-reservoir-foundation system used in ABAQUS and b) non-linear results of joint opening (upstream face) and damage distribution (downstream face) under the 1994 Northridge earthquake.

Following the developments in this field, the methods used today for analysing the seismic response of large concrete dams are based on time domain procedures, using acceleration time histories as inputs. Thus, the performance of the dam under strong earthquakes can be analysed considering the structural non-linearities, which are acceptable according to modern criteria, unlike in traditional pseudo-static analysis or in linear dynamic analysis. Nevertheless, the seismic capacity evaluation must be conducted based on sensitive engineering judgement, in order to meet the general requirements and performance criteria provided in the guidelines of ICOLD and in the regulations of countries.

The seismic design and safety assessment of large concrete dams is usually conducted by performing multiple time history seismic analyses, using appropriate acceleration time histories to analyse both current and failure scenarios. Ideally, the acceleration time histories are obtained based on the design ground motion parameters from specific seismic hazard analysis for the dam site, for both the OBE and the SEE, and the seismic response is calculated for the intended scenarios, using several generated accelerograms (with distinct frequency content). Otherwise, the seismic calculations can be carried out according to the principals of Incremental Dynamic Analysis (Vamvatsikos & Cornell, 2002), using one or more generated accelerograms from appropriate response spectra, which are then scaled to obtain seismic actions with various peak ground accelerations, corresponding to weaker or stronger ground motions.

These are more classical approaches, which allow to achieve valuable results and to draw assertive conclusions on the seismic capacity of dams, for example as done in LNEC for seismic safety assessment of Ribeiradio dam (S. Oliveira, Silvestre, & Câmara, 2014) and Cahora Bassa dam (LNEC, 2009). However, the need to conduct multiple calculations for different excitation levels and to analyse different scenarios will result in longer calculation times, particularly if non-linear analyses are carried out.

Alternatively, the seismic performance of dams can be evaluated based on the Endurance Time Analysis (ETA) method. This a seismic analysis pushover procedure used to estimate the seismic response of the dam under a pre-designed intensifying seismic load (Estekanchi et al., 2004; Mashayekhi, Estekanchi, & Vafai, 2019; Mashayekhi, Estekanchi, Vafai, et al., 2019; Nozari & Estekanchi, 2011), which ideally should increase linearly with time. The aim is to subject the dam to earthquake ground motion from a low excitation level, with structural behaviour within the linear domain, to a medium excitation level, where significant structural non-linearities start to occur, and finally to a high excitation level, ultimately causing dam failure. The evolution in the dam structural response can be analysed in a single time history analysis, by analysing the results in multiple time steps along the process. Essentially, based on this procedure, the endurance limit is determined as the duration the structure can endure under the intensifying seismic action.

Not only does this approach enables to achieve a good assessment of the seismic capacity of concrete dams, as shown in various studies (Hariri-Ardebili et al., 2014; Hariri-Ardebili & Mirzabozorg, 2014; Meghella & Furgani, 2014; Valamanesh et al., 2011), but it is also highly efficient when compared to the traditional approach, thus significantly reducing the computational demands.

Finally, it is important to mention experimental seismic studies, carried out using physical models on shaking tables, which, although expensive and somewhat impractical when compared to numerical analyses, make it possible to obtain valuable experimental data for various purposes, namely to support seismic design and safety assessment, to investigate possible solutions of seismic reinforcement, and to provide results for validating and calibrating numerical models (Gomes, 2010; Rosça, 2008; R. Wang, 2016; R. Wang et al., 2018; Zhou et al., 2000).

In this work, a methodology for seismic safety assessment of large arch dams is proposed (Fig. 2.33), using the Endurance Time method and considering appropriate performance criteria. Essentially, the seismic response is calculated under a pre-designed intensifying seismic action, and the dam performance is evaluated based on the evolution of tensile and compressive damage. The goal is to determine the endurance

limits that correspond to the duration of the seismic action (and the respective acceleration level) that the dam can withstand without presenting unacceptable levels of damage.

The adopted performance criterion is related to the amount of damage at the upstream and downstream faces of the dam, and particularly along the thickness of the main cantilevers: basically, the occurrence of significant volumes in which concrete failure propagates across the entire thickness of the cantilevers is considered as unacceptable. Regarding tensile damage, associated here with the OBE, this situation could compromise the structural integrity of the dam, and thus require the interruption of normal operating conditions for repairs. In terms of compressive damage, which is associated with the SEE, such a scenario could originate concrete crushing and ultimately result in collapse and in an uncontrolled release of water from the reservoir. This approach was considered in order to meet the requirements defined for large dams under the OBE and the SEE in the current seismic design and safety guidelines (Wieland, 2016).

This method is illustrated in Fig. 2.33. The performance endurance limits are determined as the peak ground acceleration values from which dam performance becomes unacceptable, namely: a_d^+, the acceleration value from which tensile failure starts occurs in extensive areas, and a_d^-, the peak acceleration that causes concrete crushing under compression in key parts of the dam body. In summary, the seismic safety of the dam is ensured under the OBE, if $a_{OBE} < a_d^+$, and under the SEE, provided that $a_{SEE} < a_d^-$.

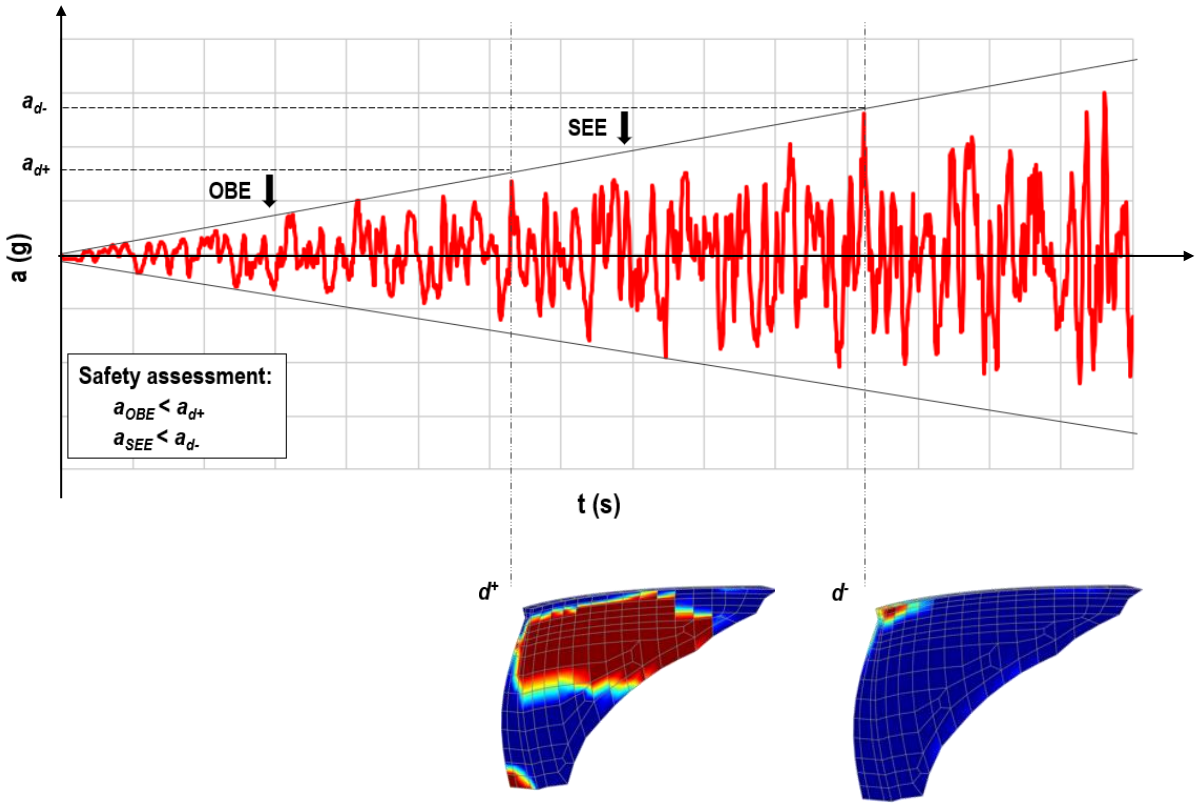

Fig. 2.33 Schematic representation of the proposed methodology for seismic safety evaluation of large concrete dams, using the Endurance Time method and considering the evaluation of tensile and compressive damages.

2.4.4 ON SEISMIC RECORDS

The seismic behaviour monitoring of large concrete dams under low, medium, or high intensity earthquakes (Fig. 2.34), by means of trigger-event seismic monitoring systems or continuous dynamic monitoring systems, can be very useful to gather acceleration records for characterizing earthquake ground motion and, if there is available equipment, the spatial variation along the dam base and the free-field, as well as for evaluating the seismic response, based on acceleration time histories measured in several points of the dam body. Furthermore, the combined use of measured accelerations and of results from reference numerical models can provide valuable data, not only to check if the performance of the dam is according to what was expected, but also to calibrate and update numerical models of the dam-reservoir-foundation system, enabling to investigate fundamental aspects regarding numerical modelling such as dam-water interaction, seismic input modelling, and damping. Examples of studies based on measured and computed accelerations on large concrete dams can be found in are referred in section 2.5.1

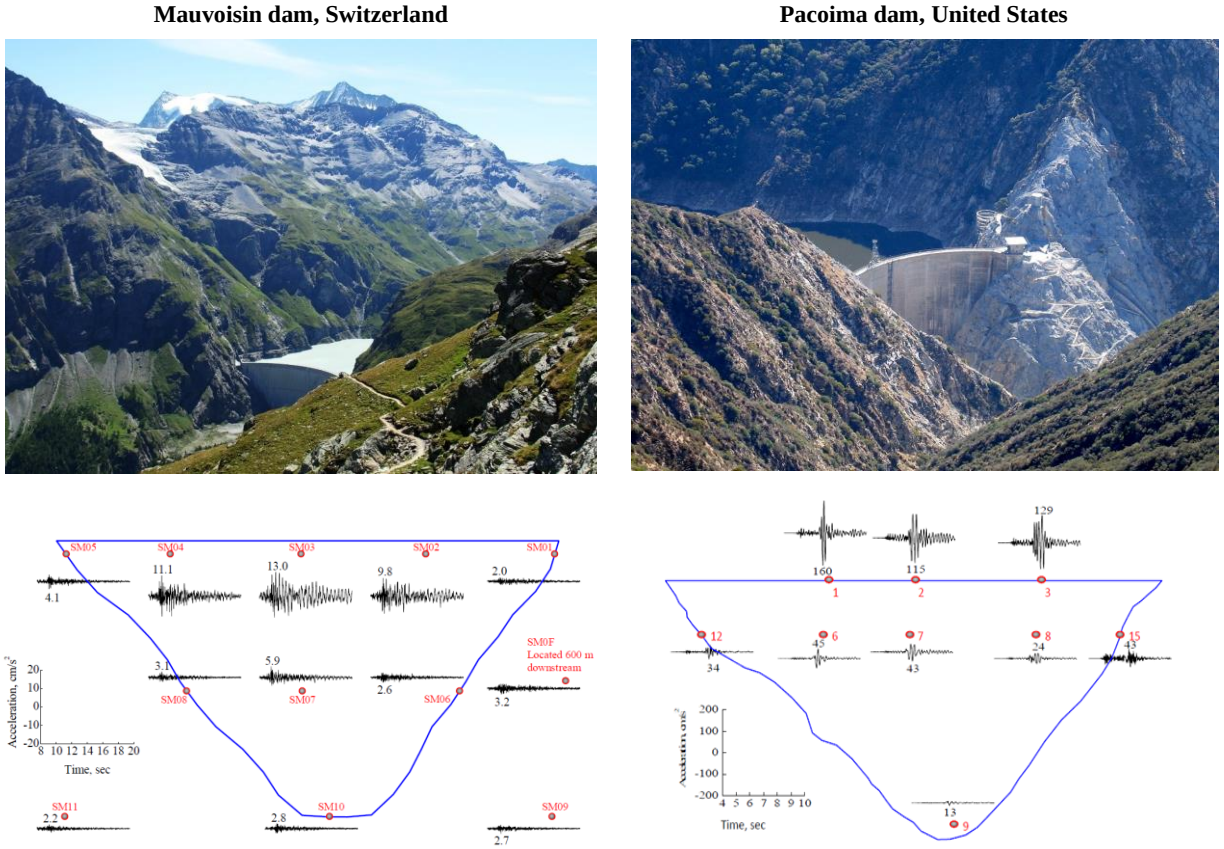

Fig. 2.34 Measured accelerations on large concrete dams during earthquakes (Chopra & Wang, 2012): a) records in Mauvoisin dam (upstream-downstream direction), during the magnitude 4.6 Valpelline earthquake of March 31, 1996; and b) records in Pacoima dam (upstream-downstream or radial direction), during the magnitude 4.3 earthquake of January 13, 2001.

Although the popularity of automatic dynamic monitoring systems has been increasing and the required equipment is becoming not only more advanced but also more affordable, considerable challenges continue to arise in this field, since the development and installation of monitoring systems requires time and specific

expertise, and the proper analysis of acceleration records needs knowledge and specific processing tools. For these reasons, available seismic records on large concrete dams throughout the world continue to be insufficient today, specially under strong earthquakes, thus making it important to continue investing in trigger-event or continuous dynamic monitoring systems, hopefully to obtain more records of seismic accelerations, as well as in methodologies and tools for processing and analysing seismic data.

Furthermore, it can of great value for the dam engineering community to develop international platforms for sharing data of seismic records on dams all over the world. This is the case of DamQuake, a project presented in (Robbe & Humbert, 2019), with the goal of building "an international database of dam response records under seismic loading", which would allow users to evaluate measured data, carry out quick analyses on selected records, and compare them with records obtained for other structures, aiming to increase knowledge on the complex seismic response of dams.

2.5 MODELLING AND MONITORING THE DYNAMIC BEHAVIOUR OF CONCRETE DAMS

As mentioned previously, it is essential to evaluate the performance of large concrete dams in normal operating conditions, to control structural health over time, and under earthquake ground motion, by monitoring seismic response and performing seismic behaviour prediction analyses for current and failure scenarios, ultimately aiming to ensure structural safety and optimal operation conditions. Therefore, both modelling and monitoring the dynamic behaviour of large concrete dams are very important to deepen knowledge on dam behaviour for different scenarios, to support and improve the design of new dams, and also to provide useful data for developing better monitoring systems and for updating existing numerical models or helping the development of new ones, ultimately working towards to increase dam safety.

However, the current state-of-knowledge of dam engineering was only possible due to the significant research activities and the numerous studies and research projects developed for many decades in these two fields. As such, a brief historical overview is provided, along with mention to important advances and references to studies of interest in modelling the dynamic behaviour of dam-reservoir-foundation systems, as well as to cases of seismic records, dynamic vibration tests, and dynamic monitoring systems for large concrete dams.

2.5.1 MODELLING THE DYNAMIC BEHAVIOUR OF DAM-RESERVOIR-FOUNDATION SYSTEMS

Modelling the dynamic behaviour of dam-reservoir-foundation systems, particularly under seismic loads, has been for many decades one of the most important subjects in dam engineering, posing significant challenges for structural engineers and researchers in this field. The most used behaviour prediction models are finite element numerical models, although mention should be made to reduced scale physical models.

The study of the dynamic behaviour of concrete dams began in the first half of the 20th century, a time when the first large concrete dams were built, by performing behaviour analysis using simplified mathematical models and tests on physical models.

During this period, many theoretical studies were performed for supporting design and safety verification of dams using mathematical models based on considerable simplifying hypotheses, which are reviewed in detail in (Serafim, 1958). Among others, it is worth mentioning the research conducted by Westergaard, including a paper on arch dam analysis by the traditional method of trial loads (Westergaard, 1931) and especially his pioneer work dedicated to water pressures on dams during earthquakes (Westergaard, 1933), where he proposed the pseudo-static method for seismic analysis of dam-reservoir systems and a solution to calculate the hydrodynamic pressure on gravity dams with vertical upstream faces (Fig. 2.35). The pseudo-static method was used during several decades for seismic design of dams (as mentioned in 2.4), while the solution for calculating hydrodynamic pressures is still used to this day to simulate the reservoir hydrodynamic behaviour in the classic added water mass models (see 3.2 for further details).

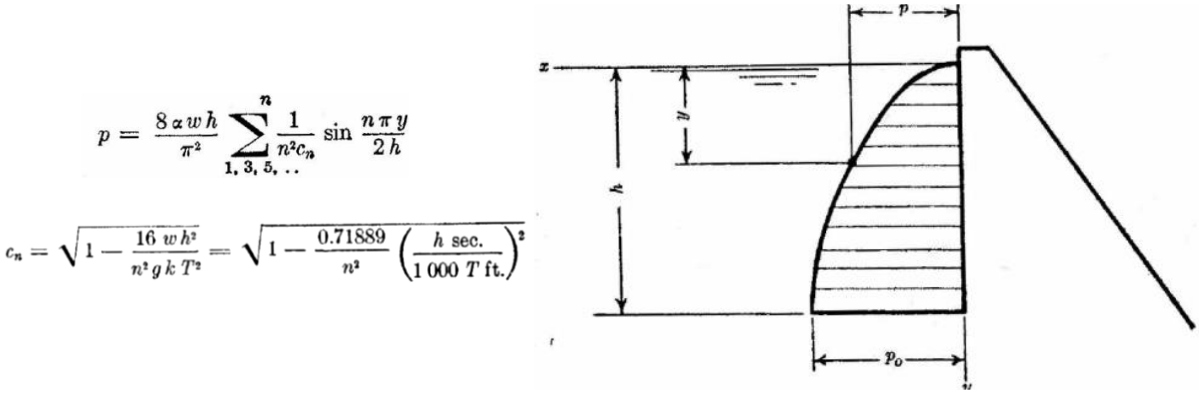

Fig. 2.35 Water pressure distribution on a gravity dam. Exact solution proposed by (Westergaard, 1933).

On the other hand, physical models started to be developed and used for analysing the behaviour and supporting the design of concrete dams in the 1920s, namely with an experimental study on the concrete arch Stevenson Creek Test dam (COADI, 1922; Westergaard, 1928). Over the next two decades, experimental studies were performed in the United States, namely for the iconic Hoover dam (USBR, 1930), as well as in France (Anclair, 1936) and in Italy (Oberti, 1946). In Portugal, the first test with a physical dam model was performed in LNEC to study the Santa Luzia arch dam (Rocha & Serafim, 1948).

Computation capabilities were still quite limited in the 1950s/60s/70s, and due to the evolution of model construction techniques and testing methodologies, experimental tests and physical models became quite popular in dam engineering. Of note is the contribute given by LNEC in this field, where physical models were used to analyse current scenarios, e.g. response under the hydrostatic pressure (Fialho, 1955) and self-weight loads (Serafim & Costa, 1961), and failure scenarios, including the concrete strength decrease (Rocha & Serafim, 1958) and the seismic load increase (Borges et al., 1963; J. Pereira & Ravara, 1973). Furthermore, a research program carried out at the University of California, in Berkeley, succeeded in developing and testing reduced scale models in shaking tables, namely to investigate the non-linear behaviour of a monolith of Koyna dam and of a jointed arch section (Niwa & Clough, 1980, 1982), which

provided valuable insight on the non-linear response of concrete dams. Relevant experimental tests on reduced scale models were also carried out worldwide, namely in China, Japan, and Italy (Hall, 1988).

Around this time, important experimental studies were also conducted based on electric analogue procedures in order to investigate the hydrodynamic pressures on concrete dams during earthquakes, first on gravity dams (Zangar, 1952) and later on arch dams (Zienkiewicz & Nath, 1963).

Nevertheless, numerical methods started to be used in the early 1950s, and the first references to the application of the FEM are made in the scope of research conducted for development of the United States aerospace industry, as described in (Clough, 1991; Clough & Wilson, 1999). Among the first applications of the FEM in Civil Engineering is dam behaviour modelling in the 1960s, including initial studies for gravity dams (Clough, 1962; Clough & Wilson, 1962) and then for arch dams (Pedro, 1967). In parallel with the appearance of the first computers, the FEM underwent significant developments (Zienkiewicz & Cheung, 1967) and it started being applied for vibration analysis (Zienkiewicz, 1967; Zienkiewicz et al., 1965) and later to solve fluid-structure coupled problems (Belytschko, 1977, 1980; Daniel, 1980; Olson & Bathe, 1983; Zienkiewicz & Bettess, 1978; Zienkiewicz & Taylor, 1985).

Following the important advances in computer technology and the development of more advanced numerical models that took place especially from the 1980s onwards, physical models became less and less used considering that their construction and testing was neither practical nor economical. Therefore, significant research on numerical modelling the dynamic behaviour o dam-reservoir-foundation-systems was carried out.

For example, Chopra and colleagues such as Tan, Fok, Fenves and Hall carried out several studies on the dynamic behaviour of gravity or arch dam-reservoir-foundation systems (Fig. 2.36), particularly under seismic loads, with significant contributions regarding the influence of water compressibility, hydrodynamic and foundation interaction effects, and reservoir bottom absorption on the structural seismic response (Chakrabarti & Chopra, 1973; Chopra & Chakrabarti, 1981; Chopra & Tan, 1992; Fenves & Chopra, 1983; Fok & Chopra, 1986b, 1986a, 1987; Tan & Chopra, 1995a, 1995b, 1996). As a result of these works, the first version of the EACD-3D program was developed (Fok et al., 1986).

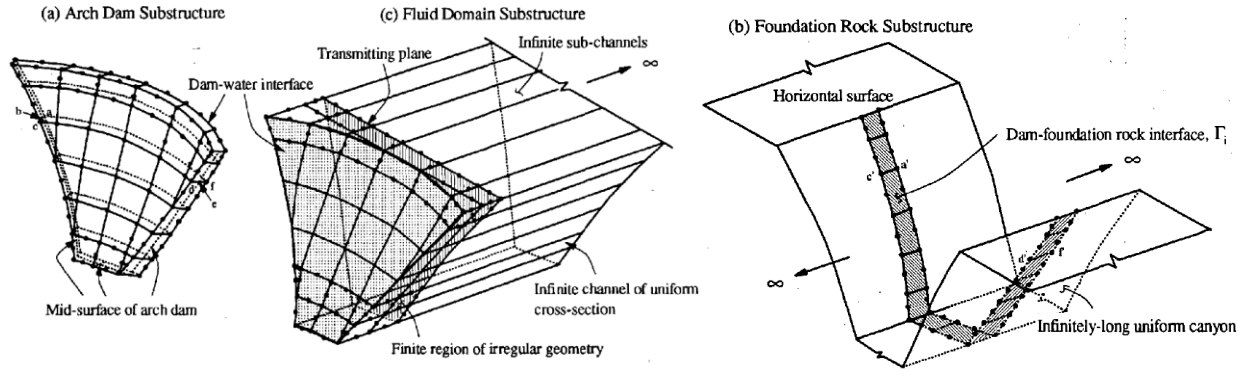

Fig. 2.36 Dam-reservoir-foundation system: arch dam, fluid, and foundation substructures (Tan & Chopra, 1995b).

With respect to the non-linear seismic behaviour of concrete dams (Fig. 2.37), important advances were made in the late 1980s, during the 1990s, and in the first years of the 21st century, and valuable research was conducted considering the non-linear behaviour of joints, in order to investigate the influence in the dam structural response (Clough, 1980; Fenves et al., 1992; Hall, 1998; Lau et al., 1998; C. Zhang et al., 2000), as well as the behaviour of concrete up to failure, aiming to predict the occurrence of damage under strong earthquakes (Cervera et al., 1995; El-Aidi & Hall, 1989a, 1989b; Espandar & Lotfi, 2003; Faria, 1994; Faria et al., 1998; Valliappan et al., 1999; Vargas-Loli & Fenves, 1989).

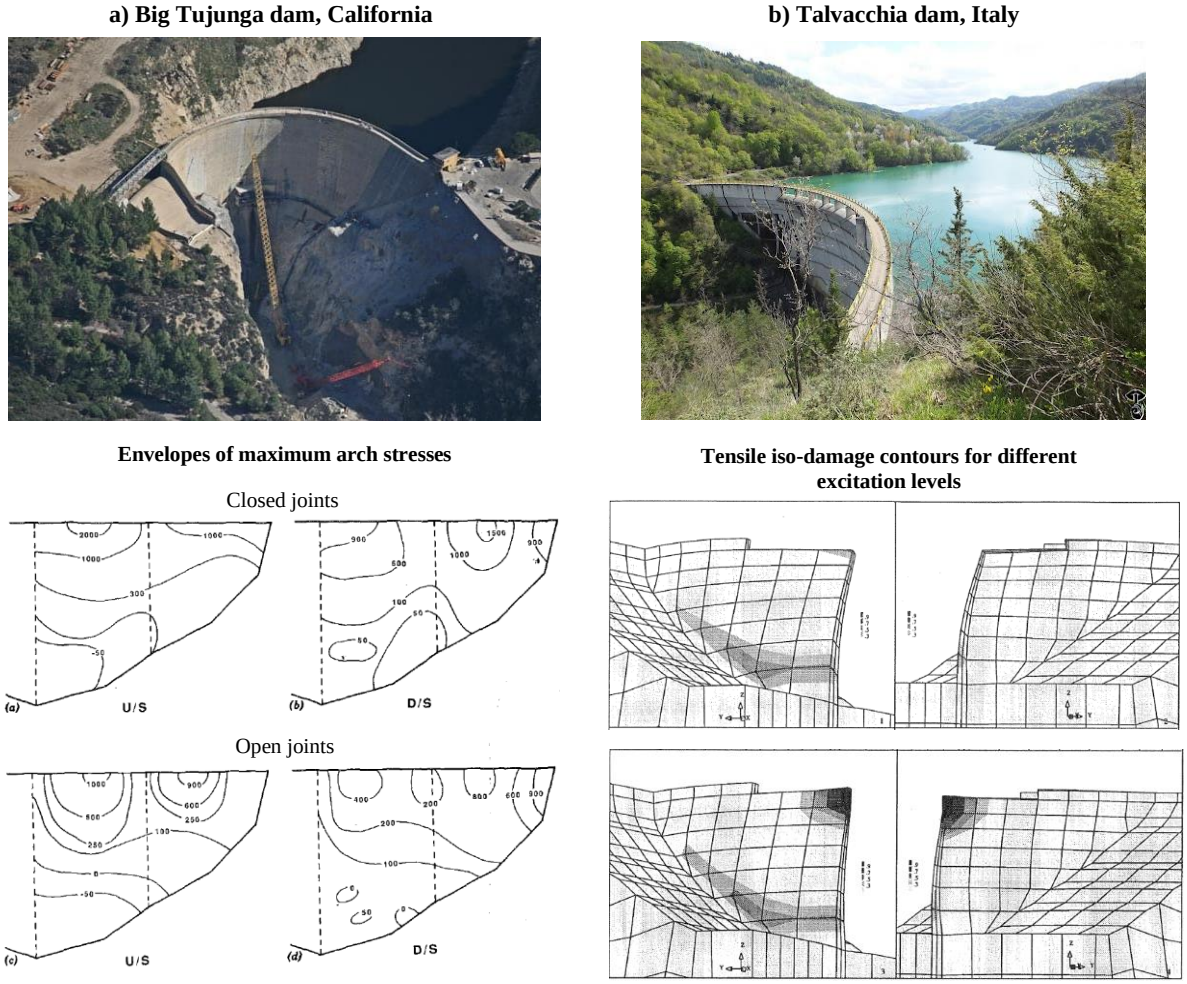

Fig. 2.37 Non-linear seismic analysis of arch dams: a) Big Tujunga dam, influence of joint movements on the maximum arch stresses (Fenves et al., 1992); b) Talvacchia dam, damages on upstream and downstream faces for different excitation level (Cervera et al., 1995).

In Portugal, the FEM was first introduced by (Pedro, 1967) for analysing the behaviour of dams in LNEC. Following this breakthrough, significant research was carried out for dynamic behaviour modelling of dam-reservoir-foundation systems, with focus on modal analysis and seismic response analysis of Portuguese and foreign large concrete dams (Câmara, 1989; Pedro, 1977; Pedro et al., 1996; Pedro & Câmara, 1986; Pedro & Pereira, 1979; Pina, 1988; Serafim & Oliveira, 1987). It is also worth mentioning the use of the DEM in LNEC, initially applied for studying dam foundations (Lemos, 1987, 1999) and latter implemented

for arch dam analysis (Lemos, 1998) as a new module for the program 3DEC. Furthermore, the FEM was used for analysing the behaviour of both gravity and arch dams in (Delgado, 1984; Faria, 1994).

Over the last two decades there was a considerable evolution in terms of computer technology, particularly in terms of processing speed and storage memory. This progress, in addition to the accumulated knowledge from decades of considerable research, enabled the development of increasingly advanced models and of more refined meshes for simulating and analysing the behaviour of dam-reservoir-foundation systems.

As such, there have been many research studies of interest regarding the dynamic behaviour of gravity and arch dam-reservoir-foundation systems, with emphasis on the structural response under seismic loads, carried out by researchers and dam engineers all over the world. In this context, it is worth referring those concerned on investigating crucial numerical modelling aspects of dam-reservoir-foundation systems and their influence on the modal parameters and on the seismic response (Fig. 2.38), including the coupled dam-reservoir interaction and other hydrodynamic effects (Bouaanani & Lu, 2009; Bouaanani & Renaud, 2014; Gogoi & Maity, 2010; Goldgruber et al., 2013; Küçükarslan, 2004; Küçükarslan et al., 2005; Miquel & Bouaanani, 2010; Sani & Lotfi, 2010), the influence of foundation dynamic behaviour and damping mechanisms (Arabshahi & Lotfi, 2008; D.-H. Chen et al., 2012; Hariri-Ardebili & Mirzabozorg, 2013; Lokke & Chopra, 2018; C. Zhang et al., 2009). Other numerical studies have been performed for analysing the influence of reservoir water level variations (Alegre, Oliveira, et al., 2019; Hariri-Ardebili & Mirzabozorg, 2011; Sevim et al., 2012), canyon (Maeso et al., 2004) and reservoir geometry (Millán et al., 2007), and the consideration of the ground motion spatial variation (Alves & Hall, 2006; Chopra & Wang, 2010; Maeso et al., 2002; J.-T. Wang & Chopra, 2010).

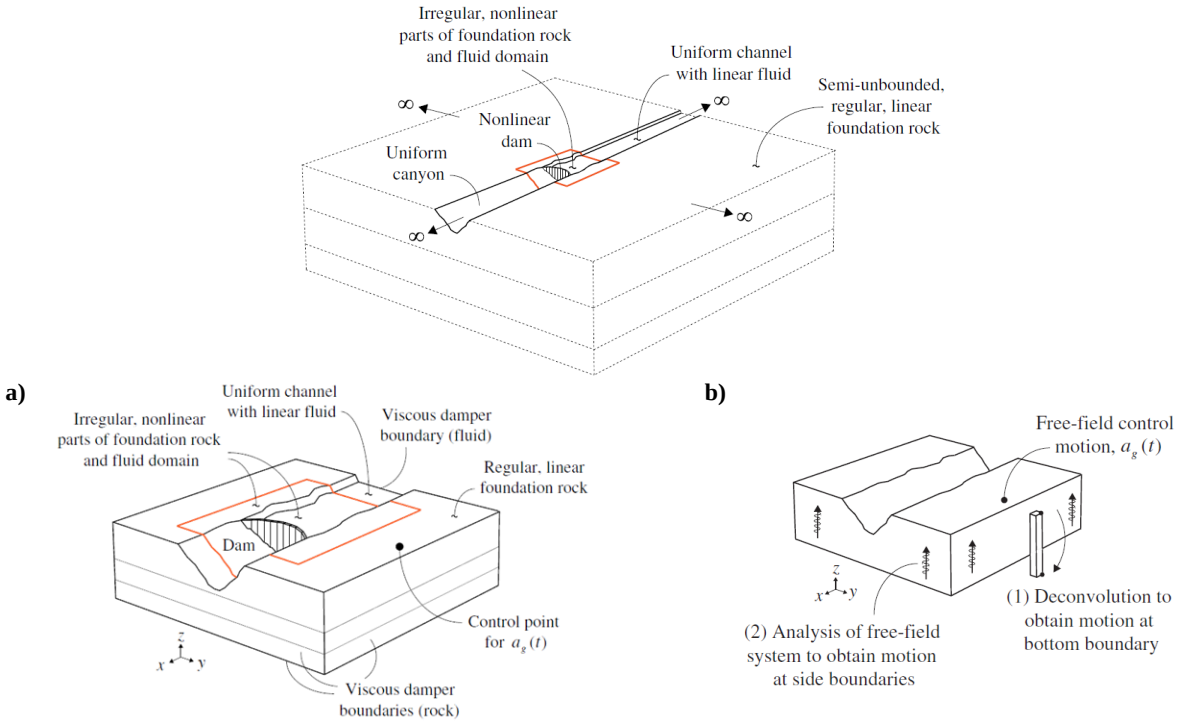

Fig. 2.38 Three-dimensional semi-unbounded dam-reservoir-foundation system: a) dam-reservoir-foundation system with truncated foundation and fluid domains for modelling using a finite element discretisation; and b) possible method to obtain free-field earthquake motion (Lokke & Chopra, 2018)

Significant work has also been conducted based on the comparison between numerical results from finite element analyses and experimental results from monitoring data, including: (i) studies dedicated to the analysis of the natural frequencies and modal configurations of dam-reservoir-foundation systems (Fig. 2.39) (Lemos et al., 2008; Mivehchi & Ahmadi, 2004; S. Oliveira et al., 2010, 2012; S. Oliveira, Silvestre, Espada, et al., 2014), in particular to evaluate the influence of the reservoir water level in the modal parameters (Alegre, Carvalho, et al., 2019; Alegre, Oliveira, et al., 2020; S. Oliveira & Alegre, 2018; Proulx et al., 2001; Sevim et al., 2012) or to calibrate and update the numerical models (Calcina et al., 2014; García-Palacios et al., 2016; Makha & Moyo, 2012); and (ii) studies for seismic response analysis during real seismic events (Fig. 2.40), not only to investigate fundamental aspects such as the required damping to fit computed and recorded accelerations (Proulx et al., 2004; Proulx & Darbre, 2008; Robbe, 2017; Robbe et al., 2017) but also the spatial variation of the ground motion used as input (Alves & Hall, 2006; Chopra & Wang, 2010; Koufoudi et al., 2018; J.-T. Wang & Chopra, 2010).

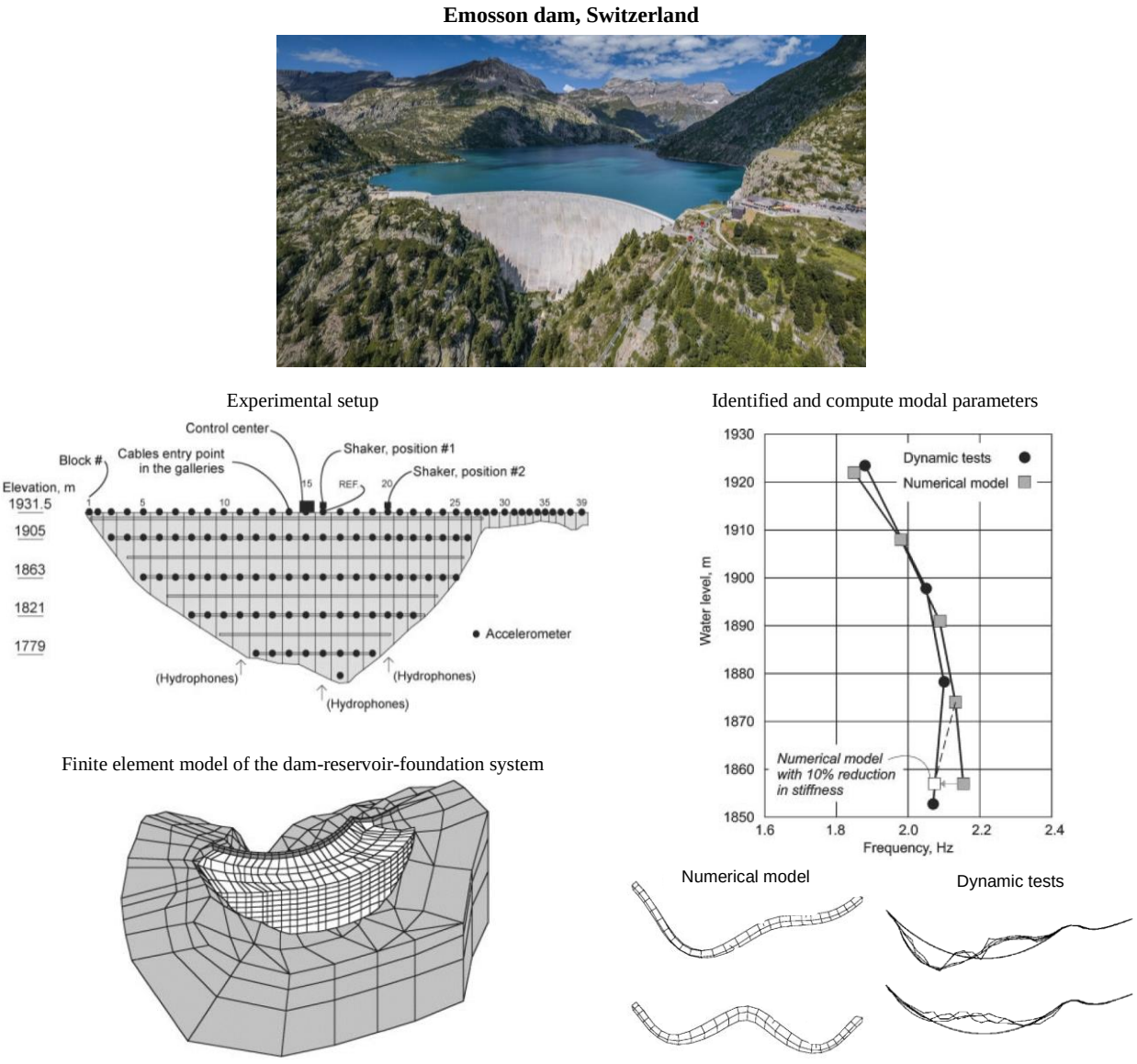

Fig. 2.39 Study on the dynamic behaviour of Emosson dam, Switzerland. Experimental setup, numerical model, and comparison of natural frequencies (considering water level effects) and mode shapes (Proulx et al., 2001).

Punt-Dal-Gall dam, Switzerland

Finite element model of the dam-reservoir-foundation system

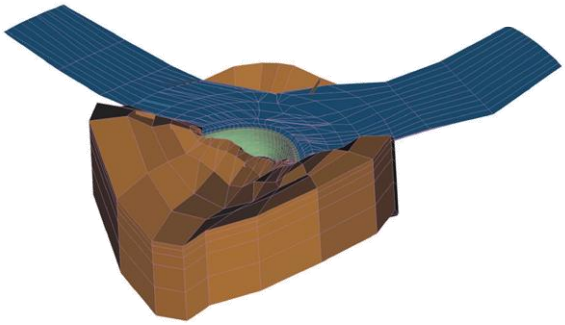

Comparison between measured and computed seismic response

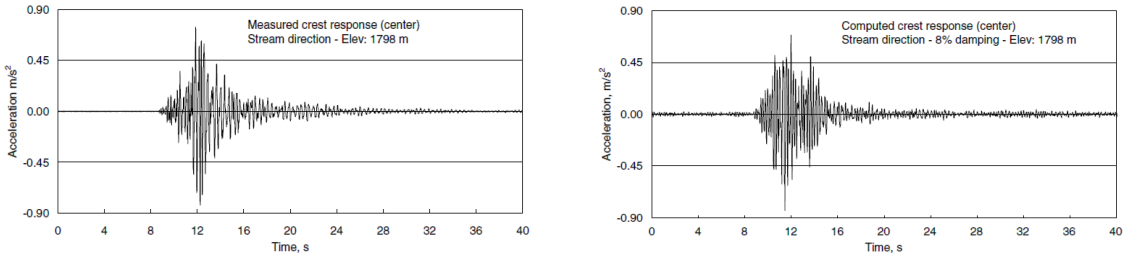

Fig. 2.40 Seismic response of Punt-Dal-Gall dam, Switzerland. Finite element model of the dam-reservoir-foundation system and comparison between measured and computed accelerations at the crest (Proulx et al., 2004).

Furthermore, taking into consideration the increasing structural safety demands and the relevance of proper seismic design and safety assessment, more numerical simulations have been carried out for non-linear seismic analysis of large concrete arch dams under strong earthquakes (Fig. 2.41), namely to analyse the non-linear joint behaviour and the influence on the dams structural response (Hariri-Ardebili et al., 2014; Mirzabozorg et al., 2013; J.-T. Wang et al., 2012; C. Zhang et al., 2009), to predict and analyse the occurrence of concrete failure (Hariri-Ardebili & Mirzabozorg, 2011, 2013, 2014; R. Wang, 2016), as well as to evaluate both joint and material nonlinearities (Alegre, Oliveira, et al., 2020; Alegre & Oliveira, 2020; Goldgruber, 2015; Hariri-Ardebili & Mirzabozorg, 2012b; J.-T. Wang et al., 2013).

Finally, although their use has decreased significantly over time in detriment of numerical models, experimental tests using physical models of dams continued to be performed over the past two decades for analysing the behaviour of large concrete dams, considering the useful experimental information that can be provided, as a complement to numerical results (recall Fig. 2.23). Thus, experimental studies of note include shaking table tests for seismic response analysis under strong earthquakes, namely a test carried out for the Portuguese Odiáxere arch dam, in LNEC (Gomes, 2010; Rosça, 2008), several studies for the design of ultra-high arch dams built in China (R. Wang, 2016; R. Wang et al., 2018; Zhou et al., 2000; Zou et al., 2006), among others (Mridha & Maity, 2014; H. Wang & Li, 2006, 2007), as well as for evaluating the influence of dam-water interaction (Mendes & Oliveira, 2007) and the influence of water level variations (Sevim et al., 2012) or of vertical joint movements in the modal parameters of the dam-reservoir-foundation systems (S. S. Wang et al., 2015).

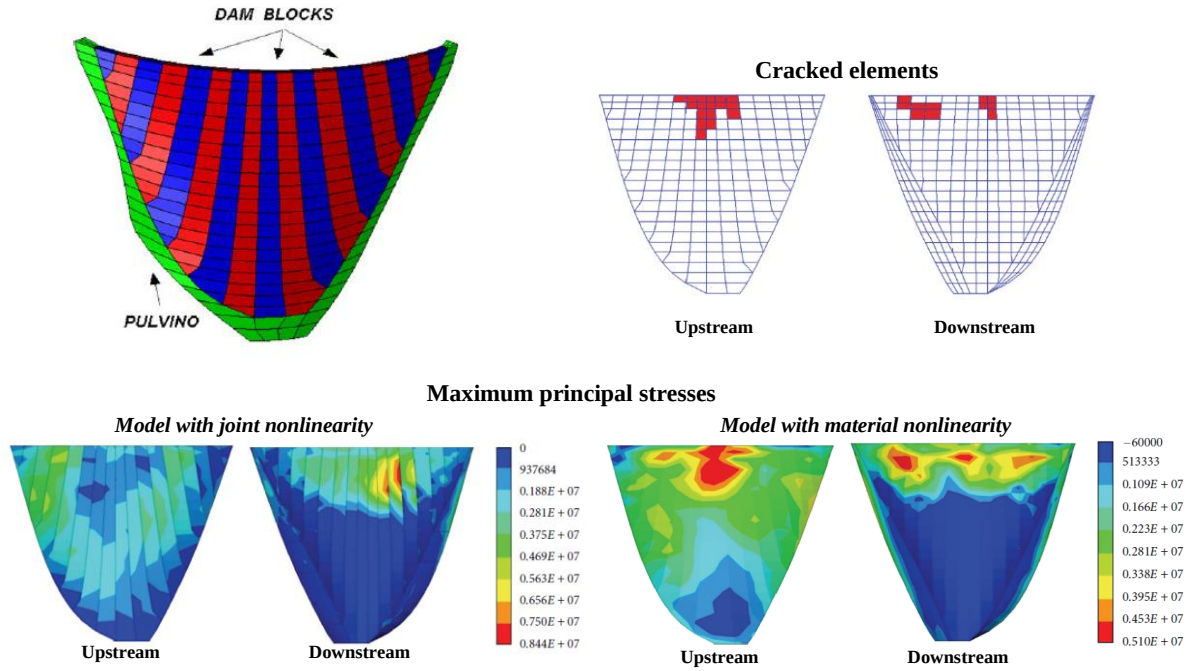

Fig. 2.41 Non-linear seismic response of Dez dam (203 m high): maximum principal stresses considering joint nonlinearity or material nonlinearity, and cracked elements (Hariri-Ardebili & Mirzabozorg, 2012a).

2.5.2 SEISMIC MONITORING OF LARGE CONCRETE DAMS

The monitoring of the dynamic behaviour of large concrete dams is carried out by measuring and analysing vibrations, aiming to evaluate the dynamic response during seismic events and/or to estimate the main modal parameters, and it has become a fundamental part of dam safety control. Significant work has been conducted in this field, not only in what concerns the seismic behaviour monitoring, particularly during strong seismic events (addressed in the current section), but also regarding the performance of forced and ambient vibration tests and, more recently, the installation of continuous dynamic monitoring systems (topics covered in the following sections).

From an early stage, one of the main concerns regarding dynamic behaviour analysis and safety assessment of dams has been their performance under seismic loads, as referred previously. Therefore, strong motion devices, or accelerographs, were installed in several large concrete dams throughout the years, enabling the measurement of acceleration time histories during moderate to strong earthquake ground motion.

One of the first instrumented concrete dams was the 221 m high Hoover arch dam, in the United States, where three accelerographs were installed in 1937, enabling the recording of several earthquakes over the years (USCOLD, 1977). The strongest ground motion was of 0.075g, at a free-field site 600 m away from the dam, and the peak acceleration reached 0.2g at the crest. An iconic case study is the 133 m high Pacoima arch dam. During the 1971 San Fernando earthquake, of magnitude 6.6, peak ground accelerations of 1.25g (horizontal) and of 0.7g (vertical) were recorded in a device installed at the top of the left bank. These accelerations gave clear indications on the vibration amplification caused by the topography of the canyon and ridge (Alves, 2004; Hall, 1998). After that, an array of 17 accelerometers were installed in the dam body, at the base, and at both abutments (Fig. 2.42). Later, during the 1994 Northridge earthquake of

magnitude 6.7, peak ground accelerations around 0.5g were recorded at the base of the dam, while extreme earthquake motion was measured near the crest of the dam, around 2.3g (the largest ever recorded in a large concrete dam), and at the top of the left bank with the older accelerometer, about 1.6g.

Pacoima dam, California

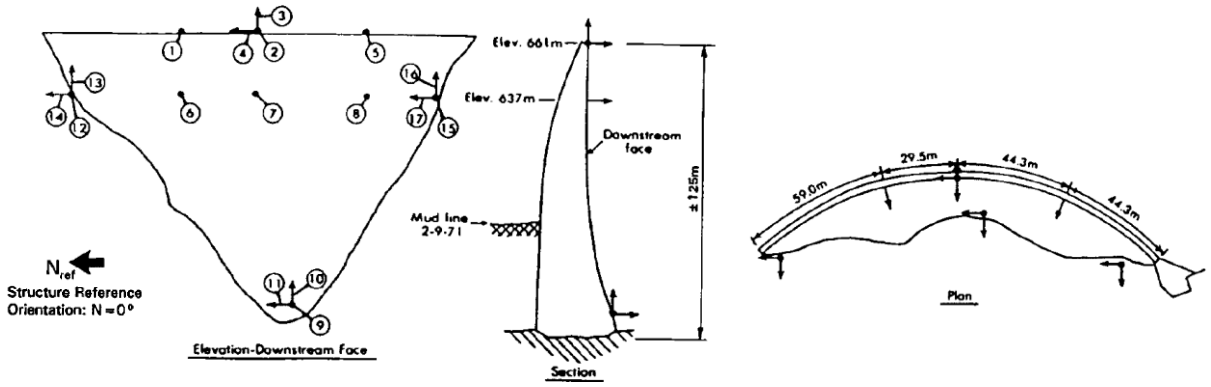

Fig. 2.42 Location of the 17 accelerometers installed in Pacoima dam in 1977 (Chopra & Wang, 2010).

In Switzerland, during the 1990s, trigger-event accelerograph arrays were installed on several large concrete dams, namely in the 285 m high Grande-Dixence gravity dam (285 m high), and in the Mauvoisin (250 m high), Emosson (180 m high), and Punt-dal-Gall (130 m high) arch dams (Darbre, 1995). The main goals were to monitor the overall seismic behaviour during seismic events, investigate response patterns, and establish a set of records for identifying input motions and for providing valuable data to calibrate finite element models (Darbre, 1995; Proulx & Darbre, 2008). Twelve triaxial accelerographs were installed in in Mauvoisin dam (Fig. 2.43), seven in Punt-dal-Gall dam, six in Grande-Dixence dam, and four in Emosson dam. Examples of seismic events that triggered the accelerographs were the 1996 Valpelline earthquake of magnitude 4.6 in Mauvoisin dam (recall Fig. 2.34), and the 1999 Bormio earthquake of magnitude 4.9 detected in Punt-dal-Gall dam.

Mauvoisin dam, Switzerland

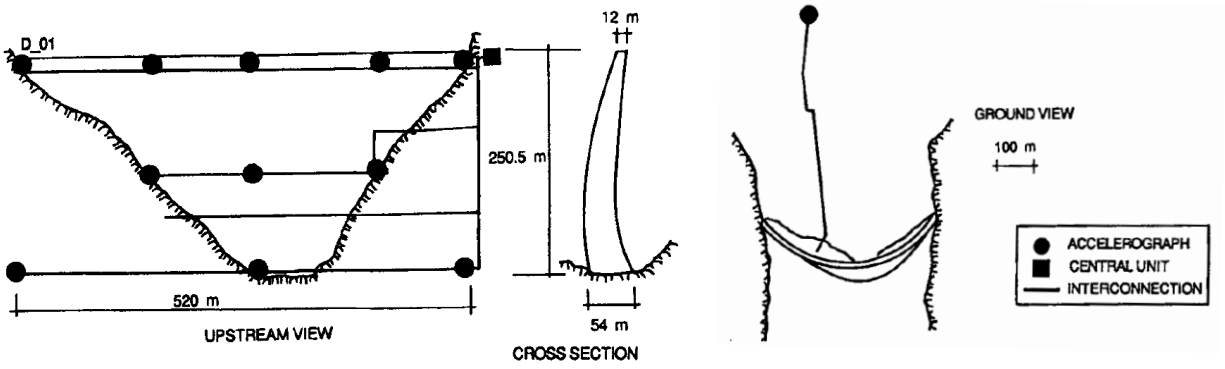

Fig. 2.43 Strong-motion array at the Mauvoisin arch dam (Darbre, 1995).

Other examples of large concrete dams where strong motion devices were installed are described in the 1970s and 1980s are described in (Hall, 1988), including Lower Crystal Springs, Big Dalton, Gibraltar and Big Tujunga dams, in the United States, Xinfengjian dam in China, Tagokura, Kurobe and Nagawado dams, in Japan, Koyna dam, in India, and Ambiesta and Talvacchia dams, in Italy.

In Portugal, several trigger-event devices for measuring seismic vibrations have been installed on large concrete dams (Fig. 2.44), including on the Aguieira multiple-arch dam (89 m high), one of the first instrumented dams in Portugal in the 1980s, as well as on the Alqueva arch dam (96 m high), the Alto Ceira II arch dam (46 m high), and the Ribeiradio arch-gravity dam (83 m high).

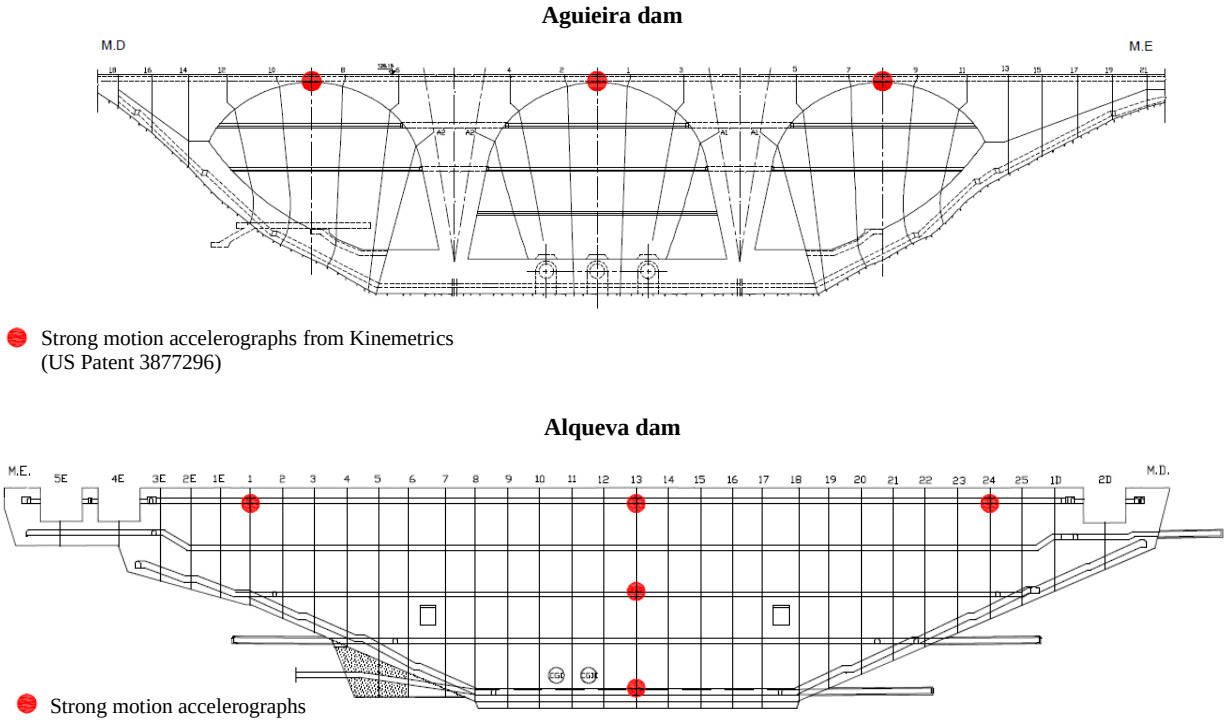

Fig. 2.44 Strong motion devices in Aguieira dam (installed in the 80s) and in Alqueva dam (installed in the late 90s).

Over the past 20 years, there are more examples of strong-motion instrumentation installed in large concrete dams. For example, in 2000, a seismic monitoring system composed of 10 strong motion recorders was installed in Enguri dam (GeoSIG, 2009a), a 272 m high arch structure. This dam is located in Georgia, in the Caucasus, one of the most active seismic regions in the Alpine-Himalayan collision belt. Later, in 2001, a seismic monitoring setup including six triaxial and six uniaxial accelerographs was implemented in the 240 m high Ertan arch dam, in China (Fig. 2.45). This seismic monitoring system recorded over 20 earthquakes over the years, including the 2008 Wenchuan and PanZhiHua earthquakes (Yang et al., 2017).

With respect to strong motion records on large concrete dams, there are several well-known cases in literature worth mentioning (USSD, 2014). In Xinfengjian dam, a 105 m high gravity dam in China, during an aftershock of a reservoir-triggered earthquake of magnitude 6.1 that occurred in 1962, the peak

acceleration at the crest reached 0.54g. In turn, for the 103 m high Koyna gravity dam, in India, the recorded peak ground accelerations in the lower gallery reached 0.63g, 0.49g, and 0.34g in the cross-valley, upstream-downstream, and vertical directions, during the magnitude 6.5 Koyna earthquake in 1967, which occurred 12 km away from the dam.

Some years later, in 1976, the magnitude 6.5 Gemona-Friuli earthquake caused maximum accelerations of 0.36g in the right abutment of the Ambiesta arch dam (60 m high), in Italy, which was at 22.5 km from the epicentre. As for Rapel arch dam (112 m high), in Chile, peak free-field accelerations of 0.31g were recorded near the dam, in the cross-valley direction, during magnitude 7.8 Santiago Earthquake in 1985, which occurred at 45 km from the dam. More recently, maximum accelerations of 0.21g occurred in this dam because of the magnitude 8.8 Maul earthquake in 2010, with epicentre at 231 km from the dam site. During the magnitude 7.6 Chi-Chi earthquake in Taiwan, in 1999, peak ground accelerations around 0.5g were recorded at less than 500 m from Shih Kang gravity dam, while peak crest accelerations reached 0.86g at the 180 m high Techi arch dam. In China, 2008, the magnitude 8 Wenchuan earthquake caused peak ground accelerations of 0.5g to 0.6g at the base of the 156 m high concrete faced rockfill Zipingpu dam, while records at the crest are around 1g, while the magnitude 5.7 PanZhiHua earthquake induced peak accelerations of 0.08g at the dam base and of around 0.68g at the crest of 240 m high Ertan arch dam (Fig. 2.45), which was at 57 km from the epicentre (Yang et al., 2017).

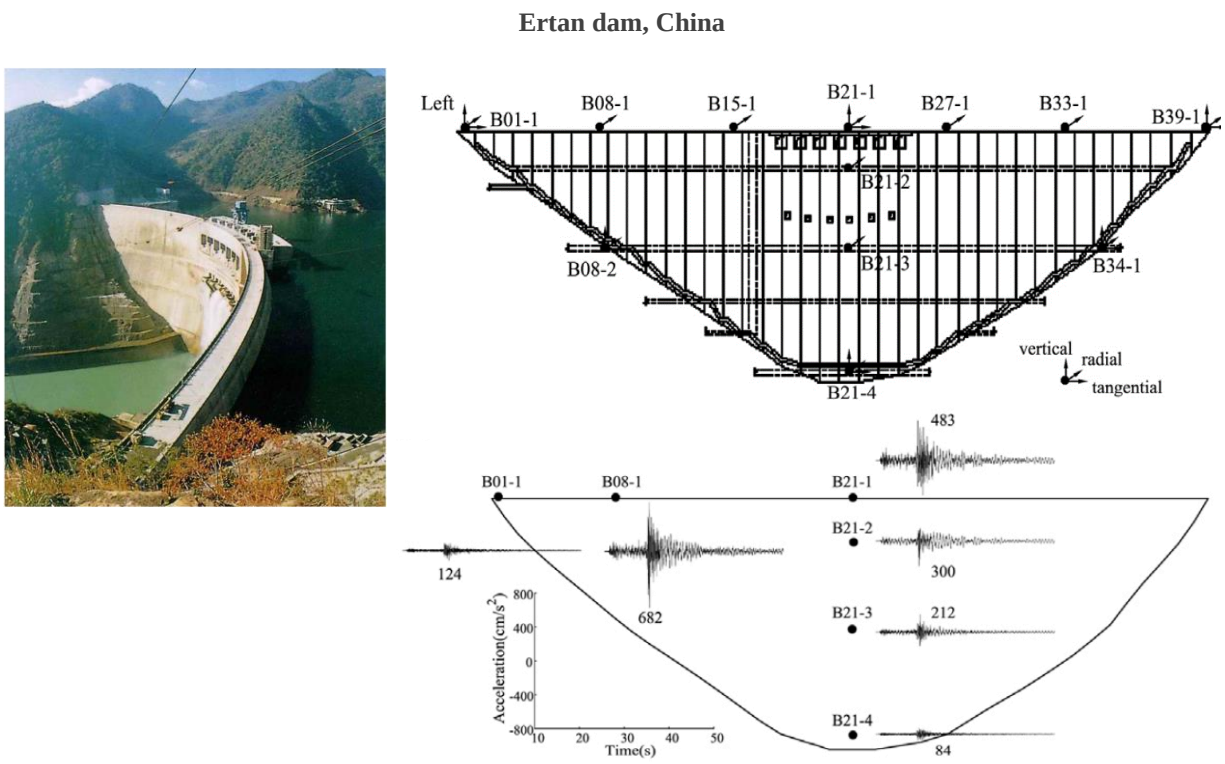

Fig. 2.45 Seismic monitoring system installed in Ertan dam, China. Acceleration time histories recorded during the 2008 PanZhiHua earthquake (Yang et al., 2017).

Some of the most important earthquake motions recorded on large concrete dams have occurred in Japan in the past 20 years (USSD, 2014). For example, during the magnitude 6.7 Western-Tottori Prefecture earthquake in 2000, peak accelerations of 0.62g and of 1.16g were measured underground and at the surface of the Hino Observation Station, located at about 20 m from the 14 m high Uh gravity dam. Furthermore, at the 46 m high Kasho gravity dam, located at less than 5 km from the epicentre, the peak ground accelerations at the lower gallery were around 0.54g, which were amplified to a maximum of 2.09g at the crest. Later, in 2007, Noto Hanto earthquake of magnitude 6.7 caused peak seismic vibrations in the upstream-downstream direction of around 0.2g at the base and of 0.87g at the crest of the 52 m high Hakkagawa gravity dam, which was at 14 km from the epicentre. More recently, in 2011, the 77 m high Takou gravity dam, located at more than 110 km from the epicentre, experienced significant earthquake motion during an aftershock (magnitude 7.1) of the magnitude 9 Tohuku earthquake (the main earthquake caused a power failure): the peak ground accelerations in the foundation were of 0.29g, 0.38g and 0.27g in the cross-valley, upstream-downstream, and vertical directions, respectively, and the maximum accelerations at the crest were 2.04g, 1.79g, and 1.33g, in the same directions.

2.5.3 DYNAMIC VIBRATION TESTS ON LARGE CONCRETE DAMS

Dynamic vibration tests consist essentially of field tests conducted for estimating the main modal parameters (natural frequencies, mode shapes, and damping ratios) from measured vibrations, with the goal of evaluating the performance of dams under dynamic loads. The analysis of these dynamic properties can also provide useful insight on the dynamic behaviour of the dam-reservoir-foundation system.

As referred previously, there are two types of field tests: forced vibration tests, in which dams are excited using eccentric mass vibrations or hydraulic shakers, and ambient vibration tests, where the response of the dam is measured under dynamic excitations from ambient and/or operational sources, like the wind, traffic, operation of power groups, etc. The dynamic vibrations are measured in various locations of the dam body using accelerometers and modal parameters are estimated using modal identification methods.

The first field tests on large concrete dams were forced vibration tests, aiming to provide additional data to better understand their dynamic behaviour and to calibrate and validate numerical models. A large number of forced vibration tests were carried out over the years, particularly during the 1970s and 1980s, when some of the most relevant works in this field were conducted (Hall, 1988).

For example, several studies using data from field tests were carried out on concrete dams in the United States. On Pine Flat dam, a 131 m high gravity dam, natural frequencies and mode shapes were identified based on the measurements from various tests throughout the year of 1971 (Rea et al., 1972). Forced vibration testing was also performed for Pacoima dam after the 1971 San Fernando Earthquake, namely to calibrate the existing finite element model, as well as to analyse the main modal parameters before and after repairs on the left abutment (Hall, 1988). As for the case of Morrow Point dam (Fig. 2.46a), a 143 m high arch structure, measured accelerations and water pressures in 1985 were compared with finite element results in a pioneer study, not only to investigate the influence of water compressibility, but also to calibrate

the numerical model (Duron & Hall, 1988). Furthermore, experimental data measured in 1982 and 1986 on the 93 m high Monticello arch dam (Fig. 2.46b) was used for studying the influence of the reservoir level and water compressibility effects on the modal parameters (Clough & Ghanaat, 1987; Roehm, 1971).

References and results of other important early forced vibration tests are provided in (Hall, 1988), including those carried out on the Kurobe and Nagawado arch dams, in Japan, on the Ambieste arch and Talvacchia gravity-arch dams, in Italy, and on the Techi arch dam, in Taiwan.

a) Morrow Point dam, Colorado **b) Monticello dam, California**

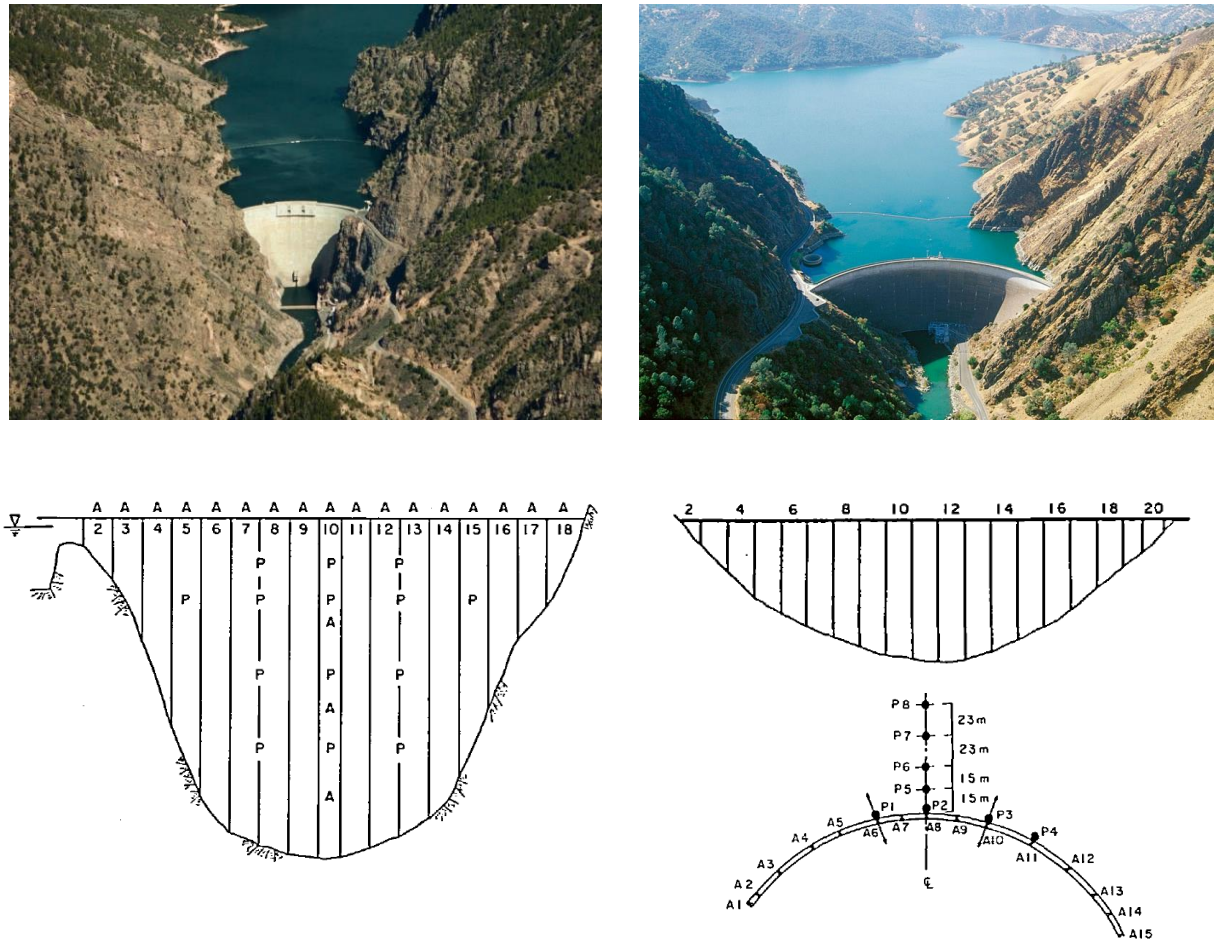

Fig. 2.46 Forced vibration tests on Morrow Point dam and on Monticello dam, United States. Upstream elevations and locations of devices used to measure accelerations (A) and dynamic pressures (P).

Forced vibration tests were also performed out for two Chinese dams in 1982, in the scope of a research program that aimed to investigate the effects of reservoir and foundation interaction on the dynamic behaviour of arch dams and to update the existing finite element models. The studied dams were Xiang Hong Dian dam, a 87.5 m high gravity arch structure (Clough, Chang, Houqun, Stephen, Wang, et al., 1984), and Quan Shui dam (Fig. 2.47), a 80 m high thin double curvature arch dam (Clough, Chang, Houqun, Stephen, Ghanaat, et al., 1984).

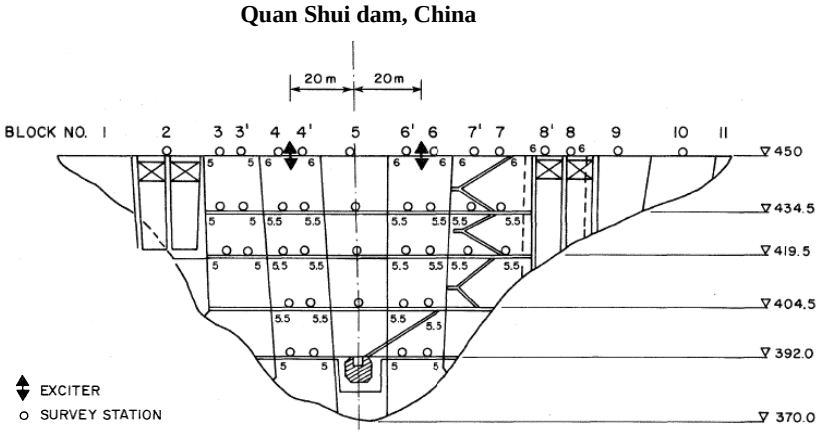

Fig. 2.47 Forced vibration test on Quan Shui dam. Upstream view showing the positions of the shaker and of the recording devices.

In Europe, forced vibration tests were carried out in 1978 and 1979 on the Wimbleball buttress dam (50 m high), in England, in order to investigate the effects of rising water level on the identified natural frequencies (Severn et al., 1980). Forced vibration tests were conducted for the 180 m high Emosson arch dam in Switzerland, first in 1980, to analyse the modal parameters and calibrate the numerical model (Deinum et al., 1982), and later in 1997/1998, to analyse the influence of reservoir level variations and to investigate dam-reservoir-foundation interaction in numerical modelling (Proulx et al., 2001). In 1996, a well-known set of field tests were conducted for the 46 m high Norsjo dam, in Sweden, where the response was measured in the form of a 270 point grid, aiming to detect several mode shapes and update a finite element model based on experimental data (Cantieni et al., 1998).

In Canada, an extensive forced vibration testing project was conducted on Outardes 3 gravity dam, aiming to evaluate the state-of-the-art numerical methods available at the time for modelling dam-reservoir-foundation interaction, by comparing experimental results and numerical results obtained with two- and three- dimensional models (Proulx & Paultre, 1997). More recently, forced vibration tests were carried out on the 1314 m long Daniel-Johnson multiple-arch-buttress dam (Fig. 2.48), in order to detect natural frequencies and mode shapes to be used as a basis for updating the numerical model (Gauron et al., 2017).

In Portugal, particularly in LNEC, there was a strong tradition regarding the performance of forced vibration tests to characterize the dynamic behaviour of some of the most important dams in the country. This tradition dates back to the 1960s, a time where an eccentric mass vibrator was built in LNEC. After that, forced vibration field tests were conducted on several Portuguese dams, namely on Aguieira, Alto Lindoso, Crestuma, Cabril, Alto Ceira, and Alqueva dams (Câmara et al., 1993; Gomes & Oliveira, 1994; Pina & Gomes, 1996; Portugal & Caetano, 1992). More recently, in LNEC, forced vibration tests were carried out on the Cahora Bassa dam (Gomes & Carvalho, 2014), in Mozambique, and on the new Baixo Sabor (Gomes & Lemos, 2016) and Alto Ceira II (Gomes et al., 2016) dams, in Portugal.

Daniel-Johnson dam, Canada

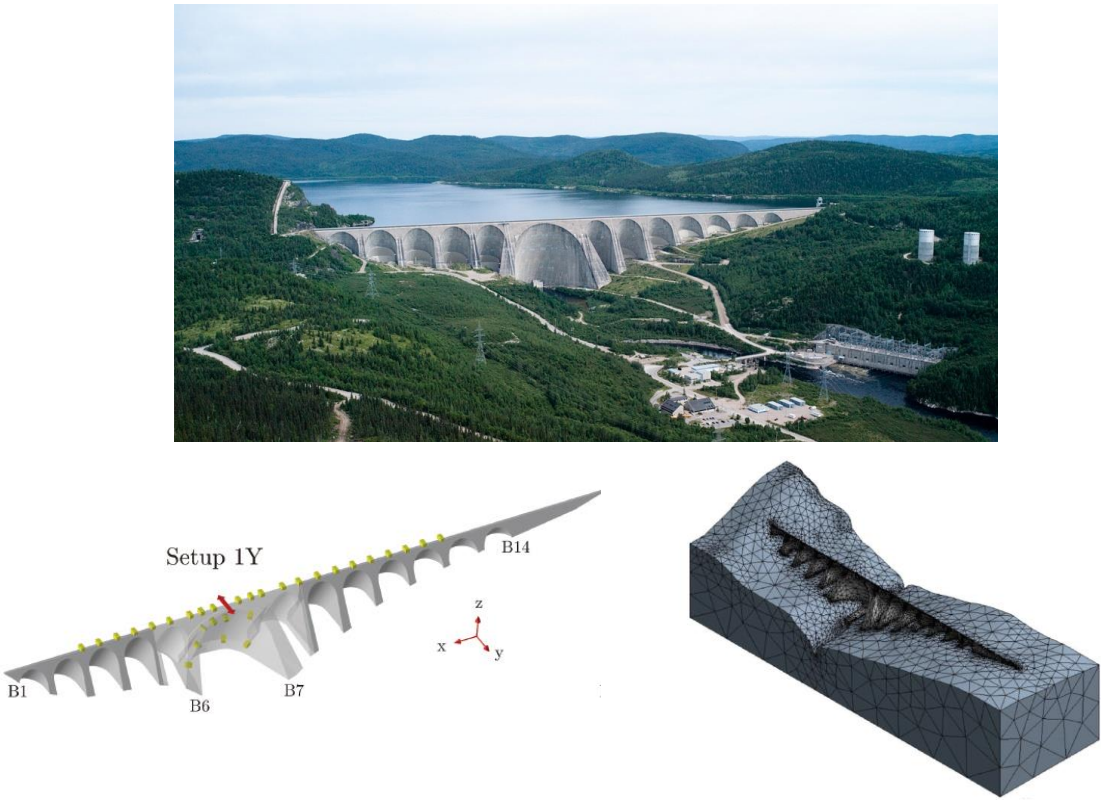

Fig. 2.48 Forced vibration test on Daniel-Johnson dam, Canada. Upstream view, positions of the shaker and accelerometers, and finite element model.

Although forced vibration tests enabled to achieve useful results on the dynamic behaviour of dams and to calibrate and validate numerical models of dam-reservoir-foundation systems, their use was not practical nor economical, and so they could only be carried out from time to time. Furthermore, since ambient vibration tests could be performed under ambient/operational excitation without disturbing the normal operation of dams, and considering not only the advances in data acquisition and measuring technology but also the development of methods for OMA, this type of field tests started to be performed on many dams, especially since the 1990s, Overall, conducted studies aimed at numerical model calibration, evaluation of the effects of water level variations, and, more recently, structural health monitoring.

One of the reported attempts on ambient vibration testing was conducted on Emosson arch dam, in 1980. Ambient measurements were made during a period of 12 hours, and the estimated natural frequencies and mode shapes were compared with results from previous forced vibration tests and with results from finite element models (Deinum et al., 1982). Later, two visits for ambient vibration tests on the Contra arch dam (200 m high) were carried out, in 1982 and 1985, under different reservoir conditions. The modal parameters extracted from the measured response were compared with results from finite element analysis, and the results showed the increase in the natural frequencies with the decrease of the reservoir water level (Brownjohn et al., 1986).

Around the same time, studies based on ambient vibration data were carried out for Techi arch dam (180 m high), in Taiwan (Clough et al., 1982), and for Xiang Hong and Quan Shui dams, in China (Clough, Chang,

Houqun, Stephen, Ghanaat, et al., 1984; Clough, Chang, Houqun, Stephen, Wang, et al., 1984). The natural frequencies were estimated from ambient vibration data for different reservoir water levels to demonstrate the influence of the water level in the frequency values, and then compared with previous forced vibration results and finite element results.

Mauvoisin dam, in Switzerland, was the subject of two experimental studies of great interest (Fig. 2.49). First, in 1995/1996, seven series of ambient vibration measurements were completed, over a period of 16 months between June 1995 and October 1996 (water levels varying from 13 to 127 m below the crest), with the goal of evaluating the influence of the reservoir level variations in the dynamic properties of the dam-reservoir-foundation system, considering the effects of the water mass and closing of contraction joints (Darbre et al., 2000). In this study, the authors recommended the continuous measurement of vibrations over a long period to improve this type of analysis. Therefore, some years later, an automated measurement system was installed in Mauvoisin dam and ambient vibrations were recorded twice a day between December 1998 and June 1999 (a total water level variation of 97.6 m). The obtained results confirmed the effect of the water level variations on the natural frequencies of the dam-reservoir-foundation system and showed the potential of continuously monitoring vibrations monitoring for safety evaluation purposes (Darbre & Proulx, 2002). This study marked the beginning of long-term ambient vibration monitoring.

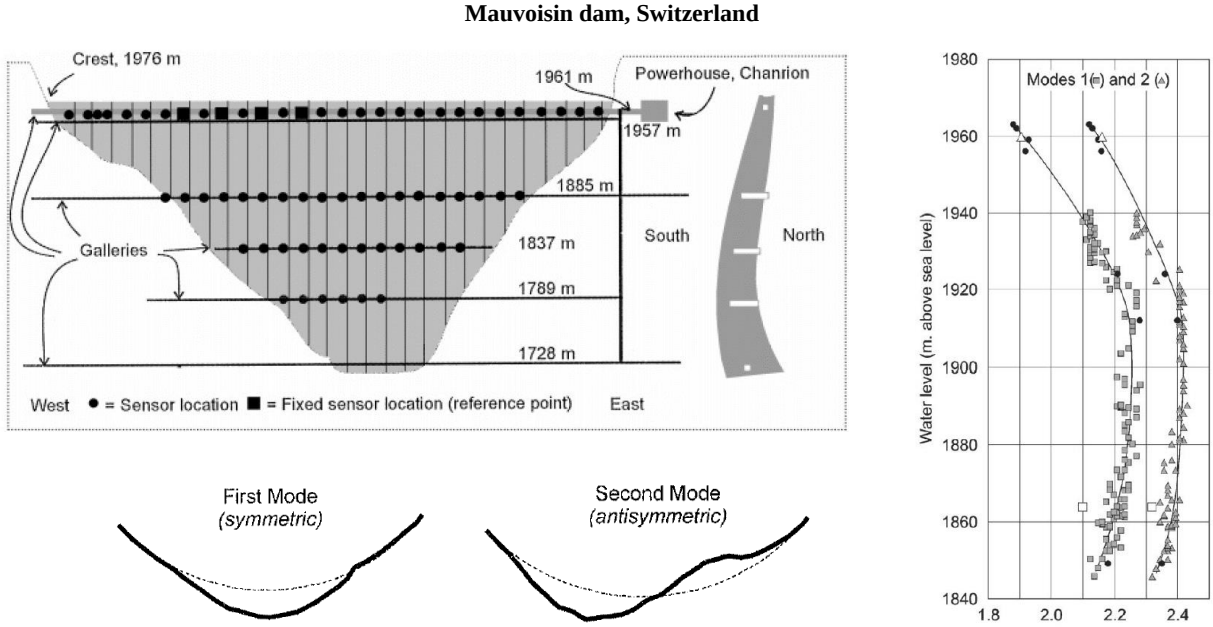

Fig. 2.49 Ambient vibration testing of Mauvoisin dam, Switzerland. Experimental setup with movable and reference measurement points (Darbre et al., 2000), and identified frequencies and mode shapes.

Ambient vibration tests were also performed on large concrete dams for calibrating and validating finite element models based on experimental data, including the cases of the 43 m high Hermitage gravity dam, in Jamaica (Brownjohn, 1990), the 59 m high Ruskin gravity dam, in Russia (Kemp, 1996; Kemp et al., 1995), and the 56 m high Claewern stone-faced concrete gravity dam, in Wales (Daniell & Taylor, 1999).

For the 122.5 m high Fei-Tsui arch dam, in Taiwan, the modal parameters obtained from ambient field measurements where consistent with those estimated using seismic response data (Loh & Wu, 1996). Later, during the winter of 1999 and autumn of 2000, several ambient vibration tests were conducted on two Iranian dams under different ambient and operational conditions, and the obtained frequencies and mode shapes were used to verify the results obtained using numerical models (Mivehchi et al., 2003; Mivehchi & Ahmadi, 2004).

In Portugal, in the scope of the research studies carried out in LNEC, three ambient vibration tests were conducted on Cabril arch dam (132 m high) between 2002 and 2003. To summarize, the estimated modal parameters were analysed and compared with results from finite element models of the dam-reservoir-foundation system, with a view to study the influence of the reservoir water level and of the contraction joints on the dynamic behaviour in normal operating conditions, to evaluate the influence of the intake tower on the modal identification of the dam, and to calibrate the numerical models (Mendes et al., 2004; Mendes & Oliveira, 2009; S. Oliveira et al., 2004; S. Oliveira, Rodrigues, Campos Costa, et al., 2003). Results obtained in these studies provided important insight on the dam dynamic performance and contributed to the development of the continuous dynamic monitoring system installed a few years later in Cabril dam (Mendes, 2010; Mendes et al., 2007; S. Oliveira et al., 2010, 2011).

In South Africa, ambient vibration survey tests were performed on two arch dams, Roode Elsberg dam (72 m high) and Kouga dam (69 m high), aiming to obtain the modal parameters of these dams to be used as reference values for posterior long-term dam safety monitoring (Bukenya, Moyo, & Oosthuizen, 2012; Bukenya, Moyo, Beushausen, et al., 2012; Moyo et al., 2013; Moyo & Oosthuizen, 2010). Therefore, six sets of ambient vibration tests were completed on Roode Eslberg dam, between December 2008 and April 2010, while two field tests were done on Kouga dam, in April 2010 and September 2010, under different seasonal and reservoir conditions. Results from the tests on Roode Eslberg dam motivated the installation of a continuous dynamic monitoring system for structural health monitoring, and hence an additional test was performed on September 2013 (Bukenya et al., 2014).

In Japan, it is worth mentioning the long-term ambient vibration tests performed on two large concrete dams. In Hitotsuse dam, a 130 m high arch dam, an automated system was installed for the ambient vibration campaign that was carried out for five years, from August 2006 to November 2011 (Fig. 2.50). After the first year, the estimated modal parameters were compared with those obtained in forced vibration tests conducted 40 years earlier, to confirm that they had not changed: thus, those results were assumed as reference to calibrate the numerical model of the dam and for future studies aiming at damage detection (Okuma et al., 2008). At the end of the long-term vibration monitoring campaign, it was confirmed that the seasonal changes of the natural frequencies were strongly influence by the reservoir water level and temperature changes (Okuma et al., 2012). With respect to Ohkura dam, an 82 m high double-arch structure, accelerations and temperatures were continuously recorded for over three years, between June 2010 and October 2013. The achieved results clearly showed that the evolution of the natural frequencies of the first two vibration modes clearly was influenced by the reservoir water level and thermal variations over time (Ueshima et al., 2017).

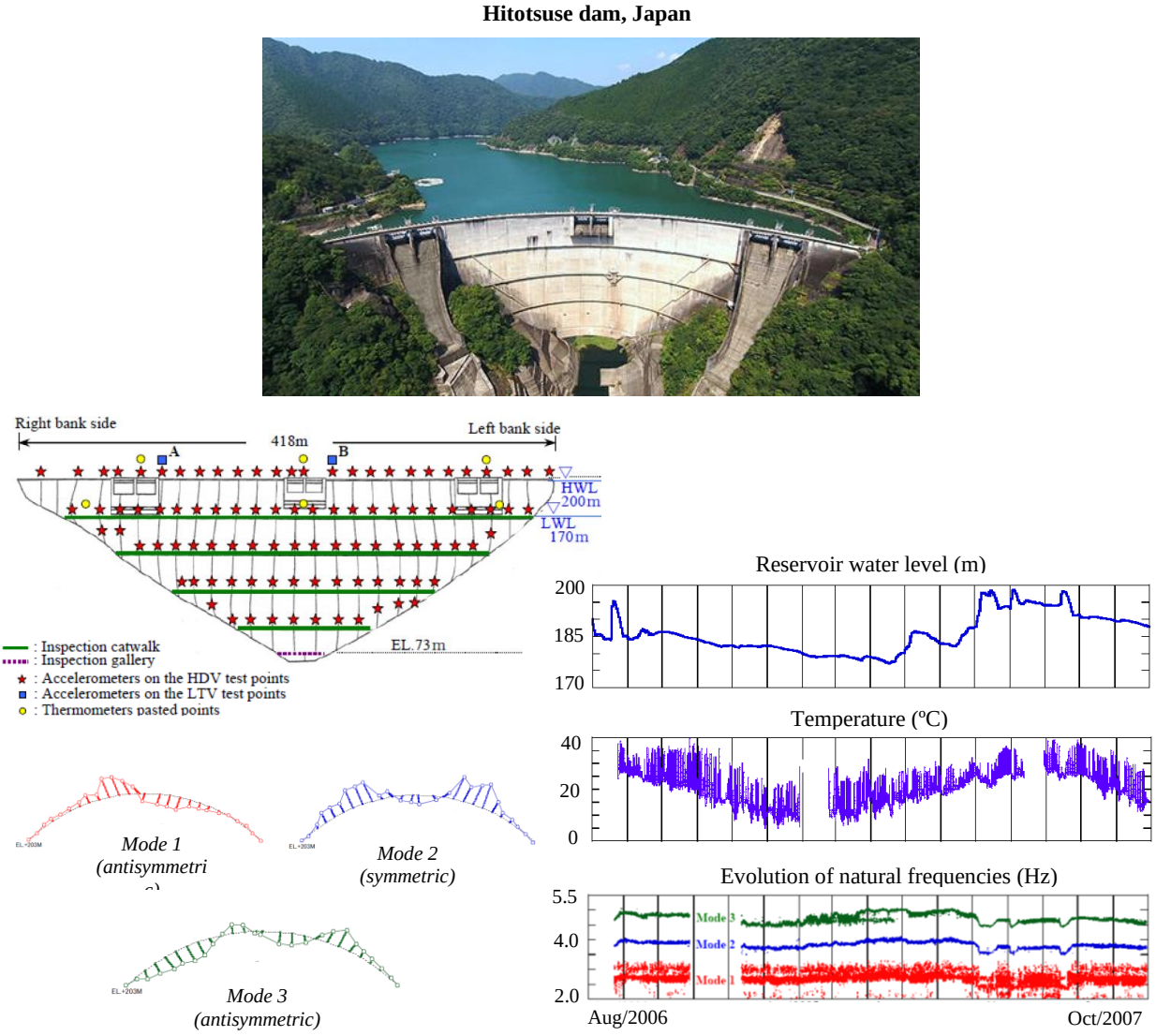

Fig. 2.50 Setup of the automated system installed in Hitotsuse dam for long-term ambient vibration testing. Water level and temperature variations and evolution of the first three vibration modes (Okuma et al., 2008, 2012).

There are also several other noteworthy studies conducted over the last decade based on ambient vibration results. For the case of the 201 m high Berke arch dam, in Turkey, a set of ambient vibration tests were performed in May 2009. The obtained experimental results were used to calibrate finite element model of the dam-reservoir-foundation system, used for seismic behaviour analysis (Sevim, Bayraktar, et al., 2011). Two ambient vibration tests were carried out on the 57 m high Punta Gennarta arch dam, in Italy, in two different operational conditions, namely at the beginning of autumn (October 2012) and at the end of Winter (March 2012), with the goal of evaluation the effects produced by different reservoir water levels on the identified dynamic properties. The estimated modal parameters were compared with results obtained using a finite element model of the dam-reservoir-foundation system (Calcina et al., 2014). For Karun IV dam, in Iran, the modal parameters are estimated based on ambient measurements and on seismic response records, which are compared with results from numerical models in order to assess the used modal identification method (Tarinejad et al., 2016). On the 62 m high Tajera arch dam, two ambient vibration

tests were conducted under different ambient and water level conditions. The estimated frequencies, mode shapes, and damping ratios were estimated using OMA techniques, and then used for updating the finite element modal of the dam-reservoir-foundation system, to be used for structural health monitoring or for seismic analysis (García-Palacios et al., 2016). A recent work mentions a long-term project for monitoring the natural frequencies of the 232 m high Chirkey arch dam (Fig. 2.51), based on vibration measurements carried out from January 2015 to December 2016. The identified modal parameters were compared with finite element results. This study allowed to evaluate the influence of the reservoir water level on the evolution of the natural frequencies, and motivated the proposal of a method for monitoring the structural health of the dam (Liseikin et al., 2020).

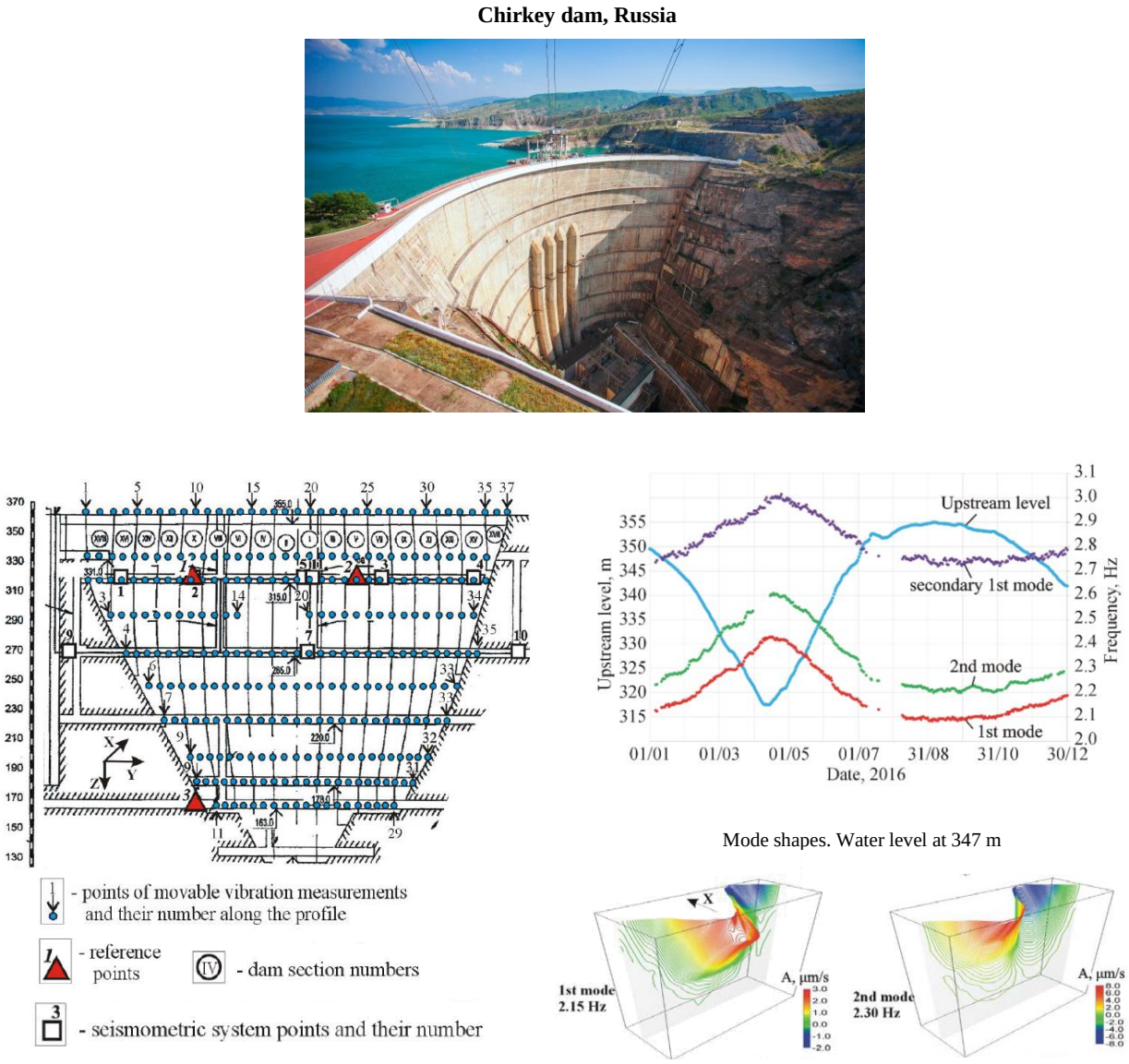

Fig. 2.51 Setup of the monitoring scheme installed in Chirkey dam for measuring ambient vibrations and seismic vibrations. Water level variation and evolution the natural frequencies during 2016, and mode shapes of the first two vibration modes (Liseikin et al., 2020).

2.5.4 CONTINUOUS DYNAMIC MONITORING SYSTEMS INSTALLED IN LARGE CONCRETE DAMS

In addition to data from seismic monitoring, the results achieved in ambient vibration tests, particularly the long-term campaigns that allowed the analysis of the dynamic behaviour of dams under different operating conditions, provided additional insight on the value of vibration-based results for studying the dynamic response of dam-reservoir-foundation systems, considering water level and thermal variations, and possibly for detecting structural changes in the dam due to ageing or deterioration phenomena. Therefore, based on the knowledge acquired over decades of experimental and numerical studies, and taking into consideration the increasing demands regarding dam surveillance and safety control assessment (ICOLD, 2018), automated continuous dynamic monitoring systems started to be developed and installed in several large concrete dams worldwide, including new dams and older dams, most built decades ago and suffering from deterioration problems, aiming to evaluate their performance in normal operating conditions and during seismic events.

The first reported case occurred in Portugal, in 2008, with the installation of a pioneer system in Cabril dam (Fig. 2.52), a 132 m high double curvature arch dam in operation since 1954, for seismic behaviour monitoring and structural health monitoring over time (Mendes, 2010; S. Oliveira, 2002). This dynamic monitoring system was designed in LNEC, based on data gathered from previous vibration tests and numerical calculations, aiming at measuring vibrations under ambient/operation excitations and during seismic events. The implemented monitoring scheme includes sixteen uniaxial accelerometers, positioned along the two upper galleries of the dam, and three triaxial accelerometers, two installed near the dam-rock interface at both banks, and another at the top of the central section (measuring devices from Kinemetrics). This dam is one of the case studies of this thesis (further details are provided in chapter 5.2). Several studies using both monitoring data and numerical results have been performed over the past decade for Cabril dam, to characterize the dynamic properties of the dam-reservoir-foundation system and their evolution over time, to assess structural health, and to analyse the seismic response (Alegre et al., 2021; Alegre, Carvalho, et al., 2019; Alegre, Robbe, et al., 2020; S. Oliveira et al., 2010, 2011, 2012; S. Oliveira, Silvestre, Espada, et al., 2014; S. Oliveira & Alegre, 2020, 2018, 2019b).

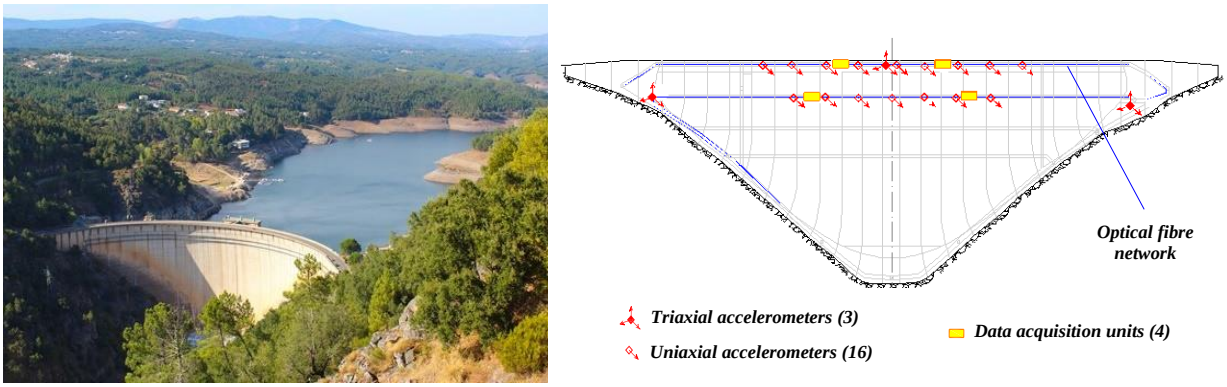

Fig. 2.52 Cabril dam, Portugal. Downstream view and the pioneer continuous dynamic monitoring system, in operating since 2008 (Mendes, 2010).

Later, in 2010, a continuous dynamic monitoring system was installed in Cahora Bassa dam (Fig. 2.53), a 170 m high thin double curvature arch dam that started operating in 1974, in Mozambique. The goal of this project was to continuously measure ambient and seismic vibrations in order to monitor dam performance in normal operating conditions and during earthquake events (E. Carvalho et al., 2014; E. Carvalho & Matsinhe, 2014). The system includes ten uniaxial accelerometers from Kinemetrics, deployed along the upper gallery of the dam, and three triaxial accelerometers, one at the downstream base and two in the rock mass, in both banks. Examples of studies on the dynamic behaviour of Cahora Bassa dam can be found in (Alegre et al., 2021; Alegre, Carvalho, et al., 2019; Alegre, Oliveira, et al., 2020). This dam is the other case study of this work (more details are given in chapter 5.3).

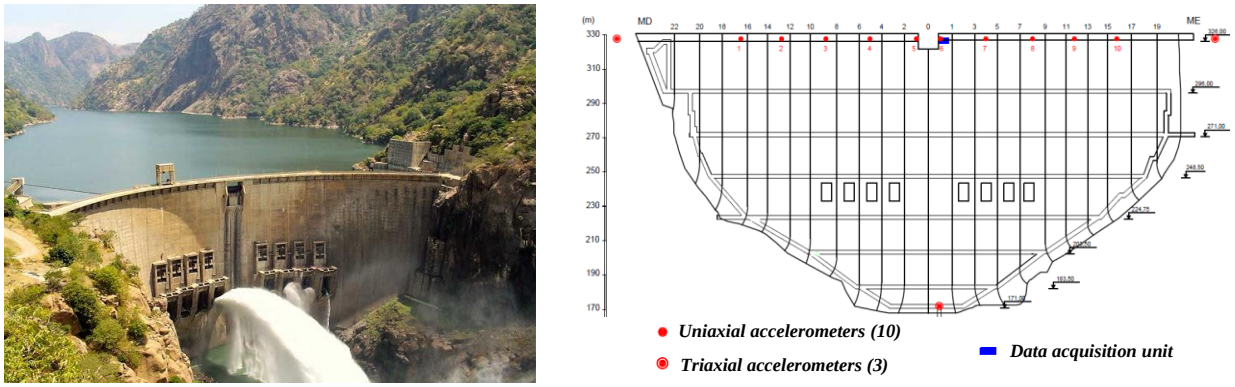

Fig. 2.53 Cahora Bassa dam, Mozambique. Downstream view and continuous dynamic monitoring system, installed in 2010 (Alegre, Carvalho, et al., 2019).

Roode Elsberg dam, in South Africa, is a double curvature arch dam with a maximum height of 72 m, which entered in operation over 50 years ago. After a series of ambient vibration tests, conducted between 2008 and 2013, a simple permanent ambient vibration monitoring system was installed in the dam (Fig. 2.54), in December 2013, in order to control the evolution of the dynamic properties of the dam over time, under different environmental conditions (Bukenya, 2020; Bukenya et al., 2014; Bukenya & Moyo, 2017). The monitoring scheme consists of three triaxial accelerometers from GeoSig, placed on top of the dam crest. Their location was determined based on results from the previous ambient vibration campaigns.

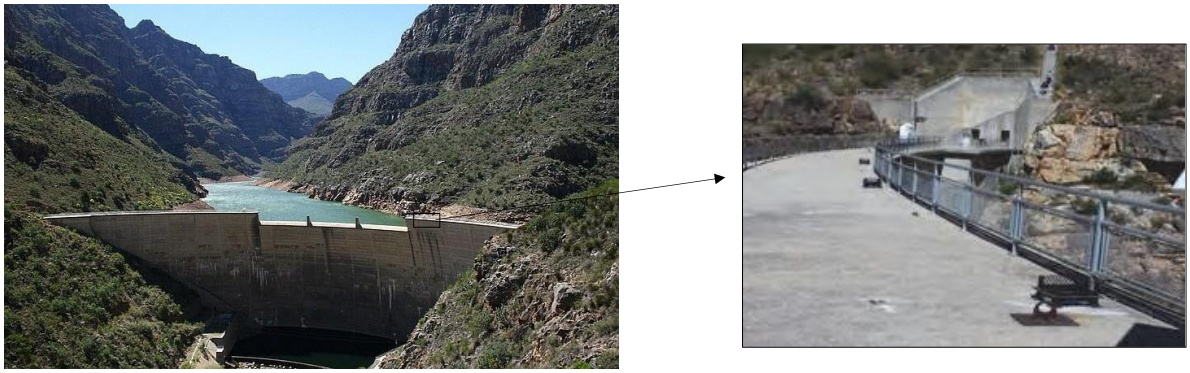

Fig. 2.54 Roode Elsberg dam, South Africa. Downstream view and location of the installed accelerometers in December 2013 (Bukenya, 2020).

The investment in long-term dynamic monitoring of large concrete dams continued in Portugal a few years later with the installation of continuous monitoring systems in two recently constructed dams. Both monitoring projects were developed aiming to determine the dynamic properties of the dams and assess their evolution over time, to study seismic behaviour, and to characterize the seismic action.

Baixo-Sabor dam is a 123 m high double curvature arch dam, located near the Vilariça fault, in a zone of low to moderate seismicity. The dynamic monitoring system (Fig. 2.55) was developed for an accurate long-term continuous characterization of the dam behaviour, and it has been in operation since the first filling of the reservoir, in December 2015 (Gomes et al., 2018; S. Pereira, 2019; S. Pereira et al., 2018, 2017). The monitoring setup is comprised of twenty uniaxial accelerometers, installed along three galleries of the dam. Also, as part of a seismic monitoring project for the Baixo Sabor Hydropower Scheme, there are six triaxial accelerometers installed in the dam body, one at the downstream base, and other 3 located around the reservoir. All equipment was provided by GeoSIG.

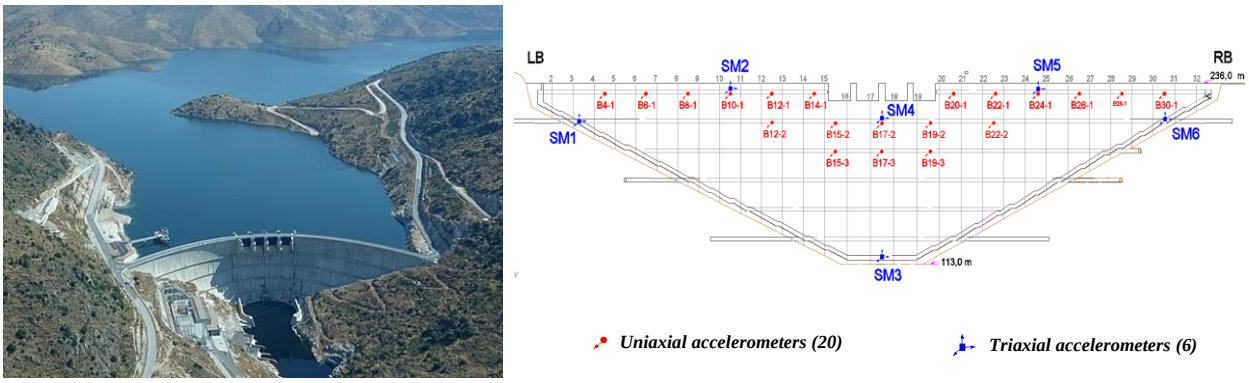

Fig. 2.55 Baixo Sabor dam, Portugal. Downstream view and continuous dynamic monitoring system, in operation since the first filling of the reservoir [adapted from (Gomes et al., 2018)].

Foz Tua dam is also a double-curvature arch dam, with a maximum height of 108 m, whose first reservoir filling took place between June 2016 and June 2017. A complete dynamic monitoring system (Fig. 2.56) was installed in the dam to measure ambient/operational vibrations and seismic vibrations (S. Pereira, Magalhães, Gomes, et al., 2021; Silva Matos, Tavares de Castro, Gomes, & Figueiredo, 2019; Silva Matos, Tavares de Castro, Gomes, Faria, et al., 2019). The system, in full operation since the beginning of 2019, is composed of 12 uniaxial accelerometers and 6 triaxial accelerometers, positioned along the two upper galleries of the dam, and 1 triaxial accelerometer located at the drainage gallery of the dam, and it also includes 4 remote stations deployed in the surrounding region.

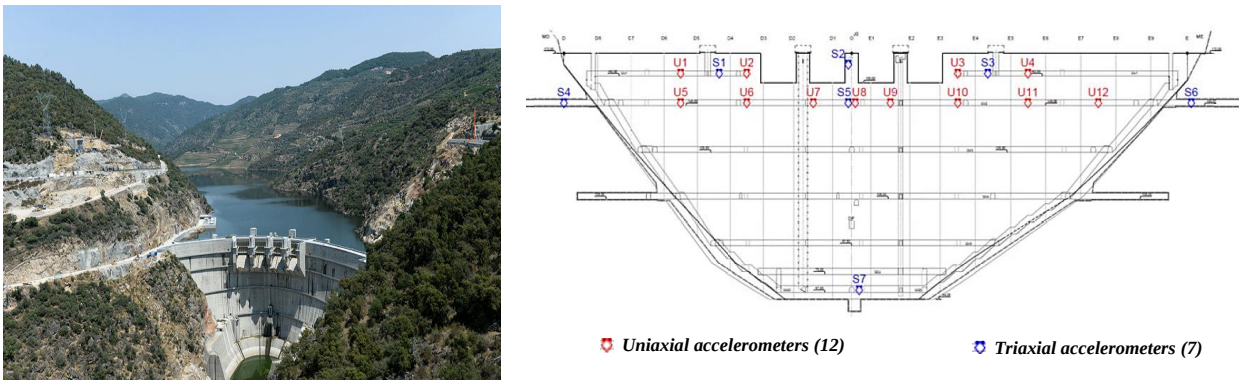

Fig. 2.56 Foz Tua dam, Portugal. Downstream view and continuous dynamic monitoring system, in operation since 2019 (Silva Matos, Tavares de Castro, Gomes, Faria, et al., 2019).

In this scope, reference should be made to other cases of large concrete dams around the world which were instrumented with equipment for recording seismic motions and ambient dynamic vibrations, as seen in (GeoSIG, 2021). For example, on Enguri arch dam (271.5 m high), in operation since 1987 in Georgia, ten uniaxial accelerometers were installed, in addition to the ten strong motion recorders that had been previously implemented in 2000 (Fig. 2.57).

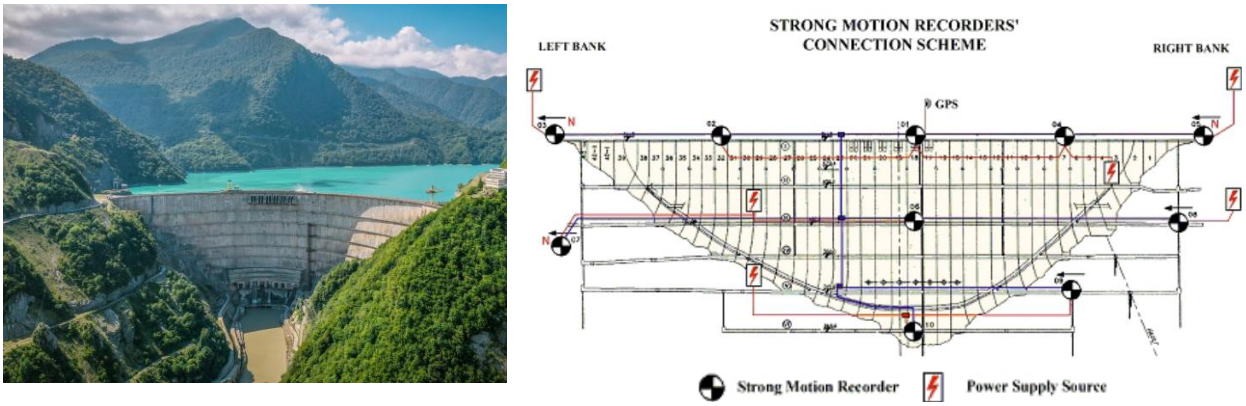

Fig. 2.57 Enguri dam, Georgia. Downstream view and scheme of seismic monitoring system (GeoSIG, 2009b).

As for the case of Beli Iskar gravity dam (Fig. 2.58a), a 51 m high and 533 m long structure put into service in 1948 in Bulgaria, the monitoring system includes three triaxial accelerometers and three strong-motion recorders. Another example is the 191 m high and 909 m long Xiangjiaba gravity dam (Fig. 2.58b), in operation since 2012 on the Yangtze River, In China, which has been instrumented with eighteen earthquake recorders and eighteen triaxial accelerometers.

a) **b)**

Fig. 2.58 Other examples of dams currently under continuous vibrations monitoring: a) Beli Iskar dam, Bulgaria, and b) Xiangjiaba dam, China (GeoSIG, 2021).

It is also relevant to mention the DEMS project (Dam Earthquake Monitoring System), undertaken by the Korean Water Resources Corporation in 2006, aiming to operate and manage a network of recording devices for a safe management of dams (Fig. 2.59). In the scope of this project, measuring devices for recording mainly seismic motions but also other ambient vibrations were installed in 23 concrete dams (GeoSIG, 2021).

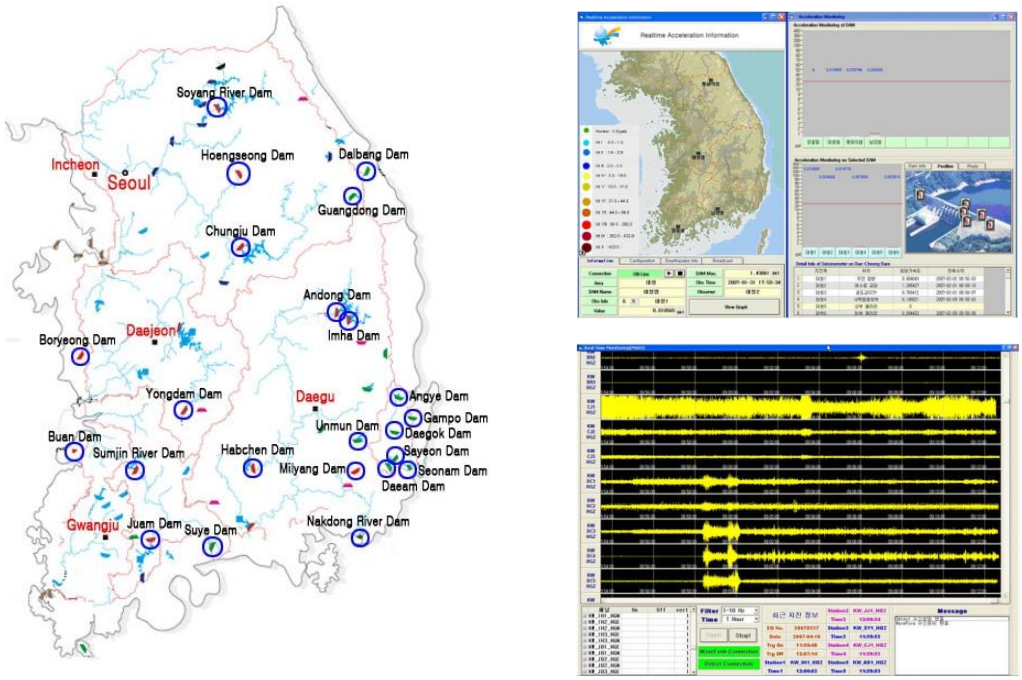

Fig. 2.59 Monitoring network of 23 dams in South Korea as part of the DEMS project (GeoSIG, 2021).

2.6 FINAL CONSIDERATIONS

The current chapter was dedicated to large concrete dams and to their dynamic behaviour, with focus on dam safety, particularly in what concerns the structural safety control during the operation phase and the seismic safety assessment. Also, a complete overview was presented on modelling the dynamic behaviour of dam-reservoir-foundation systems and on monitoring vibrations in large concrete dams, supported by references to several studies of interest.

Large concrete dams are civil engineering structures that play a key role in the management of fresh-water resources, and they are generally associated with high potential risks. Furthermore, dams are special structures that are part of a complex dam-reservoir-foundation system, whose dynamic properties can be affected, for example, by reservoir water level or temperature variations, ageing and concrete deterioration phenomena, and joint movements.

Therefore, aiming to have a comprehensive understanding on the dynamic behaviour of large concrete dams, as well as to ensure the best operational and safety conditions for recent dams and for dams built several decades ago, it is fundamental a) to analyse their dynamic performance in normal operating conditions and during seismic events, for structural health monitoring and seismic monitoring, and b) to (re)evaluate their performance under strong earthquake ground motion, according to modern seismic design and performance criteria, for seismic safety assessment.

In this context, it is worth stressing the need to continue investing in research projects that contribute to the advancement of knowledge in dam engineering, particularly in terms of numerical modelling the dynamic behaviour of dam-reservoir-foundation systems and of long-term continuous vibrations monitoring of large concrete dams.

With respect to numerical modelling, advanced finite element numerical models should be developed to enable a proper simulation of the dynamic response of dam-reservoir-foundation systems for the scenarios that can occur over the lifetime of dams, involving variations of the static and dynamic loads, changes in dynamic properties to reservoir level or thermal variations, and perhaps structural alterations due to deterioration processes and/or joint movements. Furthermore, there is also room for improvement at the level of the finite element-based formulations commonly used for modal analysis and seismic response analysis of dam-reservoir-foundation systems, which are in essence solid-fluid coupled problems, a subject that is covered in detail in Chapter 3.

Regarding monitoring vibrations on dams, it is of paramount importance to continue installing automated continuous dynamic monitoring systems in large concrete dams, to enable a permanent long-term evaluation of their performance, particularly for older dams, possibly suffering from deterioration problems, and/or dams located in zones of high seismicity. In addition, although the companies that develop and supply the equipment for these types of systems have started to take an interest in the software component, there is still a clear need to complement monitoring systems by implementing appropriate software tools, adapted and optimized to each dam, for management and analysis of monitoring data, with

a view to enhance their operation and enable the retrieval of valuable information. This type of software is presented in chapter 4.

Knowing that structural safety control should be based on the analysis and interpretation of the measured behaviour and on its comparison with behaviour prediction models, it is also regarded important to work towards the implementation of methodologies and graphical tools that allow for a simple and intuitive comparison between experimental and numerical results (as shown in the application studies of Chapter 5). This will enable to get of useful information for owners, engineers, or other entities responsible for dam safety, in order to support informed management and help make better and timely decisions. Bearing in mind the intent of integrating numerical models in the software component for continuous dynamic monitoring systems, finite element programs should be not only reliable but also efficient, for an accurate and quick comparison with the observed behaviour.

Finally, both the seismic design of new dams and for (re)evaluation of the seismic safety of older dams (designed according to outdated seismic design criteria and analysis methods), adequate methods for seismic safety assessment should be implemented, preferably based on efficient analysis procedures, using advanced finite element models, and considering appropriate criteria, enabling to obtain reliable results and to appropriately evaluate the performance of dams (see application studies in Chapter 5).

CHAPTER 3

MODELLING THE DYNAMIC BEHAVIOUR OF DAM-RESERVOIR-FOUNDATION SYSTEMS

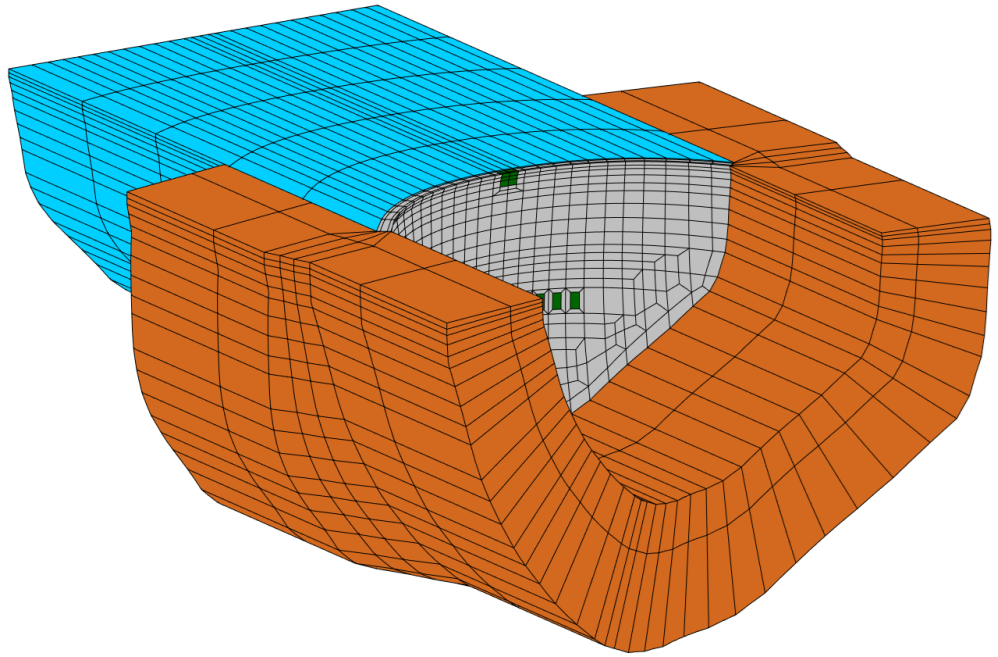

3. MODELLING THE DYNAMIC BEHAVIOUR OF DAM-RESERVOIR-FOUNDATION SYSTEMS

3.1 INTRODUCTION

The development of advanced numerical models is of great importance to study the dynamic behaviour of large concrete dams and to support the safety control in the different stages of their lifetime, namely when used in combination with monitoring data. To this day, this subject continues to represent one of the greatest challenges for dam engineers, given that large concrete dams are structures with complex geometry, including different types of joints and discontinuities, and considering that their behaviour is strongly conditioned by the interaction with the reservoir and the foundation (Câmara, 1989; Chopra, 2012; Fenves et al., 1992; Pedro & Câmara, 1986), since dams are part of a global dam-reservoir-foundation system. Therefore, there is an obvious need to continue the research work in this field and to keep investing in the development of reliable models for modal analysis and for linear or non-linear seismic analysis of dam-reservoir-foundation systems, aiming to properly simulate the dynamic behaviour of large concrete dams.

A coupled model is adopted in this work to simulate the dynamic behaviour of the dam-reservoir-foundation system, based on a finite element formulation in displacements (dam and foundation) and hydrodynamic pressures (reservoir) and considers the dam-water dynamic interaction and the propagation of pressure waves in the reservoir. The main goal of the current chapter is to present the developed calculation methods, which are based on a new approach to solve the coupled problem, namely for modal analysis and for linear and non-linear seismic analysis. The coupled model and the numerical methods are implemented in *DamDySSA*, a 3D finite element program for dynamic analysis of concrete dams.

Subchapter 3.2 presents a state-of-the-art review, by describing the types of models currently used for considering dam-water dynamic interaction and for foundation behaviour and seismic input modelling. The available numerical methods for modal analysis and for calculating seismic response are addressed. After that, with a view to present the mathematical notation and the basis for the proposed finite element formulations, section 3.3 is dedicated to the fundamental equations of Solids Mechanics and their application to structural analysis and dynamic behaviour analysis, while section 3.4 addresses the fundamental concepts and properties associated with joint behaviour. Then, subchapter 3.5 describes the coupled problem and the corresponding finite element formulation in displacements and pressures that governs the dynamic behaviour of the dam-reservoir-foundation system. With respect to the calculation methods developed in this work, section 3.6 presents the state-space formulation for coupled complex modal analysis, considering generalized damping, section 3.7 describes the coupled time-stepping procedure linear seismic response calculation, and section 3.8 covers the proposed method for non-linear seismic analysis and describes the constitutive models used for simulating joint movements and concrete damage (under tension and compression). After that, section 3.9 presents the program *DamDySSA*, including the algorithm and graphical user interface, as well as the main results achieved in several tests for validation of the developed model. Section 3.10 describes the module developed for automatic introduction of joints in finite element meshes of dams, incorporated in the program *Dam3DMesh*.

3.2 STATE-OF-THE-ART

Significant research was carried out on the numerical modelling of the dynamic behaviour of concrete dam-reservoir-foundation systems (Fig. 3.1) over the decades, leading to the development of various models and formulations based on the Finite Element Method (Zienkiewicz et al., 2013), and to a considerable number of relevant numerical studies (recall 2.5.1). A state-of-the-art review is presented here.

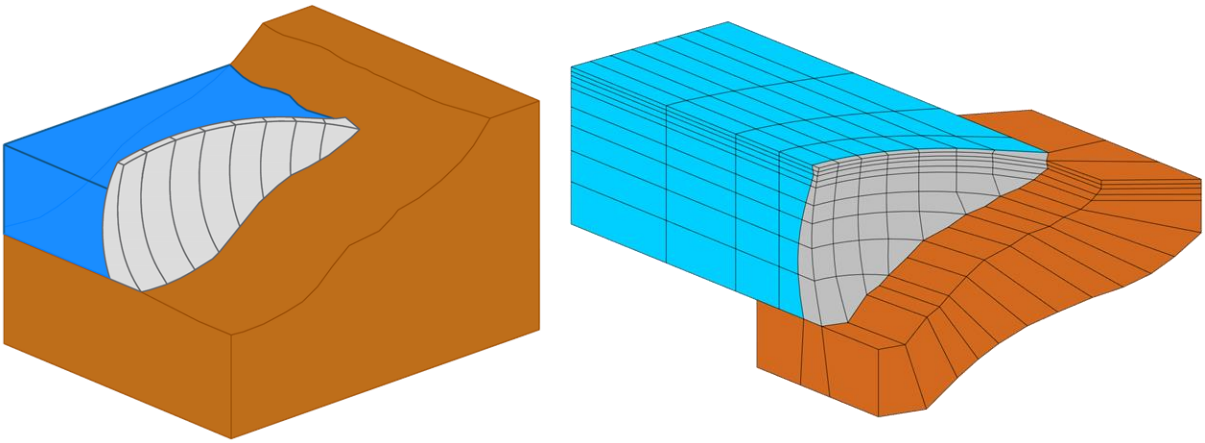

Fig. 3.1 Dam-reservoir-foundation system and example of 3D finite element model with discretized reservoir.

For simulating the dam-reservoir dynamic interaction and the hydrodynamic effects there are essentially two types of models: added mass models and coupled models (Fig. 3.2).

The classic added water mass models use displacement-based formulations for the dam and foundation (solid domain) and consider the reservoir mass effect by calculating added masses equivalent to the hydrodynamic pressures on the dam-reservoir interface, based on the pioneer solution proposed by Westergaard (1933). Although simple and efficient, this type of model neglects water compressibility and hydrodynamic effects, which can influence dam behaviour (Chopra & Hall, 1982; Fok & Chopra, 1986b; Goldgruber et al., 2013; Robbe et al., 2017; Tiliouine & Seghir, 1998). Also, since Westergaard's solution was prescribed for rigid gravity dams, the added water mass effect is overestimated on curved and flexible dams (Alegre et al., 2017), and thus the use of reduction factors is required for arch dams (H. Chen, 2014).

Coupled models are based on finite element formulations for the dam and foundation (solid) and reservoir (fluid) domains (Zienkiewicz & Bettess, 1978). In this case, two approaches can be adopted. The first approach consists in using a displacement-based formulation for both the solid and fluid, treating the fluid as an elastic solid with negligible shear modulus (Belytschko, 1977, 1980; Hamdi et al., 1978; Zienkiewicz & Bettess, 1978). The nodal displacements are the degrees of freedom of the entire dam-reservoir-foundation system, and the water is assumed as an elastic solid with negligible shear modulus. Although simpler in principle, given that the solid and the fluid are treated in the same way, this type of approach results in problems of larger dimensions (reduced computational efficiency) and may lead to numerical instabilities. As for the second approach, the coupled model is formulated in displacements for the solid

domain and in hydrodynamic pressures or velocity potentials for the reservoir domain (Fok et al., 1986; Hall & Chopra, 1980; Zienkiewicz & Bettess, 1978), and proper boundary conditions are adopted to simulate the dam-reservoir motion coupling, the free surface null pressure condition, the propagation of pressure waves with radiation at the far-end of the reservoir, and the reservoir bottom absorption (Bouaanani & Lu, 2009; Lokke & Chopra, 2018; Zienkiewicz et al., 2013). This method is more complex, as it requires the definition of specific interfaces and equilibrium conditions, but it saves calculation time and computational storage particularly for large scale problems. Coupled models with either pressure- or velocity potential-based formulations have been widely used and successfully applied in several studies. A coupled model in displacements and pressures is considered in the present work.

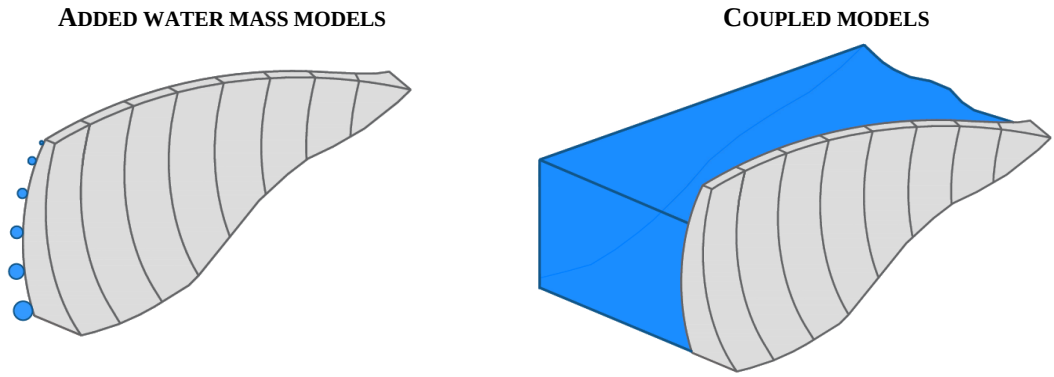

Fig. 3.2 Models used for simulating water-structure dynamic interaction: added water mass and coupled models.

Regarding the foundation behaviour, there are several types of approaches, considering either a massless foundation or a foundation with mass (Fig. 3.3).

The simplest approach is based on the use of a massless foundation model (Clough, 1980), assuming that the dam is supported by a deformable foundation block with a rigid boundary at the base and disregarding the effects of wave propagation through the foundation and the radiation damping (only the foundation flexibility is considered). For this type of model, the substructure method can be used to calculate the foundation block as an elastic and massless substructure, considering an equivalent condensed stiffness matrix at the dam-rock interface (Fenves et al., 1989; Fok et al., 1986; Fok & Chopra, 1986a). The seismic input can be applied directly at the dam base, either as uniform ground motion or spatial variating ground motion (J.-T. Wang & Chopra, 2010), or by generating specific free-field motions at the dam-foundation interface (Alves, 2004; Alves & Hall, 2006).

As an alternative, there are energy dissipating foundation models that considering the foundation mass. These models simulate the wave propagation and radiation effects in the rock mass, e.g., using viscous-spring boundaries (Lysmer & Kuhlemeyer, 1969; C. Zhang et al., 2009) or transmitting boundaries (Liao et al., 1984) in the truncated foundation limits, or by applying a finite-boundary element method (Chopra & Tan, 1992; Dominguez & Maeso, 1992). The seismic input modelling can be achieved using different methods. In the incident wave method, the seismic input is applied at the foundation base after being

determined by a deconvolution analysis (Reimer, 1973) to a free-field motion; then, the spatial varying ground motion histories at the dam-foundation interface are determined by compression and shear waves vertically propagating from the foundation base (Lokke & Chopra, 2018; C. Zhang et al., 2009). As for the free-field approach, the free-field motions can be applied directly at the dam base (Clough & Penzien, 2003), if available, or by employing an equivalent force scheme to generate the ground motion at the dam-foundation surface (J.-T. Wang et al., 2013).

Several studies have shown that neglecting foundation inertia and radiation damping can lead to an overestimation of stresses in the dam body (D.-H. Chen et al., 2012; Fok & Chopra, 1986b; Hariri-Ardebili & Mirzabozorg, 2013; Mirzabozorg et al., 2012; C. Zhang et al., 2009) if no additional damping source is considered. However, when using massless foundation models, a damping matrix proportional to the foundation stiffness matrix can be introduced at the dam-rock interface, as considered in this work. Furthermore, the massless approach is simpler and more efficient, saving storage memory and calculation time. It is also relevant to mention that the consideration of a spatially varying seismic input can affect the structural response of dams, which is more noticeable for higher intensity seismic excitations (Chopra & Wang, 2010; Mirzabozorg et al., 2013).

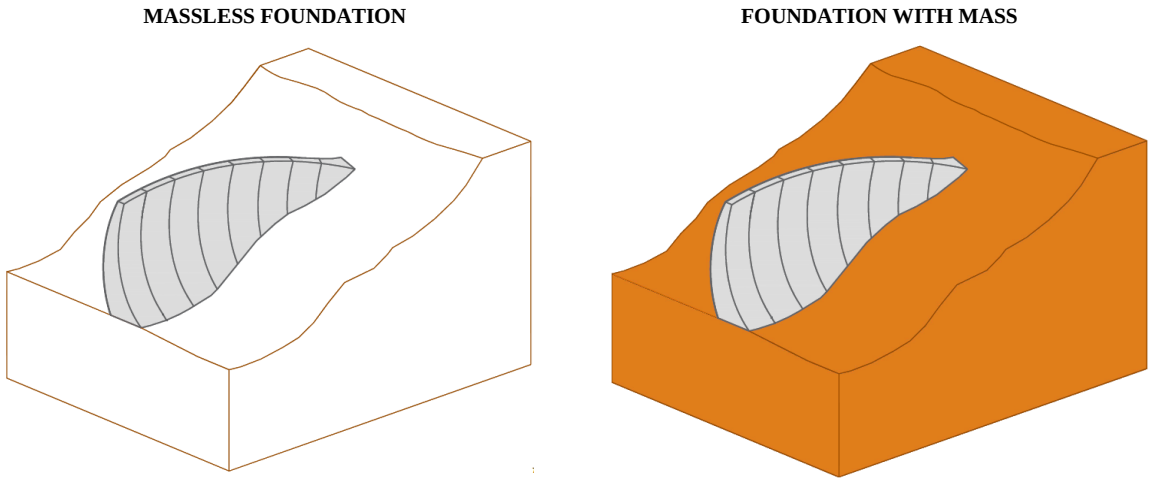

Fig. 3.3 Models used for simulating foundation behaviour: massless foundation and foundation with mass.

The studies on the dynamic behaviour of dam-reservoir-foundation systems may involve modal analysis (Fig. 3.4), to compute the main modal parameters (natural frequencies, mode shapes, and modal damping), and seismic response analysis (Fig. 3.5), considering either linear behaviour or non-linear behaviour (joint movements and concrete damage), in order to calculate the global system response (displacements and stresses in the dam body and hydrodynamic pressures in the reservoir).

For modal analysis, it is necessary to solve the eigenproblem of the discretized dam-reservoir-foundation system. For problems using the classic added water mass models, assuming null or proportional damping the eigenproblem is symmetric (Zienkiewicz & Cheung, 1967) and the free vibration solution can be obtained by solving a standard eigenproblem with real eigenvalues and eigenvectors (Clough & Penzien,

2003; Zienkiewicz et al., 2013) - stationary modes are determined (Cahghey & O'Kelly, 1965). If the hypothesis of generalized (non-proportional) damping is assumed, a state-space formulation written in terms of the displacements and velocities should be used (Mendes, 2010; S. Oliveira et al., 2011; S. Oliveira, Silvestre, Espada, et al., 2014) to solve an eigenproblem with complex eigenvalues and eigenvectors, which enables to obtain non-stationary modal configurations (Veletsos & Ventura, 1986).

As for coupled models the problem becomes non-symmetric due to the fluid-structure coupling term (Zienkiewicz & Bettess, 1978) and hence the previous methods cannot be directly applied (Zienkiewicz et al., 2013). In this case, the traditional approach that is usually adopted involves the determination of an equivalent symmetric form of the eigenproblem for the dam-reservoir-foundation system (without damping), from which real eigenvalues and eigenvectors are then calculated (Daniel, 1980; Felippa, 1988; Lotfi, 2005; Ohayon, 1979; Ohayon & Valid, 1984; Sani & Lotfi, 2010; Zienkiewicz et al., 2013). As an alternative, a new state-space approach is proposed in this thesis in order to perform the coupled modal analysis of the entire system, considering generalized damping, and thus solve an eigenproblem with complex eigenvalues and eigenvectors.

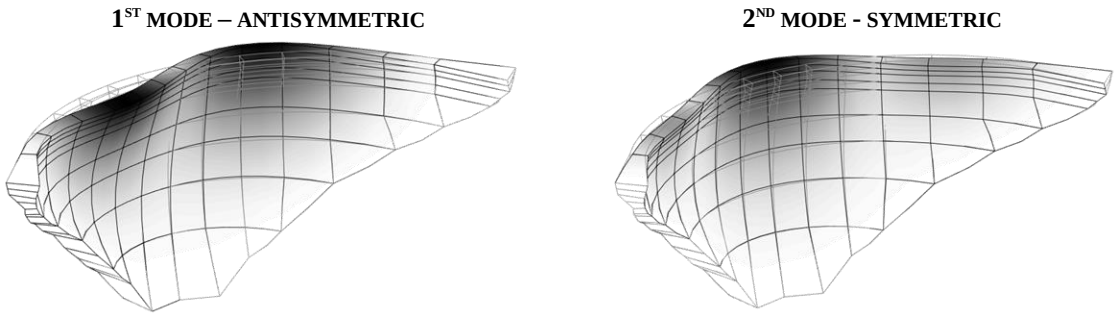

Fig. 3.4 Modal configurations of a large arch dam. First (antisymmetric) and second (symmetric) vibration modes.

Regarding the linear seismic analysis dam-reservoir-foundation systems, in studies using added water mass models the solution over time can be obtained assuming two different approaches (Chopra, 2017; Clough & Penzien, 2003; Zienkiewicz et al., 2013), namely a) based on the modal decomposition method, by calculating the response as a linear combination of the modes - good results can be achieved with a reduced number of modes, even for problems with many degrees of freedom, or b) considering time-stepping methods for numerical integration in time domain, e.g. based on the based on the Euler (Euler, 1768), Newmark (Newmark, 1959) or Wilson methods (Wilson, 1968) or on other single step algorithms (Zienkiewicz et al., 1984).

For seismic analysis using coupled models, the problem is non-symmetric and thus the modal decomposition method is not computationally viable for large problems. Therefore, time-stepping procedures are required to calculate the dynamic solution for the coupled system. Similarly to modal analysis, the solutions that are usually adopted are based on the initial separation of the solid and fluid equations in order to obtain an equivalent symmetric form and hence solve the problem (Zienkiewicz et al., 2013; Zienkiewicz & Taylor, 1985). As such, it is proposed in this thesis an efficient time-stepping

procedure, based on the Newmark method, to directly solve the coupled dynamic equation of the entire system with generalized damping.

For modelling non-linear seismic behaviour, numerical time-stepping procedures should be combined with iterative methods, developed to solve non-linear problems (Clough & Penzien, 2003; Zienkiewicz et al., 2014). Examples of these methods include the Newton-Raphson method, which solves the problem as a succession of changing linear systems, or the stress-transfer method (also known as modified Newton-Raphson), considering the use of the elastic stiffness matrix and the application of artificial forces equivalent to the unbalanced stresses arising in the dam due to joint and/or material non-linear behaviour.

With regard to the seismic behaviour of arch dams (the type considered for the application studies of this work), for low intensity earthquakes, commonly measured and inducing low amplitude vibrations (Alegre, Carvalho, et al., 2019; Chopra & Wang, 2010; Proulx et al., 2004; Proulx & Darbre, 2008; J.-T. Wang & Chopra, 2010), the numerical simulations can be conducted assuming linear-elastic behaviour for concrete and that the joints remain closed. However, under high intensity earthquakes considerable deformations can occur, leading to the contraction joints opening, and the subsequent stress redistributions (H. Chen, 1994; Clough, 1980; Fenves et al., 1992; Hall, 1998; Lau et al., 1998; Niwa & Clough, 1982), and simultaneously resulting in the appearance of high tensile and compressive stresses, which may cause damage in concrete (Cervera et al., 1995; Espandar & Lotfi, 2003; Faria et al., 1998; Valliappan et al., 1999). As such, proper models are required for non-linear seismic analysis of arch dams, ideally considering the effects due to joint movements and tensile and compressive concrete damage. Therefore, this work proposes a complete method for non-linear seismic analysis that combines a time-stepping procedure with the stress-transfer method, using an isotropic constitutive damage model for concrete, with two independent damage variables for tension and compression, and a non-linear joint model based on the Mohr-Coulomb criterion, to simulate opening/closing and sliding movements.

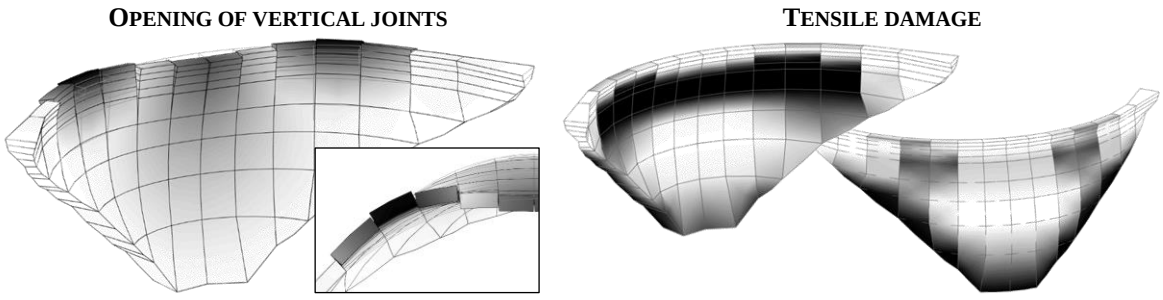

Fig. 3.5 Non-linear seismic response of an arch dam. Deformed shape (vertical joint openings) and tensile damage.

There are several finite element programs used in current practice for linear and non-linear dynamic analysis of concrete dams, based on the models and methods described above, including EACD-3D (J.-T. Wang & Chopra, 2008), ANSYS (ANSYS Inc., 2020), ABAQUS (Dassault Systèmes Simulia Corp., 2020), ADINA (ADINA R & D Inc., 2020), DIANA (DIANA FEA BV., 2020), and the open-source software Code_Aster (http://www.code-aster.org); mention should also be made to the discrete element program 3DEC (Itasca

Consulting Group Inc., 2020). Nevertheless, one of the main goals of this work is not only the development of calculation methods for modal analysis and linear/non-linear seismic analysis, but also the implementation in a finite element program for dynamic analysis of concrete dams (*DamDySSA*). The computational implementation of these methods can yield several benefits, since it allows a deeper knowledge and control over all variables and algorithms, which can be constantly updated and optimized. Also, graphical outputs can be adapted to the goals of the intended studies, e.g., to perform adequate comparisons with dynamic monitoring results, for dynamic behaviour analysis and for supporting structural health control, or to carry out seismic performance and safety evaluations. The proposed formulations and the referred program are presented in this chapter.

3.3 FUNDAMENTAL EQUATIONS OF SOLID MECHANICS. DYNAMIC BEHAVIOUR

In any structural analysis problem, the main goal is to characterize the behaviour of the structure by calculating the displacements, stresses, and strains under a set of applied forces, knowing its geometry, material properties and boundary conditions. Under dynamic loads, the structural behaviour must be known for each time instant. This section aims to present the mathematical notation and the bases for the formulations described in the following sections.

Considering a generic three-dimensional structure, e.g., a concrete arch dam, under dynamic excitation, the main unknown is the displacements vector, to be determined in every point *P* of the structure volume at each time instant *t*, which is defined as

$$\underset{\sim}{u} = \underset{\sim}{u}(x_1, x_2, x_3, t) = \begin{bmatrix} u_1(x_1, x_2, x_3, t) \\ u_2(x_1, x_2, x_3, t) \\ u_3(x_1, x_2, x_3, t) \end{bmatrix} \tag{3.1}$$

The corresponding stress and strain states at that same point can be described by the stress $\underline{\sigma}$ and strain $\underline{\varepsilon}$ second order tensors. Their components relatively to the global axis can be presented in 3×3 symmetric matrices, or be conveniently gathered by 6×1 vectors using Voigt notation, which is useful for computational programming, as

$$\underset{\sim}{\sigma} = \begin{bmatrix} \sigma_{11} \\ \sigma_{22} \\ \sigma_{33} \\ \sigma_{23} \\ \sigma_{31} \\ \sigma_{12} \end{bmatrix} \quad ; \quad \underset{\sim}{\varepsilon} = \begin{bmatrix} \varepsilon_{11} \\ \varepsilon_{22} \\ \varepsilon_{33} \\ 2\varepsilon_{23} \\ 2\varepsilon_{31} \\ 2\varepsilon_{12} \end{bmatrix} \tag{3.2}$$

Aiming to solve the dynamic structural problem, the fundamental equations of Solids Mechanics can be used to establish the relations between displacements, stresses, and strains. For a three-dimensional case,

15 equations are defined, including six compatibility differential equations, that relate displacements and strains, six algebraic constitutive relations for stresses and strains, and three differential equilibrium equations between mass forces and stresses.

Starting with the displacements and strains, the relation between the three displacement components and the normal and shear strain terms is given by

$$\begin{bmatrix} \varepsilon_{11} \\ \varepsilon_{22} \\ \varepsilon_{33} \\ 2\varepsilon_{23} \\ 2\varepsilon_{31} \\ 2\varepsilon_{12} \end{bmatrix} = \begin{bmatrix} \frac{\partial}{\partial \mathrm{x}_1} & 0 & 0 \\ 0 & \frac{\partial}{\partial \mathrm{x}_2} & 0 \\ 0 & 0 & \frac{\partial}{\partial \mathrm{x}_3} \\ 0 & \frac{\partial}{\partial \mathrm{x}_3} & \frac{\partial}{\partial \mathrm{x}_2} \\ \frac{\partial}{\partial \mathrm{x}_3} & 0 & \frac{\partial}{\partial \mathrm{x}_1} \\ \frac{\partial}{\partial \mathrm{x}_2} & \frac{\partial}{\partial \mathrm{x}_1} & 0 \end{bmatrix} \begin{bmatrix} u_1 \\ u_2 \\ u_3 \end{bmatrix} \tag{3.3}$$

Considering $\underline{\boldsymbol{L}}$ to be a differential operator, the compatibility equation is thus written

$$\underset{\sim}{\varepsilon} = \underline{\boldsymbol{L}} \cdot \underset{\sim}{u} \tag{3.4}$$

As for the stresses and strains, for isotropic materials the constitutive relations between all six stress and strain components are defined as follows

$$\begin{bmatrix} \sigma_{11} \\ \sigma_{22} \\ \sigma_{33} \\ \sigma_{23} \\ \sigma_{31} \\ \sigma_{12} \end{bmatrix} = \begin{bmatrix} K+\frac{4}{3}G & K-\frac{2}{3}G & K-\frac{2}{3}G & & & \\ K-\frac{2}{3}G & K+\frac{4}{3}G & K-\frac{2}{3}G & & \underline{0} & \\ K-\frac{2}{3}G & K-\frac{2}{3}G & K+\frac{4}{3}G & & & \\ & & & G & 0 & 0 \\ & \underline{0} & & 0 & G & 0 \\ & & & 0 & 0 & G \end{bmatrix} \begin{bmatrix} \varepsilon_{11} \\ \varepsilon_{22} \\ \varepsilon_{33} \\ 2\varepsilon_{23} \\ 2\varepsilon_{31} \\ 2\varepsilon_{12} \end{bmatrix} \tag{3.5}$$

where E is Young's modulus and ν is Poisson's ratio, while the shear modulus G and the bulk modulus K are obtained as

$$G = \frac{E}{2(1+\nu)}; \quad K = \frac{E}{3(1-2\nu)} \tag{3.6}$$

Therefore, assuming null initial deformations, the constitutive equation with the elasticity matrix $\underline{D}$ yields

$$\underset{\sim}{\sigma} = \underline{D} \cdot \underset{\sim}{\varepsilon} \tag{3.7}$$

Regarding the stress-force equilibrium, in each point of the material equilibrium is achieved if the sum of all forces in any direction is equal to zero. Hence, the equilibrium equation that relates the six stress components and the three mass body force terms is given by

$$\underline{\boldsymbol{L}}^T \underset{\sim}{\sigma} + \underset{\sim}{f} = \underset{\sim}{0} \tag{3.8}$$

where the term $\underline{\boldsymbol{L}}^T \underset{\sim}{\sigma}$ represents the stress gradient and $\underset{\sim}{f} = \underset{\sim}{f}(x_1, x_2, x_3, t)$ is the vector of body forces, defined as

$$\underset{\sim}{f} = \rho \underset{\sim}{g} - c\dot{\underset{\sim}{u}} - \rho(\ddot{\underset{\sim}{u}}_b + \ddot{\underset{\sim}{u}}) \tag{3.9}$$

The body forces include the gravity forces $\rho \underset{\sim}{g}$, where ρ (kN/m^3) is the material density and $\underset{\sim}{g}$ (m/s^2) is the gravity acceleration, and the forces induced by dynamic motion, including damping forces, $-c\dot{\underset{\sim}{u}}$, and inertia forces, $-\rho(\ddot{\underset{\sim}{u}}_b + \ddot{\underset{\sim}{u}})$, where c is the specific material damping (kN.s/m/m^3), $\dot{\underset{\sim}{u}}$ and $\ddot{\underset{\sim}{u}}$ are the relative velocities and accelerations, and $\ddot{\underset{\sim}{u}}_b$ is the rigid body acceleration, which is equal to the acceleration applied at the base of the structure; for seismic analysis, the seismic accelerations $\underset{\sim}{a}_s$ can be applied at the base of the structure and the inertia forces become $-\rho(\ddot{\underset{\sim}{u}} + \underset{\sim}{a}_S)$.

Finally, by substituting eq. (3.4) into eq. (3.7) and the resulting one into eq. (3.8), the equilibrium equation can be established in terms of the displacements and the body forces, considering the material properties in the elasticity matrix, which must be verified for all points belonging to the structure domain Ω and for all instants in time *t*,

$$\underline{\boldsymbol{L}}^{\mathrm{T}} \left(\underline{D} \underline{\boldsymbol{L}} \underset{\sim}{u} \right) + \underset{\sim}{f} = \underset{\sim}{0}, \quad \forall\, P(x_1, x_2, x_3) \in \Omega, \ \forall\, t \tag{3.10}$$

This is Navier's differential equation for structural analysis, based on a classic displacement formulation, and it can be used for calculating the dynamic response of a dam-reservoir-foundation system (Fig. 3.6), by solving an Initial and Boundary Values Problem, which requires both spatial and time integration.

For more complex problems involving three-dimensional behaviour and/or fluid-structure interaction, as is the case of dam-reservoir-foundation systems, the use of numerical methods is required to approximate the solutions for the corresponding differential equations (E. A. Oliveira & Pedro, 1986), since analytical solutions are only possible for elementary problems. A viable solution is the Finite Element Method (Zienkiewicz et al., 2013), widely used for solving problems in several fields, including structural analysis, fluid behaviour, heat conduction, etc., due to its potential to simulate an extensive range of boundary and/or initial value problems and to ensure computational robustness when applied to large problems, which require models comprising a great amount of data.

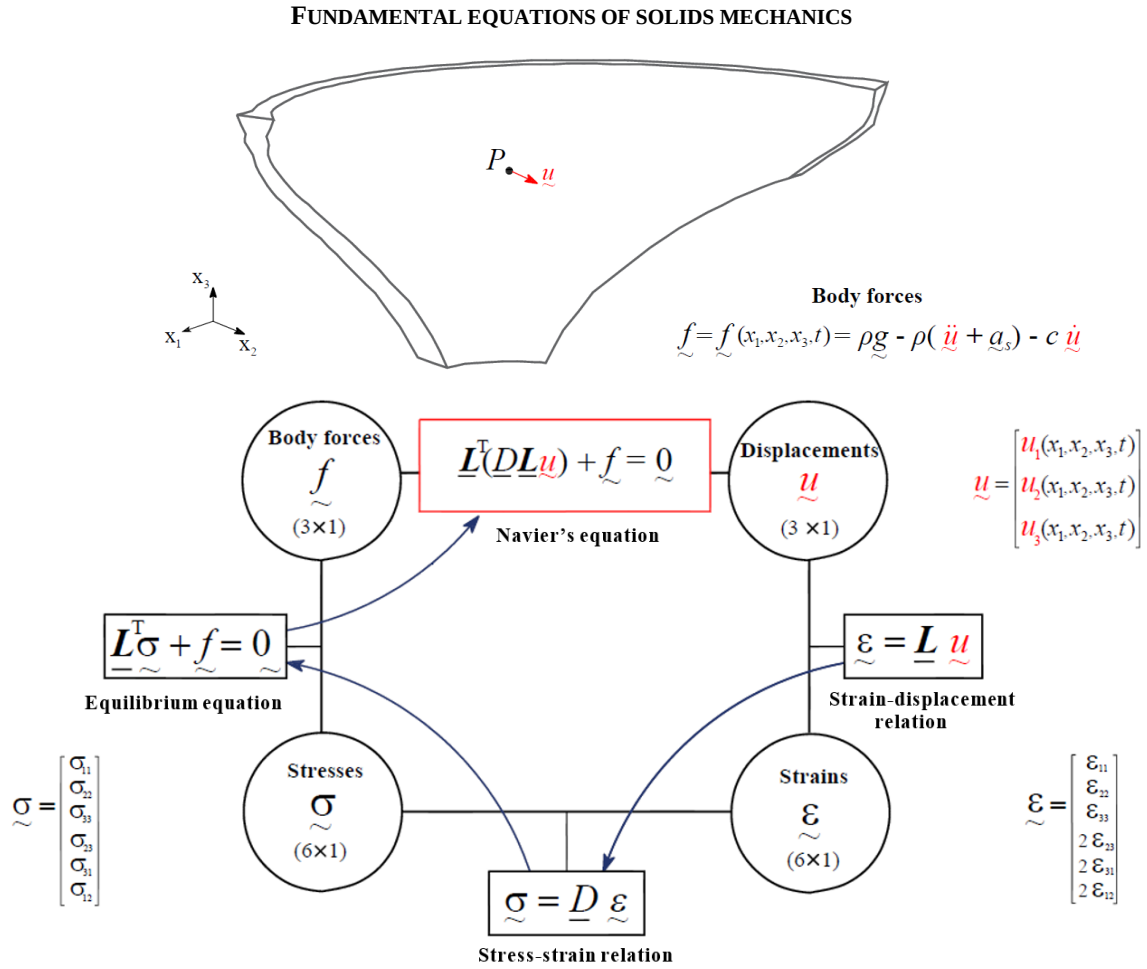

Fig. 3.6 Three-dimensional structure: concrete arch dam. Fundamental equations of Solid Mechanics.

3.4 FUNDAMENTAL CONCEPTS ON JOINT BEHAVIOUR

Large concrete dams are structures that can have different types of discontinuities, like joints or cracks (Fig. 3.7). For example, arch dams are structures typically constructed as cantilever monoliths separated by vertical contraction joints, which can present a curved and flat surface or a plain surface containing shear keys of different shapes and sizes (Fig. 3.8). Some dams also have a peripheral joint separating the dam body from the pulvino, a concrete mass supporting the dam, which extends over the entire length of the structure. Furthermore, important cracks can arise in the dam body or along the dam base, due to water pressure, thermal variations, or strong earthquakes. There can also be several types of discontinuities in the foundation, although this subject is not considered in this work.

Under static loads, dams are generally under compression due to the hydrostatic water pressure, and thus, the vertical joints remain closed while the resulting forces are transmitted along the arches to the abutments. During a strong earthquake, however, significant dynamic motion may occur, and thus tensile stresses can arise in the arch direction. Therefore, adjacent cantilevers may move relatively to each other, leading to the opening/closing of the vertical joints and to shear sliding at the surfaces of joints. In that case, there is a significant release of arch stresses and a redistribution of the forces to the cantilevers (Clough, 1980; Fenves

et al., 1992; Lau et al., 1998; Niwa & Clough, 1982); this can also cause a loss of global dam stiffness, hence changing the natural vibration frequencies. Furthermore, some dams may have cracked zones, which, despite being under control in normal operating conditions (Alegre, Carvalho, et al., 2019; S. Oliveira & Alegre, 2019a), can also influence the structural response of the dam.

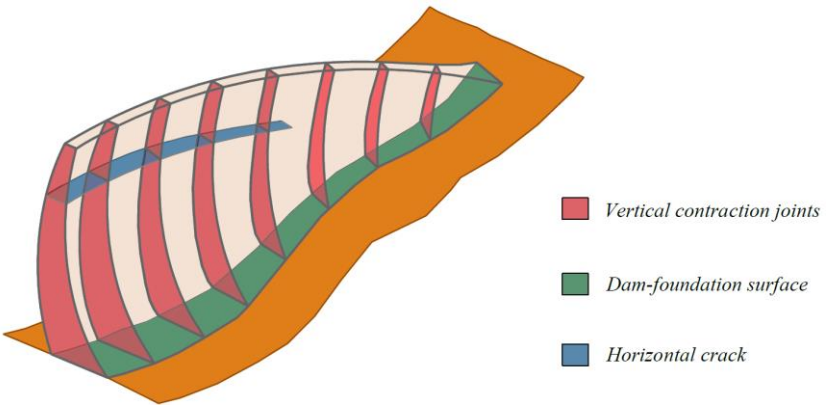

Fig. 3.7 Arch dam. Vertical contraction joints, horizontal crack, and dam-foundation surface.

In extraordinary circumstances, the scenario of sliding along the dam base, either at the dam-foundation or dam-pulvino surface, must also be accounted for. The collapse scenario due to sliding along the base, commonly studied for gravity dams, is very unlikely to occur in the case of arch dams due to the considerable arch effect. Nevertheless, during a high-intensity earthquake, if there are important uplift pressures at the base and/or deterioration along the insertion interface that result in a reduction of the shear resistance, small shear slippage may occur and cause damage to the grout and drainage curtains.

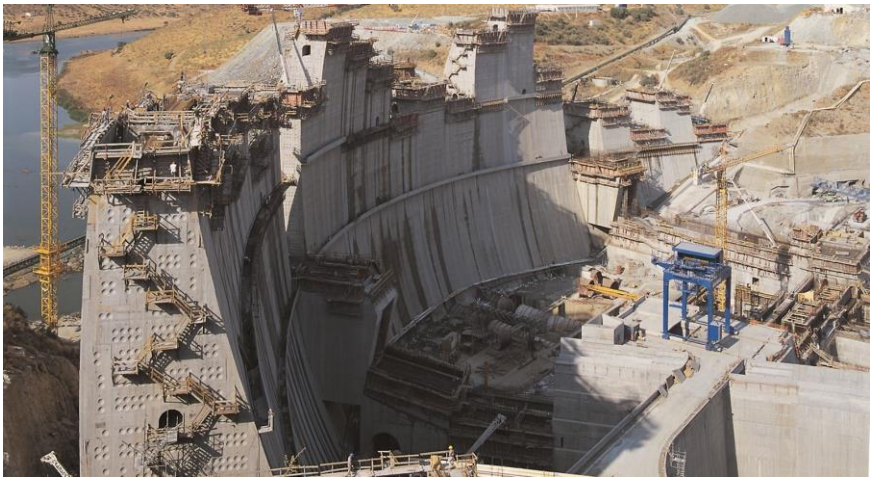

Fig. 3.8 Alqueva dam during construction. View of a contraction joint with shear keys of hemispherical shape.

Bearing in mind the above considerations, in addition to the fundamental equations describing the behaviour of solids presented in the previous section, the subject of joint behaviour is addressed here, as they might have an important influence in the structural response of dams.

Joints are essentially interfaces that act as discontinuities in the continuum, physically separating adjacent continuous structural elements (Fig. 3.9), which consist of two coincident faces: a lower face (face 1) and an upper face (face 2). Under a certain external load, relative displacements Δu may occur between the faces, namely normal Δu_{N} and tangential Δu_{T} displacements. Considering a local tri-orthogonal coordinate system (t_1, t_2, t_3), with two axes contained in the tangential plane and an axis in the normal direction to the joint plane, the displacements vector for any point a point belonging to the joint is given by

$$\Delta \underset{\sim}{u} = \begin{bmatrix} \Delta u_{\mathrm{T},1} \\ \Delta u_{\mathrm{T},2} \\ \Delta u_{\mathrm{N}} \end{bmatrix} \tag{3.11}$$

The corresponding stress and strain states are defined by the following vectors

$$\underset{\sim}{\sigma} = \begin{bmatrix} \tau_1 \\ \tau_2 \\ \sigma_{\mathrm{N}} \end{bmatrix} \quad ; \quad \underset{\sim}{\varepsilon} = \begin{bmatrix} \gamma_1 \\ \gamma_2 \\ \varepsilon_{\mathrm{N}} \end{bmatrix} \tag{3.12}$$

where τ_1 and τ_2 are the two shear stresses and σ_{N} is the normal stress, while γ_1 and γ_2 indicate the shear strains and ε_{N} represents the normal strain. For a joint with a unit area section, assuming an infinitesimal thickness w_j, the compatibility relations between the shear and normal strains and the relative displacements yield

$$\gamma_1 = \frac{\Delta u_{\mathrm{T},1}}{w_j} \quad ; \quad \gamma_2 = \frac{\Delta u_{\mathrm{T},2}}{w_j} \quad ; \quad \varepsilon_{\mathrm{N}} = \frac{\Delta u_{\mathrm{N}}}{w_j} \tag{3.13}$$

while the constitutive relation between stresses and strains is defined as follows

$$\begin{bmatrix} \tau_1 \\ \tau_2 \\ \sigma_{\mathrm{N}} \end{bmatrix} = \begin{bmatrix} G & 0 & 0 \\ 0 & G & 0 \\ 0 & 0 & E \end{bmatrix} \begin{bmatrix} \gamma_1 \\ \gamma_2 \\ \varepsilon_{\mathrm{N}} \end{bmatrix} \tag{3.14}$$

Assuming that there is an isotropic joint filling material with a Young's modulus *E* and a shear modulus *G*, the normal $\mathrm{K_N}$ and shear $\mathrm{K_T}$ stiffness (kN.m^{-1}/m^2) of the joint become

$$\mathrm{K_N} \approx \frac{E}{w_j} \quad ; \quad \mathrm{K_T} \approx \frac{G}{w_j} \tag{3.15}$$

Therefore, considering the normal and shear stiffness and the compatibility relations in (3.13), the relation between stresses and relative displacements becomes

$$\begin{bmatrix} \tau_1 \\ \tau_2 \\ \sigma_N \end{bmatrix} = \begin{bmatrix} K_T & 0 & 0 \\ 0 & K_T & 0 \\ 0 & 0 & K_N \end{bmatrix} \begin{bmatrix} \Delta u_{T,1} \\ \Delta u_{T,2} \\ \Delta u_N \end{bmatrix} \tag{3.16}$$

which can be presented in a compact form, using the joint elasticity matrix $\underline{D}_j$, as

$$\underset{\sim}{\sigma} = \underline{D}_j \, \Delta \underset{\sim}{u} \tag{3.17}$$

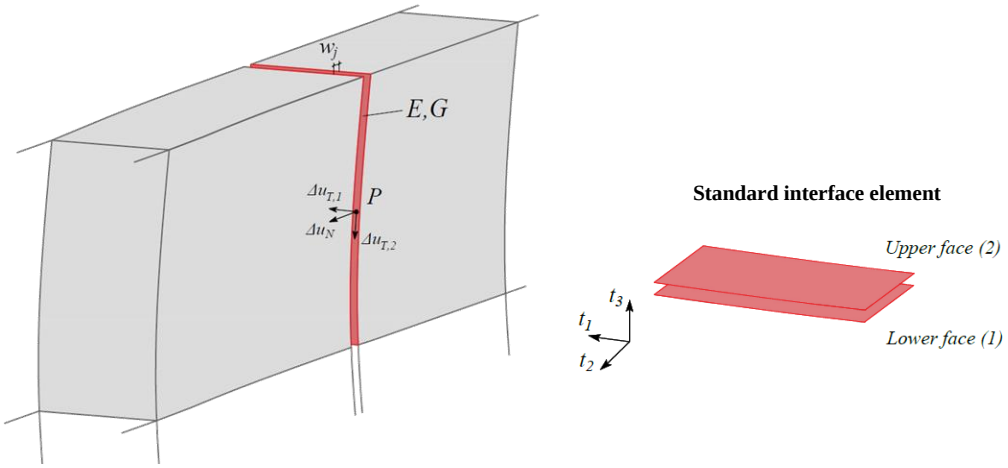

Fig. 3.9 Example of an interface element for a vertical contraction joint in an arch dam.

3.5 DYNAMIC BEHAVIOUR OF THE DAM-RESERVOIR-FOUNDATION SYSTEM: COUPLED PROBLEM AND FINITE ELEMENT FORMULATION

Under dynamic loads, concrete dams vibrate together with the foundation and the reservoir. Therefore, the dynamic motion of the solid domain (dam-foundation) and of the fluid domain (reservoir) and the interaction between all parts must be considered in order to analyse the dynamic behaviour of the entire dam-reservoir-foundation system. As mentioned in (Zienkiewicz & Bettess, 1978), this is a fluid-structure interaction problem in which the fluid motion is assumed to remain small while interaction is substantial. In such cases, generation of pressures in the reservoir is influenced by structural motion.

In this thesis, the numerical modelling of the dam-reservoir-foundation system is achieved based on a coupled model, using a finite element formulation in displacements and pressures (Zienkiewicz & Bettess, 1978) to simulate the dam-water dynamic interaction and the propagation of pressure waves in the reservoir, and on the massless approach (Clough, 1980) to simulate the foundation behaviour. The hypothesis of isotropic materials is assumed for the solid domain, while the impounded water in the reservoir is an inviscid and compressible fluid (Zienkiewicz et al., 2013).

3.5.1 COUPLED PROBLEM WITH SOLID-FLUID INTERACTION

The dynamic behaviour of a dam-reservoir-foundation system (Fig. 3.10) is described by a coupled problem with initial and boundary values, including the governing differential equations for the solid domain Ω_s (dam and foundation) and for the fluid Ω_w domain (reservoir),

$$\underline{\underline{\boldsymbol{L}}}^{\mathrm{T}}\left(\underline{\underline{\boldsymbol{D}}}\,\underline{\underline{\boldsymbol{L}}}\,\underset{\sim}{u}\right)+\underset{\sim}{f}=\underset{\sim}{0},\quad \forall\, P_s(x_1,x_2,x_3)\in\Omega_s,\ \forall\, t \tag{3.18}$$

$$\nabla^2 p-\frac{\ddot{p}}{c_w^2}=0,\quad \forall\, P_w(x_1,x_2,x_3)\in\ \Omega_w,\ \forall\, t \tag{3.19}$$

and considering specific boundary conditions, prescribed at the main interfaces of the system,

$$\begin{cases}\underset{\sim}{u}=\underset{\sim}{0} & ,\Gamma_f\\ \underset{\sim}{\mathbf{t}}=\underset{\sim}{n}_{\Gamma_1}^{\mathrm{T}}\gamma_w h_w & ,\Gamma_1\end{cases}\qquad \begin{cases}\dfrac{\partial p}{\partial \underset{\sim}{n}_{\Gamma_1}}=-\rho_w\,\underset{\sim}{n}_{\Gamma_1}^{\mathrm{T}}\,\ddot{\underset{\sim}{u}} & ,\Gamma_1\\ \dfrac{\partial p}{\partial \underset{\sim}{n}_{\Gamma_2}}=\underset{\sim}{n}_{\Gamma_2}^{\mathrm{T}}\ddot{\underset{\sim}{u}}=0 & ,\Gamma_2\end{cases}\qquad \begin{cases}p=0 & ,\Gamma_3\\ \dfrac{\partial p}{\partial \underset{\sim}{n}_{\Gamma_4}}=-\dfrac{1}{c_w}\,\dot{p} & ,\Gamma_4\end{cases} \tag{3.20}$$

The unknowns of the coupled problem are the displacement vector, $\underset{\sim}{u}=\underset{\sim}{u}(x_1,x_2,x_3,t)$, for points P_s in the solid domain, and the hydrodynamic pressure value, $p=p(x_1,x_2,x_3,t)$, for points P_w of the fluid domain. To simplify the notation, the spatial and time indexes are omitted unless necessary.

For the solid domain, the Navier's equilibrium equation (3.18) is considered. As referred previously, the vector of body forces, $\underset{\sim}{f}=\underset{\sim}{f}(x_1,x_2,x_3,t)$ (kN/m^3), includes the gravity, inertia and damping forces. For dynamic analysis under seismic excitation, the body forces become $\underset{\sim}{f}=\rho_s\,\underset{\sim}{g}-\rho_s(\ddot{\underset{\sim}{u}}+\underset{\sim}{a}_S)-c_s\dot{\underset{\sim}{u}}$, where $\dot{\underset{\sim}{u}}$ and $\ddot{\underset{\sim}{u}}$ denote the velocity and acceleration vectors, ρ_s (kg/m^3) represents the mass density of the solid materials (if the massless foundation approach is adopted, $\rho_s=0$ is used for the foundation materials), $\underset{\sim}{g}$ (m/s^2) is the gravity acceleration vector, c_s (kN.s/m/m^3) indicates the specific material damping, and lastly $\underset{\sim}{a}_S=\underset{\sim}{a}_S(x_1,x_2,x_3,t)$ (m/s^2) represents the seismic accelerations (considering a massless foundation model, the seismic input can be applied either at the base of the foundation block Γ_f or at the dam base Γ_b).

For the fluid domain, the pressure wave equation (3.19) is derived assuming the hypothesis of inviscid and compressible fluid (Zienkiewicz et al., 2013), where c_w (m/s) is the speed of sound in water (speed of pressure waves propagation). For dam reservoirs, the speed of sound in water can vary between 1400 m/s and 1500 m/s, depending on the average water temperature (Alegre, Carvalho, et al., 2019).

Regarding the boundary conditions of the coupled dam-reservoir-foundation system (Fig. 3.10), a displacement boundary condition is defined by prescribing null displacements, $\underset{\sim}{u}=\underset{\sim}{0}$, for the points at the base of the foundation block Γ_f, while a stress boundary condition is considered by applying forces, $\underset{\sim}{\mathbf{t}}=\underset{\sim}{n}_{\Gamma_1}^{\mathrm{T}}\gamma_w h_w$, at the upstream face of the dam Γ_1, to simulate the reservoir hydrostatic pressures. The boundary conditions for simulating fluid behaviour and fluid-structure interaction are the same as in (Zienkiewicz et al., 2013). In order to consider the solid-fluid motion coupling, dam-water interaction is considered by relating pressure gradients to structural accelerations at the dam-reservoir interface Γ_1, while

at the reservoir bottom Γ_2, it is assumed that only horizontal motion exists. Moreover, a radiation boundary is introduced at the far end of the reservoir Γ_4, assuming outgoing pressure waves only, and a null pressure condition is prescribed at the free surface of the reservoir Γ_3. The normal vector to each interface Γ_i is given by $\underset{\sim}{n}_{\Gamma_i}$.

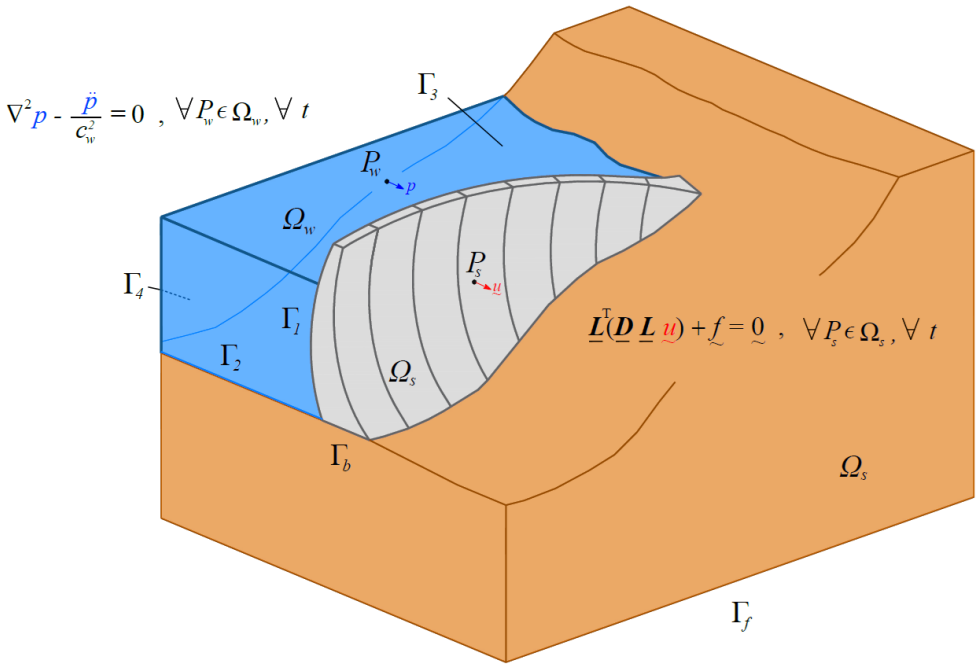

Fig. 3.10 Modelling the dynamic behaviour of the dam-reservoir-foundation system. Governing equations and main system interfaces.

To define the discrete formulation for the described coupled problem and thus calculate the numerical solution based on the Finite Element Method, some standard steps must be taken (Zienkiewicz et al., 2013). Initially, the governing equations of the dam-reservoir-foundation system, (3.18) and (3.19), are transformed from the strong (differential) form to the corresponding weak (integral) form, considering the prescribed boundary conditions in (3.20). Then, the continuous domain of the entire system is discretized into finite elements, connected by nodal points. Finally, the FEM approach, based on the concept of finite element interpolation functions, is used to establish the discrete equilibrium equations that describe the structural motion of the dam and the hydrodynamic behaviour of the reservoir.

COUPLED PROBLEM: WEAK FORMULATION

As part of the FEM procedure, first it is necessary to establish the equivalent weak or integral form of the governing equations of motion for the solid (3.18) and fluid (3.19) domains, e.g. using either Weighted Residual Methods or Variational Principles (Zienkiewicz et al., 2013). After integration by parts and substitution of the prescribed boundary conditions (3.20), the weak form is obtained for each part of the coupled system.

Accordingly, for the solid (dam-foundation) domain the weak form is

$$\int_{\Omega_s} \underset{\sim}{v}_u \left[\underline{L}^{\mathrm{T}} \underline{D} \underline{L} \underset{\sim}{u} + \left(\rho_s \underset{\sim}{g} - \rho_s (\ddot{\underset{\sim}{u}} + \underset{\sim}{a}_S) - c_s \dot{\underset{\sim}{u}} \right) \right] d\Omega - \int_{\Gamma_1} \underset{\sim}{v}_u^{\mathrm{T}} \underset{\sim}{n}_{\Gamma_1} p \, \mathrm{d}\Gamma - \int_{\Gamma_1} \underset{\sim}{v}_u^{\mathrm{T}} \underset{\sim}{\mathbf{t}} \, \mathrm{d}\Gamma = 0 \tag{3.21}$$

while for the fluid (reservoir) domain the weak form is given by

$$\int_{\Omega_w} \left[\underset{\sim}{v}_p \frac{1}{c_w^2} \ddot{p} + \left(\nabla \underset{\sim}{v}_p \right)^{\mathrm{T}} (\nabla p) \right] d\Omega + \int_{\Gamma_1} \underset{\sim}{v}_p \rho_w \underset{\sim}{n}_{\Gamma_1}^{\mathrm{T}} \ddot{\underset{\sim}{u}} \, \mathrm{d}\Gamma + \int_{\Gamma_3} \underset{\sim}{v}_p \frac{1}{g} \ddot{p} \, \mathrm{d}\Gamma + \int_{\Gamma_4} \underset{\sim}{v}_p \frac{1}{c_w} \dot{p} \, \mathrm{d}\Gamma = 0 \tag{3.22}$$

where the integral over the surface Γ_1 is related to the solid-fluid motion coupling at the dam-reservoir interface, and the terms $\underset{\sim}{v}_u$ and $\underset{\sim}{v}_p$ are the so-called arbitrary or test functions (the term virtual displacements is also used in Portuguese literature).

3.5.2 DISCRETIZED SYSTEM: FINITE ELEMENT FORMULATION IN DISPLACEMENTS AND PRESSURES

In the present work, the dam-reservoir-foundation system is discretized using displacement-based finite elements for the dam and the foundation, with three displacement degrees of freedom per node, and pressure-based finite elements for the reservoir, considering a single pressure degree of freedom per node (Fig. 3.11). The number of degrees of freedom of the entire system n is obtained by adding the displacement n_s and pressure n_p degrees of freedom, $n = n_s + n_p$. Hexahedral type finite elements (6 faces), namely isoparametric elements with 20 nodes, are used for the continuum, i.e., dam, foundation, and reservoir, and compatible interface elements with 16 nodes are used for the discretisation of the main interfaces, including the dam-foundation interface and other discontinuities as vertical contraction joints and cracks.

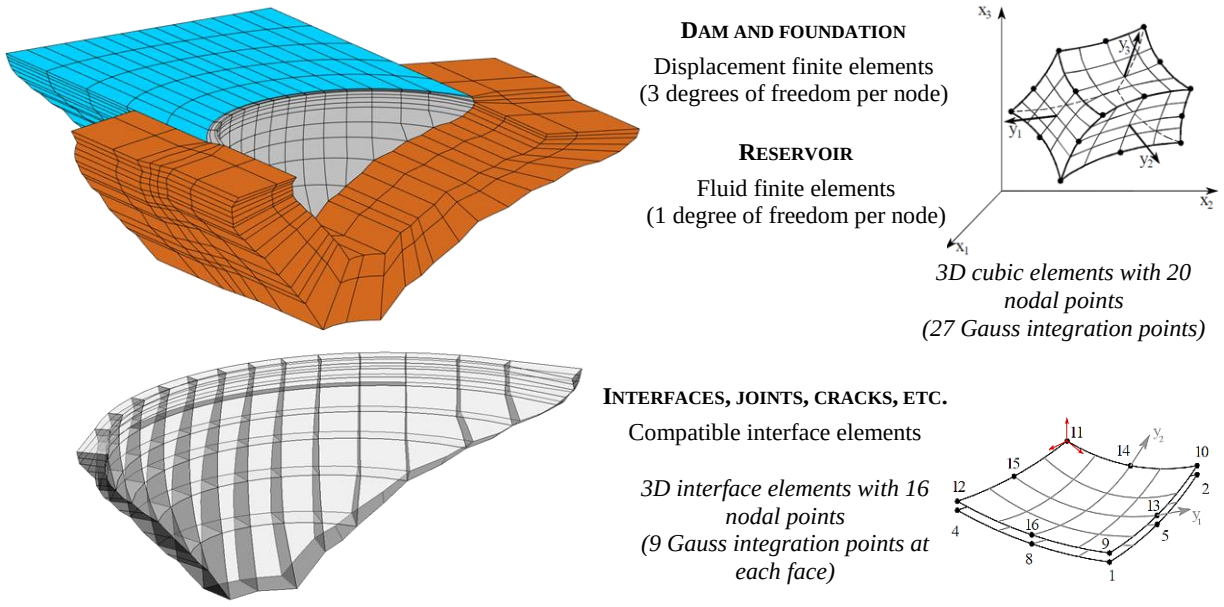

Fig. 3.11 Discretized dam-reservoir-foundation system and types of finite elements used.

The FEM procedure requires the definition of approximation functions to achieve the numerical solutions for all nodal points of the discrete solid-fluid system (Zienkiewicz et al., 2013). Considering the coupled problem to be discretized in the standard manner, the displacements vector on each point in the solid domain is approximated as

$$\underset{\sim}{u} = \underline{\mathrm{N}}_u \, \underset{\sim}{u}^{\mathrm{e}} \tag{3.23}$$

and similarly, the pressure value on each point within the reservoir domain is approximated as

$$p = \underline{\mathrm{N}}_p \, \underset{\sim}{p}^{\mathrm{e}} \tag{3.24}$$

where $\underset{\sim}{u}^{\mathrm{e}}$ and $\underset{\sim}{p}^{\mathrm{e}}$ are the nodal parameters, while $\underline{\mathrm{N}}_u$ and $\underline{\mathrm{N}}_p$ are matrices containing the appropriate interpolation functions (Zienkiewicz et al., 2013).

For the discretized solid domain, based on the displacement approximation, strain- and stress-displacement relations can be written as

$$\underset{\sim}{\varepsilon} = \boldsymbol{L} \, \underline{\mathrm{N}}_u \, \underset{\sim}{u}^{\mathrm{e}} = \underline{\mathrm{B}}_u \, \underset{\sim}{u}^{\mathrm{e}} \tag{3.25}$$

$$\underset{\sim}{\sigma} = \underline{D} \, \boldsymbol{L} \, \underline{\mathrm{N}}_u \, \underset{\sim}{u}^{\mathrm{e}} = \underline{D} \, \underline{\mathrm{B}}_u \, \underset{\sim}{u}^{\mathrm{e}} \tag{3.26}$$

where $\underline{\mathrm{B}}_u$ is the matrix containing the derivatives of the displacement interpolation functions. Also, if interface elements are considered, the relative displacements for every point in the interface can be approximated as

$$\Delta \underset{\sim}{u} = \underline{\mathrm{T}}_j \underline{\mathrm{N}}_j \, \underset{\sim}{u}^{e,j} \tag{3.27}$$

where $\underset{\sim}{u}^{e,j}$ are the nodal parameters for all nodes of both faces of the interface element, $\underline{\mathrm{T}}_j$ represents a matrix to account for the transformation from the local tri-orthogonal system to the global coordinate system, and $\underline{\mathrm{N}}_j$ is the matrix that contains appropriate interpolation functions, which is defined to get the differences between the nodal displacements in coincident nodes in the lower and upper faces of the interface element (Fenves et al., 1992).

In order to define the dynamic equations for the discretized system, the solid (3.21) and fluid (3.22) equations in weak form can be established at an elementary level, considering the volume domain Ω^e and the boundaries Γ^e of the elements. The displacement approximation (3.23) can be introduced in the elementary solid weak equation to determine the elementary mass, damping and stiffness matrices as

$$\underline{\mathrm{m}}^e = \int_{\Omega_s^e} \rho_s \, \underline{\mathrm{N}}_u^{\mathrm{T}} \, \underline{\mathrm{N}}_u \, d\Omega \,; \quad \underline{\mathrm{c}}^e = \int_{\Omega_s^e} \mu_s \, \underline{\mathrm{N}}_u^{\mathrm{T}} \, \underline{\mathrm{N}}_u \, d\Omega \,; \quad \underline{\mathrm{k}}^e = \int_{\Omega_s^e} \underline{\mathrm{B}}_u^{\mathrm{T}} \, \underline{D} \, \underline{\mathrm{B}}_u \, d\Omega \tag{3.28}$$

Similarly, substitution of the pressure approximation (3.24) into the elementary fluid domain weak equation leads to the corresponding mass, damping and stiffness components,

$$\underline{\mathrm{S}}^{e} = \int_{\Omega_w^e} \underline{\mathrm{N}}_p^{\mathrm{T}} \frac{1}{c_w^2} \underline{\mathrm{N}}_p \, d\Omega_f \; ; \quad \underline{\mathrm{R}}^{e} = \int_{\Gamma_{4e}} \underline{\mathrm{N}}_p^{\mathrm{T}} \frac{1}{c_w} \underline{\mathrm{N}}_p \mathrm{d}\Gamma \; ; \quad \underline{\mathrm{H}}^{e} = \int_{\Omega_w^e} \nabla \underline{\mathrm{N}}_p^{\mathrm{T}} \nabla \underline{\mathrm{N}}_p \, \mathrm{d}\Omega_w^e \tag{3.29}$$

The solid-fluid coupling matrix, which establishes the correlation between pressures in the reservoir and motion in the dam on the dam-reservoir boundary, is given by

$$\underline{\mathrm{Q}}^{e} = \int_{\Gamma_1^e} \underline{\mathrm{N}}_u^{\mathrm{T}} \underset{\sim}{n}_{\Gamma_1} \underline{\mathrm{N}}_p \, \mathrm{d}\Gamma \tag{3.30}$$

Regarding the interface elements, taking into account the approximation for relative displacements in interface elements, the elementary interface stiffness matrices are obtained as follows

$$\underline{\mathrm{k}}_j^{e} = \int_{\Gamma_j^e} \underline{\mathrm{N}}_j^{\mathrm{T}} \underline{\mathrm{T}}_j^{\mathrm{T}} \underline{D}_j \underline{\mathrm{T}}_j \underline{\mathrm{N}}_j \; d\Gamma \tag{3.31}$$

In addition, the static loads may include, e.g., the dam self-weight (SW), obtained from the gravity body forces $\rho_s \underset{\sim}{g}$, and the hydrostatic pressure (HP), resulting from the stress forces $\underset{\sim}{\mathbf{t}} = \underset{\sim}{n}_{\Gamma}^{\mathrm{T}} \gamma_w h_w$ at the upstream face. The corresponding elementary nodal forces are defined as

$$\underset{\sim}{\mathrm{f}}_{SW}^{e} = \int_{\Omega_s^e} \underline{\mathrm{N}}_u^{\mathrm{T}} \rho_s \underset{\sim}{g} \, d\Omega \; ; \quad \underset{\sim}{\mathrm{f}}_{HP}^{e} = \int_{\Gamma_1^e} \underline{\mathrm{N}}_u^{\mathrm{T}} \underset{\sim}{n}_{\Gamma_1}^{\mathrm{T}} \gamma_w h_w \, \mathrm{d}\Gamma \; . \tag{3.32}$$

The above elementary matrices are obtained by calculating the volume and surface integrals. Integration over each element or surface domain is performed by numerical quadrature, e.g. based on the Gauss integration method, accounting for the mapping from local coordinates (at the element level) to global coordinates (Zienkiewicz et al., 2013).

The global matrices and force vectors of the discrete solid (dam-foundation) and fluid (reservoir) domains are calculated by assembling the element contributions, resulting in the solid and fluid dynamic equations,

$$\underline{\mathrm{m}} \, \underset{\sim}{\ddot{\mathrm{u}}} + \underline{\mathrm{c}} \, \underset{\sim}{\dot{\mathrm{u}}} + \underline{\mathrm{k}} \, \underset{\sim}{\mathrm{u}} = \underset{\sim}{F}_s + \underline{\mathrm{Q}} \, \underset{\sim}{\mathrm{p}} \tag{3.33}$$

$$\underline{\mathrm{S}} \, \underset{\sim}{\ddot{\mathrm{p}}} + \underline{\mathrm{R}} \, \underset{\sim}{\dot{\mathrm{p}}} + \underline{\mathrm{H}} \, \underset{\sim}{\mathrm{p}} = \underset{\sim}{F}_w - \rho_w \underline{\mathrm{Q}}^{\mathrm{T}} \, \underset{\sim}{\ddot{\mathrm{u}}} \tag{3.34}$$

The mass, damping and stiffness matrices for the solid domain are, $\underline{\mathrm{m}}$, $\underline{\mathrm{c}}$ and $\underline{\mathrm{k}}$ ($\mathrm{n_s}\times\mathrm{n_s}$), while the corresponding terms for the fluid domain are $\underline{\mathrm{S}}$, $\underline{\mathrm{R}}$ and $\underline{\mathrm{H}}$ ($\mathrm{n}_p\times\mathrm{n}_p$). The coupling matrix associated with water-structure motion coupling is $\underline{\mathrm{Q}}$ ($\mathrm{n}_p\times\mathrm{n_s}$) (Zienkiewicz & Bettess, 1978). The solid and fluid nodal force vectors are given by $\underset{\sim}{F}_s = \underset{\sim}{F}_s(t)$ ($\mathrm{n_s}\times1$) and $\underset{\sim}{F}_w = \underset{\sim}{F}_w(t)$ ($\mathrm{n_s}\times1$). For example, the solid forces may include

those due to static loads, such as the dam self-weight and the hydrostatic pressure on the upstream face, and to dynamic loads, e.g., seismic excitation or harmonic vibrations from operational sources.

Finally, the coupled equation of the discretized dam-reservoir-foundation system is defined as

$$\begin{bmatrix} \underline{\mathrm{m}} & \underline{0} \\ \rho_w \underline{\mathrm{Q}}^{\mathrm{T}} & \underline{\mathrm{S}} \end{bmatrix} \begin{bmatrix} \ddot{\underset{\sim}{\mathrm{u}}} \\ \ddot{\underset{\sim}{\mathrm{p}}} \end{bmatrix} + \begin{bmatrix} \underline{\mathrm{c}} & \underline{0} \\ \underline{0} & \underline{\mathrm{R}} \end{bmatrix} \begin{bmatrix} \dot{\underset{\sim}{\mathrm{u}}} \\ \dot{\underset{\sim}{\mathrm{p}}} \end{bmatrix} + \begin{bmatrix} \underline{\mathrm{k}} & -\underline{\mathrm{Q}} \\ \underline{0} & \underline{\mathrm{H}} \end{bmatrix} \begin{bmatrix} \underset{\sim}{\mathrm{u}} \\ \underset{\sim}{\mathrm{p}} \end{bmatrix} = \begin{bmatrix} \underset{\sim}{F}_s \\ \underset{\sim}{F}_w \end{bmatrix} \tag{3.35}$$

For the particular case of dynamic behaviour under seismic loads, and omitting other excitation sources, the solid and fluid forces become $\underset{\sim}{F}_s = -\underline{\mathrm{m}}\ \underline{s}\ \underset{\sim}{a}_S$ and $\underset{\sim}{F}_w = -\rho_w\ \underline{\mathrm{Q}}^{\mathrm{T}}\ \underline{s}\ \underset{\sim}{a}_S$, where $\underset{\sim}{a}_S = \underset{\sim}{a}_S(t)$ (3×1) is the seismic input, which includes three acceleration time histories in the upstream-downstream, cross-valley and vertical directions, and $\underline{s}$ (n_s×3) is a matrix to uniformly distribute the seismic accelerations by all degrees of freedom,

$$\underline{s} = \begin{bmatrix} 1 & 0 & 0 \\ 0 & 1 & 0 \\ 0 & 0 & 1 \\ & \vdots & \end{bmatrix} \tag{3.36}$$

Thus, the above coupled equation can be expressed as

$$\begin{bmatrix} \underline{\mathrm{m}} & \underline{0} \\ \rho_w \underline{\mathrm{Q}}^{\mathrm{T}} & \underline{\mathrm{S}} \end{bmatrix} \begin{bmatrix} \ddot{\underset{\sim}{\mathrm{u}}} + \underline{s}\,\underset{\sim}{a}_S \\ \ddot{\underset{\sim}{\mathrm{p}}} \end{bmatrix} + \begin{bmatrix} \underline{\mathrm{c}} & \underline{0} \\ \underline{0} & \underline{\mathrm{R}} \end{bmatrix} \begin{bmatrix} \dot{\underset{\sim}{\mathrm{u}}} \\ \dot{\underset{\sim}{\mathrm{p}}} \end{bmatrix} + \begin{bmatrix} \underline{\mathrm{k}} & -\underline{\mathrm{Q}} \\ \underline{0} & \underline{\mathrm{H}} \end{bmatrix} \begin{bmatrix} \underset{\sim}{\mathrm{u}} \\ \underset{\sim}{\mathrm{p}} \end{bmatrix} = \begin{bmatrix} \underset{\sim}{0} \\ \underset{\sim}{0} \end{bmatrix} \tag{3.37}$$

or, by placing the mass forces due to the seismic accelerations on the right-hand side, as

$$\begin{bmatrix} \underline{\mathrm{m}} & \underline{0} \\ \rho_w \underline{\mathrm{Q}}^{\mathrm{T}} & \underline{\mathrm{S}} \end{bmatrix} \begin{bmatrix} \ddot{\underset{\sim}{\mathrm{u}}} \\ \ddot{\underset{\sim}{\mathrm{p}}} \end{bmatrix} + \begin{bmatrix} \underline{\mathrm{c}} & \underline{0} \\ \underline{0} & \underline{\mathrm{R}} \end{bmatrix} \begin{bmatrix} \dot{\underset{\sim}{\mathrm{u}}} \\ \dot{\underset{\sim}{\mathrm{p}}} \end{bmatrix} + \begin{bmatrix} \underline{\mathrm{k}} & -\underline{\mathrm{Q}} \\ \underline{0} & \underline{\mathrm{H}} \end{bmatrix} \begin{bmatrix} \underset{\sim}{\mathrm{u}} \\ \underset{\sim}{\mathrm{p}} \end{bmatrix} = \begin{bmatrix} -\underline{\mathrm{m}}\ \underline{s}\ \underset{\sim}{a}_S \\ -\rho_w\ \underline{\mathrm{Q}}^{\mathrm{T}}\ \underline{s}\ \underset{\sim}{a}_S \end{bmatrix} \tag{3.38}$$

In this thesis, based on the proposed calculation methods, the goal is to solve the coupled problem in order to calculate the dynamic response of the solid-fluid system as a whole, assuming natural viscous damping in the solid and radiation damping in the reservoir. Therefore, the discrete dynamic equation of the dam-reservoir-foundation system with generalized damping becomes

$$\underline{\mathrm{M}}\ \ddot{\underset{\sim}{\mathrm{q}}} + \underline{\mathrm{C}}\ \dot{\underset{\sim}{\mathrm{q}}} + \underline{\mathrm{K}}\ \underset{\sim}{\mathrm{q}} = \underset{\sim}{F} \tag{3.39}$$

considering the coupled unknown given by

$$\underset{\sim}{\mathrm{q}} = \underset{\sim}{\mathrm{q}}(t) = \begin{bmatrix} \underset{\sim}{\mathrm{u}} \\ \underset{\sim}{\mathrm{p}} \end{bmatrix} \tag{3.40}$$

The global mass, damping and stiffness matrices are $\underline{M}$, $\underline{C}$ and $\underline{K}$ (n×n) and the global nodal force vector is $\underset{\sim}{F} = \underset{\sim}{F}(t)$ (n×1). The unknown vector $\underset{\sim}{q} = \underset{\sim}{q}(t)$ includes the displacements vector $\underset{\sim}{u} = \underset{\sim}{u}(t)$ (n_s×1) and the hydrodynamic pressures vector $\underset{\sim}{p} = \underset{\sim}{p}(t)$ (n_p×1).

The substructure method is used in the implemented model in order to simulate the foundation block as an elastic and massless substructure: a condensed foundation stiffness matrix is calculated and assembled in matrix $\underline{k}$, at the dam-foundation interface nodes, and similarly, a foundation damping matrix, proportional to the stiffness, is incorporated in matrix $\underline{c}$. Based on this method, the degrees of freedom of the solid domain become only those associated with the dam, thus reducing the total degrees of freedom of the problem and increasing computational efficiency.

The proposed methods for solving the dynamic coupled problem of the dam-reservoir-foundation system are presented in the following subchapters, namely for modal analysis (subchapter 3.6), linear seismic analysis (subchapter 3.7) and non-linear seismic analysis (subchapter 3.8).

3.6 STATE-SPACE FORMULATION FOR MODAL ANALYSIS

A new state-space approach is proposed for coupled modal analysis of the dam-reservoir-foundation system, considering generalized damping (e.g., this allows the definition of zones with different material properties or under dissimilar deterioration states). The goal is to solve a complex eigenproblem and calculate the main modal parameters, i.e., natural frequencies, damping ratios, and modal configurations.

The state-space formulation requires the definition of a new variable, $\underset{\sim}{v}$, which is the first time derivative of the coupled unknown, hence including the derivatives of the displacements and pressures,

$$\underset{\sim}{v} = \dot{\underset{\sim}{q}} = \begin{bmatrix} \dot{\underset{\sim}{u}} \\ \dot{\underset{\sim}{p}} \end{bmatrix} \tag{3.41}$$

By introducing this new variable into the problem, the second order equation of motion of the coupled system (3.39) can be equivalently presented as a set of two first order equations

$$\begin{cases} \underline{M}\,\dot{\underset{\sim}{v}} + \underline{C}\,\underset{\sim}{v} + \underline{K}\,\underset{\sim}{q} = \underset{\sim}{F} \\ \underset{\sim}{v} = \dot{\underset{\sim}{q}} \end{cases} \tag{3.42}$$

Then, multiplication of the first equation by the inverse of the global mass matrix leads to

$$\begin{bmatrix} \dot{\underset{\sim}{q}} \\ \dot{\underset{\sim}{v}} \end{bmatrix} = \begin{bmatrix} \underline{0} & \underline{I} \\ -\underline{M}^{-1}\underline{K} & -\underline{M}^{-1}\underline{C} \end{bmatrix} \begin{bmatrix} \underset{\sim}{q} \\ \underset{\sim}{v} \end{bmatrix} + \begin{bmatrix} \underset{\sim}{0} \\ \underline{M}^{-1}\underset{\sim}{F} \end{bmatrix} \tag{3.43}$$

Therefore, the state-space dynamic equation of motion of the coupled system is written as

$$\dot{\underset{\sim}{x}} = \underline{A}\,\underset{\sim}{x} + \underline{P} \tag{3.44}$$

where $\underline{A}$ (2n×2n) is the state matrix, which includes the mass, damping and stiffness of the dam-reservoir-foundation system, and $\underline{P}$ $(2n \times 1)$ is the state force vector. The state-space unknown of dynamic coupled problem, $\underset{\sim}{x} = \underset{\sim}{x}(t)$ (2n×1), comprises the displacements and pressures and the respective time derivatives,

$$\underset{\sim}{x} = \begin{bmatrix} \underset{\sim}{q} \\ \underset{\sim}{v} \end{bmatrix} = \begin{bmatrix} \underset{\sim}{u} \\ \underset{\sim}{p} \\ \dot{\underset{\sim}{u}} \\ \dot{\underset{\sim}{p}} \end{bmatrix} \tag{3.45}$$

Based on the proposed state-space approach, the coupled eigenproblem of the discretized dam-reservoir-foundation system is

$$\left[\underline{A} - \lambda\,\underline{I}\right]\underset{\sim}{\phi} = \underset{\sim}{0} \tag{3.46}$$

where λ denotes a single eigenvalue and $\underset{\sim}{\phi}$ represents the respective eigenvector. Since the adopted coupled model considers fluid-structure interaction and generalized (or non-proportional) damping, the eigenvalues and eigenvectors are complex conjugate pairs. The eigenvalue pairs λ_n and $\bar{\lambda}_n$ are defined as

$$\lambda_n = -\xi_n\omega_n + \mathrm{i}\,\omega_n\sqrt{1-\xi_n^2}\;; \quad \bar{\lambda}_n = -\xi_n\omega_n - \mathrm{i}\,\omega_n\sqrt{1-\xi_n^2} \tag{3.47}$$

where ω_n is the undamped natural frequency and ξ_n denotes the modal damping ratio. The corresponding eigenvector pairs, $\underset{\sim}{\phi}_n$ and $\bar{\underset{\sim}{\phi}}_n$ (2n×1), contain complex modal coordinates for all n degrees of freedom of the discretized system,

$$\underset{\sim}{\phi}_n = \underset{\sim}{a}_n + i\underset{\sim}{b}_n\;; \quad \bar{\underset{\sim}{\phi}}_n = \underset{\sim}{a}_n - i\underset{\sim}{b}_n \tag{3.48}$$

The eigenvalues can be presented in a diagonal matrix $\underline{\lambda}$ (2n×2n) as

$$\underline{\lambda} = \begin{bmatrix} \lambda_1 & & & & \\ & \bar{\lambda}_1 & & & \\ & & \ddots & & \\ & & & \lambda_n & \\ & & & & \bar{\lambda}_n \end{bmatrix} \tag{3.49}$$

while the eigenvectors are stored in the state modal matrix $\underline{\Phi}$ (2n×2n), represented by

$$\underline{\Phi} = \begin{bmatrix} \underline{\Phi}_{\mathrm{q}} \\ \underline{\Phi}_{\mathrm{v}} \end{bmatrix} \tag{3.50}$$

where the sub-modal matrices $\underline{\Phi}_{\mathrm{q}}$ and $\underline{\Phi}_{\mathrm{v}}$ (n×2n) comprise all the eigenvector pairs

$$\underline{\Phi}_{\mathrm{q}} = \begin{bmatrix} \underset{\sim}{\phi}_1 & \overline{\underset{\sim}{\phi}}_1 & \cdots & \underset{\sim}{\phi}_{\mathrm{n}} & \overline{\underset{\sim}{\phi}}_{\mathrm{n}} \end{bmatrix}; \quad \underline{\Phi}_{\mathrm{v}} = \begin{bmatrix} \lambda_1 \underset{\sim}{\phi}_1 & \overline{\lambda}_1 \overline{\underset{\sim}{\phi}}_1 & \cdots & \lambda_{\mathrm{n}} \underset{\sim}{\phi}_{\mathrm{n}} & \overline{\lambda}_{\mathrm{n}} \overline{\underset{\sim}{\phi}}_{\mathrm{n}} \end{bmatrix} \tag{3.51}$$

Lastly, the main modal parameters of the dam-reservoir-foundation system can be calculated from the complex eigenvalues and eigenvectors. For a generic vibration mode *n*, the undamped ω_n and damped $\omega_{d,n}$ natural frequencies and the modal damping ratio ξ_n are calculated as

$$\omega_n = |\lambda_n|; \quad \omega_{d,n} = \omega_n \sqrt{1-\xi_n^2} \tag{3.52}$$

$$\xi_n = \frac{-\mathrm{Re}(\lambda_n)}{|\lambda_n|} \tag{3.53}$$

The modal oscillatory motion $\underset{\sim}{\phi}_n$ for all displacement and pressure degrees of freedom is obtained as

$$\underset{\sim}{\phi}_n(t) = \underset{\sim}{\phi}_n \, e^{\lambda_n t} + \overline{\underset{\sim}{\phi}}_n \, e^{\overline{\lambda}_n t} \tag{3.54}$$

The modal configurations are graphically represented by calculating modal displacement time histories and 3D mode shapes, enabling the representation of the modal oscillation of the dam and of the reservoir modal pressure variations (Fig. 3.12). Based on the adopted coupled model, since generalized damping is considered, non-stationary modes can be obtained from the complex eigenvectors (Veletsos & Ventura, 1986) - this type of modal configuration has been identified from vibrations measured on large concrete dams before (Alegre, Carvalho, et al., 2019; S. Oliveira et al., 2011, 2012; S. Oliveira, Silvestre, Espada, et al., 2014), and the same is shown later in the present work.

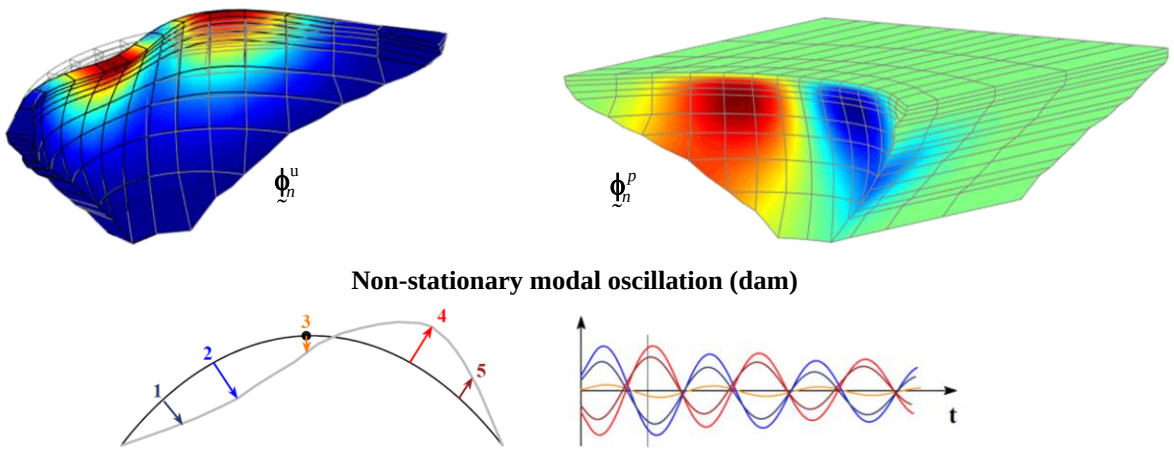

Fig. 3.12 Modal analysis for a coupled model, considering generalized damping. Example of a complex vibration mode (non-stationary): dam oscillation and reservoir hydrodynamic pressures.

3.7 TIME-STEPPING METHOD FOR LINEAR SEISMIC RESPONSE ANALYSIS

A time-stepping formulation based on the Newmark method (Newmark, 1959) is developed for linear seismic analysis of the dam-reservoir-foundation system. The aim is to directly the coupled dynamic equation (3.39) in time domain and compute the response of the discretized system in displacements and pressures. Assuming null initial conditions, the problem is defined at each time step t+Δt as,

$$\underline{\underline{M}}\,\underset{\sim}{\ddot{q}}_{t+\Delta t} + \underline{\underline{C}}\,\underset{\sim}{\dot{q}}_{t+\Delta t} + \underline{\underline{K}}\,\underset{\sim}{q}_{t+\Delta t} = \underset{\sim}{F}_{t+\Delta t} \tag{3.55}$$

The proposed time-stepping method follows the basic ideas of the original Newmark method, where the solutions for displacements and velocities at t+Δt are obtained from Taylor series expansions, while the accelerations are assumed to vary linearly within each time step (Newmark, 1959). By applying the same principles to the coupled problem allows the definition of approximate solutions for the coupled unknown $\underset{\sim}{q} = \underset{\sim}{q}(t)$ and the respective velocities $\underset{\sim}{\dot{q}} = \underset{\sim}{\dot{q}}(t)$ at the end of a generic time interval [t; t+Δt], as follows

$$\begin{aligned} \underset{\sim}{q}_{t+\Delta t} &= \underset{\sim}{q}_t + \Delta t \cdot \underset{\sim}{\dot{q}}_t + \Delta t^2 \cdot \left(\frac{1}{2} - \beta\right) \cdot \underset{\sim}{\ddot{q}}_t + \Delta t^2 \cdot \beta \cdot \underset{\sim}{\ddot{q}}_{t+\Delta t} \\ \underset{\sim}{\dot{q}}_{t+\Delta t} &= \underset{\sim}{\dot{q}}_t + \Delta t \cdot (1-\gamma) \cdot \underset{\sim}{\ddot{q}}_t + \Delta t \cdot \gamma \cdot \underset{\sim}{\ddot{q}}_{t+\Delta t} \end{aligned} \tag{3.56}$$

The Newmark parameters β and γ indicate the weighting contributions of the values of the coupled accelerations, , at the beginning ($\underset{\sim}{\ddot{q}}_t$) and at the end ($\underset{\sim}{\ddot{q}}_{t+\Delta t}$) of the time interval, in the values of both $\underset{\sim}{q}_{t+\Delta t}$ and $\underset{\sim}{\dot{q}}_{t+\Delta t}$. In the developed formulation these parameters are taken to be $\lambda = 1/2$ and $\beta = 1/4$, meaning that the constant acceleration hypothesis is adopted and that the Newmark method is unconditionally stable, with no artificial damping (Clough & Penzien, 2003).

Considering the above approximations, the coupled dynamic equation of the discretized dam-reservoir-foundation system at t+Δt (3.55) is expressed in terms of the coupled unknown $\underset{\sim}{q}_{t+\Delta t}$ as

$$\left(\alpha_0 \underline{\underline{M}} + \alpha_1 \underline{\underline{C}} + \underline{\underline{K}}\right) \underset{\sim}{q}_{t+\Delta t} = \underset{\sim}{F}_{t+\Delta t} + \underline{\underline{M}}\left(\alpha_0 \underset{\sim}{q}_t + \alpha_2 \underset{\sim}{\dot{q}}_t + \alpha_3 \underset{\sim}{\ddot{q}}_t\right) + \underline{\underline{C}}\left(\alpha_1 \underset{\sim}{q}_t + \alpha_4 \underset{\sim}{\dot{q}}_t + \alpha_5 \underset{\sim}{\ddot{q}}_t\right) \tag{3.57}$$

where the auxiliary constants α_i, defined by Newmark in (1959), are

$$\begin{aligned} &\alpha_0 = \frac{1}{\beta \Delta t^2} \quad ; \quad \alpha_1 = \frac{\gamma}{\beta \Delta t} \quad ; \quad \alpha_2 = \frac{1}{\beta \Delta t} \quad ; \quad \alpha_3 = \frac{1}{2\beta} - 1 \\ &\alpha_4 = \frac{\gamma}{\beta} - 1 \quad ; \quad \alpha_5 = \frac{\Delta t}{2} \cdot \left(\frac{\gamma}{\beta} - 2\right) \quad ; \quad \alpha_6 = (1-\gamma) \cdot \Delta t \quad ; \quad \alpha_7 = \gamma \cdot \Delta t \end{aligned} \tag{3.58}$$

Gathering terms on equation (3.57) enables to define the equivalent “stiffness” matrix and force vector

$$\underline{\underline{K}}^* = \alpha_0 \underline{\underline{M}} + \alpha_1 \underline{\underline{C}} + \underline{\underline{K}} \quad ; \quad \underset{\sim}{P}^*_{t+\Delta t} = \underset{\sim}{F}_{t+\Delta t} + \underline{\underline{M}}\left(\alpha_0 \underset{\sim}{q}_t + \alpha_2 \underset{\sim}{\dot{q}}_t + \alpha_3 \underset{\sim}{\ddot{q}}_t\right) + \underline{\underline{C}}\left(\alpha_1 \underset{\sim}{q}_t + \alpha_4 \underset{\sim}{\dot{q}}_t + \alpha_5 \underset{\sim}{\ddot{q}}_t\right) \tag{3.59}$$

and therefore, to establish the equivalent coupled dynamic equation of the dam-reservoir-foundation system

$$\underline{\underline{K}}^{*} \cdot \underset{\sim}{q}_{t+\Delta t} = \underset{\sim}{P}^{*}_{t+\Delta t} \tag{3.60}$$

Based on the proposed time-stepping method, considering null initial conditions, $\underset{\sim}{q}(0) = \underset{\sim}{0}$, $\dot{\underset{\sim}{q}}(0) = \underset{\sim}{0}$ and $\ddot{\underset{\sim}{q}}(0) = \underset{\sim}{0}$, the coupled response $\underset{\sim}{q} = \underset{\sim}{q}(t)$ is calculated by solving the above equation for each time step t+Δt. First, $\underset{\sim}{q}_{t+\Delta t}$ is computed at t+Δt, using only the variables available at the beginning of the time interval and the values of the nodal forces at t+Δt. Then the value of $\dot{\underset{\sim}{q}}_{t+\Delta t}$ and $\ddot{\underset{\sim}{q}}_{t+\Delta t}$ are calculated accordingly. The dynamic response of the dam-reservoir-foundation system in displacements and pressures (Fig. 3.13) is obtained by extracting the corresponding time histories, $\underset{\sim}{u} = \underset{\sim}{u}(t)$ and $\underset{\sim}{p} = \underset{\sim}{p}(t)$, from $\underset{\sim}{q} = \underset{\sim}{q}(t)$.

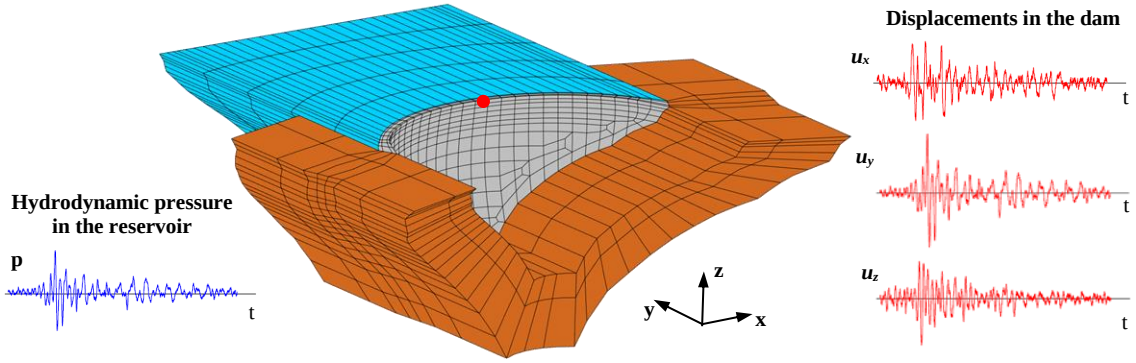

Fig. 3.13 Computed seismic response: displacements and hydrodynamic pressures time histories.

For structural analysis of the dam, accurate deformed shapes and stress fields are required. Considering this method is based on a finite element formulation, the approximation of the solution in each node gives a proper representation of the displacement field over the discretized dam domain (good results can be achieved even using simpler finite element meshes of dams). Furthermore, aiming to evaluate the stress fields in the dam body, it is very important to ensure that the principal stresses are represented in a realistic way, knowing that these are continuous within the material; this can be achieved by calculating the stress tensors (and the respective principal stress components) for all Gauss integration points within every finite element of the dam mesh, as follows

$$\underset{\sim}{\sigma}_{P_G} = \underline{\underline{D}}\ \underline{\underline{B}}_{P_G}\ \underset{\sim}{u}^{e} \tag{3.61}$$

Similarly, for the evaluation of stresses in joints, the stress tensors containing the normal and shear components, can be calculated for all Gauss points in both faces of the interface elements as

$$\underset{\sim}{\sigma}_{P_{G,j}} = \underline{\underline{D}}_{j}\ \underline{\underline{B}}_{P_{G,j}}\ \underset{\sim}{u}^{e}_{j} \tag{3.62}$$

3.8 TIME-STEPPING METHOD FOR NON-LINEAR SEISMIC ANALYSIS, CONSIDERING JOINT MOVEMENTS AND CONCRETE DAMAGE

A complete time-stepping method is proposed for non-linear seismic analysis of arch dam-reservoir-foundation systems, considering the opening/closing and sliding joint movements and tensile and compressive damage in the dam.

The goal is to compute the non-linear response of the discretized system in time domain. However, structural non-linearities are expected to alter the stiffness of the dam and hence non-linear dam behaviour must be simulated within each time step t+Δt. Therefore, the developed approach combines the previous time-stepping method with a non-linear iterative method, in order to account for the redistribution of unbalanced stresses in the dam body (3.8.1), considering appropriate constitutive models for joints (3.8.2) and for concrete (3.8.3).

In the developed model, structural non-linear behaviour is simulated using the Modified Newton's iterative method (de Borst & Sluys, 1999; Zienkiewicz et al., 2014), also referred to as stress-transfer or initial stress-method. Based on this method, the linear-elastic dam stiffness matrix, computed a priori, is used throughout the entire calculation process[3], while the loads are increased by applying additional fictitious forces on the dam, in order to reproduce the redistribution of unbalanced stresses that occurs due to joints and/or concrete non-linear behaviour. Thus, considering the application of a vector of unbalanced nodal forces $\underset{\sim}{\Psi}$, the coupled dynamic equation (3.39) of the dam-reservoir-foundation system becomes

$$\underline{M}\,\underset{\sim}{\ddot{q}} + \underline{C}\,\underset{\sim}{\dot{q}} + \underline{K}\,\underset{\sim}{q} = \underset{\sim}{F} + \underset{\sim}{\Psi} \tag{3.63}$$

Following the time-stepping procedure based on the Newmark method, described in section 3.7, the non-linear dynamic equation at each time step t+Δt is written as

$$\underline{M}\,\underset{\sim}{\ddot{q}}_{t+\Delta t} + \underline{C}\,\underset{\sim}{\dot{q}}_{t+\Delta t} + \underline{K}\,\underset{\sim}{q}_{t+\Delta t} = \underset{\sim}{F}_{t+\Delta t} + \underset{\sim}{\Psi}_{t+\Delta t} \tag{3.64}$$

and it can be simply expressed using the equivalent form

$$\underline{K}^{*}\,\underset{\sim}{q}_{t+\Delta t} = \underset{\sim}{P}^{*}_{t+\Delta t} + \underset{\sim}{\Psi}_{t+\Delta t} \tag{3.65}$$

where the equivalent global "stiffness" $\underline{K}^{*}$ and nodal force vector $\underset{\sim}{P}^{*}_{t+\Delta t}$ are the same as in eq. (3.59), and $\underset{\sim}{\Psi}_{t+\Delta t}$ represents the vector of total unbalanced forces (obtained at the end of the stress-transfer process conducted within each time step, as explained next).

Based on the proposed non-linear method, the non-linear coupled response $\underset{\sim}{q} = \underset{\sim}{q}(t)$ is calculated by solving the equivalent equation for each time step t+Δt. For non-linear structural analysis of the dam (Fig. 3.14),

[3] Newton's iterative method is commonly used to deal with non-linear structural behaviour. There are several variants to this method which require the recalculation of a tangent stiffness matrix in every iteration or once every *n* iterations. Although of rapid convergence, such techniques can be significantly demanding computationally, particularly for problems of large dimensions.

the displacements time histories are extracted from the coupled unknown. Then, based on a finite element formulation, the stresses are calculated for every Gauss point of the interface elements, using eq. (3.62), and non-linear joint behaviour is analysed based on the constitutive model presented in 3.8.2. Moreover, the stress state of the dam is evaluated by computing the stress tensors for all Gauss points, using the approximation defined in eq. (3.61), and concrete non-linear behaviour is simulated based on the constitutive damage model for concrete (3.8.3), considering both tensile and compressive damage.

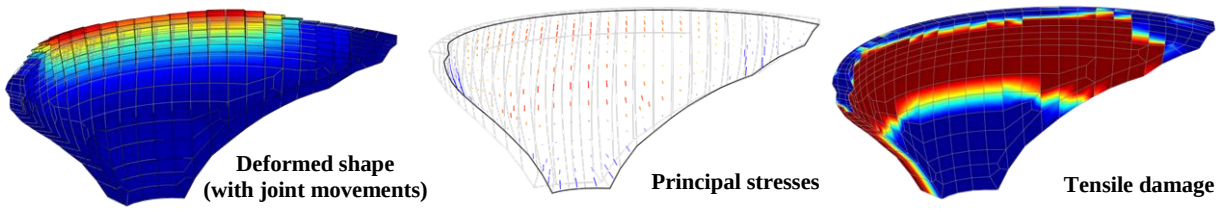

Fig. 3.14 Non-linear dam seismic response: deformed shape, principal stresses field and tensile damage.

3.8.1 STRESS-TRANSFER PROCESS: UNBALANCED FORCES AND CONVERGENCE CRITERIA

The stress-transfer iterative process is conducted within each time step t+Δt and it results in the calculation of the unbalanced nodal forces $\underset{\sim}{\Psi}_{t+\Delta t}$, which are calculated by summing the partial terms that arise in each iteration n, $\underset{\sim}{\Psi}_{t+\Delta t} = \sum \underset{\sim}{\Psi}_n$.

In practice, in order to simulate non-linear dam behaviour considering both joint movements and concrete damage, the stress-transfer process is divided into two iterative sub-processes. These sub-processes are performed consecutively: the first, to model the effects due to non-linear joint behaviour under normal and shear stress, and the second, to account for tensile and compressive damage in concrete. As such, the partial unbalanced forces in every iteration *n* are defined as

$$\underset{\sim}{\Psi}_n = \begin{bmatrix} \underset{\sim}{\Psi}_J + \underset{\sim}{\Psi}_C \\ \underset{\sim}{0} \end{bmatrix}_n \tag{3.66}$$

where $\underset{\sim}{\Psi}_J$ and $\underset{\sim}{\Psi}_C$ are the nodal forces associated with unbalanced stresses that arise due to joints and concrete non-linear behaviour, respectively. The unbalanced stresses are computed as the difference between the installed stresses and material strength, using the appropriate constitutive models for the joints (3.8.2) and for concrete (3.8.3).

The convergence of the stress-transfer process is verified at the end of each iteration, with the goal of evaluating structural equilibrium (de Borst & Sluys, 1999; Zienkiewicz et al., 2014). If the dam has enough resistant capacity to support the applied loads, being able to redistribute the unbalanced stresses, equilibrium is reached, and the non-linear iterative process is convergent. Otherwise, overall equilibrium is not achieved and the process diverges. This convergence verification is usually carried out by analysing the computed unbalanced forces $\underset{\sim}{\Psi}_{t+\Delta t,n}$ or the corresponding displacements $\underset{\sim}{u}^{\Psi}_{t+\Delta t,n}$, which are compared with

a predefined tolerance value. The technique adopted in the proposed method aims to control the convergence of the stress-transfer process (Fig. 3.15) based on the "unbalanced displacements" vector, which is obtained at the end of iteration *n* as

$$\begin{bmatrix} \underset{\sim}{u}^{\Psi}_{t+\Delta t,n} \\ \underset{\sim}{0} \end{bmatrix} = \underline{K}^{*^{-1}} \underset{\sim}{\Psi}_{t+\Delta t,n} = \underline{K}^{*^{-1}} \begin{bmatrix} \underset{\sim}{\Psi}_J + \underset{\sim}{\Psi}_C \\ \underset{\sim}{0} \end{bmatrix}_{t+\Delta t,n} \tag{3.67}$$

Essentially, these "unbalanced displacements" are compared with those computed in the first iteration, and the relation between their norms must be smaller than the tolerance value μ (e.g., $\mu = 10^{-7}$). Based on this criterion, the non-linear iterative process is convergent if the displacements associated with the unbalanced forces decrease from iteration to iteration, until they become small enough to be disregarded. In that case, global equilibrium is reached at t+Δt, the stress-transfer process ends, and the dynamic calculation will move on to the next time step. Otherwise, the process diverges if the unbalanced stresses, and hence the corresponding forces, increase consecutively over several iterations, resulting in unreasonable values for the "unbalanced displacements". Thus, structural equilibrium will not occur. In summary, the adopted stress-transfer convergence criterion can be expressed as

$$\begin{cases} \underset{n\to\infty}{Norm} < \mu & \rightarrow convergence \\ \underset{n\to\infty}{Norm} > \mu & \rightarrow divergence \end{cases}, \qquad \underset{n}{Norm} = \frac{\| \underset{\sim}{u}^{\Psi}_{t+\Delta t,n} \|}{\| \underset{\sim}{u}^{\Psi}_{t+\Delta t,n=1} \|} \tag{3.68}$$

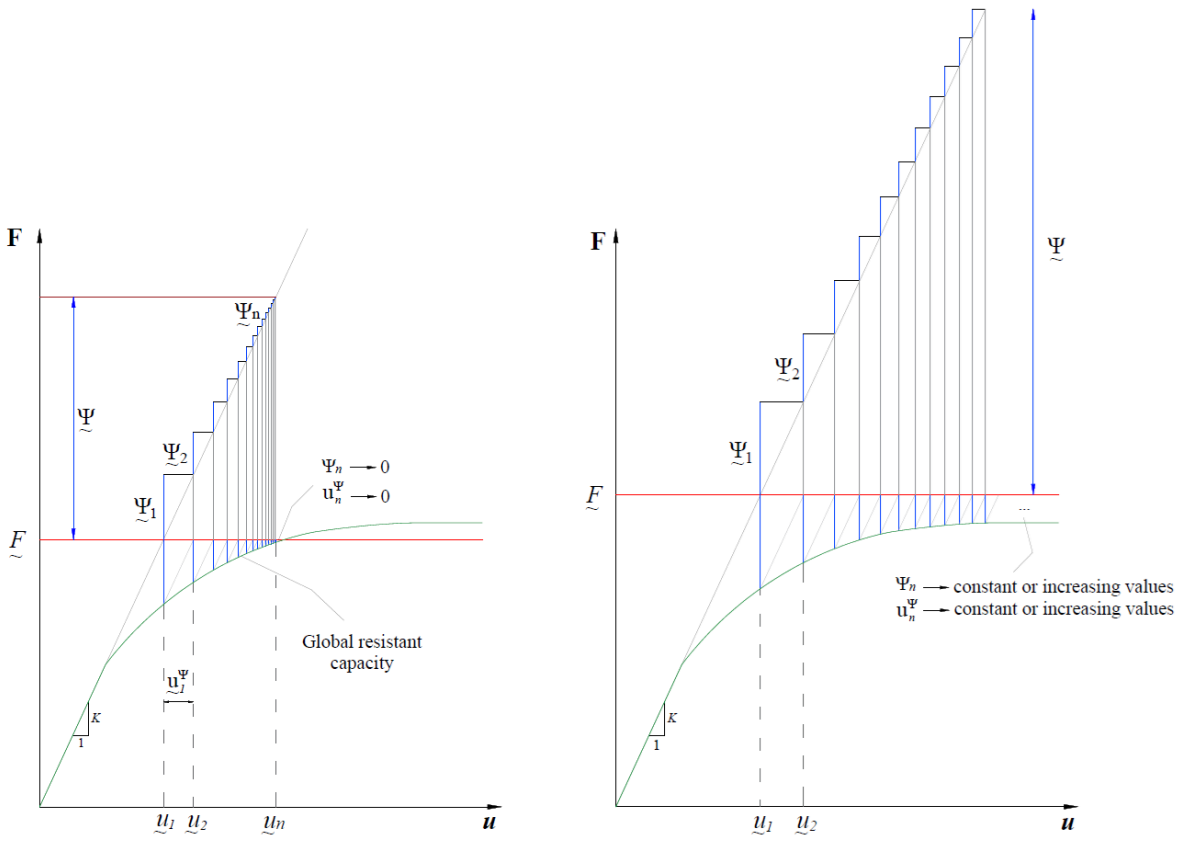

Fig. 3.15 Stress-transfer iterative method. Scheme representing a global applied force-displacement equilibrium for convergent and divergent processes (the time step index is omitted as a simplification).

3.8.2 CONSTITUTIVE MODEL FOR NON-LINEAR JOINT BEHAVIOUR

The non-linear joint behaviour of joints is simulated in this work using a constitutive model based on the Mohr-Coulomb failure criterion and considering appropriate normal and shear stress-displacement laws to simulate opening/closing and sliding movements, assuming that joints cannot develop high tensile stresses (Fenves et al., 1992; Lau et al., 1998).

In this model[4], the main properties are the elastic properties of the joint material (recall subchapter 3.4), namely the namely the normal K_N and shear K_T stiffness, and the strength properties, which are the cohesion c and the friction angle ϕ. Moreover, in order to evaluate the admissibility of the stress state installed in a generic point of the joint surface[5], given by $\underset{\sim}{\sigma} = \left[\tau_1 \quad \tau_2 \quad \sigma_N\right]^T$, it is convenient to consider the normal stress value σ_N and an equivalent positive shear stress value $\tau = \sqrt{\tau_1^2 + \tau_2^2}$, to be compared with the joint material strength.

Regarding the stress thresholds that bound linear elastic behaviour, based on the Mohr Coulomb criterion the normal tensile strength f_t and the shear strength τ_R, always positive valued, are defined as

$$f_t = c \cdot \frac{2\cos(\phi)}{1+\sin(\phi)} \tag{3.69}$$

$$\tau_R = c + |\sigma_N| \cdot \tan(\phi) \tag{3.70}$$

As seen in the above equations, the joints resist to opening and sliding movements by friction and cohesion, while the resistance to shear forces also depends on the applied normal stress (the dilatancy effect is not considered). The cohesion can be equal to zero, to represent flat and/or smooth joints, or have a specific value, to account for a certain degree of resistance to sliding (e.g., in arch dams, the contact surfaces between adjacent blocks may include shear keys to increase resistance to shear forces). Assuming the hypothesis of null cohesion (Fig. 3.16), the normal tensile strength f_t is equal to zero and the joint opens under tensile forces, while the shear strength τ_R becomes proportional to the normal compression. Otherwise, if cohesion is considered (Fig. 3.17), then the joint resists to tensile forces to some extent, while the resistance to shear forces increases.

Regarding joint behaviour under normal stresses, under compression the joint closes and therefore it behaves linearly. However, under tension the joint opens once the tensile strength is reached, $\sigma_N \geq f_t$. In what concerns the response under shear stress, considering an applied normal stress σ_a, joint behaviour is linear until the corresponding shear strength is exceeded, $\tau \geq \tau_R$, and henceforth, shear sliding occurs. When the joint is closed, the friction between the two faces is more effective and hence the shear resistance τ_R increases.

[4] The interfaces are simulated in the finite element meshes using compatible interface elements with 16 nodes (recall Fig. 3.11).
[5] Considering a local orthogonal coordinate system, it is assumed that displacement in direction *i* only produces stress in direction *i* (Fenves et al., 1992).

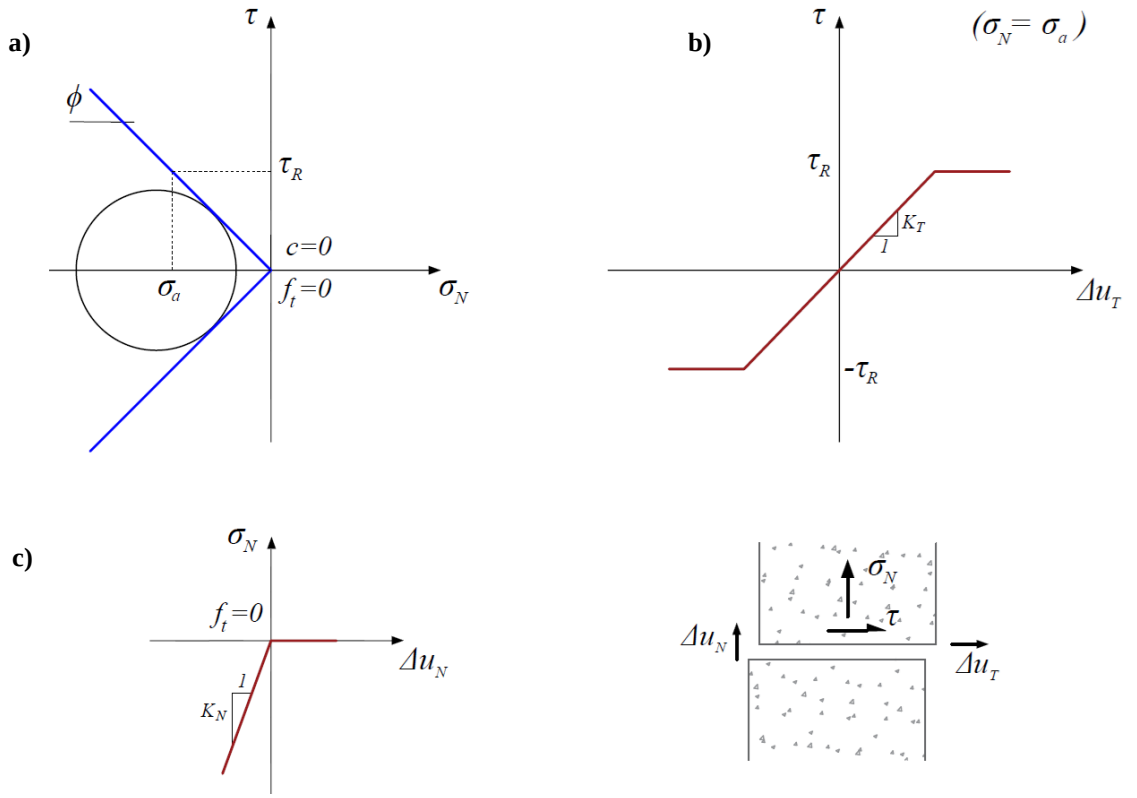

Fig. 3.16 Joint model used to simulate non-linear behaviour, assuming null cohesion: a) Mohr-Coulomb failure criterion, and b) shear stress-displacement law and c) normal stress-relative displacement law.

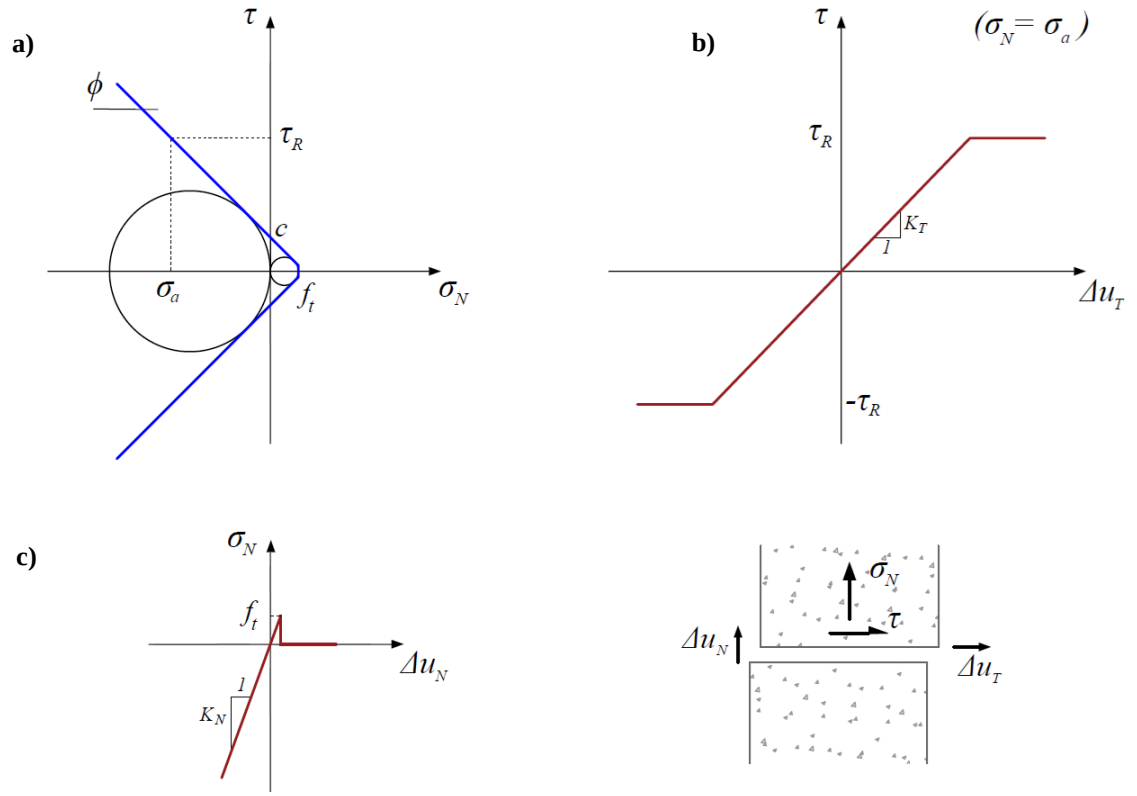

Fig. 3.17 Joint model used to simulate non-linear behaviour, considering cohesion: a) Mohr-Coulomb failure criterion, and b) shear stress-displacement law and c) normal stress-relative displacement law.

Concerning its implementation in the developed non-linear time-stepping method, the joint constitutive model is incorporated into the global stress-transfer iterative process. Furthermore, the fact that it is based on simple stress-relative displacement relations simplifies its use in the finite element code, since nodal displacements are easily obtained for the nodes of the surface elements in the dynamic calculations.

Therefore, the stress tensor that includes normal and shear components, $\underset{\sim}{\sigma} = \begin{bmatrix} \tau_1 & \tau_2 & \sigma_{\mathrm{N}} \end{bmatrix}^{\mathrm{T}}$, can be calculated for all Gauss points on both faces of all surface elements. Then, knowing the joint material elastic and strength properties, the applied normal σ_{N} and equivalent shear τ stresses are compared with the tensile f_t and shear τ_R strength at each point. In case the material strength is exceeded, the corresponding unbalanced stresses are calculated, $\sigma_{\mathrm{N}} > f_t \rightarrow \sigma_{\Psi,\mathrm{N}} = f_t - \sigma_{\mathrm{N}}$ and $\tau > \tau_R \rightarrow \tau_{\Psi} = \tau_R - \tau$. After that, knowing that the equivalent unbalanced shear stress τ_{Ψ} is decomposed into two tangential components, $\tau_{\Psi,1}$ and $\tau_{\Psi,2}$, the vector of unbalanced normal and shear stresses at each point of the joint is $\underset{\sim}{\sigma}_{\Psi} = \begin{bmatrix} \tau_{\Psi,1} & \tau_{\Psi,2} & \sigma_{\Psi,\mathrm{N}} \end{bmatrix}^{\mathrm{T}}$. Finally, the vector of unbalanced forces of the surface element

$$\underset{\sim}{\Psi}_J^e = \int_{\Gamma_j^e} \underline{\mathrm{N}}_j^{\mathrm{T}} \, \underline{\mathrm{T}}_j^{\mathrm{T}} \underset{\sim}{\sigma}_{\Psi} \, d\Gamma \tag{3.71}$$

is calculated using the Gauss integration method (as explained in section 3.5.2), and the global vector of unbalanced forces due to non-linear join behaviour $\underset{\sim}{\Psi}_J$ is calculated by summing all the element contributions (Zienkiewicz et al., 2013).

3.8.3 CONSTITUTIVE DAMAGE MODEL FOR CONCRETE

The non-linear behaviour of concrete up to failure is simulated based on a three-dimensional isotropic constitutive damage model with strain-softening, considering two independent scalar damage variables, d^+ for tension and d^- for compression. (Faria, 1994; S. Oliveira, 2000; S. Oliveira & Faria, 2006). This damage model is able to reproduce crack formation and propagation under tension, and it can also cope with 3D confinement under compression (S. Oliveira, 2000), based on the fundamental concepts of Continuum Damage Mechanics[6] (CDM) and of Fracture Mechanics[7]. These are two fundamental features to account for in non-linear seismic analysis of concrete dams, given that considerable tensions and compressions may occur in the dam body under strong earthquakes.

Concrete is a material with high compressive strength that presents a fragile behaviour under tension. Its instantaneous failure process is characterized by a softening phenomenon, i.e. a post-peak stress strength

[6] Continuum Damage Mechanics, introduced by Kachanov (1958), describes the evolution of the irreversible deterioration phenomenon that occurs inside a given material under applied forces that exceed its strength, from the undamaged state to the occurrence of macroscopic cracks, resulting in a reduction of its intrinsic stiffness.

[7] Fracture Mechanics is a field that studies the propagation process of existing cracks in materials, accounting for the energy release and softening phenomena, in order to describe the non-linear behaviour of structural elements with macroscopic discontinuities up to failure (Bažant & Oh, 1983; Hillerborg, 1985).

decrease, combined with a global stiffness decrease, due to the increase of internal damage (e.g., formation and growth of microcracks) and the accumulation of irreversible strains (Faria, 1994; S. Oliveira, 2000).

In Continuum Damage Mechanics, the state of internal damage of a certain material can be characterized and quantified based on internal damage variables (Kachanov, 1958, 1986). Considering a material point of initial elemental area A, the application of external loading can lead to the formation and growth of micro-cracks due and consequently to a reduction of the "effective" resisting area $\tilde{\mathrm{A}}$, which is determined by subtracting the damaged area A_d to the initial undamaged area. Therefore, the damage variable *d* represents the surface density of material defects at a local level,

$$d = \frac{\mathrm{A}_d}{\mathrm{A}} = 1 - \frac{\tilde{\mathrm{A}}}{\mathrm{A}} \tag{3.72}$$

and its value ranges from 0, representing an undamaged or intact state, to 1, when failure occurs. Damage can only increase, given the irreversible nature of the internal material deterioration process. For a material with internal damage *d*, the stress installed at the resisting area $\tilde{\mathrm{A}}$ is referred to as effective stress $\tilde{\sigma}$ (Lemaitre, 1984), to be distinguished from the true stress, σ (Fig. 3.18).

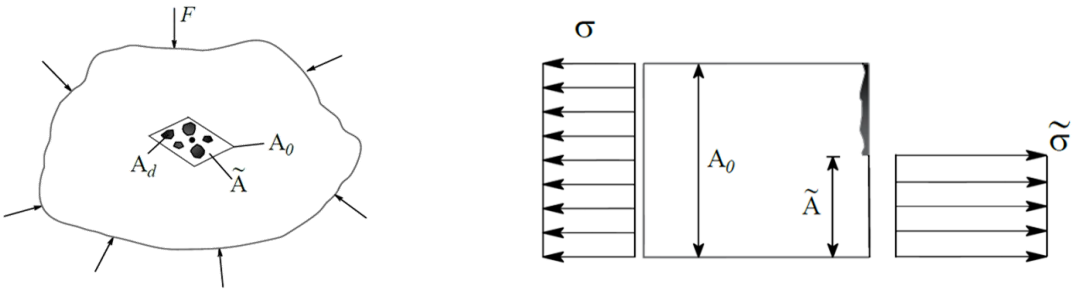

Fig. 3.18 Material with internal damage: effective area and effective and true stress (S. Oliveira, 2000).

The stress-strain constitutive relation can be written in terms of the effective stress as, $\tilde{\sigma} = E \cdot \varepsilon$, as done for an undamaged material (Lemaitre & Chaboche, 1978), or in terms of the true stress, $\sigma = (1-d) E \cdot \varepsilon$, considering the damage value, where E is the material Young's modulus and ε is the strain value. Generalizing for a three-dimensional problem, the effective stress tensor $\tilde{\underline{\sigma}}$ is given by $\tilde{\underline{\sigma}} = \underline{D} \cdot \underline{\varepsilon}$, where $\underline{D}$ the elasticity matrix and $\underline{\varepsilon}$ stands for the strain tensor. Therefore, assuming a material with internal isotropic damage *d*, the non-linear constitutive relation can be defined as

$$\underline{\sigma} = (1-d)\tilde{\underline{\sigma}} = (1-d)\underline{D} \cdot \underline{\varepsilon} \tag{3.73}$$

The implemented constitutive model aims to simulate concrete non-linear behaviour with strain-softening under both tensile and compressive stresses, which naturally involve dissimilar features (the accumulation of irreversible strains is not incorporated). As such, to characterize the state of internal damage of concrete, two independent scalar damage variables are considered: d^+, for damage under tension, and d^-, for damage

under compression (Faria, 1994; S. Oliveira, 2000; S. Oliveira & Faria, 2006). Furthermore, the effective stress tensor $\tilde{\underline{\sigma}}$ is decomposed into tensile and compressive effective stress tensors, $\tilde{\underline{\sigma}}^{+}$ and $\tilde{\underline{\sigma}}^{-}$, represented in the space of the principal stresses and directions (Faria et al., 1998).

The formulation of a realistic constitutive model must be consistent from a thermodynamic point of view, to properly represent the irreversible naturel of material deterioration. For the present model, this requirement leads to the postulation of a free energy potential ψ that must verify the fundamental thermodynamic condition $\psi \geq 0$, using an expression similar to the specific elastic strain energy (Mazars & Pijaudier-Cabot, 1989) that is related to the area underneath an uniaxial stress-strain diagram. Taking into account that the energy dissipation can never decrease during the material deterioration process, then the Clausius-Duhem inequality, $-\dot{\psi} + \underline{\sigma}^{\mathrm{T}} \dot{\underline{\varepsilon}} \geq 0$, must be fulfilled (Lubliner, 1972).

Therefore, from the defined free energy potential (Faria et al., 1998), considering the decomposition of the effective stress tensor tensile $\tilde{\underline{\sigma}}^{+}$ and compressive $\tilde{\underline{\sigma}}^{-}$ stresses, and the use of two independent scalar damage variables d^{+} and d^{-}, the constitutive damage law is simply defined as (S. Oliveira & Faria, 2006)

$$\mathrm{e}\,\underline{\sigma} = (1-d^{+})\,\tilde{\underline{\sigma}}^{+} + (1-d^{-})\,\tilde{\underline{\sigma}}^{-} \tag{3.74}$$

where the damage variables are always $d^{+} \geq 0$ and $d^{-} \geq 0$, in order to in order to properly represent the irreversible nature of material deterioration.

This non-linear constitutive law enables the calculation of the true stresses $\underline{\sigma}$ at any material point, knowing the tensile and compressive components of the effective stress, and considering an internal damage state characterized by the isotropic tensile and compressive damage variables. To facilitate the interpretation of this constitutive law, stress-strain diagrams for uniaxial tension and compression are presented in Fig. 3.19, where f_0^{+} and f_0^{-} indicate the maximum admissible tension and compression for linear elastic behaviour, as determined in a standard uniaxial tests, while f_t and f_c are the peak tensile and compressive stresses.

With regard to the implementation of the constitutive damage model, the fact that it is based on a clear stress-strain relation makes it perfectly suitable to be used in a finite element code, since the displacements (and hence stresses and strains) can be easily obtained, thus allowing a simple calculation of the required internal variables. In this work, the damage model is implemented as part of the stress-transfer iterative process for non-linear dam behaviour simulation. Therefore, from the nodal displacements calculated at each time step t+Δt in the dam body, the strain tensors and the effective stresses are easily computed for all Gauss points of every dam finite element. Then, if concrete strength is exceeded, the tensile and compressive damage variables are obtained based on appropriate damage evolution laws (as described next), and the and the real stress tensor is obtained using the constitutive damage law in eq. (3.74). After that, the unbalanced stresses are computed as the difference between the effective and true stress tensors, $\underline{\sigma}_{\Psi} = \underline{\sigma} - \tilde{\underline{\sigma}}$. At last, the corresponding elementary unbalanced forces,

$$\underline{\Psi}_{C}^{e} = \int_{\Omega_s^e} \underline{\mathrm{B}}_{u}^{\mathrm{T}} \underline{\sigma}_{\Psi}\, d\Omega \tag{3.75}$$

are calculated using the Gauss integration, and then the global vector of unbalanced forces due to non-linear concrete behaviour $\underset{\sim}{\Psi}_C$ is determined by assembling all element contributions (Zienkiewicz et al., 2013).

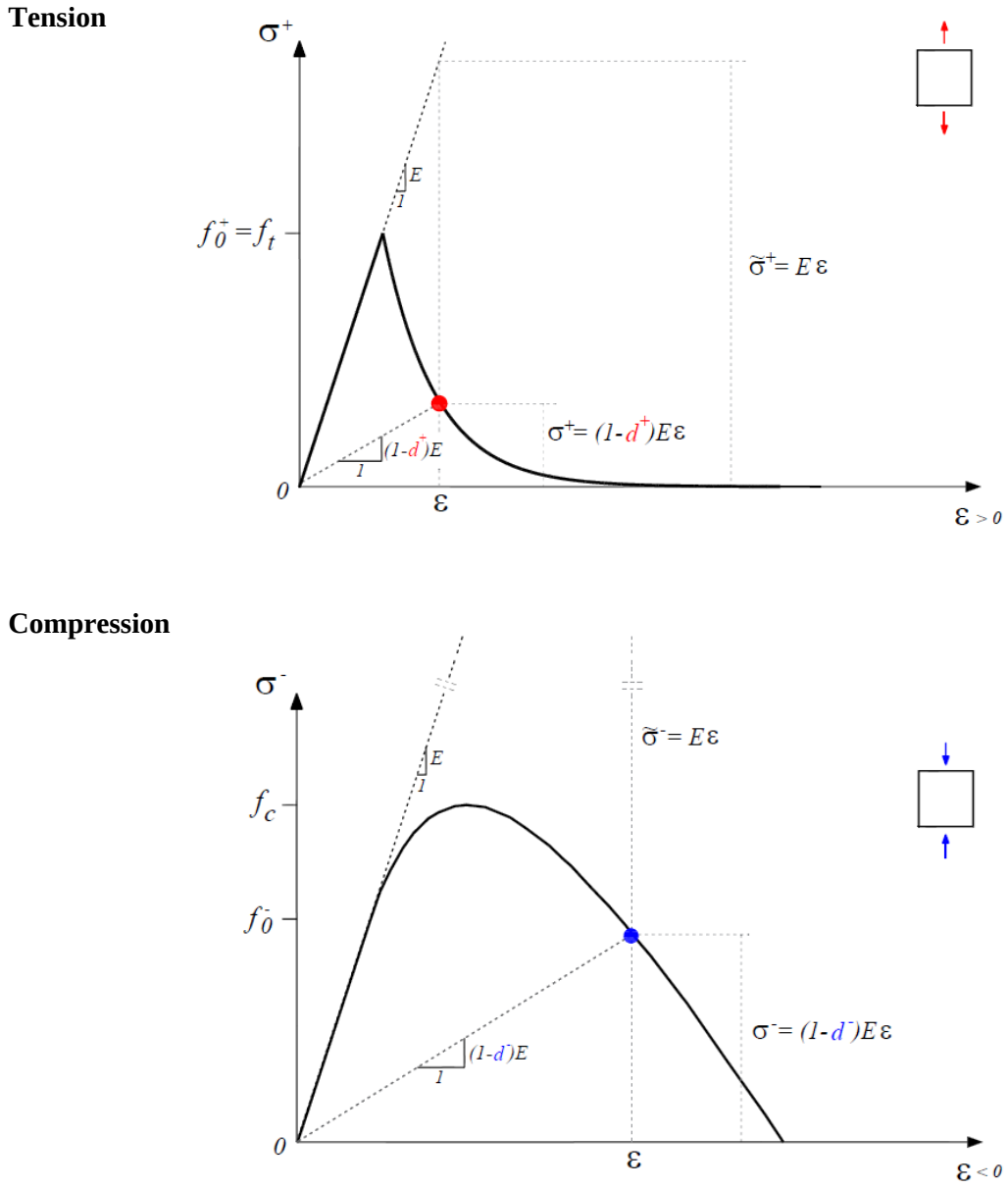

Fig. 3.19 Constitutive damage model with two independent damage variables. Stress-strain diagrams for uniaxial tension and compression.

DAMAGE CRITERIA AND DAMAGE EVOLUTION LAWS

In order to simulate the evolution of the concrete deterioration process, the constitutive model includes specific damage criteria and damage evolution laws, to bound linear elastic behaviour and to control the progression of both tensile and compressive damage. This is a consistent damage formulation which incorporates a "memory" feature that accounts for the irreversible nature of the damage process (S. Oliveira, 2000; S. Oliveira & Faria, 2006).

The bounding surfaces of the linear elastic domain are determined based on specific stress thresholds. To enable the comparison with general stress states, and considering the partition of the effective stress tensor $\tilde{\underset{\sim}{\sigma}}$ into its tensile $\tilde{\underset{\sim}{\sigma}}^{+}$ and compressive $\tilde{\underset{\sim}{\sigma}}^{-}$ components, it is convenient the use of equivalent effective stresses $\tilde{\tau}$, quantified by positive scalar values (Faria & Oliver, 1993; Simo & Ju, 1987). Concerning behaviour under tension, the equivalent effective tensile stress is expressed as

$$\tilde{\tau}^{+} = \sqrt{\left(\tilde{\underset{\sim}{\sigma}}^{+}\right)^{\mathrm{T}} \underline{D}^{-1} \tilde{\underset{\sim}{\sigma}}^{+}} \tag{3.76}$$

and the tensile threshold is defined as (Faria et al., 1998)

$$r_0^{+} = \frac{f_0^{+}}{\sqrt{E}} \tag{3.77}$$

As for behaviour under compression, assuming a bounding surface based on the Drucker-Prager yield criterion, the equivalent effective compressive stress is given by

$$\tilde{\tau}^{-} = \sqrt{\sqrt{3}(\mathrm{K}\,\tilde{\underset{\sim}{\sigma}}_{oct}^{-} + \tilde{\tau}_{oct}^{-})} \tag{3.78}$$

and the compressive threshold is determined as

$$r_0^{-} = \sqrt{\frac{\sqrt{3}}{3}(K.f_0^{-} + \sqrt{2}.\left|f_0^{-}\right|)} \tag{3.79}$$

where K is a material property related to the yield surface, while $\tilde{\underset{\sim}{\sigma}}_{oct}^{-}$ and $\tilde{\tau}_{oct}^{-}$ are the normal and shear components of the octahedral stress obtained from tensor $\tilde{\underset{\sim}{\sigma}}^{-}$.

Regarding the damage criterion, it is assumed that the damage process begins once the equivalent stress exceeds the linear elastic threshold, $\tilde{\tau}^{\pm} > r_0^{\pm}$. From that moment on, structural analysis is performed assuming non-linear behaviour, and the stress thresholds $r_k^{\pm}$ are redefined as the greatest values ever reached by the respective equivalent stresses $\tilde{\tau}^{\pm}$. Subsequently, the deterioration process will progress and hence the damage variables increase when the new equivalent effective stresses surpass the last stress threshold, $\tilde{\tau}_{k+1}^{\pm} > r_k^{\pm}$ (Lemaitre, 1984). Based on this criterion (Faria, 1994; S. Oliveira, 2000; S. Oliveira & Faria, 2006) the stress thresholds and the damage values are constantly updated throughout the non-linear calculation, enabling to control the evolution of the damage phenomenon and simultaneously to account for its irreversibility. In summary, the damage criteria for both tension and compression are as follows

$$\begin{cases} \tilde{\tau}_{k+1}^{\pm} \le r_0^{\pm} & \rightarrow \quad \mathrm{d}^{\pm} = 0 & \rightarrow \quad r_{k+1}^{\pm} = r_0^{\pm} & (\textit{linear domain}) \\ \tilde{\tau}_{k+1}^{\pm} > r_k^{\pm} & \rightarrow \quad d_{k+1}^{\pm} \ge d_k^{\pm} > 0 & \rightarrow \quad r_{k+1}^{\pm} = \max(r_k^{\pm}; \tilde{\tau}_{k+1}^{\pm}) & (\textit{non-linear domain}) \end{cases} \tag{3.80}$$

In what concerns damage progression, appropriate evolution laws are used for tensile and compressive damage variables (Faria, 1994; S. Oliveira, 2000; S. Oliveira & Faria, 2006), with a view to reproduce the phenomena that occur in concrete up to failure, namely of softening under tension and of hardening followed by softening under compression.

Considering the behaviour under tension, the stress-strain constitutive law has an ascending branch, for the linear elastic domain, followed by a post-peak descending branch to simulate softening until failure. Assuming an exponential softening branch, the evolution of the scalar tensile damage variable yields

$$d^{+} = 1 - \frac{r_0^{+}}{\tilde{\tau}^{+}} e^{\mathrm{A}^{+}\left(1-\frac{\tilde{\tau}^{+}}{r_0^{+}}\right)} \tag{3.81}$$

where A^{+} is a parameter fixed to ensure an appropriate dissipation of the tensile fracture energy G_f during the fracture process.

In what concerns the behaviour up to failure under compression, the constitutive stress-strain relation is characterized by a linear ascending branch until the maximum uniaxial stress is exceeded, followed by a hardening branch, and, after surpassing the peak compressive stress, by a descending curve to simulate softening. Accounting for both hardening and softening phenomena under compression, the evolution law of the scalar compressive damage variable is defined as

$$d^{-} = 1 - \frac{r_0^{-}}{\tilde{\tau}^{-}}(1-\mathrm{A}^{-}) - \mathrm{A}^{-} e^{\mathrm{B}^{-}\left(1-\frac{\tilde{\tau}^{-}}{r_0^{-}}\right)} \tag{3.82}$$

where A^{-} and B^{-} are parameters defined by adjusting the numerical stress-strain curve with an experimental one for uniaxial compression, to guarantee an adequate energy dissipation during the compressive crushing process.

FRACTURE PROCESS AND STRAIN LOCALIZATION

Considering the lower tensile strength of concrete and its fragile behaviour under tension, it is required to properly simulate the cracking growth process leading to fracture. When the tensile strength is exceeded, the strain-softening and internal damage increase due to the formation/growth of microcracks. According to the fundamentals of Non-Linear Fracture Mechanics, this happens in a microcracking zone located at the crack tip, spread over a band of width w_b[8], the so-called Fracture Process Zone (Fig. 3.20).

The fracture process originates a certain amount of energy, associated with crack formation/growth, which must be fully dissipated in the distributed cracking band (Hillerborg et al., 1976). The surface energy

[8] The width of the Fracture Process Zone is a constant material property and depends on the maximum concrete aggregate dimension. For example, in large concrete dams aggregates of large dimensions (around several cm) are used, and a cracking band width of about 1 m can be assumed.

involved in the crack growth can be considered as a material property, referred to as fracture energy G_f (kN.m/m^2). The energy dissipated per volume unit is the specific fracture energy g_f (kN.m/m^3), given by

$$g_f = G_f / w_b \tag{3.83}$$

Furthermore, the crack propagation depends on the stress installed at the crack tip. Therefore, it is possible to establish a correlation between this stress and the dissipated energy, by regarding the area under the stress-strain diagram as the specific fracture energy g_f (Bažant & Oh, 1983; Pietruszczak & Mróz, 1981).

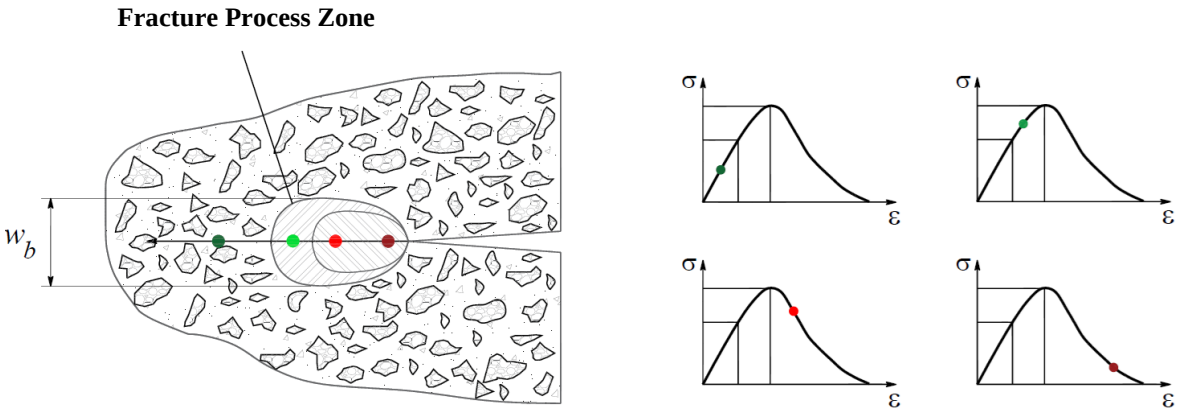

Fig. 3.20 The Fracture Process Zone. Different stress-strain states (S. Oliveira, 2000).

As mentioned previously, during the concrete fracture under tensile stresses, the strain-softening phenomena and consequently damage evolution are localized inside the Fracture Process Zone. For this reason, it is necessary to use constitutive models with softening, which, however, is a feature that involves considerable numerical difficulties due to the localization phenomenon (Bažant & Cedolin, 1979; Bažant & Oh, 1983).

If the non-linear analysis is performed adopting a finite element discretisation and using a constitutive model with softening based on principles resembling the Smeared Crack Approach, as done in this work, then each crack is thought to be distributed over a band inside the finite element and the fracture energy G_f is dissipated on an artificial cracking bandwidth or characteristic length w_b^* (Bažant & Oh, 1983). Usually, given that stresses and damage values are computed at all Gauss quadrature points, the value of the bandwidth is related to their volume (or weight). This can lead to numerical solutions strongly dependent on the mesh refinement, a problem commonly referred to as lack of objectivity of numerical solutions (S. Oliveira & Faria, 2006), a problem that must be wisely accounted for in order to be minimized or avoided (Bažant & Cedolin, 1979; Bažant & Oh, 1983).

For small-scale problems, where very refined meshes are used, the Fracture Process Zone comprises various finite elements, and failure can be localized in zones of null volume. In this case, localization limiters are adopted to make sure that cracking occurs in a minimum volume (Bažant & Planas, 1998; Jirásek, 2002).

For large-scale problems, as is the case for large concrete dams, due to limitations imposed by limited computational capacity, the use of less refined meshes is required. Here, the dimension of the finite elements (and hence associated with Gauss points) is significantly greater than the real cracking bandwidth (S. Oliveira, Faria, et al., 2003; S. Oliveira & Faria, 2006). For this type of problem, in order to ensure an adequate dissipation of the fracture energy G_f, the area below the stress-strain curve must fulfil the condition in eq. (3.83). Therefore, in order to achieve objectivity, it is necessary to use a special constitutive law, associated with an artificial specific fracture energy g_f^*, and, regarding a certain finite element discretisation, to adopt an artificial dimension for the Fracture Process Zone w_b^*, hence guaranteeing that

$$G_f = g_f w_b = g_f^* w_b^* \tag{3.84}$$

The artificial cracking bandwidth w_b^* can be simply calculated based on the size of the finite element where failure occurs, $w_b^* = \sqrt{V^e}$, or using a consistent formulation that also considers the cracking orientation (S. Oliveira, Faria, et al., 2003; S. Oliveira & Faria, 2006; Oliver, 1989). In some cases, it might be possible to adopt a mesh discretisation such that the volumes of the Gauss points are of the same order of magnitude as the dimension of the real FPZ, $w_b^* \approx w_b$; consequently, the real stress-strain diagrams could be used.

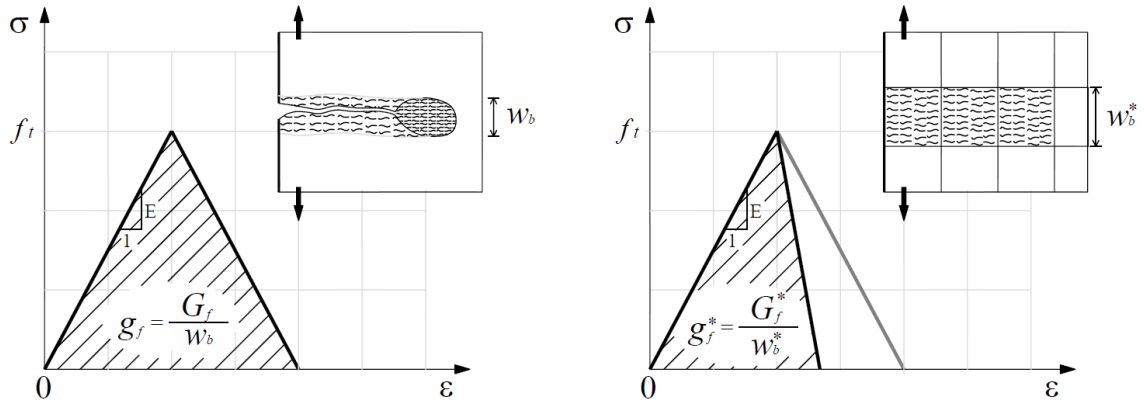

Fig. 3.21 Fracture process: smeared approach. Real and artificial constitutive law and fracture energy (S. Oliveira & Faria, 2006).

3.9 *DAMDYSSA4.0*: FINITE ELEMENT PROGRAM FOR DYNAMIC ANALYSIS OF CONCRETE DAMS

DamDySSA is a 3D finite element program developed in MATLAB for dynamic analysis of concrete dams. This program has been under continuous development for several years in LNEC, in the scope of extensive research conducted at the Concrete Dams Department on modelling the dynamic behaviour of dam-reservoir-foundation systems. The numerical methods proposed in this thesis were implemented in the code of the program (Alegre, 2015; S. Oliveira et al., 2015), which is updated to the new version, *DamDySSA4.0*.

The dynamic behaviour of the dam-reservoir-foundation system is simulated based on the coupled model described in subchapter 3.5, using a finite element formulation in displacements (dam and foundation) and in hydrodynamic pressures (reservoir), and considering specific boundary conditions to account for the dam-water dynamic interaction and the propagation of pressure waves in the reservoir. Generalized damping is considered, with viscous Rayleigh damping being calculated element by element in the solid domain (enabling the definition of areas with different materials or under dissimilar states of deterioration) and energy dissipation due to radiation in the fluid domain. The substructure method is used to compute the foundation block as an elastic and massless substructure, with stiffness and damping components introduced the dam-foundation interface, hence increasing computational efficiency The main loads that can be selected for structural analysis are the dam self-weight (SW), the hydrostatic pressure at the upstream face (HP), and the seismic load (SEISMICL), considering a seismic input composed by three accelerograms.

This new version of the program now includes three modules for dynamic analysis of concrete dams, namely for: (i) complex modal analysis with generalized damping, using the state-space formulation proposed in 3.6; (ii) linear seismic response analysis, based on the coupled time-stepping procedure described in 3.7; and (iii) non-linear seismic analysis, using the time-stepping formulation and the stress-transfer method presented in 3.8, considering non-linear constitutive models to simulate joint movements and tensile and compressive damage in concrete. The algorithm of the program is presented in Fig. 3.22.

In order to run the intended calculations *DamDySSA* requires, as input, a specific Excel data file containing all data on the mesh of the dam-reservoir-foundation system, including the coordinates of nodes, the definition of the solid and fluid 3D elements and the interface elements, the elastic properties of the dam and foundation materials, the water properties, and the strength properties needed for the non-linear constitutive models of both concrete and joints. The water level is chosen as an input by the user and thus the reservoir mesh is automatically readjusted accordingly. The program also needs an additional file with the acceleration time histories that define the seismic input.

As for the main outputs, *DamDySSA* provides: (i) the frequency values and modal configurations for several vibration modes, computed using the modal analysis module; and (ii) the coupled response time histories (displacements and pressures), 3D deformed shapes, fields of principal stresses, displacements and stresses envelopes, and damage distributions, calculated using the linear or non-linear seismic analyses modules.

3.9.1 GRAPHICAL USER INTERFACE

After the implementation of the proposed methods into the finite element code of *DamDySSA*, a graphical user interface was developed using the GUIDE tool in MATLAB. The aim was not only to develop an interactive and easy-to-use executable version of the program, allowing numerical simulations to be conducted in a simple way and to facilitate the analysis and interpretation of the results, but also to provide a tool that can be used in the future in LNEC, by researchers and by master and doctoral students, to analyse the dynamic behaviour of concrete dams, to support structural health monitoring and to conduct seismic safety studies. The main menus and panels of this graphical interface are shown in Fig. 3.23 to Fig. 3.29.

DAMDYSSA4.0

Data input. Finite element coupled model

1. Read input data files: mesh data (coordinates, elements), material properties (dam, foundation, reservoir), and seismic input
2. Reservoir mesh: select reservoir level and automatically readjust reservoir mesh
3. Compute foundation substructure
4. Calculate the solid ($\underline{m}$, $\underline{c}$, $\underline{k}$), fluid ($\underline{S}$, $\underline{R}$, $\underline{H}$), and coupling ($\underline{Q}$) matrices, and assemble the global mass $\underline{M}$, damping $\underline{C}$, and stiffness $\underline{K}$ matrices of the dam-reservoir-foundation system

Dynamic analysis

5. Complex modal analysis
   - 5.1. Select number of modes N_{MOD} (reduced modal analysis)
   - 5.2. State-space formulation: dam-reservoir-foundation system with generalized damping
     - 5.2.1. Calculate the coupled state matrix $\underline{A}=\begin{bmatrix} \underline{0} & \underline{I} \\ -\underline{M}^{-1}\underline{K} & -\underline{M}^{-1}\underline{C} \end{bmatrix}$
     - 5.2.2. Solve the eigenproblem $\left[\underline{A}-\lambda\,\underline{I}\right]\underset{\sim}{\phi}=\underset{\sim}{0}$
     - 5.2.3. Vibration mode n: compute the natural frequency ω_n , damping ratio ξ_n , and modal configuration $\underset{\sim}{\varpi}_n$
   - 5.3. Present results: natural frequencies; oscillatory motion time histories and 3D modal configurations (dam and reservoir)
6. Linear seismic analysis
   - 6.1. Select load combination (SW; HP; SEISMICL) and calculate the vector of nodal forces $\underset{\sim}{F}$
   - 6.2. Define null initial conditions $\underset{\sim}{q}(0)=\underset{\sim}{0}$, $\dot{\underset{\sim}{q}}(0)=\underset{\sim}{0}$, $\ddot{\underset{\sim}{q}}(0)=\underset{\sim}{0}$ and calculate the constants α_i for Newmark's method
   - 6.3. Compute the equivalent stiffness matrix, $\underline{K}^{*}=\alpha_0\underline{M}+\alpha_1\underline{C}+\underline{K}$
   - 6.4. Time-stepping procedure: calculate the response of dam-reservoir-foundation system [step t+Δt]
     - 6.4.1. Compute the equivalent force, $\underset{\sim}{P}^{*}_{t+\Delta t}=\underset{\sim}{F}_{t+\Delta t}+\underline{M}\left(\alpha_0\underset{\sim}{q}_t+\alpha_2\dot{\underset{\sim}{q}}_t+\alpha_3\ddot{\underset{\sim}{q}}_t\right)+\underline{C}\left(\alpha_1\underset{\sim}{q}_t+\alpha_4\dot{\underset{\sim}{q}}_t+\alpha_5\ddot{\underset{\sim}{q}}_t\right)$
     - 6.4.2. Solve the equation $\underline{K}^{*}\cdot\underset{\sim}{q}_{t+\Delta t}=\underset{\sim}{P}^{*}_{t+\Delta t}$ to calculate the coupled response $\underset{\sim}{q}_{t+\Delta t}$
     - 6.4.3. Compute the first- and second-time derivatives: $\dot{\underset{\sim}{q}}_{t+\Delta t}$ and $\ddot{\underset{\sim}{q}}_{t+\Delta t}$
     - 6.4.4. Repeat for the next time step
   - 6.5. Calculate the displacements $\underset{\sim}{u}$, velocities $\dot{\underset{\sim}{u}}$ and accelerations $\ddot{\underset{\sim}{u}}$, and the hydrodynamic pressures $\underset{\sim}{p}$
   - 6.6. For each dam finite element: compute the elastic stress tensors $\underset{\sim}{\sigma}$ for all Gauss points
   - 6.7. Present results: response time histories for selected points; 3D deformed shapes and stress fields, displacements and stresses envelopes
7. Non-linear seismic analysis
   - 7.1. Same as 6.1 and 6.2
   - 7.2. Initialize damage variables, d^{+} and d^{-} , and stress thresholds, r^{+} and r^{-}
   - 7.3. Time-stepping procedure: calculate the response of dam-reservoir-foundation system [step t+Δt]
     - 7.3.1. Same as 6.4.1 and 6.4.2

Fig. 3.22 Algorithm of the new version of the program *DamDySSA4.0*.

7.3.2. Obtain the response in displacements $\underset{\sim}{q}_{t+\Delta t} \rightarrow \underset{\sim}{u}_{t+\Delta t}$ for the iterative process

7.3.3. Stress-transfer iterative process 1 – joint non-linear behaviour (iteration n+1)

- Calculate non-linear displacements: first iteration, $\underset{\sim}{u}_{NL} = \underset{\sim}{u}_{t+\Delta t}$; next iterations, $\underset{\sim}{u}_{NL} = \underset{\sim}{u}_{n+1}$
- For each joint element:
  - Read joint material elastic and strength properties (K_N, K_T, c and ϕ) and the nodal displacements $\underset{\sim}{u}^{e}_{NL}$
  - For each Gauss point: compute elastic stresses $\underset{\sim}{\sigma}$, verify non-linear behaviour, and calculate the unbalanced stresses $\underset{\sim}{\sigma}_{\Psi}$
  - Calculate the elementary unbalanced nodal forces $\underset{\sim}{\Psi}^{e}_{J,n+1}$
- Assemble the unbalanced forces $\underset{\sim}{\Psi}_{J,n+1}$
- Verify the convergence of the iterative process 1: $\underset{n}{Norm} = \|\underset{\sim}{u}^{\Psi}_{t+\Delta t,n}\| / \|\underset{\sim}{u}^{\Psi}_{t+\Delta t,n=1}\| < \mu$
- Update the non-linear response at t+Δt, by solving $\underline{K}^{*} \cdot \underset{\sim}{q}_{t+\Delta t} = \underset{\sim}{P}^{*}_{t+\Delta t} + \underset{\sim}{\Psi}$
- Repeat all previous steps for the next iteration until convergence is achieved

7.3.4. Stress-transfer iterative process 2 – concrete non-linear behaviour (iteration n+1)

- Compute non-linear displacements: first iteration: $\underset{\sim}{u}_{NL}$ from iterative process 1; subsequent iterations: $\underset{\sim}{u}_{NL} = \Delta\underset{\sim}{u} = \underset{\sim}{u}_{n+1} - \underset{\sim}{u}_{n}$ (displacement increment)
- Read data from iteration n (all Gauss points): damage variables, d_n^{+} and d_n^{-}, stress thresholds, r_n^{+} and r_n^{-}, and effective stress tensors $\tilde{\underset{\sim}{\sigma}}$
- For each dam element
  - Load concrete elastic and strength properties ($E, \nu, \underline{D}$; f_0^{+}, G_f, w_f; $f_0^{-}, f_{0,2}^{-}, f_c^{-}$) and the nodal displacements $\underset{\sim}{u}^{e}_{NL}$
  - Compute parameters for tensile/compressive damage evolution laws r_0^{+}, A^{+}; r_0^{-}, B^{-}, A^{-}
  - For each Gauss point: calculate effective stresses $\tilde{\underset{\sim}{\sigma}}$, verify damage criteria and compute damage variables *d+* and *d-*, true stresses $\underset{\sim}{\sigma}$, and unbalanced stresses $\underset{\sim}{\sigma}_{\Psi}$
  - Calculate the elementary unbalanced nodal forces $\underset{\sim}{\Psi}^{e}_{C,n+1}$
- Assemble the unbalanced forces $\underset{\sim}{\Psi}_{C,n+1}$
- Verify the convergence of the iterative process 2: $\underset{n}{Norm} = \|\underset{\sim}{u}^{\Psi}_{t+\Delta t,n}\| / \|\underset{\sim}{u}^{\Psi}_{t+\Delta t,n=1}\| < \mu$
- Update the non-linear response at t+Δt, by solving $\underline{K}^{*} \cdot \underset{\sim}{q}_{t+\Delta t} = \underset{\sim}{P}^{*}_{t+\Delta t} + \underset{\sim}{\Psi}$
- Verify the convergence of the iterative process 2
- Repeat all previous steps for the next iteration until convergence is achieved

7.4. Determine the displacements $\underset{\sim}{u}$, velocities $\dot{\underset{\sim}{u}}$ and accelerations $\ddot{\underset{\sim}{u}}$, and the hydrodynamic pressures $\underset{\sim}{p}$

7.5. For each dam finite element: calculate the nodal displacements $\underset{\sim}{u}^{e}$, the elastic stress tensors $\underset{\sim}{\sigma}$, and the tensile d^{+} and compressive d^{-} damage values for all Gauss points

7.6. Present results: response time histories; 3D deformed shapes and stress fields, displacements and stresses envelopes, and tensile/compressive damage distributions

Fig. 3.22 Algorithm of the new version of the program *DamDySSA4.0* (continued).

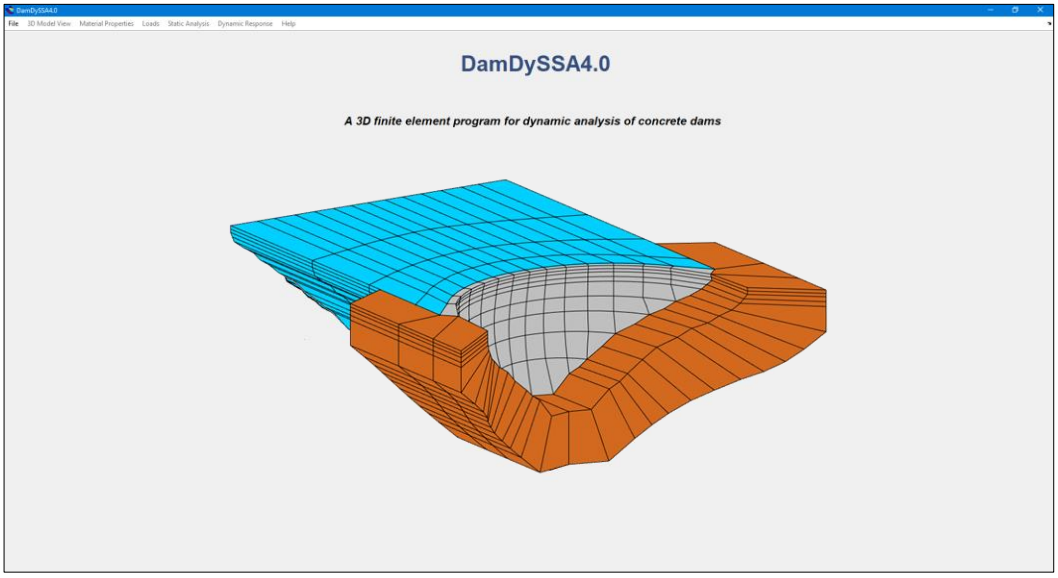

Fig. 3.23 *DamDySSA4.0*: graphical user interface. Initial opening menu.

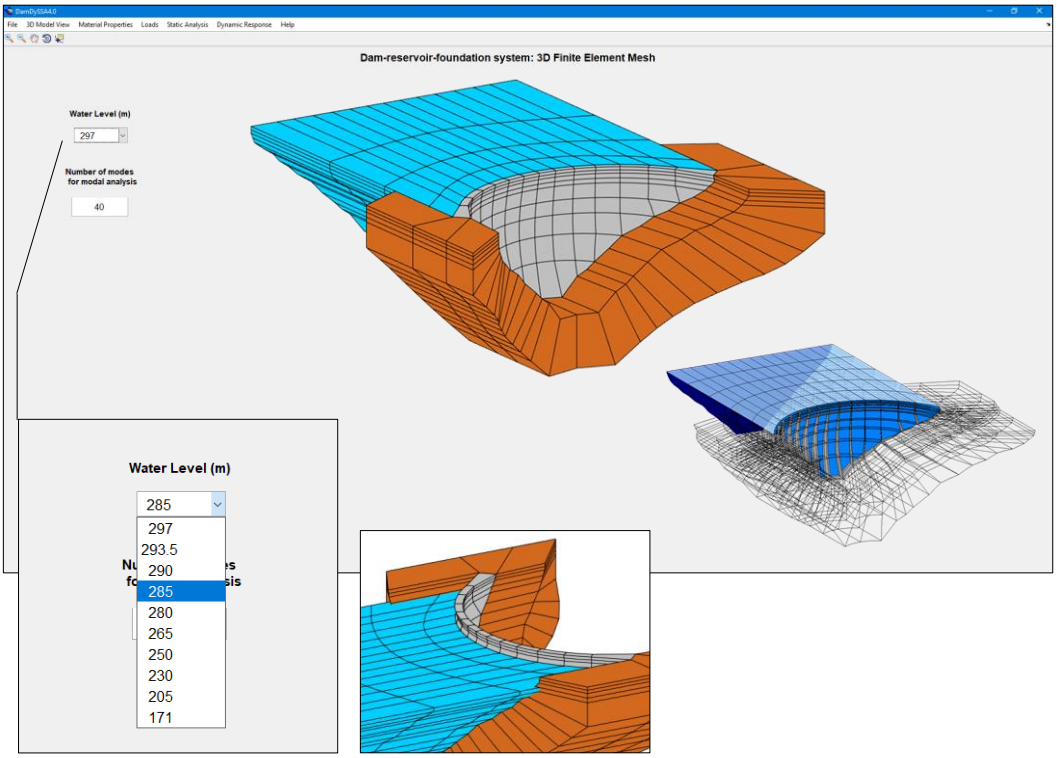

Fig. 3.24 *DamDySSA4.0*: graphical user interface. Menu with the 3D mesh of the dam-reservoir-foundation system and user inputs for selecting the reservoir water level and the number of modes for modal analysis.

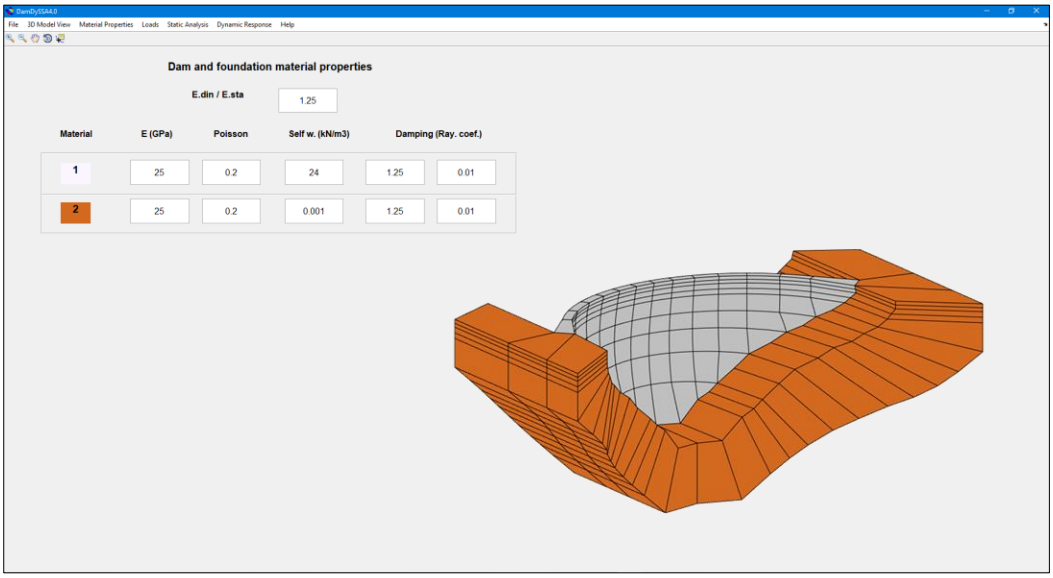

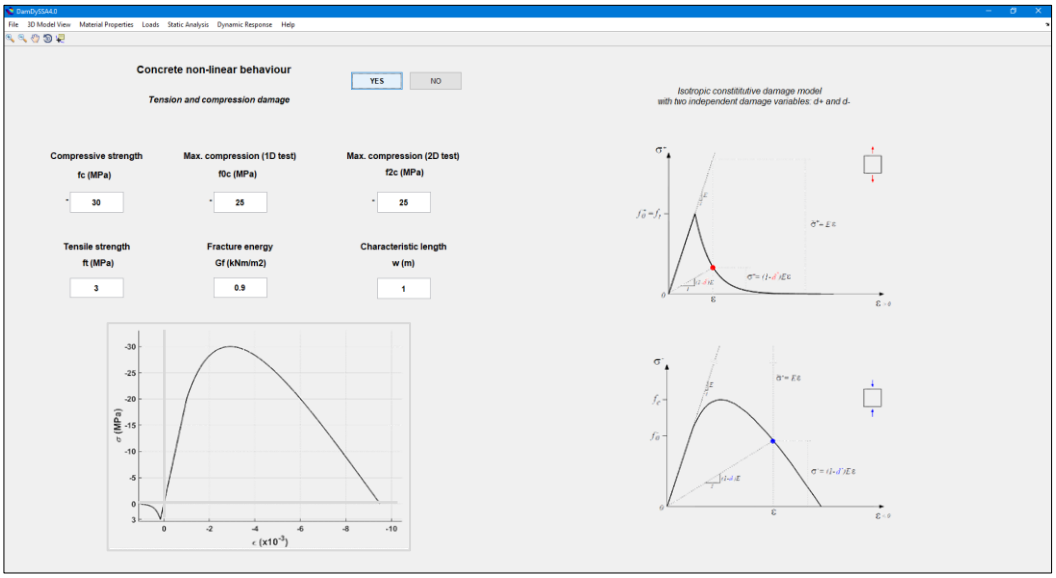

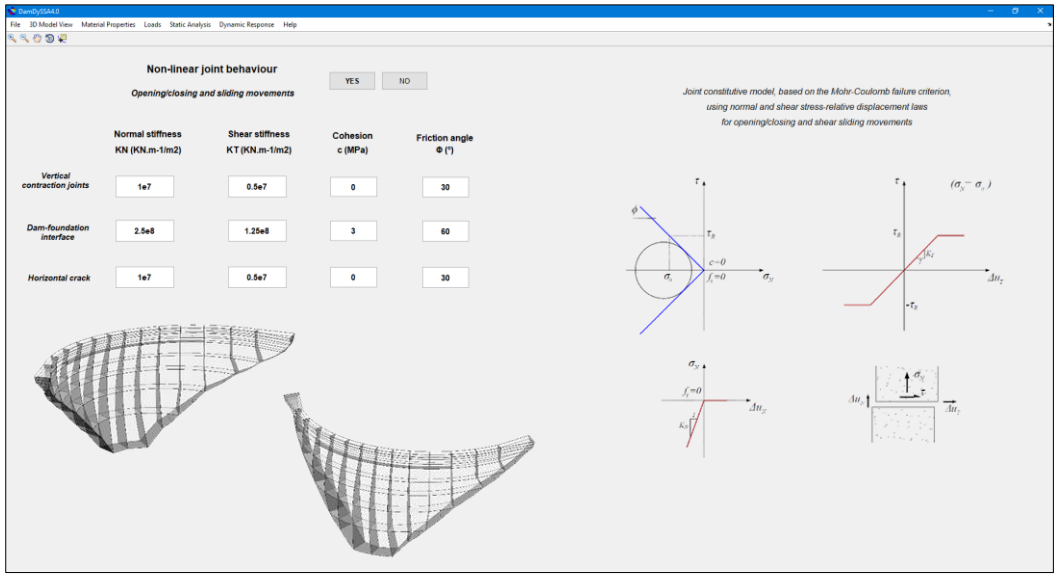

Fig. 3.25 *DamDySSA4.0*: graphical user interface. Menus with material properties. Elastic properties for dam/foundation materials. Main properties for concrete and/or joint non-linear behaviour.

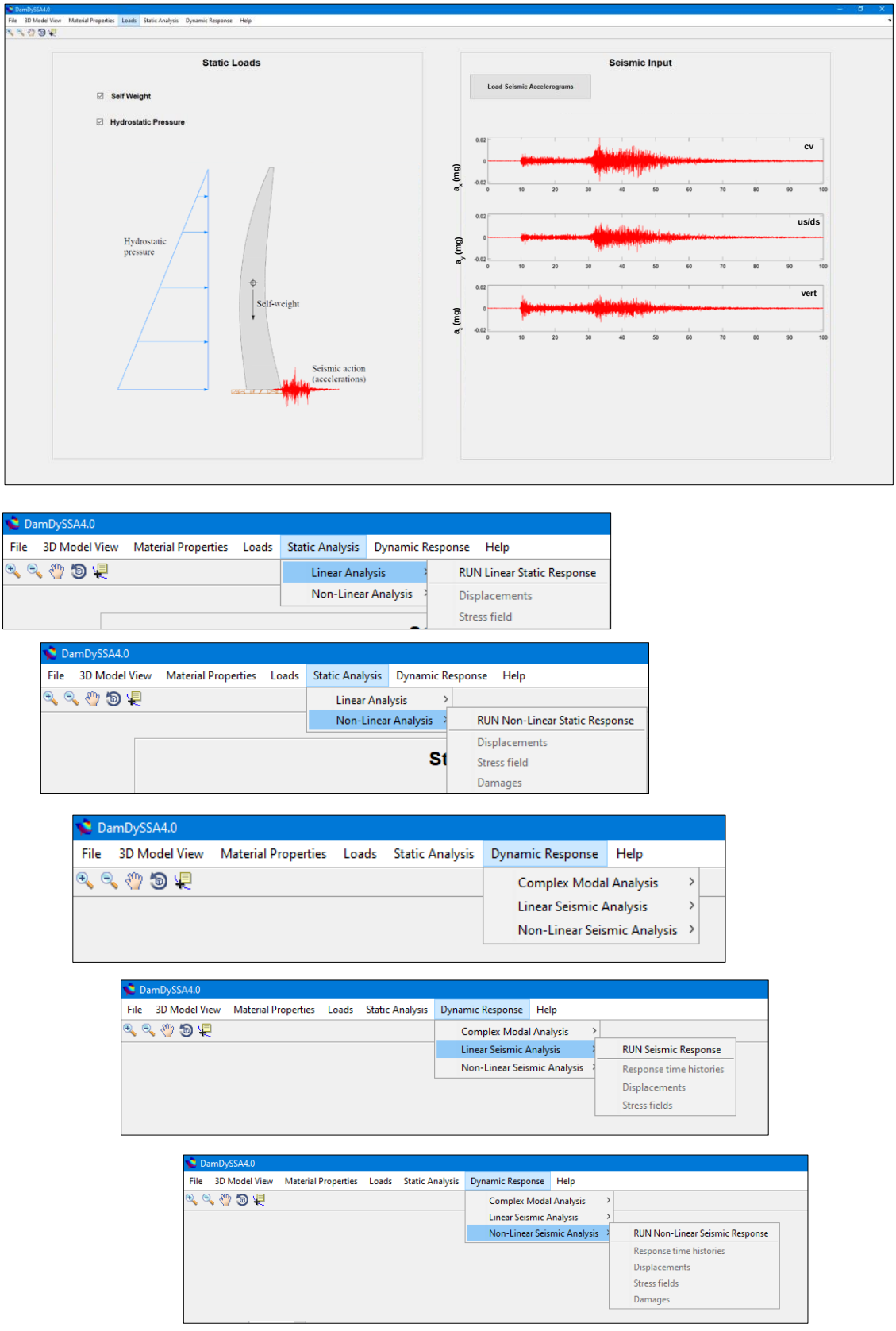

Fig. 3.26 *DamDySSA4.0*: graphical user interface. Menu to select static loads and read the seismic input. Drop-down options for static analysis (run linear or non-linear response) and for dynamic analysis (modal analysis, linear seismic analysis, or non-linear seismic analysis).

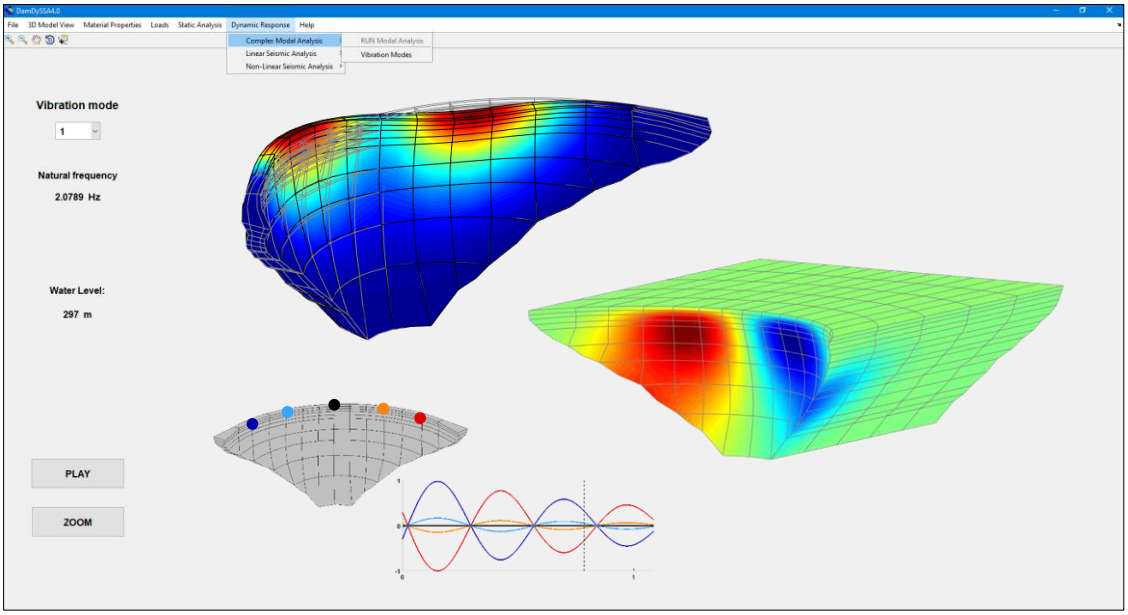

Fig. 3.27 *DamDySSA4.0*: graphical user interface. Results from dynamic analysis: complex modal analysis. Natural frequencies and modal configurations.

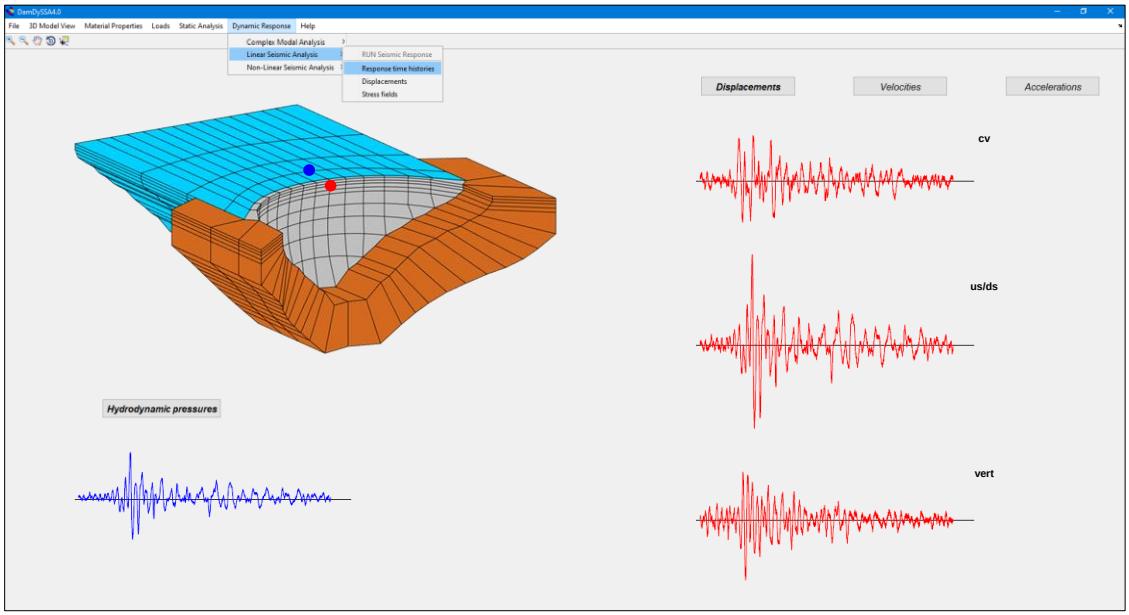

Fig. 3.28 *DamDySSA4.0*: graphical user interface. Results from dynamic analysis: linear seismic analysis. Response time histories /displacements and hydrodynamic pressures

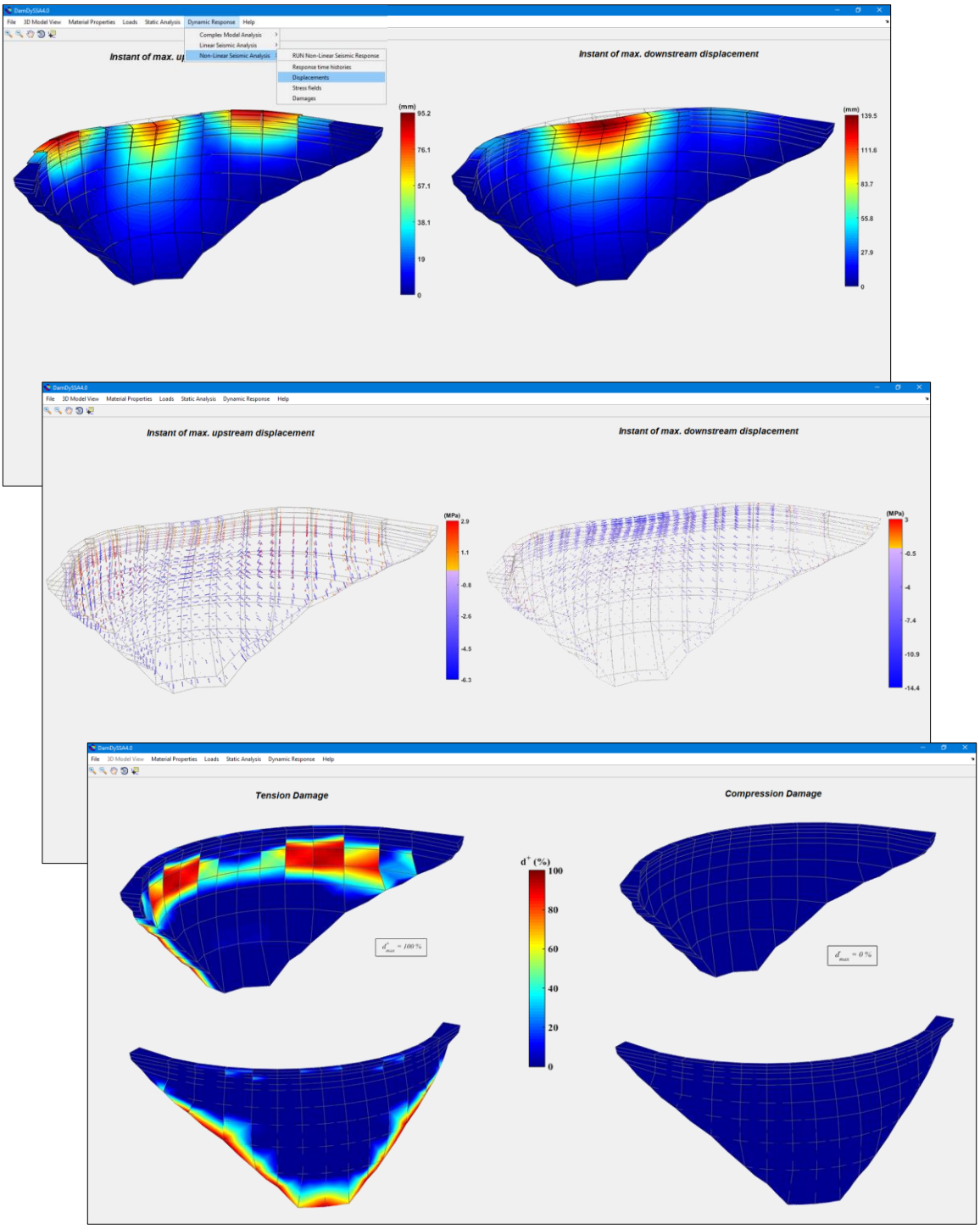

Fig. 3.29 *DamDySSA4.0*: graphical user interface. Results from dynamic analysis: non-linear seismic analysis. Displacements, stress fields, and damages.

3.9.2 TESTS CONDUCTED USING *DAMDYSSA*: VALIDATION OF THE DEVELOPED MODEL

In this work, there was a clear intention to validate the implemented model and the proposed numerical methods, as well as to show its potential for simulating the dynamic behaviour of dam-reservoir-foundation systems. Therefore, several tests carried out using the program *DamDySSA* and involving dam models are presented here. Overall, numerical results are compared with experimental data and analytical solutions.

MODAL ANALYSIS

Aiming to validate the proposed state-space formulation for modal analysis (recall subchapter 3.6), considering dam-water dynamic interaction and generalized damping, the first test consists essentially in the comparison between computed natural frequencies and mode shapes and modal identification results (see Chapter 4).

This test is carried out using experimental data obtained from continuous dynamic monitoring of namely Cabril dam (132 m high), in Portugal, and Cahora Bassa dam (171 m high), in Mozambique. As mentioned, these are the two case studies of this work, which are presented in greater detail in Chapter 5.

Regarding Cabril dam, the comparison for the first three vibration modes is shown in Fig. 3.30 and Fig. 3.31. The identified natural frequencies and mode shapes were obtained from accelerations recorded on June 16, 2018, from 16:00 to 17:00, when the water level was at el. 294 m (just 3 m lower than the crest level). The numerical analysis was performed using a model of the dam-reservoir-foundation system with the reservoir level at el. 293.5 m, as close as possible to the real water level. In the dam, the Young's modulus of concrete is 25 GPa, assuming an increase of 30% for dynamic analysis, as detected during in situ ultrasound tests (Espada, 2010). In the reservoir, the pressure waves propagation velocity is set to 1440 m/s, according to the mean reservoir water temperature.

As for Cahora Bassa dam, the comparison between numerical and experimental results is presented in Fig. 3.32 and Fig. 3.33. The experimental results were extracted from dynamic vibrations measured on August 6, 2017, between 06:00 and 07:00, with the reservoir level at el. 319.5 m (around 11.5 m below the crest). The dynamic calculation was conducted with the water level exactly 12 m below the dam crest in the dam-reservoir-foundation model. For this case, the concrete Young's modulus is 40 GPa, considering an amplification of 25% for dynamic behaviour, while the pressure waves propagation velocity in water is set to 1500 m/s.

Overall, in this comparative study it was possible to achieve a very good agreement between numerical and experimental results. Regarding natural frequencies, not only the computed frequency values for each mode are close to those extracted from dynamic monitoring data, but the differences between the values for consecutive modes are also properly reproduced. As for the modal configurations, the implemented numerical model can properly simulate symmetric and antisymmetric modal configurations. Moreover, as dam-water dynamic interaction and generalized damping are considered, complex (or non-stationary) vibration modes are calculated (for both dams, non-stationary modes are identified)

To conclude, the proposed state-space formulation, applied to solve the dynamic equation of the coupled model in displacements and pressures, is capable of accurately simulating the free vibration response of the dam-reservoir-foundation system and to get a good agreement with the measured response of both dams under ambient/operational excitations. These results required only the definition of well-known material properties and of appropriate values for the pressure waves propagation velocity.

In this context, it is important to emphasize that such promising results were not reached in previous studies, conducted for Cabril dam using the classic added water mass models (Mendes et al., 2004; S. Oliveira et al., 2011, 2012), which are based on the Westergaard formulation - this formulation, which is postulated for dams with rigid vertical upstream faces), results in an overestimation of the added water mass, thus requiring the application of empirical water mass reduction factors for analysing arch dams (H. Chen, 2014). This subject is properly addressed in one of the next tests.

LINEAR DYNAMIC RESPONSE: DISPLACEMENTS

The second test is performed to evaluate the reliability and numerical stability of the proposed time-stepping formulation (see subchapter 3.7), which was developed to solve the coupled dynamic equation in time domain and thus compute the forced dynamic response (displacements and pressures) of the dam-reservoir-foundation system.

In this test, the dynamic response in displacements, calculated using *DamDySSA*, is compared with a known solution: the static response under the self-weight load[9]. With that aim, the dynamic force input is an acceleration time history applied in the vertical direction, with constant value equal to the gravitational acceleration (9.81 m/s^2). To confirm if the dynamic calculations are correct, the steady-state response (when the oscillatory movement stabilizes after the transient state) should be equal to the static response.

The results from this comparative analysis are presented in Fig. 3.34. Once again, Cabril arch dam is used as case study, considering the same properties as before. The vertical displacement time history, calculated for the nodal point at the top of the central section in the dynamic analysis, is compared with the corresponding value obtained in the static analysis. The provided comparison shows that the value obtained at the end of the displacement time history, around 6.5 mm, perfectly matches the displacement calculated in the static response. Furthermore, a perfect agreement was achieved between the 3D deformed shape under the self-weight load and the deformed shape computed from the steady-state dynamic response under the gravitational acceleration input.

To summarize, this test has shown that the steady-state dynamic response was correctly calculated, and, as intended, demonstrated the potential and stability of the implemented time-stepping formulation for linear dynamic analysis of dam-reservoir-foundation systems.

[9] Cabril dam's response under static loads was analysed in detail in a special dam behaviour report (LNEC, 2003), using experimental observation results and finite element numerical results.

EXAMPLE 1: CABRIL DAM

Dynamic monitoring results

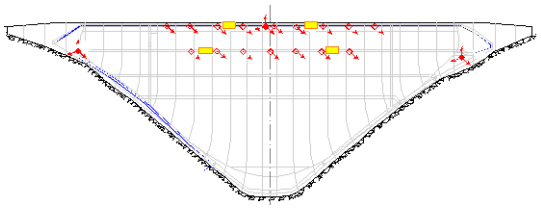

Singular value spectrum obtained from accelerations recorded on June 16, 2018, from 16:00 to 17:00, water level at el. 294 m

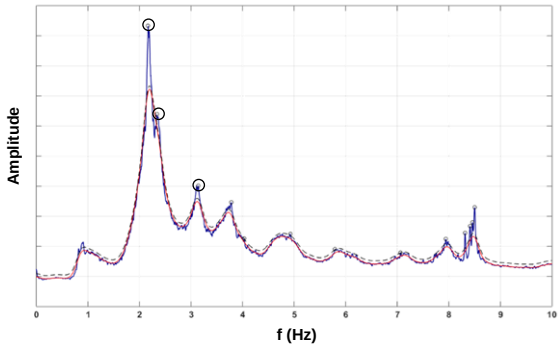

Mode 1: Antisymmetric

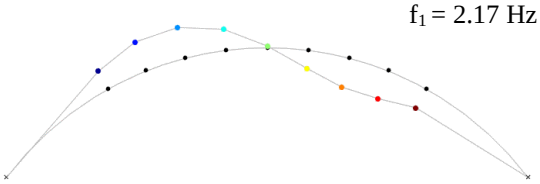

f_1 = 2.17 Hz

Mode 2: Symmetric

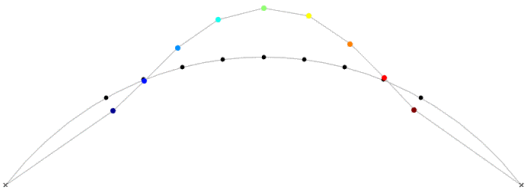

f2 = 2.34 Hz

Mode 3: Symmetric

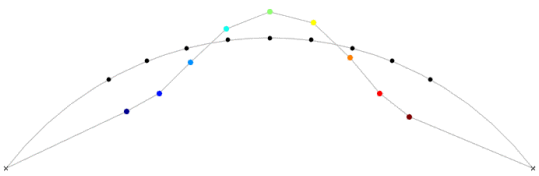

f3 = 3.14 Hz

Finite element numerical results

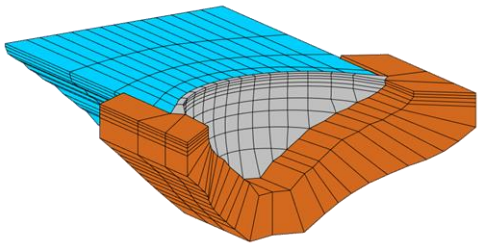

Reservoir
c_w = 1440 m/s
Water level: el. 293.5 m

Dam; Foundation
E = 25 GPa
E_{dyn} = 1.3 × E

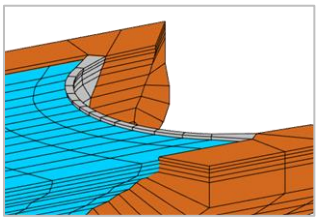

Mode 1: Antisymmetric

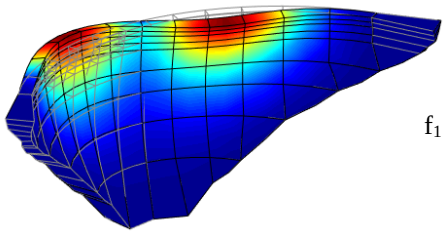

f_1 = 2.16 Hz

Mode 2: Symmetric

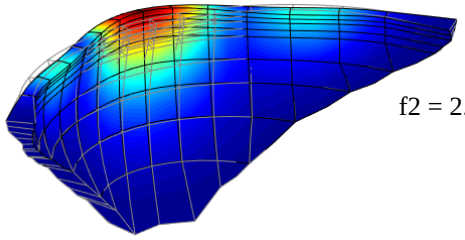

f2 = 2.31 Hz

Mode 3: Symmetric

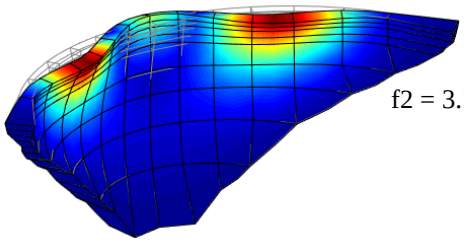

f2 = 3.11 Hz

Fig. 3.30 Test 1: modal analysis. Natural frequencies and mode shapes. Comparison between experimental and numerical results for Cabril dam.

EXAMPLE 1: CABRIL DAM

Mode 1 (stationary)

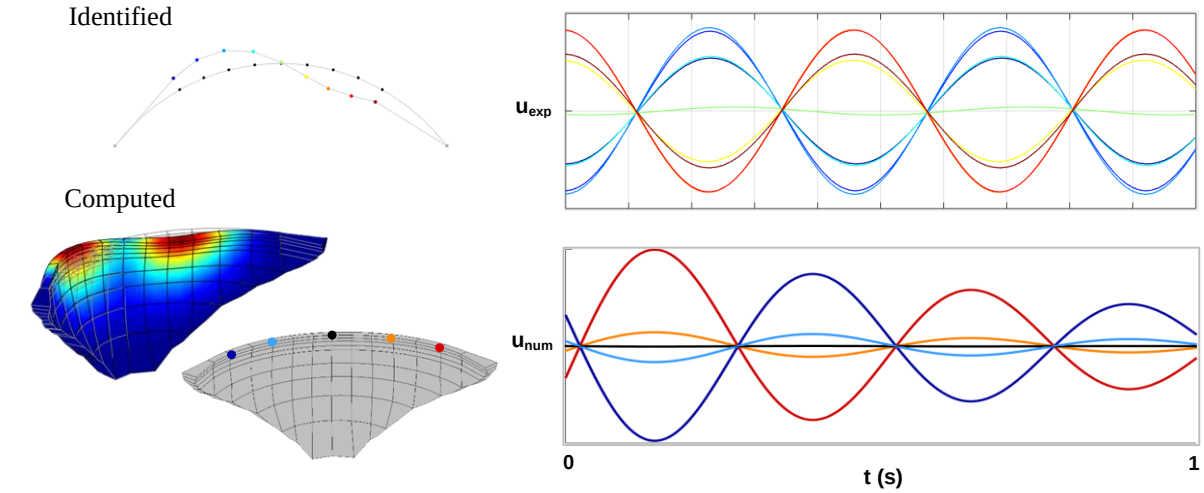

Mode 2 (non-stationary)

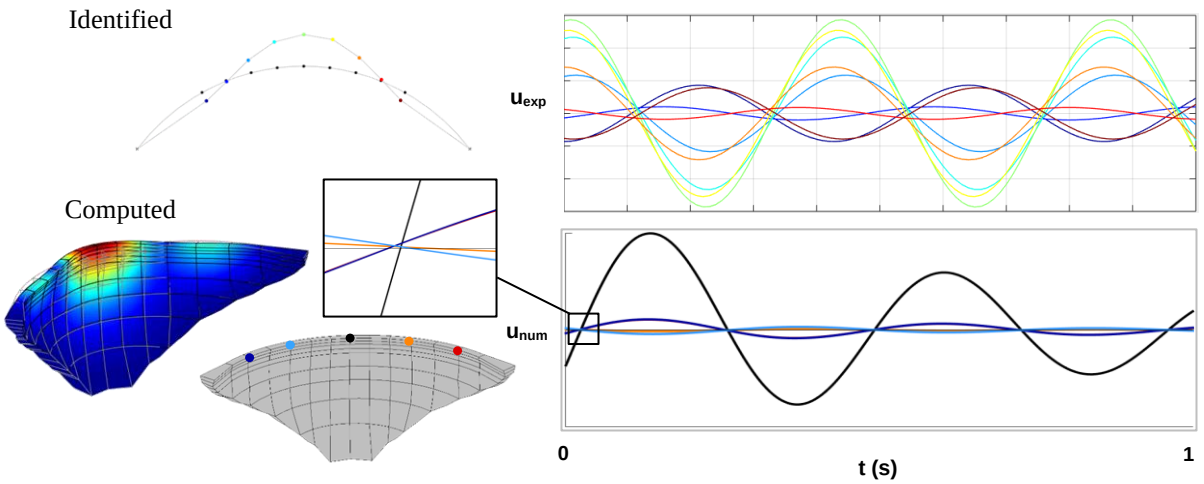

Mode 3 (non-stationary)

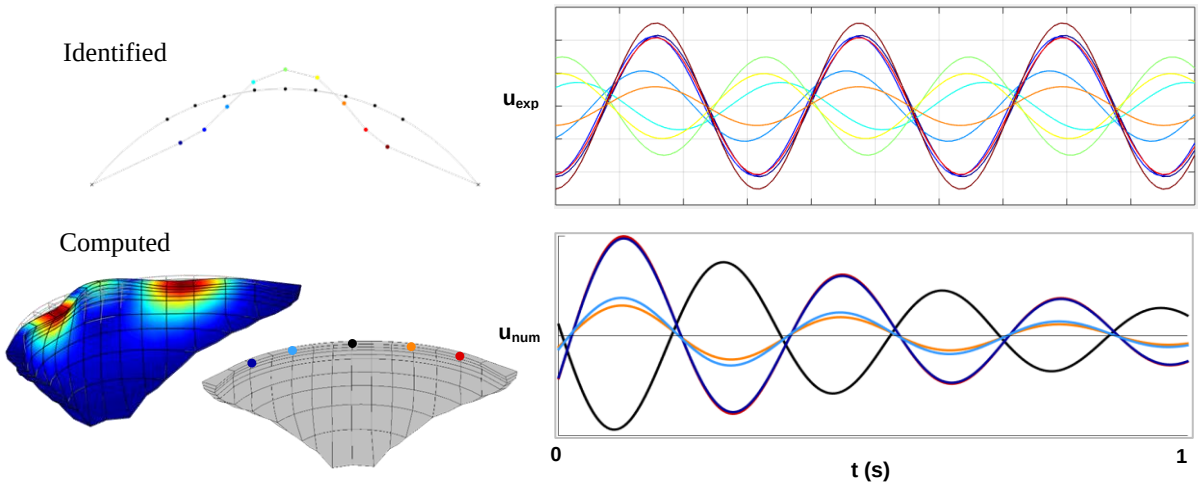

Fig. 3.31 Test 1: modal analysis. Experimental and numerical modes for Cabril dam: stationary and non-stationary modal configurations.

EXAMPLE 2: CAHORA BASSA DAM

Dynamic monitoring results

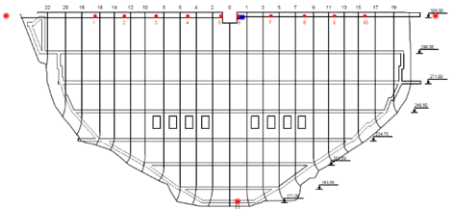

Singular value spectrum obtained from accelerations recorded on August 6, 2017, from 06:00 to 07:00, water level at el. 319.5 m

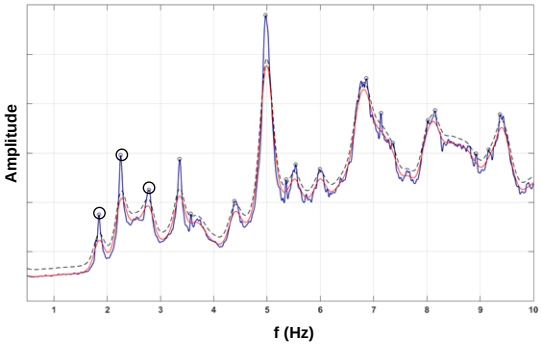

Finite element numerical results

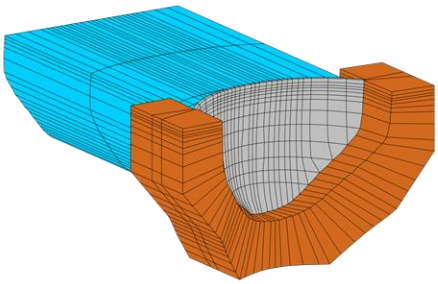

Reservoir
c_w = 1500 m/s
Water level: el. 319 m

Dam; Foundation
E = 40 GPa; E_{dyn} = 1.25×E
ν = 0.2

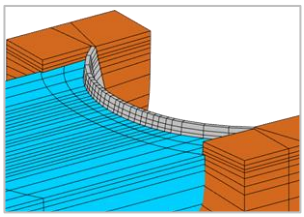

Mode 1: Antisymmetric

f_1 = 1.86 Hz

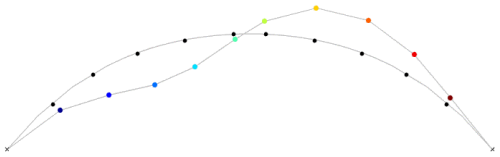

Mode 1: Antisymmetric

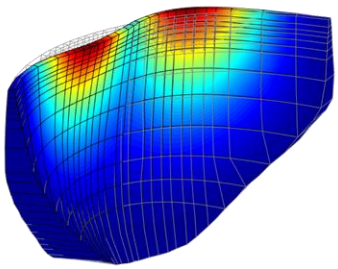

f_1 = 1.84 Hz

Mode 2: Symmetric

f2 = 2.26 Hz

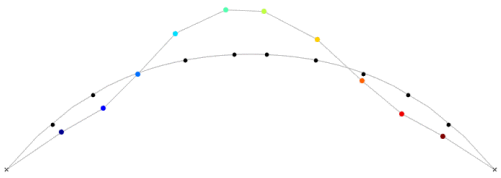

Mode 2: Symmetric

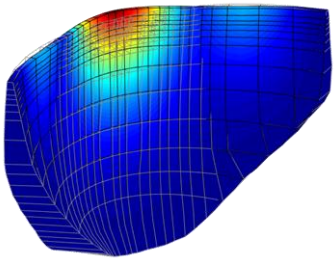

f2 = 2.25 Hz

Mode 3: Symmetric

f3 = 2.79 Hz

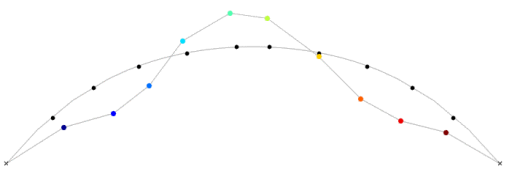

Mode 3: Symmetric

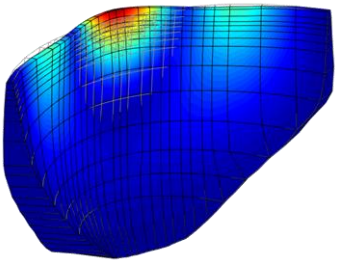

f2 = 2.74 Hz

Fig. 3.32 Test 1: modal analysis. Natural frequencies and mode shapes. Comparison between experimental and numerical results for Cahora Bassa dam.

EXAMPLE 2: CAHORA BASSA DAM

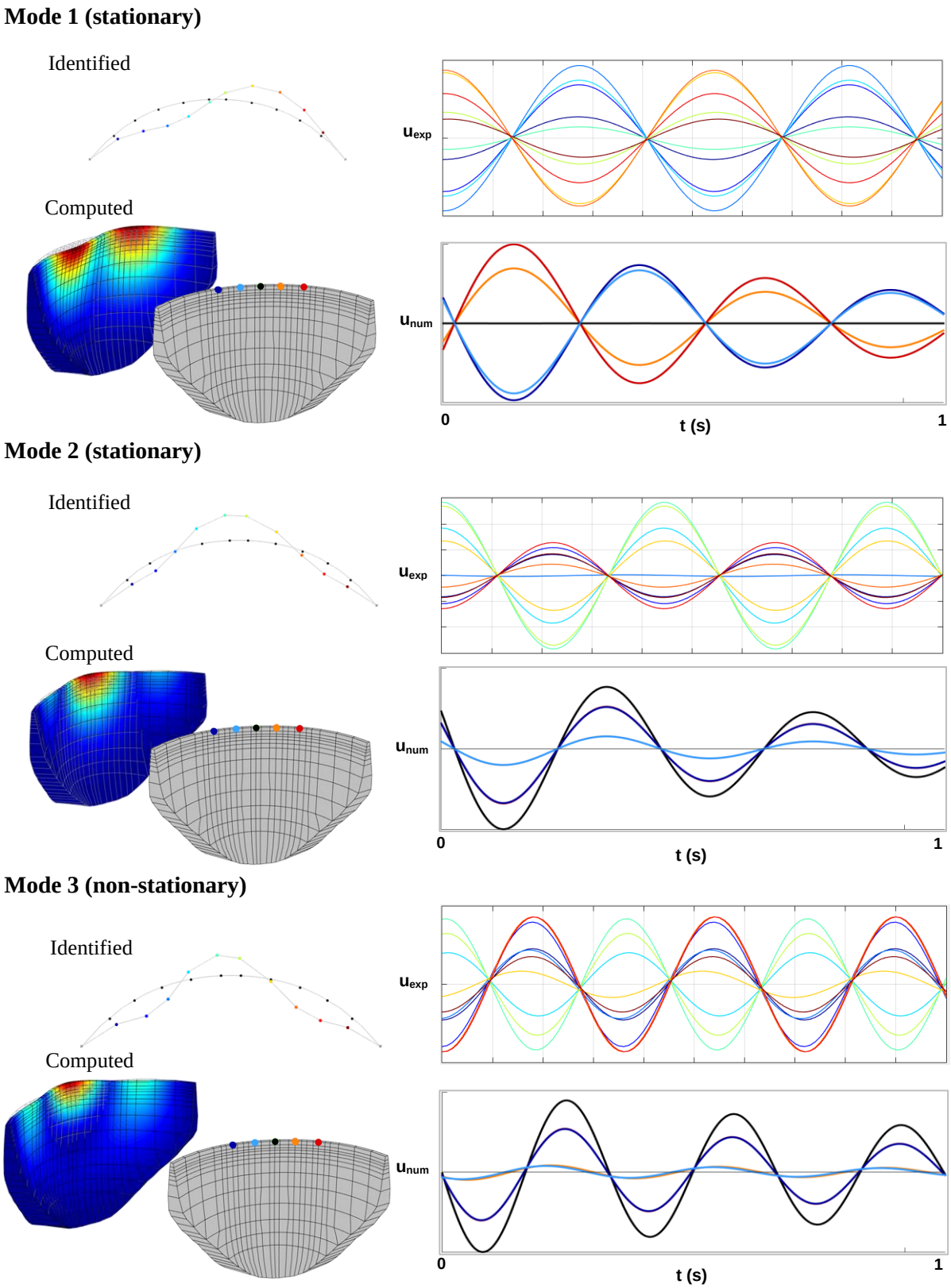

Fig. 3.33 Test 1: modal analysis. Stationary and non-stationary modes for Cahora Bassa dam.

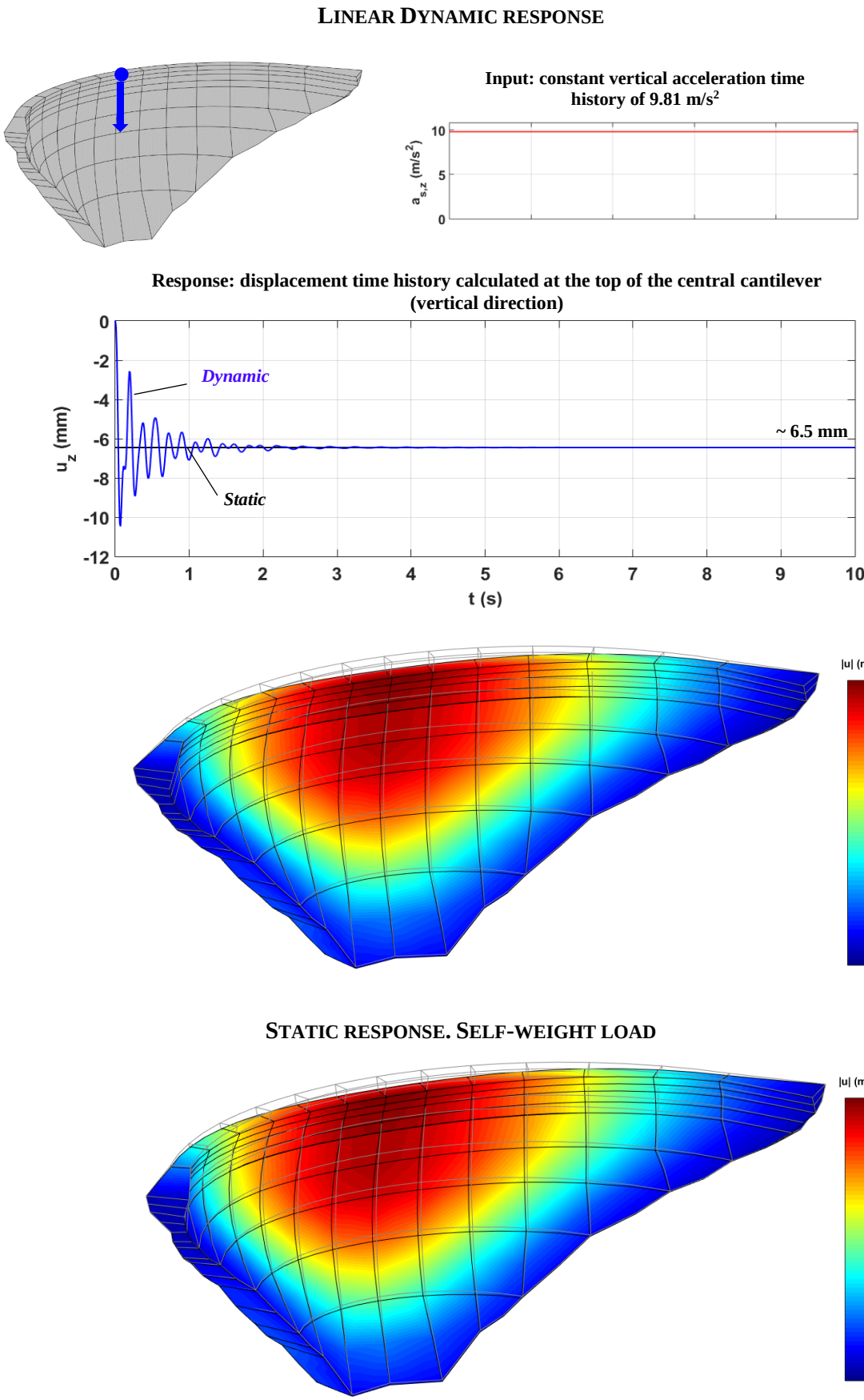

Fig. 3.34 Test 2: linear dynamic response. Displacement time history and deformed shape (steady-state response) under gravitational acceleration input. Comparison with static response.

LINEAR DYNAMIC RESPONSE: HYDRODYNAMIC PRESSURES ON DAMS

The third test is performed not only to evaluate once again the proposed coupled time-stepping formulation, but also to show the potential of the coupled model in displacements and pressures to simulate the hydrodynamic behaviour of the reservoir and dam-reservoir interaction. This test is focused on the study of hydrodynamic pressures on dams, and it is essentially divided into two parts.

The first part analyses the distributions of hydrodynamic pressures on 100 m high gravity dams with vertical and sloped upstream faces. The numerical results calculated using *DamDySSA* are compared with both analytical and experimental values (Fig. 3.35), namely: (i) with the pressure values obtained using an exact formula of Westergaard's solution (Westergaard, 1933), which assumes the hypotheses of rigid dam and incompressible fluid; and (ii) with experimental pressure curves obtained by Zangar in (1952), based on the so-called electric analog method, for upstream faces with different slopes.

WESTERGAARD'S FORMULATION

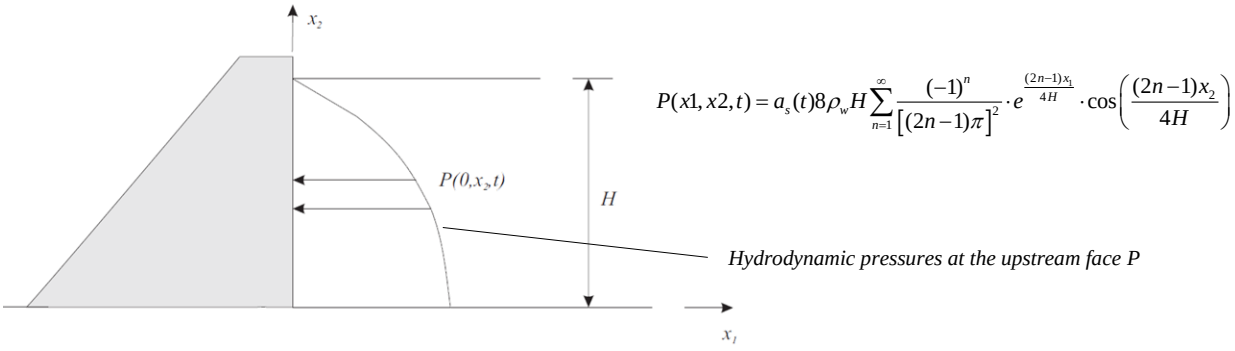

ZANGAR'S EXPERIMENTAL RESULTS

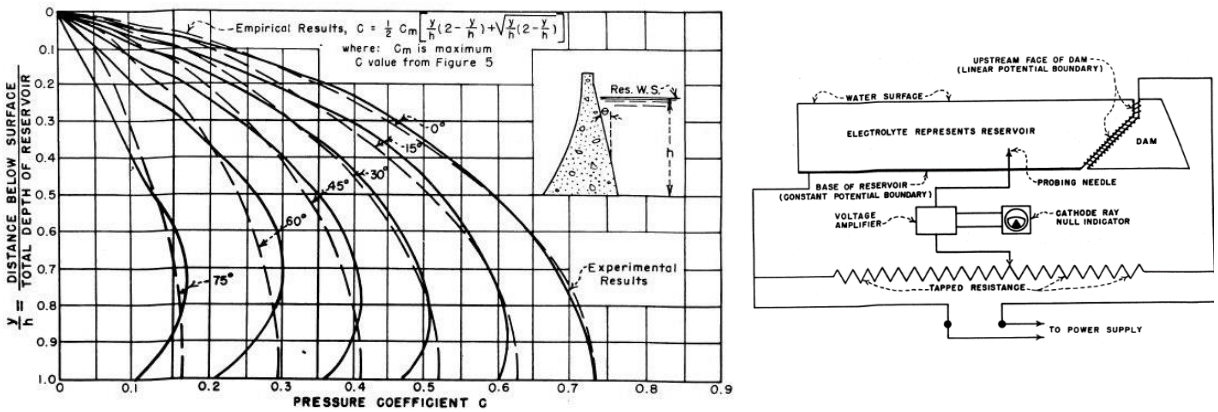

Fig. 3.35 Test 3: hydrodynamic pressures on dams. Westergaard's formulation for vertical upstream faces (Itasca Consulting Group Inc., 2019) and Zangar's experimental results for different upstream slopes (Zangar, 1952).

The dynamic analyses with *DamDySSA* are carried out using two 3D models of simple gravity dams, one with a vertical upstream surface and another with a 30º slope (Fig. 3.36). For this study, to enable a coherent comparison with the referred results, the hypothesis of rigid dam is considered by assuming a high value of Young's modulus for concrete. In the reservoir, the hypothesis of water compressibility is considered, with

fluid motion in both horizonal and in the vertical directions. As dynamic load input, an acceleration time history with constant unitary value (1 m/s^2) is applied at the base, in the upstream-downstream direction. In order to obtain the distribution of pressures in the dam-reservoir interface, the hydrodynamic pressures time histories are calculated for all nodes along the height of the upstream face of the dam and then the steady-state values are selected.

The results of this comparative study show that it was possible to achieve a very good agreement between the hydrodynamic pressures computed with *DamDySSA* (in red), for models with vertical and sloped upstream faces, and the pressure values calculated using Westergaard's formula (in blue) and the experimental curves obtained by Zangar (in black). It is therefore possible to conclude that the hydrodynamic behaviour of the reservoir and dam-reservoir interaction were properly simulated for rigid gravity dams with vertical and sloped upstream faces.

In the second part, the aim is to analyse the hydrodynamic pressures on an arch dam (Fig. 3.37). Once again, Cabril dam (132 m high) is used as application example. The hypothesis of flexible dam behaviour is assumed. As done in the first parts, the dynamic calculation is carried out using *DamDySSA*, considering an acceleration time history with constant value of 1 m/s^2 applied in the upstream downstream direction: the hydrodynamic pressures time histories are calculated at all points of the dam-reservoir interface, and subsequently the steady-state values are used to get a 3D graphical representation with the distribution of pressures in the upstream face. For comparison, the water pressures are directly computed at all nodes of the upstream face using Westergaard's solution, assuming a unitary acceleration value and considering *z* as the coordinate in the vertical axis.

These results show clear differences between the pressures computed with *DamDySSA* (coupled model) and the values calculated using Westergaard's formula, not only in terms of the pressure values but also in their distribution over the upstream face in the horizontal and vertical directions - it is interesting to note how the coupled model gives a more uniform distribution of the hydrodynamic pressures along the height of the dam, in accordance with the reservoir water level. Furthermore, the pressures obtained using Westergaard's solution, which is valid for rigid vertical upstream faces, are overestimated when compared to the values calculated with the coupled model for a flexible dam with a curved upstream face.

This observation has great value because it allows to clarify, for the first time, the need to apply an empirical added mass reduction factor (of around 50 to 70%) when using the classic added water mass models based on Westergaard's hypothesis, as has been recommended in this field for dynamic analysis of arch dams (H. Chen, 2014). For the case of Cabril dam, the pressures calculated with Westergaard's solution are overestimated by about 30%, on average. These results also help explain the added mass reduction factors used in previous studies (around 70%), which were defined to get the best agreement possible between identified and computed natural frequencies (Mendes et al., 2004; S. Oliveira et al., 2011, 2012)

To conclude, the results presented in this third test allowed to prove the potential of the implemented coupled model to simulate the hydrodynamic behaviour of the reservoir and the dam-water dynamic interaction. In combination with the results of the second test, it is thus possible to emphasize the capacity of *DamDySSA* to predict the dynamic behaviour of concrete dam-reservoir-foundation systems.

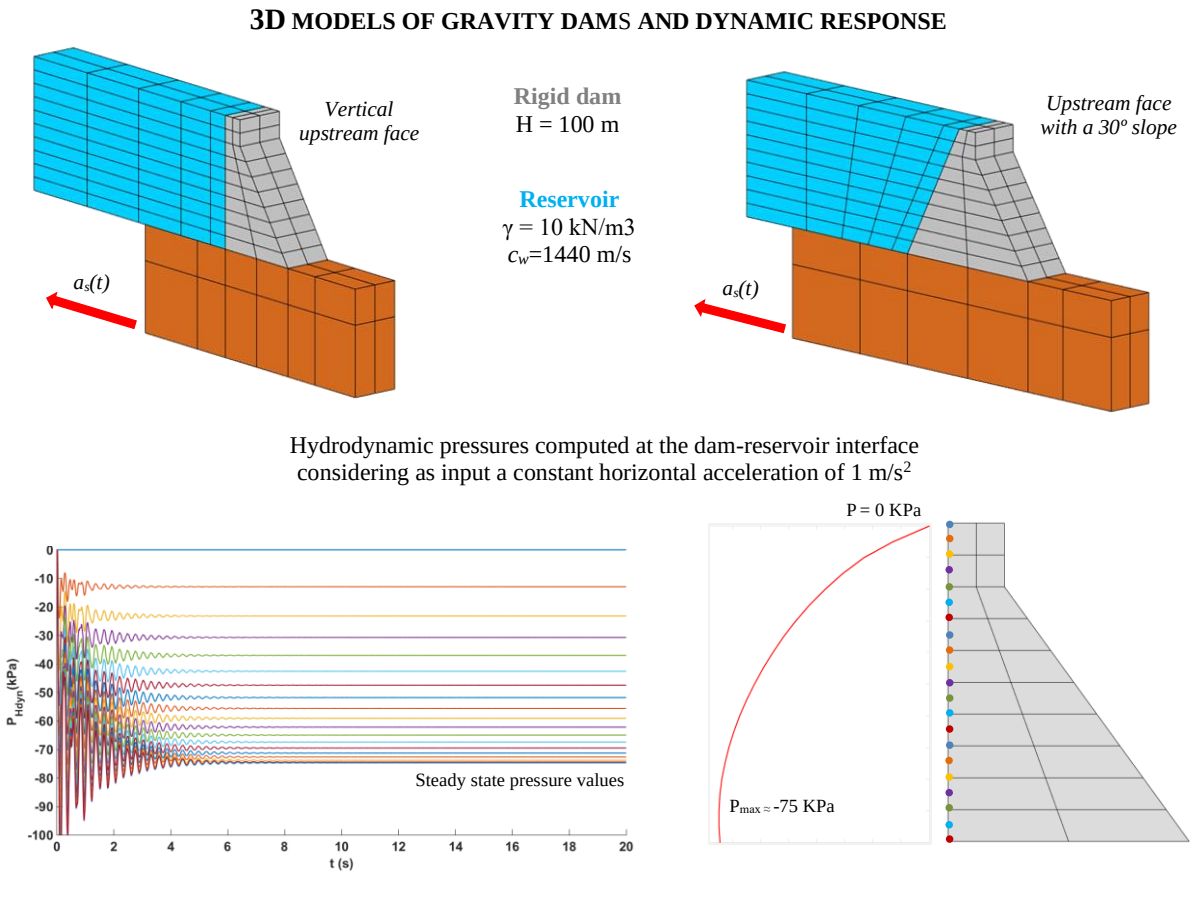

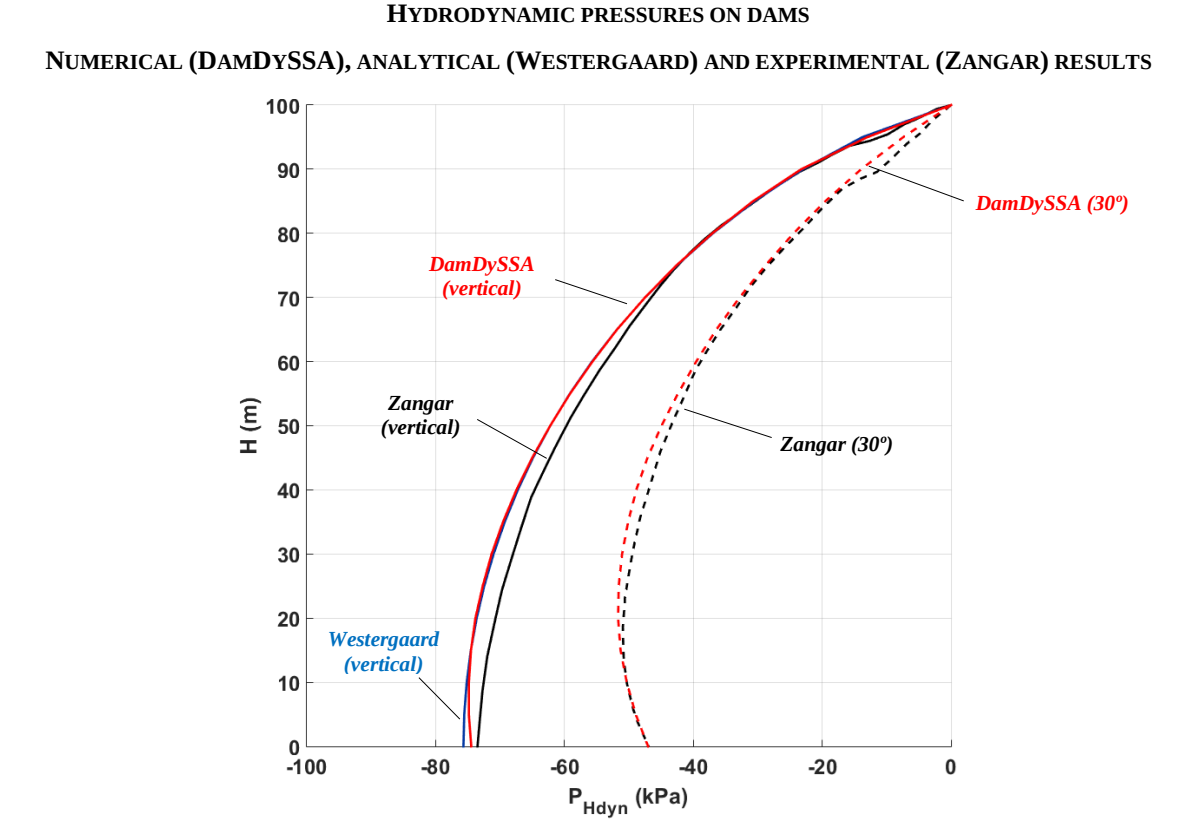

Fig. 3.36 Test 3: hydrodynamic pressures on dams. 3D models of gravity dams with vertical and sloped (30º) upstream faces. Hydrodynamic pressures time histories under constant unitary acceleration. Comparison with analytical and experimental results.

CABRIL DAM: HYDRODYNAMIC PRESSURES

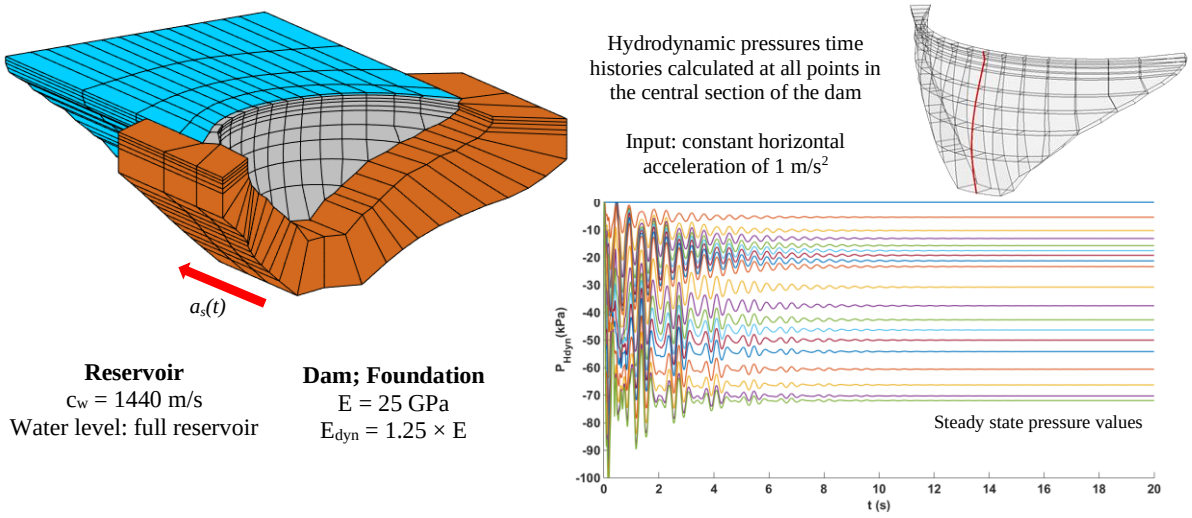

***DamDySSA*. Hydrodynamic pressures calculated at the dam-reservoir interface (steady-state values)**

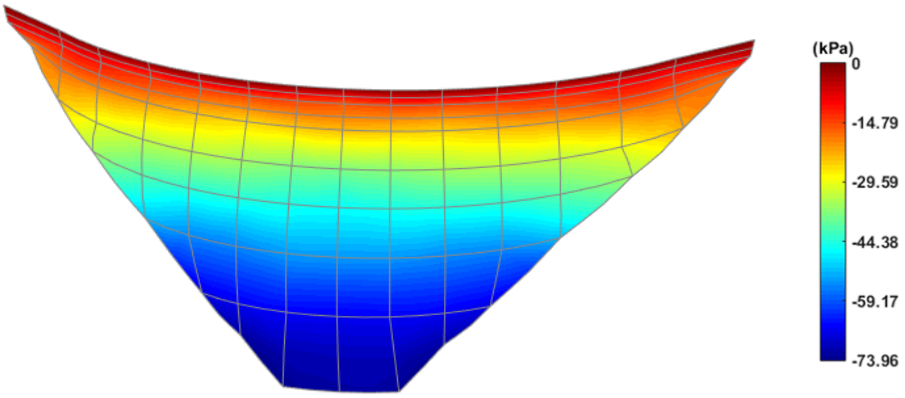

For comparison: pressures computed at all nodes of the upstream face using Westergaard's formula

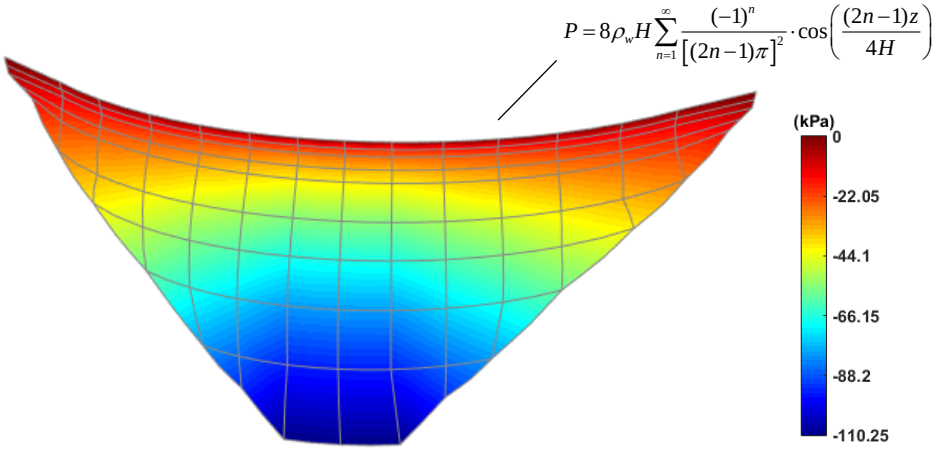

Note: In added water mass models, the added water masses are computed using Westergaards formula; however, it is common for dam engineers to use added water mass reduction factors for ach dam (0.5 to 0.7) – as shown here, such a reduction would give pressure values coherent with those obtained using coupled models

Fig. 3.37 Test 3: hydrodynamic pressures on an arch dam. Comparison of pressures obtained using a coupled model (implemented in *DamDySSA*) and pressures calculated using Westergaard's formula.

NON-LINEAR DYNAMIC RESPONSE: DISPLACEMENTS AND JOINT MOVEMENTS

The fourth and last test aims to check the stability and validate the formulation developed for non-linear seismic analysis (recall subchapter 3.8), which combines a time-stepping algorithm with the stress-transfer method, considering opening/closing and sliding joint movements and tensile and compressive damage in concrete.

It is worth reminding that the implemented non-linear constitutive model has already been properly tested, separately, elsewhere. In what concerns the joint model, it was applied to analyse the non-linear static response of a test structure and of a gravity dam for sliding scenarios, and consequently validated through the comparison with theoretical and analytical results (M. Rodrigues & Oliveira, 2019). With respect to the damage model, it has been extensively used and validated in various studies (Alegre & Oliveira, 2019; Faria, 1994; S. Oliveira, 2000; S. Oliveira, Faria, et al., 2003; S. Oliveira & Faria, 2006), namely to generate stress-strain diagrams under uniaxial loading, to analyse the static response of simple test structures and compare the results with known theoretical solutions, and to evaluate the so-called concrete strength decrease scenario for large concrete dams, including the comparison with experimental results obtained with reduced scale physical models.

What is new in this work is the incorporation of both non-linear models into a coupled finite element formulation for simulating the non-linear seismic behaviour of dam-reservoir-foundation systems. Therefore, a simple test is presented here, following the same line of thought as in the linear dynamic analysis test. This test consists of a comparison between the non-linear static response, under the self-weight load, and the non-linear dynamic response, considering as input an acceleration time history applied in the vertical direction, with a value that goes progressively from 0 to the gravitational acceleration (9.81 m/s^2) in half a second and remains constant from that moment on. Yet again, the intent is to verify if the steady-state non-linear dynamic response matches the non-linear static behaviour.

The 3D finite element model of Cabril dam, used as case study, as well as the interface elements that represent the vertical contraction joints and the dam-foundation surface can be seen in Fig. 3.38. For this study, the same Young's modulus E = 25 GPa was used for concrete. Normal and shear stiffness of $K_N = 10^7\ kN.m^{-1}/m^2$ and $K_T = 0.5\ K_N$ are considered for the vertical contraction joints, to simulate shear and normal strength that allow joint movements to occur, while higher values are defined for the dam-foundation joint to ensure it remains completely closed. The non-linear vertical displacement time history, calculated for the nodal point at the top of the central section of the dam, is compared with the corresponding vertical displacement value calculated in the non-linear static analysis. As can be observed, the steady-state value of the non-linear displacement time history is coincident with the static value.

Furthermore, the steady-state non-linear dynamic response is compared with the non-linear static response in Fig. 3.39, including the deformed shapes and representations giving the opening and sliding values of all vertical joints (in this case, as the dam is essentially under compressions, no concrete damage occurs). Overall, an excellent agreement was reached between the non-linear static response under the self-weight and the non-linear dynamic response under the gravitational acceleration input, hence demonstrating the value of the proposed formulation for non-linear dynamic analysis and the stability achieved in the

numerical solutions. It can therefore be concluded that *DamDySSA* is a reliable tool for predicting the non-linear seismic behaviour of large concrete dams under strong earthquakes.

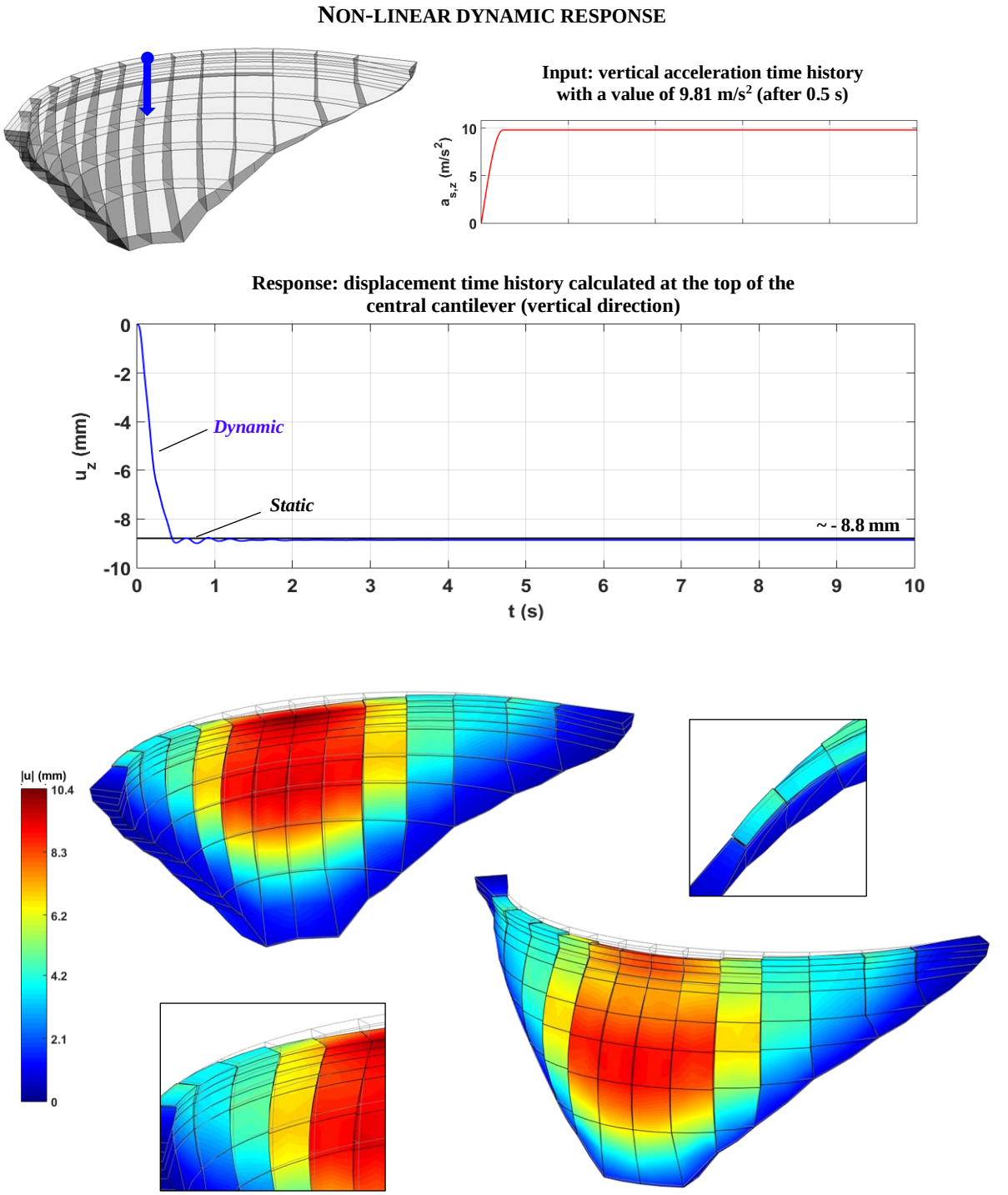

Fig. 3.38 Test 4: non-linear dynamic response. 3D dam mesh and joint elements. Displacement time history computed in non-linear dynamic analysis under a gravitational acceleration input, and 3D representation of the deformed shape with joint movements.

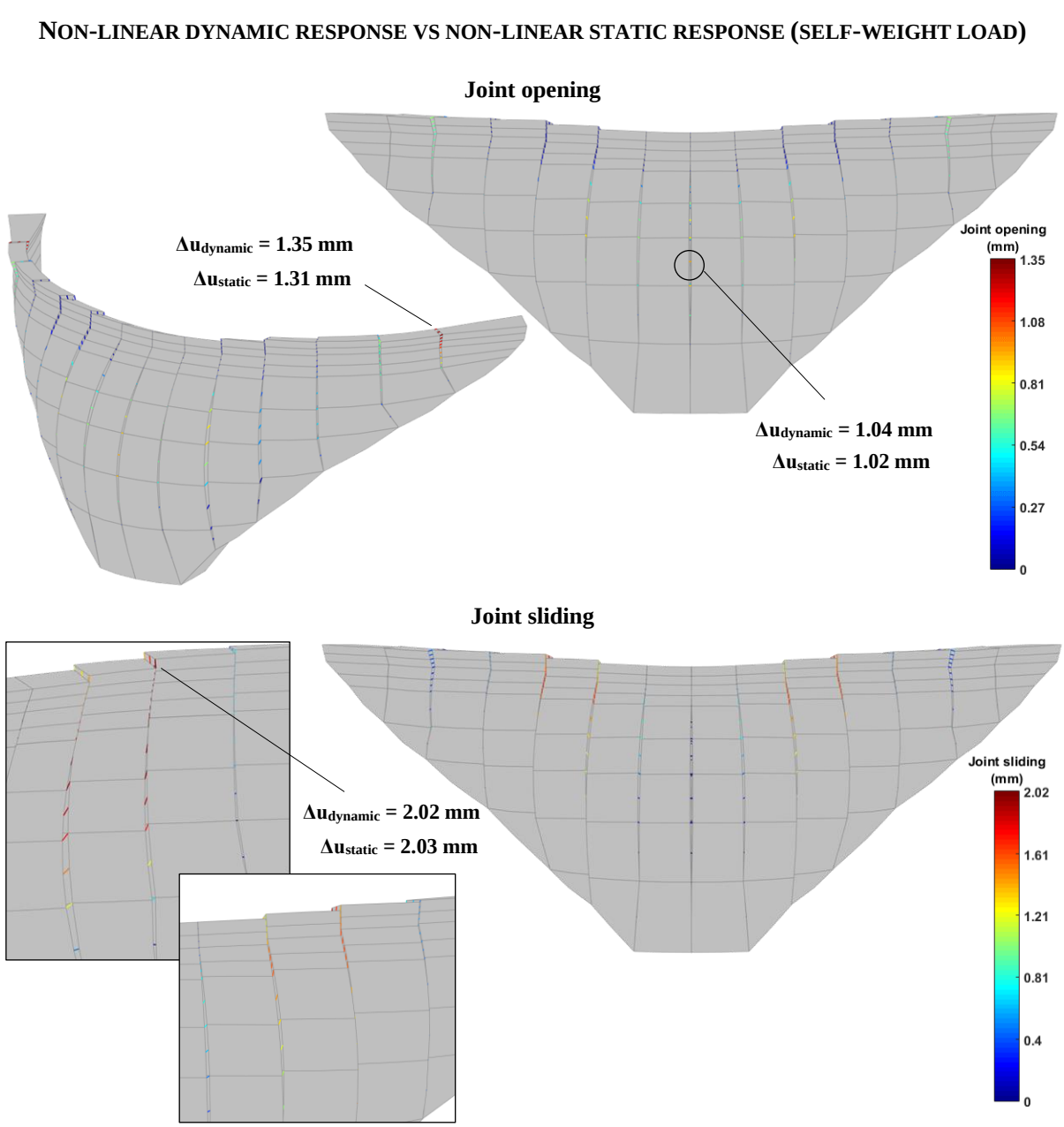

Fig. 3.39 Test 4: non-linear dynamic response: joint opening/sliding values from dynamic analysis under a gravitational acceleration input. Comparison with results from non-linear static analysis under the self-weigh load.

3.10 DAM3DMESH: AUTOMATIC MESH GENERATION

Aiming to perform the studies intended in this thesis on the dynamic behaviour of large concrete dams, and particularly to carry out the numerical calculations with *DamDySSA*, it became necessary to use realistic 3D finite element meshes. Therefore, these meshes were obtained using the program *Dam3DMesh*, developed in LNEC in the 1990s for automatic generation of 3D finite element meshes of dam-reservoir-foundation systems, considering cubic elements with 20 nodes (Fig. 3.40). As inputs, the program requires the data of a 2D plane mesh representing the front elevation of the dam from the downstream face, using quadrilateral elements with 4 nodal points, as well as the specific dam equations that define its geometry. Based on this information, first the program generates the 3D mesh of the dam, and then, depending on that

mesh, it also generates the meshes for the reservoir and the foundation block. The data on the 3D mesh of the dam-reservoir-foundation system is written on a text file, which can be reorganized into a specific Excel file to be read later by *DamDySSA*.

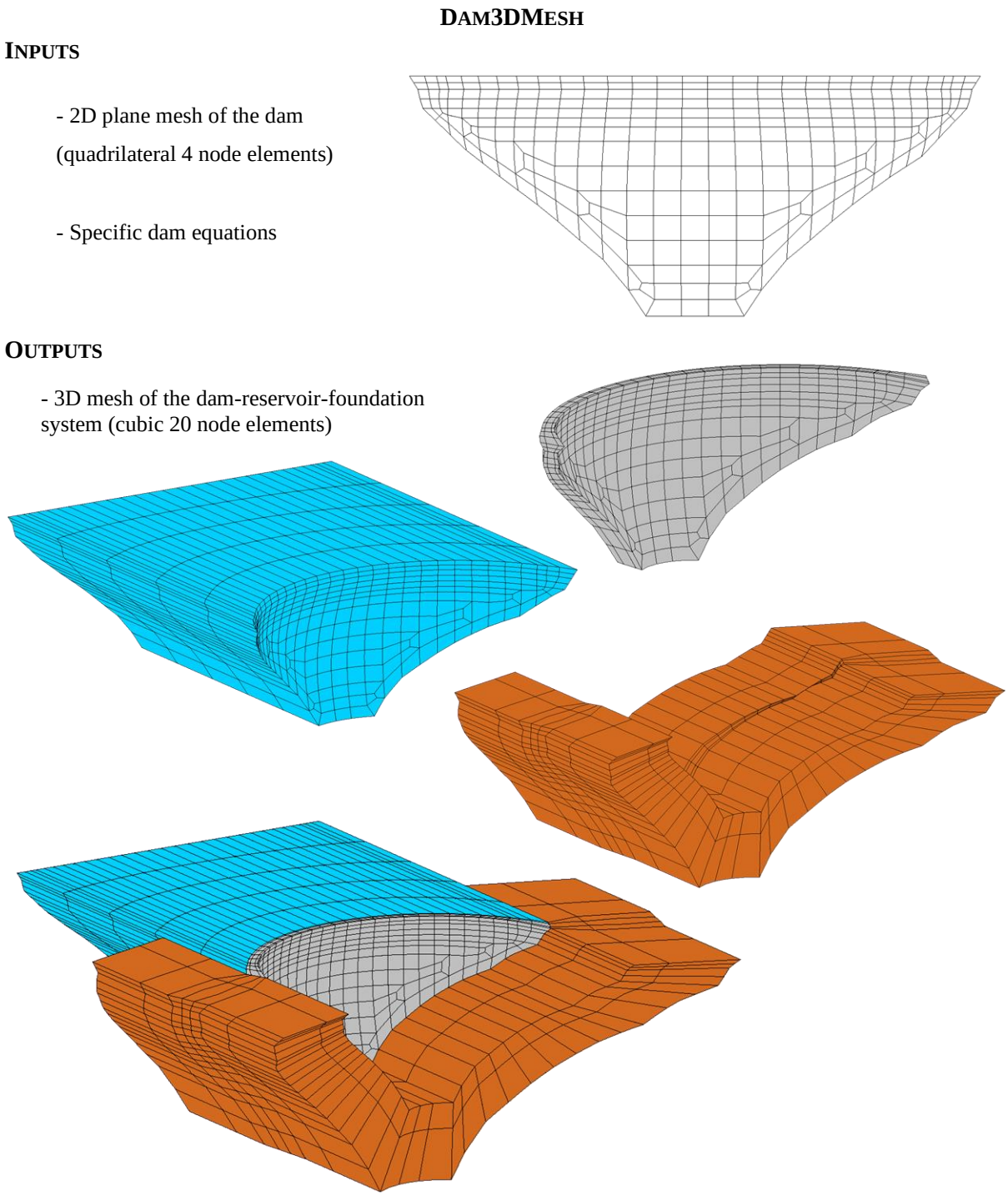

Fig. 3.40 *Dam3DMesh*. Inputs and outputs.

In the scope of this thesis, considering the goal of performing non-linear seismic simulations, a new module was developed for *Dam3DMesh* to automatically introduce joints in the finite element mesh of the dam

(Fig. 3.41). As input, this new module requires only the Excel data file with the data on the 3D mesh of the 3D dam-reservoir-foundation system, to which it is only necessary to add a list with the elements of the blocks or cantilevers composing the dam body; if required, additional lists of elements to simulate cracks or other discontinuities can also be given. Then, through a set of consecutive programming routines, the implemented code provides a list of joints elements, which includes the number of each element and the corresponding face, namely: (i) along the dam base, to define the dam-foundation surface; (ii) in the contacts between adjacent cantilevers, to introduce the vertical contraction joints; and (iii) between specific elements in the dam body, to reproduce existing cracks or other discontinuities.

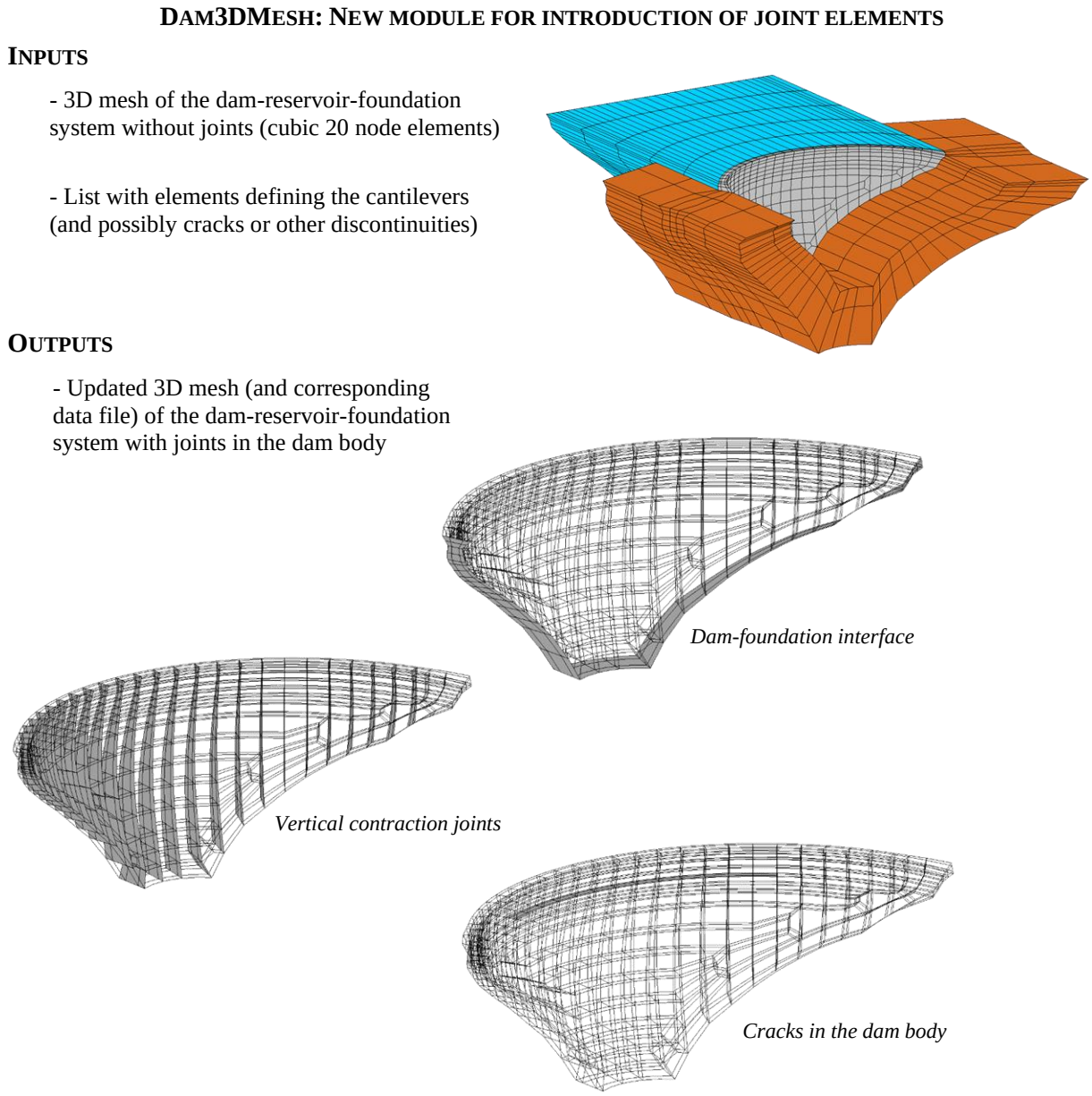

Fig. 3.41 New module for *Dam3DMesh*: introduction of joint elements in 3D finite element meshes.

3.11 FINAL CONSIDERATIONS

The current chapter was dedicated to the numerical modelling of the dynamic behaviour of dam-reservoir-foundation systems, and the main goal was the presentation of the finite element-based formulations for modal analysis, linear seismic analysis, and non-linear seismic analysis.

The chapter started with a comprehensive state-of-the-art review, which described the principal types of models used to simulate dam-reservoir dynamic interaction and hydrodynamic effects - added water mass models or coupled models in displacements and pressures/velocity potentials with radiation in the reservoir -, and to simulate the dam-foundation interaction and the foundation behaviour – massless foundation or foundation with mass and radiation energy dissipation.

The advantages and disadvantages of the different approaches used in current practice were referred. For example, traditional added water mass models are simpler and do not require the reservoir discretisation, but neglect water compressibility and other hydrodynamic effects. Consequently, added water mass reduction factors are recommended for dynamic analysis of arch dams. On the other hand, coupled models require the reservoir discretisation, leading to larger problems, and the definition of specific boundary conditions. However, these boundary conditions enable the proper simulation of dam-water dynamic interaction and radiation damping. Regarding the Foundation, models based on the massless approach do not account for the foundation inertia nor the radiation damping, which can alter the dam stress state if no additional damping source is considered. Nevertheless, massless foundation models are simple, and a damping component can be applied at the dam-rock interface. Also, the use of the substructure method to consider the foundation block as an elastic massless substructure enables to achieve highly efficient models. Various types of models combining the different modelling approaches have been used successfully in the past but coupled models with massless or massed foundations usually lead to the best results. A coupled model with massless foundation was considered in this thesis.

After that, the provided review addressed the mathematical formulations that are usually used to perform modal analysis and to calculate the forced dynamic response, both for symmetric problems, as is the case of the classic added water mass models, and for non-symmetric problems, case of coupled problems, considering either linear or non-linear behaviour. Overall, classic solutions from Structural Dynamics can be adopted to solve problems using added water mass models with proportional damping, whereas the formulations commonly used to solve dynamic equations of coupled problems require special procedures that treat the solid and fluid separately and/or neglect the generalized (or non-proportional) damping matrix.

Therefore, in this work it was decided to develop a complete finite element formulation in displacements and pressures calculate the global dynamic response the dam-reservoir-foundation system, by solving the coupled dynamic equation and considering generalized damping.

A state-space formulation was adopted for coupled modal analysis of the dam-reservoir-foundation system, resulting in the calculation of complex eigenvalues and eigenvectors. Complex eigenproblems are typical of dynamic systems described by non-symmetric matrices, such as those resulting from structure-fluid

coupled analysis and/or from the use of damping matrices non-proportional to the mass and stiffness. Physically, complex eigenvectors correspond to the calculation of non-stationary vibration modes.

A time-stepping coupled formulation was proposed for numerical integration in time domain, based on the application of the Newmark method to the global dynamic equation, in order to calculate the response of the dam-reservoir-foundation system in displacements and pressures, under applied dynamic loads. For seismic analysis, acceleration time histories are used as input.

In addition, a complete formulation was also developed for non-linear dynamic analysis, by combining the referred time-stepping procedure with the stress-transfer iterative method, which enables the simulation of non-linear structural behaviour. Aiming to use this finite element formulation for non-linear seismic analysis of arch dams, a strain-softening constitutive damage model with two independent damage variables was implemented to simulate concrete failure under tension and compression, and a joint constitutive model, based on the Mohr-Coulomb failure criterion and considering normal and shear stress-relative displacement laws, was used to account for opening/closing and sliding movements.

The formulations proposed in this chapter were implemented in the new version of the finite element program *DamDySSA*, developed for dynamic analysis of concrete dams. In the course of this work, the first version a new interactive graphic interface was developed for this program, with a view to simplify its use, as well as the analysis and interpretation of the results.

Regarding the developed formulations, it is important to highlight their simplicity and elegance, which has facilitated the implementation into the pre-existing finite element code of *DamDySSA*, as well as their computational efficiency, despite considering hydrodynamic displacements and pressures as variables.

Moreover, it is worth emphasizing that the development of the referred formulations and their implementation in *DamDySSA*, instead of opting to use a commercial software, brought numerous advantages for this work. On the one hand, this allowed to obtain a deeper knowledge of the formulations and of the behaviour intended to simulate, and, at the same time, to ensure complete control over all variables and lines of code, which could be corrected or updated whenever necessary. On the other hand, it was necessary to develop several graphical tools from scratch, which enabled to optimize and adapt the figures according to the goals of the studies to be conducted. Examples include figures representing the evolution of natural frequencies or with the modal configurations, to be compared with experimental results obtained from continuous dynamic monitoring systems, as well as high-quality 3D representations of deformed shapes, stress fields, and damage distributions, to ensure a proper evaluation of the non-linear seismic behaviour and particularly for seismic safety assessment.

Finally, the chapter ended with several tests on the dynamic behaviour of dam-reservoir-foundation systems, namely to analyse modal parameters, displacements and hydrodynamic pressures, and joint movements, involving the comparison of numerical results with experimental results or analytical solutions. The results achieved in these tests enabled to validate the proposed formulations and show the potential of the program *DamDySSA*. Therefore, *DamDySSA* was used to carry out the numerical calculations for the application studies on the dynamic behaviour of two large arch dams, presented in Chapter 5.

CHAPTER 4

SEISMIC AND STRUCTURAL HEALTH MONITORING OF LARGE CONCRETE DAMS

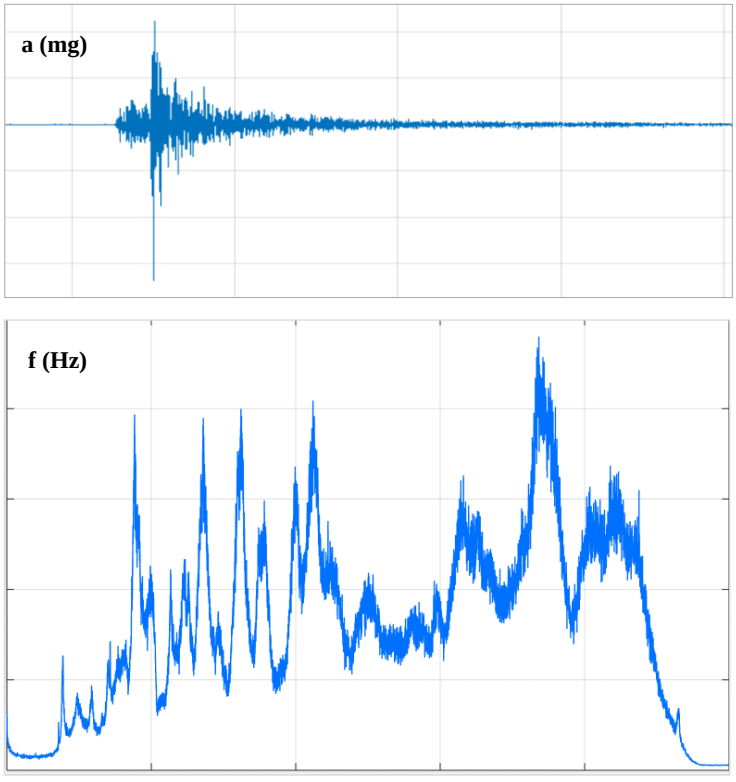

4. SEISMIC AND STRUCTURAL HEALTH MONITORING OF LARGE CONCRETE DAMS

4.1 INTRODUCTION

The observation and analysis of the dynamic behaviour of large concrete dams is essential for increasing knowledge on the response of dam-reservoir-foundation systems and for supporting structural safety control, something that has been widely recognised for decades as a result of the considerable research conducted on monitoring vibrations on large dams (recall subchapter 2.5). Furthermore, the concept of Seismic and Structural Health Monitoring (SSHM) has emerged and asserted itself on a global level over the past years, not only due to the needs of owners, managers and users, but also to the inherent advantages of SSHM and the useful data that can be provided (Limongelli & Çelebi, 2019).

Therefore, considering the importance of evaluating the performance of dams in normal operating conditions and during seismic events (ICOLD, 2018, 2019b), the installation of SSHM systems (Fig. 4.1) has been proposed and undertaken for new and old large concrete dams worldwide, as described in detail in section 2.5.4. Nevertheless, in parallel with the continuous evolution in the technology for measuring vibrations and for data acquisition and storage, important challenges continue to arise in this field, particularly in what concerns the software component, which is essential to ensure a proper operation of monitoring systems and thus to provide useful data for dynamic behaviour analysis, particularly when monitoring data is used in combination with modelling results (Alegre, Carvalho, et al., 2019; S. Oliveira et al., 2011, 2012; S. Oliveira & Alegre, 2018), and for informed decision making (S. Oliveira & Alegre, 2020). The need to complement these systems by developing programs adapted and optimized to each dam is highlighted, aiming to perform tasks such as automatic and continuous management and analysis of monitoring data.

In this scope, the aim in this chapter is to present the programs developed to integrate and complement the software component of continuous dynamic monitoring systems installed in large concrete dams, comprising computational tools for automatic analysis and management of continuous monitoring data and for automatic identification of modal parameters.

As for the contents of the current chapter, subchapter 4.2 presents a state-of-the-art review on SSHM systems, with emphasis on their use for continuous dynamic monitoring of large concrete dams. This includes three sections, namely, to address the main goals and advantages of this type of system for dam safety control, general considerations regarding monitoring schemes and the hardware used, and important aspects on their installation and operation. The following two subchapters describe the software developed in this work. Subchapter 4.3 presents the program *DamSSHM*, developed for automatic analysis and management of continuous dynamic monitoring data, which is implemented for testing in the SSHM system installed in Cabril dam. Detailed descriptions are provided regarding the four modules of the program and the tasks executed by each one, including the reading of the data files, the analysis and management of the acceleration records, the automatic detection of dynamic vibrations during seismic events, and the automatic maintenance of the server storage. Subchapter 4.4 is focused on the program *DamModalID*, developed for automatic modal identification and optimized for the identification of modal parameters for

dams. First, a brief review on Operational Modal Analysis (OMA) is given, and the main modal identification methods are referred. Then, general remarks on signal processing and frequency-domain modal identification are addressed. After that, the modal identification method implemented in *DamModalID* is presented in detail, which is based on the frequency domain decomposition method, and complemented by new techniques proposed in this work for automatic selection of spectral and for enhancing modal parameter estimation of dams. Finally, the algorithm and the developed graphical user interface of *DamModalID* are shown.

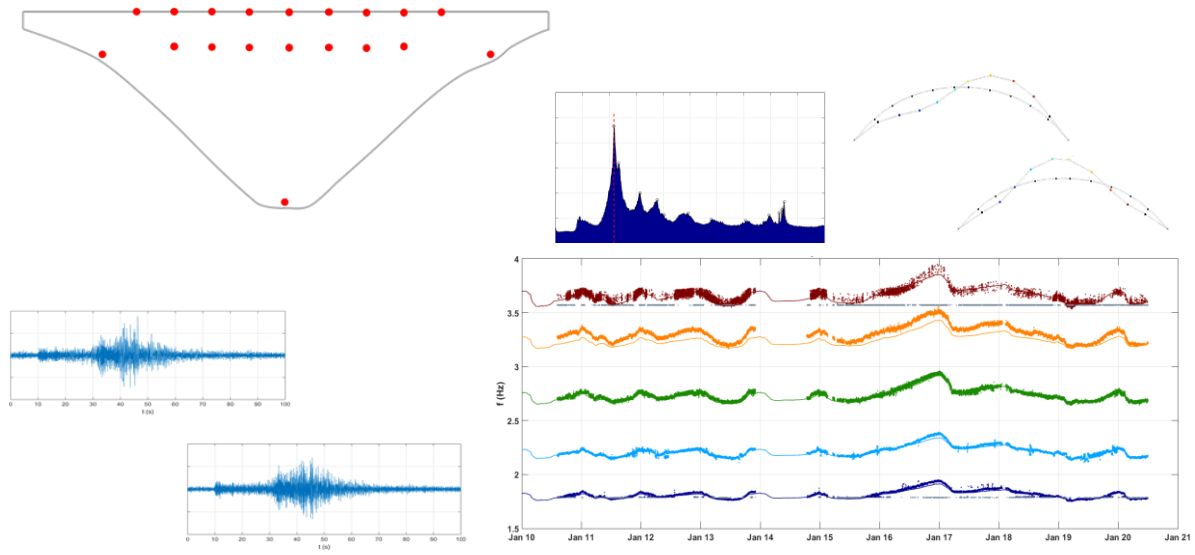

Fig. 4.1 Representation of an SSHM scheme for a large dam. Seismic acceleration records and modal identification results (mode shapes and evolution of natural frequencies over time).

4.2 STATE-OF-THE-ART: SSHM SYSTEMS FOR LARGE CONCRETE DAMS

The concept of Seismic and Structural Health Monitoring (SSHM) refers to the implementation of a set of procedures and strategies aiming to characterize the dynamic behaviour of structures based on their response to ambient/operational vibrations and to seismic vibrations, recorded using a permanent monitoring network, and consequently to provide useful information for controlling structural integrity and for supporting informed management.

Nowadays, the dynamic behaviour monitoring and the structural safety control of many large structures all over the world, such as tall buildings, long-span bridges, large dams and other important structures, is based on methods that use data retrieved from Seismic and Structural Health Monitoring (SSHM) systems (Limongelli & Çelebi, 2019). When installed, configured, and operated correctly, these systems enable the continuous evaluation of structural performance in normal operating conditions and during extraordinary events such as earthquakes, and can be a valuable asset to assess structural health conditions as well as serviceability and functionality. Namely, data from continuous dynamic monitoring can be used to analyse the seismic response under earthquakes of various intensities and study the evolution of modal parameters

over time. Possibly, damage detection, often associated with stiffness losses, can be performed by comparing the measured response with a reference state or with numerical models calibrated based on that reference state. Furthermore, the permanent surveillance of this type of structures can be fundamental (Limongelli, 2020), on one hand, because there is a need for effective maintenance interventions, to ensure that normal service conditions are not affected and that structural integrity is maintained, and, on the other, given that hazards from the natural or man-made environment, such as earthquakes or floods, can result in emergency situations that have to be dealt with efficiency, to reduce service interruption and prevent or minimize environmental, material and human damages. Despite the significant investment required and the challenges still posed in this field (Limongelli, 2019), SSHM systems have proven to be a superior alternative to traditional observation and monitoring methods and are capable of providing useful results for different types of structures, including large dams, bridges, high-rise buildings and towers and historical monuments (Li et al., 2016; Limongelli & Çelebi, 2019). In addition, the evolution and increasing efficiency of monitoring equipment for continuous vibrations measurement and acquisition and of hardware for data storage and management enable to design sophisticated and reliable permanent monitoring systems.

The popularity of SSHM methodologies for dam safety control has suffered an important growth over the past 10 to 15 years, which is well evidenced by the number of dams instrumented with continuous dynamic monitoring systems all over the world today (Fig. 4.2), as addressed in section 2.5.4, namely for new large dams, to evaluate their behaviour since the first filling of the reservoir, and for older dams, built decades ago and possibly suffering from deterioration problems.

Cabrill dam (1954), Portugal, 132 m high

Baixo-Sabor dam (2016), Portugal, 123 m high

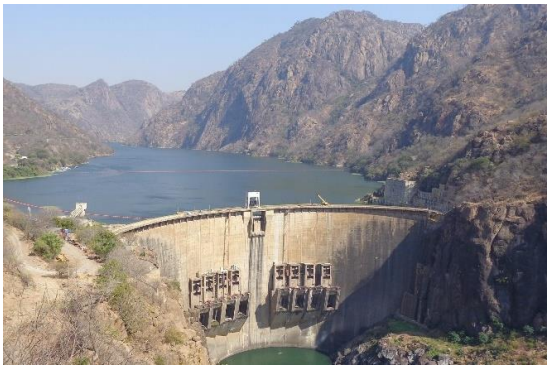

Cahora Bassa dam (1974), Mozambique, 171 m high

Rood Elsberg dam (1969), South Africa, 72 m high

Fig. 4.2 Large concrete dams currently under continuous dynamic monitoring using SSHM systems.

This was fostered by the undeniable advantages of continuous dynamic monitoring, both for analysing the response of dam-reservoir-foundation systems and to support safety control studies, as well as by the increasing safety requirements from dam owners and from the researchers and engineers responsible for dam safety. In addition, the use of SSHM systems makes it possible to meet the recommendations on the need for continuously monitoring of the performance of large concrete dams in normal operating conditions and during seismic events (ICOLD, 2018, 2019b).

4.2.1 MAIN GOALS AND ADVANTAGES

In what concerns the application of SSHM systems for monitoring the dynamic behaviour of large concrete dams (Fig. 4.3), the monitoring scheme should ideally be designed to measure vibrations in the dam body, in as many positions as possible, at several points along the dam-foundation surface, mainly at the dam base, and, if possible, in the free field (Darbre, 1995), aiming to continuously evaluate their performance in normal operating conditions and when seismic events occur (Alegre, Carvalho, et al., 2019; Bukenya & Moyo, 2017; S. Oliveira & Alegre, 2019a). Therefore, this type of systems must be configured with a high dynamic range, to ensure an accurate measurement of both low amplitude accelerations, induced by ambient and operational vibrations or by lower intensity earthquakes, and high amplitude accelerations, caused by strong earthquakes or other extraordinary events (Mendes, 2010).

With the abovementioned goal in mind, these monitoring systems should be installed using cutting-edge and quality hardware for automatic data measurement and acquisition, including digitizers, recorders, transducers, accelerometers, data concentrators, etc., which are usually provided by specialized companies like Kinemetrics, Inc. (https://kinemetrics.com/), GeoSIG Ltd. (https://www.geosig.com/) and Nanometrics (https://www.nanometrics.ca/). Nevertheless, it is vital to complement the hardware component with suitable software, adapted and optimized to each dam and the respective monitoring system, to process, manage and analyse monitoring data (Alegre, Oliveira, et al., 2020; S. Oliveira & Alegre, 2020, 2018).

In order to obtain useful data for dynamic behaviour analysis and taking the SSHM goals into consideration, the software component should include tools for automatic identification of modal parameters, i.e. natural frequencies, mode shapes and damping ratios, and for automatic detection of vibrations induced by seismic events, which must be distinguished from those induced by the operation of gates and turbines, as well as modules that allow the comparison with results from reference numerical models in a simple and expeditious way.

According to the experience accumulated in this field, particularly in recent studies carried out in LNEC on the dynamic behaviour of Cabril dam and Cahora Bassa dam, the combined use of experimental results retrieved from SSHM data and of numerical results from advanced finite element models have proven to be really useful, namely: (i) to study the evolution of the modal parameters over time, enabling to evaluate the effects of reservoir water level variations (Alegre, Carvalho, et al., 2019; Bukenya & Moyo, 2017; Darbre & Proulx, 2002; Okuma et al., 2012; S. Oliveira et al., 2012; Proulx et al., 2001) and/or thermal variations (Ueshima et al., 2017) on the dynamic response of the dam-reservoir-foundation system; (ii) to

assess the effects due to the ageing of dams or to perform damage detection based on the evolution of natural frequencies (Alegre, Oliveira, et al., 2020; S. Oliveira & Alegre, 2020), by comparing the observed behaviour at a certain point in time with a specific reference state or with the behaviour simulated using a reference numerical model (calibrated for that same reference state); (iii) to evaluate possible damages or other structural effects caused by strong earthquakes, by analysing the dynamic performance in normal operating conditions before and after the seismic events; and iv) to analyse the acceleration time histories recorded during seismic events, in order to characterize the seismic actions and to analyse the response during low, medium or high intensity earthquakes, with focus on the amplification of peak accelerations from the base to the top of the dam (Alegre, Robbe, et al., 2020; Chopra & Wang, 2010; S. Oliveira & Alegre, 2020; Proulx & Darbre, 2008; Robbe, 2017; Robbe et al., 2017).

This SSHM methodology, based on the comparison of measured and computed responses under ambient/operational vibrations and seismic vibrations, can be a very important source for increasing knowledge on the dynamic behaviour of large concrete dams, in terms of both modal analysis and seismic response analysis. Furthermore, valuable data can be gathered to provide additional insight on the response of dam-reservoir-foundation systems, namely in what concerns the dam-water dynamic interaction, the effects of water level or thermal variations in the dynamic properties, the response in accelerations and the damping mechanism for earthquakes of different intensities, etc., which are fundamental aspects to take into account in numerical modelling. This data can therefore be used for calibrating and validating existing models or help in the development of new ones, which will then be used as reference models for structural health monitoring, or for simulating different scenarios, in order to support the design of new dams or to carry out safety assessment of existing dams. Finally, in the scope of dam safety control, valuable information can also be provided to owners and to entities responsible for safety control and health monitoring, enabling cost-effective and condition-based decisions to be made in a timely fashion, for ordinary maintenance needs and for management of eventual emergency situations.

4.2.2 MONITORING SCHEME AND MAIN COMPONENTS

The definition of the overall architecture of an SSHM system for a large concrete dam should be carried out carefully for each specific case. The monitoring scheme should be designed based on results obtained with dynamic behaviour prediction models, such as finite element numerical models, as well as on experimental data gathered from forced and/or ambient vibration tests, previously performed on site (Limongelli & Çelebi, 2019). Therefore, it is possible to determine the best location for the measuring equipment in order to characterize the dynamic response of the dam in normal operating conditions and during seismic events, by positioning the sensors in zones of the dam body where the most significant oscillatory movements are expected, as well as to characterize the seismic accelerations arriving at the dam site, by placing accelerometers along the dam base or in the free field.

SSHM SYSTEMS FOR LARGE CONCRETE DAMS

Hardware

- Accelerometers, digitizers, data concentrators, electric/optical signal converters, cables for data transmission
- Local computer server and hard drives for data storage
- Internet connection and devices to enable remote access

Software

- Data acquisition and management
- Automatic detection of seismic vibrations and modal identification

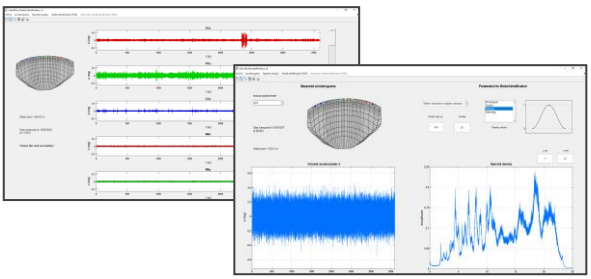

- Finite element modelling: modal analysis and seismic analysis

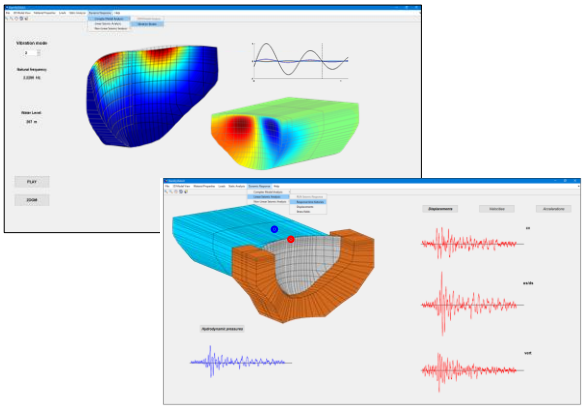

Combined use of experimental and numerical results

- Evolution of natural frequencies (Hz) over time

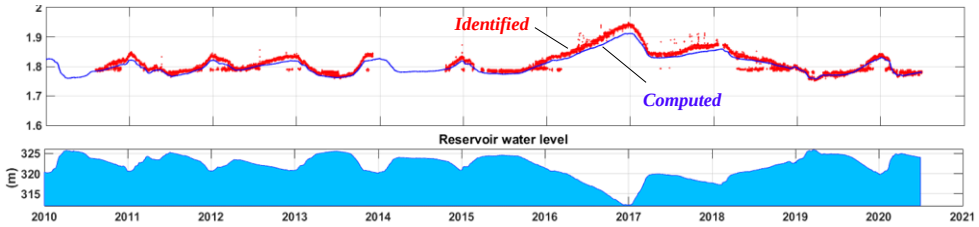

- Seismic accelerations (mg)

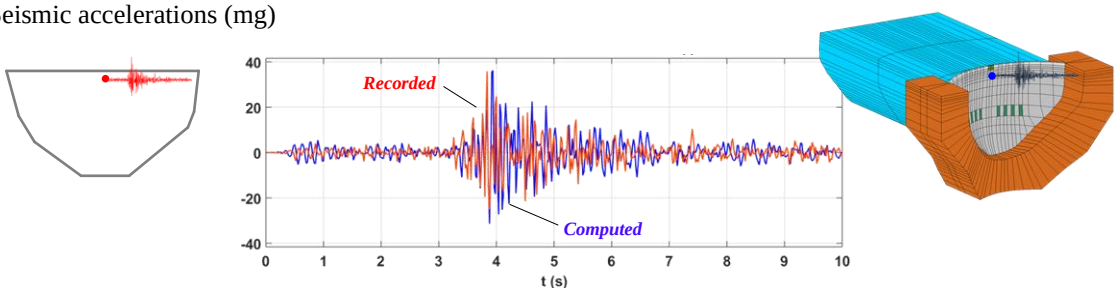

Fig. 4.3 SSHM systems for large concrete dams. Main hardware and software components and results.

The regular solutions of monitoring schemes of SSHM systems comprise a reasonable number of accelerometers, which are installed in the upper zone of the dam, usually near the crest, and also close to the dam-foundation interface, e.g., at the base (central section) and/or near the abutments (Fig. 4.4). However, the ideal solution would be to install a large number of sensors, not only near the crest but also at other elevations along the height of the dam, which would allow for a more accurate modal identification of the frequencies and modal configurations of the vibration modes, particularly those associated to higher frequencies (Cantieni, 2005; Cantieni et al., 1998; Darbre et al., 2000). Moreover, it would be very advantageous to deploy several accelerometers along the insertion, not only near the dam-foundation interface, but also in the free-field, to better characterise the seismic action and its propagation along the rock mass from different directions, enabling to further investigate the phenomenon of the ground motion spatial variation (Alves, 2004; Chopra & Wang, 2010; Koufoudi et al., 2018).

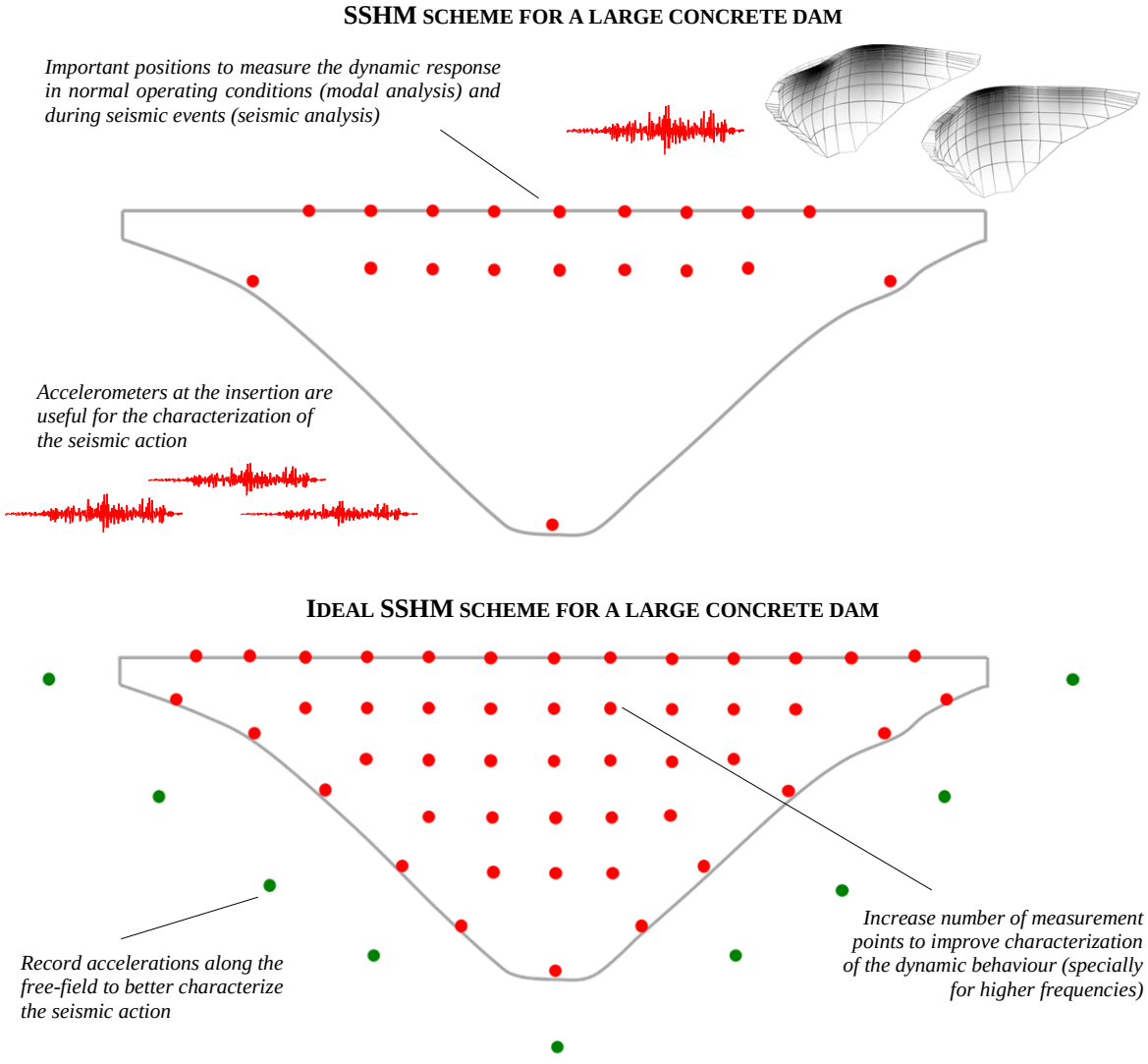

Fig. 4.4 Schematic representation of common and ideal solutions of monitoring schemes for large concrete dams.

In what regards the instrumentation, it is necessary to perform a cost-benefit analysis and to evaluate the equipment available on the market, aiming to provide the system with the best solutions according to the available funds. It is also fundamental to assess the metrological requirements for the quantities to be measured, namely the dynamic range, the sensitivity, the admissible uncertainties, and the sampling frequency (Cantieni, 2001; Cantieni et al., 1994, 1998; Darbre et al., 2000; de Smet et al., 1998; Pietrzko & Cantieni, 1994). Other relevant features to consider when choosing accelerometers are the hysteresis, the cross-axis sensitivity, and the thermal drift. Furthermore, the equipment in general must be reliable and durable, have mechanical ruggedness, to resist the imposed actions and environmental conditions during their operation, and be protected from damages caused by power surges and voltage spikes (e.g., due to lightning), to keep the system in operation.

As the name indicates, an SSHM system is installed in a large concrete dam aiming to measure the seismic response and to assess its structural health condition. Considering these purposes, it is therefore recommended the use of force-balance accelerometers, including triaxial accelerometers, set for recording accelerations in the cross-valley, upstream-downstream and vertical directions, and uniaxial accelerometers, for measuring vibrations in the upstream-downstream or radial direction.

Usually, the triaxial sensors are especially useful for characterizing the seismic action and the dam response during a seismic event, while the uniaxial sensors are best suited for gathering data to study the dynamic behaviour of the dam in normal operating conditions, by recording ambient/operational vibrations. Therefore, the accelerometers should be configured differently: the uniaxial accelerometers with a lower full-scale range (e.g. of ± 0.25g), given the lower amplitude of vibrations from ambient/operational sources, while the triaxial accelerometers must have a higher range (e.g. from 0.5g to 4g), to enable recording of accelerations under seismic events with different intensities and to avoid saturation under a strong earthquake (Mendes, 2010; S. Oliveira & Silvestre, 2017). In this way, the uniaxial sensors ensure greater accuracy when recording low amplitude vibrations from ambient/operational sources, while also being able to measure low amplitude seismic vibrations, depending on the earthquake intensity and on the distance from its epicentre to the dam site. Moreover, provided that triaxial accelerometers are installed near the dam-rock interface and at the top of dam near the crest, where the maximum response values are expected according to the prediction models (Alegre, Robbe, et al., 2020; Chopra & Wang, 2010; Proulx & Darbre, 2008; Robbe, 2017; Robbe et al., 2017), it is possible to accurately evaluate the base-to-top amplification factors of peak accelerations.

In what concerns data acquisition units, the most recent solutions available include equipment with several functionalities and advantages. These units, specifically developed for continuous monitoring systems, have multiple channels for connection of several measurement sensors and are able to acquire and store data with high sampling rates and excellent resolution. Furthermore, they also allow to create and manage databases and to establish communications via internet for remote access and control of the units installed on site. Some of these solutions even include their own software or dedicated webservers to allow remote access and perform diagnostic and maintenance tests. Currently, there are several solutions of measuring

equipment and data acquisition available on the market for seismic response monitoring and/or for structural health monitoring, provided by specialised companies in the field (Fig. 4.5).

Fig. 4.5 Examples of available equipment for SSHM systems. Accelerometers and data acquisition units.

In order to establish the connection between the measuring sensors and the data acquisition units, optical-fibre cables or wireless networks can be used, as alternatives to classic electrical cables with copper conductors. In the particular case of the optical-fibre cables, these are an excellent solution for implementation in a large concrete dam monitoring system, considering that this type of cables are able to avoid electromagnetic problems in locations where power surges occur (a common situation in dams), offer protection during thunderstorms, and are suitable for transmitting data over long distances (Garrett, 2007). Moreover, the use of optical fibres has become more common over the years and their availability in the market has increased, hence their cost has decreased. As for wireless networks, if designed properly, they could permit higher distances between sensors, lower energy consumption and no need of further devices to ensure data synchronization (Lynch, 2007). Also, the data recorded on the data acquisition units should be continuously stored in local or remote data repositories and synchronised with computer servers at the

workplaces to enable the creation of databases and to carry out proper dam behaviour analyses, via proper, high-quality Internet connections.

In the case of a large concrete dam, the aim is to continuously measure vibrations at various locations, with high sampling frequencies. Thus, depending on the location and distribution of the measuring equipment along the dam galleries, the installation of several data acquisition units, which must be perfectly synchronised, may be recommended. In addition, considering that data acquisition units have limited data storage capacity, it is necessary to install a central computer server to collect and store all monitoring data. Given the significant amount of recorded data that has to be transmitted and stored, the distances to be covered and the existing constraints on the dam site, which is usually a remote site, a possible solution may be to design and implement a local network, using optical-fibre cables, to connect the referred equipment and to enable data transmission to the central server (Mendes, 2010; S. Oliveira & Alegre, 2019a). In that case, it can be beneficial to design a ring network layout, which allows for two alternative paths for data transmission between all data acquisition units and the central server; hence, in the event of any type of malfunction that prevents one of the data paths, all data can be sent in the other direction of the ring network. This design was adopted for the pioneer SSHM system installed in Cabril dam (Fig. 4.6).

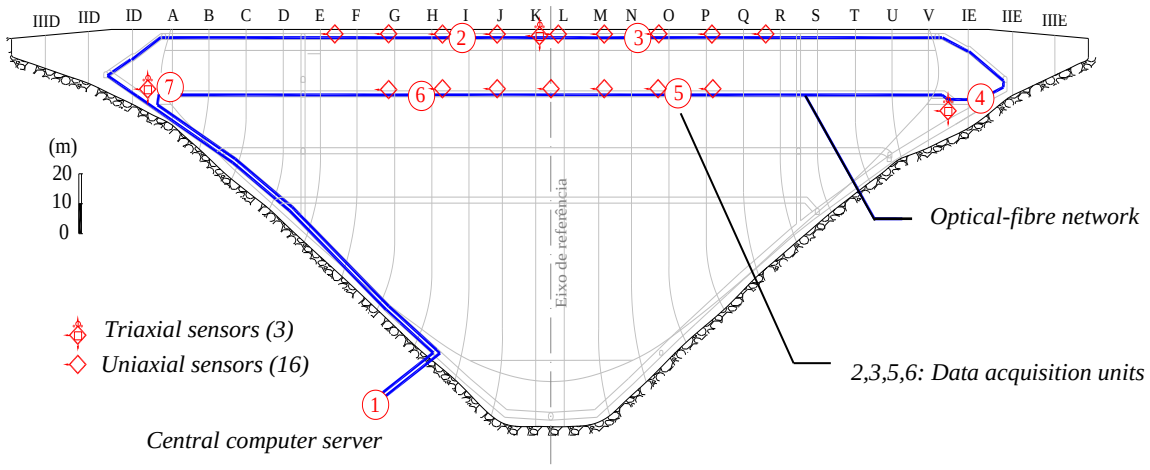

Fig. 4.6 SSHM systems installed in Cabril dam. Optical-fibre network, data acquisition units (2,3,5,6), and positions of the accelerometers. Adapted from (S. Oliveira & Silvestre, 2017).

4.2.3 INSTALLATION, OPERATION AND REQUIRED SOFTWARE

The installation of an SSHM system on a large dam involves a series of works on the dam site and of tests in the laboratory. These should be carried out carefully and follow a well-defined plan, with a view to guarantee the reliability of the system and that it functions properly during its operation. Overall, in an initial phase, the equipment for data measurement and acquisition, as well as the software for data processing, management, and analysis, should be properly configured and tested. Then, the local network for data transmission, whether optical fibre or wireless, is installed in the dam, to ensure a proper connection between the accelerometers (and maybe other measuring sensors) to the data acquisition units, and the latter

to the computer server for data storage. In addition, equipment storage boxes, where the data acquisition units and all associated accessories are assembled, are placed in the proper locations, and concrete niches are created in the dam galleries, to isolate and protect the accelerometers (Mendes, 2010; S. Oliveira & Silvestre, 2017). After that, to store/manage all monitoring data and to use appropriate software that complements the SSHM system, the computer servers for data storage must properly installed in suitable locations and ensure enough memory capacity to gather all monitoring data. Finally, all equipment can be correctly deployed and connected to the local network to form the overall monitoring system (Fig. 4.7).

Fig. 4.7 Installation of the dynamic monitoring system at Cabril dam. Uniaxial and triaxial accelerometers, equipment storage box for data acquisition units, and optical-fibre cables (S. Oliveira & Silvestre, 2017).

After completing the installation of all equipment, the operation phase of the SSHM system can begin. Nevertheless, to achieve the proposed objectives, it is essential to guarantee not only an effective control of the system over time, but also the ability to retrieve useful information from collected monitoring data.

On the one hand, given that the dam site is usually in a remote location, far from the workplace of researchers and technicians/engineers responsible for dam safety control, remote access to the system must be assured, e.g., using existing tools such as TeamViewer or Chrome Remote Desktop. Therefore, it is also essential to ensure a good, or at least stable, Internet connection, to allow all required tasks to be performed in a simple and trouble-free way, and, if necessary, to transfer data via cloud storage. In this way, it is possible to evaluate the status of the system over time, assess the need for repair/maintenance actions (ideally carried out by technicians working on the dam site), carry out software maintenance, and perform specific analyses on the latest recorded data using software suitable for seismic response and structural health condition studies. However, periodic visits to the site must also be accounted for.

On the other hand, it is important to emphasize the need to complement the SSHM systems with appropriate software for processing, managing, and analysing dynamic monitoring data collected on a continuous basis. In recent years, the specialized companies that develop and supply measuring and data acquisition equipment have also started to invest in software for data acquisition and processing, as well as in tools for analysing vibrations measured under normal operating conditions and vibrations induced by seismic events. However, dams are special structures, whose dynamic behaviour is influenced by multiple factors, and each dam has unique features. Therefore, there is a clear need to develop software, adapted and optimised for each dam and the installed SSHM system, for data processing, management, and analysis. This SSHM software, properly equipped with adequate graphical tools, will allow the retrieval of useful data, and

facilitate the analysis and interpretation of the dynamic behaviour of dams under normal operating conditions and during seismic events, as well as provide relevant information dam owners and to the entities responsible for dam safety, to support decision making in current or emergency maintenance situations.

The present work intends to contribute with the development of specific software and computational tools to complement and improve SSHM systems installed in large concrete dams, namely *DamSSHM*, for automatic data analysis and management, and *DamModalID*, for automatic modal identification. These programs are described in detail in subchapters 4.3 and 4.4, respectively.

4.3 SOFTWARE FOR MANAGEMENT AND ANALYSIS OF MONITORING DATA: *DAMSSHM*

DamSSHM is a program developed in MATLAB for automatic analysis and management of continuous vibrations monitoring data collected with SSHM systems installed in large concrete dams. The first version of *DamSSHM* was specifically designed and optimized to complement and improve the operation of the SSHM installed in Cabril dam (Mendes, 2010; S. Oliveira & Silvestre, 2017), which has been in operation since 2008 and under LNEC's supervision ever since. This program is installed in the central computer server of the system (Fig. 4.8) and it includes four modules, namely for: (i) reading data files recorded with the data acquisition units; (ii) automatic data analysis and management, (iii) automatic detection of seismic vibrations, and (iii) automatic management of storage hardware. Each module is described in detail in the following sections.

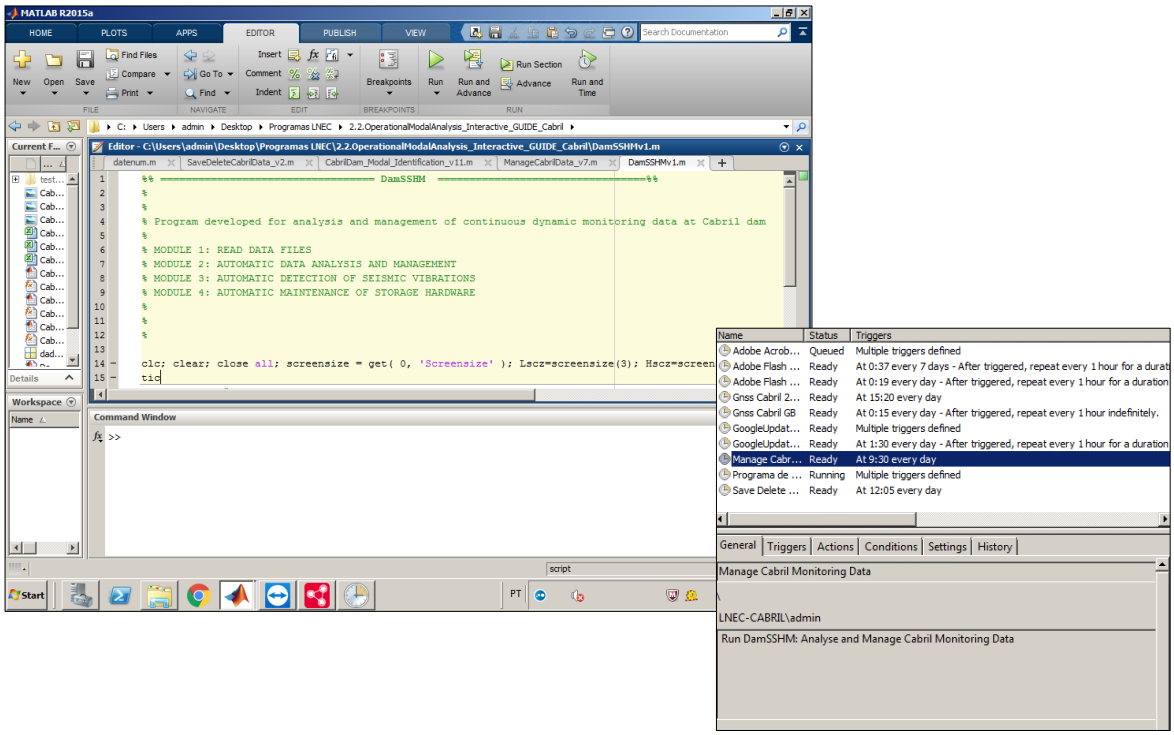

Fig. 4.8 Desktop environment of the central server installed in Cabril dam' SSHM system. MATLAB work environment showing the *DamSSHM* code and task scheduled with Windows Task Scheduler.

DamSSHM is executed automatically, every day at 9:30 am, as a specific task scheduled using the Windows Task Scheduler tool. Furthermore, a private email account, associated with the SSHM system, was created to allow the program to automatically send emails, and a Google Drive folder was configured to enable automatic cloud storage of data. Since 2018, and still in the testing phase, *DamSSHM* is working automatically and independently in Cabril dam, as shown in this chapter.

4.3.1 MODULE 1: READ DATA FILES

The automatic collection, management and analysis of continuous monitoring data is fundamental for the successful operation of an SSHM system, as previously emphasized in this chapter. In the case of Cabril dam, the data continuously recorded with the measuring sensors is collected with 4 data acquisition units (recall Fig. 4.6) and sent to the central computer server, Then, using *Cabril_Aquis*, a program developed in LabView at the Scientific Instrumentation Centre of LNEC (S. Oliveira & Silvestre, 2017; Reis & Oliveira Costa, 2009), this data is stored in 4 binary files, one for each unit, every hour. The files are saved in a pre-defined computer directory, and their names are basically sets of characters that contain information on the number of the corresponding data acquisition unit X (from 1 to 4) and on the year YY, month MM, day DD and hour HH of recording, e.g., *E01E0X@YYMMDDHH.dat*. Therefore, to take advantage of the previously carried out work, the first module of *DamSSHM* was specifically prepared to read the sets of 4 binary data files from *Cabril_Aquis* and to create matrices in MATLAB with all the acceleration records.

First, as soon as the program runs, module 1 begins by setting the date of the previous day as the analysis date and selects all files from that day in the main storage directory. For example, if the program runs on November 11, all files recorded during the 24 hours of November 10, i.e., files with the designation *E01E0X@YY1110HH.dat*, are selected. Then, for each hour of the day, the data is extracted from the 4 binary data files, using the commands *fopen* and *fread* to access and read binary files, in order to obtain the acceleration time histories (in m/s^2 or in g) for all accelerometers installed in the dam. In addition, aiming to increase the efficiency of future analyses while also maintaining the quality of the data, the original acceleration records, measured with a sampling frequency of 1000 Hz, are converted to decimated versions, considering an artificial sampling rate of 50 Hz. Finally, a moving average filter is applied to all signals to regulate the time histories by filtering unwanted noise components, thus ensuring their mean value is set to zero (see section 4.4.2 for further details).

Following these preliminary tasks, the analysis and management of the acceleration records (module 2), the automatic detection of seismic vibrations (module 3) and the maintenance of the storage hardware (module 4) can be carried out.

4.3.2 MODULE 2: AUTOMATIC DATA ANALYSIS AND MANAGEMENT

The second module of *DamSSHM* was developed both for analysing the acceleration records, aiming to detect errors and evaluate their integrity, and for management of the collected data files, with a view to perform the maintenance of the storage hardware installed on the dam site. The tasks described next are

carried out for each hour of the analysis date, i.e., using all the files selected with module 1 for the corresponding day.

In the first phase, module 2 executes a series of tasks to evaluate all the accelerations records, aiming to detect corrupt files or records with measurement errors (Fig. 4.9). These errors can be occasional, if they occur only in one or two sensors, or general, when detected in most or in all sensors. Also, errors in the data files can also be associated with problems occurring with specific data acquisition units, and, in such cases, the acceleration records of the sensors connected to those units will be corrupt. As a result of this evaluation, and to allow for a proper management of data files and accurate studies on the dam dynamic behaviour to be performed in the future, the hour under analysis is associated with a generic tag as *00000*, when no errors are detected, or with a tag like *error*, if errors are detected in a number of records considered unacceptable. Nevertheless, in case there are errors in a small number of records, say less than three, while all others are in good conditions, then the corresponding time histories are filled automatically with null values (and latter excluded from the analysis) and the hour under analysis is assumed as viable.

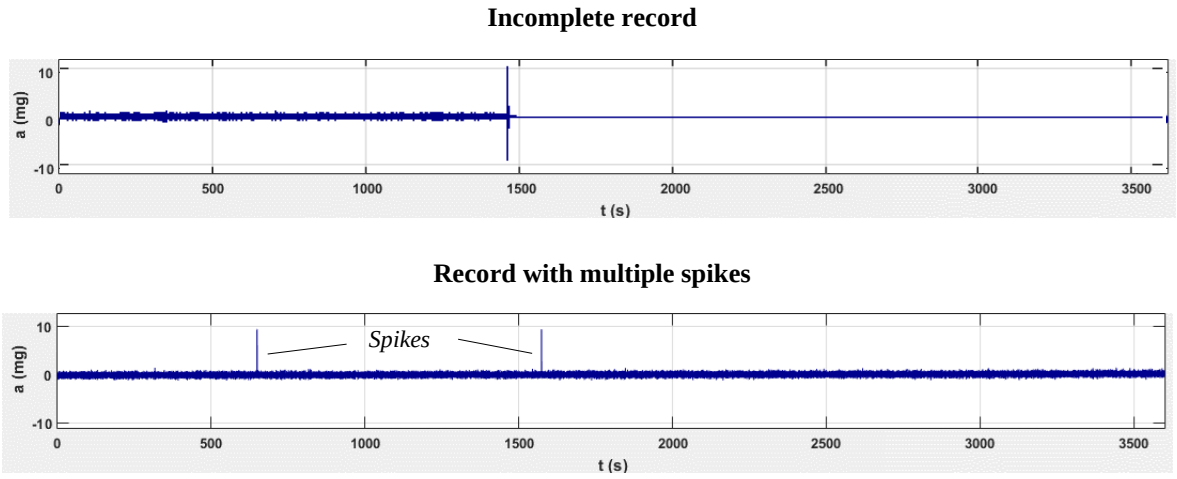

Fig. 4.9 Examples of detected records with errors from the SSHM system installed in Cabril dam.

In what concerns the system installed in Cabril dam, several types of errors have been detected during the development of this work, including records with null or constant values during all or a large part of the hour, records with single or multiple spikes and/or with several plateaus throughout the hour, and even incomplete records due to malfunctions in the sensors or the data acquisition units. These types of errors were gradually discovered over time in an empirical way, simply based on the observation of the measured acceleration time histories. Therefore, continuous updates and improvements to the code of module 2 were necessary during this period, to enable the detection of all these errors and hence achieve a reliable tool.

In the second phase, module 2 includes a code to generate new data files containing the decimated records with an artificial sample rate of 50 Hz. Essentially, for the hour under analysis a single data file is created with a new designation as *E01E01234@YYMMDDHHtag.dec*, where *YY* gives the last two digits of the year, *MM*, *DD* and *HH* indicate the month, day, and hour, while the string *tag* is replaced by *00000* if the

file is normal, or by *error*, if the file is corrupt. Each generated file is then automatically stored in an extra external storage device, acquired for that sole purpose, in a directory corresponding to the respective month *MM* and year *YY*, where all files of each day of that month are located. Moreover, copies of the new files are saved in a Google Drive folder for cloud storage (Fig. 4.10), hence enabling a direct retrieval of data once the synchronisation is complete, which currently must be done manually.

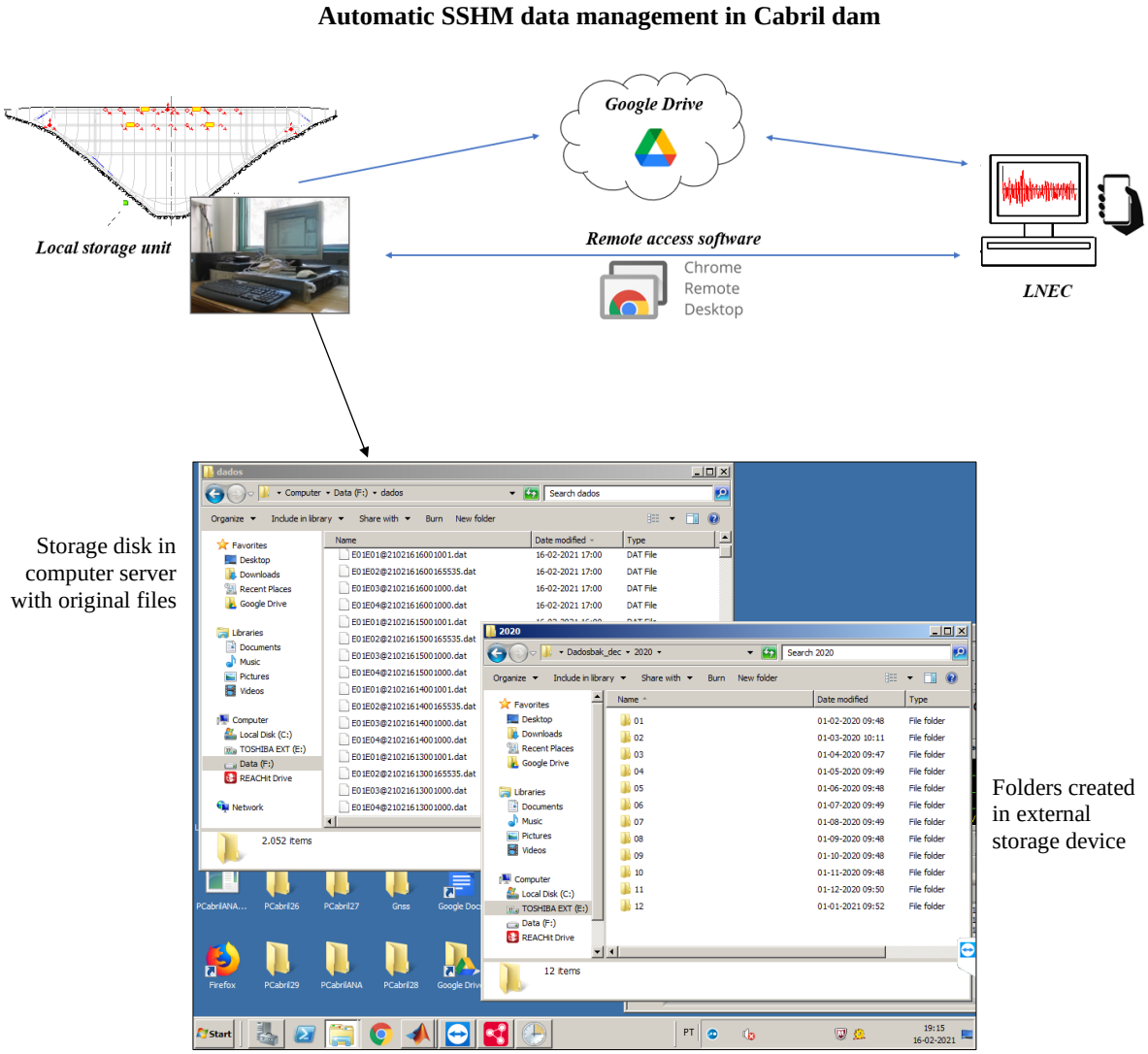

Fig. 4.10 Scheme illustrating the data management of the SSHM system of Cabril dam (top) and desktop environment of the central computer server (bottom).

This feature of *DamSSHM* is critical not only for an efficient management of the storage space of the hardware, but also for increasing the speed of data transfer to Google Drive and of its remote access. To demonstrate how significant this is, it should be noted that a set of 4 original binary data files, which include all the acceleration records for a single hour, consume a total of 370 Megabytes (MB) of storage space; for a whole month, the files would take around 265 Gigabytes (GB). This means that a 3 Terabyte (TB) storage device would be full in around 11 months, which is not at all sustainable. Therefore, the decision was made

to save backups of new files containing the records decimated to 50 Hz. In this case, the size of the file for a single hour is around 17 MB, while all files corresponding to a whole month of continuous monitoring consumes around 12.3 GB, and thus a 3 TB storage device would allow to store around 244 months (or 20 years) of data.

Finally, on a third phase, module 2 generates a series of figures and a text file with a daily summary of monitoring results, which are automatically sent by email (Fig. 4.11) for any intended recipient, e.g., researchers and engineers responsible for dam safety.

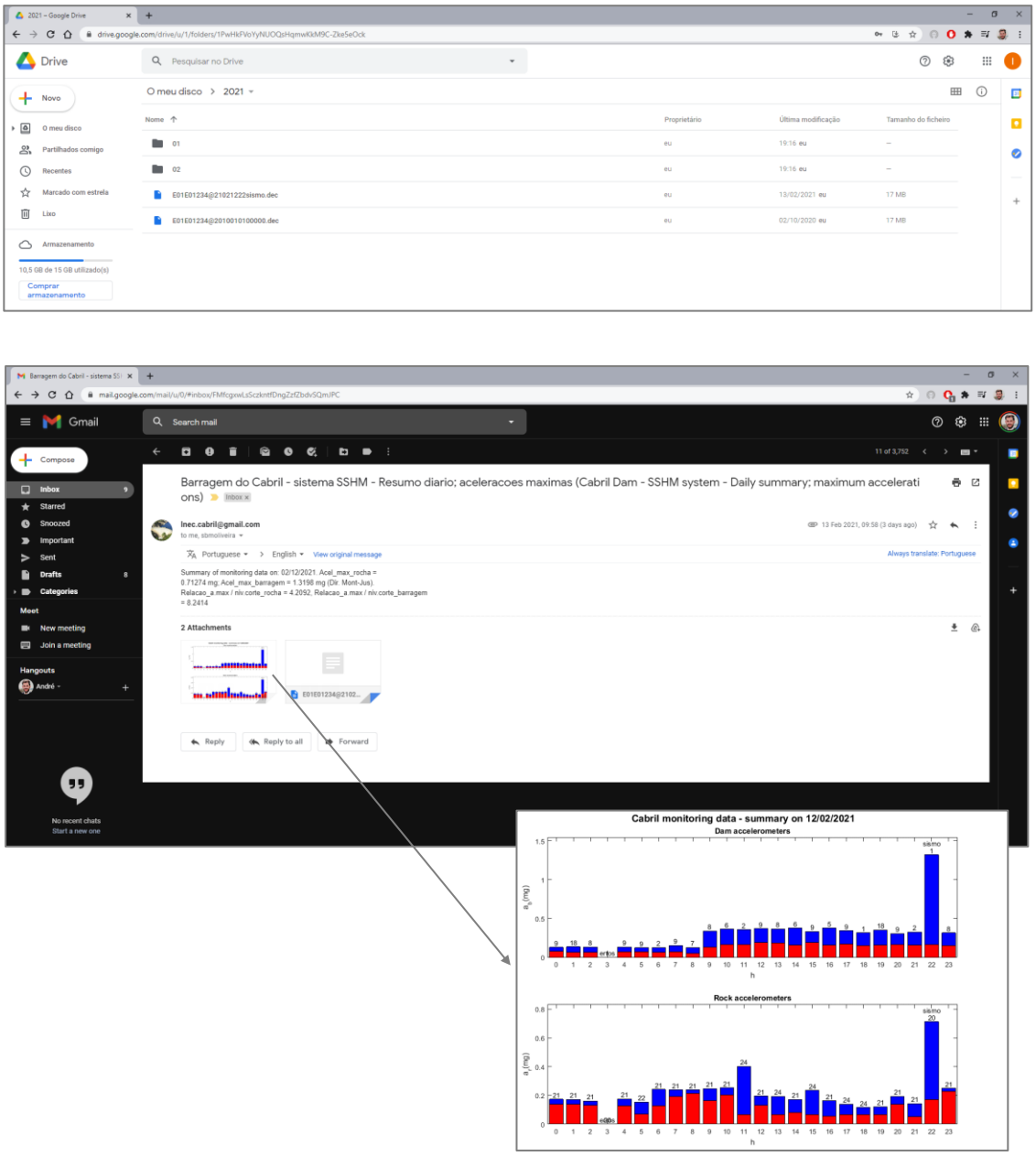

Fig. 4.11 Desktop environment of a work computer. Folders created in Google Drive with *DamSSHM* to enable remote access and example of received email.

4.3.3 MODULE 3: AUTOMATIC DETECTION OF VIBRATIONS DURING SEISMIC EVENTS

The third module of *DamSSHM* was developed for automatic detection of vibrations induced by seismic events on dams, and simultaneously to distinguish them from those induced by the operation of gates and by turbines of generator sets, based on the analysis of the acceleration records. The procedures described below are performed following module 2, namely for all hours of the date under analysis whose files are error-free or uncorrupted.

On the first phase, for each hour, module 3 includes a series of tasks that aim at evaluating certain parameters and patterns, which, based on experience, are usually observed in seismic accelerograms. These tasks are carried out for all the acceleration records measured during that hour. First, the relation between the maximum (or peak) acceleration and a specific comparison level, which is calculated as the sum of the mean value of the local maxima of the signal and the respective standard deviation, is calculated to investigate if there is a relevant increase in the amplitude of recorded vibrations. After that, the difference in seconds between the maximum acceleration, either positive- or negative- valued, and the second maximum but of opposite signal, is computed in order to evaluate if significant vibrations occur in both directions in a short period. These first two parameters can be quite important on their own for analysing patterns on acceleration records in order to detect vibrations induced by seismic events. Nevertheless, additional verification is required when analysing recorded vibrations on a large concrete dam, since the operation of the generator sets and the actions of closing/opening the spillways can induce a sudden increase in the amplitude of recorded vibrations, result in peak accelerations that could be confused with those usually measured during low intensity seismic events if only the first two parameters were evaluated. However, based on experience, the variation between the normal level of ambient vibrations and the peaks due to operational sources is more abrupt, while during earthquakes it is common to note a more gradual variation in the amplitude of vibrations before and after the peak values. Therefore, it is necessary to evaluate the gradual variation of the acceleration values, based on the gradient of the local maxima, during a certain time interval before and after the peak acceleration, aiming to increase the accuracy of the proposed method and to be able to distinguish between seismic vibrations and those induced by the operation of generator sets or spillways. At last, if the analysed parameters meet the established requirements (based on specific tolerance values) for all acceleration records, the program determines that a seismic event was detected on the dam site and module 3 continues to the following tasks; otherwise, *DamSSHM* continues to module 4.

On the second phase, if a seismic event was detected, a new tag *sismo* (which means earthquake in Portuguese) is associated with the hour under analysis, replacing the generic tag *00000*, assigned by module 2 because the file didn't have errors. Then, module 3 creates a new data file, *E01E01234@YYMMDDHHsismo.dec*, which is stored both in the directory previously created by module 2, according to the year/month, and in Google Drive folder for cloud storage. In addition, the 4 original binary data files are copied to a new folder created by module 3 in the external storage device, with a view to create backups of the original seismic accelerograms, recorded with the sampling frequency of 1000 Hz.

Finally, on the third phase, module 3 automatically sends an additional email to inform that a seismic event was detected in Cabril dam, containing figures of the acceleration time histories recorded both near the dam-rock interface and at the top of the central section (Fig. 4.12).

Since the system entered in operation at Cabril dam in 2008, only small to medium intensity earthquakes have occurred in Portugal and in adjacent zones, usually at a great distance from the dam, resulting in low amplitude vibrations at the dam site, namely of the order of magnitude of the milli-g (mg). Nevertheless, even for these earthquakes the system has been able to record the resulting seismic accelerations with great accuracy. Furthermore, throughout the development of this work, several seismic events have been automatically detected with *DamSSHM*, clearly demonstrating the potential of this module for automatic detection of seismic vibrations. Next are two examples of automatically detected seismic events. The first is an earthquake of magnitude 4.6, recorded on September 4, 2018, with the epicentre located in the abyssal region off the coast of Peniche, at about 200 km from the dam (Fig. 4.13). The second is an earthquake of magnitude 3.6, detected on February 12, 2021, which occurred to the North of Rio Maior, at round 89 km from the dam site (Fig. 4.14).

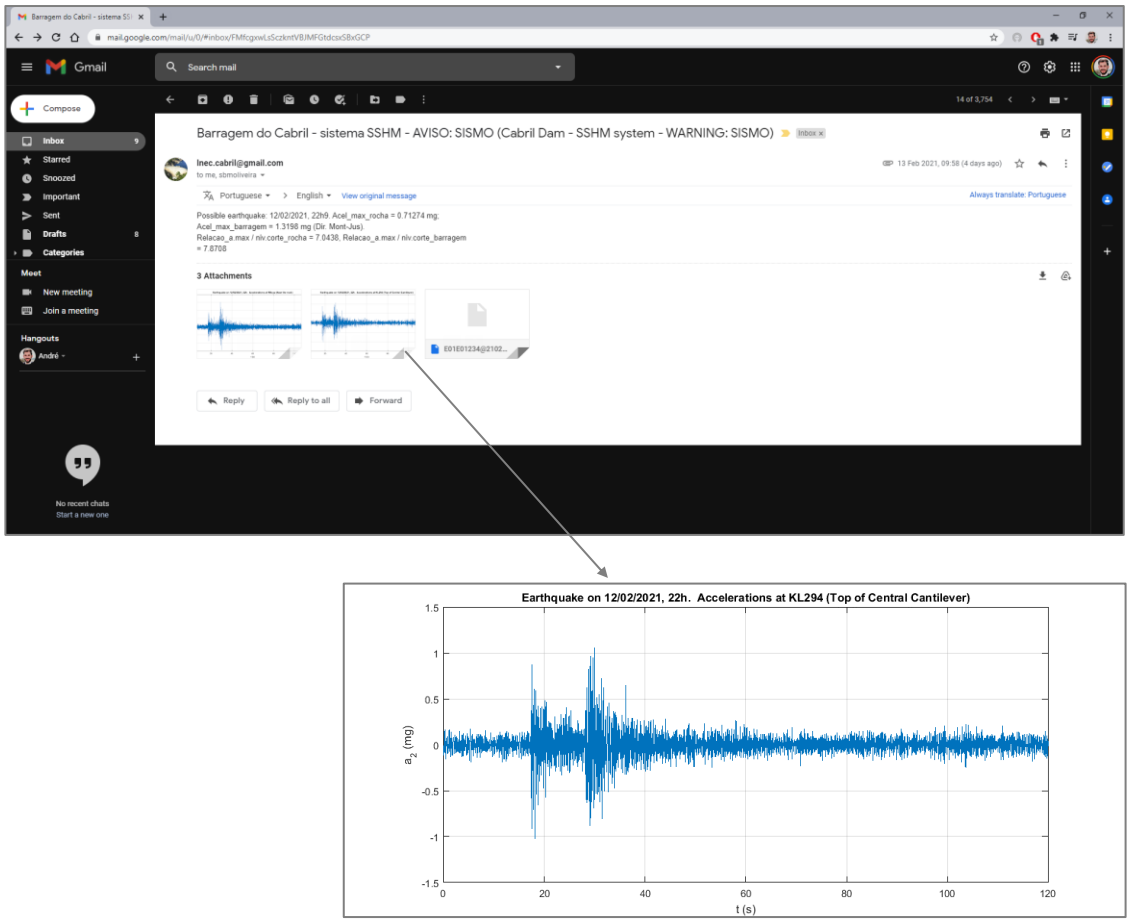

Fig. 4.12 Example of received email when a seismic event is detected in Cabril dam.

EARTHQUAKE (4.6 M) ON SEPTEMBER 4, 2018. DISTANCE: 206 km FROM CABRIL DAM

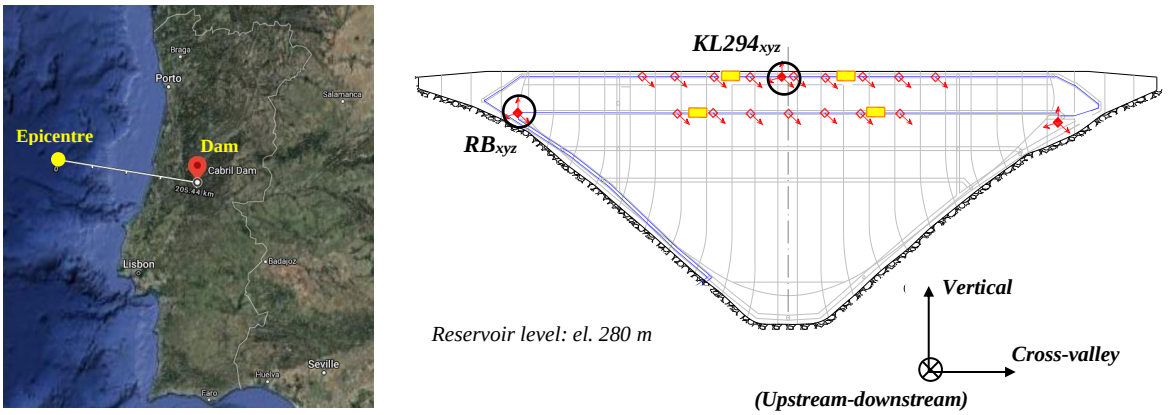

Seismic accelerations recorded near the dam-foundation interface, at the right bank (RB_{xyz})

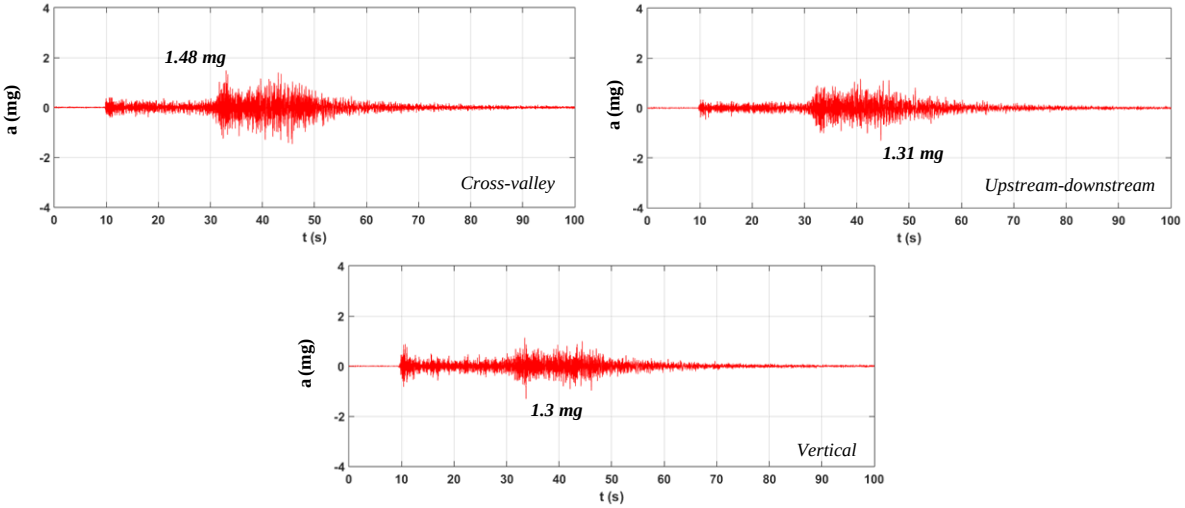

Seismic accelerations measured at the upper gallery ($KL294_{xyz}$)

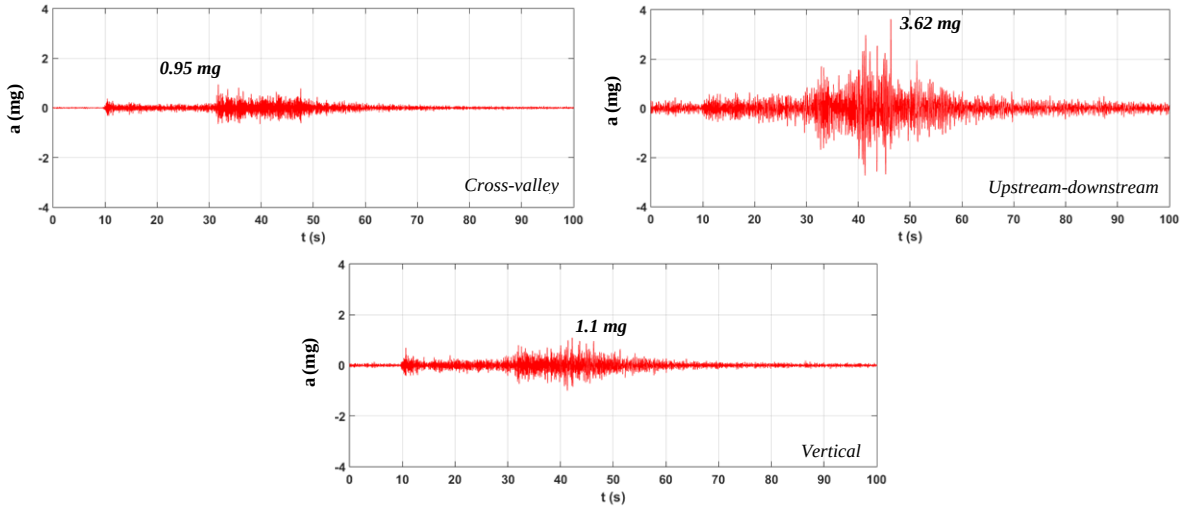

Fig. 4.13 Seismic event detected with *DamSSHM* on September 4, 2018. Recorded seismic accelerations at the dam-foundation interface and in various positions of the dam body.

EARTHQUAKE (3.6 M) ON FEBRUARY 12, 2021. DISTANCE: 206 km FROM CABRIL DAM

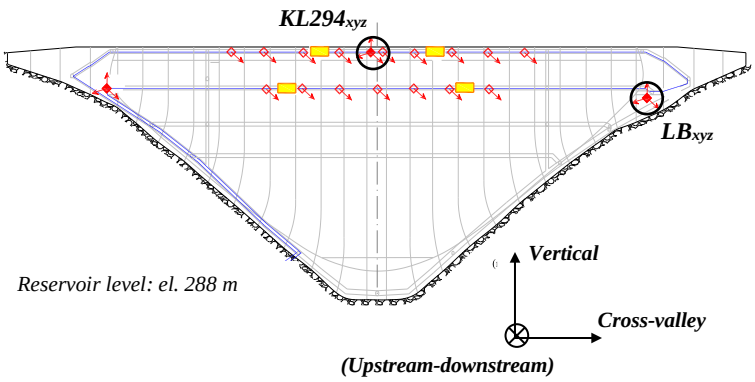

Seismic accelerations recorded near the dam-foundation interface, at the right bank (RB_{xyz})

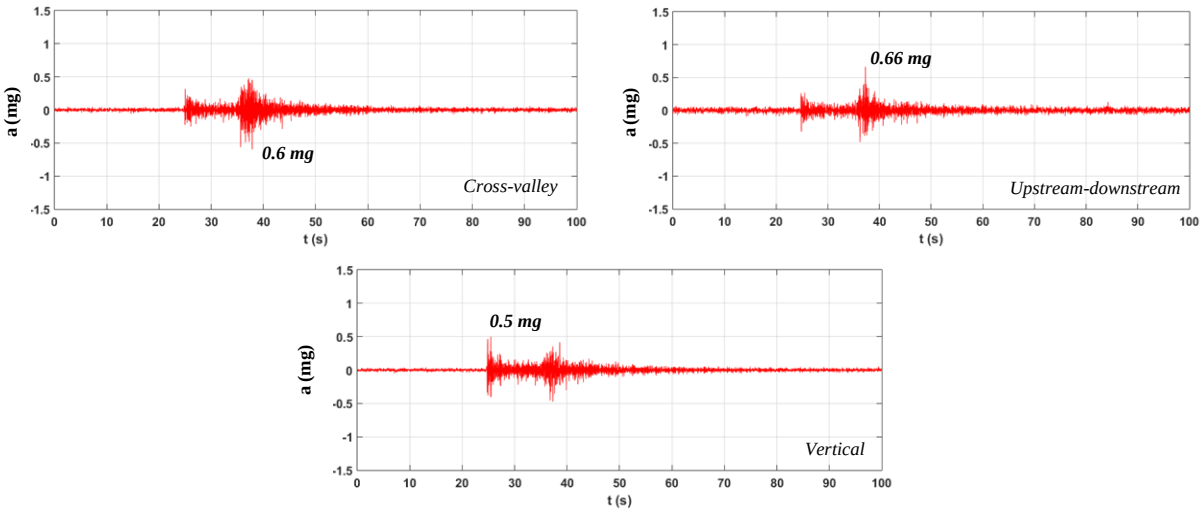

Seismic accelerations measured at the upper gallery ($KL294_{xyz}$)

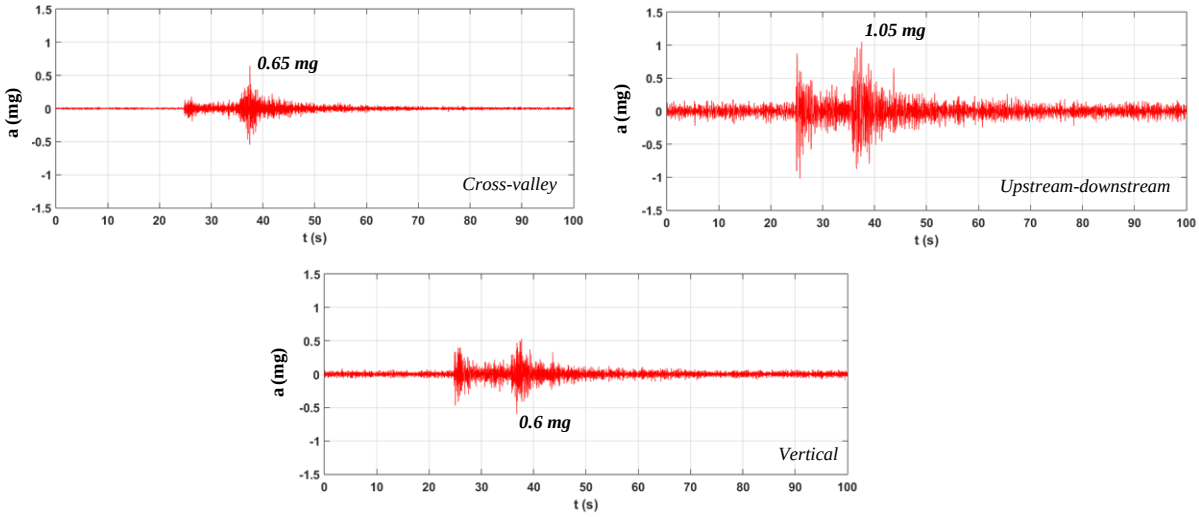

Fig. 4.14 Seismic event detected with *DamSSHM* on February 12, 2021. Recorded seismic accelerations at the dam-foundation interface and in various positions of the dam body.

4.3.4 MODULE 4: AUTOMATIC MAINTENANCE OF THE SERVER STORAGE

As described previously, modules 2 and 3 create files with the decimated acceleration records, which are much smaller in size than the original binary files and save them in both an external storage device for a backup and a Google Drive folder to allow remote access to the data. Moreover, module 3 also saves the sets of 4 binary files when seismic events are detected. These tasks are fundamental for managing, preserving, and facilitating the access to dynamic monitoring data. Nevertheless, the original files continue to be continuously saved in the central server with *Cabril_Aquis*, every hour. As mentioned, a set of 4 binary data files, containing all the acceleration records for an hour, has a total file size of 370 MB. Hence, a whole month consumes around 265 GB of storage space. Although the server in Cabril dam has an internal disk used only for data storage, this was installed more than 10 years ago and hence its capacity is only about 360 GB (enough for less than 2 months of monitoring data). Thus, it became essential to ensure that data storage on the server, and hence the system operation, are not compromised. Therefore, the fourth and last module of *DamSSHM*, was specifically prepared to perform the maintenance of the computer server installed in the Cabril dam SSHM system, through the management and elimination of data files. First, module 4 defines the analysis date to 21 days before the day when *DamSSHM* is executed, and it selects all files for every hour of that date. Then, the program saves a backup for a single hour of the analysis date, by moving the corresponding original set of 4 data files to the external storage device, namely to a new directory created for this purpose according to the year/month, in order to preserve some of the original data files. After that, the remaining files of that day are eliminated, to ensure the storage capacity of the computer server in the future (Fig. 4.15). Finally, an email with relevant information is sent, in which the total storage capacity of the server is indicated, as well as an update on used and the available storage space, to allow an effective control and maintenance of the storage hardware.

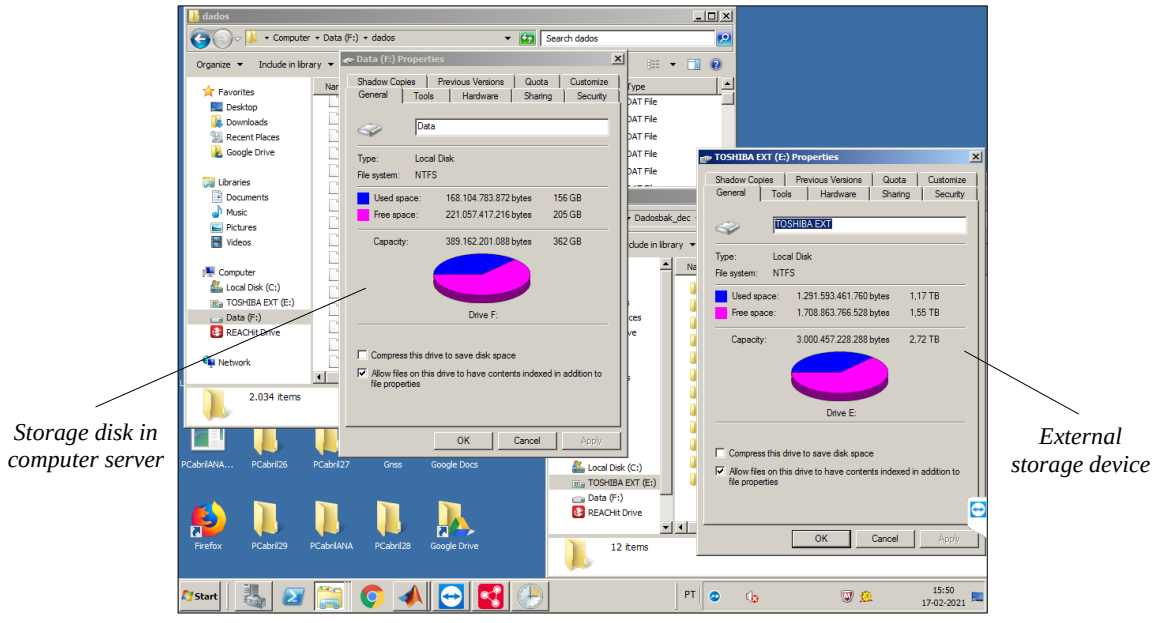

Fig. 4.15 Desktop environment of the central server installed in Cabril dam' SSHM system: available and used storage space in both the computer server disk and in the external storage device.

4.3.5 *DAMSSHM*: ALGORITHM

The algorithm of *DamSSHM*, describing all tasks currently thar are automatically executed as part of the SSHM system installed in Cabril dam, is presented in Fig. 4.16.

DAMSSHM

1. Module 1: read data files
    - 1.1. Define the analysis date (*DD/MM/YY*) to the previous day and select all corresponding data files
    - 1.2. Read monitoring data. *For each hour HH:*
        - 1.2.1. Open and read the 4 binary files
        - 1.2.2. Create matrix with all acceleration time histories (measured at 1000 Hz)
        - 1.2.3. Decimate the acceleration time histories (new sample rate of 50 Hz)
2. Module 2: Automatic data analysis and management
    - 2.1. Analyse monitoring data. *For each hour HH:*
        - 2.1.1. Identify corrupt files or detect measurement errors in the acceleration records
        - 2.1.2. Evaluate file integrity
        - 2.1.3. Normal files: attribute tag *00000;* Corrupt file: attribute tag *errors*.
    - 2.2. Management of monitoring data. *For each hour HH:*
        - 2.2.1. Create new data file with decimated acceleration record: *E01E01234@YYMMDDHHtag.dec*
        - 2.2.2. Store data file in external storage device (subfolder *MM* of folder *YY*) and in Google Drive
    - 2.3. Send email with figures and daily summary of results
3. Module 3: Automatic detection of seismic vibrations
    - 3.1. Analyse monitoring data (files without errors). *For each hour HH:*
        - 3.1.1. Evaluate specific parameters and patterns in the acceleration records
        - 3.1.2. Distinguish possible seismic vibrations from those induce be operational sources
        - 3.1.3. Assess if a seismic event has occurred: Yes – replace the tag by *sismo* and continue to 3.2; No – continue to 4.
    - 3.2. Management of files with seismic records
        - 3.2.1. Create new data file with the seismic accelerations: *E01E01234@YYMMDDHHsismo.dec*
        - 3.2.2. Store data file in external storage device (subfolder *MM* of folder *YY*) and in Google Drive
        - 3.2.3. Save the 4 original binary data files in the external storage device (subfolders *MM* and *YY* of main folder *Earthquakes*)
    - 3.3. Send email with figures of the acceleration time histories recorded both near the dam-rock interface and at the top of the central section.
4. Module 4: Automatic maintenance of the server storage
    - 4.1. Define the second analysis date (*DD/MM/YY*) to the 21 days before and select all corresponding data files
    - 4.2. Save backup of a single hour *HH*: move the set of 4 binary data files to the external storage device (subfolders *MM* and *YY* of main folder *OriginalDataBackup*)
    - 4.3. Eliminate remaining files associated with the analysis date
    - 4.4. Send email with information on the task and on the storage capacity of the computer server

Fig. 4.16 Algorithm of *DamSSHM*.

4.4 SOFTWARE FOR AUTOMATIC MODAL IDENTIFICATION: *DAMMODALID*

DamModalID is the second program developed in this work for complementing and enhancing the software component of SSHM systems installed in large concrete dams, aiming to provide data for studies on the dynamic behaviour of dam-reservoir-foundation systems and to support structural health monitoring activities (Fig. 4.17). More specifically, this program is designed to perform modal analysis based on continuous vibrations monitoring data in large concrete dams, in order to determine the natural frequencies and modal configurations of the main vibration modes. The first version, presented in this chapter, includes three modules, namely: (i) for frequency domain modal identification, based on the Frequency Domain Decomposition method with Singular Value Decomposition (FDD-SVD); (ii) to automate the selection of spectral peaks, using a new proposed technique; and (iii) to enhance modal parameter identification of dams over time, based on previous dynamic behaviour results and considering the reservoir level variations). In addition, an interactive version of the program was developed, with its own graphical user interface, to allow for periodic studies to be performed, based on data collected on specific dates and hours, and thus to analyse in detail both the acceleration records and modal identification results. *DamModalID* was properly tested by performing various studies using continuous dynamic monitoring data from two large concrete dams, namely Cabril dam Cahora Bassa dam, the two case studies of this work.

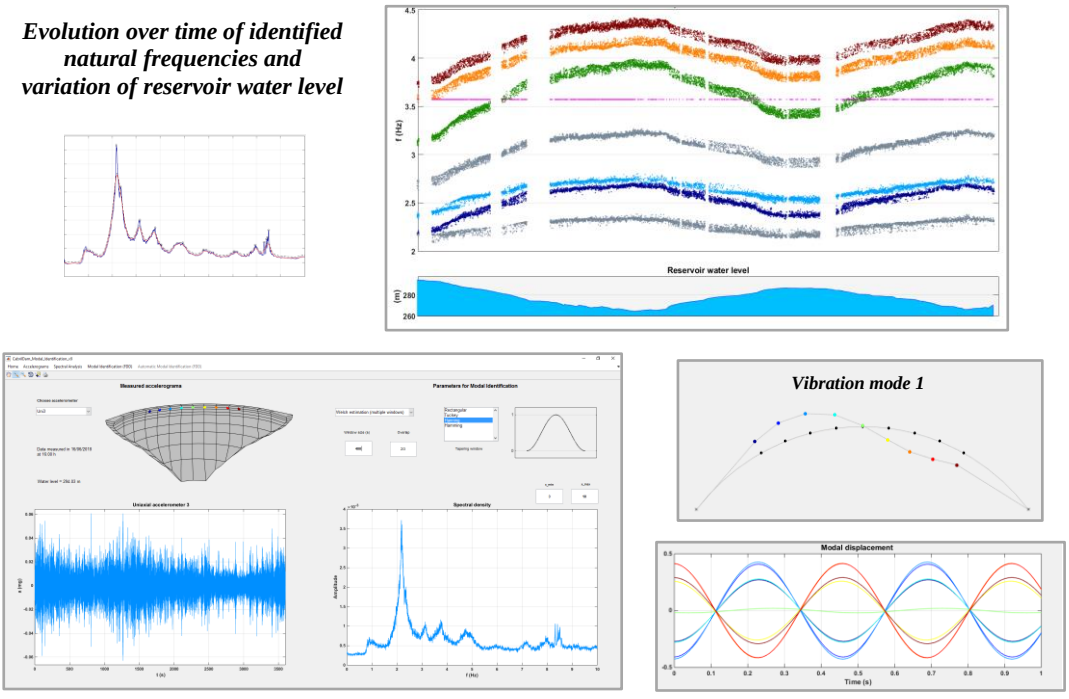

Fig. 4.17 *DamModalID*. Automatic modal identification results and version with graphical interface.

4.4.1 MODAL IDENTIFICATION: GENERAL REVIEW

The analysis of the dynamic behaviour of a structure from a modal identification perspective aims to obtain accurate estimates of its main modal parameters, i.e. natural frequencies, modal configurations, and

damping ratios, based on the measured response under certain dynamic excitations (Peeters, 2000; J. Rodrigues, 2004). The determination of modal parameters from measured vibrations in structures and their careful analysis can provide extremely useful results for evaluating their dynamic performance, for supporting structural health monitoring and vibration-based damage detection, and for validating and updating numerical models (Li et al., 2016; Limongelli & Çelebi, 2019).

The identification of the modal parameters of a structural system is a research field where extensive work has been conducted over several decades, leading to the development of well-established methods based on solid theoretical foundations. In current practice, there are two main approaches used for experimental characterization of structural dynamic behaviour, which differ essentially with respect to the origin of the dynamic excitation.

The first approach, known as Experimental Modal Analysis (EMA), or input-output modal analysis (Maia & Silva, 1997), is based on the measured dynamic behaviour of the structure (output) under one or several dynamic loads (input), which are known and controlled. The modal parameters are then estimated from the relation between the applied input and the observed dynamic response, using appropriate deterministic modal identification methods. This methodology can be applied in laboratory tests with reduced scale structures, e.g., using shaking tables, or in forced vibration tests, which entail the application of controlled excitations using special devices and the measurement of the response at various points of the structure. EMA has been successfully used for experimental identification of civil engineering structures, such as buildings, bridges and dams, by performing forced vibration tests which provided useful and insightful data on their dynamic behaviour (Cunha & Caetano, 2006; Severn, 2010). Although they can provide important experimental data, forced vibration tests can only be performed from time to time and thus do not allow for a continuous evaluation of structural dynamic performance.

The second approach, referred to as Operational Modal Analysis (OMA) or output-only modal analysis (Brincker & Ventura, 2015; Peeters, 2000; J. Rodrigues, 2004), is based on the measurement of the dynamic response under ambient or operational excitations. In this type of approach, the modal parameters are retrieved from the measured vibrations using stochastic modal identification methods, by assuming that the unknown dynamic excitation is a random excitation with white noise characteristics, i.e. a realization of a stochastic Gaussian process with zero mean value (Brincker & Ventura, 2015). As the name indicates, in OMA the dynamic behaviour of a structure is analysed in normal operating conditions, which entails the advantage of allowing dynamic monitoring without disturbing its operation, by conducting ambient vibration tests over a certain time period or by using continuous monitoring systems. It is therefore clear that the OMA methodology is perfectly appropriate for continuous dynamic monitoring. The OMA approach has been extensively used in civil engineering to characterize the dynamic behaviour of large structures and to perform vibration-based health monitoring (Li et al., 2016; Limongelli & Çelebi, 2019), namely in bridges (Brownjohn et al., 2010; Cunha et al., 2018; Magalhães et al., 2012; Y. Zhang et al., 2017), high-rise buildings and towers (Ni et al., 2009; Su et al., 2013), historical monuments (Ceravolo et al., 2019; Monti et al., 2018), and, of particular interest for this thesis, in large concrete dams (Fig. 4.18)

(Alegre, Carvalho, et al., 2019; Bukenya & Moyo, 2017; S. Oliveira et al., 2012; S. Pereira, Magalhães, Cunha, et al., 2021; S. Pereira, Magalhães, Gomes, et al., 2021).

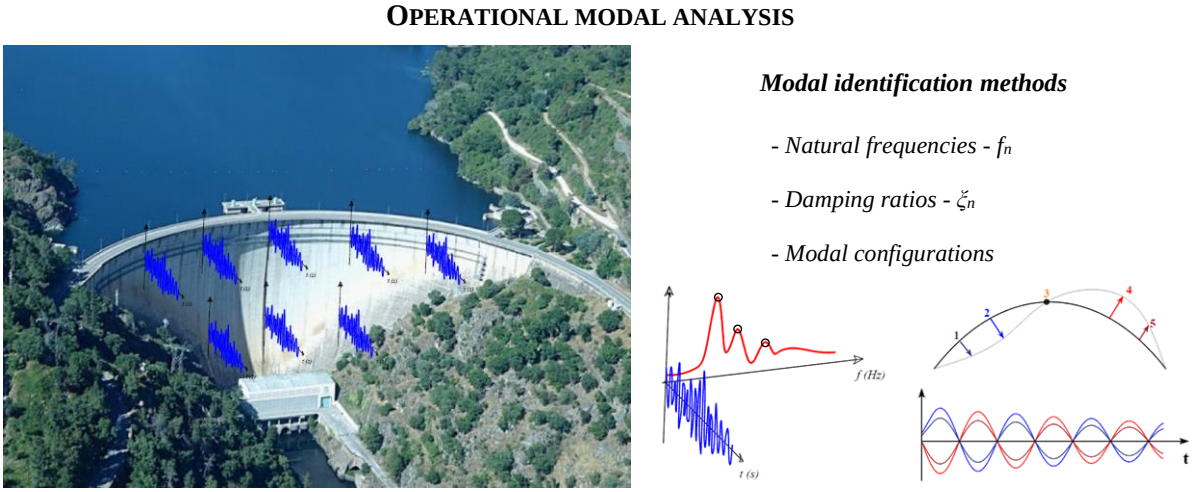

Fig. 4.18 Operational modal analysis of a large concrete dam.

Since one of the objectives of this thesis is the development of a modal identification program, as part of a software component for complementing continuous monitoring systems installed in large concrete dams, this subchapter is focused only on the OMA approach. Therefore, a brief overview of some the most popular modal identification methods available for OMA is given here, in order to provide a framework for the implemented methodology.

MODAL IDENTIFICATION METHODS FOR OPERATIONAL MODAL ANALYSIS

The characterization of the dynamic behaviour of a structure under ambient/operational excitations is usually performed using frequency-domain or time-domain modal identification methods (Brincker & Ventura, 2015; Peeters, 2000; J. Rodrigues, 2004). In practice, the identification of modal parameters of the structural system is carried out by correlating the dynamic characteristics of an idealized mathematical model with the physical properties of the system, which are extracted from the measured response: essentially, the mathematical models are fitted to or estimated from experimental measurements. The most relevant and widely used methods in current practice are summarised next.

In frequency-domain modal identification, the power spectral density (PSD) matrix (or output spectrum matrix) is obtained from the response time histories, measured in several points in the structure, and thus analysed based on non-parametric or parametric methods.

The Basic Frequency Domain (BFD) method, also known as Peak-Picking (PP) method (J. S. Bendat & Piersol, 1993; Felber, 1993), is a simple and fast non-parametric method in which the frequencies are estimated by selecting the peaks of the auto-spectra of the measured outputs, while the mode shapes can be extracted by analysing one row/column of the PSD matrices, under the condition of well separated modes

and low damping. The modal damping ratios can be determined based on the half-power bandwidth method. Being non-parametric, the PP method enables the determination of the eigenfrequencies just by evaluating features of the signal without fitting nor estimating a mathematical model. The Frequency Domain Decomposition (FDD) method, also called Complex Mode Identification Function (CMIF) method (Brincker et al., 2000; Peeters, 2000), is a more advanced non-parametric method that overcomes some limitations of the BFD method, while maintaining simplicity and efficiency. It is based on the analysis of the singular value decomposition (SVD) of the PSD matrix to identify natural frequencies and mode shapes, and it works well even for closely spaced modes. Furthermore, an enhanced version of the method, the Enhanced Frequency Domain Decomposition (EFDD), has been developed to allow for the determination of modal damping ratios, as detailed in (Brincker et al., 2001), based on the Modal Assurance Criterion (MAC) index first introduced by (Allemang & Brown, 1982). This is a quite popular method for OMA, being implemented in commercial software like ARTeMIS Modal (Structural Vibration Solutions, 2020).

In what concerns parametric methods for frequency-domain identification, these are based on the fitting of a mathematical model of the dynamic system to the output PSD matrix, on a first phase, in order to retrieve the modal parameters on a second phase. This problem can be solved based on optimization-based methods, using the linear least squares method or the Maximum Likelihood estimator (Guillaume et al., 1999), or considering stochastic subspace identification methods, using frequency-domain state space models (P. Van Overschee et al., 1997). The parametric method most used today in civil engineering applications is the poly-Least Squares Complex Frequency (p-LSCF) due to its good performance and to its implementation on the commercial software PolyMax (Peeters & Van der Auweraer, 2005).

As for time-domain modal identification, the mathematical models (and respective dynamic properties) are fitted directly to the response time histories or to the corresponding correlation functions, using parametric stochastic methods.

The Ibrahim Time Domain (ITD) method was among the first used for OMA, in which relevant information is extracted from the measured responses in multiple positions of the structure (Ibrahim, 1977; Ibrahim & Milkulcik, 1977), namely by applying the random decrement technique originally proposed in (Cole, 1968).

The time-domain methods based on Auto-Regressive (AR) models or Auto-Regressive Moving Average (ARMA) models (Andersen, 1997; Ljung, 1999) are those in which the parameters of the model are estimated either from the correlation functions of the measured output, using the Instrumental Variable method (Peeters, 2000), or by directly fitting the mathematical model to the measured signals.

The Stochastic Subspace Identification (SSI) methods are methods that identify a stochastic state space model from output-only data (Peeters, 2000; Peter Van Overschee & De Moor, 1996), being among the most popular adopted in civil engineering applications. Two main types of SSI formulation can be used, namely, the Covariance-driven Stochastic Subspace Identification (SSI-COV) and the Data-driven Stochastic Subspace Identification (SSI-DATA). Therefore, the state-space model can be estimated either from the correlation functions (or covariances) of the measured outputs, using the SSI-COV, or directly from the recorded time series, using the SSI-DATA.

4.4.2 SIGNAL PROCESSING AND FUNDAMENTAL CONCEPTS FOR FREQUENCY-DOMAIN MODAL IDENTIFICATION

In this thesis, the decision was made to implement a frequency-domain procedure in the developed modal identification program. In particular, this procedure is based on the FDD method, since this is a well-established and widely used method in current practice, which has been successfully used previously for studying the dynamic response of Cabril dam in normal operating conditions (Mendes et al., 2004; S. Oliveira et al., 2011, 2012; S. Oliveira, Silvestre, Espada, et al., 2014). Considering the main goal of subchapter 4.4 to be the presentation of said program, the purpose here is not to discuss thoroughly the subjects of data acquisition and signal processing, properly explained elsewhere (J. Bendat & Piersol, 2010; J. S. Bendat & Piersol, 1993; Brincker & Ventura, 2015), nor to present in detail the theoretical bases supporting frequency-domain modal identification and the corresponding mathematical formulations, which can be found in several works (Brincker & Ventura, 2015; Magalhães, 2010; Maia & Silva, 1997; Peeters, 2000; J. Rodrigues, 2004). Thus, the present section aims to concisely addresses some fundamental concepts deemed essential for the development of this work.

In OMA, the goal is to estimate the correlation functions (in time-domain) or the spectral densities (in frequency-domain) of the measured response, and consequently extract the physical information (modal parameters) about the structural system. Therefore, the phase of signal processing is vital, to enable the retrieval of reliable results on the dynamic response of the structure and thus to provide useful information for dynamic behaviour analysis and structural health monitoring. The application of signal processing techniques aims essentially at removing spurious components from experimental data and to amplify the most important elements hidden in the noise of measured signals. In this way, it is possible to extract important the intended information for interpretation and analysis of the physical problem.

PRE-PROCESSING

For measuring vibrations, sensors that record discrete temporal series $x(t)$ are used. Typically, these sensors record data series containing values of electrical voltage, within a predefined scale, which are proportional to the physical parameter intended to measure. Then, the required conversion to digital values is achieved using analogue-to-digital conversers. This process is denoted sampling, and the goal is to obtain a discrete sample of a physical quantity, e.g., velocity or acceleration, intending to represent the corresponding continuous signal in time domain. At this stage, as soon as the data is collected, it is vital to check its quality, to prevent the use of bad quality records for subsequent modal identification analyses. Therefore, the measured signals should be checked for clipping, dropouts, and spikes.

The obtained discrete temporal series, or data sample, of total length T, is composed of a sequence of n_T values recorded with a constant time interval Δt. A fundamental parameter is the sampling rate, or sampling frequency, which indicates the number of data values recorded per time unit, $f_s = 1/\Delta t$, in Hz. Moreover, the sampling frequency also defines the upper limit of the frequency band covered in the spectral analysis, as explained further below.

In the first instance, the definition of a very high sampling rate would seem like the best decision, in order both to obtain a temporal data series as close to the continuous signal as possible and to cover a wider frequency band. However, this would lead to the measurement and acquisition of data series with a great number of points, hence requiring a significant storage capacity and significantly demanding computational analyses, as referred in the previous subchapter regarding the Cabril dam SSHM system. Therefore, the chosen sampling frequency should be large enough so that the frequencies of the vibration modes of interest fall within the effective frequency band, hence being dependent on the type of structure, whether it is more or less stiff, and of the type of analyses to be carried out. Moreover, the characterization of seismic accelerograms and of the seismic response can be improved by using higher sampling rates. At the same time, this sampling frequency should not be so large that compromises the capability of data storage and management of data servers. Nonetheless, it is always possible to decimate oversampled series (Brincker & Ventura, 2015), to a smaller and more suitable sampling frequency, while also maintaining the quality of measured signals (Fig. 4.19).

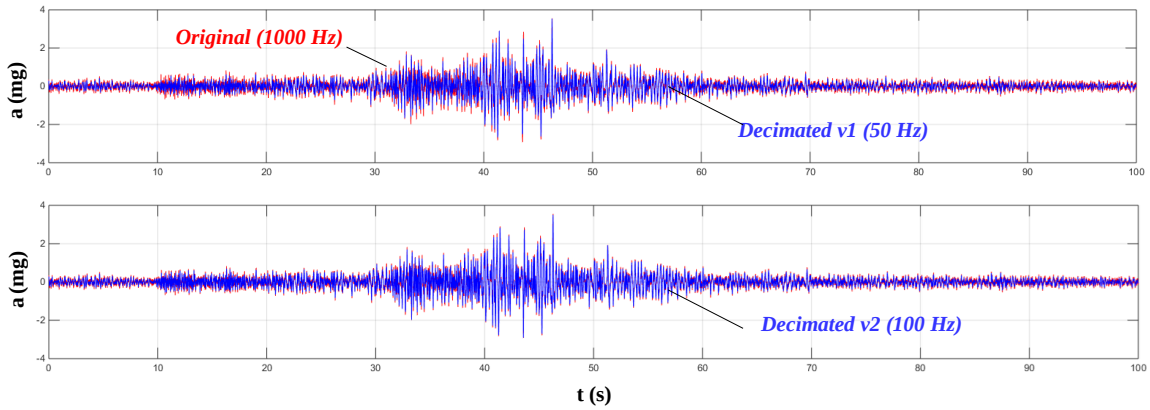

Fig. 4.19 Measured acceleration time history in Cabril dam. Original signal in red (recorded at 1000 Hz) and decimated signal (test sampling rate of 50 and 100 Hz).

It is also important to mention that, in the sampling process, it is common to obtain data series with a non-zero and/or variable mean, which is not in agreement with the principles of a stochastic analysis. This type of issue might be caused by problems in the calibration of measuring sensors, signals with excessive noise in the low frequency region, events or incidents that disturb the signals, or undesired thermal variations. If that is the case, before proceeding with data analysis, it is necessary to apply digital filters to detrend the signals (Fig. 4.20) and thus force them to have a zero mean (Brincker & Ventura, 2015). A possible solution involves the application of a moving average filter, where the detrended signal, $x^*(t)$, is obtained by removing the moving average $\mu(t)$ from the measured signal, as in $x^*(t) = x(t) - \mu(t)$. As an alternative, detrending can be achieved by segmenting the signal in shorter overlapping segments, and hence removing the mean value of each data segment. In this case, the data segments are tapered by applying a tapering window (Brincker & Ventura, 2015), to minimize continuity issues between adjacent segments and reduce leakage in Fourier transforms.

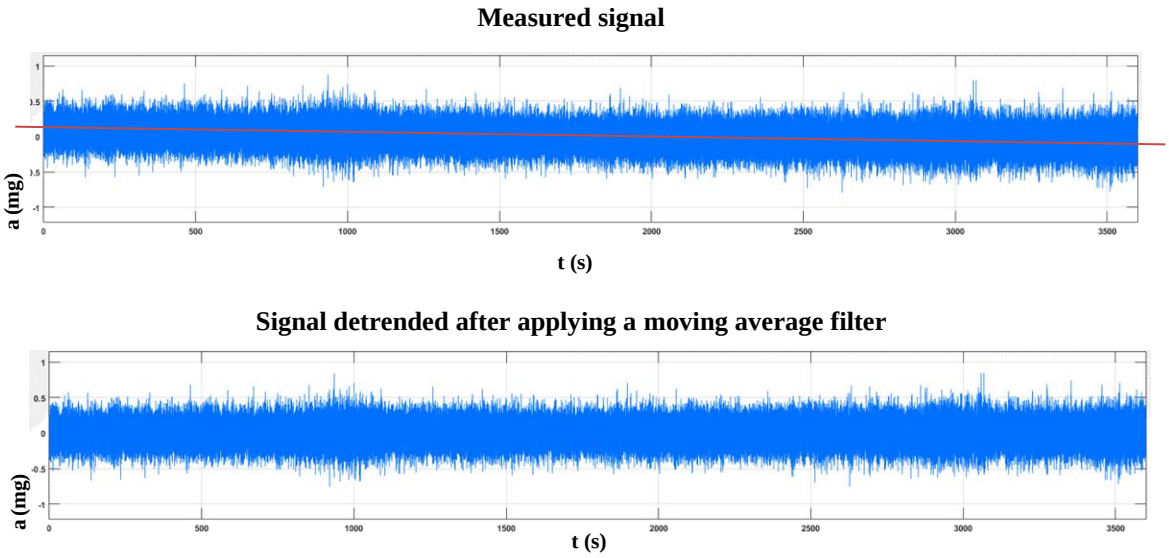

Fig. 4.20 Example of measured signal at Cahora Bassa dam before and after detrending.

TIME TO FREQUENCY DOMAIN TRANSFORMATION: DISCRETE FOURIER TRANSFORM

With the goal of retrieving useful physical information about the dynamic behaviour of a structural system from experimental measurements, the discrete temporal series can be transformed into the frequency domain, to make them more suitable for further analysis, and thus to enable the estimation of the modal parameters using frequency-domain modal identification methods.

The time to frequency domain transformation of an acceleration, velocity, or displacement time history, measured at a certain point of a structure under dynamic excitation(s), is performed by decomposing the signal into a sum of k sinusoidal waves at distinct frequencies ω_k (Fig. 4.21), each one associated with a specific amplitude $\sqrt{a_k^2 + b_k^2}$ and phase $\text{atan}\left(b_k / a_k\right)$ - these are basically the waves that compose the signal in the frequency domain. This transformation is performed using the Discrete Fourier Transform (DFT), which is a real valued function that quantifies the distribution of the energy content of a signal in the frequency domain, $X\left(\omega\right) = \mathscr{F}\left[x(t)\right]$. Usually, the DFT is obtained using the Fast Fourier Transform (FFT), a highly efficient algorithm called proposed in (Cooley & Tukey, 1965).

Given that the discrete time series is composed by a finite number of values N_t, recorded at time intervals of amplitude Δt, the DFT is calculated for discrete frequency values given by $\omega_k = k \cdot \Delta\omega$, where the frequency interval is $\Delta\omega = 2\pi/T$. The maximum frequency captured in this procedure is known as the Nyquist frequency, $f_{Nyq} = f_s/2$ (Hz), or $\omega_{Nyq} = \left(f_s/2\right)/2\pi$ (rad/s), meaning that only half of the complex values of the spectrum are covered, which corresponds to the signal frequency content between 0 and $f_s/2$ Hz (Maia & Silva, 1997).

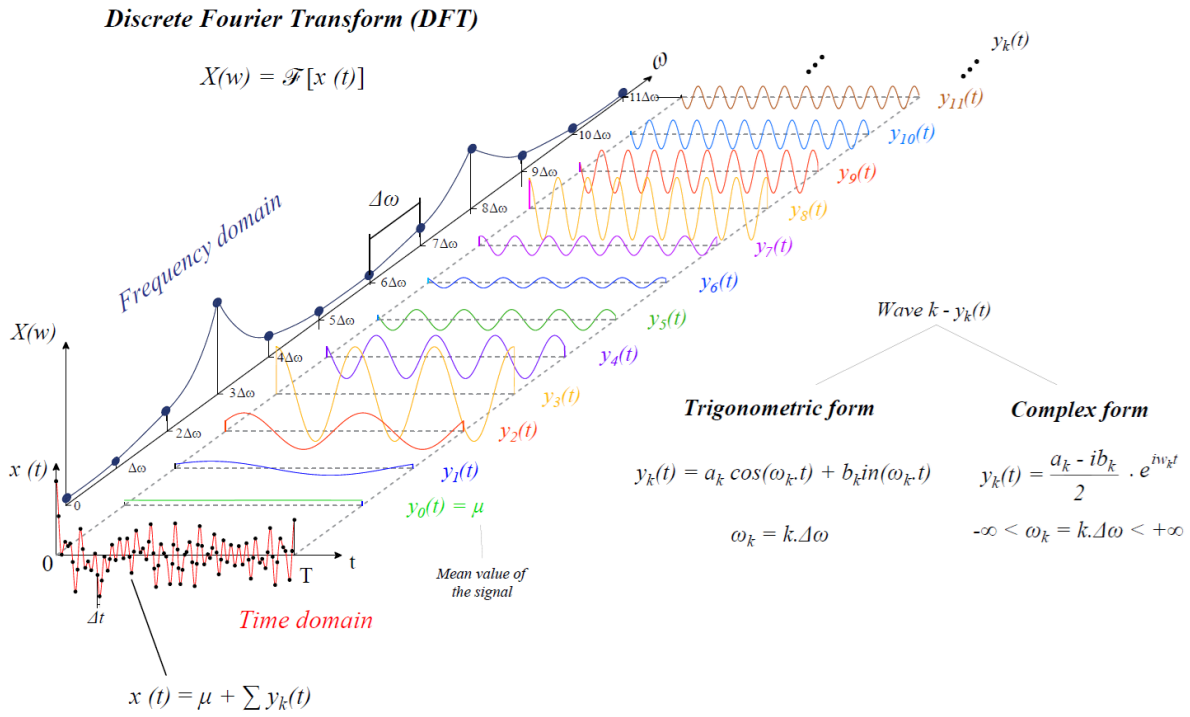

Fig. 4.21 Discrete Fourier Transform (DFT). Decomposition of a discrete signal into a sum of sinusoidal waves. [Adapted from (S. Oliveira, 2013)].

The transformation of a discrete time signal to the frequency domain can be achieved by calculating the DFT of the complete signal, as a single data segment, or considering multiple data segments (Fig. 4.22). If the full signal is used, considering that a longer data series is analysed, then spectra with higher frequency discretisation and excessive noise are obtained. Nevertheless, the resulting spectra can be smoothed to a certain extent, e.g., by applying a moving average filter, using a reduced number of adjacent points to calculate the mean in order not to eliminate the main peaks. As for the second approach, the data time series is divided into multiple, shorter segments, assuming a certain overlapping between adjacent segments, aiming at calculating a smoothed spectrum as the average of the spectra calculated for each of the data segments - this method is known as the Welch estimate (Welch, 1967), In this case, a lower frequency discretisation is achieved, since the length of each time segment T_s is shorter. Therefore, in order to ensure continuity between adjacent segments and reduce leakage errors, each data segment must be tapered using specific tapering windows w_s based on functions with different shapes, e.g. Tukey, Hamming, or Hanning windows (Maia & Silva, 1997).

Regarding computational implementation in MATLAB, the DFT of a signal $x(t)$, or of the multiple data segments, is calculated using the function $fft()$, in order the obtain the corresponding amplitude and phase spectra. However, considering that said function assumes a unitary time step by default, and that the signal is measured with a sampling frequency $f_s = 1/\Delta t$, the DFT is obtained through a line of code such as $DFT = fft\left(x(t)\right) \cdot \Delta t$.

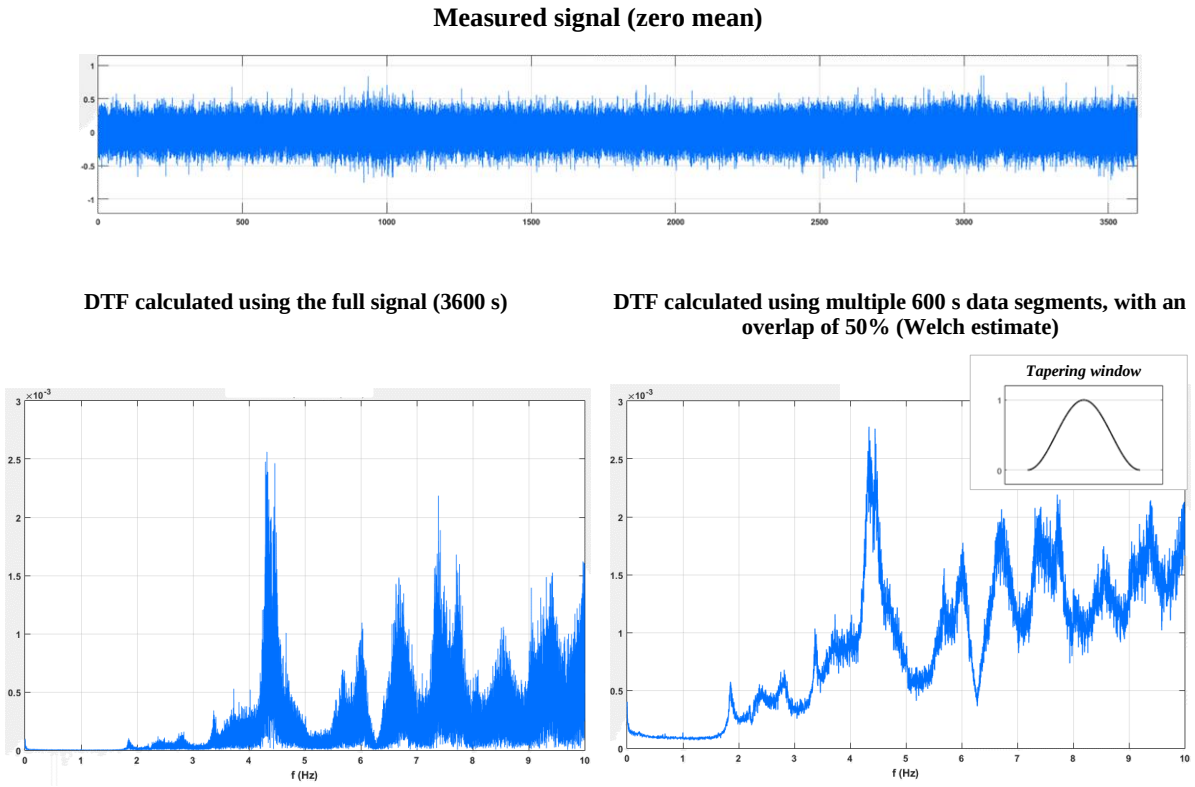

Fig. 4.22 Measured signal at Cahora Bassa dam. DTF calculated: a) using the full signal with 3600 s length; and b) using multiple data segments with 600 s length and an overlap of 0.5 (Welch estimate).

After transforming the measured signals from the time domain to the frequency domain, it is then possible to analyse the frequency content of the signals and thus retrieve useful physical information about the structural system. Even before the application of any specific modal identification method, the natural frequencies of the main vibration modes can be detected as the frequencies of the waves with greater amplitude, that is, the peaks of the amplitude spectrum. This is possible because in the frequency domain each mode has a small frequency band where it is dominant (Brincker & Ventura, 2015). Furthermore, if this technique is applied to the spectra obtained from multiple time series, recorded in a synchronized way at multiple points of the structural system, it is even possible to obtain good estimates of the modal configurations by comparing the waves associated with the selected frequencies. This spectral analysis approach constitutes the foundations of several mathematical formulations that have been developed for frequency domain stochastic modal identification of structures.

THE POWER SPECTRAL DENSITY (PSD) MATRIX

In frequency-domain modal identification the main idea is to extract the physical information of the structural system from the spectral density functions. Therefore, the majority of frequency-domain methods start with the calculation of the so-called spectral density (SD) or power spectral density (PSD) matrix $\underline{S}$, which is a matrix containing the auto-spectral density functions S_{ii} of all measured outputs, along the main diagonal, and the cross-spectral densities S_{ij} that correlate signals measured in different points i and j of the structure, in the remaining positions outside the diagonal (Fig. 4.23). The PSD matrix can be a square

matrix, with n_o rows by n_o columns, where n_o indicates the number of measured outputs, or of observed degrees of freedom, or a rectangular matrix, containing some columns of the complete matrix, where the n_r signals of the selected columns are associated with the reference sensors.

The use of a rectangular PSD matrix leads to a reduction in size, and thus to faster calculations that also require less computer memory. Also, if the reference sensors are appropriately selected this technique does not result in a loss of accuracy. Usually, this means selecting the reference signals as those that present significant modal components for all the modes to be identified. In other cases, e.g., when measuring vibrations in large structures as bridges or dams, an ideal dynamic identification process would require a significant number of experimental measurements, which is not always possible as the number of sensors is usually limited. Therefore, a solution is to define several measurement setups, by moving some sensors while keeping the reference ones in the same positions, so that all measurements records can be correlated later (Cantieni, 2005).

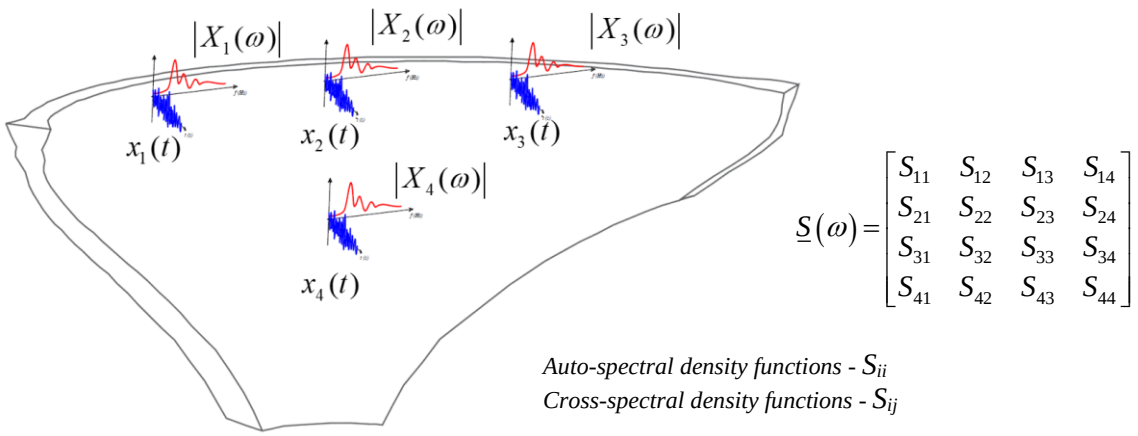

Fig. 4.23 Power Spectral Density (PSD) matrix. Example considering 4 measured signals.

The PSD matrix can be obtained using different approaches for estimating the measured signal spectra. In a first type of approach, the PSD matrix is calculated directly from the measured time series. First, the signals are divided into segments and the DFT is computed for each segment, based on the Welch estimate (using tapering windows) or on the Random Decrement Technique. Then, the PSD matrix is estimated by calculating the average of the auto-spectra or crossed spectra associated with all data segments. When the data segments are longer, frequency discretisation is increased and the leakage effect is reduced, although the number of segments used for averaging the PSD matrix is smaller. In a second type of approach, the PSD matrix is obtained through the application of the DFT to the correlation matrix, which contains the autocorrelations and the cross-correlations of the measured signals. When the DFTs are calculated considering the positive and negative parts of the correlation functions, the full spectra are obtained; if only the positive parts are used, the half-spectra are estimated instead. The fundamentals and the mathematical formulations used for estimating the PSD matrix are described in detail in the works cited above.

4.4.3 MODULE 1: FREQUENCY DOMAIN DECOMPOSITION METHOD WITH SINGULAR VALUE DECOMPOSITION (FDD-SVD)

The first module of the program *DamModalID* was developed to perform frequency-domain modal identification. The classic FDD-SVD method is used for identification of the natural frequencies and modal configurations of large concrete dams, based on continuous vibrations monitoring data recorded under ambient/operational excitation. This method was adopted because it is relatively simple to implement and it also ensures good computational efficiency, while making it possible to overcome some limitations of the BFD method. In addition, the FDD-SVD approach makes frequency-domain identification simpler, considering that all information required can be extracted from the matrices of singular values and singular vectors of the PSD matrix. This also enables the generation of plots which facilitate the analysis and interpretation of modal identification results, and the comparison with results from finite element analyses.

The FDD-SVD method is an approximate solution to the modal analysis problem, considering that modal identification is performed based on the PSD matrix, which in turn is estimated from measured discrete time series. Nevertheless, good estimates of the modal parameters can be achieved for certain conditions, namely: (i) assuming that the structure is subjected to ambient/operational dynamic excitations that are realizations of Gaussian stochastic processes with zero mean, i.e. to white noise type excitations, as in all output-only methods; (ii) for structural systems with low damping; and (iii) in the case of vibration modes with well-separated frequencies, or of modes with close frequencies, if the condition of orthogonality is respected (uncorrelated modal coordinates). For these reasons, the FDD-SVD method is a suitable solution for modal identification of dams under ambient/operational excitations, considering that dams are reasonably lightly damped structures which usually present well separated modes and/or with distinguishable modal configurations.

The fundamentals of the FDD method with SVD of the PSD matrix are presented here, and the main steps to follow for estimating the modal parameters are described. Essentially, the implementation of FDD approach consists of three main steps: (i) estimate the PSD matrix from the measured outputs, based on the Welch method; (ii) perform SVD of the PSD matrix and use the singular values and singular vectors to identify the main modal parameters; and (iii) analyse the modal identification results.

CALCULATION OF THE PSD MATRIX USING THE WELCH METHOD

The estimation of the PSD matrix from the response time histories, measured simultaneously in several points in the structure and in multiple degrees of freedom, represents the first step in the non-parametric FDD method. As mentioned in the previous section, the PSD matrix has the auto-spectral density functions S_{ii} of all measured signals along the main diagonal, and the cross-spectral densities S_{ij}, which correlate different signals, in the remaining positions. This can be a $n_o \times n_o$ square matrix, where n_o gives the number of measured outputs or observed degrees of freedom, or a $n_o \times n_r$ rectangular matrix, where n_r indicates the number of outputs referred to as reference signals. The PSD matrix can be obtained in the frequency

domain, by calculating the auto- and cross-spectral density functions for all frequency values that compose the measured temporal series. For a discrete signal $x(t)$ of length *T*, the power spectral density is

$$S(\omega) = \frac{X(\omega) \cdot \bar{X}(\omega)}{T} \tag{4.1}$$

where $X(\omega)$ and $\bar{X}(\omega)$ are the DFT and the respective conjugate of the discrete signal. Therefore, considering the concepts of auto- and cross- spectral density (J. Bendat & Piersol, 2010; Brincker & Ventura, 2015) and their application to generic time series $x_i(t)$ and $x_j(t)$, recorded at points i and j, the spectral densities can be estimated as

$$S_{ij}(\omega_k) = \frac{\bar{X}_i(\omega_k) \cdot X_j(\omega_k)}{T} \tag{4.2}$$

where $\bar{X}_i$ gives the conjugate of the DFT of signal $x_i(t)$ and X_j is the DFT of signal $x_j(t)$. The indexes associated with measured signals, i and j, go from 1 to n_o, while the number of the sinusoidal wave at frequency $\omega_k = k \cdot \Delta\omega$ goes from 0 to $N_t - 1$, where N_t is the number of sampling values of the time series.

Since the above expression is established considering its direct application to the complete signals, although a superior frequency discretisation is achieved, the resulting spectral densities would present considerable noise, as already mentioned for the calculation of the DFTs. Therefore, with the goal of obtaining smoother estimates of the auto- and cross- spectral density functions and improve the accuracy of parameter identification, the Welch method is used (Welch, 1967), i.e., the temporal series are divided into $\sim' n_s$ shorter data segments of length T_s, assuming a certain overlapping between adjacent segments, thus enabling the calculation of average spectra. Nevertheless, in order to minimize leakage errors, it is recommended the application of tapering windows w_s to the data segments, which obey to specific shape functions (J. Bendat & Piersol, 2010; Maia & Silva, 1997).

In this way, the elements of the PSD matrix $\underline{S}(\omega_k)$ are estimated for all frequency values by averaging the auto- and cross- spectral density functions obtained for each tapered data segment, using the expression

$$S_{ij}(\omega_k) = \frac{1}{n_s} \sum_{k=1}^{n_s} \left[\frac{\bar{X}_i(\omega_k) \cdot X_j(\omega_k)}{T_s \cdot \sum_{p}^{N_s} \left| w_{s,p} \right|^2 \Big/ N_s} \right]_k \tag{4.3}$$

where the wave or frequency index k ranges from 0 to $N_s - 1$, with N_s being the number of sampling values of the data segments, while the number of data segments n_s depends on the predefined overlapping between adjacent windows.

Essentially, for each frequency ω_k, the PSD matrix consists of real values along the main diagonal, which correspond to the auto spectral density functions, and of complex values in the remaining positions, which

relate to the cross-spectral density functions. According to the equation above, these values result from the multiplication of the waves that compose the measured signals in the frequency domain (obtained with the DFT).In graphical terms, it is then possible to represent the PSD matrix through plots with the amplitude and phase of the auto- and cross-spectral densities (Fig. 4.24).

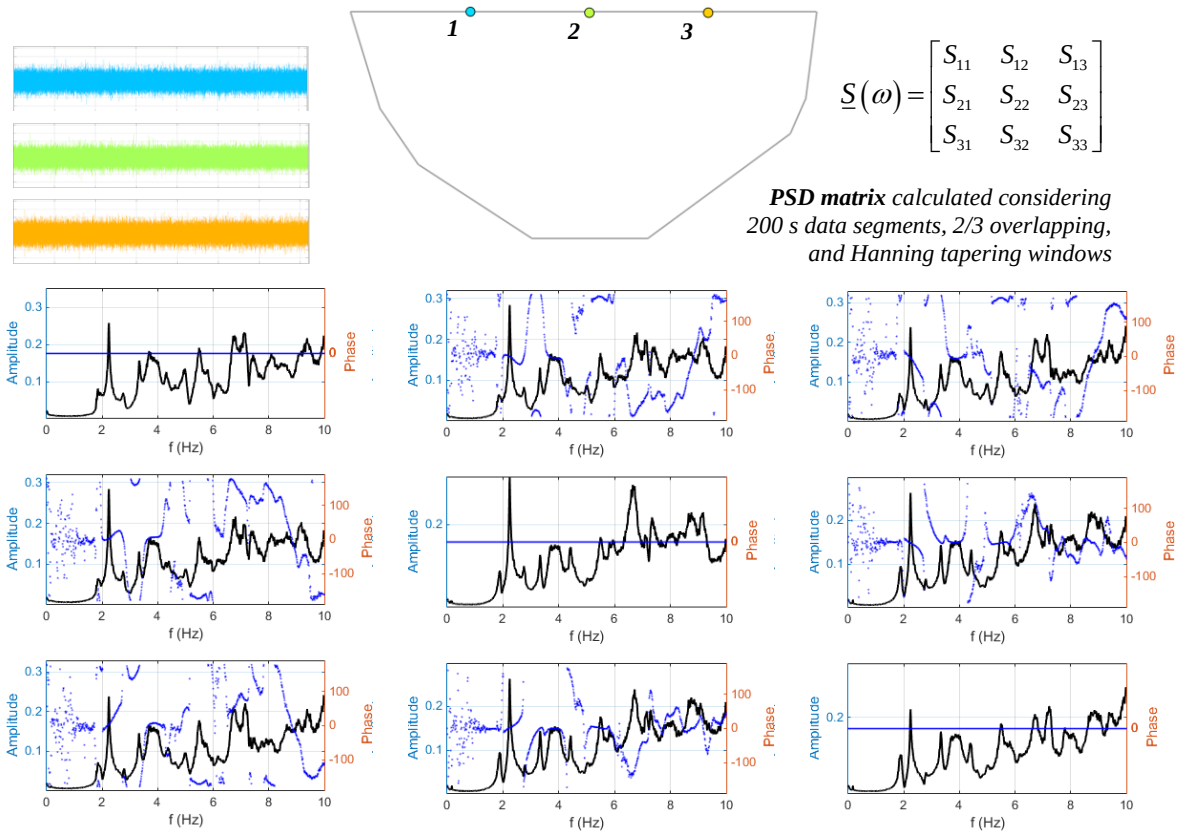

Fig. 4.24 PSD matrix calculated from three acceleration time series recorded in Cahora Bassa dam. Graphical representation: amplitude (black) and phase (blue) of the spectral densities.

Regarding the tapering data windows, there are several types of windows, based on functions with different shapes (Fig. 4.25), including Tukey, Hamming, or Hanning windows (Maia & Silva, 1997). In terms of the data segments overlapping, it is common to consider an overlapping of $2/3$ or $1/2$. According to some authors, the use of the Hanning tapering window associated with an overlapping of 2/3 results in an optimization of the use of the information hidden in the recorded time series.

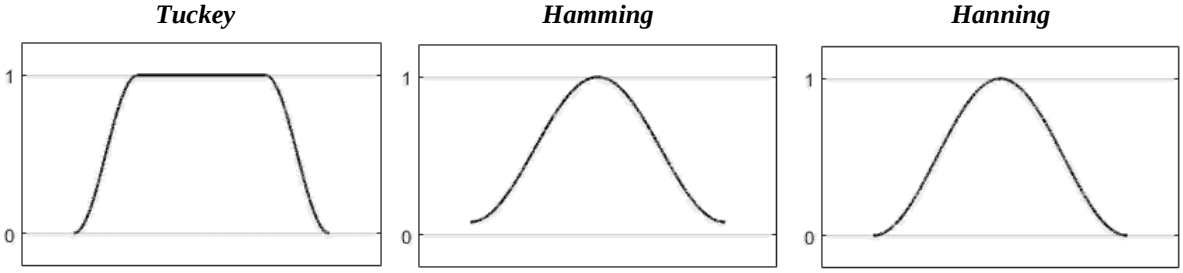

Fig. 4.25 Tapering data windows: Tukey, Hamming, and Hanning.

SINGULAR VALUE DECOMPOSITION AND MODAL PARAMETER IDENTIFICATION

Considering the hypothesis of a structural system subjected to white noise excitation, based on a modal decomposition approach the theoretical PSD matrix $\underline{G}(\omega)$ can be expressed as a superposition of the modes of the structural system (Ljung, 1999; Peeters, 2000), provided the modes are orthogonal. This theoretical matrix can be represented in a simplified way as

$$\underline{G}(\omega) = \underline{\mathrm{O}} \cdot \underline{\mathrm{A}}(\omega) \cdot \underline{\mathrm{O}}^{\mathrm{H}} \tag{4.4}$$

where $\underline{\mathrm{A}}(\omega)$ is a diagonal matrix composed of functions that depend on the natural frequencies and modal damping ratios, while $\underline{\mathrm{O}}$ is a matrix whose columns are associated with mode shapes.

On the other hand, the PSD matrix estimated from the measured signals $\underline{S}(\omega_k)$ can be decomposed by SVD as follows

$$\underline{S}(\omega_k) = \underline{\mathrm{U}}_k \cdot \underline{\mathrm{S}}(\omega_k) \cdot \underline{\mathrm{U}}_k^{\mathrm{H}} \tag{4.5}$$

where $\underline{\mathrm{U}}$ is the matrix including the singular vectors of the estimated PSD matrix, and $\underline{\mathrm{S}}$ is a diagonal matrix containing the corresponding singular values sorted in descending order, for each frequency value. The comparison between eqs. (4.4) and (4.5) shows that the singular values are associated with the natural frequencies of the structural system, and that the singular vectors can be used to determine the corresponding mode shapes (Fig. 4.26).

The singular values are associated with the ordinates of the auto-spectra of single degree of freedom systems with the same modal parameters as the modes contributing to the response of the global structural system under analysis. Therefore, for each discrete frequency value, the first singular value gives the ordinate of the spectrum associated with the dominant mode at that frequency. In case the modes are well separated, the plot of the first singular value spectrum presents amplitude peaks in the natural frequencies of the structural system, while the ordinates of the remaining singular value spectra are not significant. If two or more vibration modes are close within certain frequency band, there will be that many peaks of the first singular value spectrum in that band, and of other singular value spectra with important amplitudes.

In what concerns the modal configurations, for well-separated modes the modal shape of each mode associated with the frequencies pf the spectrum peaks can be estimated from the corresponding first singular vector, i.e., the first column of matrix $\underline{\mathrm{U}}_k$ obtained for those frequencies. Also, if there are two or more closely spaced modes, the modal configuration of the dominant mode is determined using the first singular vector, while the configurations of the other modes are evaluated based on the singular vectors corresponding to the singular values that present local peaks in the vicinity of the dominant frequency.

In what concerns the graphical representation of vibration modes, a simple procedure can be adopted. For a mode associated with a certain natural frequency ω_k, identified as the peak of the first singular value, the singular vector in the first column of the corresponding matrix $\underline{\mathrm{U}}_k$ contains, in each row, a complex number $a_n + ib_n$, which essentially can be used to get the parameters of waves $y_n(t)$ that describe the oscillatory

movement of the measurement points associated with that row of the matrix, for the natural frequency under analysis. Therefore, it is possible to obtain the modal displacement time history $y_n(t)$ for each measurement point in order to represent the vibration mode, by calculating $y_n(t) = Y_n \cdot \cos(\omega_n - \theta_n)$, where $Y_n = \sqrt{a_n^2 + b_n^2}$ is the amplitude and θ_n is the phase angle.

With respect to the implementation of the FDD-SVD method in MATLAB, the SVD of the PSD matrix can be carried out using the command *[U, S, V] = svd (A)*, where *U* gives the singular vector matrix and *S* is a diagonal singular value matrix, obtained from matrix *A*.

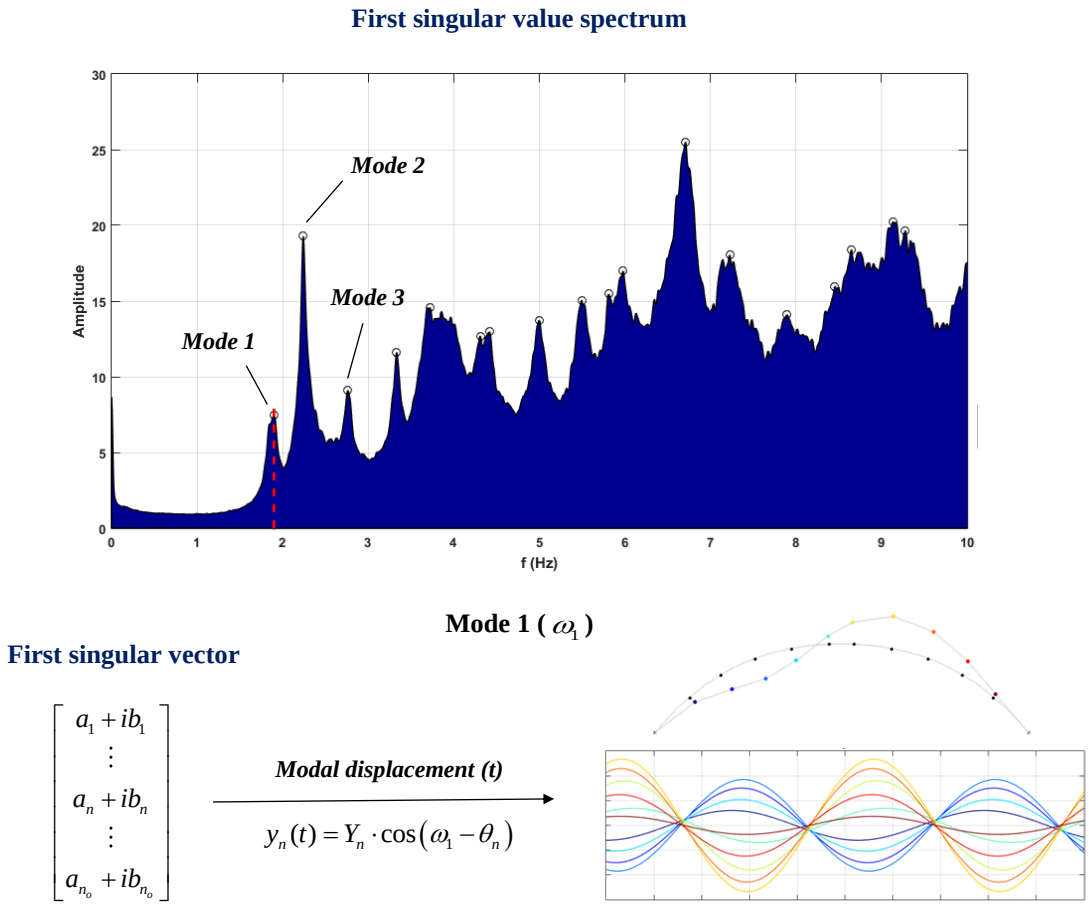

Fig. 4.26 Representation of the first singular value spectrum of the PSD matrix, estimated from measured signals at Cahora Bassa dam. Identification of natural frequencies from the spectral peaks and estimation of the first mode shape from the first singular vector.

The simplest version of the FDD method only estimates the natural frequencies and modal configurations of structural system based on the singulars values and vectors of the PSD matrix. However, for situations where damping is not an issue, this method can be use due to its user friendliness and because it gives good estimates of the modal parameters. Also denoted as peak-picking FDD, this was the first version of the method introduced by (Brincker et al., 2000). Later, an improved and more advanced version was developed, named EFDD method (Brincker et al., 2001), which allows to estimate the modal damping and to improve the accuracy in the identification of natural frequencies and mode shapes.

In this work, the decision was to implement the simplest version of the FDD method presented above, and then invest in the development of additional techniques to automate the selection of spectral peaks and to enhance the modal identification process for dams. The main reason is that the primary focus of the application studies will be on the evolution of natural frequencies and corresponding modal configurations over time, not only for dynamic behaviour analysis but also for structural health monitoring purposes. Besides, the determination of damping in dams, which are structures whose dynamic response clearly influenced by the dynamic dam-water interaction, is a topic that continues to require further developments and investigation (in general, low damping is expected under ambient/operational vibrations). Therefore, the referred techniques are described in detail in the next two subchapters.

4.4.4 MODULE 2: AUTOMATIC SELECTION OF SPECTRAL PEAKS

The second module of the program *DamModalID* was developed to complement the implemented FDD-SVD method, namely for automating the identification of natural frequencies. An original and efficient method is proposed to automatically select the peaks from singular value spectra of the PSD matrix, using a Smoothed Threshold Curve (STC) technique, and considering the distinction of modes with different modal configurations, based on the MAC index.

In the first phase of this procedure, the STC technique is applied to automatically select a set of spectral peaks from a singular value spectrum, as well as the corresponding frequency values. If necessary, the first singular value spectrum can be slightly smoothed *a priori*, in order to reduce existing noise and facilitate the peak selection: this can be done by applying a moving average filter in a consecutive way, considering a reduced number of points for averaging at each frequency value; however, the spectrum smoothing should not be exaggerated too many times, to avoid "hiding" relevant peaks. After that, the smoothed curve is obtained by calculating a significantly smoothed version of the singular value spectrum itself, using the moving average filter (Fig. 4.27). Then, a user-defined vertical shift is applied to the curve and a specific algorithm is used to automatically select the peaks of the singular value spectrum which remain above the shifted threshold curve, thus obtaining a preliminary set of frequencies $\underset{\sim}{f}_N$ of the vibration modes the structural system.

A fundamental aspect that must be accounted for, and that can greatly influence the obtained results, is the frequency resolution, which depends on the length of the data segments used to estimate the PSD matrix based on the Welch method (recall Fig. 4.22). When a higher discretisation is considered, the frequency interval, $\Delta\omega$ (rad/s) or Δf (Hz), is smaller and the spectral will likely present more noise, given that fewer averages are used to calculate the spectral densities, and thus the identification process is hampered. On the other hand, a lower frequency discretisation can limit he accuracy in the estimation of the natural frequencies corresponding to spectral peaks, since the real frequency values may not be captured.

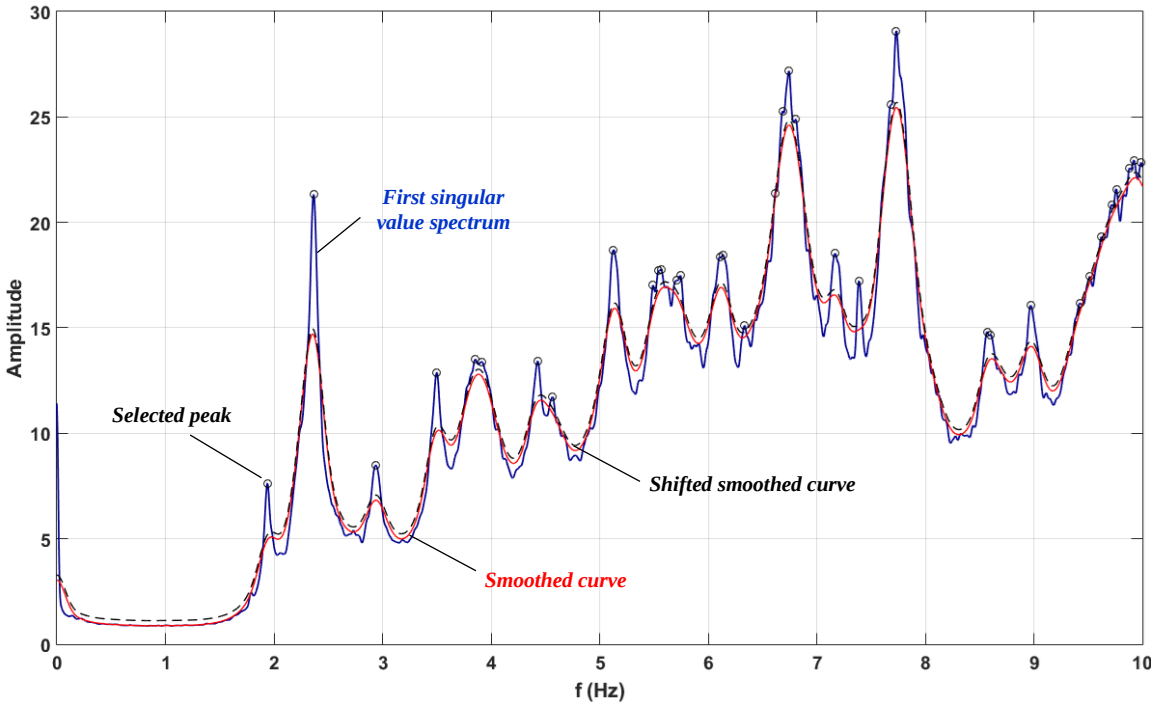

Fig. 4.27 Automatic selection of spectral peaks using the STC technique: first singular value spectrum, shifted threshold curve, and selected peaks. Example of first singular value spectrum of the PSD matrix, estimated from measured signals at Cahora Bassa dam.

In the second phase of this procedure, the mode shapes of the selected natural frequencies are evaluated in order to determine which spectral peaks are associated with true vibration modes of the structural system (Fig. 4.28), and simultaneously to distinguish closely spaced modes with different modal configurations, by establishing a minimum similitude criterion This step, inspired by the approach described in (Brincker et al., 2007), is based on analysing all modes within a predefined frequency band (or search domain), through the comparison of a reference mode with other local modes existing in its neighbourhood.

The modal configuration comparison is carried out based on the MAC index (Allemang & Brown, 1982), which measures the correlation between two mode shapes as

$$MAC_{i,j} = \frac{\left|\underset{\sim}{\phi}_i^T \underset{\sim}{\phi}_j\right|^2}{\left(\underset{\sim}{\phi}_i^T \underset{\sim}{\phi}_i\right)\left(\underset{\sim}{\phi}_j^T \underset{\sim}{\phi}_j\right)} \tag{4.6}$$

where $\underset{\sim}{\phi}_i$ and $\underset{\sim}{\phi}_j$ are the first singular vectors, retrieved from the singular vector matrices, obtained for the frequencies of modes i and j under analysis. The value of the MAC index varies from 0, when the modes are not correlated (i.e., orthogonal modes), to 1, for very similar modal configurations, which may differ only on a scale factor. Based on this index, it can be assumed that two modes have approximate modal configurations if the MAC index is higher than a certain minimum value, e.g., 0.8 or 0.9. The search domain includes the points of the singular value spectra around the peak centred at the mode under analysis: for a mode with frequency f_k, the search domain is defined as $\left[f_k - r(\Delta f); f_k + r(\Delta f)\right]$, where $r(\Delta f)$ gives the frequency range to both sides of the peak under analysis, which depends on the frequency interval Δf (Hz).

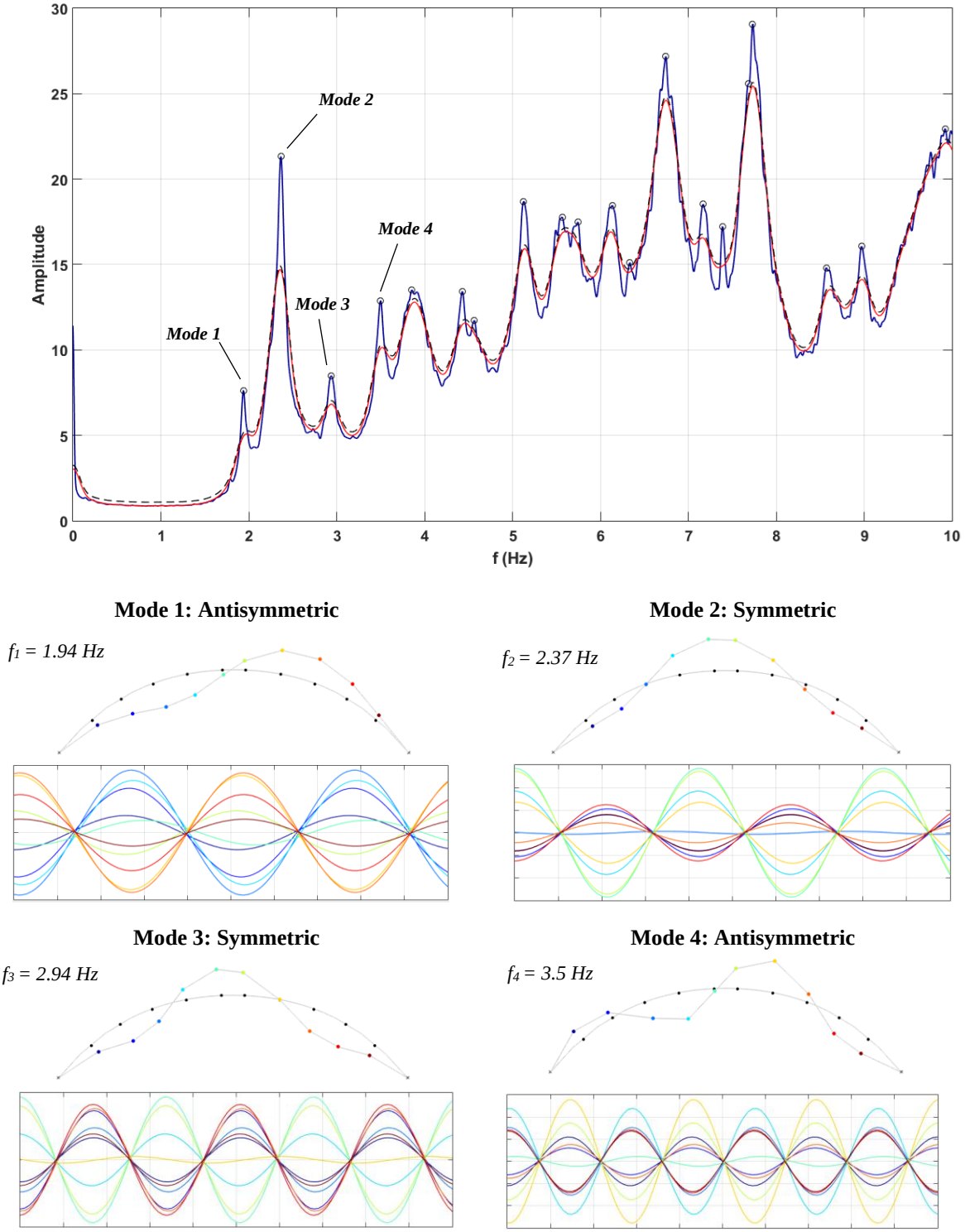

Fig. 4.28 Automatic selection of spectral peaks using the STC technique. Evaluation of modal configurations.

In practice, the analysis of the modes associated with each peak is an iterative process where, for each peak, the corresponding mode is compared to the other modes located within the search domain. Therefore, if two or more modes located within the search domain are very similar between them, $MAC_{i,j} > 0.9$, then frequency value associated to the highest local peak is selected as the natural frequency of the dominant mode with that modal configuration, while the remaining frequencies in the search domain are discarded.

Otherwise, if the modal configurations are different, then these may by closely spaced modes with different configurations, and hence those peaks are kept. With this procedure, the set of peaks and corresponding frequencies is constantly updated as modes are eliminated or selected as resonant nodes of the structural system, until a new set of natural frequencies $\underset{\sim}{f}_{N,new}$ is achieved.

It is also relevant to point out that the implemented procedure allows to separate the peaks associated with true physical modes of the structure and peaks caused by noise or harmonic excitations. In the case of large concrete dams, the operation of existing turbines of generator sets excites the structure with a well-known frequency that can be easily identified and separated from the analysis to be conducted.

The proposed method for automating peak selection, besides being efficient, has allowed to obtain good results, as shown in the examples given here and later in the application studies presented in Chapter 5. However, the success of its application depends on an adequate definition of key parameters, namely the frequency discretisation, the smoothing factor and vertical shift applied to obtain the STC, the frequency range defining the search domain, and the minimum similitude criterion based on the MAC index. Problems that may arise associated with setting these parameters have already been addressed throughout this chapter. Therefore, when intending to carry out automatic analysis of data gathered from continuous dynamic monitoring over several years, it is of utmost importance to carefully select, calibrate and test the chosen parameters, aiming to obtain reliable results for studying the evolution of the modal parameters over time.

In order to demonstrate the potential of the proposed method for automatic peak selection, Fig. 4.29 shows the evolution over time the automatically identified natural frequencies, based on continuous monitoring data collected for Cahora Bassa dam from 2010 to 2020. It is possible to see that the method enables to obtain very good results, particularly for modes with lower frequencies, given that singular value spectra usually present more noise in regions of higher frequency values. Nevertheless, 10 modes of the dam can be identified with good precision.

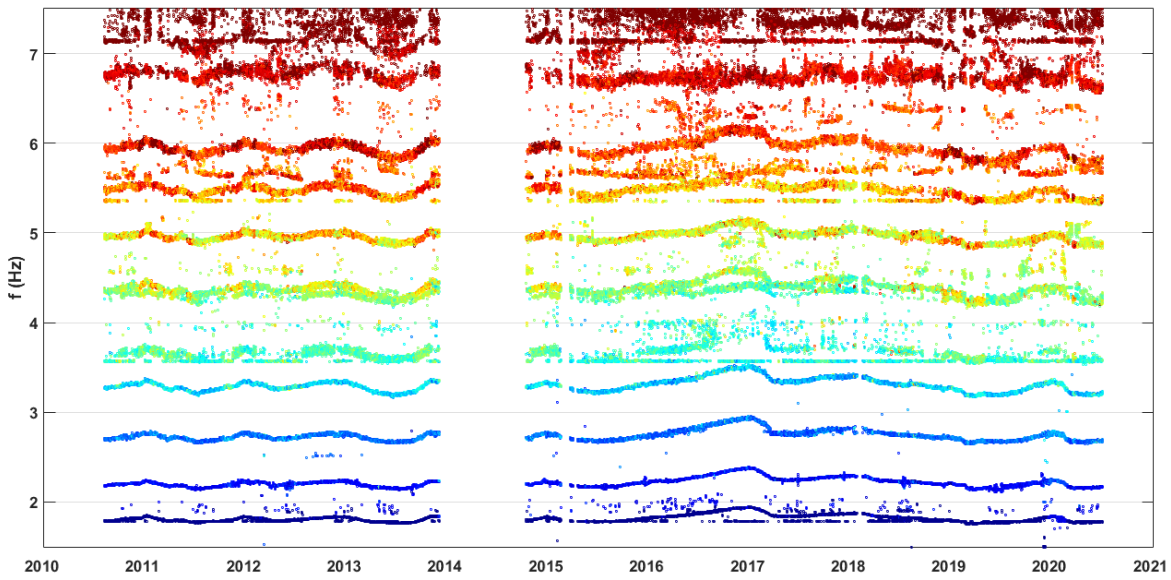

Fig. 4.29 Evolution of natural frequencies over time for Cahora Bassa dam. Modal identification test using *DamModalID* (FDD-SVD method and automatic selection of spectral peaks).

4.4.5 MODULE 3: OPTIMIZATION OF MODAL IDENTIFICATION USING FREQUENCY INFLUENCE CURVES FOR DAMS

A study on the dynamic behaviour of a large concrete dam or the assessment of its structural health over time requires an accurate identification of the modal parameters and their careful analysis. In this context, it is worth reminding the influence of the dam-reservoir interaction in the dynamic response of the dam, since water level variations resulting in alterations in the global dynamic properties of the dam-reservoir-foundation system. Essentially, for each water level a different dynamic system should be considered. On the other hand, if the powerplant is close to the dam, the operation of turbines of generator sets excites the structure with specific frequencies, which despite being well-known and easily detectable, may overlap with the real natural frequencies of the dam and difficult their identification. Therefore, under different operating periods over time, the singular value spectra estimated from the measured signals will be different, with varying modal information, hence requiring extra care in modal parameter estimation.

From another perspective, it is important to note that continuous dynamic monitoring is carried out using systems comprised of a reasonable number of sensors, which permanently record files with high sampling frequencies. As such, after several months or years it will be necessary to process, analyse and interpret a large amount of gathered data, which, in addition to the classical problem associated with efficiency, might make the analyses of the frequencies identified over time less intuitive, given the large amount of data represented in the plots.

Therefore, the third module of *DamModalID* was developed in order to enhance the modal identification process that is performed using continuous dynamic monitoring data of large concrete dams over time. The proposed method consists of an original technique based on Dam Frequency Influence Curves (DamFIC), which are used to group the frequency values associated with each vibration mode of the dam, as in a cluster analysis. The development of this method took advantage of the experience acquired in previous studies on modal parameters of dams, using both experimental results, retrieved from continuous dynamic monitoring data, and numerical results from finite element models (calibrated based on experimental data). In particular, the patterns usually observed in the evolution of the natural frequencies over time are considered, since the frequency values follow a certain variation according to the water level in the reservoir (Alegre, Carvalho, et al., 2019; Bukenya & Moyo, 2017; Darbre & Proulx, 2002; S. Oliveira et al., 2012; Proulx et al., 2001; Sevim et al., 2012). Furtheremore, the type of outputs obtained with this technique also intend to facilitate the analysis and interpretation of the results.

For each vibration mode *n* of the dam, the frequency influence curve is defined by a function that is a linear combination of exponential terms, and it enables to estimate an expected frequency value f_n^* from the reservoir water level h_w, as follows

$$f_n^*(h_w) = -a \cdot e^{\left(\frac{h_w}{Q_1}\right)} - b \cdot e^{\left(\frac{h_w}{Q_2}\right)} - c \cdot e^{\left(\frac{h_w}{Q_3}\right)} - d \cdot e^{\left(\frac{h_w}{Q_4}\right)} + f_{n,0} \tag{4.7}$$

The parameters of the functions for each mode are obtained using previous experimental data and numerical results, as mentioned. The coefficients of the exponential terms, *a*, *b*, *c*, and *d*, are calculated by fitting the function to data sets containing experimental natural frequencies and the corresponding reservoir water levels, based on the Least Squares Method. However, the frequency value for an empty reservoir scenario $f_{n,0}$ is obtained from the numerical models (due to the unavailability of experimental frequency data under these conditions). The other coefficients Q_i are values predefined in order to achieve adequate frequency curves; in this work, these are taken to be $Q_1 = 15$; $Q_2 = 20$; $Q_3 = 25$; $Q_4 = 30$. The definition of the curve parameters must be properly adapted to each dam in order to obtain the corresponding DamFIC. For example, Fig. 4.30 shows the natural frequencies automatically identified for Cahora Bassa dam, for the monitoring period between 2010 and 2020 (shown previously in Fig. 4.29), and the frequency influence curves defined in this work for 10 vibration modes.

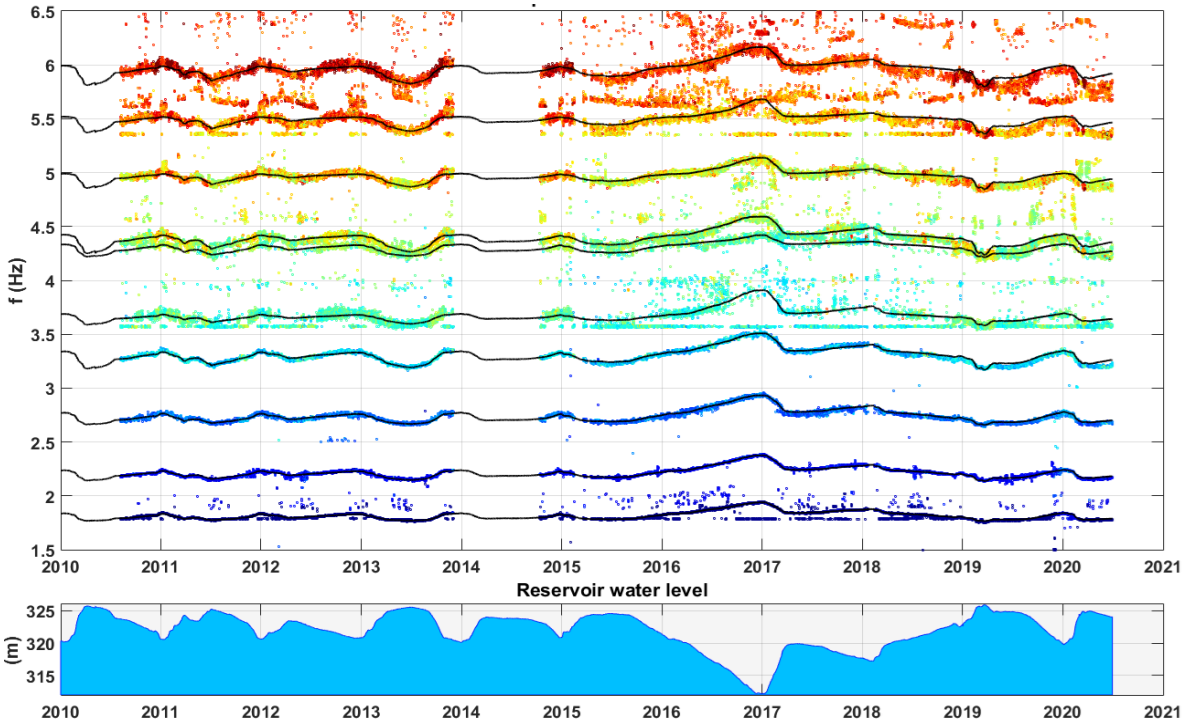

Fig. 4.30 Evolution of natural frequencies over time (Cahora Bassa dam). Example of personalised frequency influence curves (in black) for 10 vibration modes.

Based on the proposed method, the calculated frequency influence curves are incorporated in a specific algorithm that analyses the set of peaks/natural frequencies estimated before, using the FDD-SVD method and the SCT technique, aiming to select the identified frequency values that are associated with each vibration mode to be considered. In practice, for each mode *n*, with an expected frequency value $\underset{\sim}{f}_n^*$ for water level h_w, the implemented algorithm selects the peaks whose frequency values are located within a small influence search domain given by $\left[f_n^* - \lambda; f_n^* + \lambda \right]$, where λ is a predefined tolerance in Hz.

Aiming to exemplify the potential of this method, as well as the usefulness of the DamFIC for enhancing and optimising the automatic identification of natural frequencies over time for large dams, Fig. 4.31

presents updated results concerning the evolution of the natural frequencies of Cahora Bassa dam over time. These results represent the final output computed with the program *DamModalID* after applying the frequency influence curves (shown in Fig. 4.30) in the modal identification process. The evolution of natural frequencies is shown for ten dam vibration modes, as well as frequencies associated with the operation of generator sets (at 1.785 Hz and 3.57 Hz).

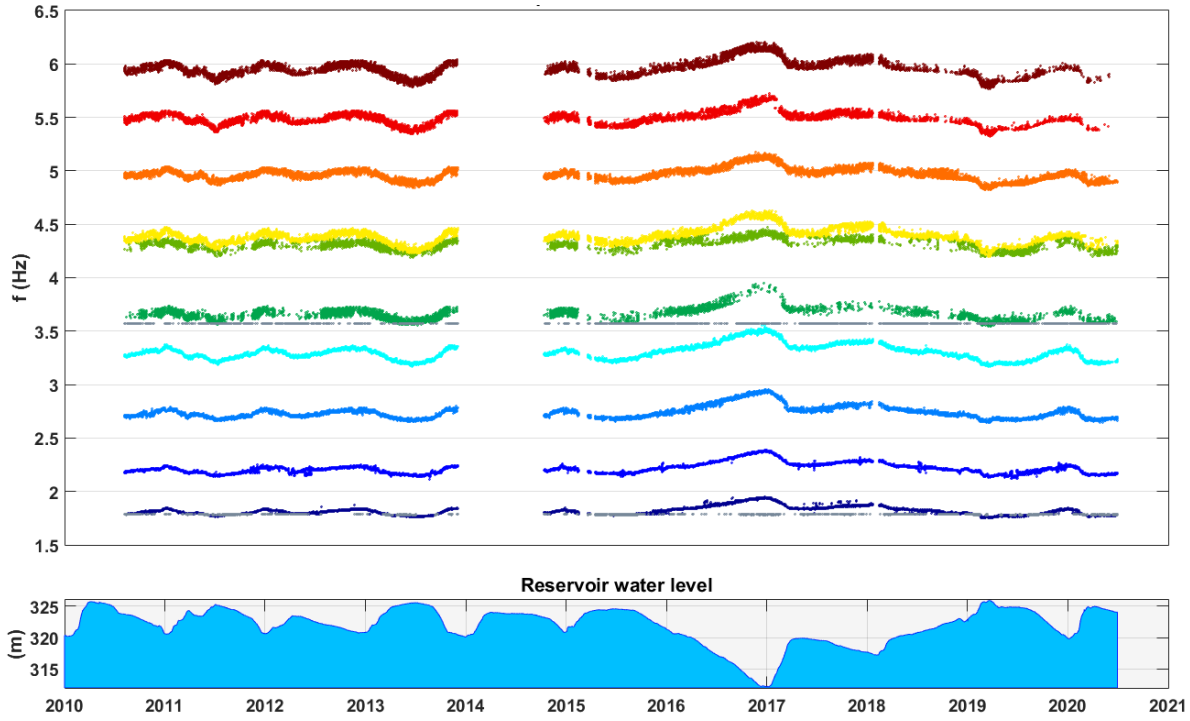

Fig. 4.31 Evolution of natural frequencies over time (Cahora Bassa dam). Modal identification test using *DamModalID* after the implementation of the DamFIC method.

4.4.6 INPUTS, OUTPUTS, ALGORITHM, AND GRAPHICAL USER INTERFACE

DamModalID is one of the programs developed in this thesis for integrating and complementing the software component of SSHM systems installed in large concrete dams (together with *DamSSHM*). The first version of the program, *DamModalID1.0*, implemented using MATLAB, includes the three modules describe before, namely: (i) module 1, for frequency-domain modal identification, based on the FDD-SVD method (section 4.4.3); (ii) for automatic selection of spectral peaks, using an original approach based on the STC technique and considering the MAC index (section 4.4.4); and (iii) for enhancing the modal identification process for dams, using a new method based on DamFIC, considering the variation of the reservoir water level over time (section 4.4.5).

In order to perform modal identification, *DamModalID* requires, as inputs, the data files collected from continuous dynamic monitoring over time, as well as an Excel or text file containing information on the observed water levels and the corresponding dates. Furthermore, to run automatically and thus analyse the data for extended monitoring periods, the program also needs the user to define some parameters in

advance, including: (i) the length and overlapping of the data segments used in the Welch estimate, for the FDD-SVD method (the time discretisation and frequency resolution depend on the measured data); (ii) the factors used to smooth the singular value spectrum and to calculate the shifted threshold curve, as well as the minimum similitude value of the MAC index, for the procedure implemented for automatic peak selection; and (iii) data sets with frequency-water level values for each vibration mode of the dam under analysis, to enable the determination of the frequency influence curves.

It is relevant to note that the program should be properly adapted to read the data files from the monitoring systems installed in each dam, since these files are most likely recorded using a different number of accelerometers, with distinct features, and with different data formats. In addition, depending on the sampling frequency and on other parameters that influence the discretisation in the time and, consequently, in the frequency domain, it may be necessary to make some changes in the referred parameters, for different case studies. Furthermore, the frequency influence curves, which depend on the variation of the reservoir water level, are defined on the basis of information gathered from experimental data and of results from finite element analyses and must therefore be adapted for each dam to be studied. In this work, with Cabril dam and Cahora Bassa dam as case studies, it was necessary to make slight adaptations in the code, namely in the parts concerning the reading of the data files and the definition of the frequency influence curves.

In what concerns the main outputs, the program is prepared to save a file with extension of the type *.mat*, including, for all evaluated hours and dates, the observed reservoir water level and a list with the values of the identified natural frequencies (in Hz), namely using: (i) the peak-picking technique only; (ii) the method for automatic peak selection; and (iii) the method for automatic peak selection and the method based on the DamFIC. Moreover, auxiliary codes were also developed to serve as a complement to the main program, in order to automatically generate figures representing the evolution of the natural frequencies over the monitoring period under evaluation (see, e.g., Fig. 4.29, Fig. 4.30, and Fig. 4.31), as well as graphical representations of the modal configurations of the main vibration modes, including figures with the modal oscillatory motion of each measuring point in the dam and figures with 2D mode shapes (as shown, e.g. in Fig. 4.28) - these auxiliary codes can be executed separately while the main program is analysing all monitoring data, in order to control the evolution of the results. This significant investment in the graphical component was carried out, on the one hand, to facilitate the analysis and interpretation of data to support both dynamic behaviour studies and structural health monitoring, and on the other hand, to simplify the comparison with results from finite element numerical models, as shown in Chapter 5.

The algorithm of *DamModalID* is presented in Fig. 4.32. Regarding the operation of the program, it is important to note that the analysis is performed hour by hour, for all available dates throughout the whole monitoring period. Thus, *DamModalID* performs 24 cycles of analysis, in which all the files associated with a particular hour are analysed consecutively: for each file, modules 1, 2 and 3 are executed to perform modal identification. Then, at the end of each hour cycle, the program saves a *.mat* file with the results for that hour. Considering the great amount of data that needs to be analysed, the program was implemented in this way to allow the evaluation of the modal identification results for the entire monitoring period as soon as the cycle for a certain hour ends, only based on the file for that hour. Furthermore, it should be made

clear that all data files must go through the processing phase (check for errors, detrend, etc.) before being analysed with *DamModalID*.

DAMMODALID

1. Read main inputs
    - 1.1. Identify the main directory with all monitoring data files and create a *data matrix* with the following information for each file: year, month, day, hour, and file name
    - 1.2. Read file with the water levels in the reservoir
    - 1.3. Read parameters for modal identification and automatic peak selection
    - 1.4. Read file with frequency-water level values to define the frequency influence curves
2. Frequency-domain modal identification *[for each hour h]*
    - 2.1. Select all rows of the *data matrix* associated with hour *H* and identify all dates/files to be analysed
    - 2.2. For each data file
        - 2.2.1. Open and read the data files from the corresponding folder
        - 2.2.2. Create a matrix with all measured acceleration time histories
        - 2.2.3. Run Module 1: FDD-SVD method
            - Estimate the PSD matrix $\underline{S}(\omega)$ from all measured signals, using the Welch method
            - Perform singular value decomposition of the PSD matrix: $\underline{S}(\omega_k) = \underline{U}_k \cdot \underline{S}(\omega_k) \cdot \underline{U}_k^H$
            - Obtain the singular value $\underline{S}(\omega_k)$ and singular vector $\underline{U}_k$ matrices
        - 2.2.4. Run Module 2: automatic peak selection
            - Calculate the smoothed threshold curve
            - Select the peaks of the first singular value spectrum above the threshold curve, and identify the corresponding frequencies $\underset{\sim}{f}_N$
            - Obtain the mode shape for each frequency value from the singular vector matrix
            - Re-evaluate the peak selection based on the mode shapes. For each peak:
                - Define the corresponding frequency f and mode shape ϕ
                - Define the search domain $[f_k - r(\Delta f); f_k + r(\Delta f)]$ and select the peaks/modes for comparison
                - Calculate the MAC index and eliminate ($MAC_{ij} < 0.8$) or select the resonant modes ($MAC_{ij} > 0.8$)
                - Update the set of selected peaks and identified natural frequencies $\underset{\sim}{f}_{N,new}$
            - Detect peaks/frequency values associated with the operation of turbines of generator sets or other equipment
        - 2.2.5. Run Module 3: optimization of modal identification for dams
            - Read the water level h_w associated with the date of the file
            - For each mode *n*:
                - Calculate the expected natural frequency f_n^*, using the predefined frequency influence curve $f_n^*(h_w)$
                - Define the influence search domain $[f_n^* - \lambda; f_n^* + \lambda]$
                - Select the peak and corresponding frequency within the search domain
                - Update the frequency vector $\underset{\sim}{f}_{N,n}$
        - 2.2.6. Save the results in the file for hour H: *ResultsMIDdata_H.mat*
    - 2.3. Repeat from 2.1

Fig. 4.32 Algorithm of *DamModalID*.

After concluding the implementation of the code for automatic modal identification based on continuous dynamic monitoring data, a graphical user interface was developed for *DamModalID* using the GUIDE tool of MATLAB. The goal was to provide an interactive and user-friendly version of the *DamModalID*, enabling to carry out studies using monitoring data recorded at specific dates and hours, and to analyse in detail not only the acceleration records but also the modal identification results. Furthermore, this version can facilitate parametric tests to be conducted, in order to calibrate and assess the parameters used for automatic modal identification. On the other hand, as in the case of *DamDySSA*, the intent was also to develop a software that can be useful in practice for integration in SSHM systems installed in large concrete dams, allowing a constant monitoring of their dynamic behaviour in real time.

In this work, two versions were developed and specifically prepared to analyse dynamic monitoring data collected with the SSHM systems installed in Cabril dam and Cahora Bassa dam, chosen as case studies. In particular, the interactive version for Cabril dam was installed for testing in the central server of the SSHM system of the dam, as done with the program *DamSSHM*. The main menus and panels of the graphical user interface developed for Cabril dam are presented next, from Fig. 4.33 to Fig. 4.36.

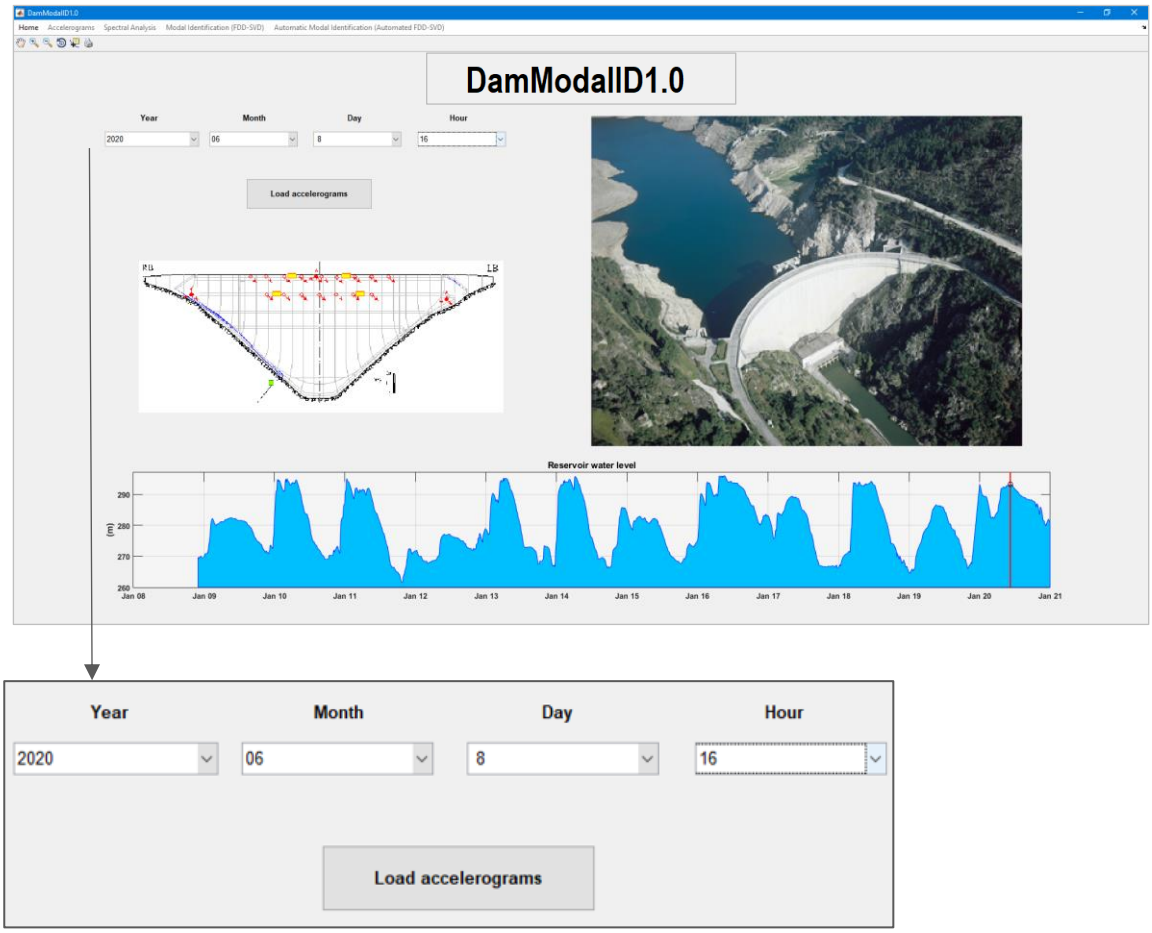

Fig. 4.33 *DamModalID*: graphical user interface. Home panel with drop-down menus to choose date and hour for analysis, and pushbutton to load the respective file with acceleration records.

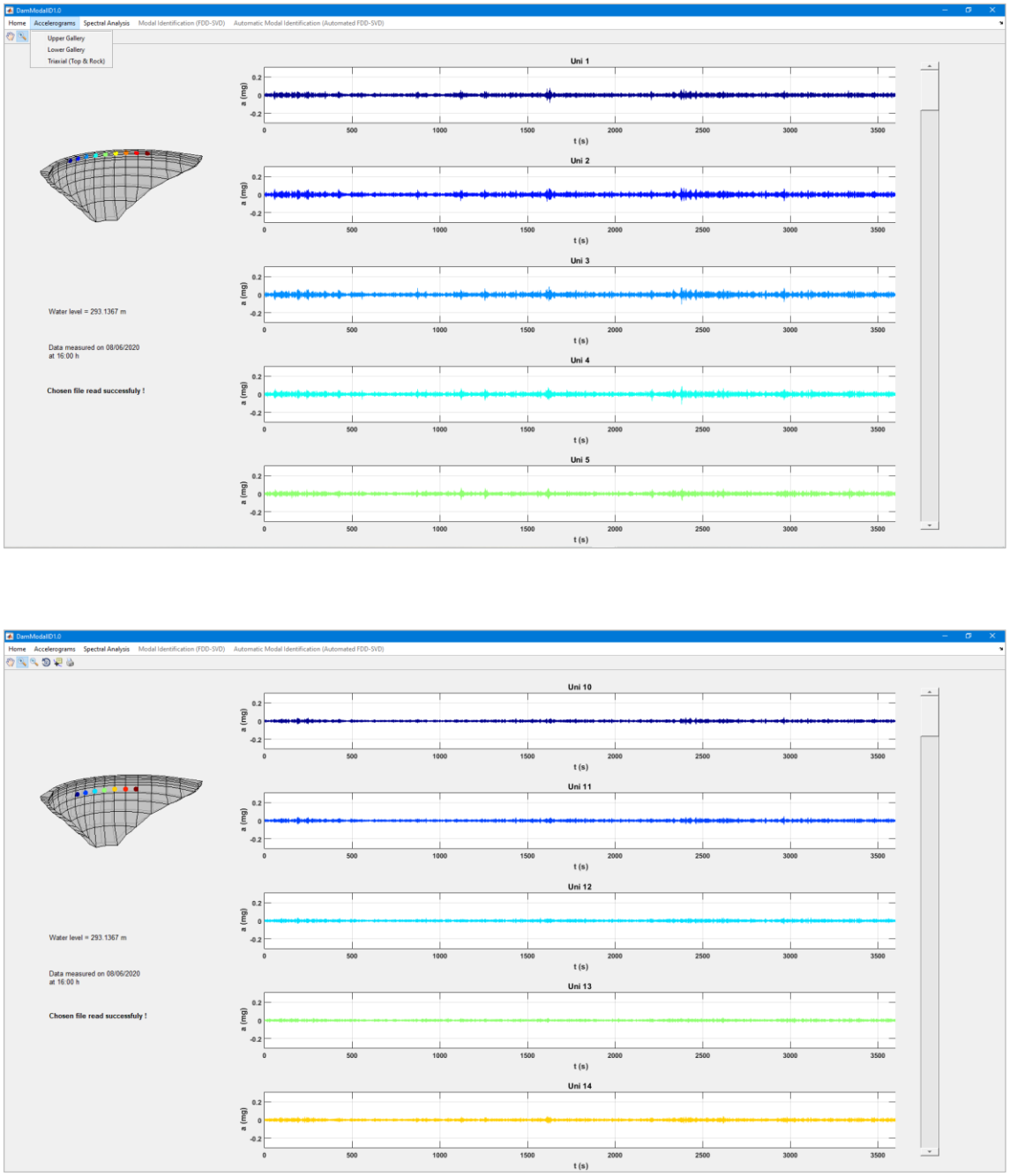

Fig. 4.34 *DamModalID*: graphical user interface. Accelerograms menu with drop-down options to show the measured accelerations with the uniaxial sensors located at the upper gallery and lower gallery, as well as with the triaxial sensors.

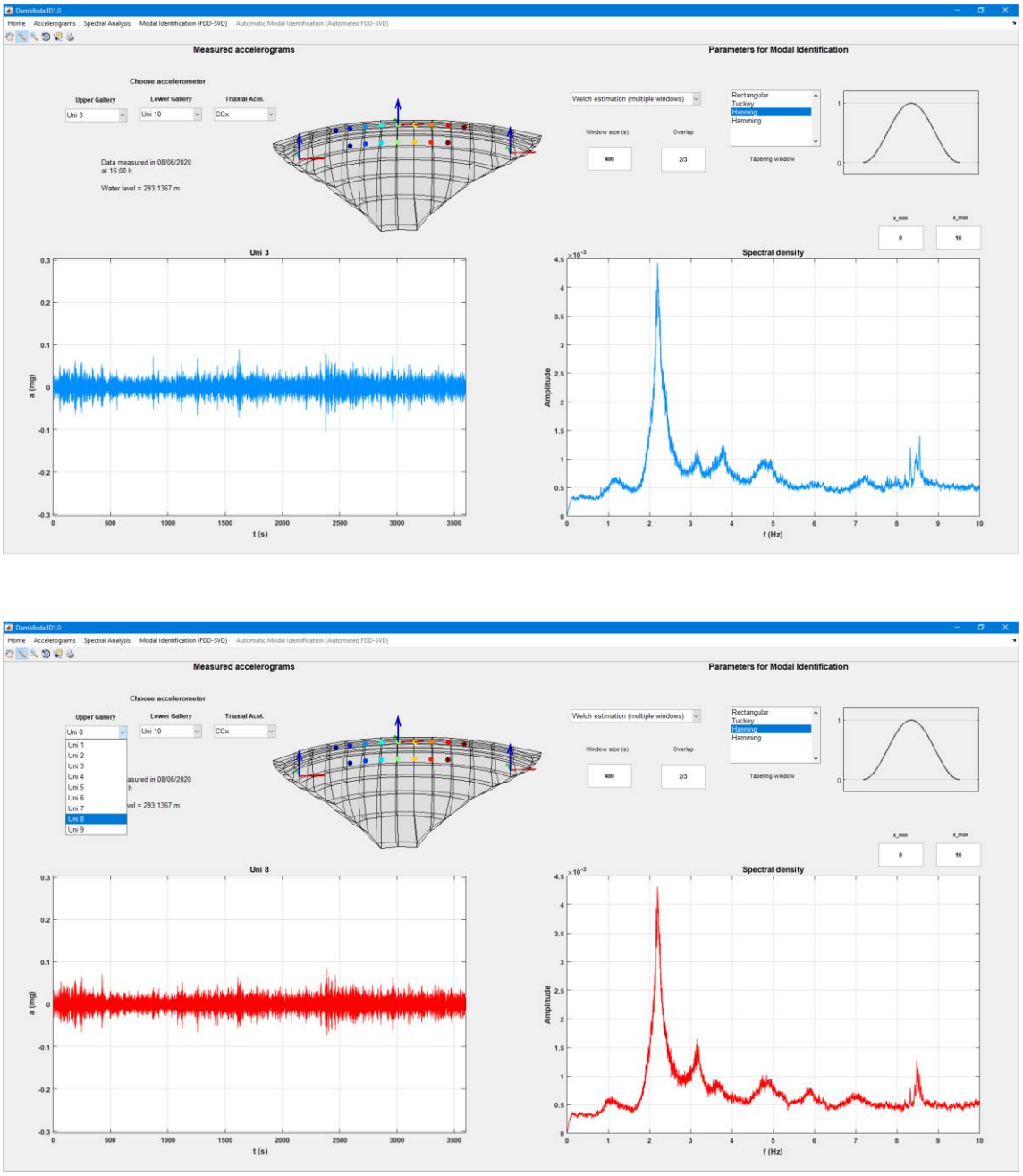

Fig. 4.35 *DamModalID*: graphical user interface. Spectral analysis menu showing the measured signals in different positions and the corresponding spectral density functions, and the parameters user for modal identification.

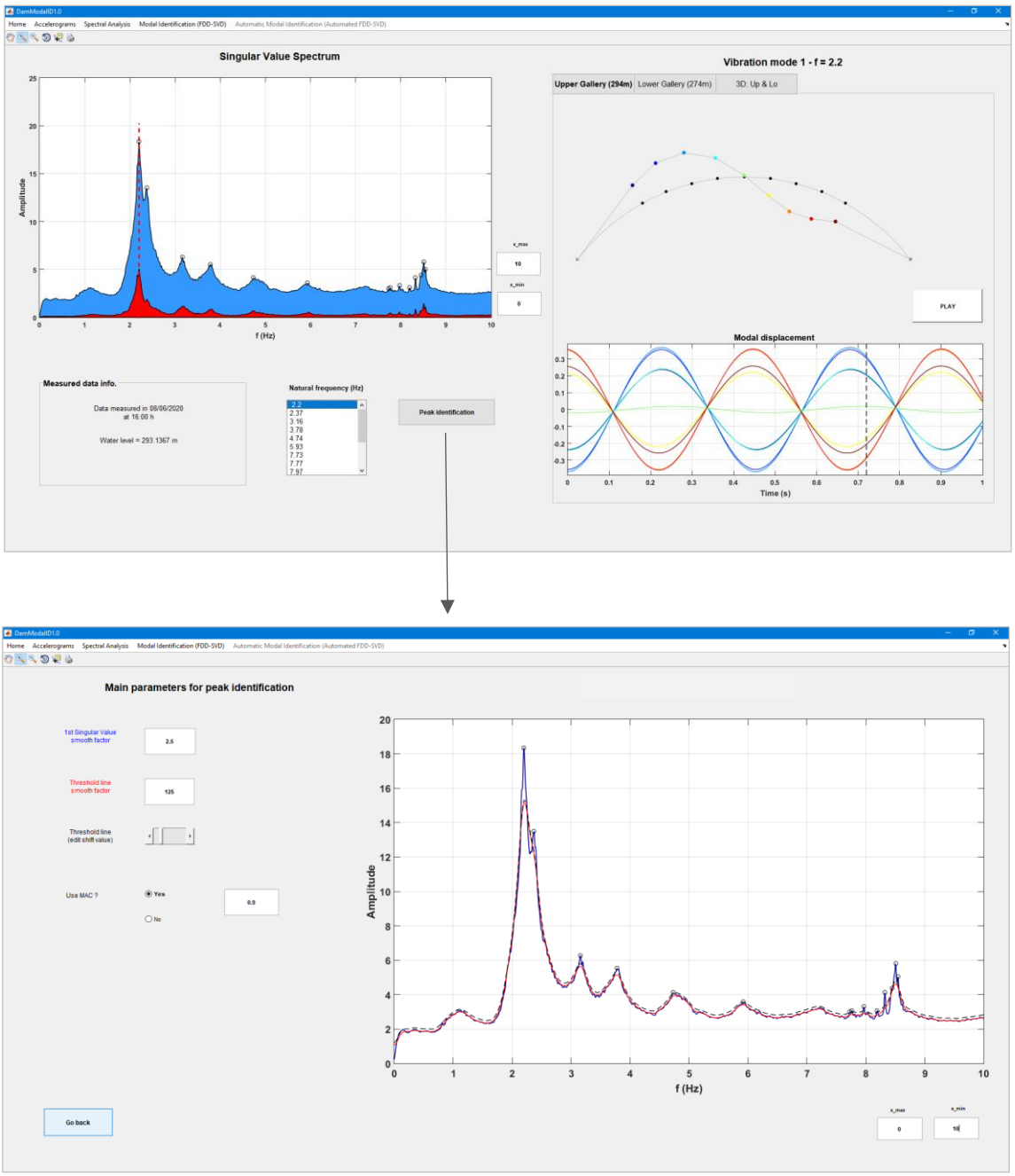

Fig. 4.36 *DamModalID*: graphical user interface. a) Menu showing the main results from modal identification using the FDD-SVD method, namely the singular value spectrum, a list with identified natural frequencies and the corresponding mode shapes; b) Additional panel representing the STC technique developed for automatic peak selection.

4.5 FINAL CONSIDERATIONS

Chapter 4 focused on the use of SSHM systems for long-term continuous vibrations monitoring on large concrete dams. This chapter began with a review about the Seismic and Structural Health Monitoring methodology and then it addressed its application for continuous dynamic monitoring of dams in detail, namely in what concerns the main goals and advantages in the scope of dam safety control, as well as important aspects that must be considered for the design of monitoring schemes, used equipment, and the installation and operation of the system

The installation of an SSHM system on a large concrete dam aims essentially to enable a permanent characterization of its performance in normal operating conditions and during seismic events, by continuously measuring ambient/operational vibrations and seismic vibrations, and to evaluate structural integrity, in order to support informed management. Thus, the use of these systems allows to meet the ICOLD recommendations regarding dam surveillance.

Ideally, SSHM systems should be developed to measure vibrations at as many points as possible, in the dam body, along the insertion (near the dam-rock interface), and in the free-field. Furthermore, to allow an accurate recording of low and high amplitude vibrations, measuring sensors should have very low self-noise and be configured with high dynamic ranges. Overall, it is recommended the use of cutting-edge, high-quality equipment for automatic data measurement and acquisition, usually provided by specialized companies.

However, it is worth stressing the need to complement these monitoring systems with suitable software for processing, managing, and analysing monitoring data, which is collected on a continuous basis, with a view to enhance their operation and obtain reliable experimental results. As shown in several studies conducted over the last decade, particularly in LNEC, the combined use of experimental results from SSHM systems and numerical results from finite element models can be of great value for increasing knowledge on the dynamic behaviour of large concrete dams, to investigate the response of dam-reservoir-foundation systems and gather data for calibrating, validating and developing numerical models, and to provide useful information to owners and to engineers and technicians responsible for dam safety.

Although the specialized companies that develop and supply the hardware have also started investing in software for SSHM systems, there continues to be a clear need for the development of computational tools for continuous dynamic monitoring data management and for modal identification of dams, which must be properly adapted and optimised for each dam, as well as for the investment in graphical tools to facilitate the comparison with finite element results. Therefore, in this work it was considered important to contribute with the development of specific software to integrate and complement the SSHM systems installed in large concrete dams, namely: *DamSSHM* and *DamModalID*.

The program *DamSSHM* was developed for automatic analysis and management of continuous dynamic monitoring data from SSHM systems, and it was implemented for testing the central server of the Cabril dam SSHM system, in 2019. *DamSSHM* is automatically executed every day at 9 a.m., and it comprises four modules to execute the following tasks: (i) read data files and apply moving average filters to the

acceleration records; (ii) carry data analysis and management, including evaluation of the integrity of records and saving decimated files to external storage units and Google Drive folders; (iii) analysis of acceleration time histories to automatically detect vibrations induced by seismic events (and distinction from those induced by the operation of gates and by turbines of generator sets), and save backups when detection is successful; and (iv) perform the maintenance of the server storage and save backups of original files. After performing these tasks, *DamSSHM* automatically sends emails with resumes of measured data and information regarding the available storage space. Furthermore, the program also sends emails when seismic vibrations are detected, which include figures of recorded acceleration time histories.

Throughout this testing period, it was demonstrated that *DamSSHM* was successfully implemented in system of Cabril dam. For example, the emails containing information summaries have been sent daily, and the performed file management has ensured that storage space is always available. In addition, many acceleration time histories, recorded during low-intensity seismic events, were automatically detected, including those used in the application study presented in section 5.2.4.

The program *DamModalID* was developed for automatic frequency domain modal identification of dams, in order to obtain the main modal parameters, including natural frequencies and mode shapes. This program includes three modules. In the first module, the classic Frequency Domain Decomposition (FDD) method with Singular Value Decomposition (SVD) was implemented, in order to calculate the spectral density matrix from measured accelerations, extract the corresponding singular values and singular vectors, and estimate the main modal parameters. The second module was developed to complement the FDD-SVD method, namely for automating the selection of spectral peaks and for distinguishing closely spaced modes, using an original method based on Smoothed Threshold Curve (STC) in combination with the MAC index. The third module was implemented aiming to enhance modal identification for dams based on Dam Frequency Influence Curves (DamFIC), which are obtained for each vibration mode using previous monitoring data and numerical results, considering reservoir level variations

The first version of a graphic user interface was developed for *DamModalID*. This interactive version of the program has also been installed in the central server of the SSHM system of Cabril dam, and it has enabled to examine acceleration records and perform modal identification tests using monitoring data collected in specific hours and dates.

The methods developed in this work were tested by using *DamModalID* to perform modal identification based on dynamic monitoring data gathered for two large concrete dams over the last decade: very good estimates were obtained for natural frequencies and their evolution over more than 10 years and for the corresponding modal configurations, thus showing the suitability of the proposed methods. These results are analysed in detail and compared with numerical results from *DamDySSA* in Chapter 5.

CHAPTER 5

APPLICATION STUDIES. DYNAMIC BEHAVIOUR OF TWO LARGE ARCH DAMS

MODAL ANALYSIS AND SEISMIC RESPONSE

CABRIL DAM, PORTUGAL

CAHORA BASSA DAM, MOZAMBIQUE

5. APPLICATION STUDIES. DYNAMIC BEHAVIOUR OF TWO LARGE ARCH DAMS: MODAL ANALYSIS AND SEISMIC RESPONSE

5.1 INTRODUCTION

Chapter 3 was dedicated to presenting the coupled finite element formulation used for simulating the dynamic behaviour of dam-reservoir-foundation systems, as well as the mathematical formulations proposed in this thesis for complex modal analysis, linear seismic analysis, and non-linear seismic analysis, which were implemented in *DamDySSA*, a finite element program developed for dynamic analysis of concrete dams. In turn, chapter 4 focused on describing the software developed in this work to integrate and complement the SSHM systems installed in large concrete dams, namely *DamSSHM*, prepared for automatic management and analysis of monitoring data, which includes a module for automatic detection of vibrations due to seismic events, and *DamModalID*, developed for frequency-domain modal identification and specifically automated and optimized for identification of modal parameters in large dams.

Following the work accomplished both at the level of numerical modelling the dynamic behaviour of dam-reservoir-foundation systems and of software for SSHM systems installed in large concrete dams, the main goal in this chapter is to use the developed programs in practical applications for studying the dynamic behaviour of two large concrete dams, with focus on modal analysis and on linear and non-linear seismic response analysis. Therefore, this chapter aims to demonstrate the potential of these programs for analysing the dynamic response of large concrete dams, to highlight the value of the combined use of numerical results from advanced finite element models and of experimental results from SSHM systems to support seismic monitoring and structural health monitoring, to present the main results from advanced non-linear seismic analyses, and to contribute for increasing knowledge on the dynamic behaviour of large arch dams by presenting results of great interest.

In this thesis, the dams chosen as case studies are the 132 m high Cabril dam, in Portugal, and the 170 m high Cahora Bassa dam, in Mozambique, two double-curvature arch dams (Fig. 5.1) which have been under continuous dynamic monitoring since 2008 and 2010, respectively. Detailed descriptions of the dams and their systems, as well as the results of the performed studies, are provided in sub-chapter 5.2, for Cabril dam, and in sub-chapter 5.3, for Cahora Bassa dam.

With regard to the application studies, this chapter presents the main results obtained from the continuous dynamic monitoring of the referred dams over the last decade, including: (i) the analysis of the evolution of the identified natural frequencies over time and the comparison with results from finite element calculations, aiming a) to study the influence of the reservoir water level variations in the dynamic response of the dam-reservoir-foundation system, and b) to provide data that can be useful for supporting structural health assessment of dams subject to deterioration phenomena; and (ii) the analysis of the seismic response, based on acceleration time histories recorded during seismic events and on results from linear seismic calculations, enabling a) the evaluation of the amplification factors between the response measured near

the dam-rock interface and the top of the dam, and b) to investigate the influence of the seismic input and of the required damping ratios for large arch dams under low to medium intensity earthquakes.

Furthermore, the current chapter also provides the most significant results from numerical simulations carried out for analysing the non-linear seismic response of large arch dams under strong earthquakes, using artificial accelerograms, in order a) to investigate the influence of opening and sliding movements of vertical contraction joints in the global seismic behaviour, based on the deformed shapes and stress fields, as well as the concrete damage distributions at the upstream and downstream faces and along the thickness, and b) to evaluate the dynamic performance of both dams under intensifying seismic excitation based on the Endurance Time method, by analysing tensile and compressive damages for different excitation levels, and therefore to assess their resistant capacity and to verify the seismic safety.

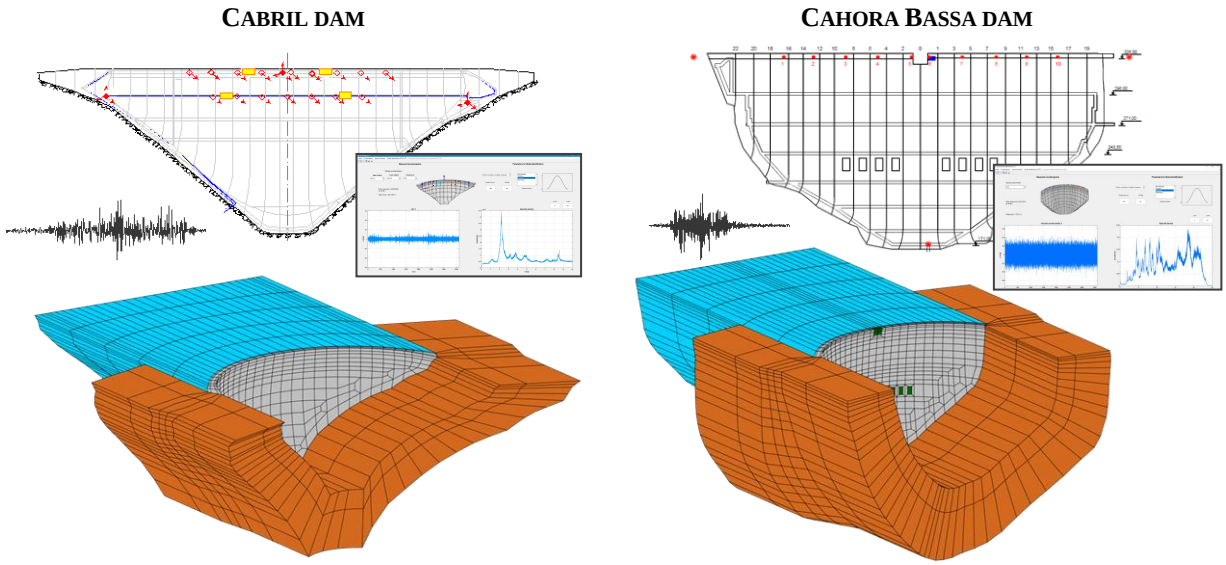

Fig. 5.1 Cabril dam and Cahora Bassa dam. SSHM systems and examples of 3D finite element models of the dam-reservoir-foundation systems.

5.2 DYNAMIC BEHAVIOUR OF CABRIL DAM

5.2.1 CABRIL DAM DESCRIPTION

THE DAM

Cabril dam is a large concrete dam in operation since 1954, being located on the Zêzere River, in the municipality of Sertã, district of Castelo Branco, Portugal (Fig. 5.2). It is the highest Portuguese dam and one of the most important in the country. A remarkable dam engineering work, Cabril dam is a 132 m high double curvature arch dam, founded on a granite mass rock foundation of good quality. The crest is at el. 297 m and its arch is 290 m long. In the central cantilever (section KL), the maximum thickness is of 20 m, at the base, and the minimum is of 4.5 m, around 7 m below the crest level, which in turn has a greater thickness. The volume of the dam body is of 360 000 m^3.

Horizontal cracks appeared at the downstream face of the dam, around el. 280 m to 290 m, during the first filling of the reservoir, caused by the crest with a larger thickness. Also, internal concrete swelling phenomena were identified in the late 1990s. Nevertheless, the dam performance has been monitored over the decades in order to monitor structural integrity, and normal operating conditions have not been affected.

As for appurtenant works, the dam has two bottom spillways, one in each riverbank, with a global maximum discharge capacity of 2200 m^3/s. Moreover, a reinforced concrete intake tower with the same height of the dam was constructed upstream of the dam, near to its surface. This tower is connected to the central cantilever via a concrete walkway at the crest level, with a joint in the contact surface. On the downstream base of the dam there is a hydropower plant with a total installed capacity of 97 MW, capable of producing a mean annual energy output of 301 GWh (CNPGB, 2021).

In what concerns the reservoir, its area is around 20 million m^2, while its effective storage is of about 615 million m^3. The water level in the reservoir usually ranges from a minimum at el. 265 m to the normal water level (NWL) at el. 294 m, while the maximum flood level (MFL) is el. 296.3 m.

SSHM SYSTEM

In Portugal, the use of dynamic monitoring systems for continuously measuring vibrations in large concrete dams began in 2008 (S. Oliveira & Alegre, 2019a), when LNEC and Energias de Portugal (EDP) made the decision to invest in the installation of a pioneer SSHM system in Cabril dam (Fig. 5.3). The goal was to monitor the performance of the dam in normal operating conditions over time and to measure its response during seismic events, enabling to gather and provide useful information for owners and engineers responsible for safety control.

The SSHM system installed in Cabril dam was designed and implemented in the scope of a long-term LNEC research program (S. Oliveira, 2002), focused on modelling and monitoring the dynamic behaviour of large concrete dams, which was supported by EDP and the Portuguese Foundation for Science and Technology (FCT). The project was developed in LNEC (Mendes, 2010; S. Oliveira & Silvestre, 2017), with collaboration from the Concrete Dams Department (DBB) and the Scientific Instrumentation Centre (CIC), and included the design of the monitoring scheme, assembling and installation of all hardware components (optical fibre networks, data concentrators, accelerometers, etc.), and the development of software for automatic data management and analysis, and for finite element numerical analysis, to which this thesis has contributed.

The monitoring scheme was developed to record accelerations at the upper part of the dam body and near the dam-rock interface, using 16 uniaxial (EpiSensor ES-U2) and 3 triaxial (EpiSensor ES-T) force balance accelerometers from Kinemetrics. The uniaxial accelerometers were configured to measure accelerations in the radial direction and are located at the upper part of the dam, distributed along two galleries: 9 in the upper gallery (el. 294 m), below the crest, and the other 7 in a second gallery (el. 275 m), below the cracked zone. As for the triaxial sensors, one is positioned in the upper gallery, in the central section, while the other two are placed in the gallery near the dam-rock interface (around el. 274 m), in both banks.

CABRIL DAM (PORTUGAL)

Downstream view

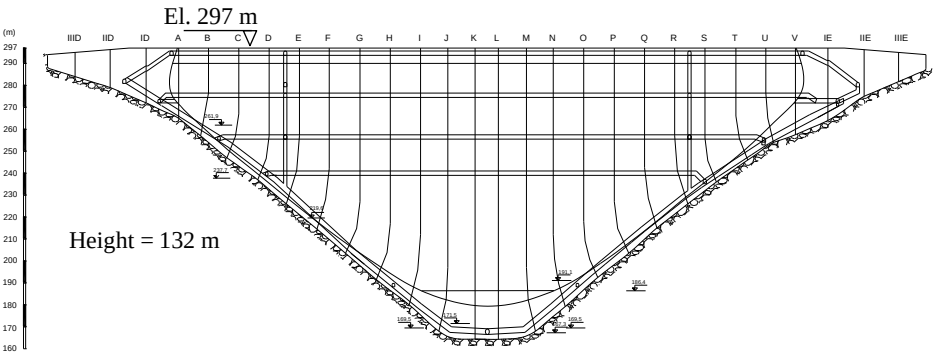

Central section

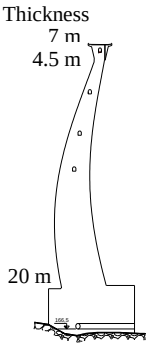

Plan view

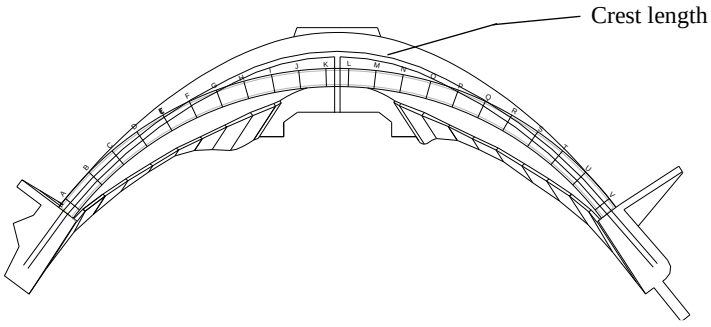

Downstream face cracking

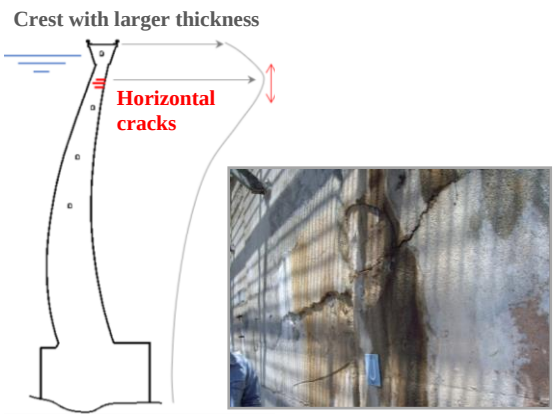

Intake tower and power plant

Fig. 5.2 Cabril dam, Portugal. Aerial view, technical drawings (downstream view, central cantilever cross section, and plan view), detail of downstream face cracking, intake tower and power plant.

Furthermore, the aim was to implement a system with a high dynamic range, capable of accurately measuring the response of Cabril dam under low amplitude ambient/operational vibrations and during low to high intensity earthquakes. Therefore, full-scale recording ranges of ± 0.25g and of ± 1g were defined for the uniaxial and triaxial accelerometers, respectively. All accelerometers are connected to a modular system, composed by four data acquisition units that gather all recorded data. In turn, the data acquisition units send the data through a local network to the central server, installed in an office at the powerplant (located at the dam toe). The connections are established by means of an optical fibre ring network. In summary, 25 signals are recorded, in 24 bit, at a sampling rate of 1000 Hz, collected and then stored in the central server, every hour.

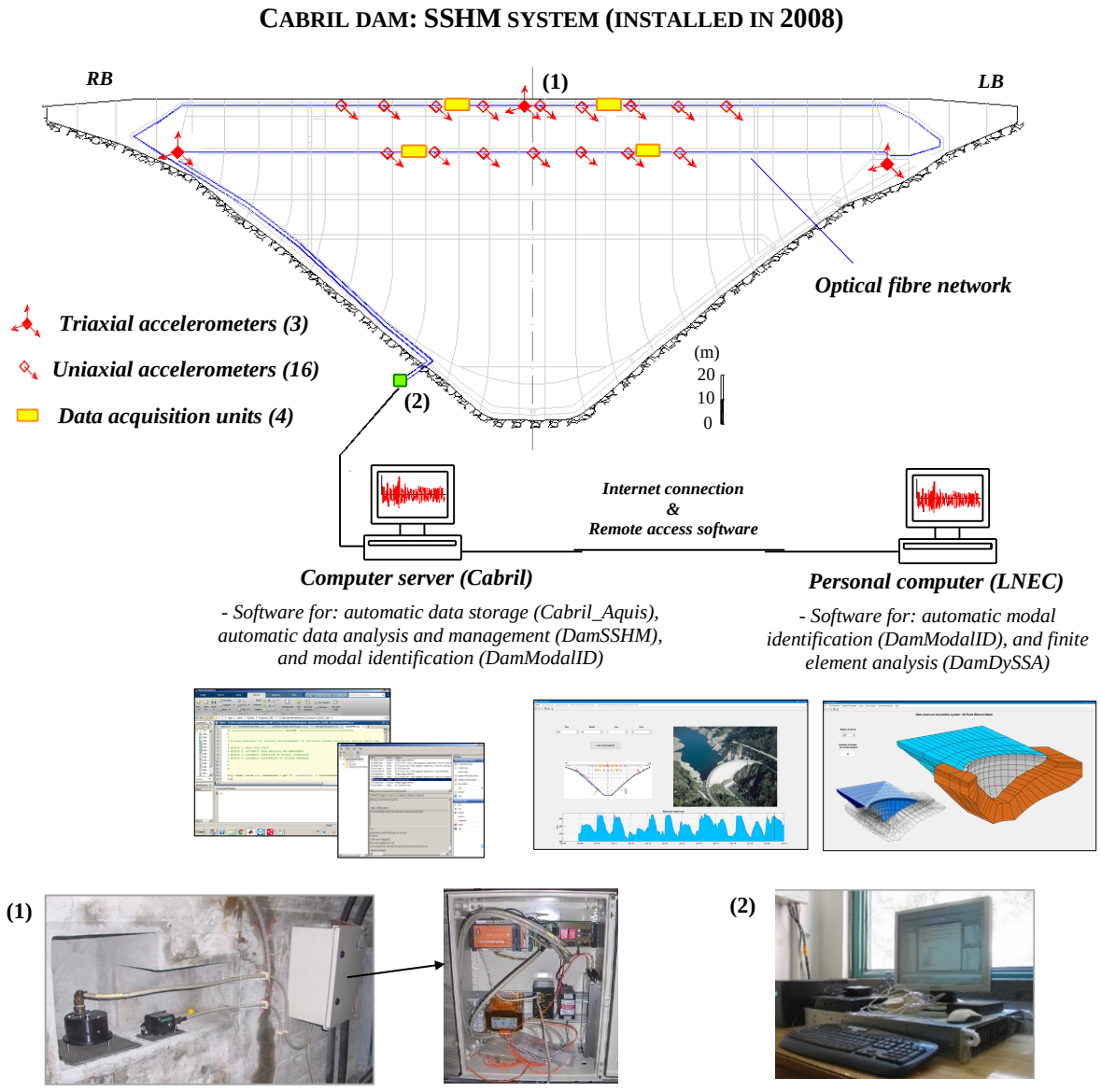

Fig. 5.3 SSHM system installed in Cabril dam. Monitoring scheme, hardware, and software elements.

Regarding the software component, which is fundamental not only to ensure a proper operation and maintenance of the system but also to provide useful data for dynamic behaviour analyses (Alegre,

Carvalho, et al., 2019; S. Oliveira et al., 2012; S. Oliveira, Silvestre, Espada, et al., 2014; S. Oliveira & Alegre, 2018) and for informed decision making (S. Oliveira & Alegre, 2020), the SSHM system of Cabril dam includes: the program *Cabril_Aquis*, to collect the measured signals and save data files, and the programs developed in this thesis and described in Chapter 4, namely *DamSSHM*, for automatic data analysis and management, and *DamModalID*, for automatic modal identification.

During the first decade, there were some periods during which the monitoring system was not active, either due to malfunctions or damages in measuring equipment or in data acquisition units. However, several visits for maintenance and repair interventions were carried during the initial phase of this thesis, and the system has been fully operational and under periodical maintenance since June 2018.

SEISMIC ACTION

Cabril dam, located in the centre of Portugal, is integrated in a national region of high seismic risk, close to some active intraplate faults, as shown in a map provided by the Portuguese Institute for Sea and Atmosphere (IPMA) (Fig. 5.4a).

In the Portuguese Standard for national implementation of Eurocode 8 (NP EN1998-1, 2010) the national territory is divided into seismic zones, depending on the local seismicity. These seismic zones are described by reference values of peak ground acceleration a_{gR}, corresponding to the reference return periods for the no-collapse requirement (475 years). For structures of a superior importance class, associated with higher return periods, the design peak ground acceleration a_g is obtained by multiplying the reference value by an importance factor (EN 1998, 2004). Knowing the reference peak ground acceleration, the ground acceleration response spectrum that represents the seismic action can be defined and suitable acceleration time histories can be generated for numerical analysis. However, Eurocode 8 does not cover special structures such as nuclear power plants and large concrete dams, which are associated with high potential risks and thus require special ground investigations and/or geological studies to be conducted in order to define the seismic action.

According to the Portuguese Standards for dam design (NPB, 1993), the Operating Basis Earthquake (OBE) and the Maximum Design Earthquake (MDE) must be considered for seismic safety verification of current and failure scenarios of large concrete dams. As such, and following the ICOLD guidelines (ICOLD, 2016a), specific seismic hazard studies must be carried out for the region where the dam is located, in order to prescribe the seismic actions for seismic design and seismic safety evaluations (Wieland, 2016, 2019b).

In the case of Cabril dam, a seismic hazard study has not yet been performed at the dam site, and thus there are no acceleration values to be used as reference in the present work. Nevertheless, a study of this type was performed for Ribeiradio dam (S. Oliveira, Silvestre, & Câmara, 2014), a large dam built 100 km to the north-northwest of Cabril dam, based on a fault rupture and seismic wave propagation model developed in LNEC (A. Carvalho, 2007). The acceleration response spectra calculated using this model enabled to confirm the suitability of the spectra used to prescribe the seismic actions in the dam design (Fig. 5.4b). For

Ribeiradio dam, peak ground accelerations of 0.06g and 0.14g were defined for the OBE and the MDE (S. Oliveira, Silvestre, & Câmara, 2014).

As mentioned before, one of the objectives of this chapter is to perform non-linear seismic analysis and seismic safety assessment of Cabril dam, which requires appropriate seismic design criteria. Taking as reference the study carried out for Ribeiradio dam and bearing in mind that Cabril dam is relatively close but located in an area of higher seismic risk, similar or perhaps higher values of peak ground accelerations can be expected. Therefore, for the application studies to be conducted in this work, peak ground accelerations of 0.1g for the OBE and of 0.2g for the MDE are assumed. However, it is worth reminding that higher values could be determined in seismic hazard studies conducted for the dam site.

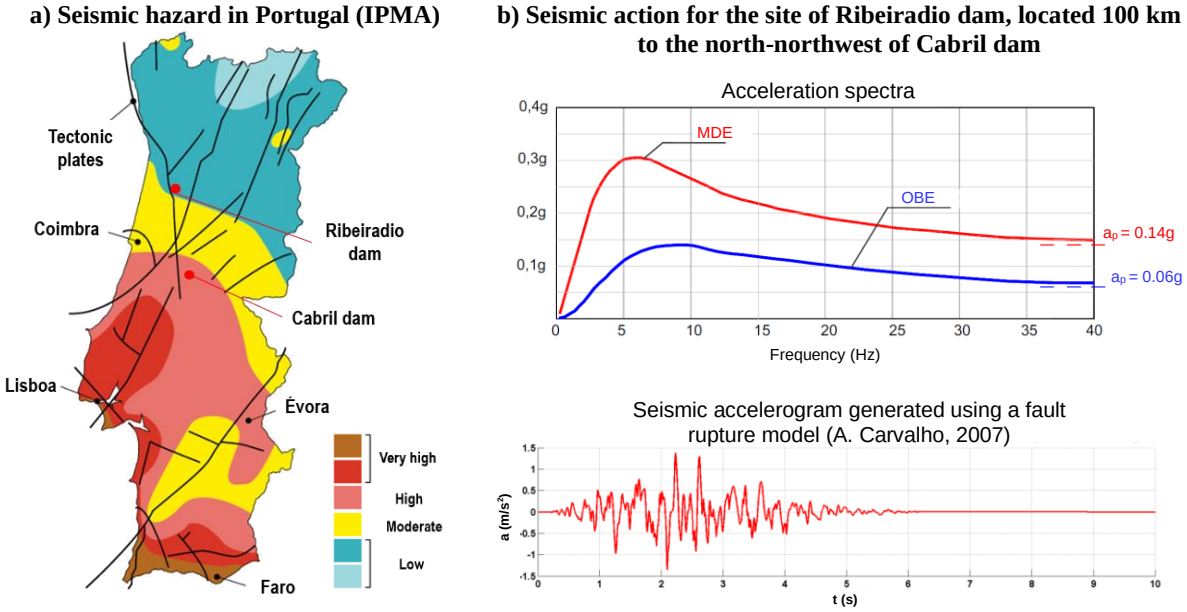

Fig. 5.4 a) Seismic hazard zones in Portugal (map from IPMA), b) Design acceleration response spectra with peak ground acceleration values for the OBE and MDE and example of generated 10 s accelerogram for a site located 100 km to the north-northwest of Cabril dam (S. Oliveira, Silvestre, & Câmara, 2014).

5.2.2 MODAL ANALYSIS: EVOLUTION OF NATURAL FREQUENCIES OVER TIME

In this section, the aim is to study the dynamic behaviour of Cabril dam under ambient/operational excitations (in normal operating conditions), for the monitoring period between 2008 and 2020. Therefore, the most important results obtained from continuous vibrations monitoring data, gathered with the SSHM system, are presented here. In particular, the evolution of the automatically identified natural frequencies over time are analysed and compared with frequency values from finite element simulations. This will enable, on the one hand, to evaluate the influence of water level variations on the dynamic response of the global dam-reservoir-foundation system, and, on the other hand, to assess the difficulties encountered in the modal identification for lower water levels due to the interaction between the dam and the intake tower. Furthermore, it is intended to demonstrate how this type of analysis can be useful for vibration-based damage detection and thus for supporting structural health monitoring of dams.

MODAL IDENTIFICATION RESULTS FROM CONTINUOUS DYNAMIC MONITORING DATA

The evolution of the identified natural frequencies for the first five vibration modes of Cabril dam is presented in Fig. 5.5. The frequencies and modal configurations estimated from the accelerations measured on two specific dates are also presented, namely on June 16, 2018, between 5 and 6 p.m., and on May 4, 2019, from 4 to 5 a.m. The modal identification results were obtained using *DamModalID*, from monitoring data collected between December 2008 and December 2020.

During the monitoring period, the reservoir level varied from el. 261.5 m to el. 295 m, i.e., 35.5 m to 2 m below the crest, a 33.5 m water level variation. Regarding temperature, the air temperature amplitude in the dam site is of only about ± 8º throughout the year, and thus the influence of thermal variations on the dam dynamic behaviour is assumed to be negligible in comparison with the influence of water level variations.

These results show that the dynamic response of the dam-reservoir-foundation system is considerably influenced by the reservoir level, since the values of the natural frequencies clearly follow the water level variations over time. Considering the maximum and minimum water levels during the period under analysis, the natural frequencies of the five modes present the following variations, where the lower values correspond to higher water levels: (i) mode 1, from 2.09 to 2.72 Hz; (ii) mode 2, between 2.31 and 2.79 Hz; (iii) mode 3, from 3.09 to 4 Hz; (iv) mode 4, between 3.55 and 4.23 Hz; and (v) mode 5, from 3.64 to 4.42 Hz. As expected, the frequency values decrease as the water level increases. It is also worth noting how this effect is more noticeable for vibration modes with higher natural frequencies, and that the first two modes have relatively close frequencies (maximum differences of about 0.2 Hz), which become closer for lower water levels. Additionally, the frequency values associated with the operation of the energy production groups, with a known rotation frequency of 3.57 Hz, are also captured.

Regarding the vibration mode shapes, the first and fifth modes are antisymmetric, while the second and third modes are symmetric. The fourth mode, approximately symmetric, is influenced by the existing horizontal cracking band in Cabril dam, and it corresponds to the vibrations of the upper blocks of the dam. Furthermore, it is relevant to note that non-stationary modes are identified (recall section 3.9.2).

In the case of Cabril dam, it is worth addressing the issue of the intake tower. For higher water levels, the tower is not in contact with the dam, as the joint between the tower and the dam opens, and hence there is not a noticeable influence in dam behaviour. However, for lower water levels, below around el. 285 m, the tower leans into the dam, resulting in dam-tower dynamic interaction and in an added mass effect that influences the response of the dam-reservoir-foundation system. This phenomenon has been studied previously, enabling the identification of vibration modes of the tower from measured vibrations in the dam (Espada, 2010; Mendes, 2010; Mendes & Oliveira, 2009). This is in line with the results obtained here, based on which it was possible to detect natural frequencies that are most likely associated to dynamic vibrations of the intake tower, since the corresponding dam mode shapes are inconclusive and do not have a clear physical meaning, and to observe how the symmetric modes seem to be particularly affected by the dam-tower interaction, namely for lower reservoir levels. Nevertheless, further investigation is required in order to fully comprehend the dam-tower dynamic interaction, ideally supported by more detailed finite

element models that includes the intake tower, to enable a proper simulation of the modes shapes of the tower-dam-reservoir-foundation system.

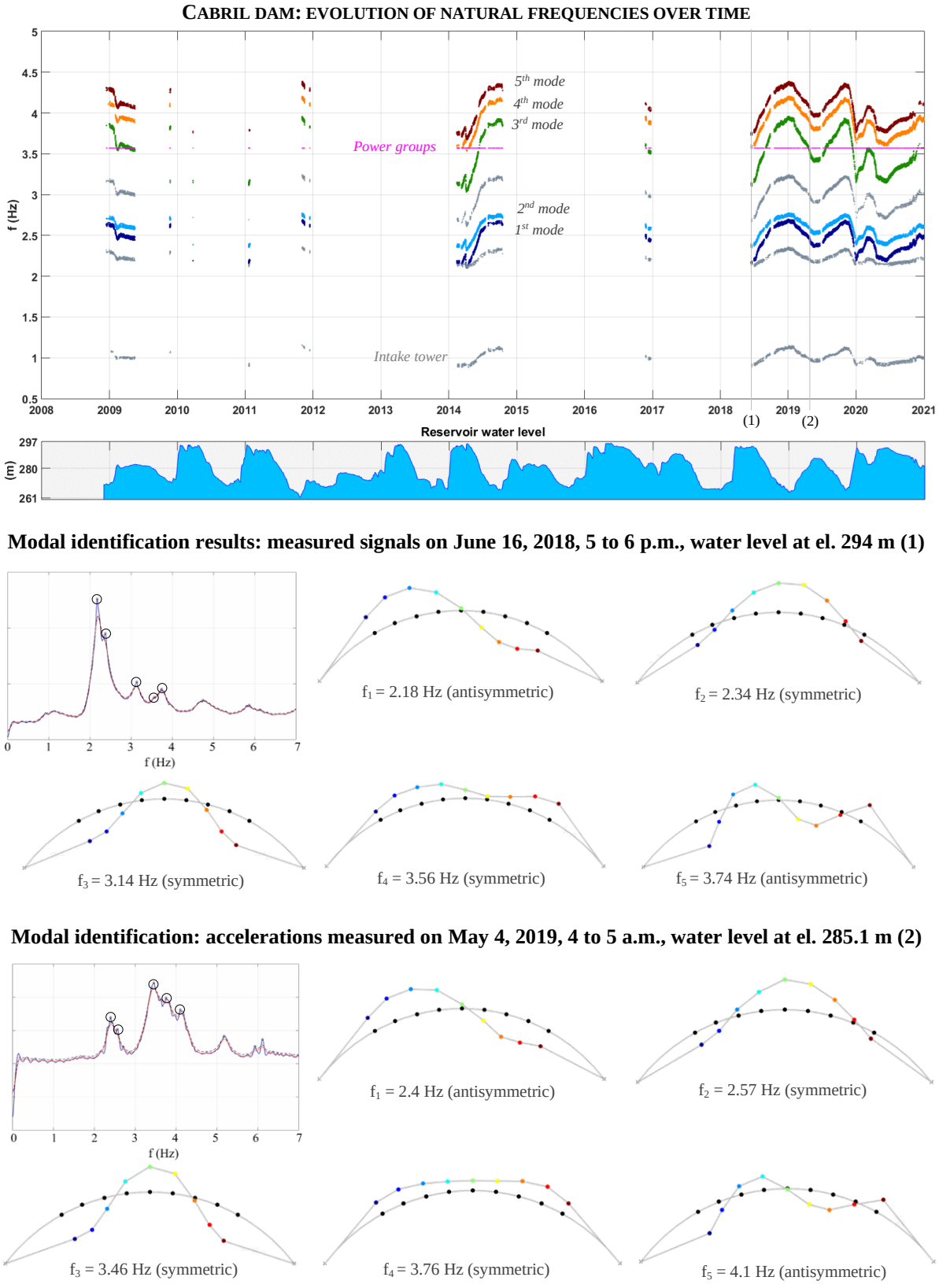

Fig. 5.5 Results from continuous dynamic monitoring of Cabril dam: evolution of identified natural frequencies over time (2008 to 2020). Singular value spectra and estimated frequencies and mode shapes for specific dates.

FINITE ELEMENT MODAL ANALYSIS AND COMPARISON WITH MODAL IDENTIFICATION RESULTS

The finite element dynamic calculations were carried out using the module of *DamDySSA* for modal analysis, based on the proposed coupled state-space formulation with generalized damping (recall subchapter 3.6), and considering the 3D finite element model of the dam-reservoir-foundation system presented in Fig. 5.6.

The dam concrete and the foundation rock are isotropic materials with linear-elastic behaviour, considering Young's modulus E = 25 GPa and Poisson's ratio $\nu = 0.2$; for dynamic calculations, a factor of 1.3 is applied to the Young's modulus. The water was assumed as a compressible fluid, with a pressure wave propagation velocity of c_w = 1440 m/s, according to a mean water temperature of around 15º C. The existing cracking band around el. 280 to 285 m is simulated in a simplified way in this work by incorporating several interface elements to form a single horizontal crack, considering linear joint behaviour (high normal and shear stiffness value are used). This a simplified model that does not incorporate the intake tower.

The adopted material properties and assumed hypotheses have been validated in previous studies carried out in LNEC, based on experimental data from the reference period in the initial monitoring phase (S. Oliveira et al., 2011, 2012; S. Oliveira & Alegre, 2018).

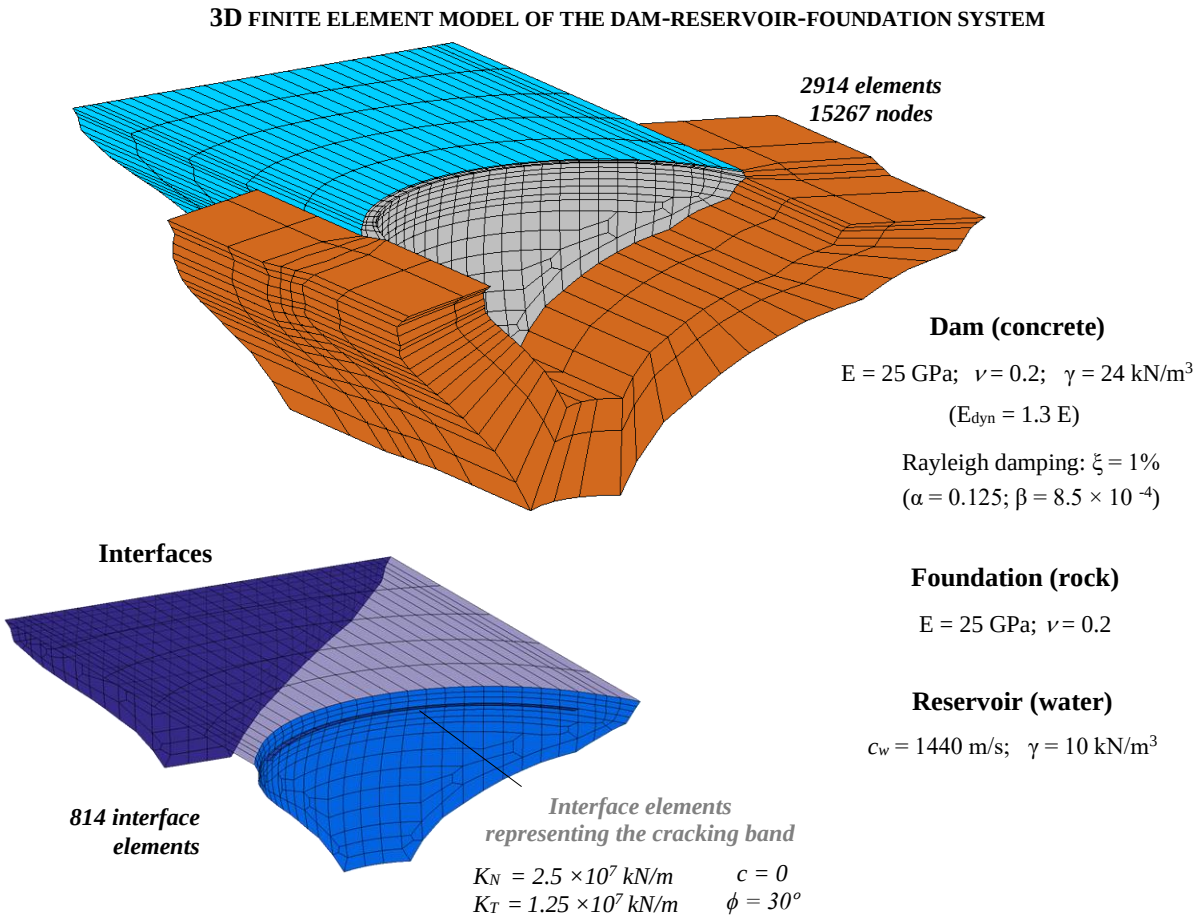

Fig. 5.6 Cabril dam. 3D finite element model of the dam-reservoir-foundation system and material properties

The comparison between the identified natural frequencies over time (coloured circles) and the calculated frequency values (coloured lines) is presented in Fig. 5.7. The computed frequencies and mode shapes for two reservoir water levels (el. 293.5 m and 285 m) are also shown for comparison with the experimental modal configurations. An additional graphical representation, where the natural frequencies are displayed according to the reservoir level, is provided in Fig. 5.8. The finite element dynamic calculations were carried out using the described linear reference model, considering various realistic water level values as input in order to define the reservoir mesh.

This comparative study shows that it was possible to achieve a very good agreement between identified and computed frequencies for all first five modes of Cabril dam, especially for higher water levels. For mode 1, a good comparison is also obtained for lower water levels, since it has an antisymmetric mode shape, with motion of null (or low) amplitude in the central section, which does not appear to be particularly affected by the intake tower. The same can be said of mode 3, which, despite being symmetric, is a mode that presents dynamic movements of higher amplitude in lateral sections of the dam, apparently reducing the influence of dam-tower interaction and resulting in a good agreement also for lower reservoir levels. Regarding mode 2, a symmetric mode with oscillatory motion of higher amplitude in the central upper part of the dam, the agreement is not as good for lower water levels due to the influence of the dam-tower dynamic interaction and to the tower added mass effect. Nevertheless, even for the second mode, the differences between identified and computed frequencies are never greater than 0.15 Hz. Concerning modes 4 and 5, despite the good comparison between experimental and numerical frequency values, there seems to be a swap in the mode shapes: the fourth mode is the symmetric one, with a modal configuration associated with the movements of the dam body above the cracked zone, and the fifth mode is a regular antisymmetric mode, while in the finite element calculations the contrary was obtained. This might be related to the interaction of the dam with the intake tower, which is not simulated in the model.

The conducted study, based on the combined use of numerical results and of experimental results obtained in normal operating conditions, was valuable to increase knowledge on the dynamic behaviour of Cabril dam under ambient/operational and to evaluate the influence of the intake tower in the modal parameters. Furthermore, the provided results allowed to show how the dynamic response of the dam-reservoir-foundation system and thus the evolution of the natural frequencies is mostly dependent on the reservoir water level variations.

The good agreement achieved between monitoring and modelling results enabled to demonstrate the suitability of the developed reference linear model for simulating the dynamic response of the dam-reservoir-foundation system of Cabril dam. However, additional studies must be conducted in the future to better understand the phenomena associated with the intake tower behaviour and the dam-tower dynamic interaction, ideally using a finite element mesh that incorporates the intake tower.

CABRIL DAM: IDENTIFIED FREQUENCIES OVER TIME VS COMPUTED FREQUENCIES

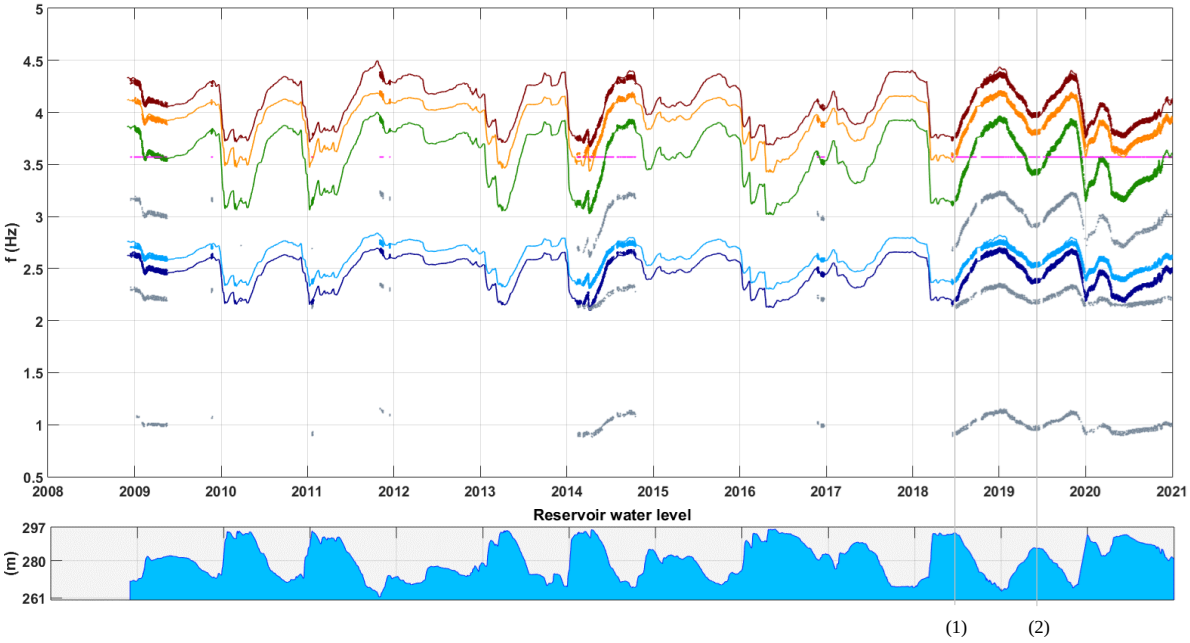

Modal analysis results considering the reservoir water level at el. 293.5 m (1)

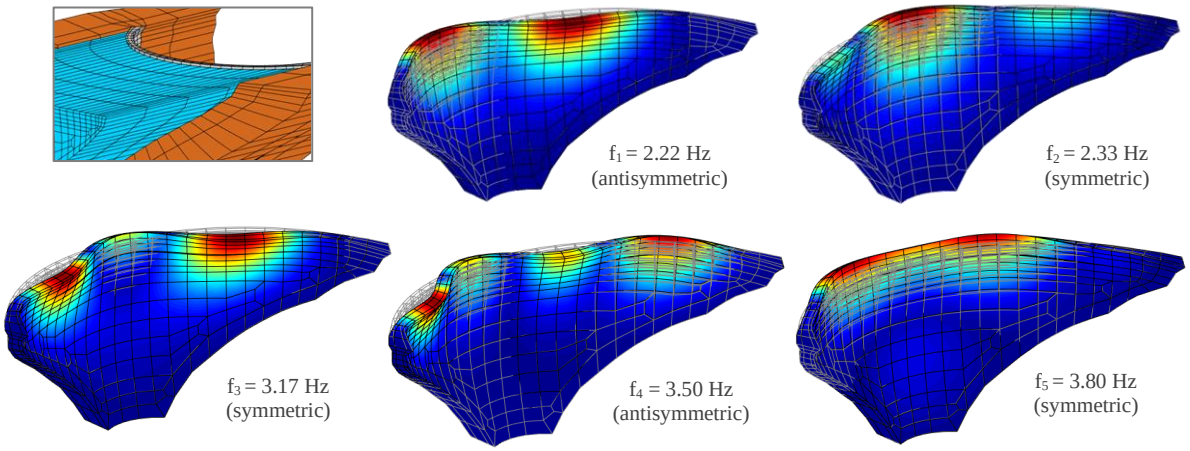

Modal analysis results considering the reservoir water level at el. 285 m (2)

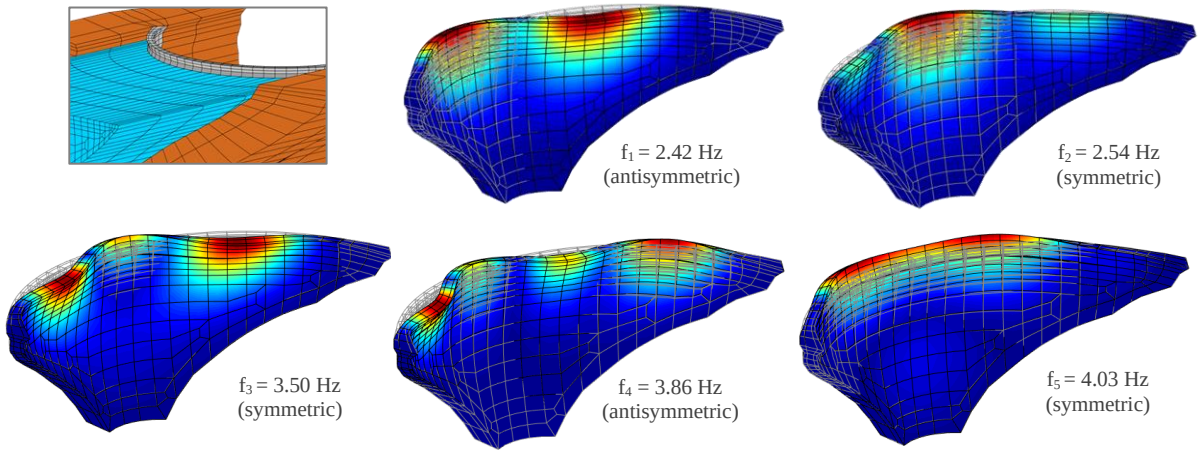

Fig. 5.7 Comparison between identified natural frequencies over time and computed frequencies for Cabril dam. Finite element modal analysis: mode shapes for two reservoir water levels.

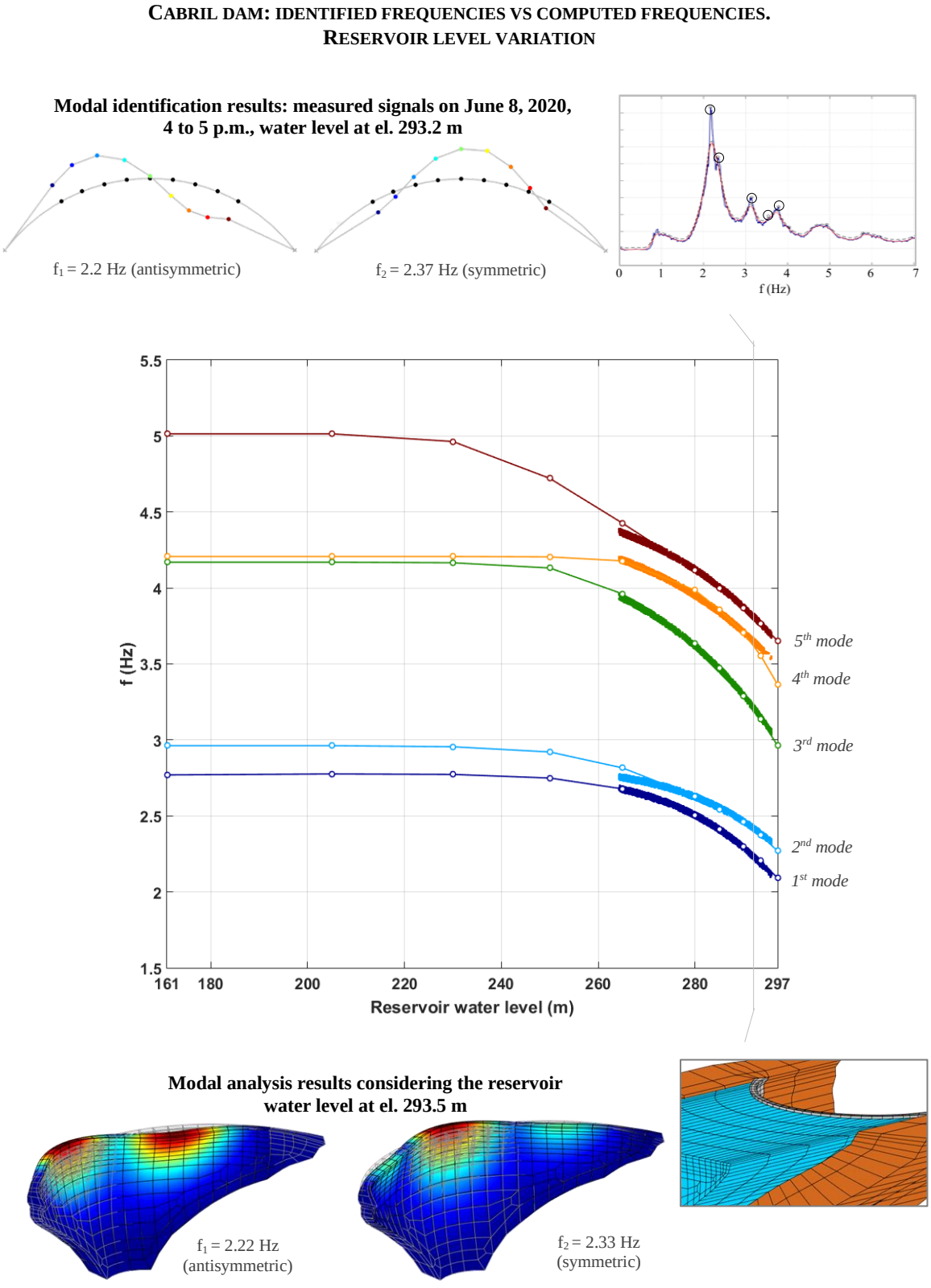

Fig. 5.8 Comparison between identified and computed natural frequencies for Cabril dam considering the reservoir water level variations.

DAMAGE DETECTION USING MEASURED VIBRATIONS AND FINITE ELEMENT RESULTS

For structural health monitoring, the natural frequencies identified based on recent data can be compared with those identified in a previous reference period or computed using reference linear models, calibrated using data from that reference period. Models that enable to simulate the process of evolutive damage can also be useful for analysing possible structural changes that occur over time.

Therefore, an additional analysis is now provided, aiming to exemplify how the combined use of results extracted from continuous vibrations monitoring and of results from finite element dynamic simulations can be of great value for evaluating structural integrity, particularly for vibration-based damage detection. With that goal, the automatically identified natural frequencies over time (in red) are compared with calculated frequencies for the first, second, and third vibration modes of Cabril dam, as well as for the mode associated with the movement of the dam body above the cracked zone (Fig. 5.9 and Fig. 5.10). In this analysis, the numerical frequency curves (in blue) are computed using: (i) a linear reference model without concrete damage, with properties calibrated using data from the early monitoring period; and (ii) a model to simulate a scenario of evolutive damage over time, assuming a gradual decrease in concrete stiffness - this is modelled in a simplified way, considering a gradual damage (d) increase from 0 to 5% over the period under analysis and a uniform deterioration over the whole dam body, with the Young's modulus of concrete becoming $E_d(t) = E \cdot (1 - d(t))$.

Based on these results, the most important observations to be made in the scope of structural health monitoring are that the frequency values extracted from recent monitoring data are equivalent to those obtained for the initial monitoring period, in late 2008 and early 2009, and that there is a good agreement between identified and computed frequencies with the linear reference model (the differences between the experimental and numerical values do not change over the ongoing monitoring period, for similar reservoir levels). Besides, the model that simulates the scenario of evolutive damage shows how the numerical frequency values start to decrease gradually, and, from a certain point, to diverge from the experimental frequencies, for all analysed vibration modes; the predicted response with this model suggests that the effects of a considerable deterioration phenomenon can be detected based on information extracted from measured vibrations.

Therefore, it is possible to state that the main modal parameters of Cabril dam have not changed over the last decade, which means that the existing cracking and swelling phenomena have not progressed significantly and hence are not affecting the structural integrity of the dam nor disturbing its regular operation in a noticeable way. Nevertheless, it is fundamental to continue performing this type of analysis on a regular basis in the future, in order to properly control the structural integrity of Cabril dam, which has been in operation for almost 70 years.

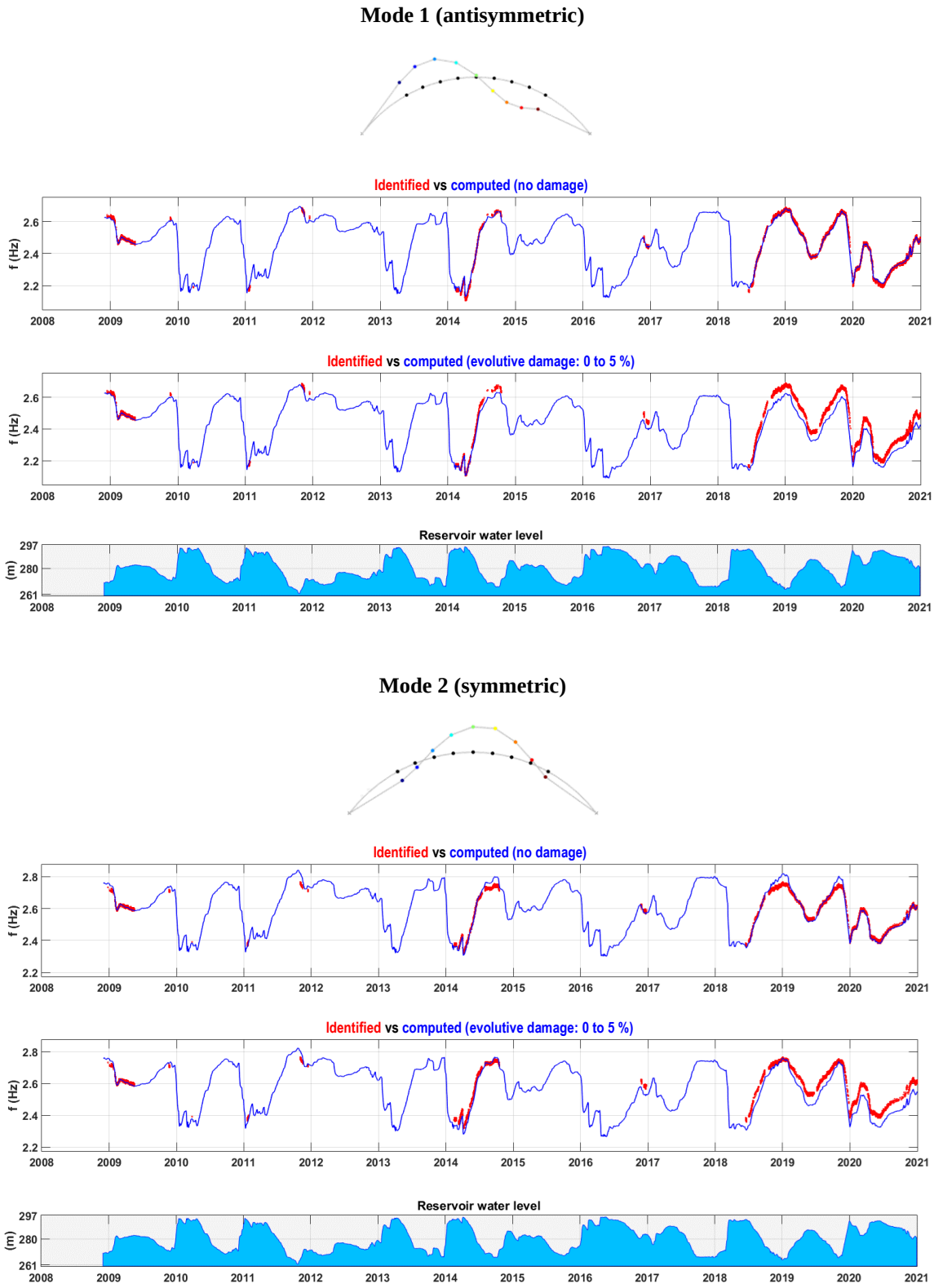

Fig. 5.9 Analysis of natural frequencies for vibration-based damage detection of Cabril dam. Evolution of identified frequencies over time (2008 to 2020) and comparison with computed frequencies using the reference model (no damage) and a model considering evolutive damage (0 to 5 %). First and second modes.

CABRIL DAM: COMPARISON FOR VIBRATION-BASED DAMAGE DETECTION

Mode 3 (symmetric)

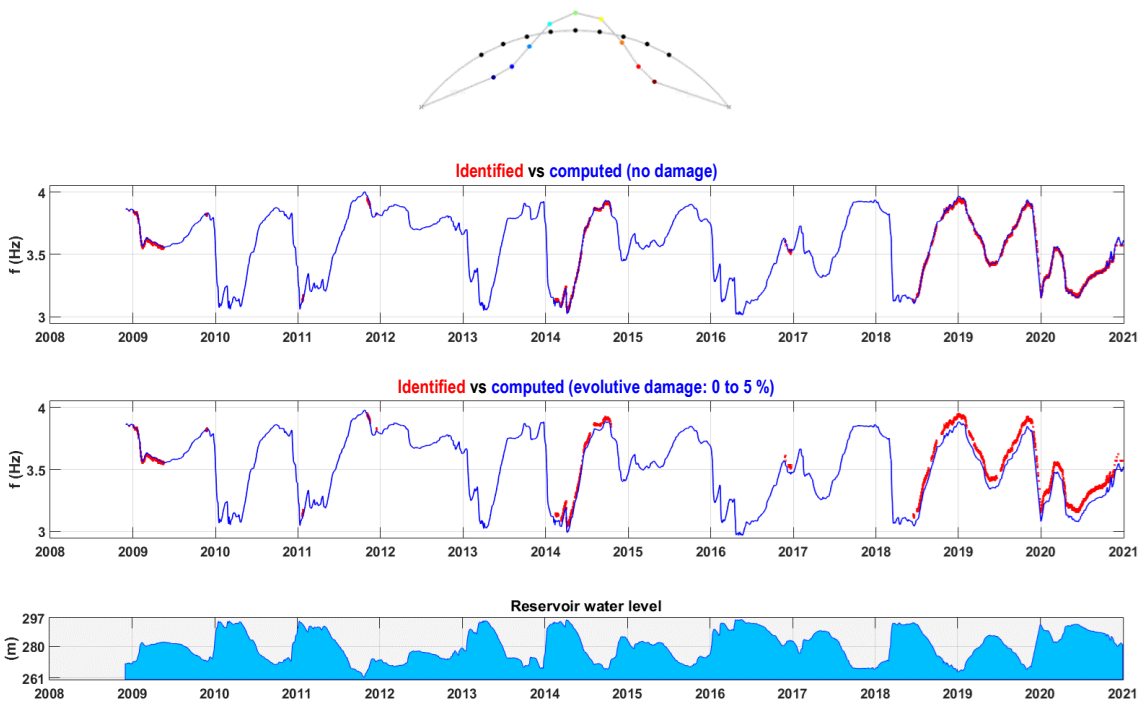

Mode influenced by movement above the horizontal cracks

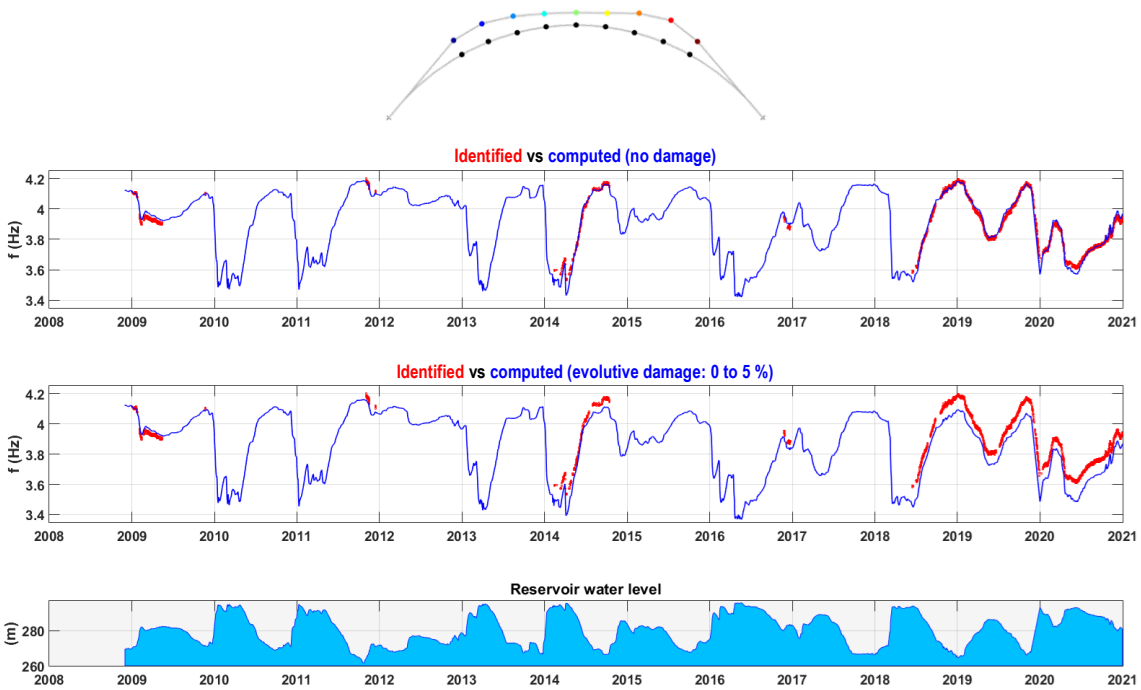

Fig. 5.10 Analysis of natural frequencies for vibration-based damage detection of Cabril dam. Evolution of identified frequencies over time (2008 to 2020) and comparison with computed frequencies using the reference model (no damage) and a model considering evolutive damage (0 to 5 %). Third mode and mode associated with the movement of the dam above the cracked zone.

5.2.3 LINEAR SEISMIC RESPONSE: MEASURED AND COMPUTED ACCELERATIONS

The measured dynamic response of Cabril dam during a real seismic event is analysed in this section. The analysis is performed based on the accelerations recorded with the SSHM system of Cabril dam near the dam-rock interface and in various points at the upper part of the dam body, which are compared with results from finite element analysis. The numerical calculations were carried out using the program *DamDySSA*, developed in this thesis, and the program *Code_Aster*, an open-source software developed by EDF (www.code_aster.org), to provide a comparison between the results of two different modelling programs and the experimental results from dam monitoring.

The purpose of this application study is to evaluate the amplification of the measured accelerations between the dam-rock interface and the crest of the dam (central section), and to discuss the use of adequate input accelerograms and damping ratios in the numerical models, in order to properly reproduce the measured dynamic response under low amplitude seismic vibrations. Therefore, it is intended to contribute not only for increasing knowledge on the seismic behaviour of Cabril dam under low to medium intensity earthquakes, but also to calibrate the linear model used for seismic response simulations.

EARTHQUAKE ON SEPTEMBER 4, 2018. MEASURED ACCELERATIONS

The seismic event detected in Cabril dam on September 4, 2018, was due to an earthquake of magnitude 4.6 that occurred in the Peniche abyssal region, off the coast of Portugal, at about 200 km from the dam site (Fig. 5.11). The seismic waves hit the dam from the west-northwest, approximately in the cross-valley direction. At the time, the water level was at el. 281.2 m, 15.8 m below the crest. This was a distant earthquake that induced low amplitude vibrations in Cabril dam, with peak values of 3.6 mg at the crest, which were recorded with great accuracy by the installed SSHM system (Fig. 5.12 and Fig. 5.13).

EARTHQUAKE (4.6 M) ON SEPTEMBER 4, 2018. DISTANCE: 206 km FROM CABRIL DAM

Fig. 5.11 Seismic event (4.6M) on September 4, 2018, automatically recorded and detected at Cabril dam.

The seismic accelerations measured with the triaxial sensor RB_{xyz} installed at the right bank near the dam-rock interface, at el. 274 m, are shown in Fig. 5.12. The recorded peak accelerations are 1.48 mg in the cross-valley direction, 1.31 mg in the upstream-downstream direction, and 1.3 mg in the vertical direction.

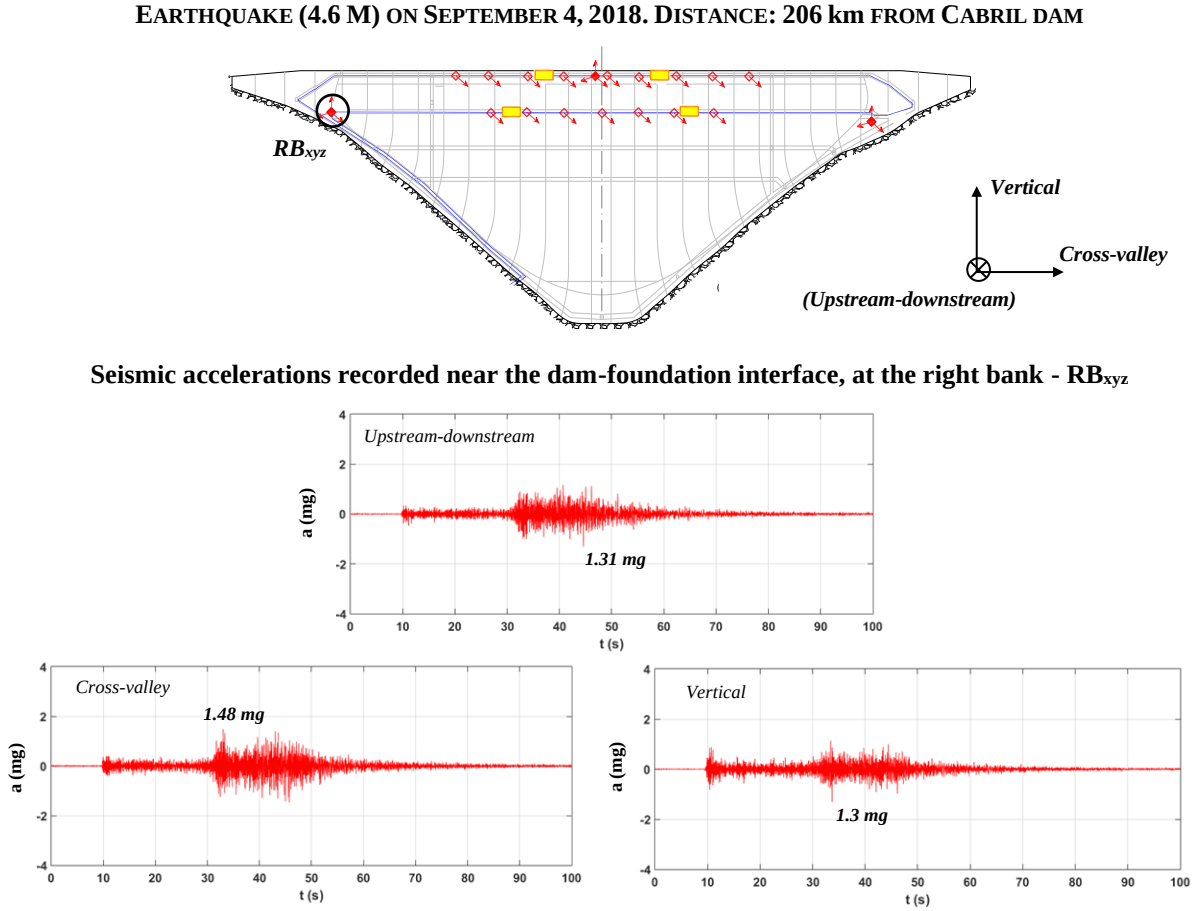

Fig. 5.12 Seismic event (4.6M) on September 4, 2018. Measured accelerations at the dam-rock interface with the triaxial sensor at the right bank RB_{xyz}.

In this application study the aim is to analyse the measured response in various positions of the dam, both in the upper gallery, at el. 294 m, and in the second lower gallery, at el. 275 m, which will then be compared with the numerical results. Fig. 5.13 presents the acceleration time histories recorded using: (i) the triaxial accelerometer $KL294_{xyz}$, located in the central section of the dam (block KL), in the upper gallery; (ii) the uniaxial accelerometers *NO294* and *QR294*, positioned in the left part of the dam (blocks NO and QR), also in the upper gallery; and (iii) the uniaxial accelerometer *KL275*, installed in the central section (block KL), in the second gallery. For this earthquake, the maximum acceleration, 3.62 mg, was recorded with sensor $KL294_{xyz}$ in the upstream-downstream direction. Compared to the peak acceleration near the abutment in the same direction (1.31 mg), the amplification factor is approximately 2.8 from the dam-rock interface to the top of the central section of the dam. Considering the maximum accelerations recorded in the radial direction with sensors *NO294* and *QR294*, amplification factors of 2.1 and 2.5 are obtained, respectively, in relation the upstream-downstream acceleration. The presented acceleration records show that the vibrations of greater amplitude were recorded in the upper part of the dam, as expected.

EARTHQUAKE (4.6 M) ON SEPTEMBER 4, 2018. DISTANCE: 206 km FROM CABRIL DAM

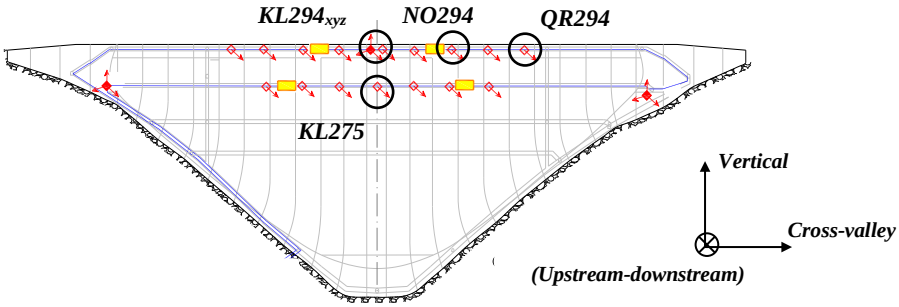

Seismic accelerations measured at the upper gallery, central section- KL294$_{xyz}$

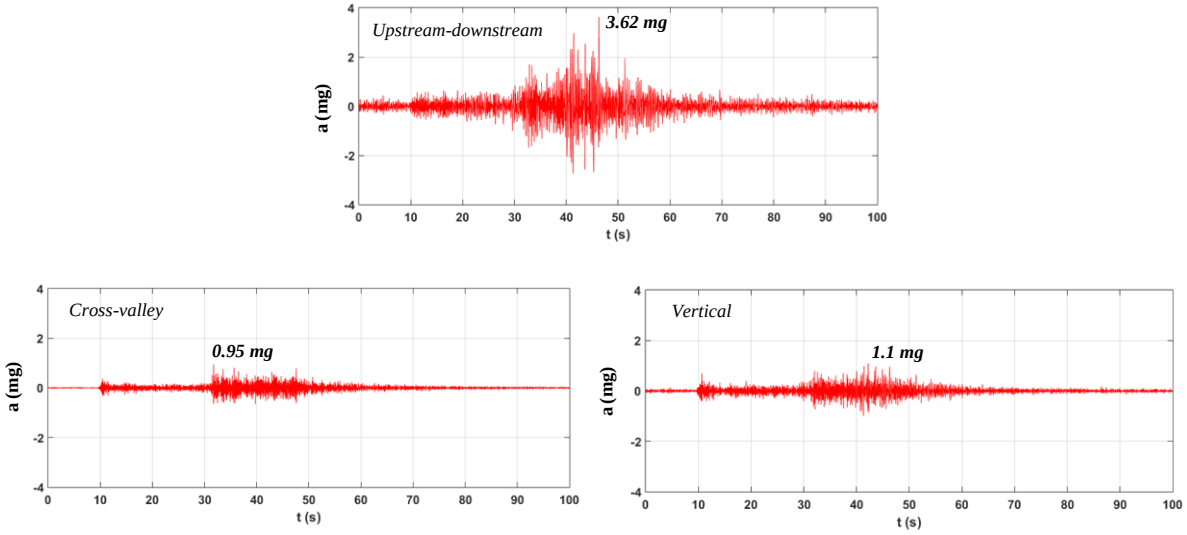

Seismic accelerations measured at the upper gallery, left part of the dam – NO294 and QR294

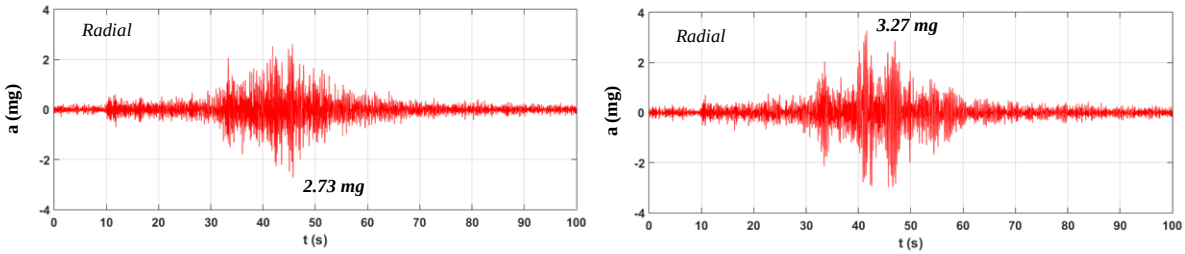

Seismic accelerations measured at the lower gallery, central section – KL275

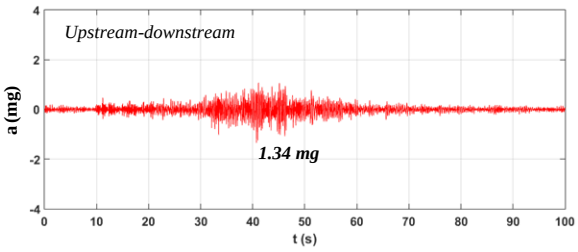

Fig. 5.13 Seismic event (4.6M) on September 4, 2018. Measured accelerations at the upper part of the dam, in the upper and lower gallery.

This analysis allowed to show not only the capability of the SSHM system installed in Cabril dam to measure vibrations induced by seismic events with great accuracy, even low amplitude vibrations due to earthquakes that occur at a long distance from the dam site, but also the value that these records can have in order to characterize the seismic action and to analyse the measured dynamic response.

FINITE ELEMENT SEISMIC ANALYSIS USING DAMDYSSA. COMPARISON WITH MEASURED RESPONSE

In order to reproduce the measured seismic response, finite element calculations were carried out using the module of *DamDySSA* for linear seismic analysis. The reference model of the dam-reservoir-foundation system used previously for modal analysis was adopted here, considering the same material properties for the dam concrete and foundation and the described horizontal crack to simulate the cracked zone (recall Fig. 5.6). Considering the low amplitude of the recorded seismic accelerations, linear behaviour is assumed for the concrete and the horizontal crack.

Aiming to consider realistic conditions in the numerical simulation of the measured response, the seismic analysis was performed by setting the model reservoir level to 17 m below the crest, at el. 280 m, as close as possible to the observed water level on the day of the seismic event (Fig. 5.14). Furthermore, the seismic accelerograms recorded with RB_{xyz} at the right bank, are used as seismic input. In *DamDySSA*, which is based on the massless approach to simulate the foundation, the seismic input is applied at the foundation base without spatial variation.

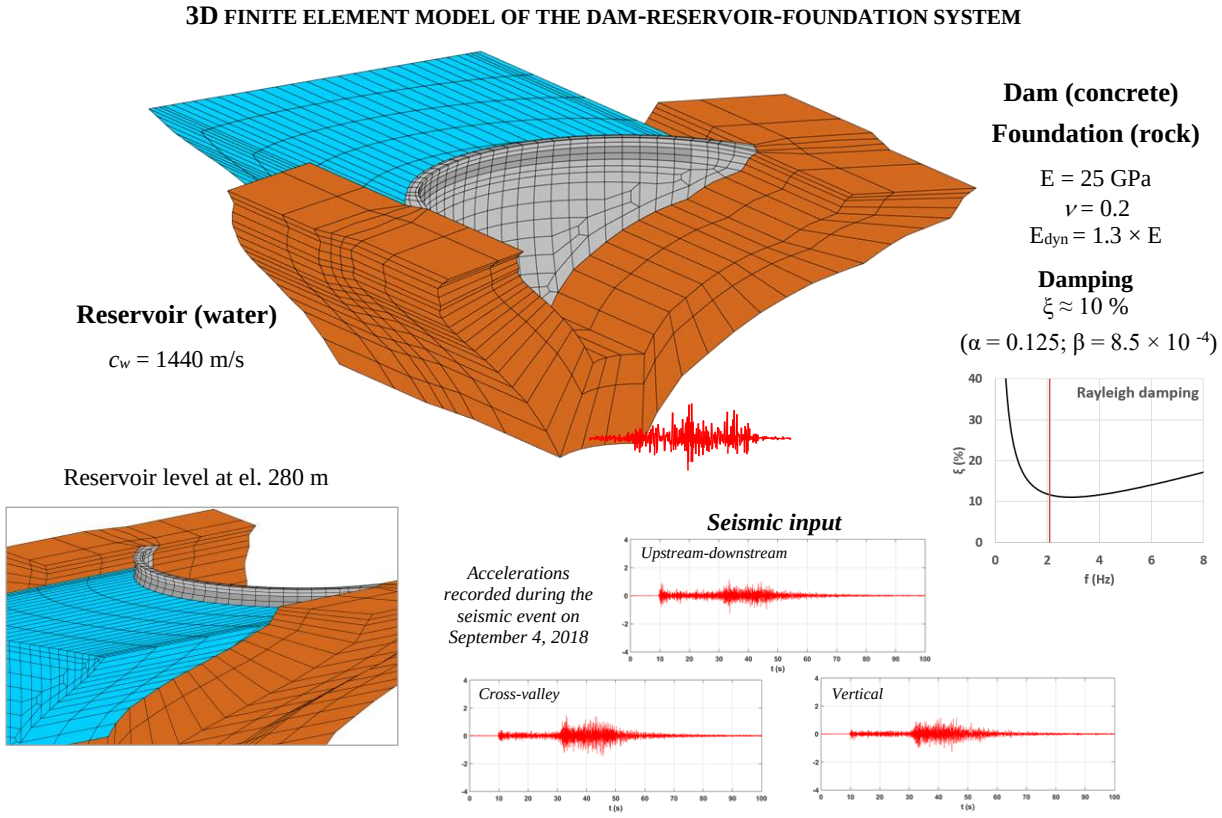

Fig. 5.14 Cabril dam. 3D finite element model of the dam-reservoir-foundation system used for linear seismic analysis and used seismic input.

For comparison with the measured computed response, the acceleration time histories were calculated in nodal points of the dam mesh equivalent to the real positions of accelerometers *KL294*$_{xyz}$, *NO294*, *QR294*, and *KL275*, as presented next.

In the case of the triaxial accelerometer *KL294*$_{xyz}$, located in the central section of the upper gallery, there is a good agreement with the numerical accelerations in the upstream-downstream direction, while in the cross-valley and vertical directions the numerical response is overestimated (Fig. 5.15). In what concerns accelerometers *NO294* and *QR294*, positioned in the left part of the dam, also in the upper gallery, it was possible to reproduce the accelerations in the radial direction quite well (Fig. 5.16). A good comparison was also achieved for the accelerograms calculated in the position of accelerometer *KL275*, installed in the central section of the second lower gallery (Fig. 5.17).

Overall, the provided results show that it was possible to reach a good agreement between the measured accelerations in Cabril dam during the seismic event on September 4, 2018, and the seismic accelerations calculated using *DamDySSA*, considering as uniform seismic input the available seismic accelerograms, i.e., those recorded near the base of the right abutment. However, in order to reproduce the measured response in Cabril dam, it was necessary to consider a damping ratio of about 10% for the frequency band around 2 to 3 Hz (frequency values of the first modes of the dam-reservoir-foundation system).

It is recognised that it would be more appropriate to use accelerations recorded at the bottom of the valley, near the dam-rock interface, as seismic input. In that case, the same good agreement would be expected when assuming a significantly lower damping value. The use of lower damping values, around 1%, has been successfully used in studies carried out for simulating the response of several large arch dams (Chopra & Wang, 2012; Proulx et al., 2004; Proulx & Darbre, 2008; Robbe, 2017; Robbe et al., 2017), in which seismic accelerograms measured at the dam base are used as inputs. This can also be observed in the application example conducted in this work for the case of Cahora Bassa dam (see section 5.3).

The analysis of the measured accelerations in Cabril dam during a low intensity seismic event and the comparison with the computed response enable some general remarks to be made, namely that additional studies are required in the future. With that purpose, it is recommended the installation of an additional triaxial accelerometer in the SSHM system of Cabril dam, more specifically at the downstream base of the dam, with a view to improve the characterization of the seismic action and to better understand the linear seismic behaviour. Moreover, it is important to recall that the dam-tower dynamic interaction can also influence the response of the dam under earthquake motion, particularly for lower reservoir water levels, and thus additional analyses should be performed in the future to evaluate the seismic response using a complete tower-dam-reservoir-foundation model.

Finally, it is worth mentioning that the numerical calculations were carried out using decimated versions of the recorded accelerograms, considering a decrease in the sampling frequency from 1000 Hz (time step $\Delta t = 0.001$) to 100 Hz ($\Delta t = 0.01$). With the program *DamDySSA*, considering the presented 3D mesh of the dam-reservoir-foundation system and the seismic input with a 0.01 s time step, the calculations took about 1 hour for every 10 seconds on a laptop with a CPU processing speed of 2.2 GHz.

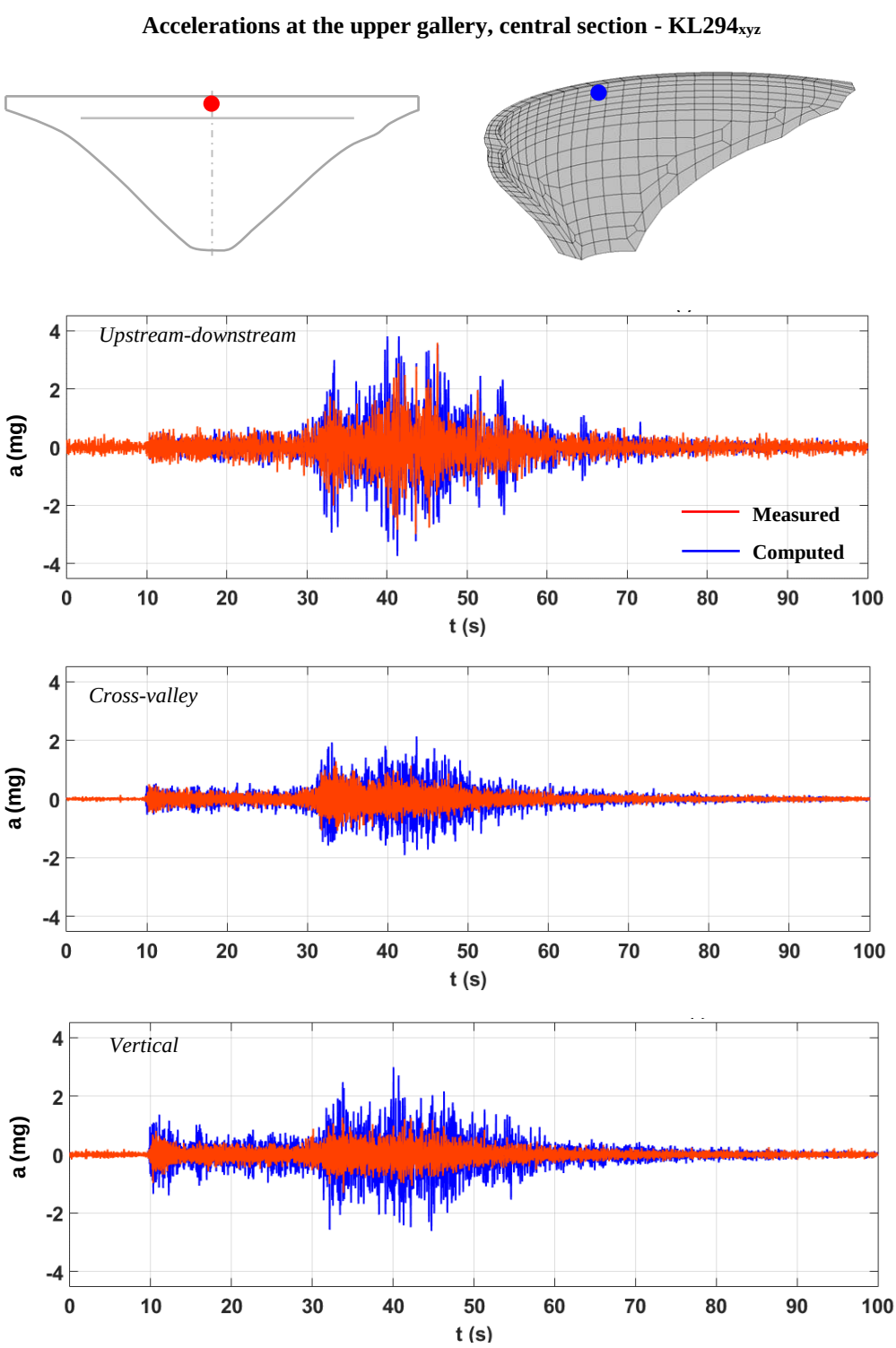

Fig. 5.15 Seismic response of Cabril dam: seismic event (4.6M) on September 4, 2018. Comparison between measured and computed accelerations - upper gallery, central section.

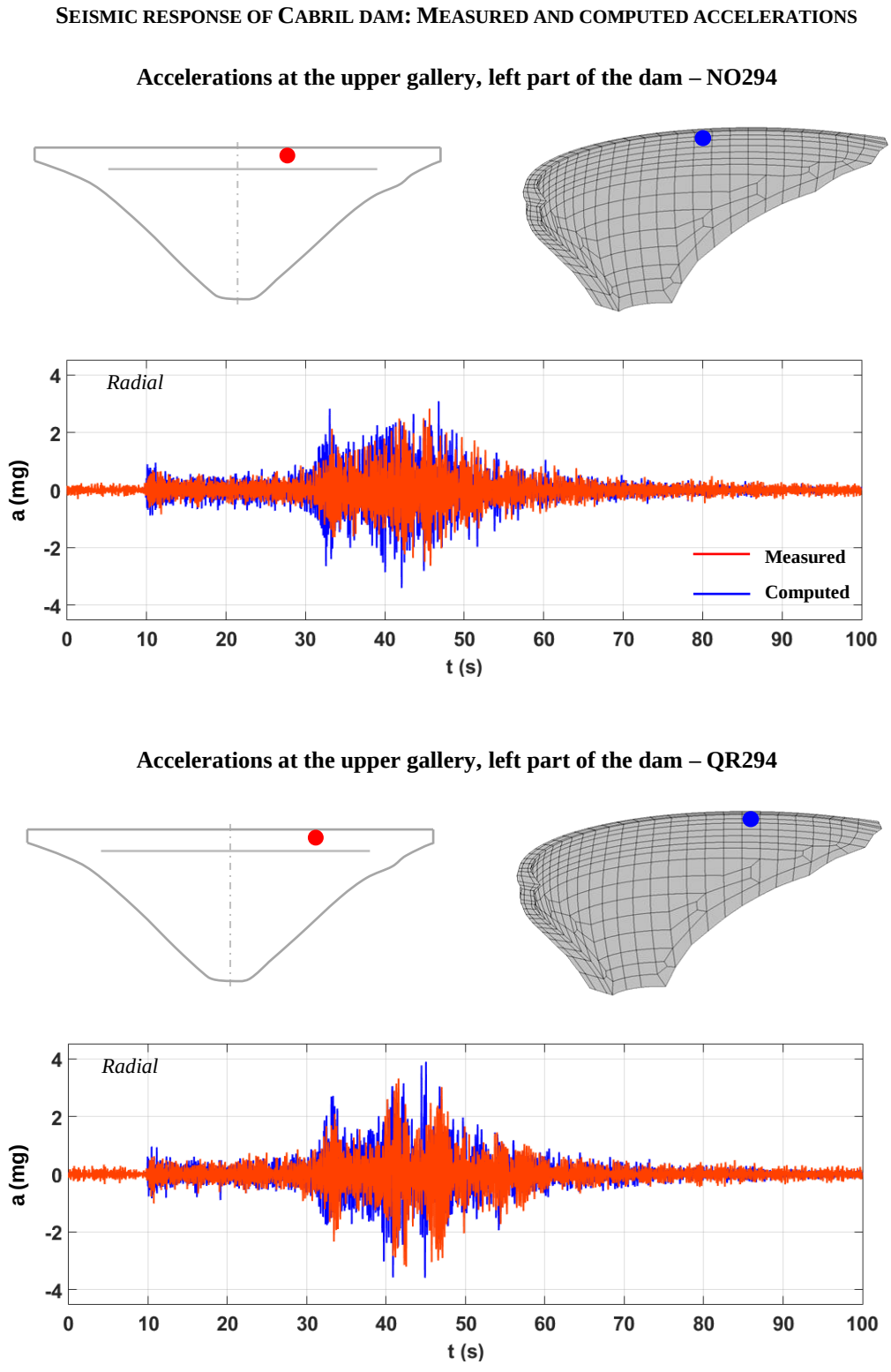

Fig. 5.16 Seismic response of Cabril dam: seismic event (4.6M) on September 4, 2018. Comparison between measured and computed accelerations - upper gallery, left part of the dam.

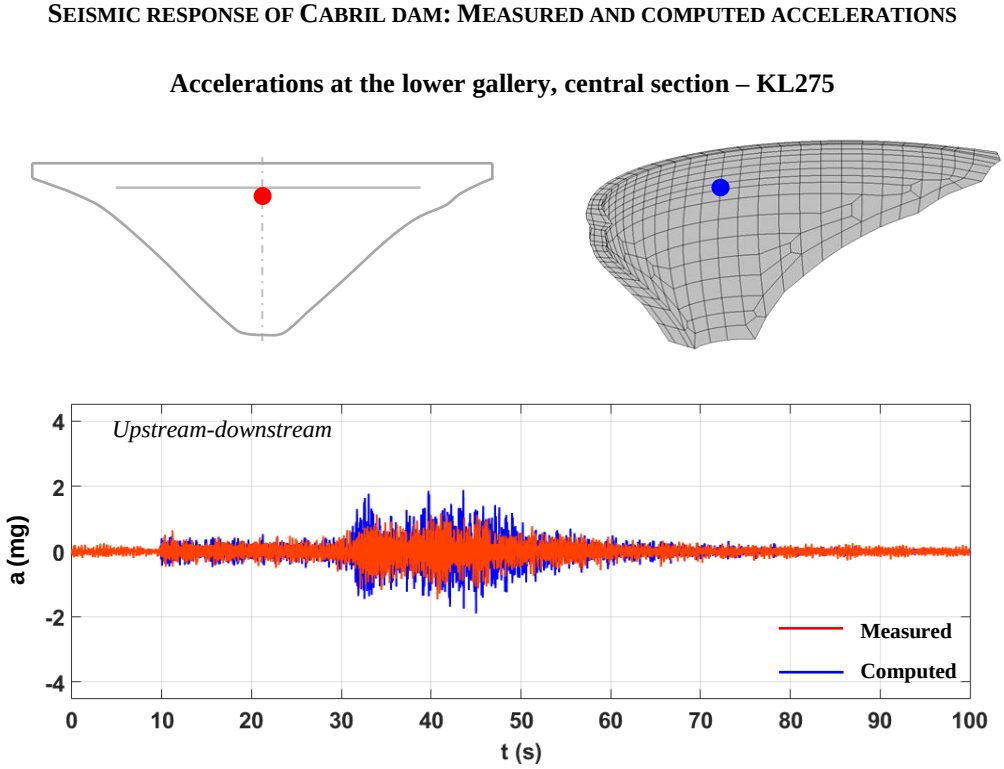

Fig. 5.17 Seismic response of Cabril dam: seismic event (4.6M) on September 4, 2018. Comparison between measured and computed accelerations - second gallery, central section.

COMPARISON WITH FINITE ELEMENT RESULTS FROM *CODE_ASTER*

A linear seismic calculation of Cabril dam was also performed using the open-source software *Code_Aster*, developed by EDF, in the scope of a study conducted in collaboration with Emmanuel Robbe[10] (Alegre, Robbe, et al., 2020). In this study, the results computed using *DamDySSA* are compared with results from *Code_Aster*, and both are compared with the measured seismic response, aiming to evaluate the suitability of the programs for linear seismic analysis of arch dams.

Code_Aster has been used to conduct various studies on the seismic response of large concrete dams, based on measured and computed accelerations (Robbe, 2017; Robbe et al., 2017), which have provided aluable information on the subject. In *Code_Aster*, the dynamic behaviour of the dam-reservoir-foundation system is simulated using potential-based fluid elements for the reservoir domain. Specific boundary conditions are established to account not only for the radiation at the far end of the reservoir domain and for fluid-structure interaction between the dam and the reservoir, but also for the rock-water interaction between the reservoir and the foundation. Furthermore, a viscous-spring boundary model (Fig. 5.18) is implemented for simulating the foundation behaviour and interaction effects, as proposed and well-described in (Robbe, 2017; Robbe et al., 2017). This model is adopted to account for the absorption of the wave energy radiation

[10] Emmanuel Robbe is a Specialist Dam Engineer at EDF, France, responsible for the safety evaluation of dams in operation and for developing numerical models.

from the dam and the foundation mass, while the seismic input is introduced as compression and shear waves vertically propagating from the bottom of the foundation block to the dam-rock interface.

The finite element calculation with *Code_Aster* was carried out using a 3D model of the dam-reservoir-foundation system; the dam mesh is the same as the one used in *DamDySSA*, while new meshes were generated for the foundation and reservoir (Fig. 5.18). The same values as before are used for the dam and foundation material elastic properties and the reservoir water level is also set to el. 280 m. In *Code_Aster*, the seismic input was introduced at the bottom of the massed foundation and subsequently calibrated in order to reproduce the accelerations recorded with triaxial accelerometer RB_{xyz} at the dam-rock interface of the right bank. Therefore, as in the calculations performed with *DamDySSA*, realistic accelerations are considered at the proper location of the model used in *Code_Aster*. To save calculation time, the simulations with this second program were performed considering a length of 50 s for the seismic accelerograms.

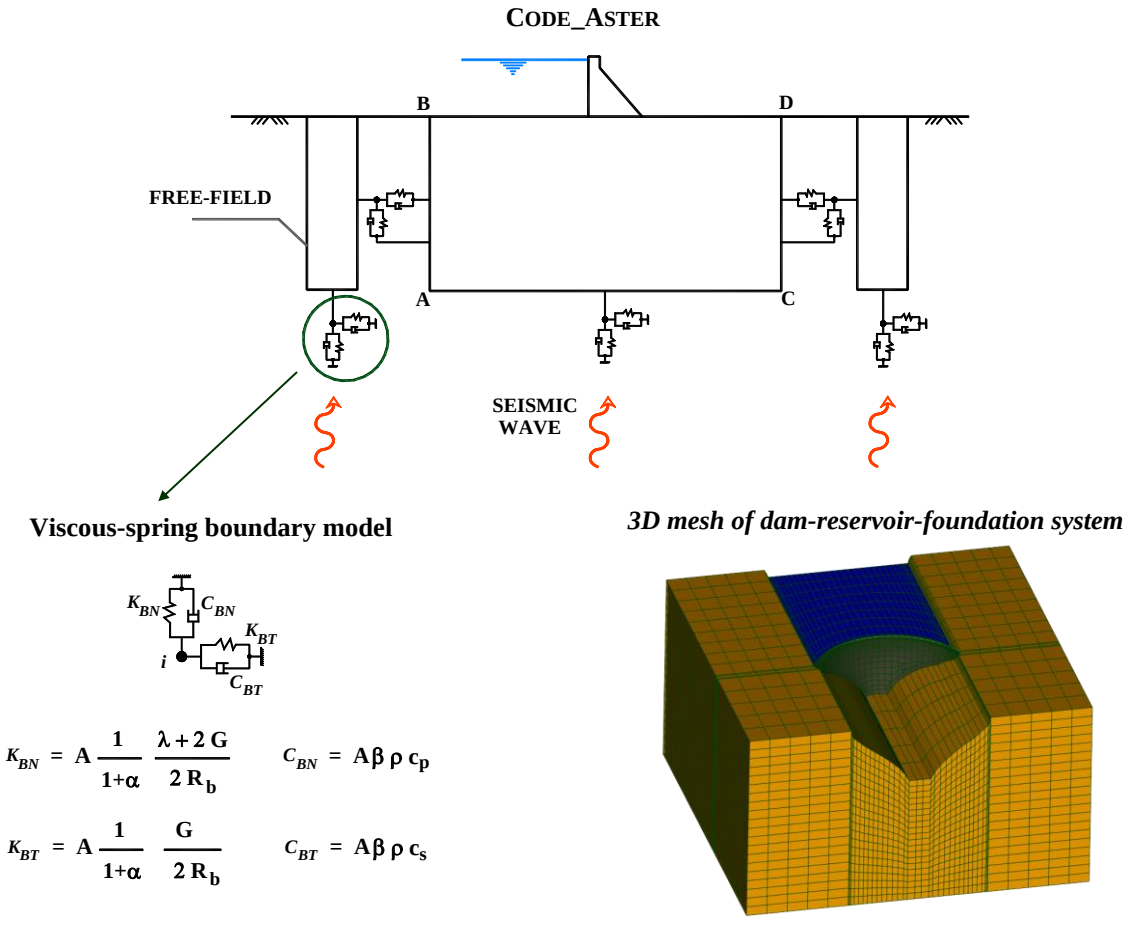

Fig. 5.18 *Code_Aster*: scheme of dam-reservoir-foundation system with viscous-spring boundary model for the foundation, and new 3D model of Cabril dam-reservoir-foundation system.

The comparison between the accelerations calculated using the programs *DamDySSA* and *Code_Aster*, and the radial acceleration time histories recorded during the earthquake event on September 4, 2018, is presented next (Alegre, Robbe, et al., 2020), namely for accelerometer $KL294_{xyz}$ (Fig. 5.19) and for accelerometers *NO294*, *QR294* and *KL275* (Fig. 5.20).

The results obtained using *Code_Aster* allow to confirm the observations made previously based on the results from *DamDySSA*: for Cabril dam, it is possible to reach a good agreement between measured accelerations and computed response, considering as input the accelerograms measured near the dam-rock interface at the right bank, but only if a higher damping ratio is used. The comparison provided in Fig. 5.19 and Fig. 5.20 allow to see that both programs, which are based on different approaches for modelling the foundation behaviour and the seismic input, lead to similar results when using a 10% damping ratio for the frequency band of the first vibration modes.

Nevertheless, it is worth noting that with *DamDySSA* it was possible to achieve a slightly better agreement between monitoring and modelling results. Therefore, this study allowed to confirm the potential of *DamDySSA* to simulate the linear seismic response of arch dams, as well as the suitability the reference model currently used for Cabril dam (even without incorporating the tower). Moreover, these new results help corroborate the conclusion that the need for high damping values to fit the computed response to the measured response might be associated with the use of input accelerations recorded at the right bank (the only that were available), hence highlighting the importance of investing in the installation of a new triaxial accelerometer at the downstream base of Cabril dam.

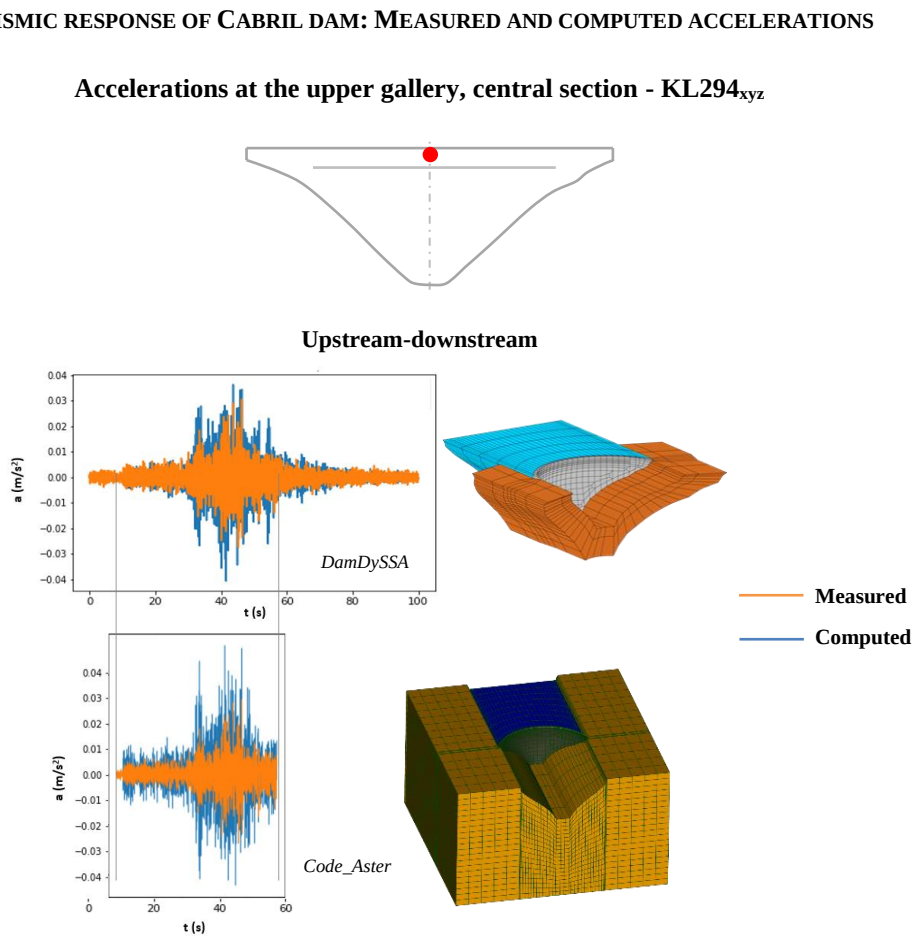

Fig. 5.19 Seismic response of Cabril dam: seismic event (4.6M) on September 4, 2018. Comparison between measured accelerations (upper gallery, central section) and numerical results from *DamDySSA* and *Code_Aster*.

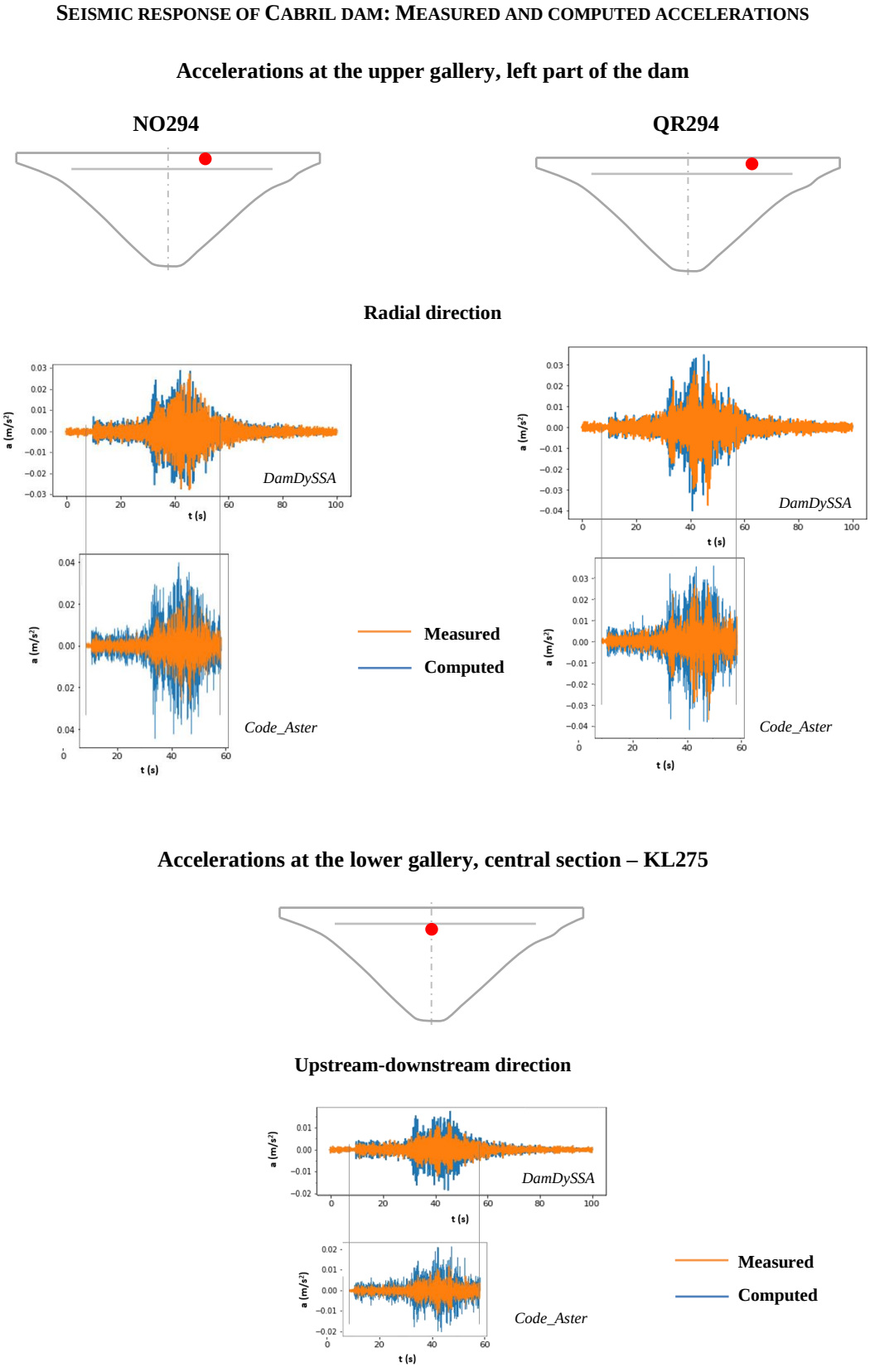

Fig. 5.20 Seismic response of Cabril dam: seismic event (4.6M) on September 4, 2018. Comparison between measured accelerations (upper gallery, left part of the dam; lower gallery, central section) and numerical results from *DamDySSA* and *Code_Aster*.

5.2.4 NON-LINEAR SEISMIC ANALYSIS CONSIDERING JOINT MOVEMENTS AND CONCRETE DAMAGE

The current section is focused on analysing the non-linear seismic behaviour of Cabril dam under strong earthquakes, considering the effects due to joint movements and the occurrence of concrete damage, based on results from numerical simulations carried out using *DamDySSA*. The presented analysis aims to investigate the influence of the opening/closing and sliding movements of the vertical contraction joints on the structural response of Cabril dam, by comparing results from linear and non-linear analyses, and to evaluate the resulting tensile and compressive damages in the dam body.

This study also intends to show the potential of the proposed method for non-linear dynamic analysis of arch dams, implemented in the program *DamDySSA*. The main results include 3D graphical representations of deformed shapes, stress fields, tensile and compressive damages in the dam body, and displacements and stresses envelopes.

The finite element calculations were performed using the 3D finite element model of the dam-reservoir-foundation system[11] shown in (Fig. 5.21). The dam concrete and foundation rock are isotropic materials, while the water in the reservoir is a compressible fluid, assuming the same properties as in the previous studies. All vertical contraction joints, the dam-rock interface, and a horizontal crack, representing the existing cracking band around el. 280 m to 285 m, are incorporated into the model, using interface elements. For non-linear analysis, a damping ratio of about 10% is considered on the frequency band around the first and second vibration modes (2 to 3 Hz).

The non-linear behaviour of concrete is simulated using the strain-softening constitutive damage law with tensile strength $f_t = 3\,\text{MPa}$ and compressive strength $f_c = -30\,\text{MPa}$ (LNEC, 2003). In order to obtain coherent stress-strain laws, which guarantee an adequate energy dissipation during material failure, a fracture energy $G_f = 0.9\,\text{kN.m}/\text{m}^2$ and an ultimate compressive strain $\varepsilon_u^- = -9.5\times10^{-3}$ are used (Alegre & Oliveira, 2019).

The opening/closing and sliding joint movements are modelled considering proper failure criteria and normal and shear stress-relative displacement laws. For the vertical contraction joints, null cohesion is assumed to enable joint opening under tensions and a 30º friction angle is used, while for the dam-rock interface joint elements with high values of cohesion and friction angle are used. Furthermore, two hypotheses are adopted for simulating the behaviour of the horizontal crack (representing the existing cracking band) under strong seismic motion, namely considering: a) a horizontal crack with higher stiffness ($K_N = 2.5\times10^7$ kN/m), in order to limit opening movements and thus allow for tensions and concrete damage to occur in that zone; and b) horizontal crack with lower stiffness ($K_N = 10^7$ kN/m) that enables opening and closing movements to occur, aiming to evaluate its influence on the global seismic response of the dam.

[11] The calculations for this study were the first to be carried out for non-linear seismic analysis of Cabril dam in this work. Thus, a coarser mesh was used to increase computational efficiency.

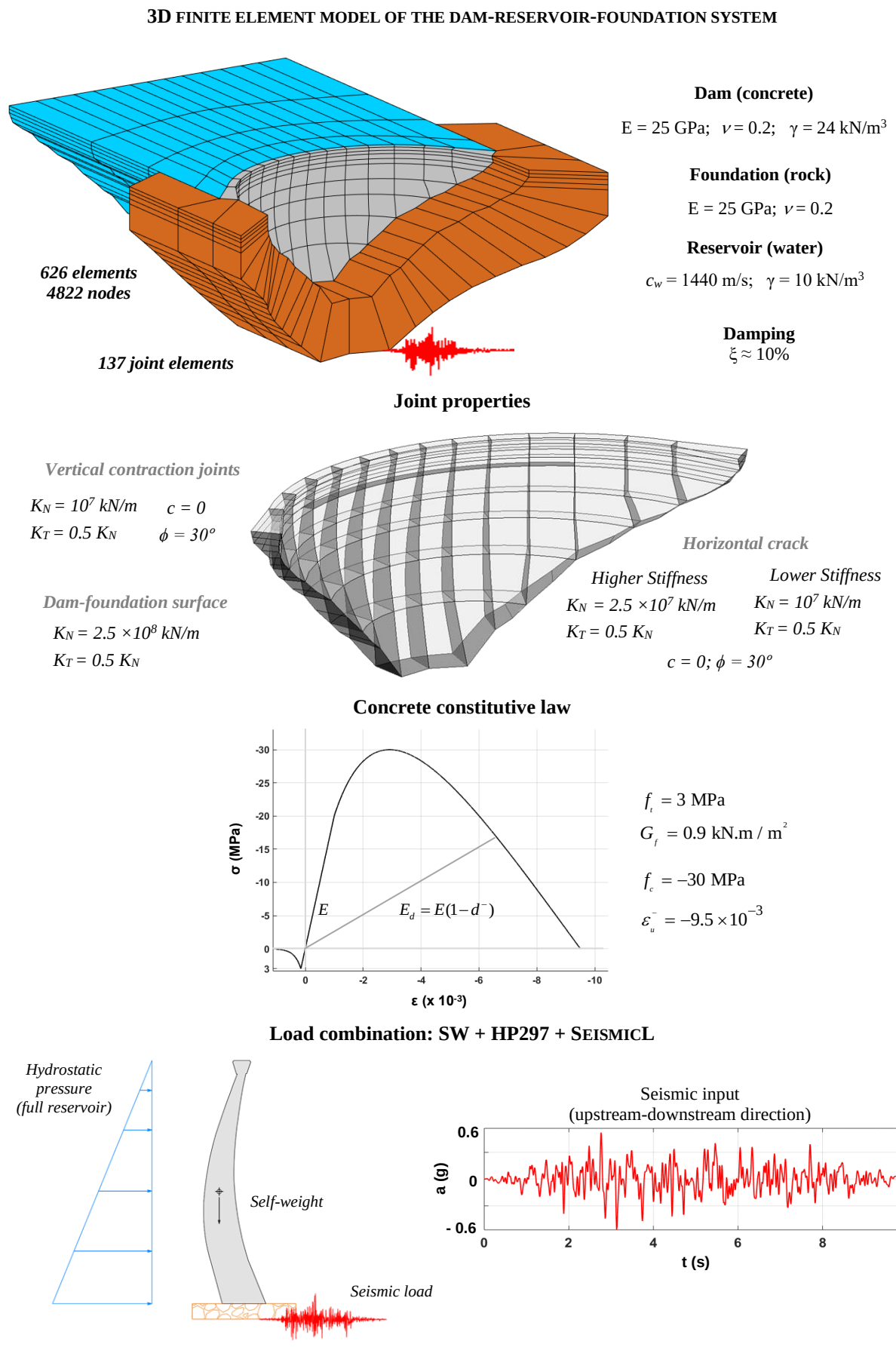

Fig. 5.21 Cabril dam. 3D finite element model of the dam-reservoir-foundation system used for non-linear seismic analysis. Material properties, joints, concrete constitutive law, load combination, and seismic input.

The seismic response of Cabril dam is analysed for the load combination including the self-weight of the dam (SW), the hydrostatic pressure for full reservoir (HP297), and a seismic load (SEISMICL) applied in the upstream-downstream direction. For this study, a 10 s artificial seismic accelerogram was generated from the response spectrum presented in Fig. 5.4, and then scaled to obtain a peak ground acceleration of 0.6g, three times greater than the excitation level assumed in this work for the MDE (0.2g).

STATIC RESPONSE: CALIBRATION OF THE CONTRACTION JOINTS STIFFNESS

The static response of Cabril dam for the load combination with the self-weight and the hydrostatic pressure (SW+HP297) is presented in Fig. 5.22, considering the use of a linear model, without joint elements, and the previous non-linear model with joints, aiming to verify the suitability of the properties assumed for the vertical contraction joints. Since tensile stresses are very low, then significant non-linearities in joints and concrete do not occur. Thus, the stress fields calculated with both models are almost equal, as intended. However, the maximum displacement calculated using the non-linear model (49.5 mm) is, as expected, slightly greater than the value computed with the linear model (44 mm). The provided results show that a good agreement was achieved between the linear and non-linear models, considering vertical joints with a normal stiffness of 2.5×10^7 kN/m.

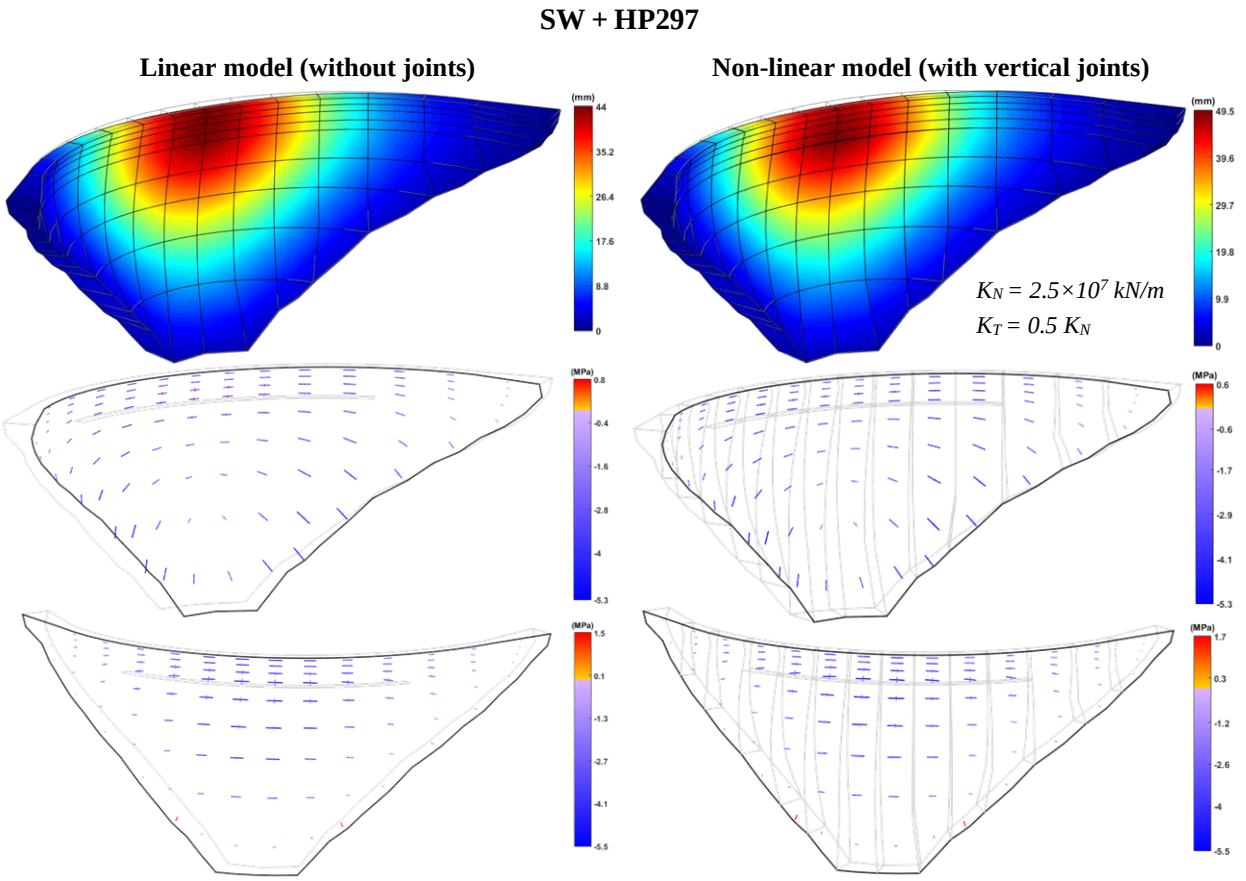

Fig. 5.22 Static response of Cabril dam for SW + HP297. Displacements and stresses calculated using a linear model without vertical joints and a non-linear model with vertical joints.

SEISMIC RESPONSE (HORIZONTAL CRACK WITH HIGHER STIFFNESS)

The seismic response of Cabril dam is analysed here for the referred dynamic load combination, considering the seismic load with a 0.6g peak ground acceleration. Results obtained using both linear and non-linear models are presented.

Starting with the linear response (Fig. 5.23), it is possible to see that the deformation of the dam is considerably influenced by the seismic motions in the upstream-downstream direction. The maximum upstream displacements are ≈ 50 mm, at the top of central section, and ≈ 60 mm, at the crest of the lateral cantilevers. The maximum downstream displacements (148.8 mm) occur at the top of the central cantilevers.

In what concerns the corresponding principal stresses fields, when the dam moves towards upstream, the higher compressions arise near the crest in the arch direction, both at the upstream face of the lateral cantilevers (- 10.3 MPa) and at the downstream surface of the central cantilevers (- 9 MPa). Important compressions also occur close to the downstream base of the lateral cantilevers (≈ - 8.7 MPa). The maximum tensile stresses are calculated in the arch direction at the top of the lateral cantilevers (6.8 MPa), at the upstream face. Considerable tensions (5.4MPa) also arise at the downstream upper part of the central cantilevers. Other relevant locations under high tensions include the upstream base of the shorter lateral cantilevers, with stresses oriented normally to the dam-rock interface (4.2 MPa), and the upper part of the downstream surface of the taller lateral cantilevers (3.5 MPa). These high tensile stresses indicate that opening/sliding movements of the vertical contraction joints and tensile damage in concrete are expected under this seismic load in the non-linear seismic simulations. At the instant of maximum downstream displacement, maximum arch compressions arise at the top of the central cantilevers (-14.8 MPa), and important compressions (- 6.3 to - 8.5 MPa) occur along the downstream face of the lateral cantilevers.

The non-linear seismic response, computed assuming the hypothesis of a horizontal crack with higher stiffness (limited opening movements), is shown in Fig. 5.24. The greater displacements at the top of the central section are now of 56.3 mm, in the upstream direction, and of 138.3 mm, in the downstream direction, values that are respectively higher and lower than those obtained in the linear analysis. The maximum displacement at the crest of the lateral cantilevers increased to 92.2 mm, where the larger joint opening movements occur (≈ 13 mm).

Regarding the non-linear stress fields, it is possible to note an overall decrease of the arch stresses due to the movements of the vertical joints, namely when the dam moves towards upstream, as well as a release of the tensions that ended up surpassing the material strength, as concrete damage occurred.

Next, to provide additional insight on the influence of the vertical joint movements on the seismic response of Cabril dam, linear and non-linear seismic response envelopes are presented.

Regarding the displacements envelopes (Fig. 5.25), the radial displacement values under the static loads are greater for the case of nonlinear behaviour, as shown previously in the linear response analysis (Fig. 5.22). The linear displacements envelope shows that the seismic motion at the top of the central section has a semi-amplitude more than two times larger than the static displacement value, both in the upstream

(91 mm) and downstream (103 mm) directions. By comparison, the non-linear response allows to see that there is an increase of the semi-amplitude towards upstream, to about 100 mm, and a decrease of the semi-amplitude towards downstream, to around 88 mm. These differences, already noted by comparing Fig. 5.23 and Fig. 5.24, are most likely due to the influence of the horizontal crack: in Cabril dam, the radial displacements at the crest level tend to increase in the upstream direction, while at the horizontal crack level they tend to increase in the opposite direction. However, the global displacement amplitude is slightly lower in the non-linear response, which might be due to the damping hypothesis considered for the interface elements used to model the contraction joints and horizontal crack (interface damping matrices proportional to the stiffness matrices are considered).

With respect to the arch and cantilever stresses envelopes (Fig. 5.25, Fig. 5.26 and Fig. 5.27), the comparison between linear and non-linear results enables to see how the vertical contraction joints non-linear behaviour influenced the structural response of Cabril dam. When the dam moves towards upstream, the opening joint movements result in an overall decrease of the compressive and tensile arch stresses at the upper part of the dam, namely at the top of the central cantilevers, where there was a reduction of the tensions from about 8 MPa (linear) to less than 3 MPa (non-linear) at the upstream face, and of around 5.5 MPa (linear) to 2.3 MPa (non-linear) at the downstream surface. Nevertheless, the release of the arch stresses originated a stress redistribution process that contributed to a global increase of the cantilever stresses, namely of tensions and compressions along the upstream surface of the lateral cantilevers, of the tensions at the upper part of the downstream face of dam, and of the maximum compressions (9.7 MPa) along the downstream base.

As mentioned before, it is worth emphasizing that the vertical and cantilever tensions end up surpassing the adopted concrete tensile strength (3 MPa) and, as a result, high tensile damage occurs near the downstream base, along the insertion, and in the upper part of the dam, at the downstream face (Fig. 5.28). Damage values of 100% are calculated in some points, indicating the locations where concrete failure has occurred. However, concrete failure is mostly superficial and does not propagate across the thickness of the cantilevers. The provided results show that the release of the arch stresses at the top of the dam prevented the occurrence of concrete damage there. Additionally, despite the significant deformations towards downstream, the maximum compressions are much lower than concrete compressive strength (30 MPa) and hence there was no compressive damage.

To summarise, this seismic analysis showed that the considered 0.6g seismic load caused dynamic motions of significant amplitude, resulting in important movements of the vertical contraction joints that clearly influenced the seismic behaviour of Cabril dam, as well as in high tensions in concrete, which lead to the occurrence of concrete failure, in particular at the upper part of the downstream face and along the upstream base, although this remained closer to the dam surface.

The conducted study demonstrated not only the suitability of the finite element model used for the Cabril dam-reservoir-foundation system, but also the potential of the program *DamDySSA* to simulate the non-linear seismic behaviour of large arch dams, considering simultaneously the effects due to joint movements and concrete damage.

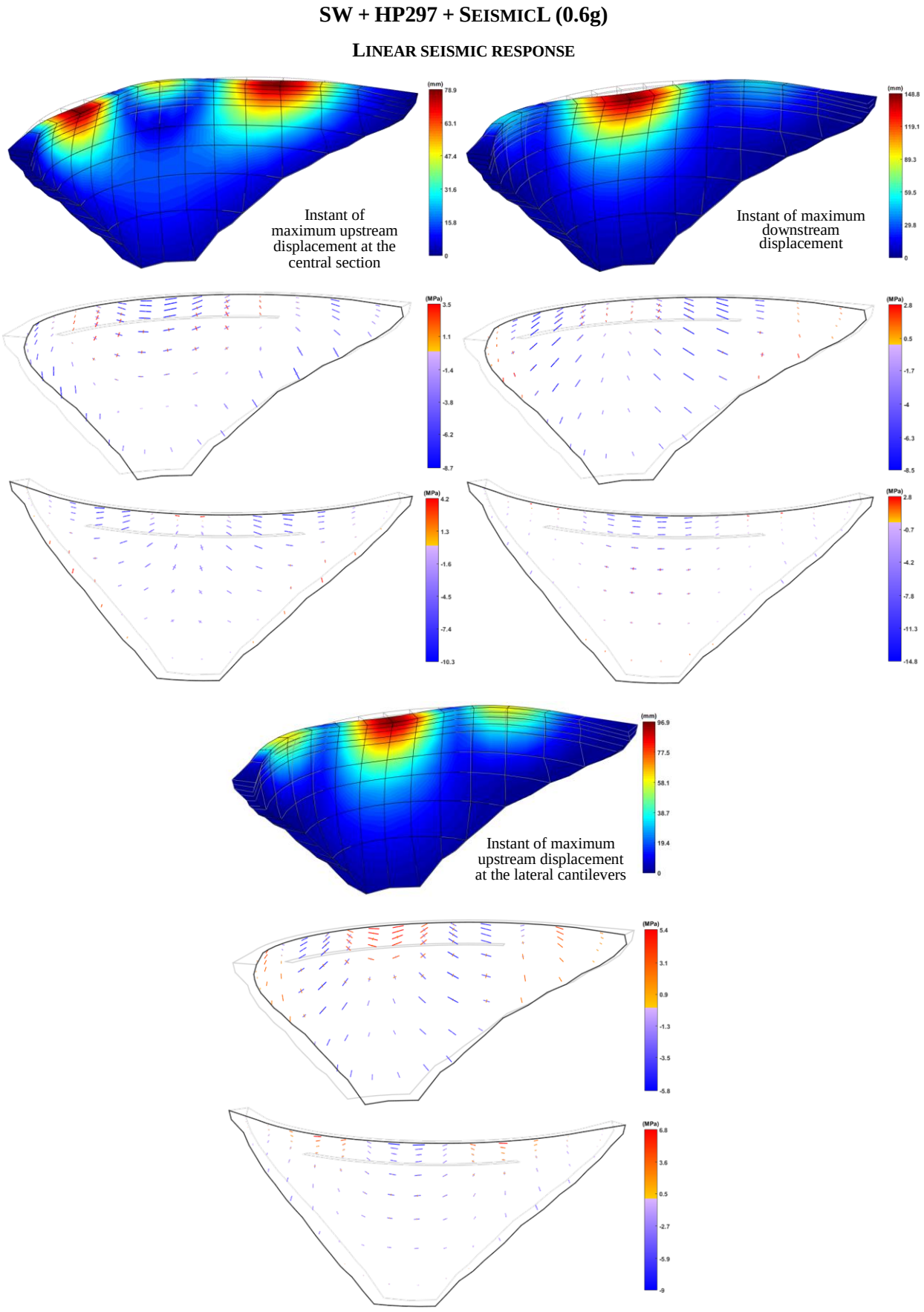

Fig. 5.23 Linear seismic response of Cabril dam for SW + HP297 + SEISMICL (0.6g). Displacements and principal stresses.

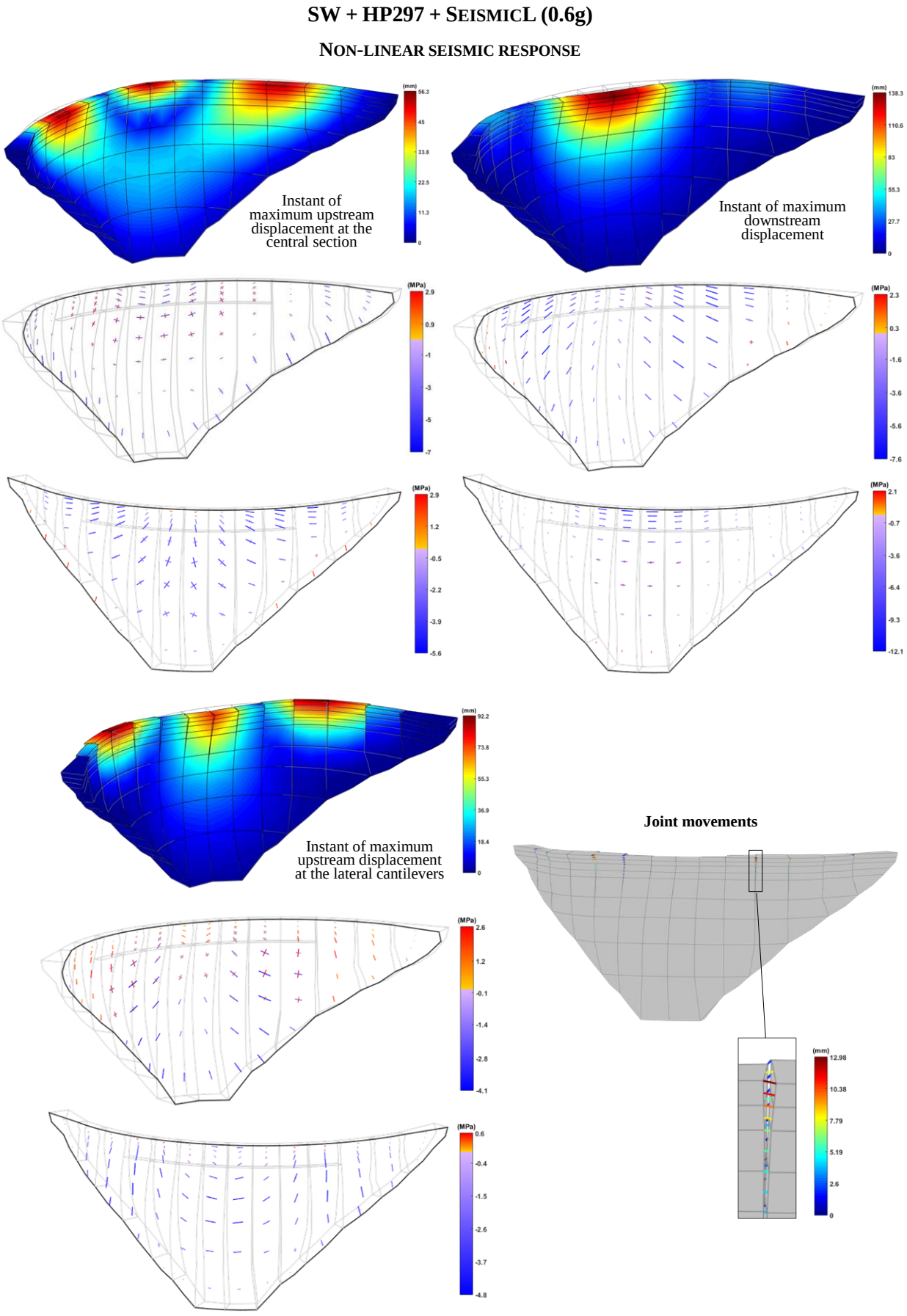

Fig. 5.24 Non-linear seismic response of Cabril dam for SW + HP297 + SEISMICL (0.6g). Horizontal crack with higher stiffness. Displacements, principal stresses, and joint movements.

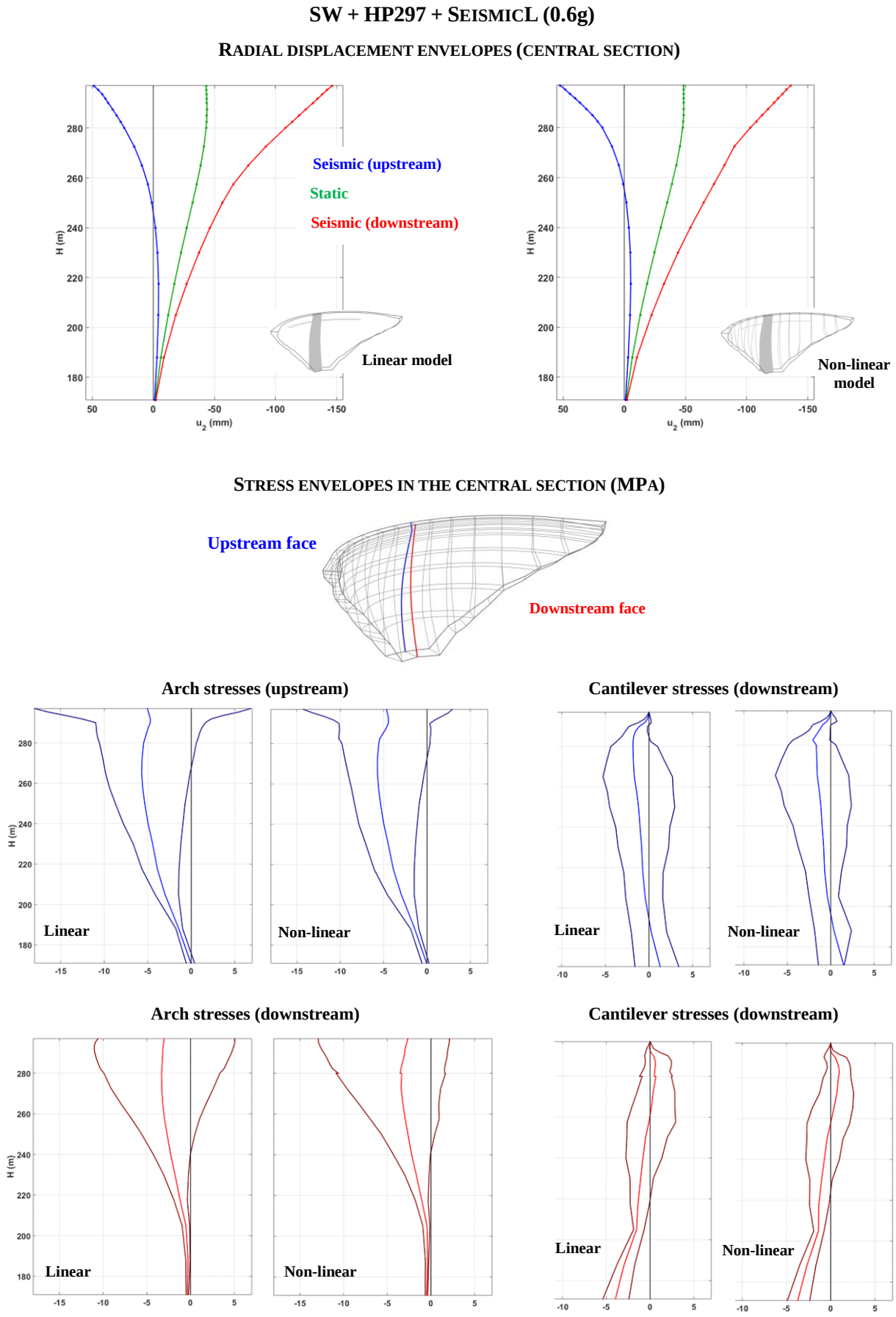

Fig. 5.25 Linear and non-linear seismic response of Cabril dam for SW + HP297 + SEISMICL (0.6g). Horizontal crack with higher stiffness. Radial displacements and arch/cantilever stresses envelopes.

SW + HP297 + SEISMICL (0.6g)

ARCH STRESSES ENVELOPES

Linear **Non-Linear**

Upstream face

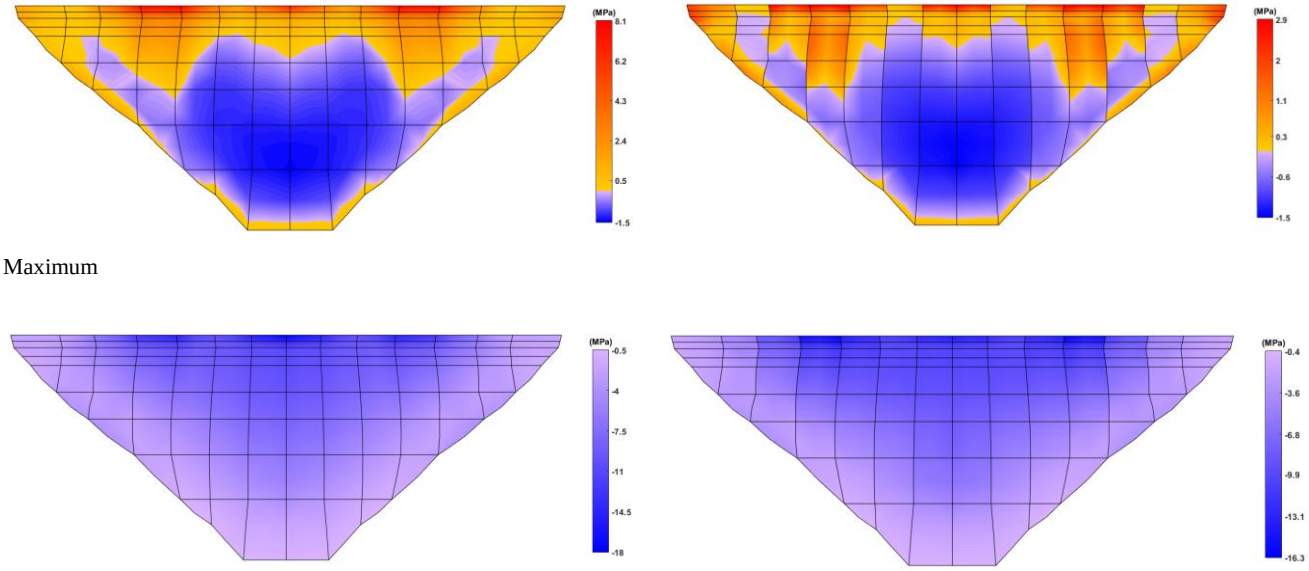

Maximum

Minimum

Downstream face

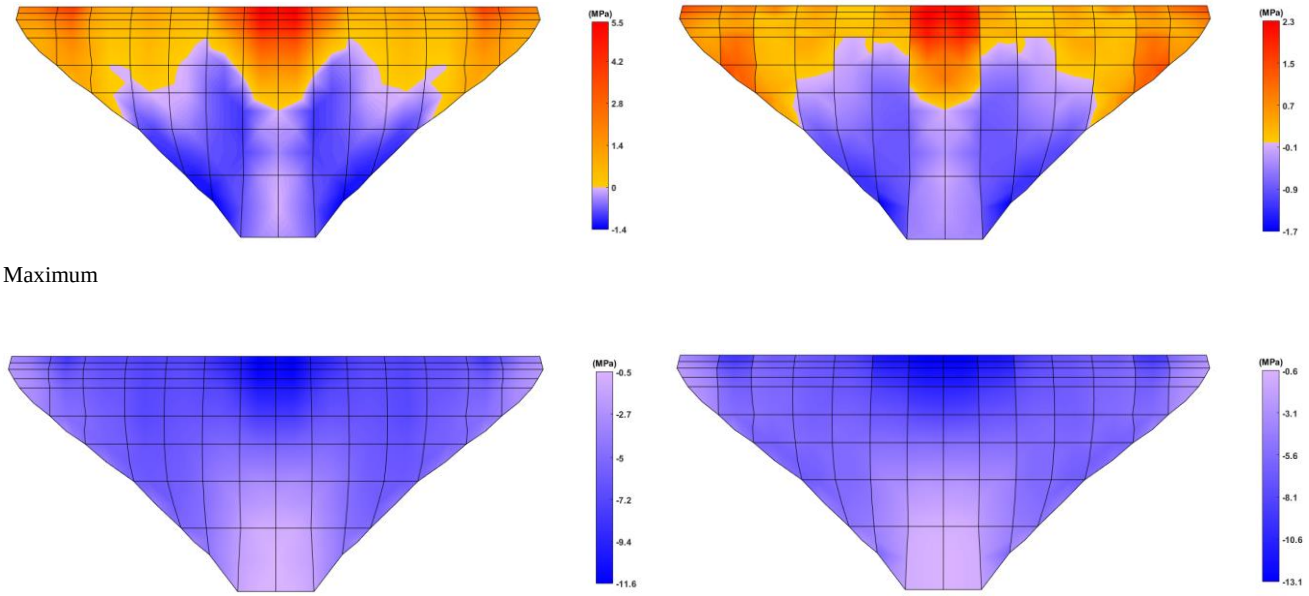

Maximum

Minimum

Fig. 5.26 Linear and non-linear seismic response of Cabril dam for SW + HP297 + SEISMICL (0.6g). Horizontal crack with higher stiffness. Arch stresses envelopes.

SW + HP297 + SEISMICL (0.6g)

CANTILEVER STRESSES ENVELOPES

Linear **Non-Linear**

Upstream face

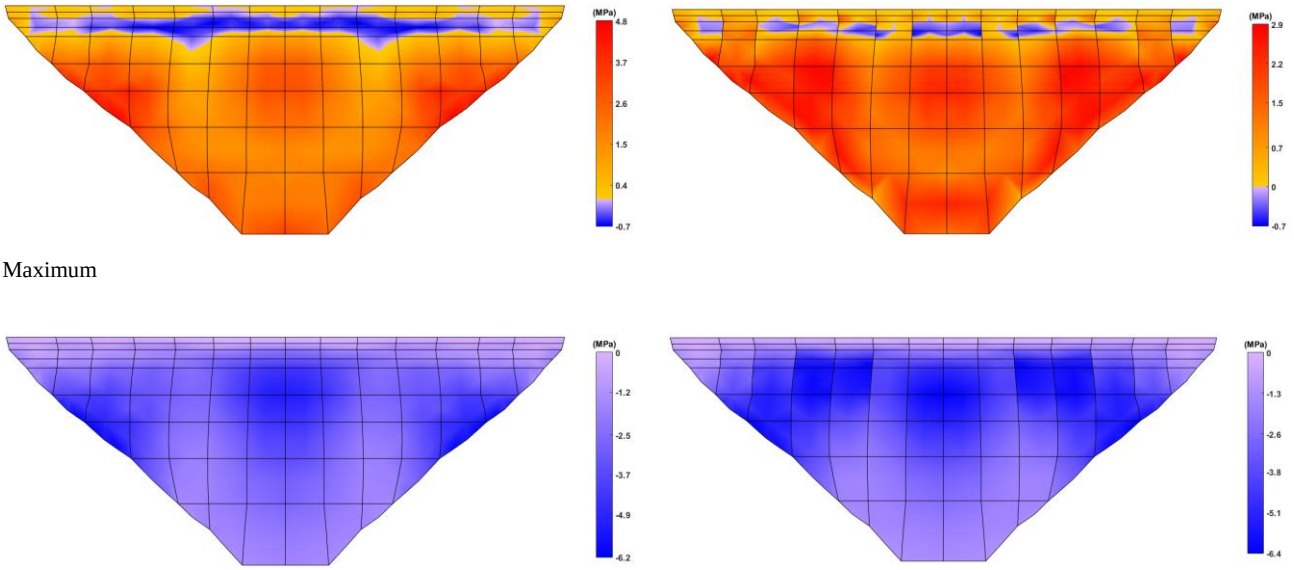

Maximum

Minimum

Downstream face

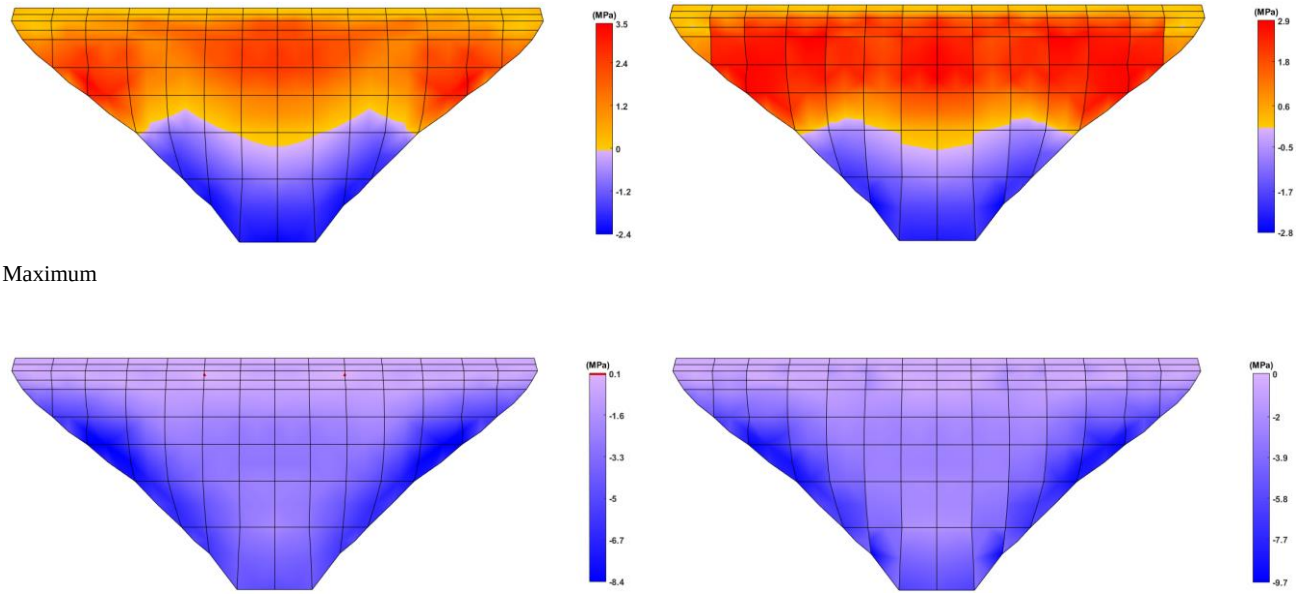

Maximum

Minimum

Fig. 5.27 Linear and non-linear seismic response of Cabril dam for SW + HP297 + SEISMICL (0.6g). Horizontal crack with higher stiffness. Cantilever stresses envelopes.

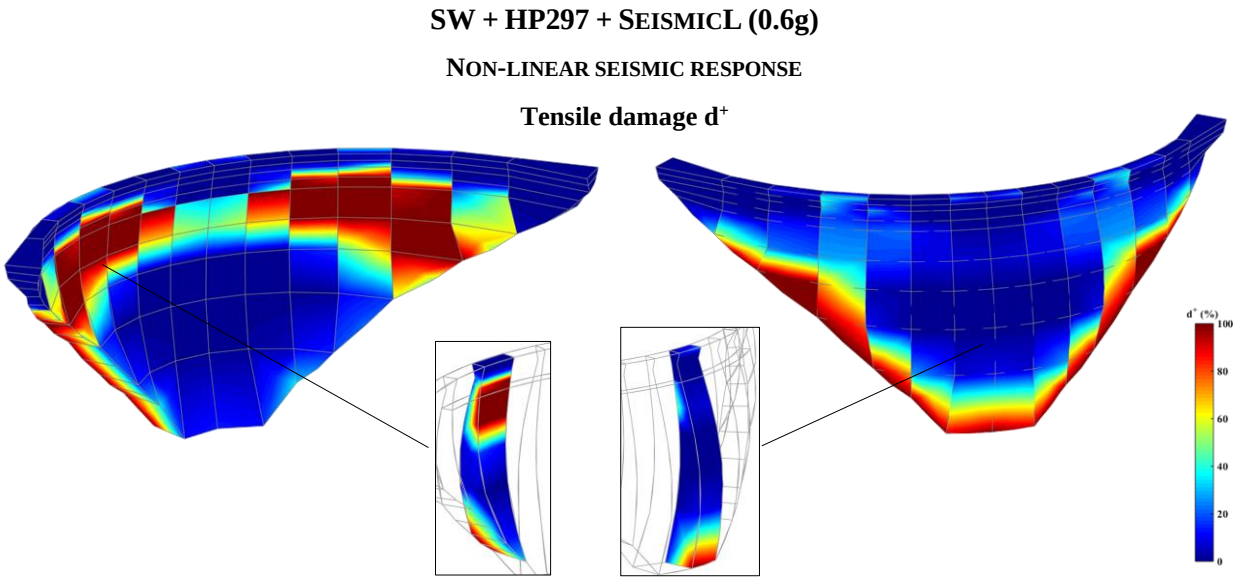

Fig. 5.28 Non-linear seismic response of Cabril dam for SW + HP297 + SEISMICL (0.6g). Horizontal crack with higher stiffness. Tensile damage.

SEISMIC RESPONSE (HORIZONTAL CRACK WITH LOWER STIFFNESS)

The existing cracking band in Cabril dam was incorporated into the model in a simplified way, considering a single horizontal crack. In the previous analysis, higher stiffness properties were adopted to limit joint movements and thus allow high tensions and concrete damage to arise in that part of the dam. However, it was also assumed worthy to simulate the case of a horizontal crack with lower normal stiffness (opening and closing movements can occur), to investigate the impact of possible movements of the cracking band in the seismic response of Cabril dam; in that case, besides concrete damage, a strong earthquake could also lead to the instability of the blocks above the cracked zone. Therefore, the non-linear seismic response, calculated considering a horizontal crack with lower stiffness values, is presented (Fig. 5.29).

In comparison with the previous analysis, there is an increase of the maximum upstream displacements in the central section, from 56.3 mm to around 60 mm, precisely when the largest horizontal crack opening occurs (≈ 8.8 mm). As for the corresponding stress fields, the most important aspect to note is the decrease of the vertical tensions in the surrounding blocks along the crack, at the downstream face, especially in the central section where the opening movements of the horizontal crack are larger (Fig. 5.29). Therefore, there is a decrease in the tensile damage distribution around that zone. However, the deformation of the blocks above the horizontal crack originates new tensile stresses, resulting in tensile damage at the upstream and especially at the downstream faces, particularly in the blocks closer the edges. When the dam moves towards downstream, the vertical contraction joints and the horizontal crack close, and thus the structural response is very similar to that presented before. These results show how the opening movements of the horizontal cracking band can influence the seismic response of Cabril dam.

Both analyses enabled to highlight the importance of properly simulating the cracked zone for evaluating the seismic behaviour of Cabril dam. To summarize, the non-linear simulations can be performed assuming a horizontal crack with high stiffness, resulting in tensile damage to arise around the crack, or a horizontal

crack with low stiffness (which can open), in which case such damages do not occur but the blocks above the crack could suffer larger overturning movements.

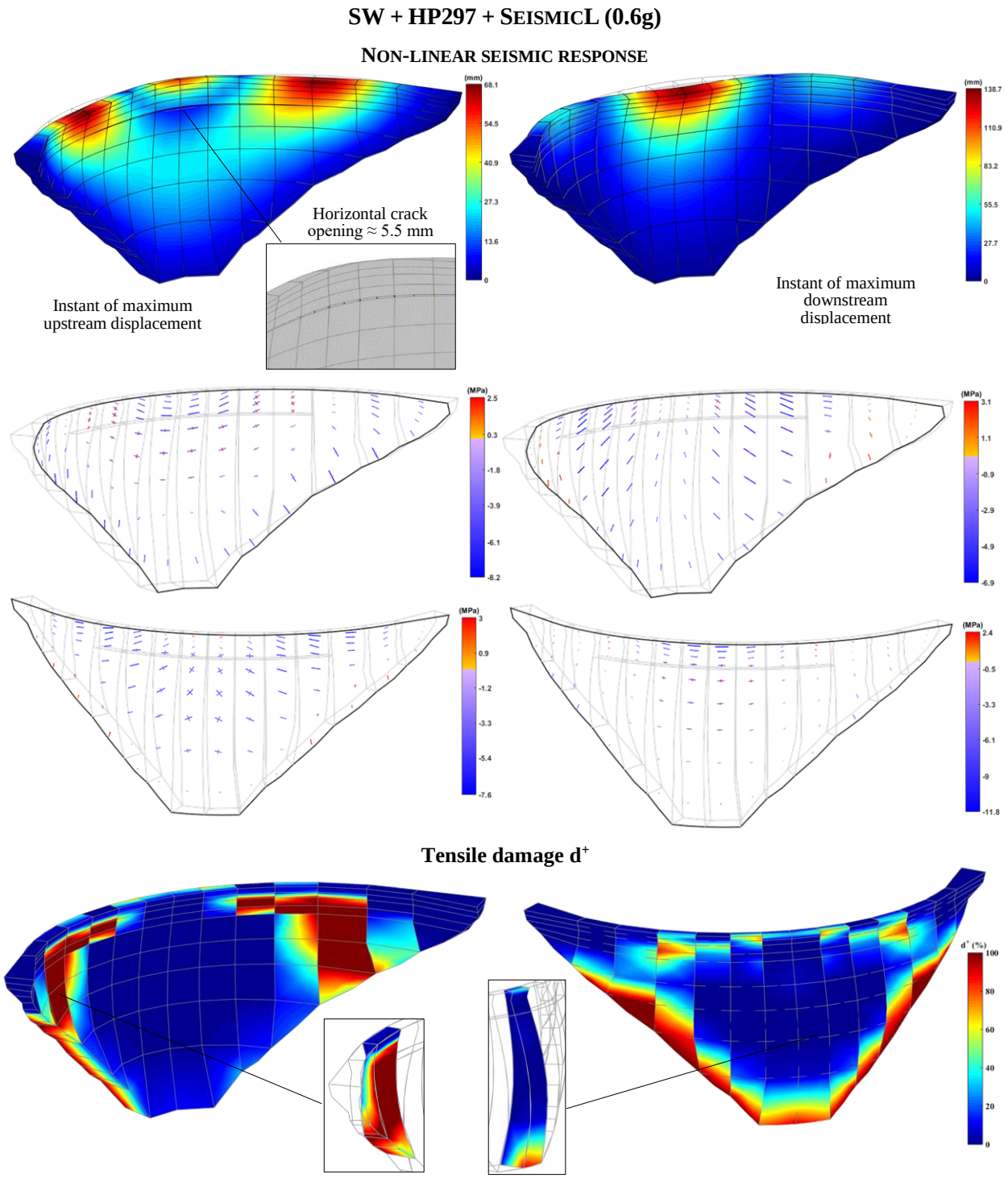

Fig. 5.29 Non-linear seismic response of Cabril dam for SW + HP297 + SEISMICL (0.6g). Horizontal crack with lower stiffness. Displacements, principal stresses, and tensile damage.

5.2.5 SEISMIC SAFETY ASSESSMENT. ENDURANCE TIME ANALYSIS

The non-linear seismic behaviour of Cabril dam is analysed in this section based on the safety assessment methodology proposed in this work (section 2.4.3), using the Endurance Time method (Estekanchi et al., 2004) and considering appropriate performance criteria (Wieland, 2016). The main goal is to evaluate the performance of the dam under an intensifying seismic load, by examining the evolution of tensile and compressive damages for increasing excitation levels. The performance endurance limits are defined as the peak accelerations that the dam can withstand until an unacceptable damage state occurs.

The finite element calculations were conducted using *DamDySSA*, considering the 3D finite element model of the dam-reservoir-foundation system presented in Fig. 5.30. This is an updated version of the reference model used for modal analysis and linear seismic analysis of Cabril dam, now taking into account the non-linear behaviour of concrete and the incorporation of all vertical contraction joints, the horizontal crack (the hypotheses of higher and lower stiffness are simulated), and the dam-foundation interface. The same constitutive models and the material properties used and calibrated in the previous section are adopted here.

Although good results were achieved in the previous section using a coarser mesh with only one element in thickness in the dam body, for studies that require a greater accuracy in the characterization of damage distributions, the use of more refined meshes with two or more elements in thickness is recommended, in order to improve the simulation of the damage not only along the upstream and downstream faces but also its propagation through the dam blocks. This motivated the use of this new finite element model.

The load combination includes the self-weight of the dam (SW), the hydrostatic pressure for full reservoir (HP297), and a seismic load (SEISMICL) applied in the upstream-downstream direction. For this study, the seismic input was an artificially designed intensifying acceleration time history[12] prepared for Endurance Time Analysis, with peak accelerations increasing from around 0.1g to 1.5g in 15 s.

STATIC RESPONSE

The results of the non-linear response under static loads are presented first (Fig. 5.31). The maximum displacement (54.3 mm) is calculated at the central upper part of the dam, around el. 280 to 285 m (where the horizontal crack is located), with an important component towards downstream due to the applied water pressures at the upstream face. The stress fields show that the dam is globally under compressions, which means that, overall, the self-weight of the dam is able to compensate the tensions induced by water pressures. The greater compressions are calculated at the downstream base, normally oriented to the insertion (- 7.5 MPa), and at the upper part of the upstream face, in the arch direction (- 6 MPa). However, high tensions arise at the upstream base of the dam, normal to the insertion, resulting in concrete tensile damage. Moreover, since the dam moves towards downstream, there is a small opening of the horizontal crack (≈ 1 mm) that causes a reduction of the vertical tensions that would arise in that zone.

[12] The original intensifying acceleration time history was provided for the 15th International Benchmark Workshop on Numerical Analysis of Dams, organized by ICOLD, for seismic analysis of a large concrete dam (Salamon et al., 2021).

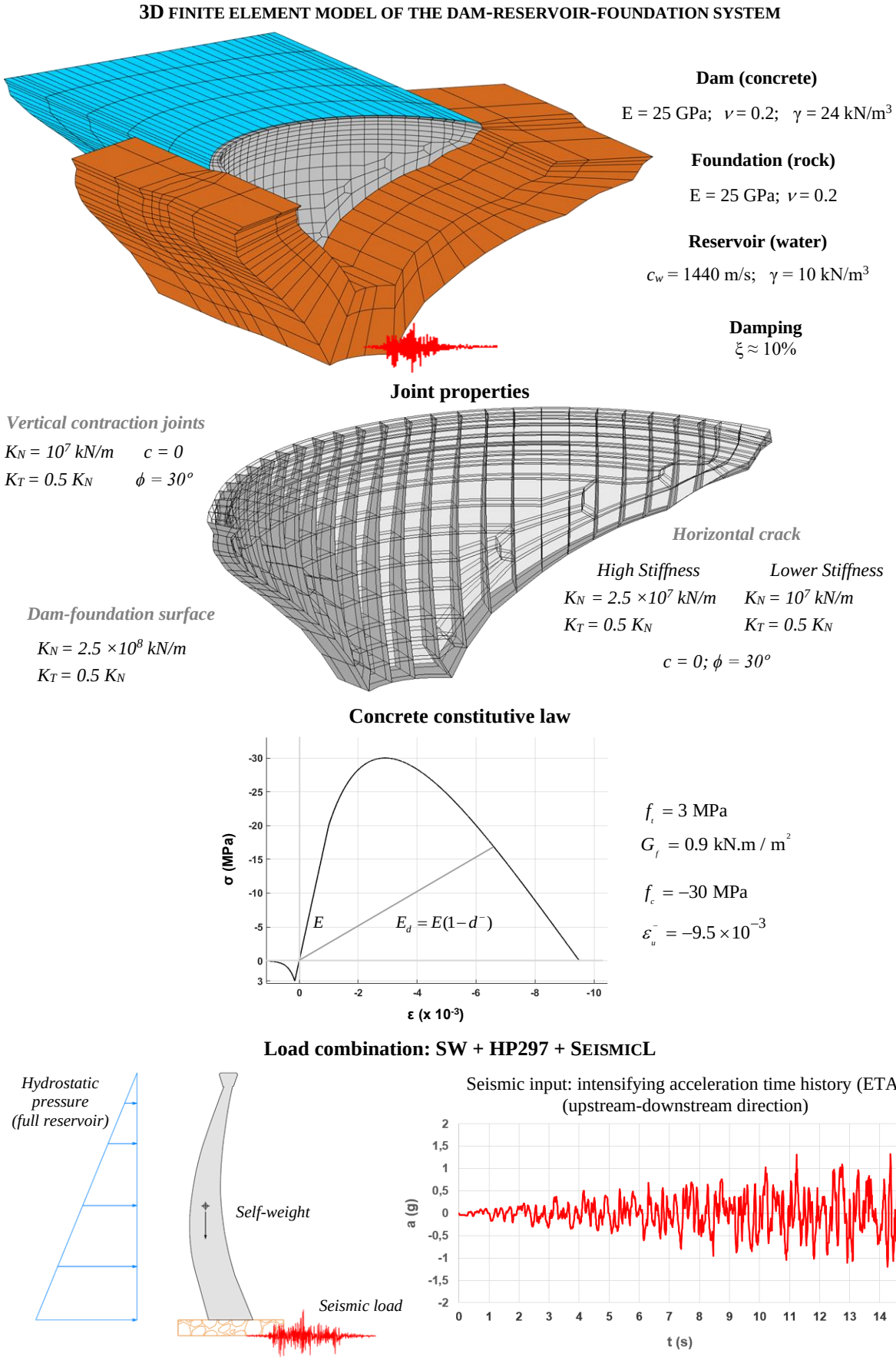

Fig. 5.30 New 3D model of the dam-reservoir-foundation system used for non-linear seismic analysis of Cabril dam. Properties, joints, concrete constitutive law, and intensifying seismic input.

In comparison with the previous analysis, carried out using a coarser mesh, the non-linear response calculated with a more refined mesh shows that larger displacement values were obtained, as expected. Greater values are also obtained for principal stresses, considering that the elements are smaller and thus numerical integration is performed at points closer to the dam base or to the upstream/downstream surfaces.

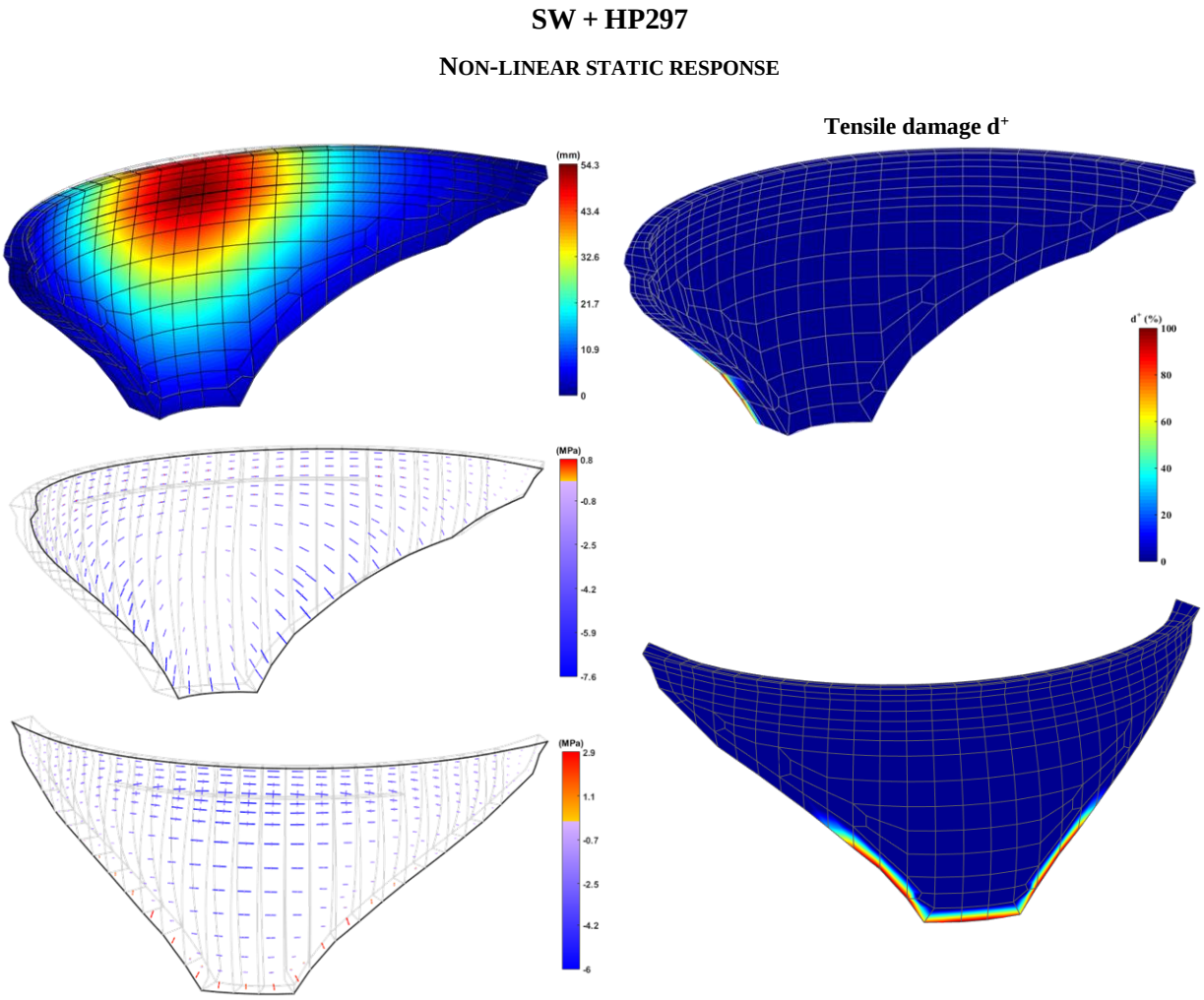

Fig. 5.31 Non-linear static response of Cabril dam for SW + HP297. Displacements, principal stresses, and tensile damage.

ENDURANCE TIME ANALYSIS (HORIZONTAL CRACK WITH HIGHER STIFFNESS)

The non-linear seismic performance of Cabril dam is evaluated here for the load combination SW + HP297 + SEISMICL, assuming the hypothesis of horizontal crack with high stiffness. The main results are presented at the end of various seconds of analysis, corresponding to increasing excitation levels.

Until t = 2 s (Fig. 5.32), the seismic action causes maximum dynamic motions with semi-amplitudes of about 38 mm towards upstream and of 42 mm towards downstream, whereas the displacement due to the static load combination SW+HP297 is of 54 mm in the downstream direction. Therefore, the maximum displacement in the upstream direction is still towards downstream (≈ 12 mm) in relation to the initial

undeformed position, while the maximum downstream displacement is 91.9 mm, both computed at the top of the central section. At this time, no significant joint opening or sliding movements occurred.

With respect to the stress fields, the higher tensions arise along the upstream base of the dam, normally oriented to the insertion, where the first signs of concrete damage occur. In turn, the greater compressions occur at the downstream base (- 9 MPa), normally oriented to the insertion, and at the upper part of the central cantilevers (- 8.1 MPa), in the arch direction, when the dam moves towards downstream; since the installed compressions are much lower than the concrete compressive strength, there is no compressive damage to report until t = 2 s.

Moving on, until t = 4 s (Fig. 5.33) the structural response of the dam has changed significantly. The greater displacements at the top of the central section are now of around 25 mm in the upstream direction and of 165.4 mm in the downstream direction. However, the maximum displacements in the upstream direction are now compute at the top of the shorter lateral cantilevers (83.9 mm), where the larger joint openings occur (≈ 8 mm).

As for the non-linear stress fields, when the dam moves towards downstream and the greater displacements occur at the central part of the dam, there is an increase of tensile cantilever stresses in the downstream face of most cantilevers, around the horizontal crack (since its opening movements are limited, due to higher stiffness value adopted, these tensile stresses are not released). Furthermore, when the greater displacements occur at the lateral parts of the dam, the opening of the vertical contraction joints are now large enough to release the arch stresses at the top, resulting in an increase of vertical compressions (upstream) and tensions (downstream) along the height of the lateral cantilevers. As a result, besides the growth of concrete failure along the upstream base, new areas with high tensile damage have appeared at the downstream face of the lateral cantilevers; nevertheless, even for the shorter cantilevers, where the damaged areas are wider, tensile damage is mostly superficial.

On the other hand, as the dam moves in the downstream direction, maximum arch compressions are calculated at the top of upstream face of the central cantilevers (- 15.4 MPa), which are still about half the value of the compressive strength, while important compressive stresses arise along the height of the lateral cantilevers (- 8 to 9.8 MPa). Once again, there is no compressive damage.

Then, until t = 6 s it is possible to see that there was a considerable increase in the non-linear structural response (Fig. 5.34). Significant upstream displacements were computed along the upper part of the dam, with maximum values of 163.9 mm at the crest of the lateral cantilevers, resulting in large joint opening (9.89 mm) and sliding (19.34 mm) movements.

Regarding the corresponding stress fields, the opening of the vertical contraction joints led to the release of arch stresses at the top of the dam, resulting in an increase of the cantilever stresses at the upstream and downstream faces of each cantilever monolith, especially on the taller ones. Therefore, in addition to the damages that occurred until this time, there was an important growth of tensile damage at the downstream face of the central cantilevers, at the upper part, as well as at the upstream face of the lateral cantilevers. For this excitation level, there are some areas where concrete failure due to tensile damage propagates

across the whole thickness of the cantilevers, particularly on the shorter lateral cantilevers. where these areas are more widespread.

Finally, to enable an overall evaluation of the seismic performance of Cabril dam under the intensifying acceleration time history, the evolution of tensile (Fig. 5.35) and compressive (Fig. 5.36) damage distributions during the seismic analysis are provided.

The presented results show that until t = 5 s the tensile damage state is acceptable, since concrete failure is mostly superficial and does not propagate across the thickness of the cantilevers. However, between t = 5 s and t = 6 s there is a considerable increase of zones with high tensile damage at the upstream and downstream faces, and that concrete failure starts to propagate from upstream to downstream in large areas of the dam body, particularly in the lateral cantilevers. Although this situation would not be expected to cause the collapse of the dam, this damage state could compromise structural integrity and require the interruption of the dam normal operation for repair and maintenance interventions. Therefore, in this case the performance endurance limit associated with tensile damage should be t = 5 s, corresponding to a peak acceleration around 0.5g, 5 times the value assumed in this work for the OBE (0.1g).

Furthermore, it is worth noting that until the previous endurance limit, no compressive damage was calculated. For the case of Cabril dam, compressive damage stars to arise only after t = 11 s, while the first occurrence of concrete failure under compression is reported only when the dam is subjected to peak accelerations of around 1.4g. Thus, considering the adopted performance criterion pertains to the occurrence of compressive failure crossing the cantilevers from upstream to downstream in key areas, the endurance limit for Cabril dam would be higher than t = 14 s, corresponding to a peak acceleration that is 7 times higher than the assumed MDE (0.2g), which demonstrates an impressive resistant capacity of Cabril dam in terms of compressive stresses.

As a final remark, the results obtained in these studies indicate that the structural safety of Cabril dam would be easily verified in possible seismic safety assessment studies to be carried out in the future, in case similar or even higher values than those assumed here for the OBE (0.1g) and for the MDE (0.2g) were used.

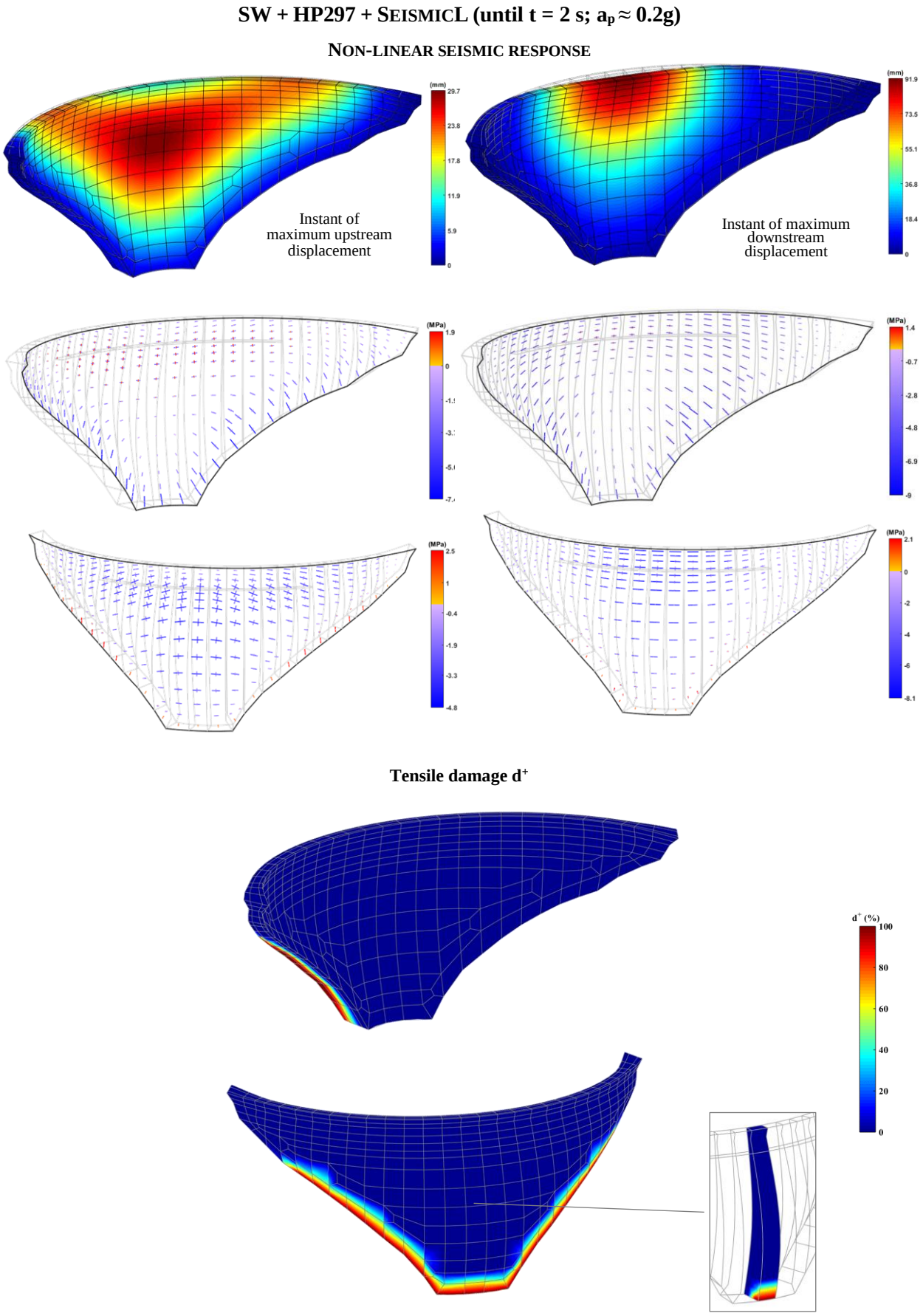

Fig. 5.32 Non-linear seismic response of Cabril dam for SW + HP297 + SEISMICL (until t = 2 s; ap ≈ 0.2g). Horizontal crack with higher stiffness. Displacements, principal stresses, and tensile damage.

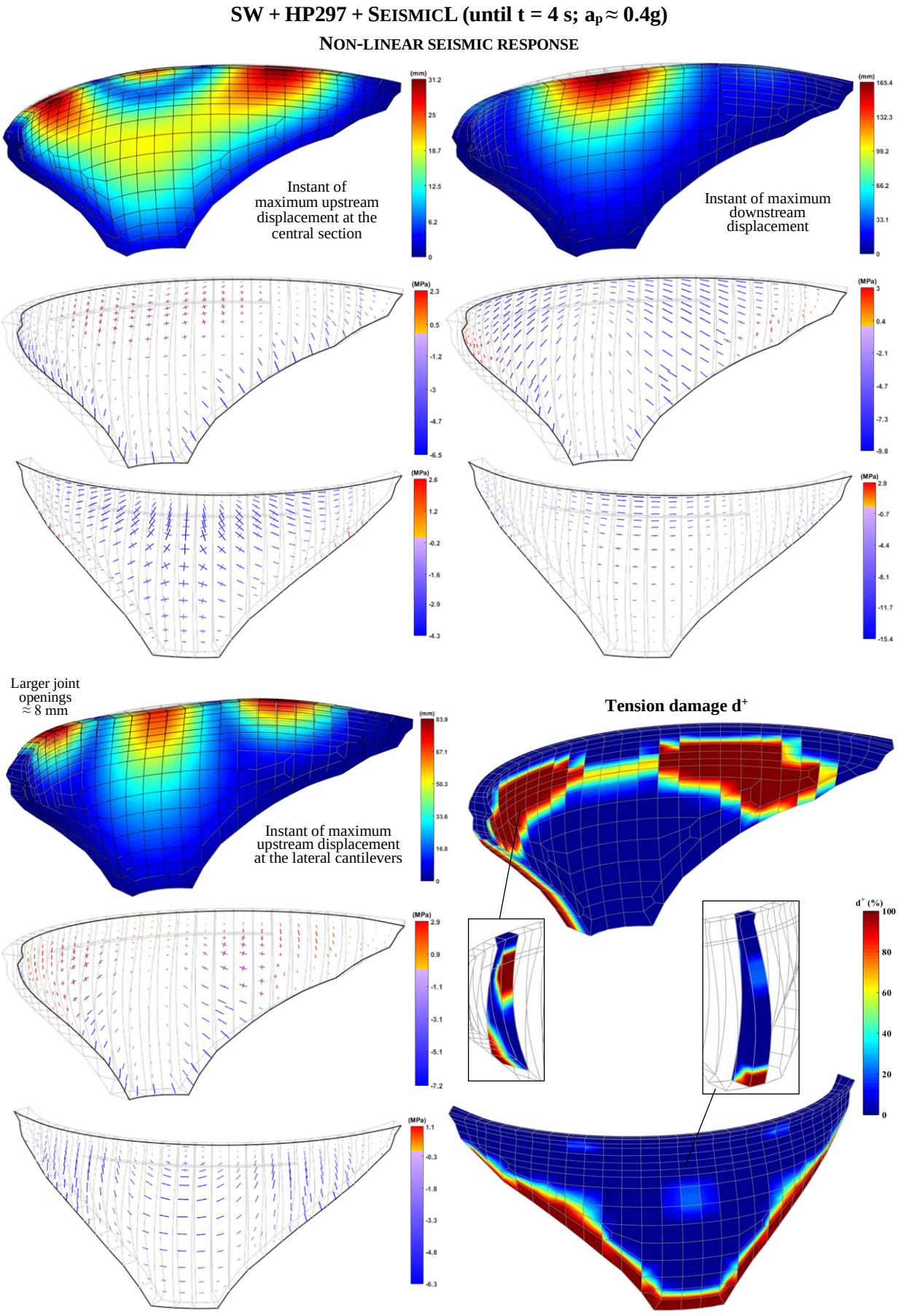

Fig. 5.33 Non-linear seismic response of Cabril dam for SW + HP297 + SEISMICL (until t = 4 s; ap ≈ 0.4g). Horizontal crack with higher stiffness. Displacements, principal stresses, and tensile damage.

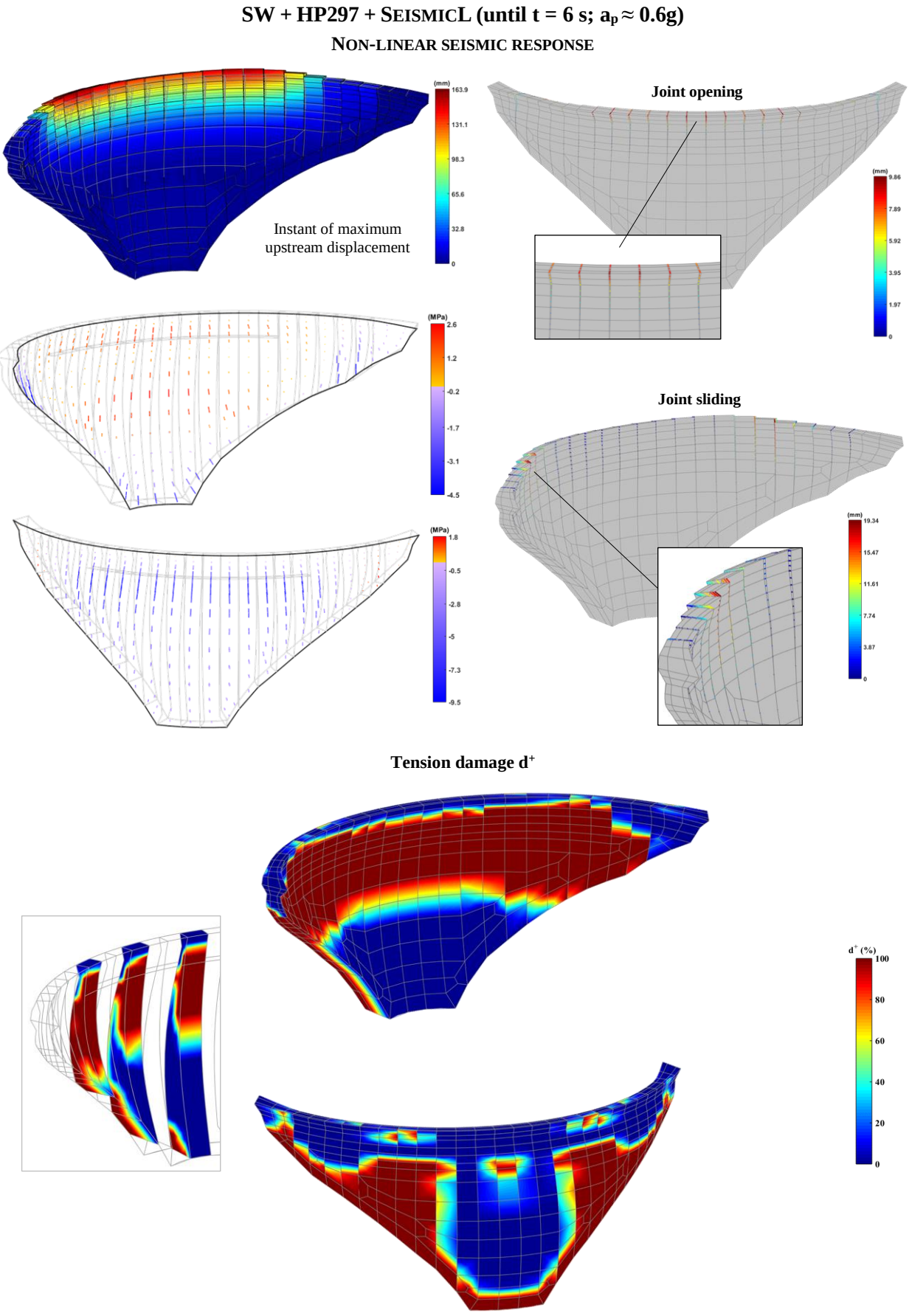

Fig. 5.34 Non-linear seismic response of Cabril dam for SW + HP297 + SEISMICL (until t = 6 s; ap ≈ 0.6g). Horizontal crack with higher stiffness. Displacements, principal stresses, joint movements, and tensile damage.

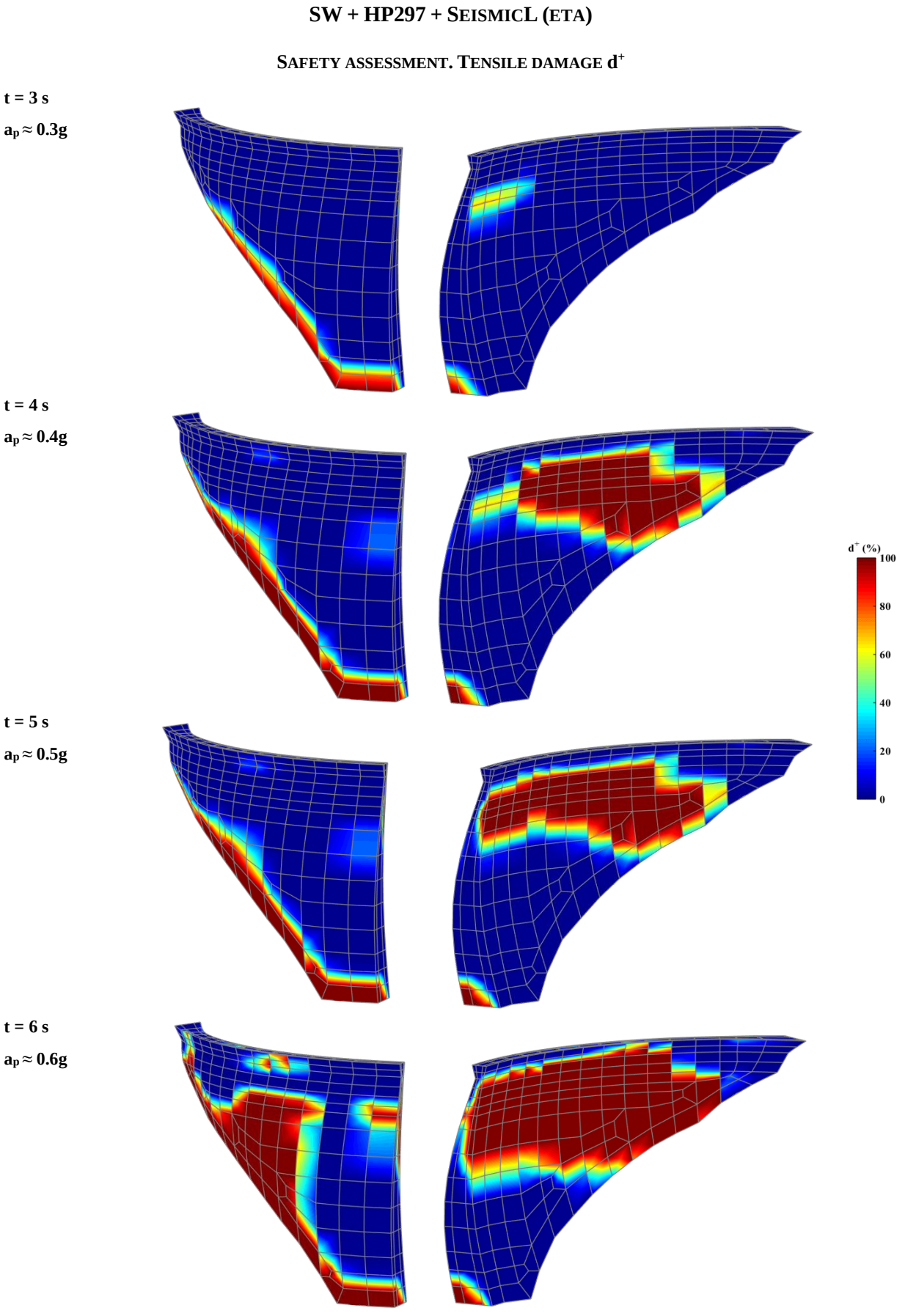

Fig. 5.35 Non-linear seismic response of Cabril dam for SW + HP297 + SEISMICL. Horizontal crack with higher stiffness. Tensile damage for consecutive excitation levels.

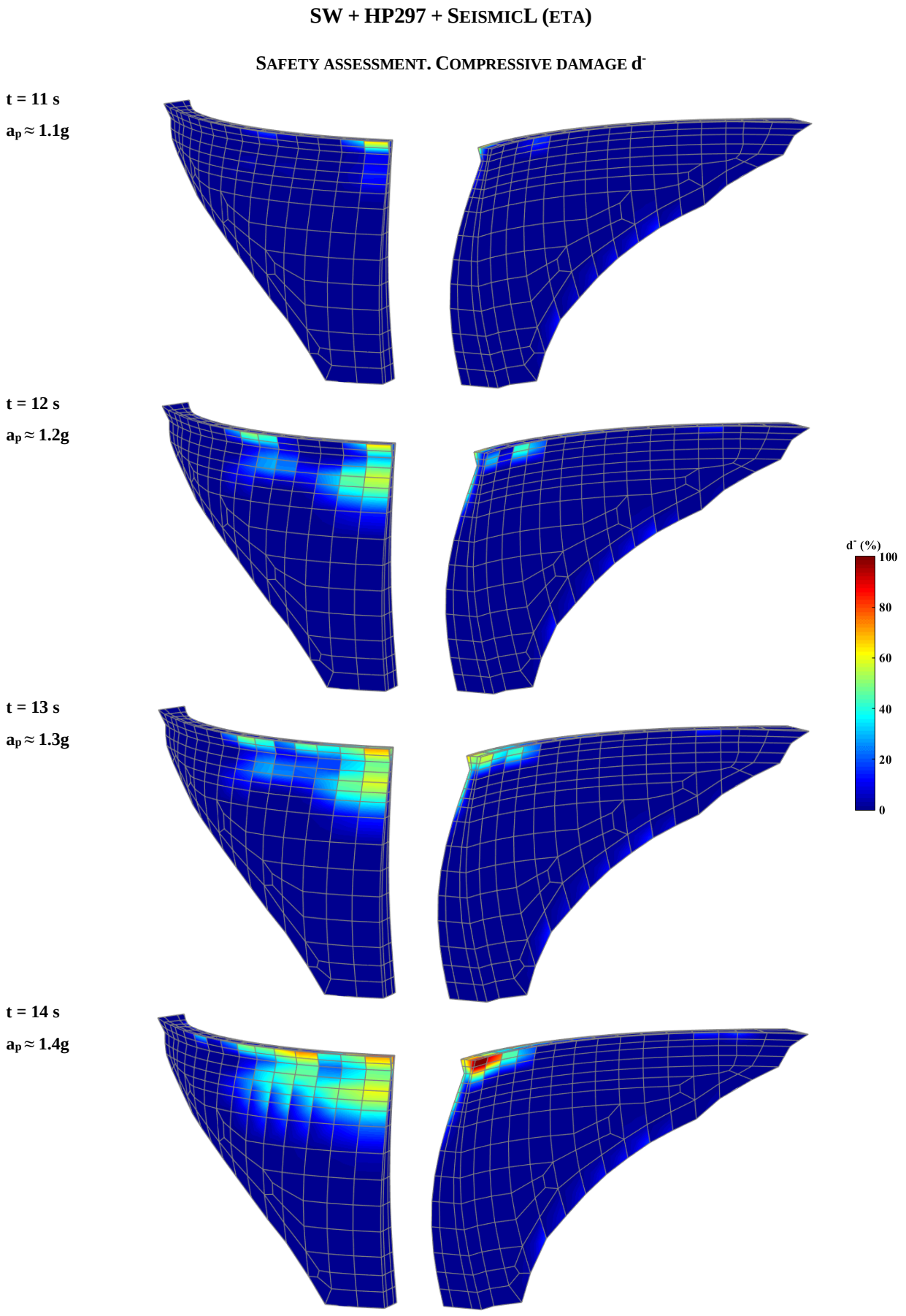

Fig. 5.36 Non-linear seismic response of Cabril dam for SW + HP297 + SEISMICL. Horizontal crack with higher stiffness. Compressive damage for consecutive excitation levels.

ENDURANCE TIME ANALYSIS (HORIZONTAL CRACK WITH LOWER STIFFNESS)

The studies conducted in the previous subchapter allowed to investigate the influence of the opening movements of the horizontal crack in the seismic response of Cabril dam and thus to demonstrate the importance of properly simulating its non-linear behaviour. Therefore, the seismic performance of Cabril dam under an intensifying seismic load is evaluated again, now considering the hypothesis of horizontal crack with lower stiffness.

Overall, when the dam moves towards downstream, the horizontal crack closes and the structural response is similar to that obtained assuming a higher horizontal crack stiffness. As such, the results provided here show only the instants of maximum upstream displacements, in order to highlight the differences considering both hypotheses.

Until t = 2 s, the structural response of the dam is not significantly different from the previous analysis (Fig. 5.37). However, the displacement field is altered by the opening of the horizontal crack, which leads to an increase in the displacements at the top in the upstream direction. In what concerns the stress fields, the horizontal crack movements result in a decrease of the vertical tensions in the area surrounding the crack, as expected. Simultaneously, this leads to an increase of tensile stresses at the upstream base, originating greater tensile damage. There is no compressive damage.

However, until t = 4 s, the influence of the horizontal crack movements become more noticeable (Fig. 5.38). Now, the largest horizontal crack openings are of about 20 mm, leading to an increase in the maximum upstream displacements at the top of the central cantilevers to around 50 mm, which is about two times those obtained assuming a horizontal crack with higher stiffness.

In this case, due to the larger horizontal crack movements, there is a more significant release of the cantilever tensions at around the crack area, the downstream face. Nevertheless, the deformations suffered by the blocks above the crack induce the appearance of new tensions at the upper part of some blocks, namely those located in the inflexion point seen in the deformed shape (low tensile damage values start to appear). Simultaneously, vertical tensions occur on the upstream side of the cracked zone, which caused high tensile damage values. There is also an increase in the compressions installed at the downstream base, normal to the insertion, and at the upper part of the upstream face of the lateral cantilevers, approximately in the arch direction.

At last, for t = 6 s, there was a notorious increase in the non-linear response, which is very different from the response calculated considering the horizontal crack with higher stiffness. In this case there is a considerable deformation of the upper part of the dam, namely of the blocks above the horizontal crack: the maximum displacements (253.8 mm) were calculated at the crest of the central blocks (Fig. 5.39), which are much greater than those in the rest of the dam body. This behaviour is clearly due to the considerable opening of the horizontal cracks, which reaches maximum values of 91.68 mm.

The stress redistribution processes induced by the joint movements resulted in an increase of tensions and compressions along the upstream base, in the upstream and downstream sides of the lateral cantilevers, thus leading to a growth of the areas under concrete failure. In addition, there is a considerable increase of the

tensile damage in the blocks above the crack, which propagate across the thickness. On the other hand, it is worth noting the absence of damage in the area below the crack since the vertical stresses are released when the horizontal crack opens.

Finally, the evolution of tensile (Fig. 5.40) and compressive (Fig. 5.41) damage distributions are presented for several time steps during the seismic analysis, to allow for a global evaluation of the seismic performance of Cabril dam.

With respect to the tensile damage evaluation (Fig. 5.40), in comparison with the results obtained assuming a horizontal crack with higher stiffness, it is possible to see that, overall, the opening movements of the horizontal crack resulted in a significant decrease of the vertical tensile stresses and hence of tensile damage at the downstream face, below the crack, and at the same time, to the appearance of new damages at the upstream face, around the cracked zone. Nevertheless, similarly to the previous analysis, there is an important increase of tensile damage between t = 5 s and t = 6 s at both upstream and downstream faces, and concrete failure starts to propagate from upstream to downstream along the height of the shorter lateral cantilevers and in the blocks above the crack. Therefore, the performance endurance limit for tensile damage is once again a peak acceleration of approximately 0.5g.

As for compressive damage, in comparison with the results obtained in the previous analysis, the accumulated damage distributions (Fig. 5.41) enable to see that there was a clear decrease of arch compressions at the upper part of the dam, hence preventing the occurrence of compressive failure near the crest. In this case, the first noticeable damages, with values close to 100%, arise only after t = 13s, and there is not significant compressive failure to report after that, which means that the endurance limit for compressive damage would be higher than 15 s, corresponding to peak accelerations greater than 1.5g.

In conclusion, the results obtained here allow to reinforce the conclusion that Cabril dam presents an impressive resistant capacity under strong earthquakes. Furthermore, since the opening movements of the horizontal crack are enabled in this second analysis, it is relevant to emphasize that, although the largest openings are of almost 20 cm, these movements occur at downstream side of blocks with a base width of about 6 to 7 m; therefore, although this scenario is not considered in this work, the instability of said blocks would not be expected until the established endurance limit.

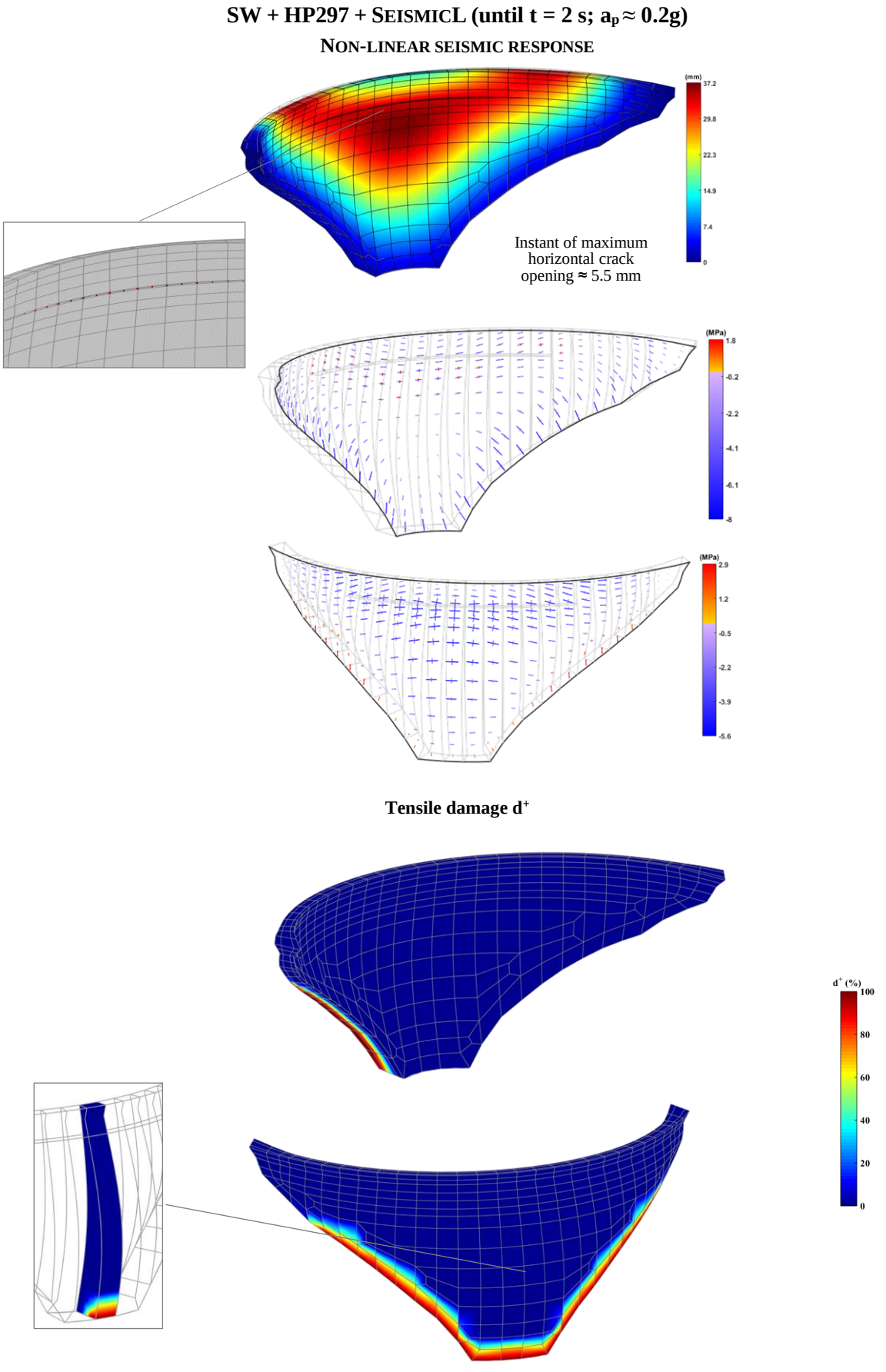

Fig. 5.37 Non-linear seismic response of Cabril dam for SW + HP297 + SEISMICL (until t = 2 s; $a_p \approx 0.2g$). Horizontal crack with lower stiffness. Displacements, principal stresses, joint movements, and tensile damage.

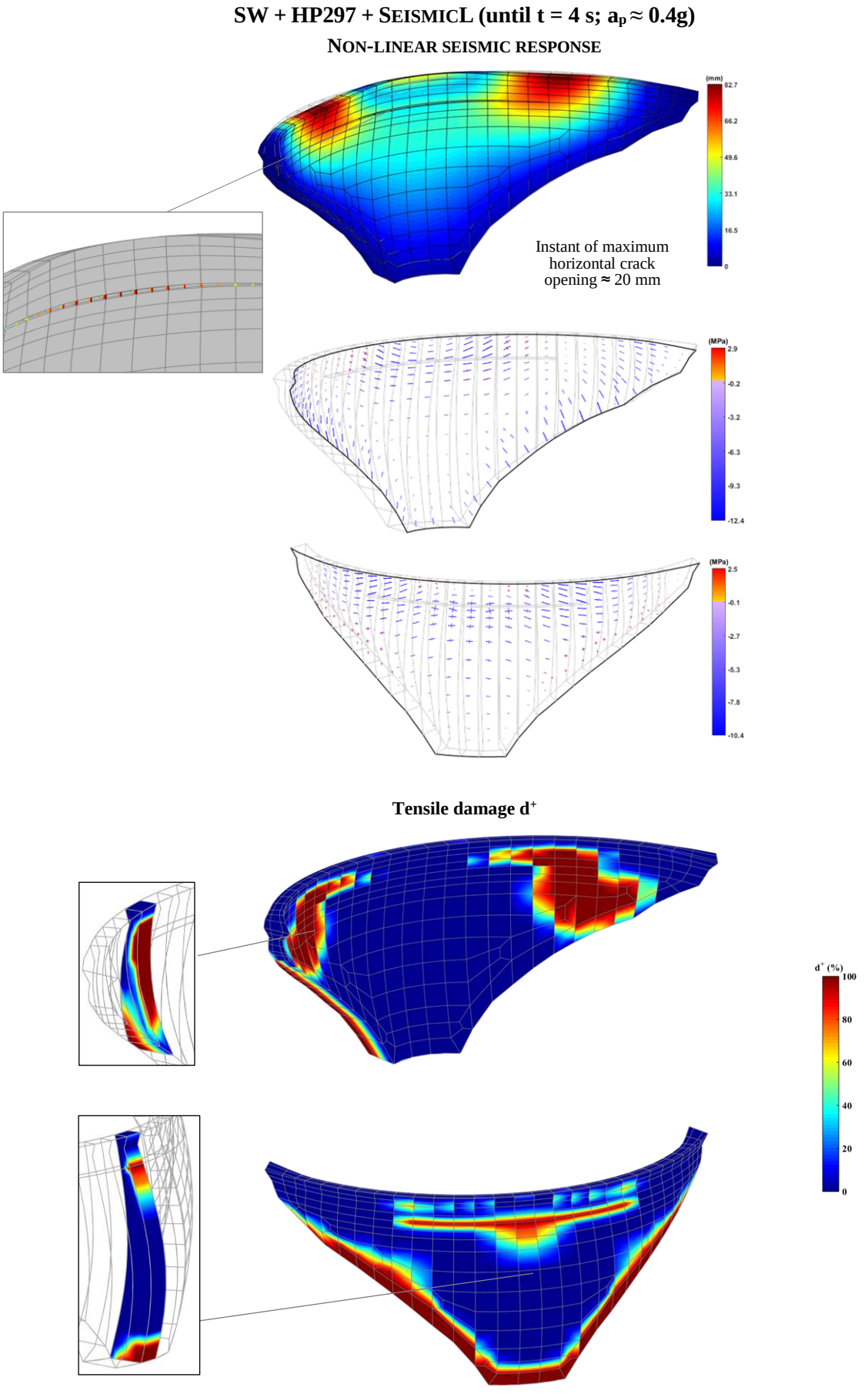

Fig. 5.38 Non-linear seismic response of Cabril dam for SW + HP297 + SEISMICL (until t = 4 s; $a_p \approx 0.4g$). Horizontal crack with lower stiffness. Displacements, principal stresses, joint movements, and tensile damage.

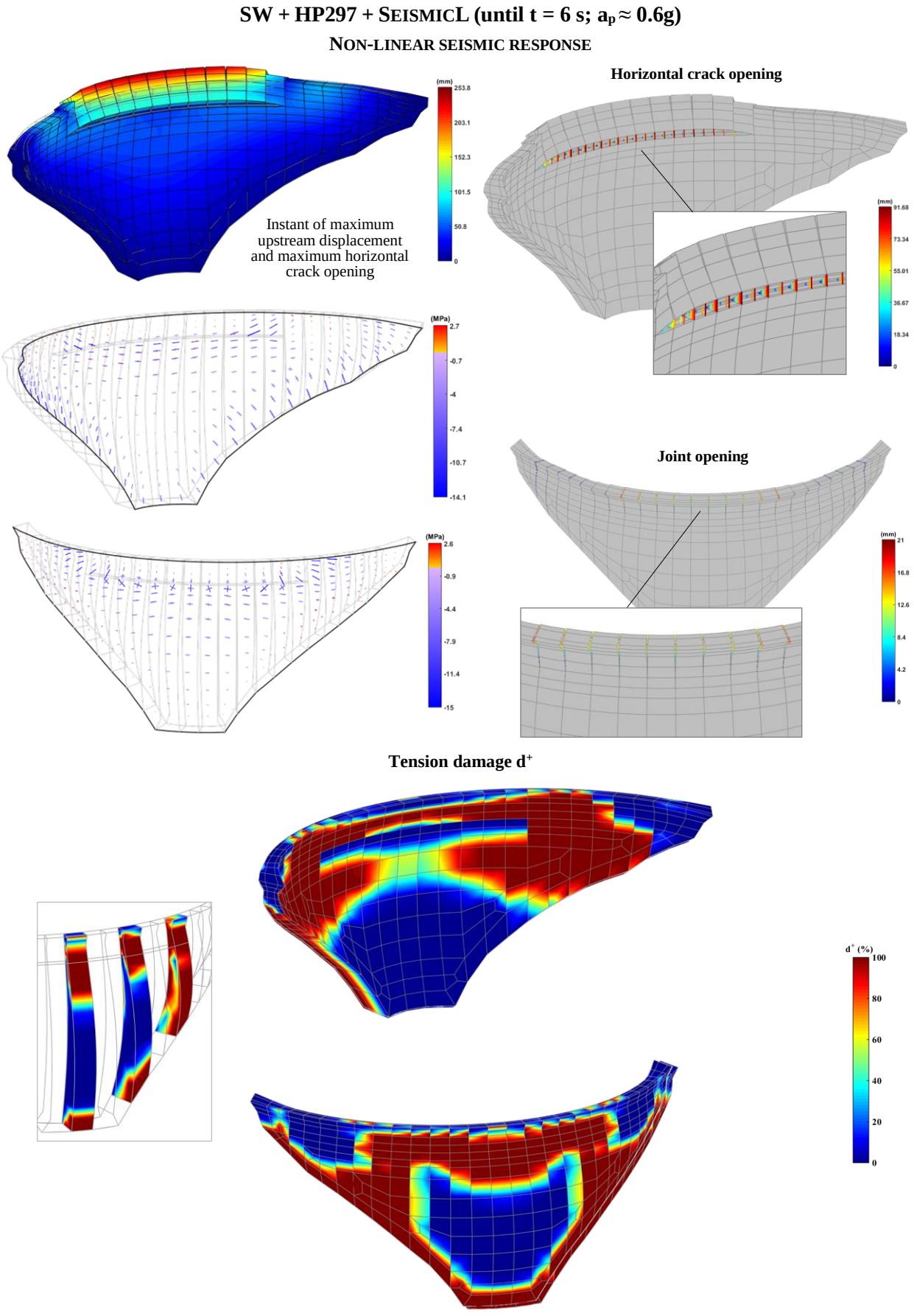

Fig. 5.39 Non-linear seismic response of Cabril dam for SW + HP297 + SEISMICL (until t = 6 s; $a_p \approx 0.6g$). Horizontal crack with lower stiffness. Displacements, principal stresses, joint movements, and tensile damage.

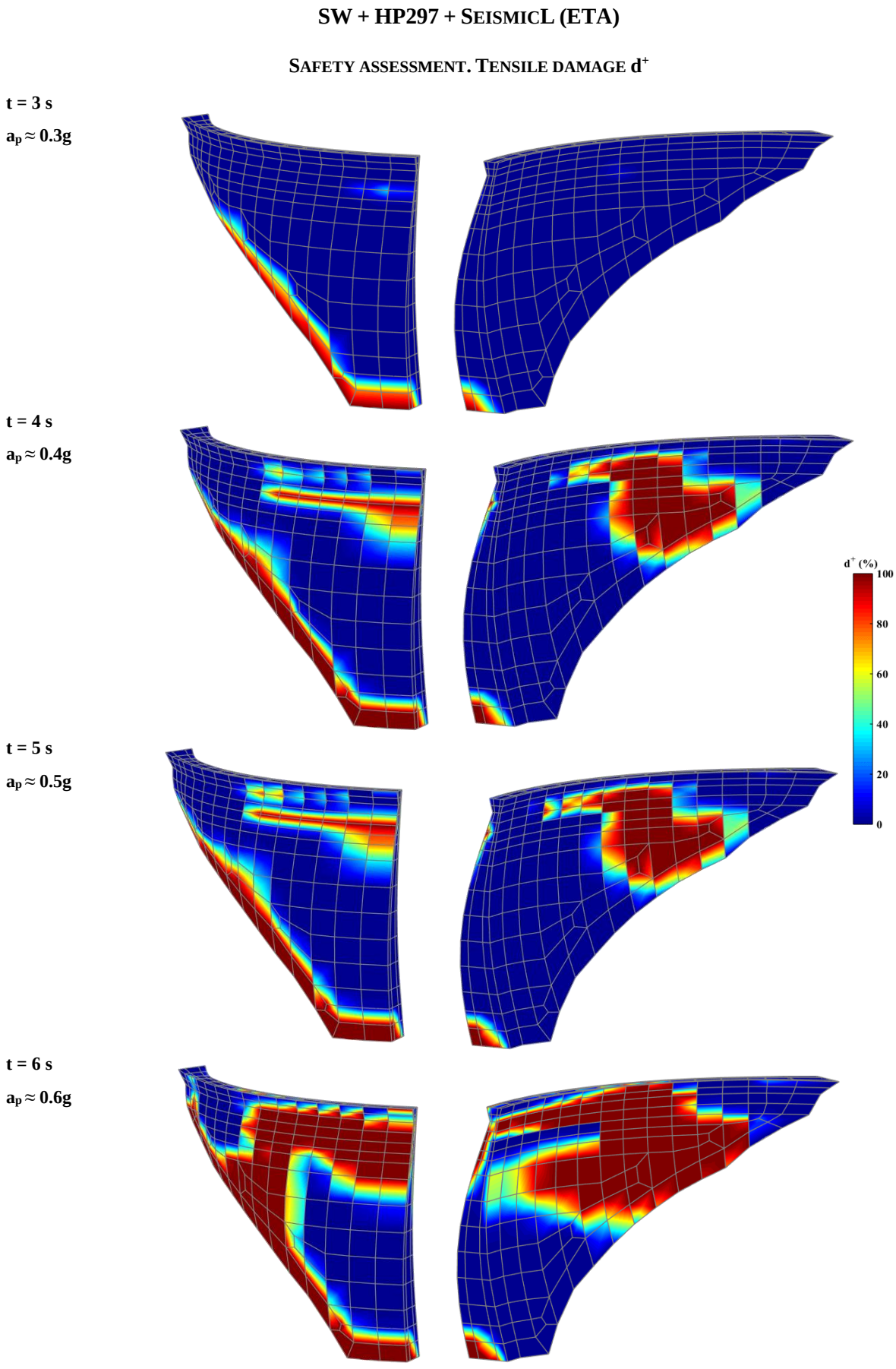

Fig. 5.40 Non-linear seismic response of Cabril dam for SW + HP297 + SEISMICL. Horizontal crack with lower stiffness. Tensile damage for consecutive excitation levels.

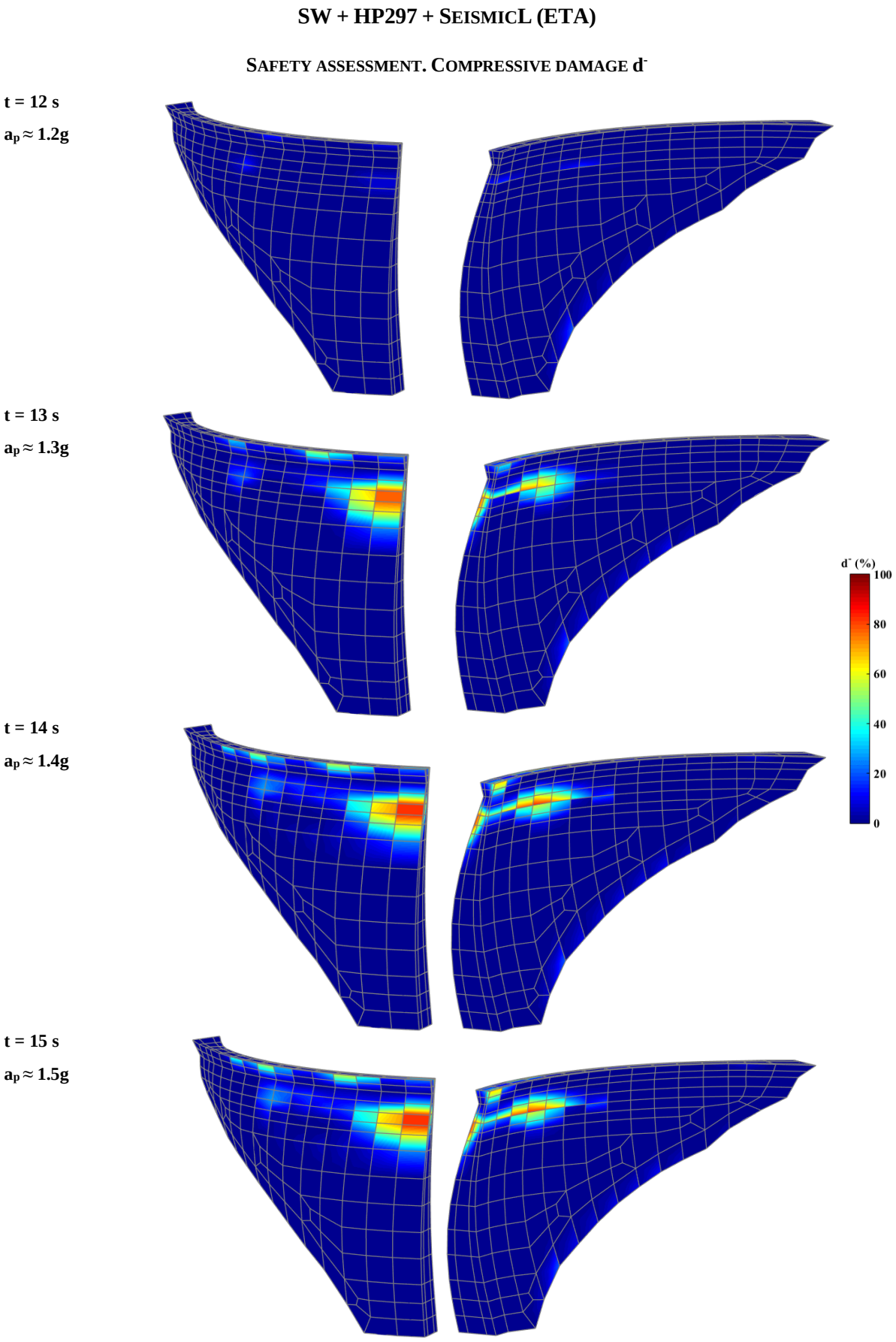

Fig. 5.41 Non-linear seismic response of Cabril dam for SW + HP297 + SEISMICL. Horizontal crack with lower stiffness. Compressive damage for consecutive excitation levels.

5.3 DYNAMIC BEHAVIOUR OF CAHORA BASSA DAM

5.3.1 CAHORA BASSA DAM DESCRIPTION

THE DAM

Cahora Bassa dam is a large concrete dam (Fig. 5.42) that was built from 1969 to 1974 on the Zambezi River, in the Tete province, near Songo, in Western Mozambique. This is a thin 170 m high double curvature arch dam with a 303 m long crest. The thickness of the central cantilever ranges from 23 m at the base to 4 m at the crest, which presents a particular half-hollow geometry. One of the highest dams on the African continent, reaching a maximum elevation at el. 331 m, this dam was constructed on a gneissic granite rock mass of very good quality.

A concrete swelling phenomenon was detected in Cahora Bassa dam in the 1980s, which is evidenced by a typical cracking pattern that can be seen at the crest, as detailed in the figure. However, the behaviour of the dam has been monitored over the years and normal operating conditions have not been affected.

Regarding appurtenant works, the dam has one control surface spillway and eight half-height spillways, with a total discharge capacity of 14 000 m^3. Moreover, the dam has several concrete ribs at the upstream face that go from the crest to the half-height spillways, which are used for lowering and lifting the corresponding floodgates when necessary.

The hydroelectric power station, built at the same time of dam construction, is located on the south bank of the river, and it has a total installed capacity of 2075 MW, provided by five 415 MW Francis Turbines, making it the largest hydroelectric scheme in southern Africa.

As the name indicates, the dam impounds Lake Cahora Bassa, a 270 km long lake, which is 30 km wide at is widest point, that extends to the Mozambique - Zimbabwe/Zambia border, thus forming a 55.8 billion m^3 reservoir with a surface area of 2 739 km^2 at full supply level.

SSHM SYSTEM

In Africa, the continuous dynamic monitoring of large concrete dams started in 2010, when Hidroelétrica de Cahora Bassa (HCB) decided to install an SSHM system in Cahora Bassa dam (E. Carvalho et al., 2014; E. Carvalho & Matsinhe, 2014; E. Carvalho & Tembe, 2012) to enable the continuous evaluation of its behaviour in normal operating conditions, as well as to measure the response in accelerations during seismic events. The goal was to develop a system for collecting and providing valuable data to owners and engineers responsible for safety control. Therefore, the system was designed to continuously record accelerations in various positions at the top of the dam body, near the base, and in both banks (Fig. 5.43).

The monitoring scheme includes 10 uniaxial accelerometers (EpiSensor ES-U2), prepared to measure vibrations in the radial direction, located in the upper gallery, at el. 326 m (5 m below the crest), and 3 triaxial sensors (EpiSensor ES-T), two placed in the right and left banks, and the third one positioned at the dam base, in the central section.

CAHORA BASSA DAM (MOZAMBIQUE)

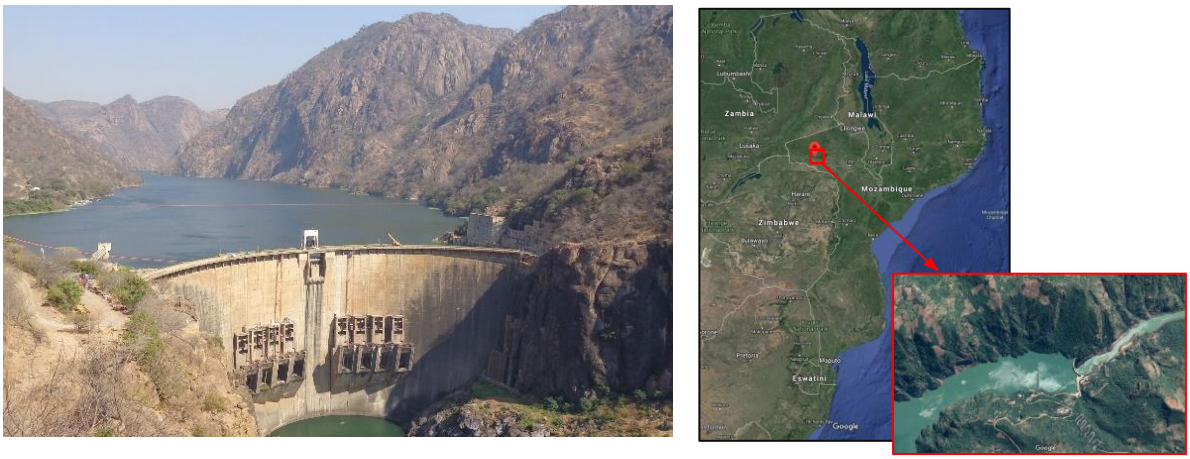

Downstream view

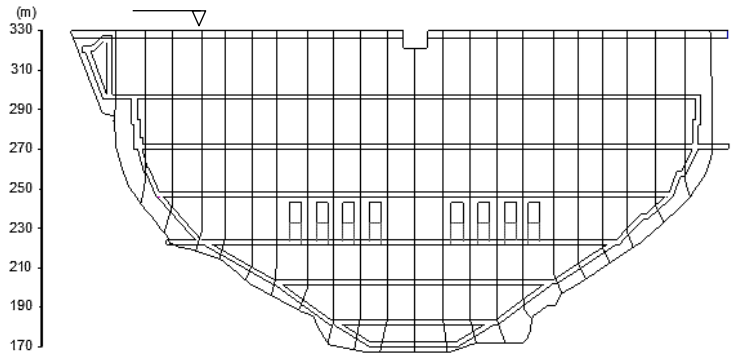

Cross section

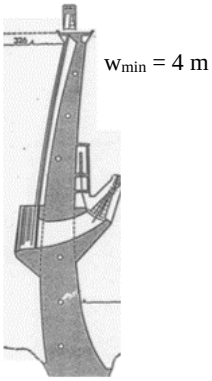

Plan view

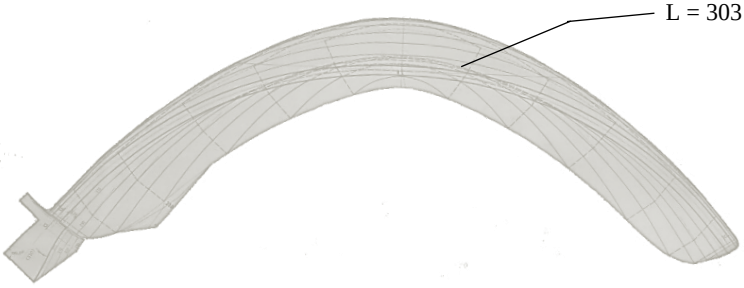

Upstream view

Detail of cracking pattern at the crest

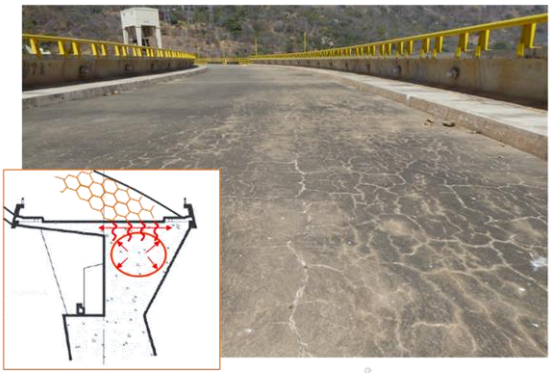

Fig. 5.42 Cahora Bassa dam, Mozambique. Aerial view, technical drawings (downstream view, central cantilever cross section, and plan view), upstream view, and crest detail.

Furthermore, in order to achieve a system with a high dynamic range and thus enable the accurate measurement of the response of the dam under low amplitude ambient/operational vibrations and during low to high intensity earthquakes, extremely low noise sensors with a full-scale recording range of ± 1g were used. All sensors are connected to a single 24-channel Granite unit from Kinemetrics for data acquisition/digitalization, through a local optical fibre network. Basically, 19 acceleration time histories are continuously recorded in 24 bit, every hour, at a sampling rate of 50 Hz, and then transmitted to the computer server in the dam control centre. Regarding the software component, an essential part of any SSHM system, there are specific tools installed in the computer server that were designed to automatically collect the measured signals and save data files. To carry out the studies intended in this work, automatic modal identification is performed using the developed program *DamModalID*.

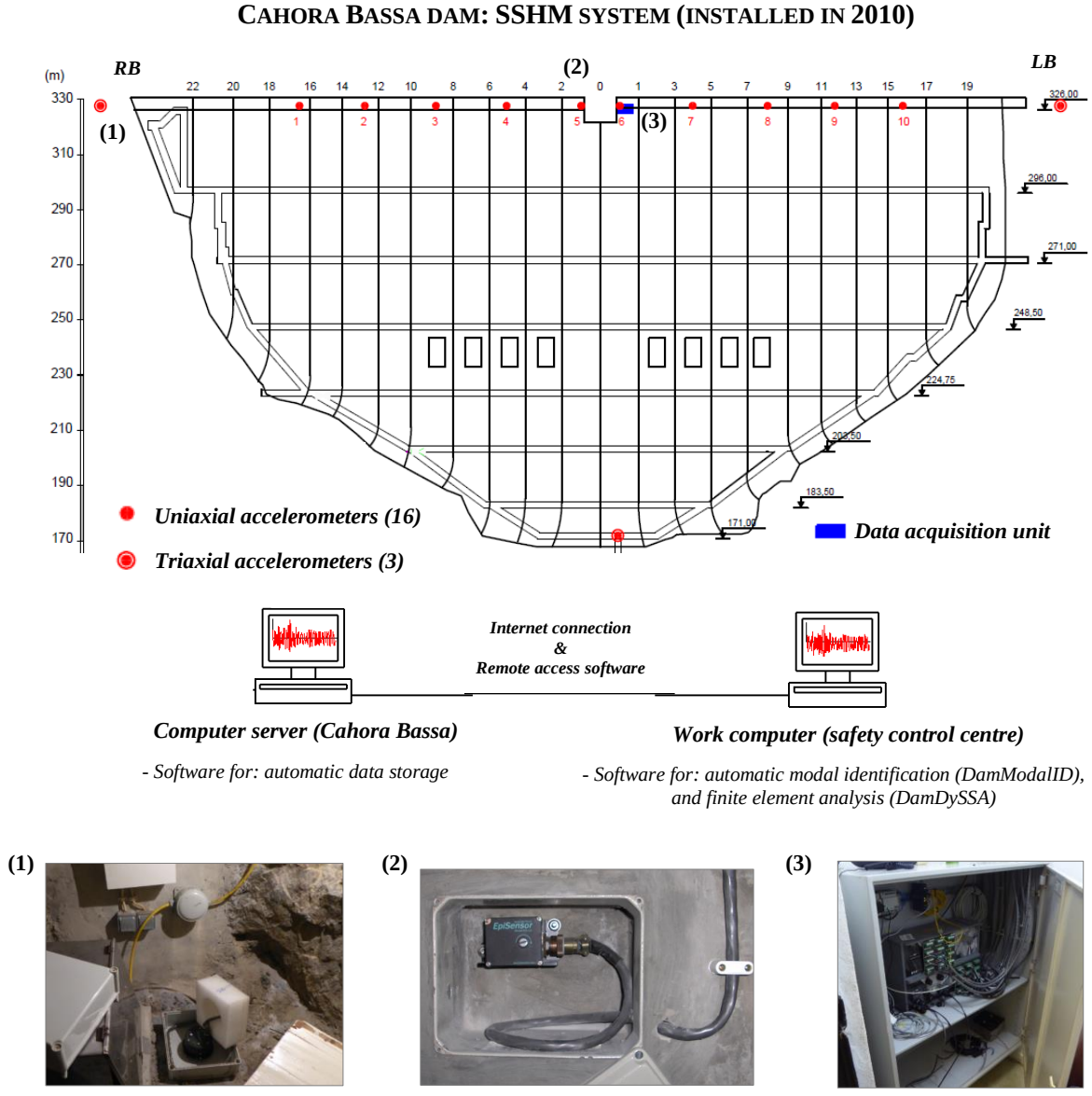

Fig. 5.43 SSHM system installed in Cahora Bassa dam. Monitoring scheme. Hardware and software components.

SEISMIC ACTION

Cahora Bassa dam is located in an earthquake hazard area, not far from the East African Rift system, an approximately 4500 km long system that extends from the Red Sea to the Indic Ocean, across Mozambique (Fig. 5.44). This is an active continental rift that is responsible for most earthquake events in Eastern Africa.

In terms of the seismic safety assessment of Cahora Bassa dam, the recommendations of the Portuguese Standards for dam design (NPB, 1993) can be followed (LNEC, 2009). Therefore, the Operating Basis Earthquake (OBE) and the Maximum Design Earthquake (MDE) must be considered for the evaluation of both current and failure scenarios.

According to HCB, the excitation levels to consider for the seismic analysis of the dam are those determined in a study that evaluated the seismic hazard for the Cahora Bassa dam area (Li-EDF-KP, 2001). In that document, the values of the horizontal peak ground accelerations are a_h = 0.076g for the OBE and a_h = 0.102g for the MDE. These values are used as reference for the seismic analyses to be carried out in this work.

a) East African Rift System **b) Map of earthquakes since 2001**

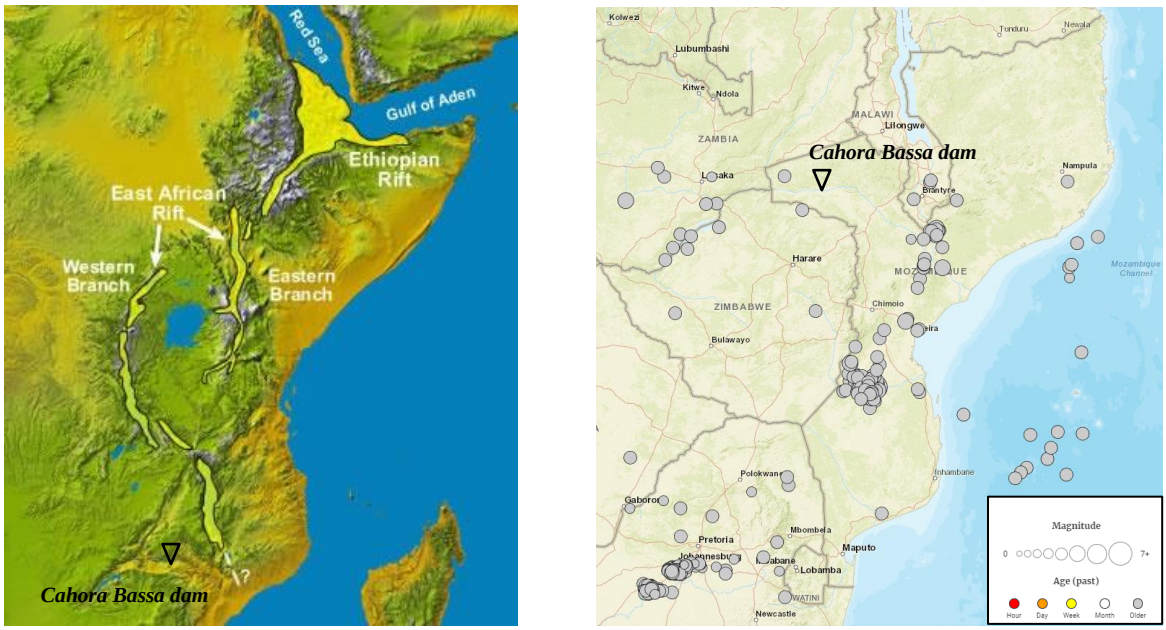

Fig. 5.44 a) East African Rift System (https://geology.com/articles/east-africa-rift.shtml) and b) Map of earthquakes of magnitude greater than 3 since 2001 (https://earthquake.usgs.gov/earthquakes/map).

5.3.2 MODAL ANALYSIS: EVOLUTION OF NATURAL FREQUENCIES OVER TIME

This section presents a study on the dynamic behaviour of Cahora Bassa dam under ambient/operational vibrations, during the monitoring period between 2010 and 2020. The main results retrieved from continuous dynamic monitoring data in normal operating conditions are provided, with focus on the evolution of the automatically identified natural frequencies over time. The modal identification outputs

are compared with results from finite element modelling, aiming to investigate the influence of reservoir level variations on the dynamic behaviour of the Cahora Bassa dam-reservoir-foundation system, as well as to further demonstrate how this type of approach can be valuable to perform vibration-based damage detection and help in the assessment of structural integrity of large concrete dams.

MODAL IDENTIFICATION RESULTS FROM CONTINUOUS DYNAMIC MONITORING DATA

The evolution of the identified natural frequencies of Cahora Bassa dam over time is presented for ten vibration modes in Fig. 5.45. The frequency values were extracted from continuous vibrations monitoring data, measured between August 2010 and June 2020, using *DamModalID*. The singular value spectra and the corresponding frequency values and modal configurations, estimated from the vibrations recorded on June 26, 2013, between 1 and 2 p.m., and on February 11, 2017, from 4 to 5 a.m., are also provided.

During this monitoring period, the reservoir water level varied from el. 312 m to el. 326 m, i.e., between 19 to about 5 m below the crest level, which represents a maximum reservoir level variation of 14 m. In Cahora Bassa dam the temperature semi-amplitude at the dam site is around ± 4º C throughout the year, and thus the influence of thermal variations was not considered in this study.

The displayed results show that the dynamic behaviour of the dam is clearly influenced by the reservoir water level, as expected: the higher the water level, and hence the global mass of the dam-reservoir-foundation system, the lower the frequency values. For example, the natural frequency of mode 1 varies between 1.76 and 1.95 Hz, while for mode 4 the frequency values range from 3.18 Hz to 3.51 Hz (these values correspond to the maximum and minimum observed reservoir levels). The influence of the reservoir level is more noticeable for vibration modes with higher frequencies. In what regards the mode shapes, modes 1 and 4 are antisymmetric, while modes 2 and 3 are symmetric. The fifth mode is a symmetric one where all measurement points move towards the same direction.

In the case of Cahora Bassa dam, which is a thin double curvature arch dam, it was possible to obtain singular value spectra with reduced noise, thus facilitating the automatic spectral peak selection and enabling to identify the natural frequencies of ten dam vibration modes for different water levels with good accuracy. In addition, the figure displays the identified frequencies associated with the operation of the power groups, at 1.785 and 3.57 Hz, values that are close to the frequencies of the first and fifth modes for higher water levels.

FINITE ELEMENT MODAL ANALYSIS AND COMPARISON WITH MODAL IDENTIFICATION RESULTS

The dynamic simulations were performed using the *DamDySSA* module for modal analysis and the 3D finite element model of the dam-reservoir-foundation system shown in Fig. 5.46. The dam concrete and the foundation rock are assumed as isotropic materials with linear elastic behaviour, considering Young's modulus E = 40 GPa and Poisson's ratio ν = 0.2. For dynamic behaviour analysis, it is considered E_{dyn} = 1.25 E (Alegre, Carvalho, et al., 2019).

CAHORA BASSA DAM: EVOLUTION OF NATURAL FREQUENCIES OVER TIME

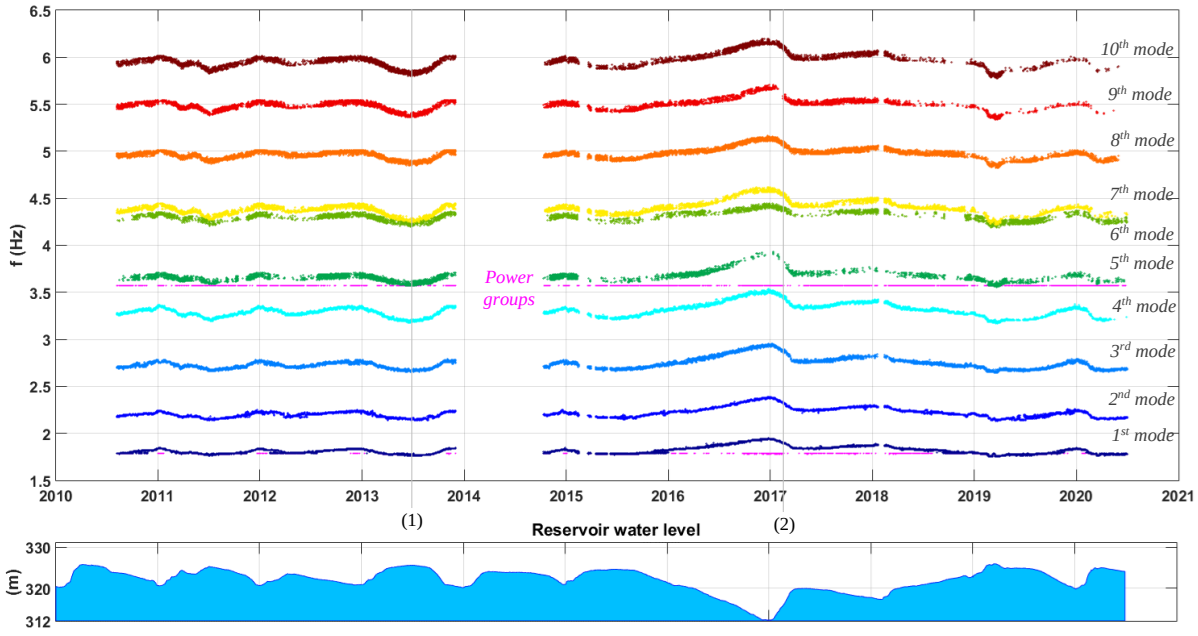

Modal identification results: measured signals on June 26, 2013, 1 to 2 p.m., water level at el. 325.6 m (1)

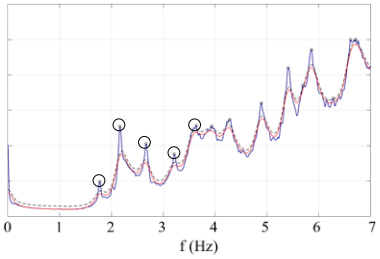

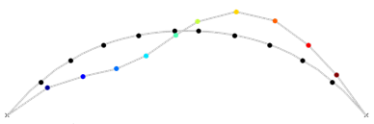

f_1 = 1.77 Hz (antisymmetric)

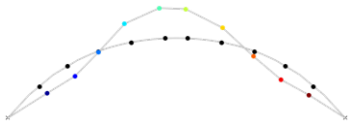

f_2 = 2.17 Hz (symmetric)

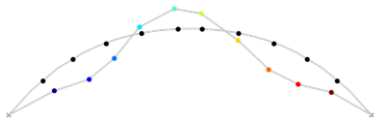

f_3 = 2.67 Hz (symmetric)

f_4 = 3.21 Hz (antisymmetric)

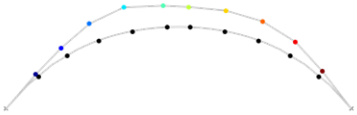

f_5 = 3.64 Hz (symmetric)

Modal identification: accelerations measured on February 11, 2017, 2 to 3 p.m., water level at el. 315 m (2)

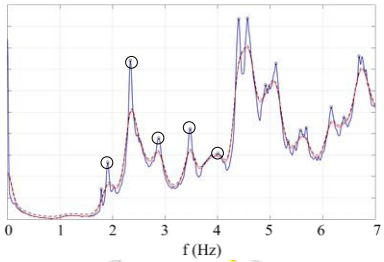

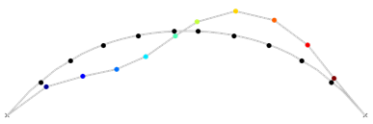

f_1 = 1.91 Hz (antisymmetric)

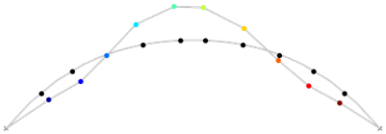

f_2 = 2.34 Hz (symmetric)

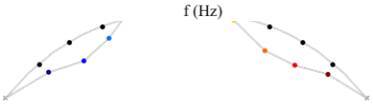

f_3 = 2.88 Hz (symmetric)

f_4 = 3.48 Hz (antisymmetric)

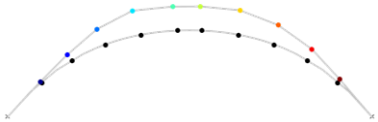

f_5 = 4.01 Hz (symmetric)

Fig. 5.45 Results from continuous dynamic monitoring of Cahora Bassa dam: evolution of identified natural frequencies over time (2010 to 2020). Singular value spectra and estimated frequencies and mode shapes for specific dates.

The reservoir water is assumed as a compressible fluid, with an average pressure wave propagation velocity c_w = 1500 m/s, in accordance with the water temperature in the reservoir (mean value of about 25ºC) (Rocha e Silva et al., 2005). In the current finite element model the half-hollow crest, the concrete ribs at the upstream face, and the geometry of the spillways are considered in a simplified way, by defining locally adapted values of specific mass and Young's modulus for the respective finite elements.

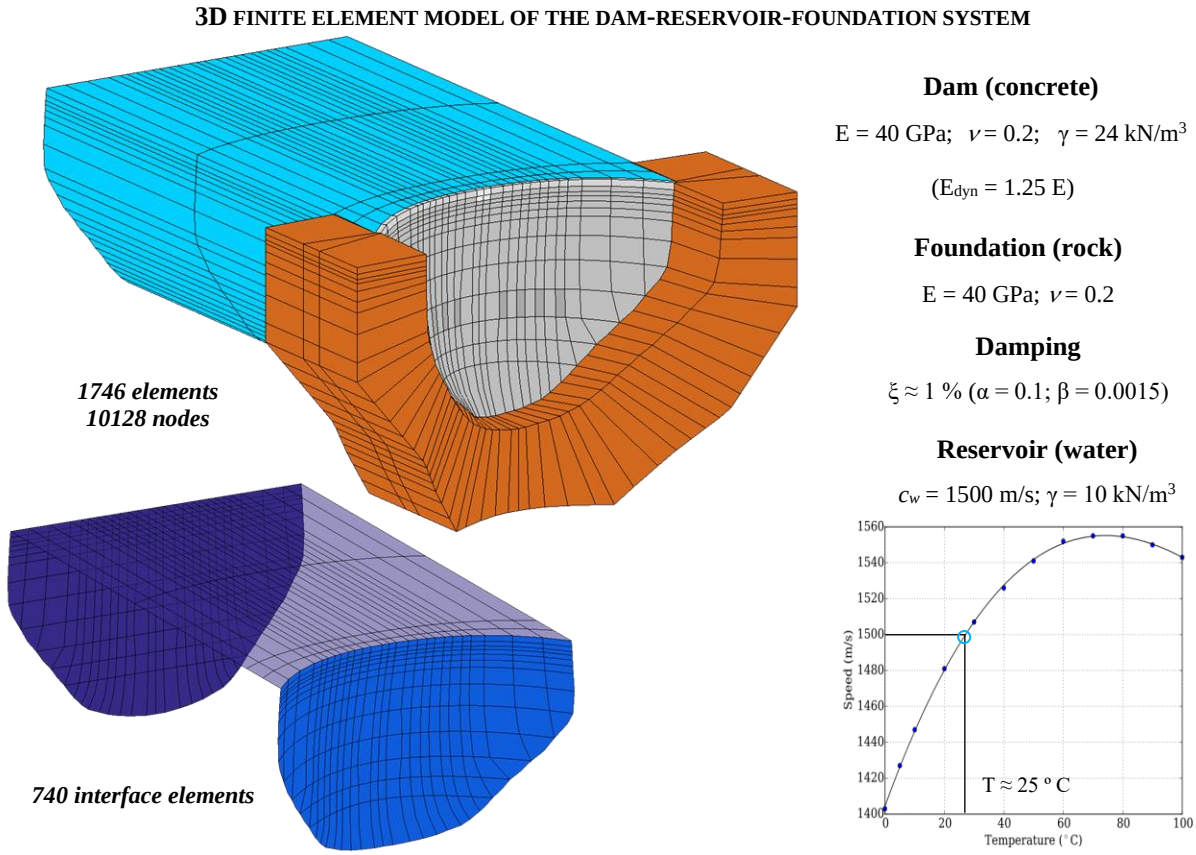

Fig. 5.46 Cahora Bassa dam. 3D finite element model of the dam-reservoir-foundation system. Material properties.

The comparison between the identified natural frequencies of Cahora Bassa dam over time and the computed frequency curves is presented in Fig. 5.47, for the first five vibration modes. The frequency values and modal configuration, calculated for two different reservoir water levels (el. 326 m and 315 m), are also shown. A new graphical representation with the frequency values represented in function of the reservoir water level is provided in Fig. 5.48. For this study, the finite element dynamic simulations were carried out assuming different water level values as inputs in the linear model of the dam-reservoir-foundation system, in order to obtain the numerical frequency curves associated with the reservoir level.

The results show that a good agreement was achieved between identified and calculated frequencies, particularly for the first three and the fifth modes, by increasing the dynamic Young's modulus in 30% and by setting the pressure wave propagation velocity to c_w = 1500 m/s. Regarding the modal configurations, the numerical model enabled to properly reproduce the shapes of the first (antisymmetric), second (symmetric), and third (symmetric) modes, for higher and lower water levels.

CAHORA BASSA DAM: EVOLUTION OF IDENTIFIED FREQUENCIES OVER TIME VS COMPUTED FREQUENCIES

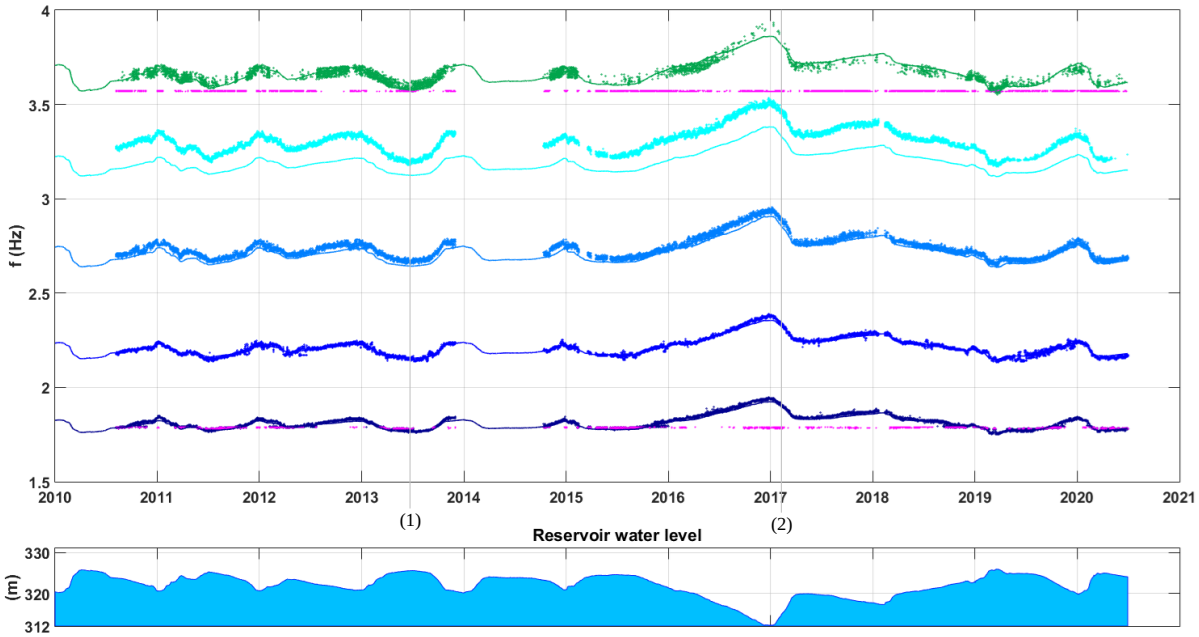

Modal analysis results considering the reservoir water level at el. 326 m (1)

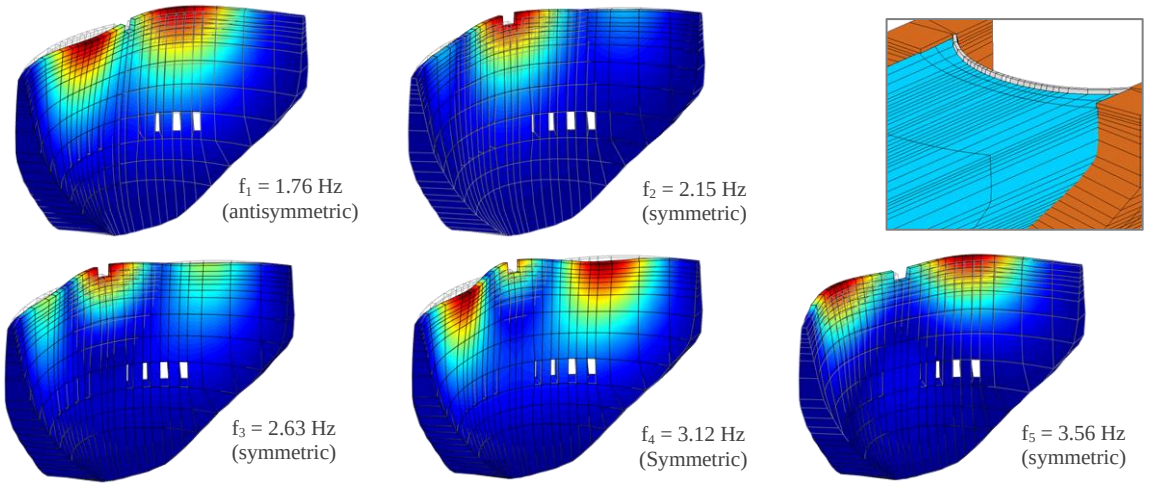

Modal analysis results considering the reservoir water level at el. 315 m (2)

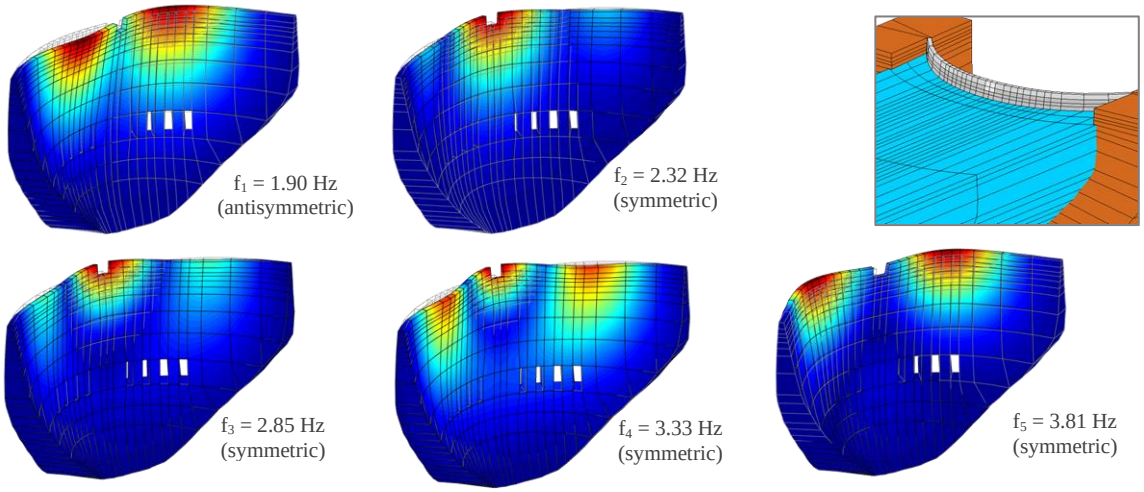

Fig. 5.47 Comparison between identified natural frequencies over time and computed frequencies for Cahora Bassa dam. Finite element modal analysis: mode shapes for two reservoir water levels.

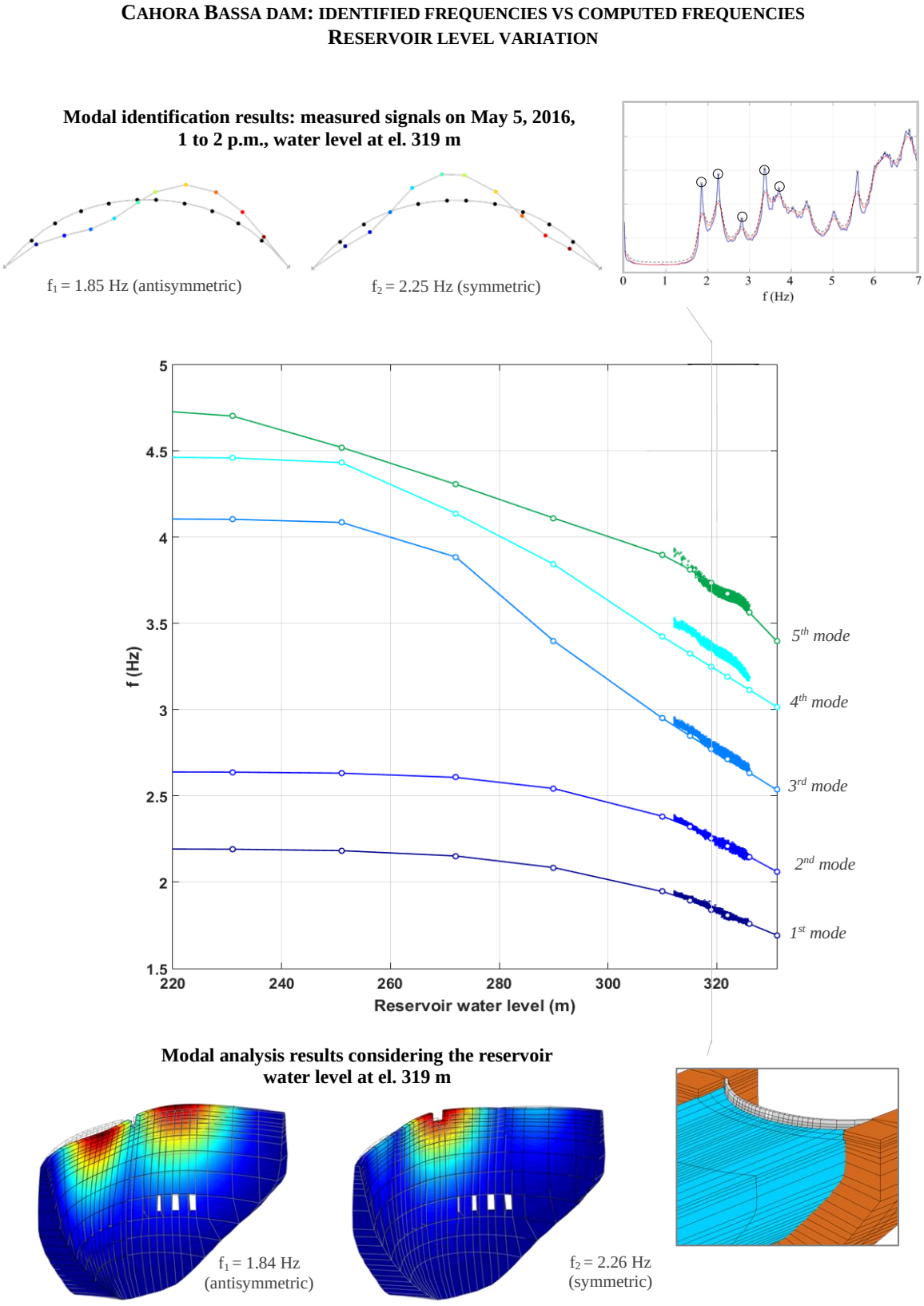

Fig. 5.48 Comparison between identified and computed natural frequencies for Cahora Bassa dam considering the reservoir water level variations.

In summary, this comparative study was of great value to increase knowledge on the dynamic response of Cahora Bassa under ambient/operational excitations, by providing a set of results based on a decade of monitoring data. First, these results have shown that the evolution of the natural frequencies of Cahora Bassa dam over time are mostly dependent on the reservoir level variations. Second, the good agreement obtained between modal identification outputs and finite element results allows to demonstrate once again the value of the linear reference model to predict the dynamic response of the dam-reservoir-foundation system of Cahora Bassa dam. Third, and despite the promising results, it could be interesting to improve the current numerical model in order to represent the geometry in greater detail, particularly in what concerns the half-hollow crest and the spillways geometry, and to propose the installation of more accelerometers, allowing to optimise the estimation of modal configurations and improve the characterization of modes with higher frequencies.

DAMAGE DETECTION USING MEASURED VIBRATIONS AND FINITE ELEMENT RESULTS

Aiming to emphasize the value of the combined use of experimental data from SSHM systems and of results obtained using advanced finite element models for structural health evaluations, an analysis using graphical representations developed to support vibration-based damage detection is presented next (Fig. 5.49). The automatically identified natural frequencies over time (red circles) are compared with the calculated frequencies (blue lines) for the first and second vibration modes of Cahora Bassa dam. As proposed previously in the application study for Cabril dam, the numerical frequency curves are computed using: (i) the reference model without damage; and (ii) a model to simulate evolutive damage over time, considering a gradual increase of the damage value (d) from 0 to 5% over the last ten years, and assuming, in a simplified way, a gradual decrease in the concrete Young's modulus, $E_d(t) = E \cdot (1 - d(t))$.

From this comparative study, it is worth highlighting that the modal parameters obtained from monitoring data gathered in the last year are very close to those identified during the early monitoring period, for similar water levels. In addition, for both vibration modes, a very good agreement is achieved between identified and computed values when using the linear model without damage (calibrated for the initial monitoring period taken as reference), which seems to indicate that there are no signs of relevant structural changes due to concrete deterioration. However, in the numerical simulation for the scenario of evolutive damage, there is a significant decrease in the computed natural frequencies over a period of 10 years that was not detected by examining the identified frequencies; this shows that the effects of a considerable deterioration phenomenon could possibly be detected using vibration-based data.

In conclusion, this study points to the fact that the behaviour of Cahora Bassa dam in normal operating conditions has not suffered important alterations over the last decade, which could mean that the existing deterioration phenomenon is not affecting the structural health of the dam in a noticeable way so far. However, Cahora Bassa dam will reach 50 years in operation in 2024, hence making it essential to continue to evaluate dam behaviour regularly based on this type of analysis, in order to support structural health assessment.

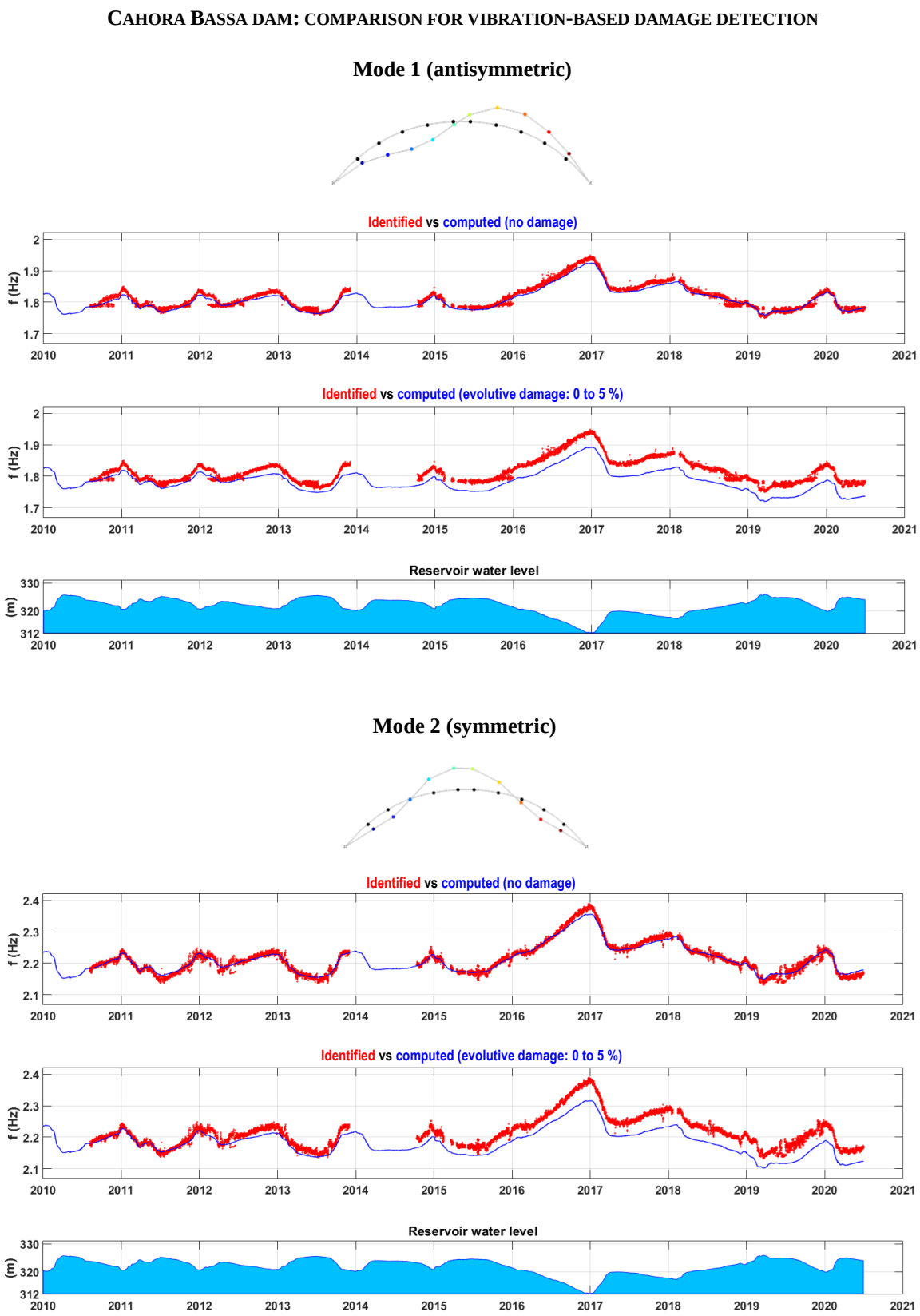

Fig. 5.49 Analysis of natural frequencies for vibration-based damage detection in Cahora Bassa dam. Evolution of identified natural frequencies over time (2010 to 2020) and comparison with computed frequencies using the reference linear model (no damage) and a test model considering evolutive damage (0 to 5%). First and second vibration modes.

5.3.3 LINEAR SEISMIC RESPONSE: MEASURED AND COMPUTED ACCELERATIONS

This subchapter presents an analysis on the seismic behaviour of Cahora Bassa dam during a seismic event detected at the dam site on June 21, 2017, using the acceleration time histories measured with the SSHM system at the base and at the top the dam, which are compared with numerical results from *DamDySSA*.

The goal is to evaluate the recorded acceleration amplification from the base to the top of the dam, and then to investigate the damping ratio that is required in the numerical model to enable an accurate simulation of the dam response under low intensity earthquakes. Thus, this study aims not only to contribute by providing results on the measured seismic response of a thin large arch dam, but also to validate the numerical model used for linear seismic response analysis of Cahora Bassa dam.

EARTHQUAKE ON JUNE 21, 2017. MEASURED ACCELERATIONS

The seismic event that was detected on June 21, 2017, in Cahora Bassa dam had an epicentre at about 32 km from the dam site (Fig. 5.51). The seismic waves arrived at the dam from the west-northwest, between the upstream-downstream and cross-valley directions. The water level on the reservoir was at el. 319.70 m (11.3 m below the crest) on the day of the earthquake. This was a close earthquake that caused relatively low amplitude vibrations in Cahora Bassa dam, with peak accelerations of about 40 mg at the crest centre.

EARTHQUAKE ON JUNE 21, 2017. DISTANCE: 32 km FROM CAHORA BASSA DAM

Fig. 5.50 Seismic event on June 21, 2017, automatically recorded and detected at Cahora Bassa dam.

The seismic acceleration time histories recorded with the triaxial sensor B_{xyz}, installed at the dam downstream base, are presented in Fig. 5.51. The maximum accelerations were 21.9 mg in the cross-valley direction, 9.03 mg in the upstream-downstream direction, and 6.1 mg in the vertical direction.

In this study the goal is to evaluate the measured response at the top of the dam and then perform the comparison with the numerical response. The seismic accelerations recorded at the upper gallery, at el. 326

m, namely with uniaxial accelerometers U_5 and U_6, located to the right and to the left of the central section, are shown in Fig. 5.52. For this earthquake, the peak acceleration recorded at the upper gallery with accelerometer U_6, was of 37.76 mg, which is slightly higher than the maximum acceleration recorded with U_5, of 35.86 mg. In this case, the acceleration amplification factor from the base to the top is of about 4.2 times, in the upstream-downstream direction.

These results show the potential of the Cahora Bassa dam SSHM system to measure vibrations induced by seismic events, enabling to record acceleration time histories in the crest gallery and near the dam-rock interface, at both right and left banks and at the bottom of the valley, which can be used to characterize the seismic actions on the dam site and to analyse the seismic behaviour of large arch dams.

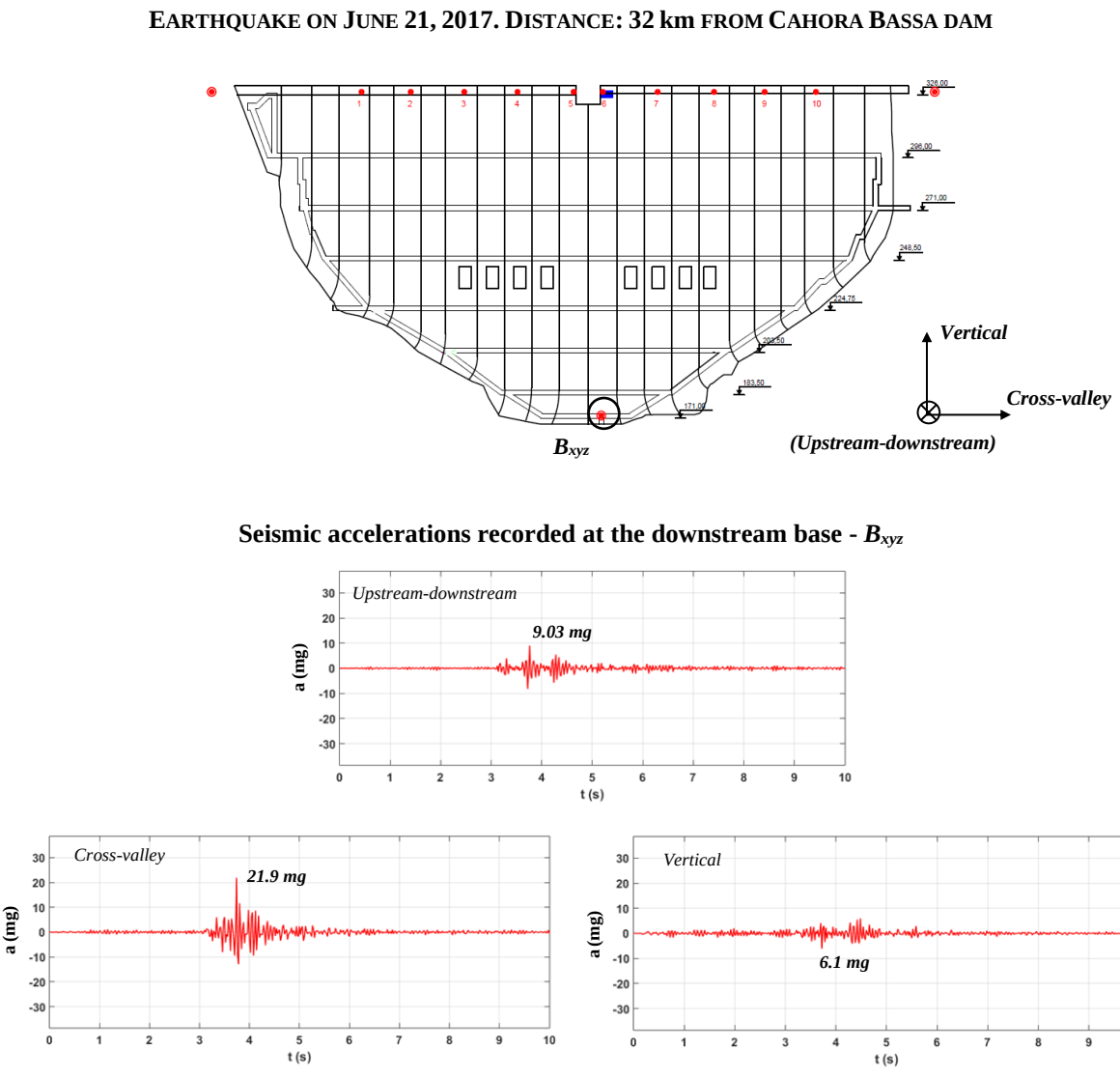

Fig. 5.51 Seismic event on June 21, 2017. Measured accelerations with the triaxial accelerometer B_{xyz} at the downstream base of Cahora Bassa dam.

EARTHQUAKE ON JUNE 21, 2017. DISTANCE: 32 km FROM CAHORA BASSA DAM

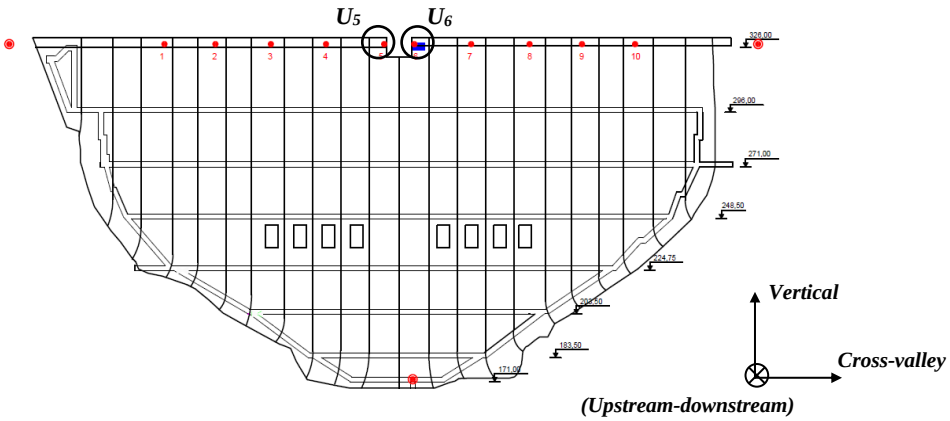

Seismic accelerations measured at the upper gallery

Right of the central section – U_5

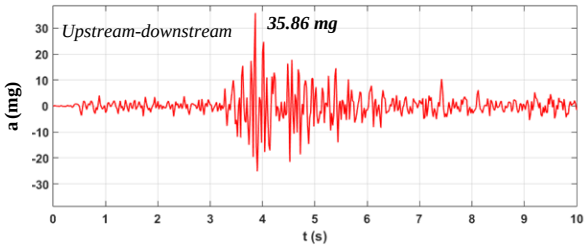

Left of the central section- U_6

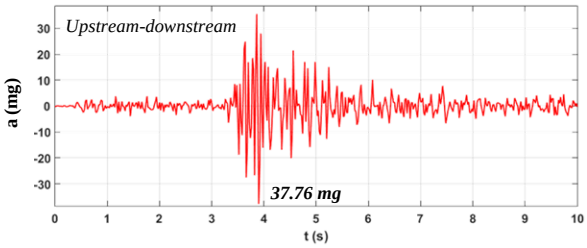

Fig. 5.52 Seismic event on June 21, 2017. Measured accelerations in the upper gallery of Cahora Basa dam with uniaxial accelerometers U_5 and U_6.

FINITE ELEMENT SEISMIC ANALYSIS AND COMPARISON WITH MEASURED RESPONSE

Aiming to simulate the measured seismic response of Cahora Bassa dam, a finite element analysis was carried out using the module of *DamDySSA* module for linear seismic analysis, considering the same model of the dam-reservoir-foundation system and material properties that were adopted for modal analysis (Fig. 5.53). Linear elastic behaviour is assumed for concrete and the model does not include any joints.

In order to consider realistic conditions in the seismic simulations, the model reservoir level was set to 12 m below the crest, at el. 319 m, as close as possible to the water level on the day of the earthquake. Additionally, the seismic accelerations recorded at the dam base with triaxial accelerometer B_{xyz} are used as seismic input. As previously mentioned, in *DamDySSA* the seismic input accelerations are applied at the base of the massless foundation without considering spatial variation.

The comparison between recorded and calculated seismic response is provided in Fig. 5.54, showing that a very good agreement was obtained for the upstream-downstream accelerations of both measurement points, U_5 and U_6, located at the upper gallery of Cahora Bassa dam. These results were achieved considering a damping ratio of about 1% for the frequency of the first vibration modes of the dam-reservoir-foundation system, assuming the Rayleigh damping parameters presented in Fig. 5.53 to calculate the damping matrices of the dam and foundation; this damping value is perfectly reasonable to be used in linear seismic

analysis of large arch dams (Chopra & Wang, 2012; Proulx et al., 2004; Proulx & Darbre, 2008; Robbe, 2017; Robbe et al., 2017).

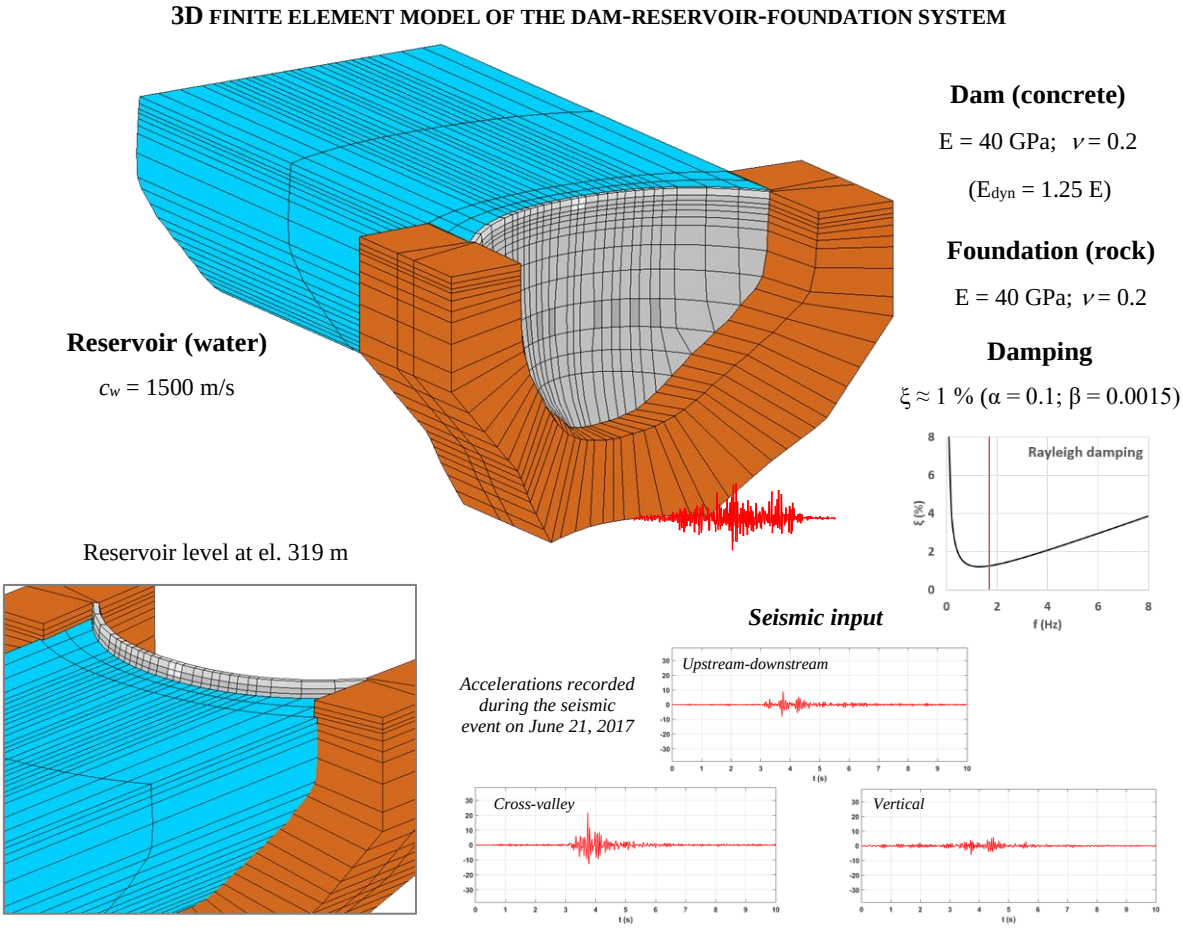

Fig. 5.53 Cahora Bassa dam. 3D finite element model of the dam-reservoir-foundation system used for linear seismic analysis and seismic input.

To summarise, the good agreement between measured and computed response for Cahora Bassa dam was achieved using as seismic input the acceleration time histories recorded at the base of the dam and considering a coherent damping ratio value of 1%. In this scope, it is worth recalling that for the case of Cabril dam, accelerations at the dam base were not available, and thus the accelerations recorded near the dam-rock interface, at a much higher elevation in the right bank, were used as seismic input. Consequently, a good agreement between measured and computed accelerations was only achieved for Cabril dam when a 10% damping ratio was used. Therefore, this study allowed to show once more the value of *DamDySSA* for linear seismic response analysis of arch dams, under low amplitude earthquakes.

Furthermore, it is relevant to remind that the model of Cahora Bassa dam used in this study is a simplified one, given that it does not consider the exact shape of the crest and does not include the half-height spillways nor the ribs at the upstream face in detail. Therefore, even considering the good agreement achieved in this study, it could be interesting to conduct additional analyses in the future to further investigate the seismic

response of Cahora Bassa dam based on recorded accelerations, ideally using a more advanced model of the dam that properly accounts for the mentioned features. In addition, not only to allow for a better characterisation of the modes of higher frequencies (as mentioned in the previous section) but also to enable a more detailed evaluation of the recorded accelerations in the dam body, it could be of great interest to install more accelerometers in other positions of the structure.

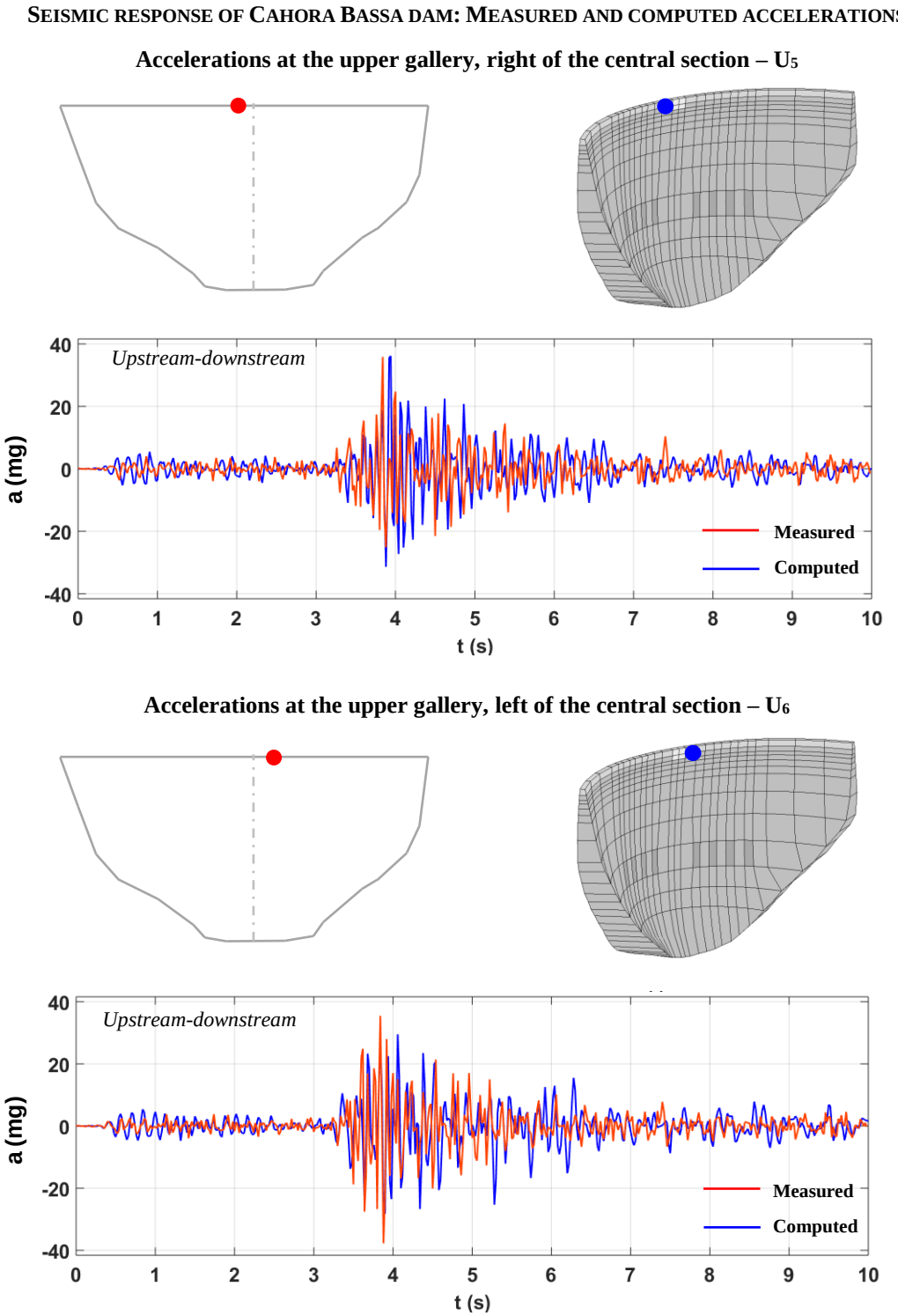

Fig. 5.54 Seismic response of Cahora Bassa dam: seismic event on June 21, 2017. Comparison between measured and computed accelerations: upper gallery, right and left of the surface spillway.

5.3.4 NON-LINEAR SEISMIC ANALYSIS CONSIDERING JOINT MOVEMENTS AND CONCRETE DAMAGE

This subchapter presents a study on the seismic response of Cahora Bassa dam under a strong earthquake, considering the movements of the vertical contraction joints and the concrete damage. The intent is to analyse the influence of the non-linear joint behaviour on the structural response of the Cahora Bassa thin large arch dam, through the comparison between linear and non-linear results, and to examine the resulting tensile and compressive damages in the dam body.

The numerical calculations were carried out using *DamDySSA*, in order to further demonstrate the potential of the developed method for non-linear dynamic analysis, considering the 3D finite element model of the dam-reservoir-foundation system shown in Fig. 5.55. This is an updated version of the model used in the previous sections for linear dynamic analysis, which now includes interface elements for simulating the vertical contraction joints and the dam-rock interface. The dam concrete and foundation rock are isotropic materials and the water in the reservoir is a compressible fluid, considering the same properties as before. A damping ratio of about 10 % is considered in order to account for a higher energy dissipation due to non-linear concrete and joint behaviour.

The behaviour of concrete up to failure is modelled using a strain-softening constitutive damage law with tensile strength $f_t = 3\,\text{MPa}$ and compressive strength $f_c = -30\,\text{MPa}$, assuming a fracture energy $G_f = 0.9\,\text{kN.m}/\text{m}^2$ and an ultimate compressive strain $\varepsilon_u^- = -9.5\times10^{-3}$. Furthermore, the opening/closing and sliding joint movements are simulated based on proper failure criteria and normal and shear stress-relative displacement laws, using adequate values for normal and shear stiffness. Null cohesion and a 30º friction angle are considered for the vertical contraction joints.

The seismic behaviour of Cahora Bassa dam is simulated for the dynamic load combination involving the dam self-weight (SW), the hydrostatic pressure for a full reservoir scenario (HP331), and a seismic load (SEISMICL) applied in the upstream-downstream direction. The seismic input is the accelerogram presented previously in the study for Cabril dam, with a duration of 10 s and a peak acceleration of 0.6g, which is six times higher than the horizontal peak ground acceleration defined for the MDE (0.102g), in accordance with the study that evaluated the seismic hazard for the area of Cahora Bassa dam (Li-EDF-KP, 2001).

STATIC RESPONSE: CALIBRATION OF CONTRACTION JOINTS STIFFNESS

The static response of Cahora Bassa dam is presented for the load combination SW+HP331 (Fig. 5.56). The calculations were carried out using the linear model without joints and the above non-linear model with joints, in order to verify the suitability of the elastic properties adopted for the vertical contraction joints. As intended, the results obtained with both models are very similar. The good agreement between linear and non-linear response was achieved assuming vertical joints with a normal stiffness of 5×10^7 kN/m, which is used from now on. Nevertheless, as expected, the maximum displacement computed using the non-linear model (42.4 mm) is slightly larger than the one obtained for the linear model (38.5 mm).

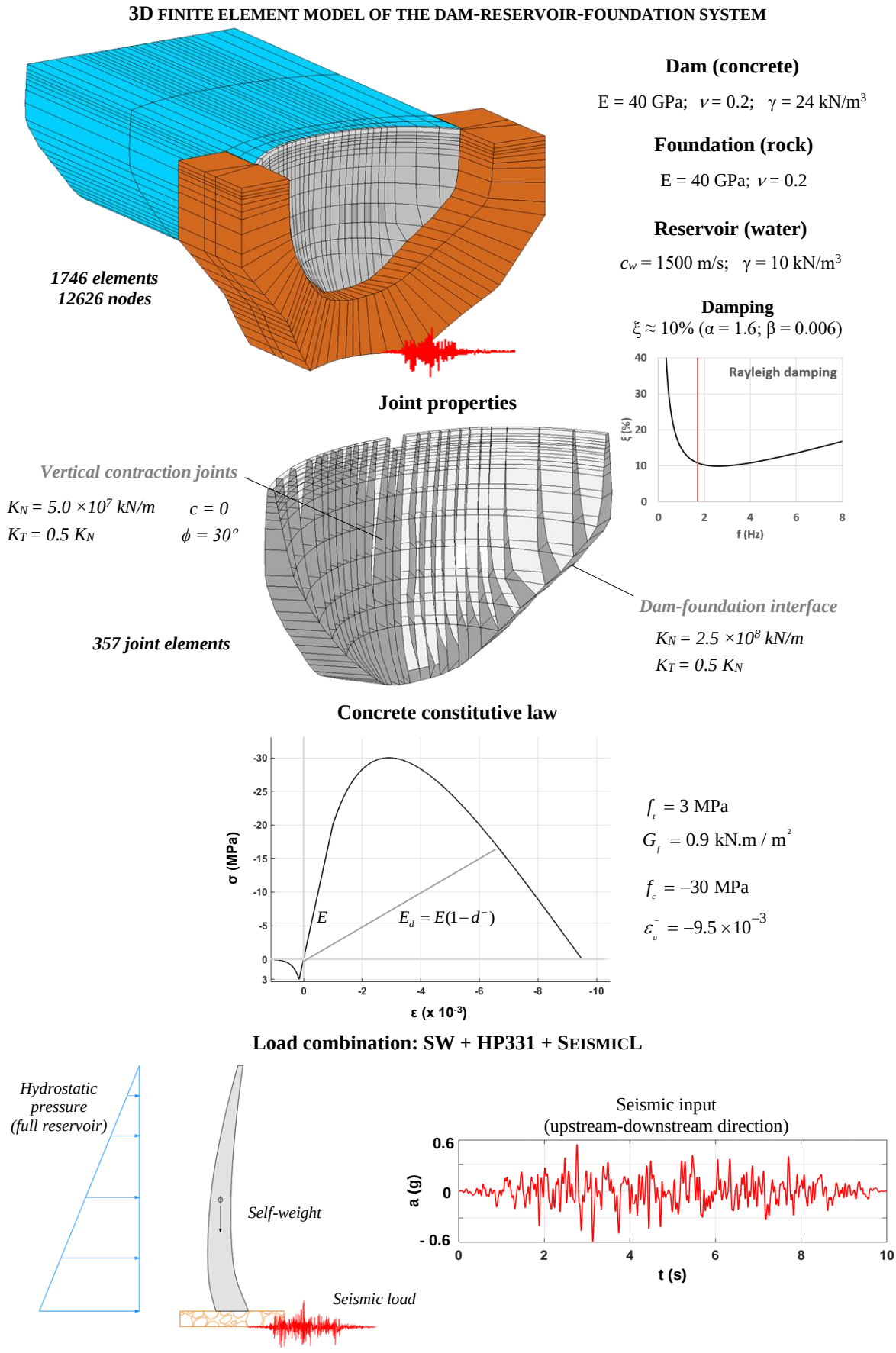

Fig. 5.55 Cahora Bassa dam. 3D finite element model of the dam-reservoir-foundation system used for non-linear seismic analysis. Properties, joints, concrete constitutive law, load combination, and seismic input.

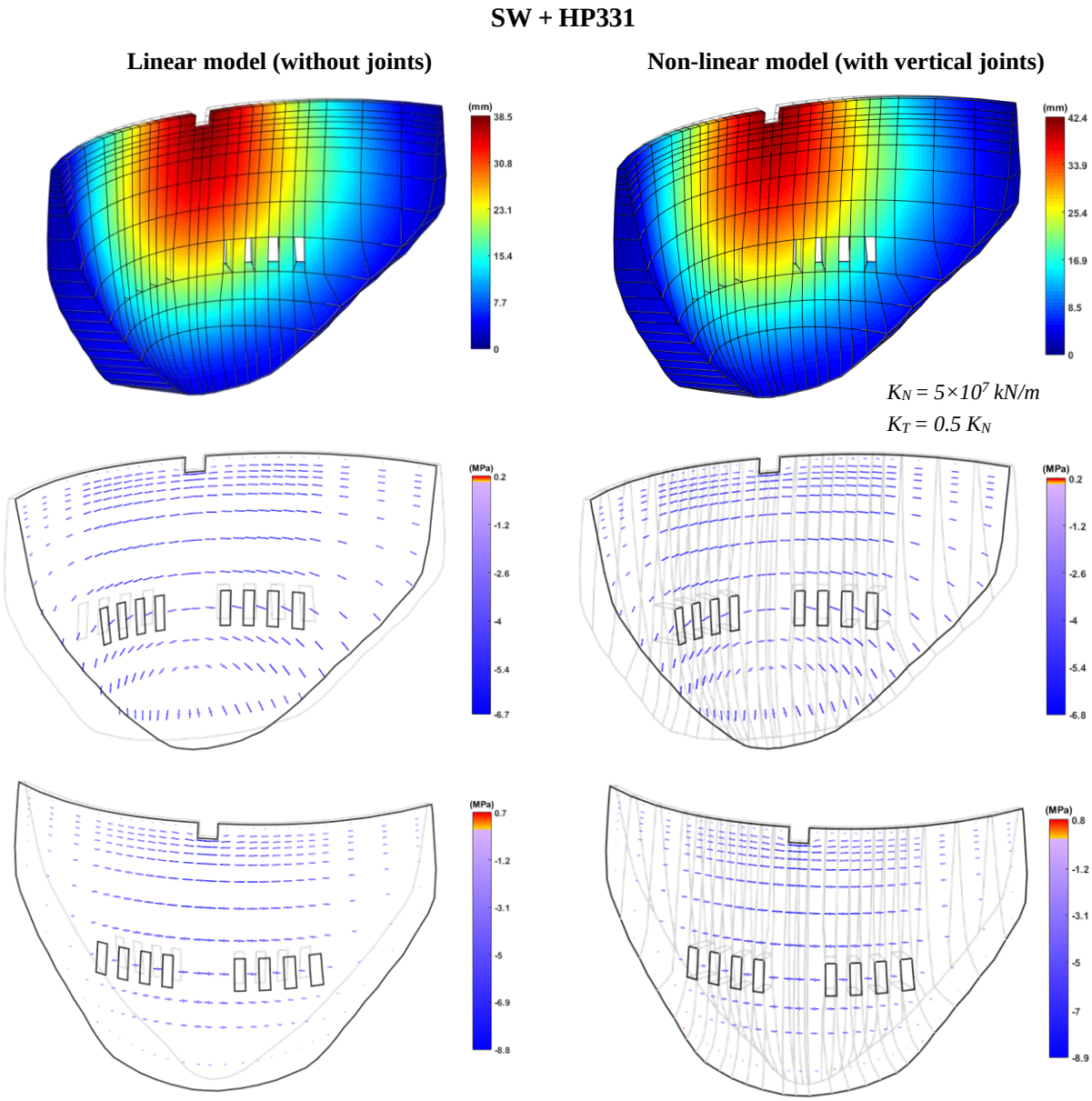

Fig. 5.56 Static response of Cahora Bassa dam for SW + HP331. Displacements and principal stresses calculated using a linear model without vertical joints and a non-linear model with vertical joints.

SEISMIC RESPONSE

The seismic response of Cahora Bassa dam under the dynamic load combination SW + HP331 + SEISMICL, considering the seismic input with a 0.6g peak acceleration, is now analysed. Results from both linear and non-linear calculations are presented.

Using the linear model without joints, the seismic response results are presented in Fig. 5.57. The dam deformation is mainly influenced by the upstream-downstream motions induced by the seismic forces. The maximum upstream displacement is 116.1 mm, and the maximum downstream displacement is 200.2 mm, both calculated at the crest centre, around the surface spillway. Large displacements in the upstream direction are also computed at the top of the lateral cantilevers (≈ 70 mm).

Regarding the respective linear stress fields, when the dam moves towards upstream, high arch compressions arise at the upper central part of the dam, below the surface spillway, both at the downstream face (- 22.3 MPa), if the maximum deformations occur at the top of the central section, and at the upstream face (- 19.9 MPa), in case the larger deformations occur at the lateral cantilevers. Important compressions, approximately in the arch direction, also arise at the upstream upper part of the cantilevers to the right and to the left of the central cantilevers (-17.1 MPa). Considerable arch tensions are calculated in the blocks around the surface spillway, at the upstream (12.7 MPa) and downstream (7.2 MPa) faces, as well as at the upper part of the lateral cantilevers, also at both the upstream (10.4 MPa) and downstream (7.4 MPa) surfaces. When the dam moves in the downstream direction, maximum arch compressions of - 28.9 MPa are computed at the upstream face, below the crest spillway. These stress values indicate that joint opening movements and concrete damage are likely to occur in the non-linear calculations.

The non-linear seismic response, simulated considering joint movements and concrete damage, is presented afterwards (Fig. 5.58). The maximum displacements calculated in the central section are now 83.1 mm, in the upstream direction, and 195.8 mm, in the downstream direction: both values are lower than those obtained in the linear analysis, which can be explained by the fact that damping has been introduced in the vertical contraction joints. In this case, the maximum displacements in the upstream direction (112.5 mm) are computed at the crest of the lateral cantilevers, when the larger joint movements occur - the maximum sliding is of 5 mm, at the top of the cantilevers adjacent to the central section, while the maximum opening is around 9 mm, at the upper part of the lateral cantilevers.

With regard to the non-linear stress fields, the results show that there was a decrease of the arch stresses at the upper part of the dam, due to the opening of the vertical contraction joints, when the dam suffers considerable deformations in the upstream direction. However, this release of arch stresses leads to an increase of cantilever stresses, particularly along the height of the lateral cantilevers. It should be noted that the maximum tensions represented here do not exceed the concrete tensile strength (3 MPa), which points to the occurrence of tensile damage. When the dam moves in the downstream direction, the vertical joints close and thus the response is similar to that obtained in the linear seismic simulation, with maximum arch compressions (-23.6 MPa) calculated at the upstream face, below the surface spillway.

To enable a deeper analysis on the influence of the joint movements on the seismic behaviour of Cahora Bassa dam, new results are provided for comparison between linear and non-linear seismic response.

First, by analysing the envelopes of radial displacements along the height of the central section (Fig. 5.59), it is possible to see that the static displacement value at the crest is larger for the case of non-linear behaviour. The linear displacement envelope shows that the seismic motion at the top of the central section is of about four times the static displacement, corresponding to semi-amplitudes of around 151 mm towards upstream and 160 mm towards downstream. However, when considering non-linear behaviour, there is a decrease in the amplitude of the displacement envelope, with semi-amplitudes of around 122 mm in the upstream direction and of 150 mm in the downstream direction. As stated previously, this is most likely related to the damping associated with the joint elements used to simulate the behaviour of the vertical contraction joints.

Next, the observation of the arch and cantilever stresses envelopes (Fig. 5.59, Fig. 5.60 and Fig. 5.61) enables to show how the opening/closing and sliding movements of the vertical contraction joints significantly influenced the seismic response of Cahora Bassa dam. Regarding the arch stress envelopes, when the dam moves in the upstream direction and the vertical contraction joints open, there is a considerable release of the arch stresses along the upper part of the dam, near the crest and below the surface spillway. This is particularly relevant in terms of arch tensions, which are considerably reduced: from 9.8 MPa (linear) to 0.8 MPa (non-linear), on the upstream face, and from 12.9 MPa (linear) to 3 MPa (non-linear), on the downstream face. In addition, the results show that the decrease of arch stresses leads to an overall increase of cantilever stresses, in particular of the tensions along the base and at the upper part of the taller cantilevers, on the upstream face, as well as along the upper half of the downstream face of the dam. Furthermore, it can be noted an increase of cantilever compressions at the upper part of the taller cantilevers, at the upstream face, and along the downstream side of the central cantilevers.

In what regards the damaged state (Fig. 5.62), the results show that the installed cantilever stresses exceed the concrete tensile strength (3 MPa), as expected, and thus high tensile damage arises along the upper half of the downstream face, and in a sort of V shape at the upper part of the taller cantilevers, at the upstream face. There are several locations where concrete failure occurs (damage values of 100%), including some zones where it has propagated across the thickness of the main cantilevers. High tensile damages appear also at the side cantilevers, close to the right and left banks, and at the upstream base. Nevertheless, it should be emphasized that the release of the arch stresses along the top of the dam prevented the occurrence of tensile damage. Furthermore, the significant compressive stresses installed at the upper part of the central cantilevers, below the surface spillway, cause compressive damage in concrete, with maximum damage values of about 60%.

To summarize, the results obtained here have shown that a 0.6g seismic load can cause significant deformations in the Cahora Bassa arch dam, originating important contraction joint movements that clearly alter the structural response of the dam. Moreover, the high tensions that arise result in considerable tensile damage at the upper part of the structure, which even crosses the entire thickness of the taller cantilevers in some areas. This tensile damage state would not be expected to cause global collapse, but it could affect its structural integrity and require repairs. In addition, since the dam globally presents very high arch compressions, compressive damage starts to arise in key locations, namely under the surface spillway. Even so, considering that Cahora Bassa dam is a very thin double curvature arch dam, this study shows that it presents a very good seismic performance under a seismic load with a peak acceleration that is six times greater than the 0.102g defined for the MDE at the dam site.

The current application study allowed to show the suitability of the model used for simulating the Cahora Bassa dam-reservoir-foundation system, as well as to further demonstrate the potential of *DamDySSA* to perform non-linear seismic analysis of arch dams, considering joint movements and concrete damage.

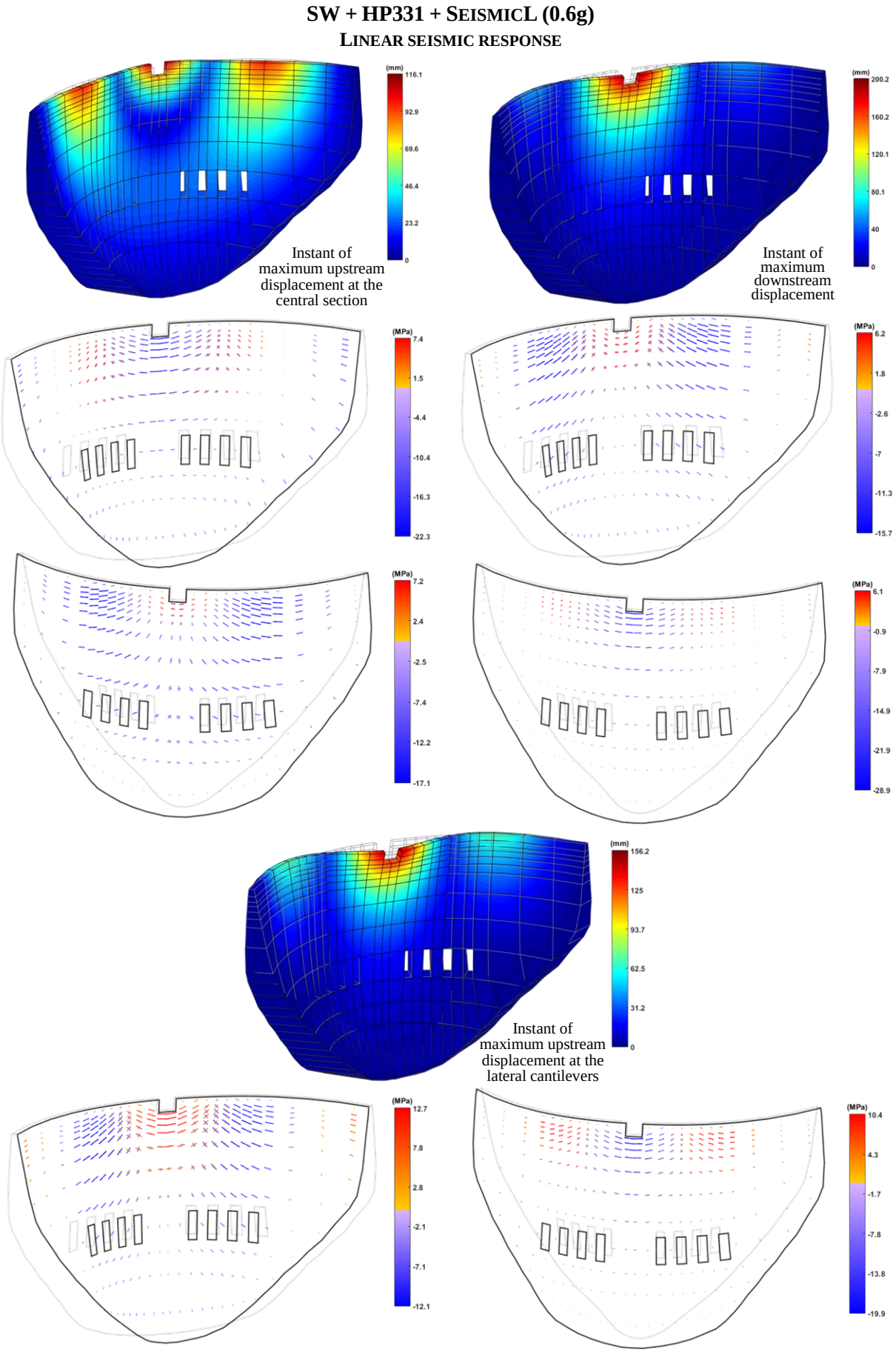

Fig. 5.57 Linear seismic response of Cahora Bassa dam for SW + HP331 + SEISMICL (0.6g). Displacements and principal stresses.

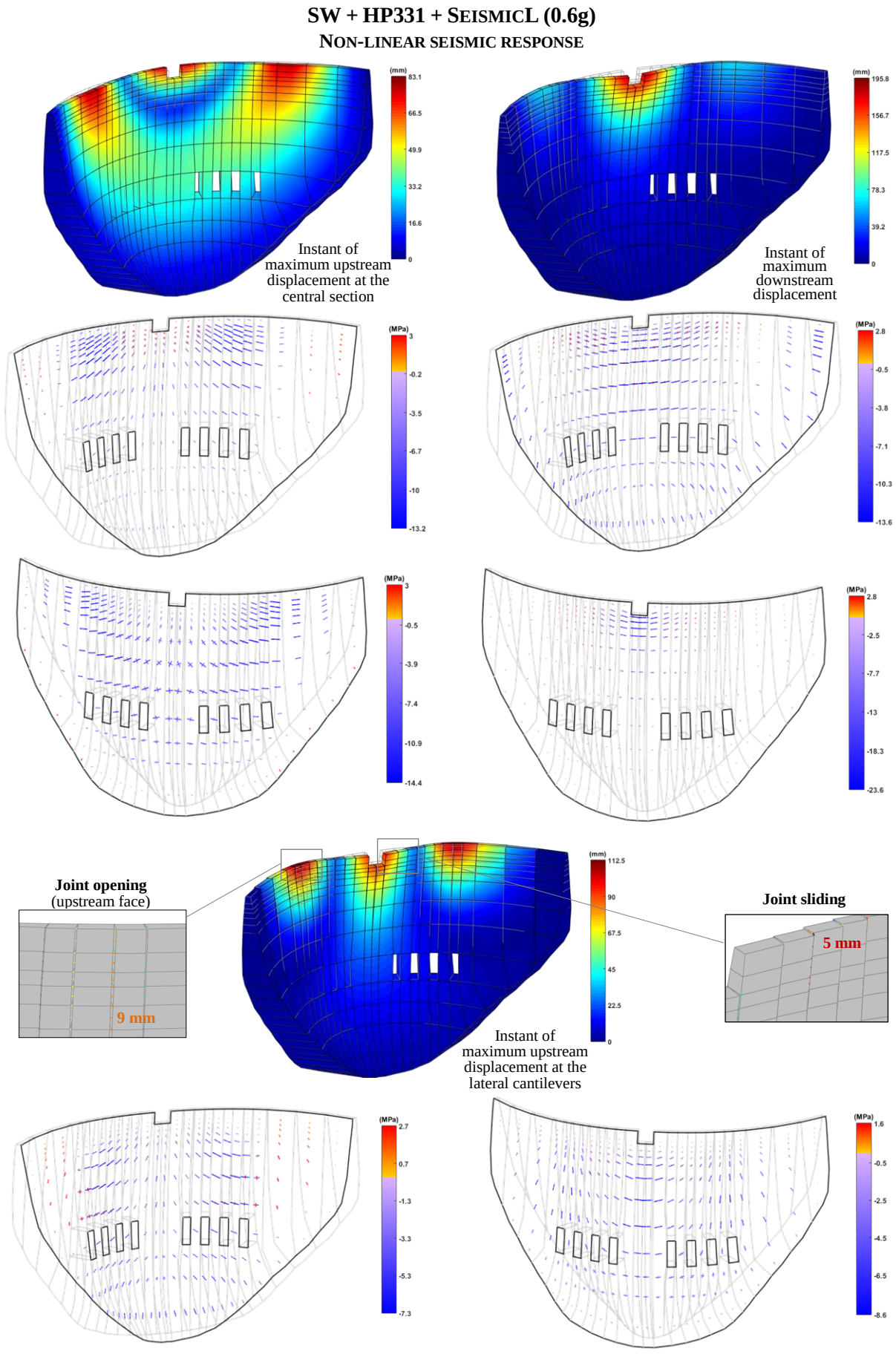

Fig. 5.58 Non-linear seismic response of Cahora Bassa dam for SW + HP331 + SEISMICL (0.6g). Displacements and principal stresses.

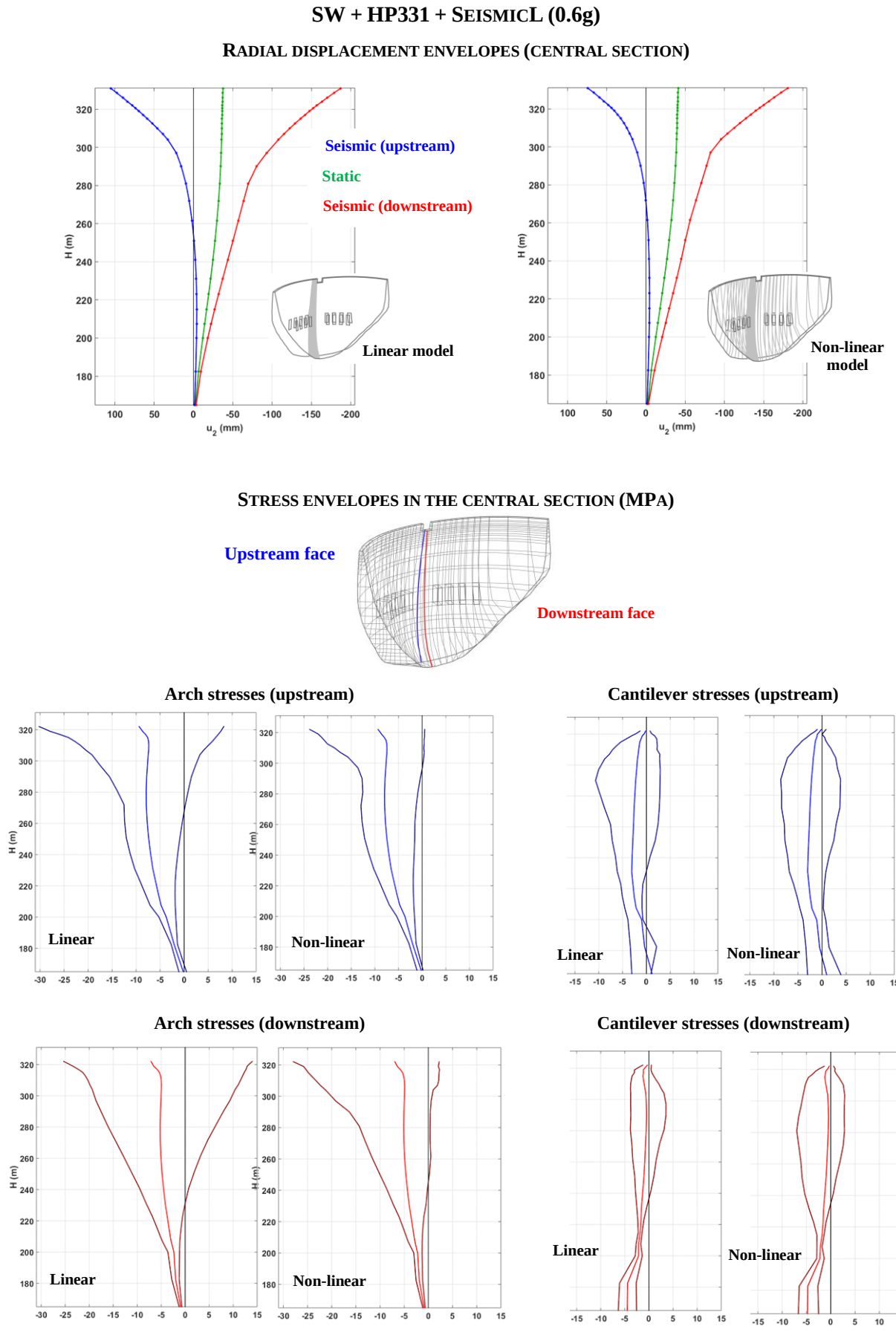

Fig. 5.59 Linear and non-linear seismic response of Cahora Bassa dam for SW + HP331 + SEISMICL (0.6g). Radial displacements and arch/cantilever stresses envelopes.

SW + HP331+ SEISMICL (0.6g)

ARCH STRESSES ENVELOPES

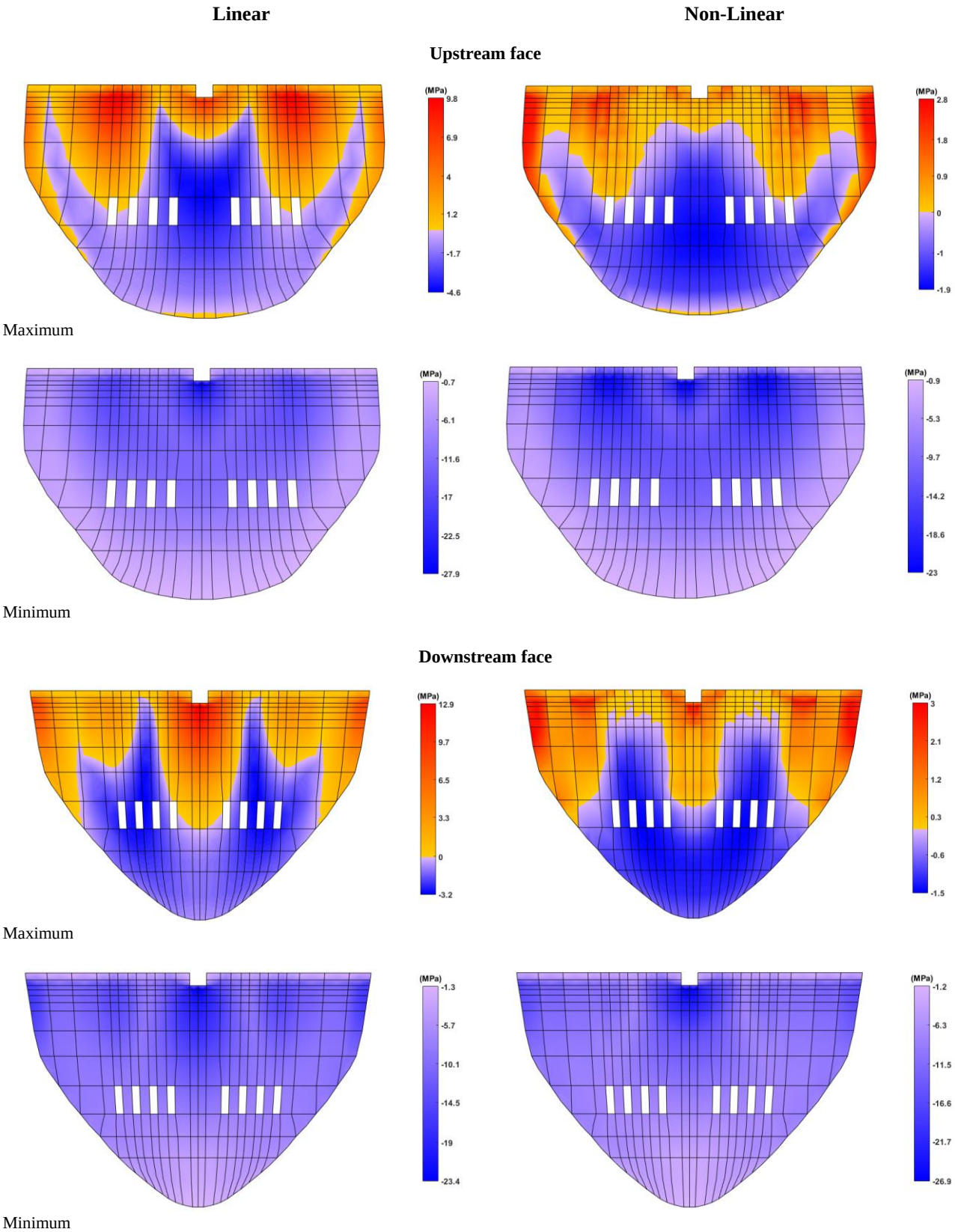

Fig. 5.60 Linear and non-linear seismic response of Cahora Bassa dam for SW + HP331 + SEISMICL (0.6g). Arch stresses envelopes.

SW + HP331+ SEISMICL (0.6g)

CANTILEVER STRESSES ENVELOPES

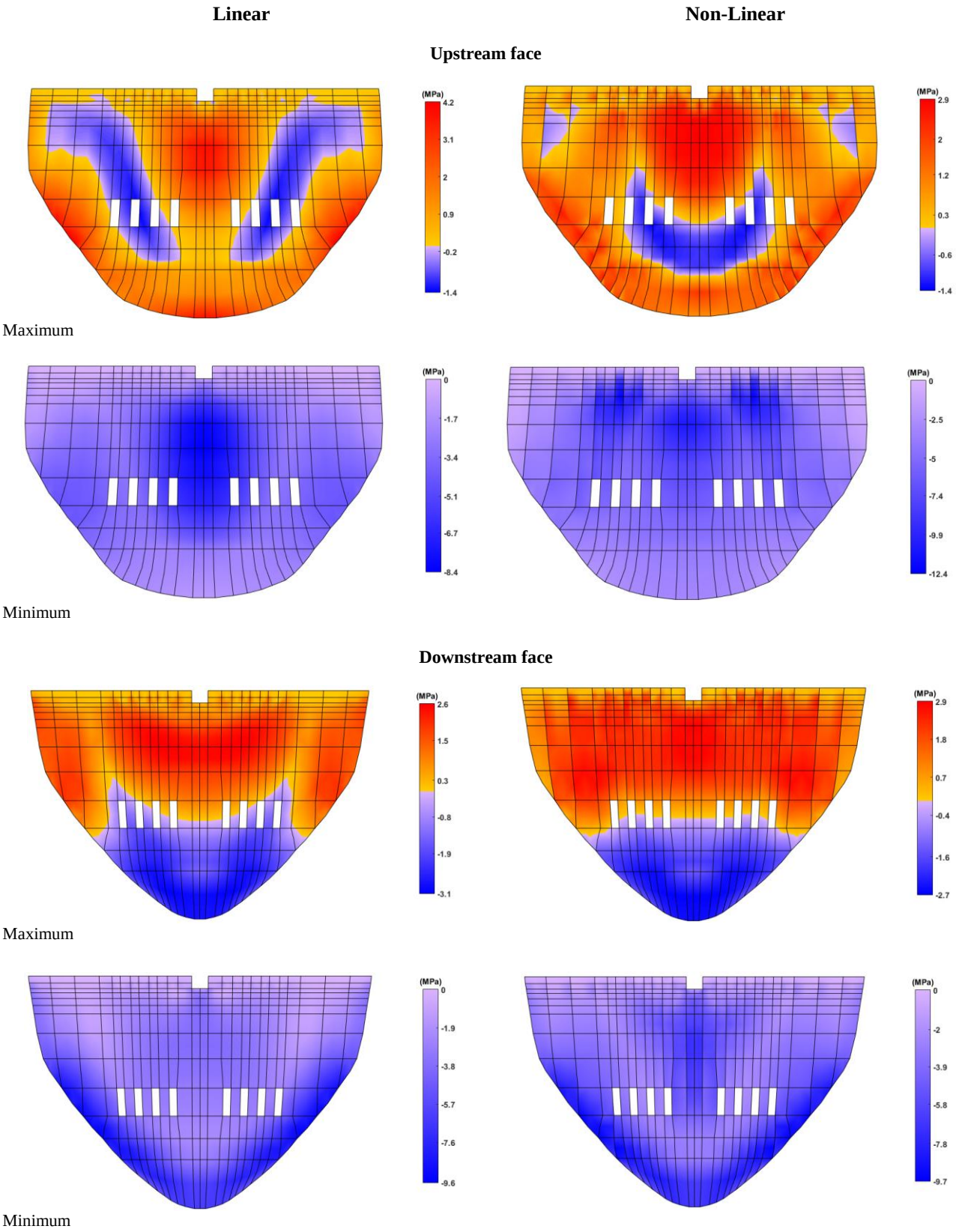

Fig. 5.61 Linear and non-linear seismic response of Cahora Bassa dam for SW + HP331 + SEISMICL (0.6g). Cantilever stresses envelopes.

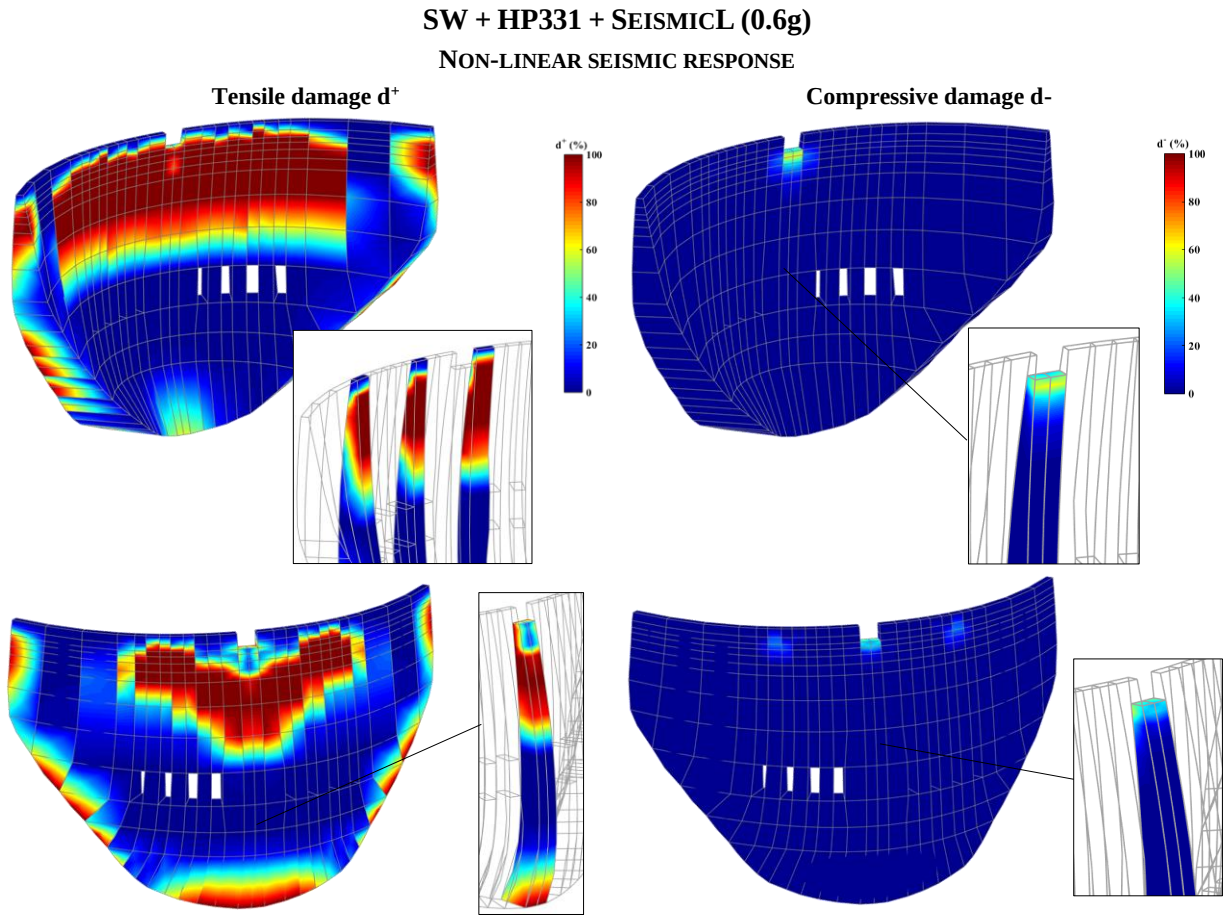

Fig. 5.62 Non-linear seismic response of Cahora Bassa dam for SW + HP331 + SEISMICL (0.6g). Tensile and compressive damage.

5.3.5 SEISMIC SAFETY ASSESSMENT. ENDURANCE TIME ANALYSIS

The non-linear seismic behaviour of Cahora Bassa dam is analysed. The proposed methodology, based on Endurance Time analysis (Estekanchi et al., 2004) and taking into consideration adequate seismic performance criteria (Wieland, 2016), is used for seismic safety assessment. The performance endurance limits are determined by evaluating the evolution of both tensile and compressive damages.

The seismic simulations were carried out using *DamDySSA* and the new 3D model of the dam-reservoir-foundation system (Fig. 5.63). This is a more refined version of the model used in the previous calculations, with three elements in thickness and a greater level of detail in the dam mesh. Despite the good results obtained previously, the decision was made to use this model in order to improve the characterization of the damage distributions, not only in the upstream and downstream faces but also along the thickness, for seismic safety assessment. The same material properties are used for the dam, the foundation, and the reservoir, as well as for simulating the non-linear behaviour of concrete and the joint movements.

The dynamic load combination considered for non-linear seismic analysis includes the dam self-weight of (SW), the hydrostatic pressure for full reservoir (HP331), and an intensifying seismic load (SEISMICL) applied in the upstream-downstream direction. The same artificial intensifying acceleration time history is used as seismic input, with peak accelerations increasing from 0.1g to about 1.5g in 15 s.

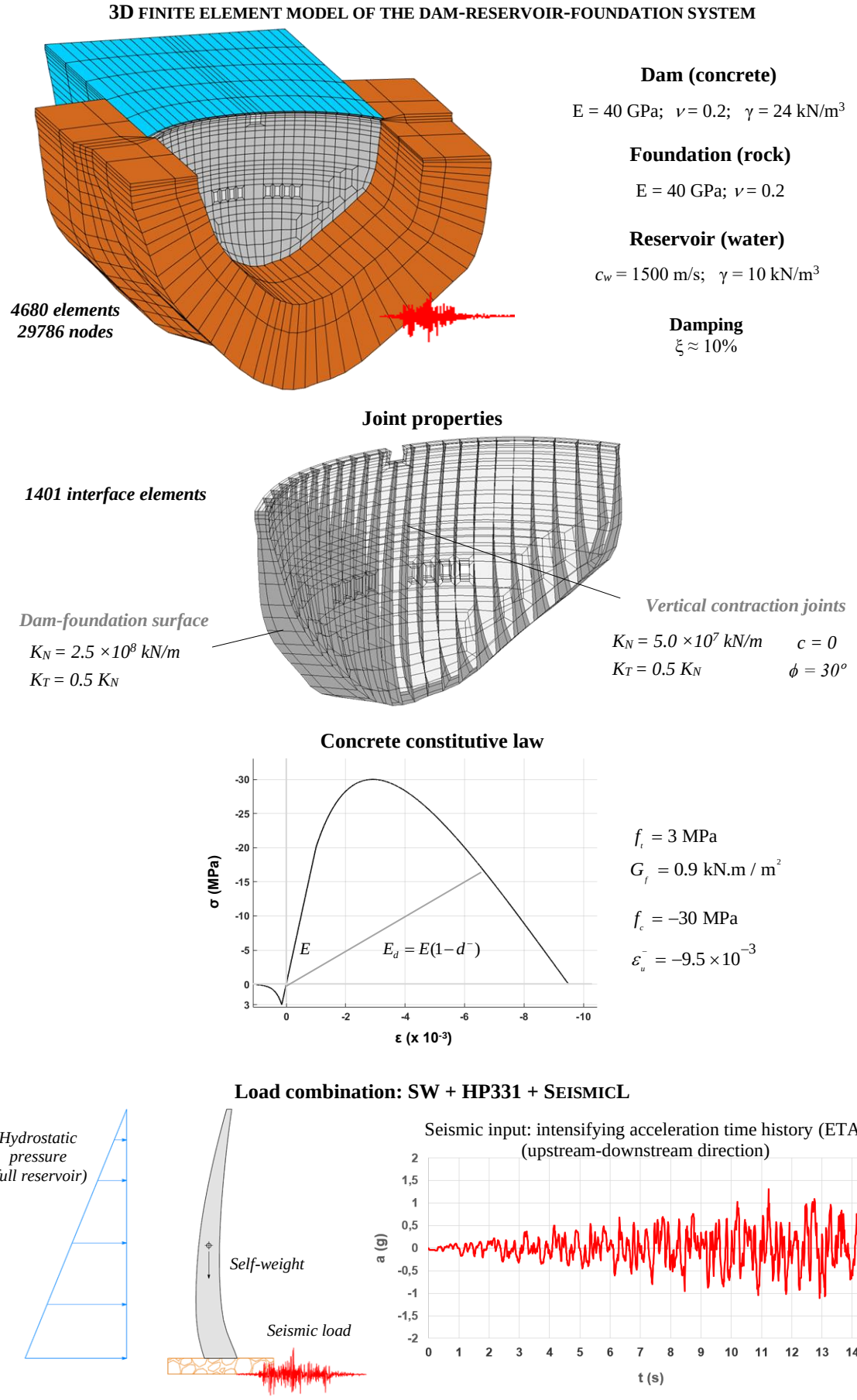

Fig. 5.63 Cahora Bassa dam. New 3D model of the dam-reservoir-foundation system used for non-linear seismic analysis. Properties, joints, concrete constitutive law, and intensifying seismic input.

STATIC RESPONSE

The non-linear response under the static load combination SW+HP331 is presented first (Fig. 5.64). The maximum displacements (45.3 mm) occur at the upper part of the central cantilevers, in the area below the surface spillway, instead of at the crest. As for the stress state, the dam is globally under compressions. The greater compressive stresses arise along the downstream base (-7.8 to -10.1 MPa), normally oriented to the insertion line, and at the upstream face of the taller cantilevers (-6.8 to -9.3 MPa), in the arch direction. Under the static loads, no compressive damage occurs. Nevertheless, high tensions arise along the upstream base, causing tensile damage with values greater than 80%. Overall, in relation to the response obtained using a coarser mesh, higher displacements and stress values were calculated here.

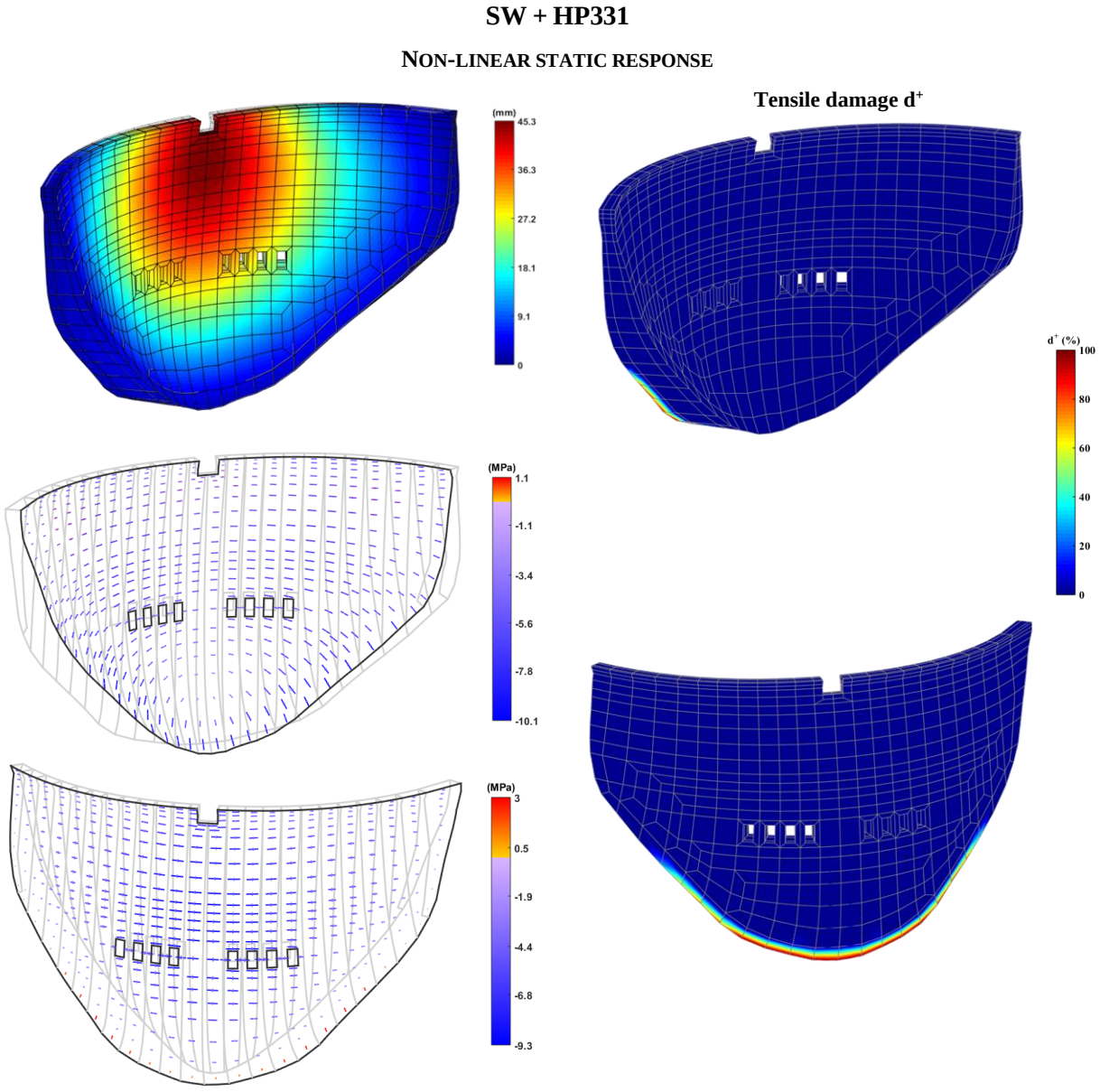

Fig. 5.64 Non-linear static response of Cahora Bassa dam for SW + HP331. Displacements, principal stresses and tensile damage.

ENDURANCE TIME ANALYSIS

The non-linear seismic response of Cahora Bassa dam is analyzed under the load combination SW + HP331 + SEISMICL, considering an intensifying seismic accelerogram, for seismic safety assessment. The main results are presented at various time steps, which are associated with increasing acceleration levels.

Up to t = 2 s (Fig. 5.65), the maximum displacements are of about 17 mm in the upstream direction and 88.7 mm in the downstream direction, both occurring at the top of the central cantilevers, around the surface spillway. Relevant joint opening and sliding movements do not occur under this excitation level.

As for the non-linear stress fields, high tensions arise along the upstream base, but they are released due to concrete damage, as seen in the tensile damage distributions. Moreover, lower tensions start to appear near the top of the lateral cantilevers (vertical direction), inducing damage values of about 50%, as well as around the surface spillway (arch direction), where low damage is noted. The maximum arch compressions (- 13.1 MPa) are calculated along the upper part of the upstream face of the lateral cantilevers, while important compressions are also computed below the surface spillway at the downstream (- 12.6 MPa) and upstream (-11.5 MPa) faces. As these values are far from the concrete compressive strength, there is no compressive damage. Furthermore, it is interesting to note that the dam mesh is not perfectly symmetric towards the abutments, which is evidenced by the differences in the furthest lateral cantilevers: higher tensions arise at the upper part of the cantilever at the left abutment.

Next, for t = 4 s, the evolution in non-linear behavior is evident, and the seismic response of the dam is considerably different than in t = 2 s. Up to this time, the maximum displacements at the top of the central section have increased to approximately 50 mm towards upstream and to 152.8 mm towards downstream. Nevertheless, the global maximum upstream displacements (117.5 mm) are computed at the crest of the lateral cantilevers, when the maximum vertical joint openings occur (13.27 mm), while the central cantilevers move in the opposite direction (Fig. 5.66).

In terms of the stress fields, when the dam moves towards upstream, with greater deformations in the central cantilevers, high tensions arise near the upper edges of the surface spillway (upstream face) and at the top of the lateral cantilevers (downstream face). In addition, if the maximum upstream motions occur at the lateral cantilevers, the vertical joints open and the subsequent release of arch stresses at the top leads to an increase of the cantilever tensions (downstream) along the upper half of the dam body. Moreover, when the dam moves in the downstream direction, the joints close and considerable tensions appear around the surface spillway (downstream face), in the arch direction, and along the height of the lateral cantilevers near the abutments, on the downstream face, as well as along the dam base and at the upper part of the lateral cantilevers, at the upstream face. The aforementioned tensions are released due to concrete non-linear behaviour: as seen in Fig. 5.67, there is an important increase of tensile failure along the upstream base, and new areas with high damage values have appeared at the downstream face of most of the taller cantilevers, around the edges of the surface spillway, and at the upper part of the downstream face of several lateral cantilevers; furthermore, damage is starting to propagate across the thickness of some blocks. With respect to compressive stresses, the greater compressions occur in the arch direction along the upper part

of the lateral cantilevers, at the upstream (- 18 to – 20.9 MPa) surface, as well as in the blocks surrounding the surface spillway, along the upstream (- 19 MPa) and downstream faces (-19.9 MPa). Since these values are still lower than the adopted compressive strength, there is no compressive damage to report.

At last, the results obtained until t = 6 s (Fig. 5.68) enable to see that there was a significant worsening in terms of non-linear dam behaviour. For this excitation level, the maximum upstream displacements (254 mm) are computed at the top of the lateral cantilevers, when the maximum joint openings occur (29 mm), while at the same time the central cantilevers move in the opposite direction. It is also relevant to note that there are instants when considerable seismic motion causes all the taller cantilevers to move in the same direction.

Furthermore, the results show that there was an extreme increase of tensile damage (Fig. 5.69), with concrete failure spreading over most of the downstream face of the dam, as well as on the upper part of the taller cantilevers and near the base, at the upstream face. Also, concrete failure has propagated through the thickness of almost all cantilevers, in significant concrete volumes. Simultaneously, the very high arch compressions arising in Cahora Bassa dam cause high compressive damage below the surface spillway (downstream face) and at the top of the lateral cantilevers (upstream face).

To finish this analysis, the evolution of tensile (Fig. 5.70) and compressive (Fig. 5.71) damage distributions are presented, aiming at a comprehensive evaluation of the Cahora Bassa dam seismic performance under the intensifying seismic action.

These tensile damage distributions tensile (Fig. 5.70) allow to verify that up to t = 5 s the damaged state is acceptable, considering that concrete failure is mainly superficial and does not cross the entire section of the most important cantilevers. Nevertheless, after that there is a significant growth of concrete failure, both at the upstream and downstream faces, including large volumes where failure propagates across the thickness of most of the cantilevers of the dam. This situation would obviously be unacceptable given that such a damaged state would compromise structural integrity and require the interruption of the normal operation of the dam for repair and maintenance action. Therefore, the performance endurance limit pertaining to tensile damage is t = 5 s, which corresponds to a peak acceleration of about 0.5g, about 6.5 times higher than the seismic action defined as OBE (0.076g) for Cahora Bassa dam.

The areas with compressive damage (Fig. 5.71) increase progressively after t = 6 s, namely at the top of the lateral cantilevers, on the upstream face, and below the surface spillway, on the downstream face, until t = 9 s, when compressive failure has propagated across the thickness of the blocks of the dam below the surface spillway. Thus, the performance endurance limit associated with compressive failure is set to t = 8 s, which corresponds to a peak acceleration of 0.8g, about 8 times greater than the defined MDE (0.102g) for Cahora Bassa dam.

As a final note, it should be emphasized that the results achieved in this Endurance Time Analysis allowed to demonstrate that Cahora Bassa dam, despite being a thin double curvature dam, presents a very satisfactory performance under strong seismic loads, resulting in endurance limits that are several times greater than the peak ground accelerations defined for the OBE (0.076g) and the MDE (0.102g).

SW + HP331 + SEISMICL (until t = 2 s; $a_p \approx 0.2g$)

NON-LINEAR SEISMIC RESPONSE

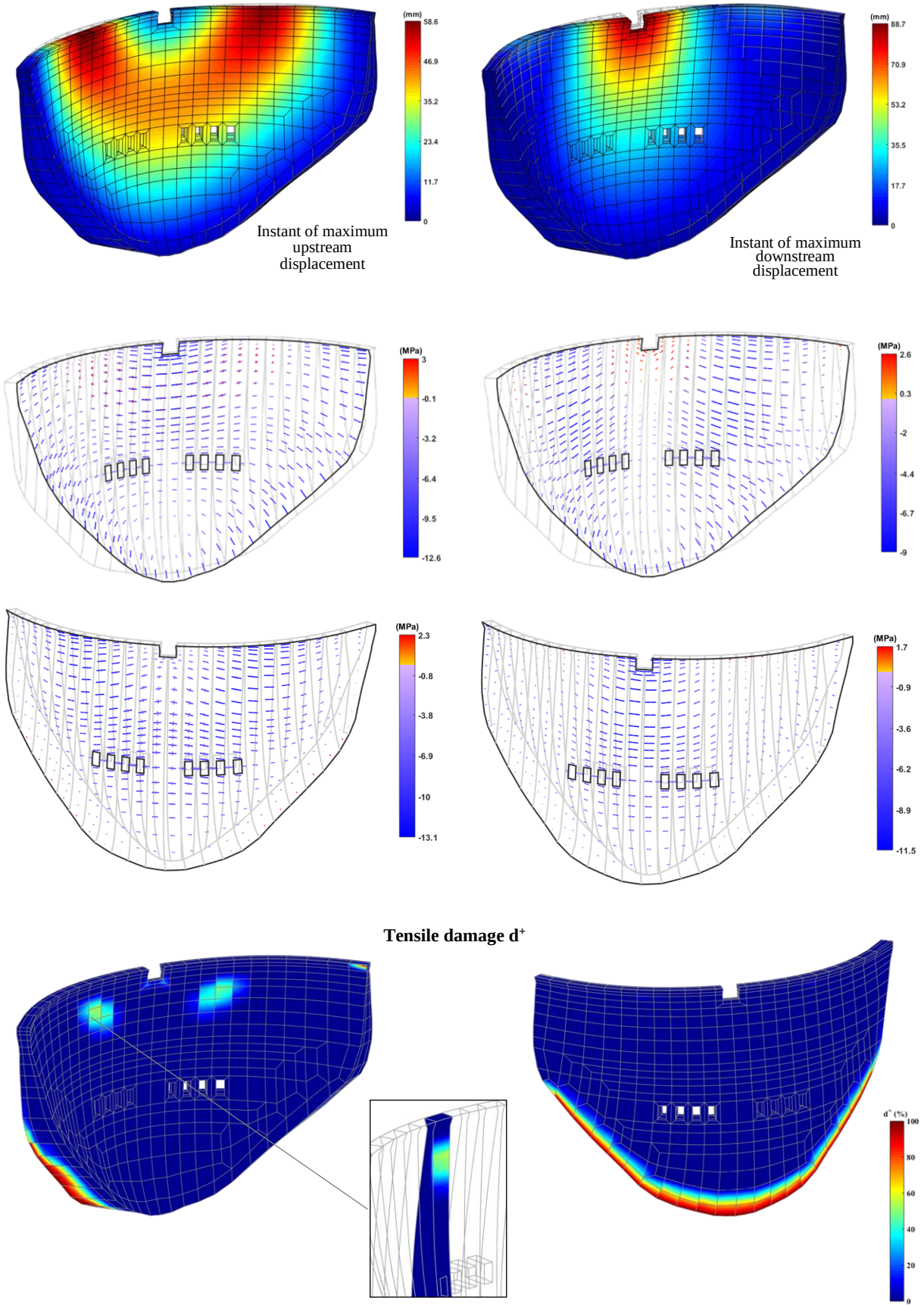

Fig. 5.65 Non-linear seismic response of Cahora Bassa dam for SW + HP331 + SEISMICL (until t = 2 s; ap ≈ 0.2g). Displacements, principal stresses, and tensile damage.

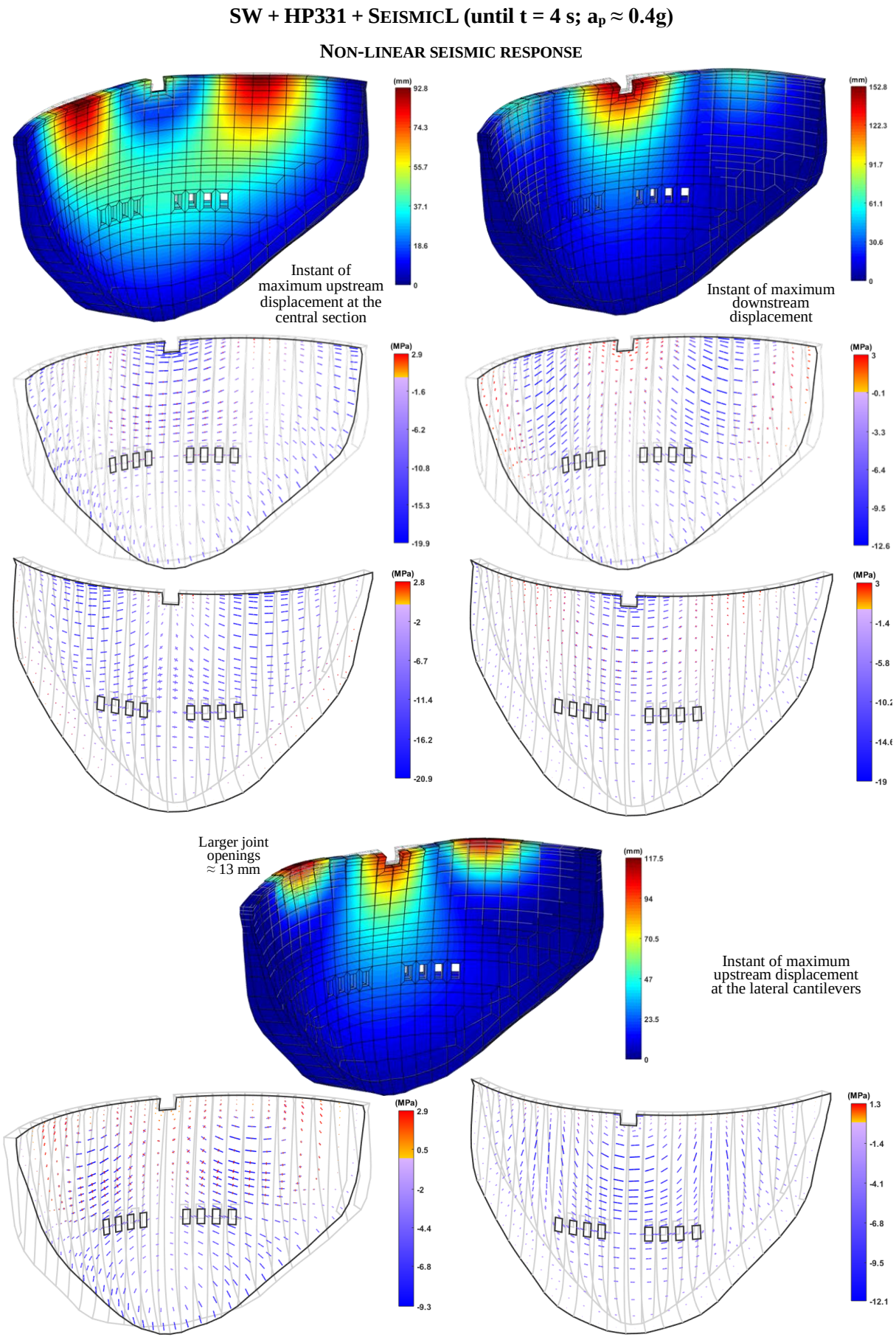

Fig. 5.66 Non-linear seismic response of Cahora Bassa dam for SW + HP331 + SEISMICL (until t = 4 s; ap ≈ 0.4g). Displacements and principal stresses.

SW + HP331 + SEISMICL (until t = 4 s; $a_p \approx 0.4g$)

NON-LINEAR SEISMIC RESPONSE

Tensile damage d^+

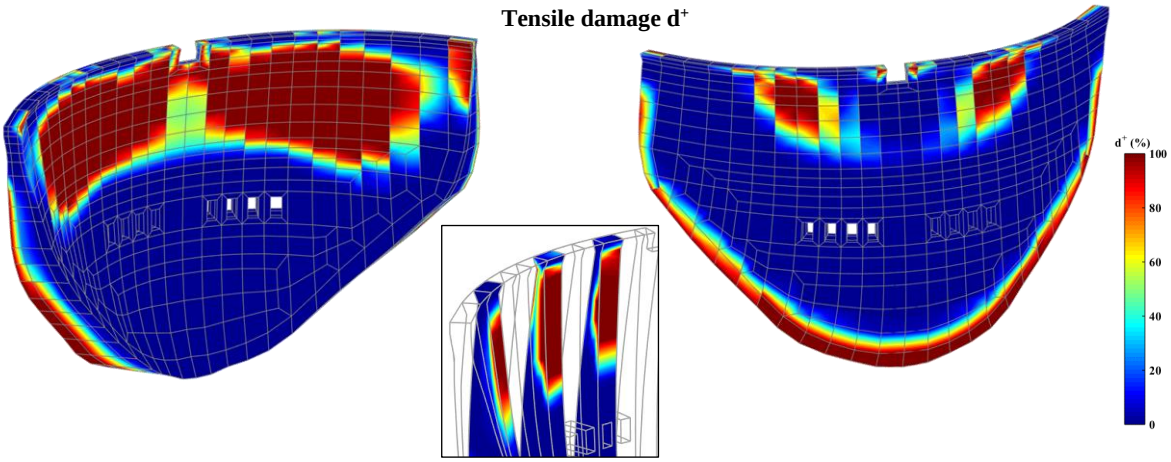

Fig. 5.67 Non-linear seismic response of Cahora Bassa dam for SW + HP331 + SEISMICL (until t = 4 s; ap ≈ 0.4g). Tensile damage.

SW + HP331 + SEISMICL (until t = 6 s; $a_p \approx 0.6g$)

NON-LINEAR SEISMIC RESPONSE

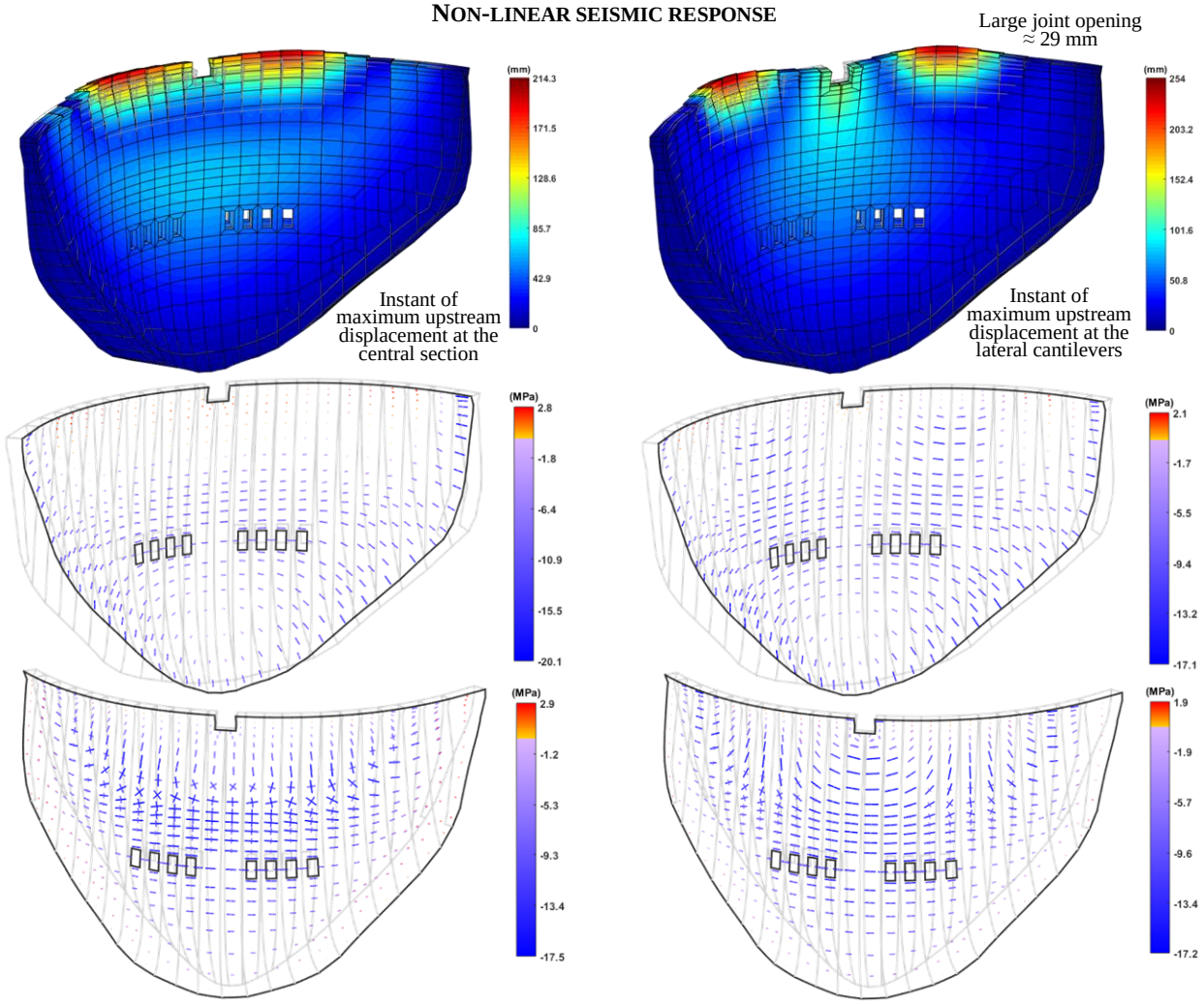

Fig. 5.68 Non-linear seismic response of Cahora Bassa dam for SW + HP331 + SEISMICL (until t = 6 s; ap ≈ 0.6g). Displacements and principal stresses.

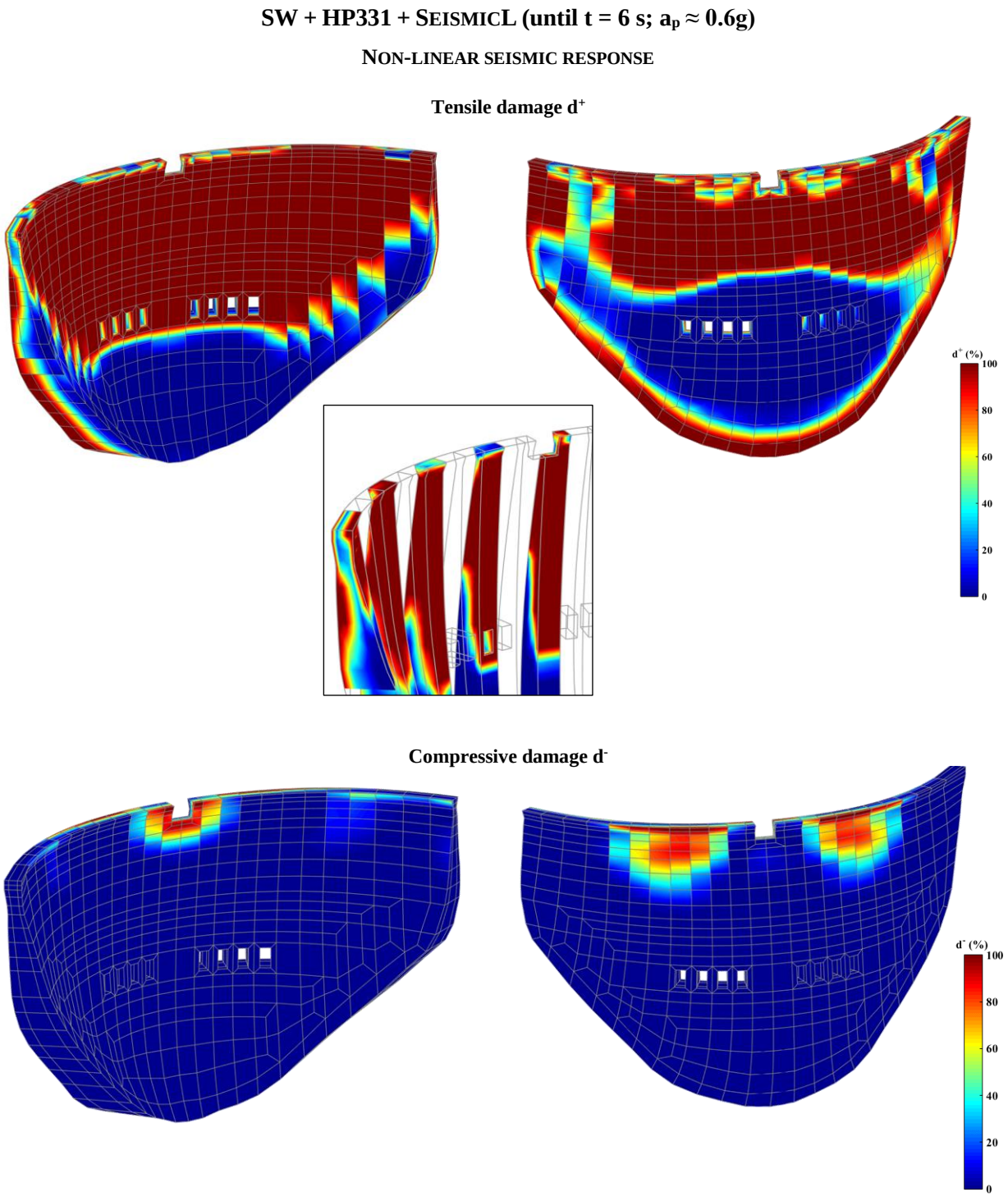

Fig. 5.69 Non-linear seismic response of Cahora Bassa dam for SW + HP331 + SEISMICL (until t = 6 s; ap ≈ 0.6g). Tensile and compressive damage.

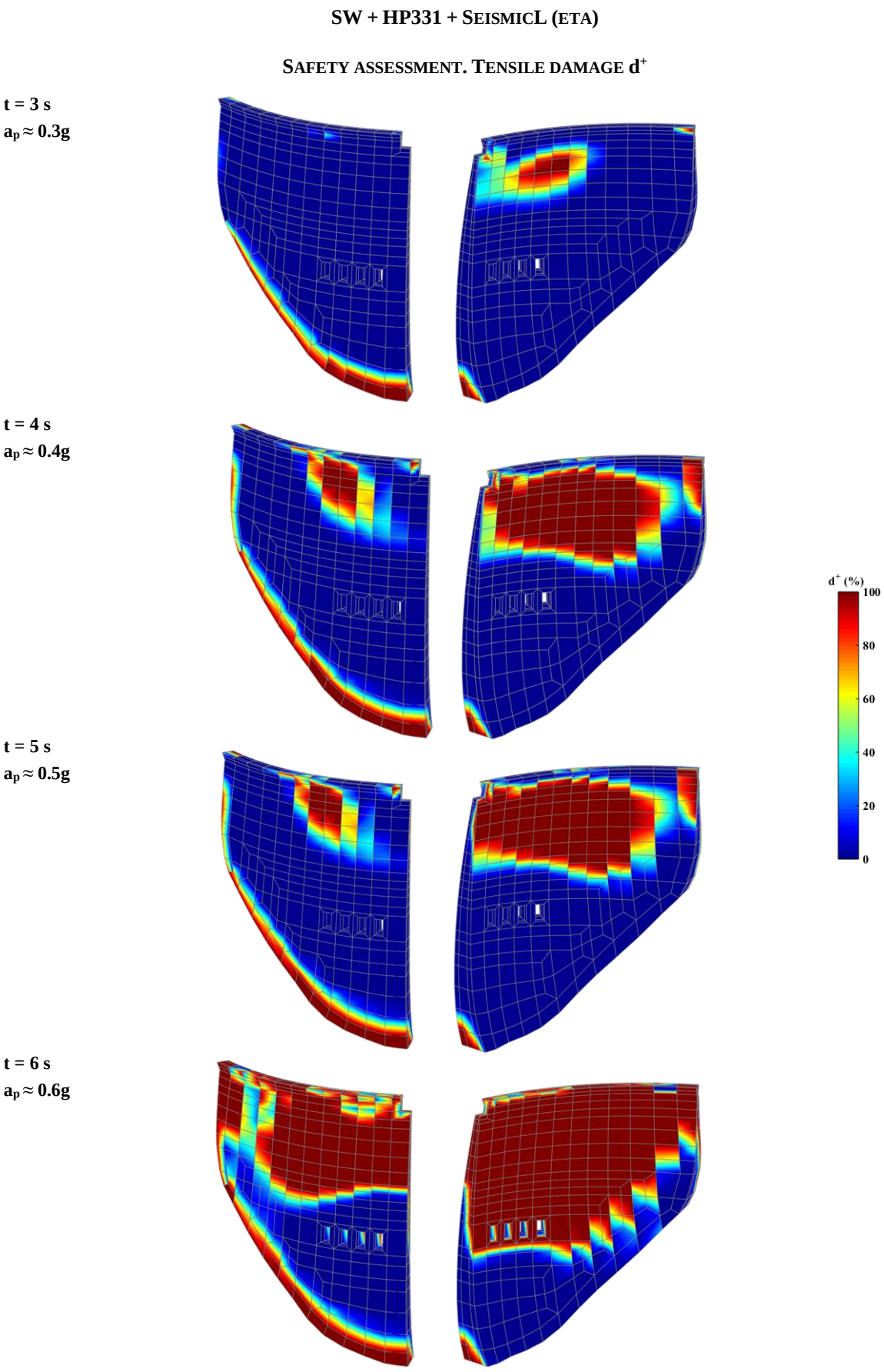

Fig. 5.70 Non-linear seismic response of Cahora Bassa dam for SW + HP331 + SEISMICL. Tensile damage for consecutive excitation levels.

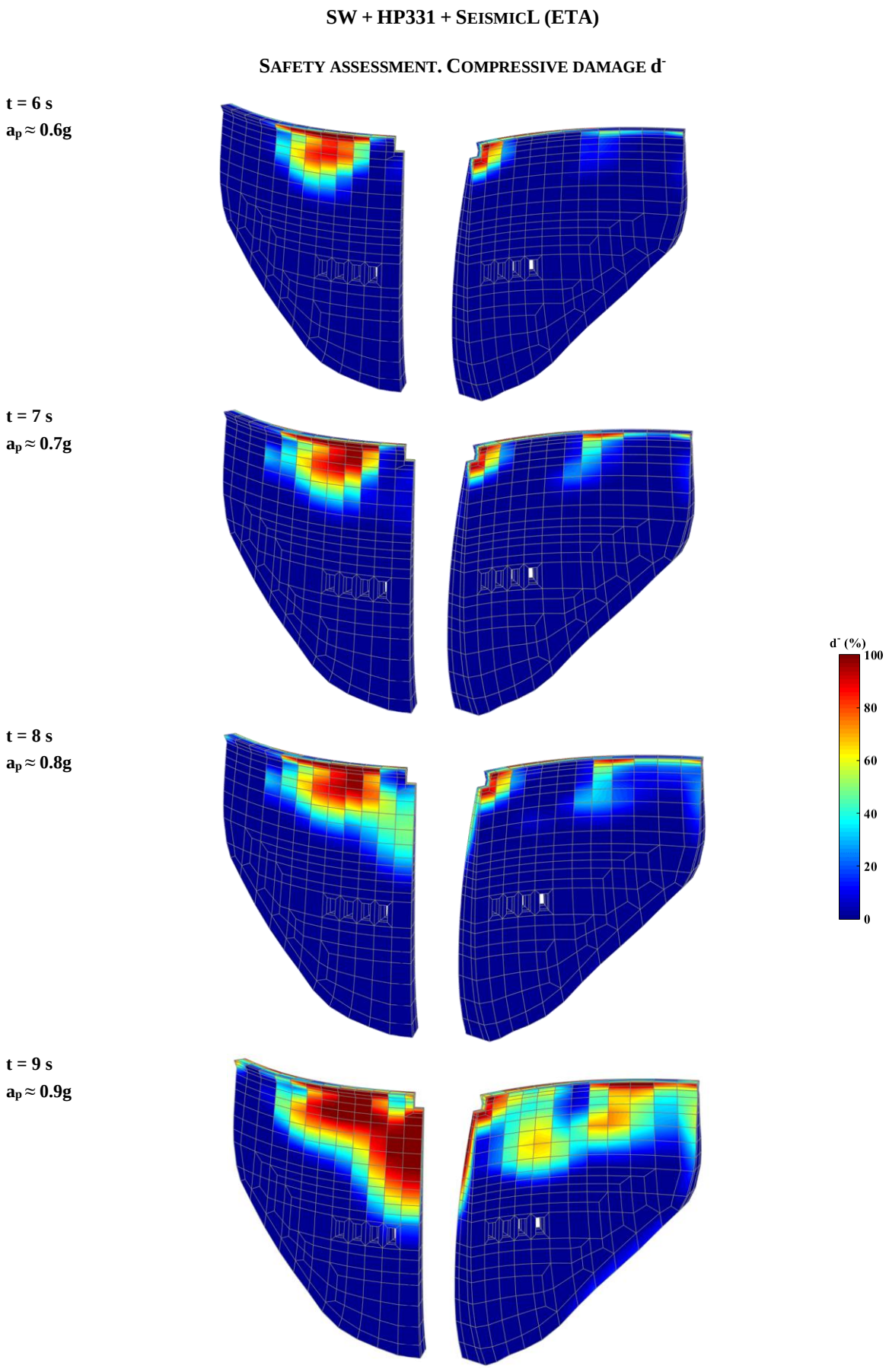

Fig. 5.71 Non-linear seismic response of Cahora Bassa dam for SW + HP331 + SEISMICL. Compressive damage for consecutive excitation levels.

5.4 FINAL CONSIDERATIONS

Following the work carried out in Chapter 3, with the development of a finite element program for dynamic analysis of concrete dams, and in Chapter 4, including the implementation of software for the detection of seismic vibrations and for automatic modal identification, the main goal of the Chapter 5 was to perform practical applications studies on the dynamic behaviour of two large arch dams.

The dams chosen as case studies for this thesis were Cabril dam (132 m high), in Portugal, and Cahora Bassa dam (170 m high), in Mozambique, two dams that have been under continuous dynamic monitoring since 2008 and 2010, respectively. Thus, this chapter was divided into two main subchapters, one dedicated to Cabril dam and the other to Cahora Bassa dam.

With respect to the performed application studies, Chapter 5 presented experimental and numerical results regarding the continuous dynamic monitoring of both dams over the last decade, and the results of finite element simulations conducted for non-linear seismic response analysis.

5.4.1 MODAL PARAMETERS AND SEISMIC RESPONSE

The main results obtained from the dynamic continuous monitoring of both dams included: (i) the analysis of the identified frequencies and mode shapes; and (ii) the study of accelerations measured on the dam body during low-intensity seismic events.

On a first phase, the evolution of the identified natural frequencies over time and the corresponding mode shapes, obtained with the program *DamModalID*, were analysed and compared with results from finite element calculations, carried out using the program *DamDySSA*.

Overall, the results achieved for both case studies clearly showed the influence of the reservoir water level variations in the dynamic properties of the dam-reservoir-foundation systems and, consequently, in the values of the natural frequencies. For the case of Cabril dam, where the global water level variation during the whole monitoring period (around 30 m) was greater than that observed in the reservoir of Cahora Bassa dam (about 14 m), the variation in the frequency values was more significant, especially for modes with higher frequencies.

For both dams it was possible to achieve a very good agreement between the identified natural frequencies over time and the frequency curves calculated using the finite element models of the dam-reservoir foundation systems, using realistic reservoir water levels as inputs and considering appropriate pressure waves propagation velocities (1440 m/s in Cabril dam and 1500 m/s in Cahora Bassa dam); this showed one of the great advantages of coupled models in displacements and pressures, in which the pressure wave propagation velocity is the only property required for the reservoir, in comparison with the classical added water mass models, which require the application of empirical added water mass reduction factors to roughly reproduce the natural frequencies. Also, in both cases the numerical models were able to properly simulate the modal configurations of the first three vibrations modes.

Despite the very good results achieved in this work, it could be useful to conduct more studies in the future to enable further investigations, namely a) for Cabril dam, to understand the intake tower behaviour and the influence of the dam-tower dynamic interaction in the dynamic properties of the dam-reservoir-foundation system, ideally using a more detailed finite element model that incorporates the tower, and b) for Cahora Bassa dam, by improving the current model to get a better representation of the dam geometry, e.g., the half-hollow crest, the spillways, and the upstream face concrete ribs, and possibly considering the installation of accelerometers in other galleries to improve the characterization of modes.

Furthermore, a new methodology was proposed for damage detection, based on the comparison between the identified natural frequencies identified from monitoring data and the frequencies values computed using linear models (calibrated for a reference period) and models that simulate the effects of evolutive damage, aiming to support structural health monitoring of large concrete dams.

For both case studies, the proposed method showed that the natural frequencies extracted from recent monitoring data were similar to the frequency values calculated using the reference models, which were calibrated based on data from the initial monitoring periods, under similar reservoir level conditions. Therefore, since the modal parameters did not change over the whole monitoring period, it was possible to conclude that the existing deterioration phenomena have not progressed significantly and thus are not affecting the performance of both Cabril dam, which has been in operation for almost 70 years, and Cahora Bassa dam, inaugurated almost 50 years ago.

On a second phase, the seismic behaviour of Cabril dam and Cahora Bassa dam was analysed based on the comparison between seismic accelerations recorded during real seismic events and acceleration time histories computed using *DamDySSA*.

The seismic response of Cabril dam was analysed for a magnitude 4.6 earthquake event that occurred on September 4, 2018, with epicentre off the coast of Portugal at 200 km from the dam site. For this earthquake, the maximum acceleration, 3.62 mg, was measured at the crest of the central section, in the upstream-downstream direction. The peak acceleration recorded at the right bank, in the same direction, was of 1.31 mg. This gives an amplification factor of 2.8 times from the dam-rock interface to the crest.

Regarding the comparative analysis, a good agreement was achieved between measured and computed response, using as seismic input the seismic accelerograms recorded at the right bank (the only available records near the dam-rock interface). However, this was only possible by considering a damping ratio of about 10% in the model, for the frequency band of the first vibration modes. Still, the same good agreement would be expected using significantly lower (and more reasonable) damping values, if accelerations recorded at the bottom of the valley were used as seismic input. Therefore, in this work it is recommended the installation of an additional triaxial accelerometer at the downstream base of Cabril dam, aiming to improve the characterization of the seismic action and to conduct further investigations using a more appropriate seismic input.

The software *Code_Aster* was also used to calculate the seismic response of Cabril dam, in order to provide and additional source of comparison, based on different modelling hypotheses. The results allowed to

corroborate the previous conclusions. It is also worth noting that it was possible to achieve a slightly better agreement between measured and computed accelerations using the program *DamDySSA*.

The seismic response of Cahora Bassa dam was analysed based on the acceleration time histories recorded during an earthquake detected at the dam site on June 21, 2017, with an epicentre at 32 km from the dam. This was a low intensity seismic event that induced low amplitude vibrations in the dam body. The peak acceleration at the downstream base was of 9.03 mg, in the upstream-downstream direction, while the maximum acceleration at the crest, 37.76 mg, occurred to the right of the central section, in the same direction. The resulting base-to-top amplification factor was of 4.2 times.

The comparative study conducted for Cahora Bassa dam showed that a very good agreement was reached between measured and computed accelerations, considering the accelerograms measured at the base of the dam as seismic input and now using a 1% damping ratio (a value coherent with those used in studies for large arch dams). In the future it could be of interest to carry out additional calculations using the abovementioned model with improved dam geometry, and to compare measured and computed accelerations at more locations of the dam body.

5.4.2 NON-LINEAR SEISMIC CALCULATIONS

This chapter provided the main results on the non-linear seismic behaviour of Cabril dam and Cahora Bassa dam. The non-linear finite element calculations were carried out using *DamDySSA*, considering opening/closing and sliding joint movements and tensile and compressive concrete damage.

On a first phase, the non-linear seismic response was analysed for a load combination including the self-weight of the dam, the hydrostatic pressure for full reservoir, and a seismic load with a peak acceleration of 0.6g. The goal was to investigate the effects due to joint movements on the structural response, by comparing results obtained using linear and non-linear models, and to evaluate the resulting damages in concrete.

The results achieved for both case studies demonstrated that the vertical contraction joint opening and sliding movements clearly influence the seismic response of large arch dams, originating stress redistribution processes. Overall, the principal stresses fields and the arch and cantilever stresses envelopes showed that the joint movements resulted in a significant release of arch stresses at the top of both dams, and, consequently, in an increase of cantilever tensions and compressions over the height of the taller lateral cantilevers, located to the right and left of the central blocks.

Regarding concrete damage, both dams presented important tensile damage along the upstream base, and at the upper part of the downstream face. In Cabril dam, tensile failure was mostly superficial, and no compressive damage occurred, which demonstrated its good seismic performance under a strong earthquake with a peak acceleration (0.6g) three times greater than that assumed for a possible MDE (0.2g). In comparison, since Cahora Bassa dam is a thinner dam, higher stresses were calculated and thus there were more extensive areas of tensile failure, which propagated across the thickness of some cantilevers. Also, low compressive damages occurred. Even so, the dam showed a good performance under a seismic

load with a peak acceleration (0.6g) six times greater than the MDE (0.1g) defined in a seismic hazard study for the dam site.

For the case of Cabril dam, the non-linear response was calculated considering two hypotheses for simulating the behaviour of a horizontal crack, incorporated to reproduce the existing cracking band, namely considering: higher stiffness values, to limit opening movements, and lower stiffness values, to enable opening movements. For higher stiffness, high vertical tensions and thus tensile damage occurred around the cracked zone, while for lower stiffness, the opening of the horizontal crack originated larger movements of the blocks above the crack but resulted in the release of the vertical tensions, therefore preventing tensile damage. Additional studies could be conducted in the future in order to further investigate the cracked zone in Cabril dam.

As for Cahora Bassa dam, more studies should be carried out using the referred updated version of the model with improved geometry.

On a second phase, the seismic performance of both dams was analysed using the safety assessment methodology proposed in this work, based on the Endurance Time analysis, by evaluating the evolution of tensile and compressive damage under intensifying seismic excitation. The adopted performance criteria are related to the extent of damage at upstream and downstream faces and along the thickness of the main cantilevers: the occurrence of significant volumes of the dam body in which concrete failure propagates across the entire thickness of the cantilevers is considered as unacceptable. Based on this methodology, the performance endurance limits were obtained for Cabril dam and Cahora Bassa dam as the peak ground acceleration values from which dam performance became unacceptable.

The calculations were carried out for a load combination including the self-weight of the dam, the hydrostatic pressure for full reservoir, and considering the application of an intensifying seismic action, with peak accelerations increasing from around 0.1g to about 1.5g in 15 s.

More refined meshes of the dams, considering three elements in thickness, were used in the performed analyses for seismic safety assessment, which enabled a better characterization of the damage distributions.

Overall, the provided results allowed to see, as expected, that there was a gradual evolution in non-linear behaviour, namely in what concerns the increase of joint opening movements as the dams moved towards upstream, resulting in the release of arch stresses at the crest and in the accumulation of cantilever stresses in certain areas, and in terms of considerable concrete damage worsening, especially under tensions.

For Cabril dam, the non-linear analysis was performed considering the referred hypotheses to simulate the horizontal crack (with higher and lower stiffness values). In both scenarios, the endurance limit of Cabril dam for tension damage was defined as 0.5g, since concrete failure was mostly superficial and did not cross the entire thickness of the cantilevers, an acceleration value 5 times greater than a possible peak acceleration for the OBE (0.1g). Under higher excitation levels, there was a considerable increase in areas under concrete failure, which started to propagate from upstream to downstream in many cantilevers; this damage state could compromise the structural integrity of the dam and require the performance of repair and maintenance interventions, thus being unacceptable. On the other hand, the endurance limit for compressive damage

would be higher than 1.4g, 7 times higher than the peak acceleration assumed for the MDE (0.2g), since concrete failure under compression occurred in key areas only after 14 s, which showed the impressive resistant capacity of Cabril dam.

As for Cahora Bassa dam, the performance endurance time limit for tension damage was defined as 0.5g, about 6.5 times the peak acceleration prescribed for the OBE (0.076g), since that until t = 5 s the concrete failure that occurred at upper part of the dam is mainly superficial. However, after that there was a considerable worsening of concrete tensile failure at both upstream and downstream faces, including large volumes where failure propagate across the whole thickness of most of the dam cantilevers. As mentioned, this situation would not be acceptable. The endurance limit for compressive damage was define as 0.8g, about 8 times the value of the MDE (0.102g), given that after t = 8 s compressive failure finally propagated from upstream to downstream in the blocks below the surface spillway, which would result in concrete crushing in that area. This situation would not be acceptable as it could result in uncontrolled release of water from the reservoir. The results of this study allowed to demonstrate that Cahora Bassa dam is a thin dam with a very good performance under strong earthquakes, since both endurance limits are several times greater than the peak acceleration value defined as MDE for the Cahora Bassa dam site.

5.4.3 CONCLUDING REMARKS

To summarise, the conducted application studies enabled to achieve results of great value and interest on the dynamic behaviour of two large arch dams. Overall, these studies allowed to show:

i) The quality of the SSHM systems installed in Cabril dam and Cahora Bassa dam, and their capacity to measure low amplitude vibrations in normal operating conditions (under ambient/operational excitation) and during low-intensity seismic events;
ii) The potential of the developed methods and thus of the modal identification program *DamModalID* to automatically identify natural frequencies and mode shapes for large concrete dams;
iii) The suitability of the finite element-based coupled methods developed for simulating the dynamic behaviour of dam-reservoir-foundation systems, including a) complex modal analysis, b) linear seismic analysis, and c) non-linear seismic analysis, considering joint movements and concrete damage, as well as the potential of the program *DamDySSA* for dynamic analysis of concrete dams;
iv) The usefulness of the proposed methodologies and the developed graphical tools, namely for a) damage detection, based on the comparison between identified and computed frequencies, to support structural health monitoring, and b) seismic safety assessment, based on the Endurance Time method and using results obtained with advanced finite element models that consider joint movements and tensile and compressive damage, to support seismic design of new dams or safety re-evaluation of older dams.

Chapter 6

CONCLUSIONS AND FUTURE RESEARCH

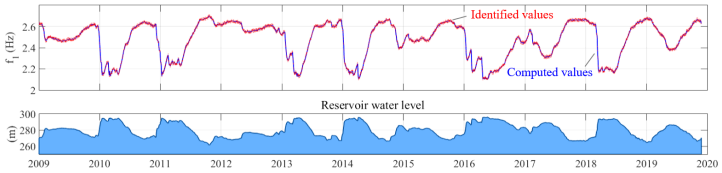

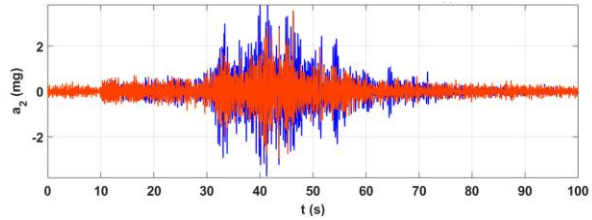

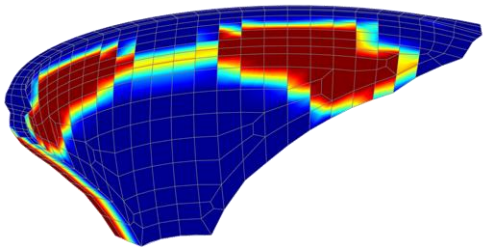

6. CONCLUSIONS AND FUTURE RESEARCH

6.1 MAIN CONTRIBUTIONS AND INNOVATIONS

The present thesis was developed with the goal of providing relevant theoretical and practical contributions to the field of dam engineering, namely for modelling the dynamic behaviour of dam-reservoir-foundation systems, including for modal analysis and seismic response analysis, and for the development of SSHM systems installed in large concrete dams, particularly for the improvement of the software component.

6.1.1 FINITE ELEMENT NUMERICAL MODELLING OF DAM-RESERVOIR-FOUNDATION SYSTEMS

In what concerns the numerical modelling of the dynamic behaviour of dam-reservoir-foundation systems, the use of a coupled model, formulated in displacements and hydrodynamic pressures, was considered. Therefore, a complete finite element-based formulation was proposed in order to solve the coupled dynamic equation governing the behaviour of the whole system, considering the effects of dam-reservoir dynamic interaction and generalized damping (including radiation damping in the reservoir).

First, a new state-space approach, considering displacements, pressures, and their time derivatives as unknowns, was proposed for coupled modal analysis of the dam-reservoir-foundation system with generalized damping, enabling the calculation of complex eigenvalues and eigenvectors (non-stationary vibration modes). Then, a coupled time-stepping method was implemented for linear seismic analysis, consisting of the direct application of the Newmark method to the dynamic equation of the whole dam-reservoir-foundation system, in order to calculate the dynamic response in displacements and pressures in time domain. Finally, a complete method was developed for non-linear seismic analysis, by combining the time-stepping formulation with the iterative stress-transfer method, considering a) the non-linear behaviour of concrete up to failure, based on a strain-softening damage model with two independent scalar damage variables (d^+ for tension and d^- for compression), e b) the opening/closing and sliding movements of joints and cracks, using a constitutive model based on the Mohr-Coulomb failure criterion and on appropriate relative displacement-stress laws.

The proposed calculations methods were implemented in the finite element program *DamDySSA*, developed for dynamic analysis of concrete. From this work resulted the latest version of this program, which now includes three calculation modules, namely for: (i) complex modal analysis, to obtain natural frequencies and mode shapes; (ii) linear seismic analysis, to calculate the response in displacement and pressures, considering acceleration time histories as seismic input; and (iii) non-linear seismic analysis, to compute the non-linear response considering joint movements and concrete damage.

Within this scope, a considerable effort was made in terms of pre- and post-processing tools, taking into account the goals of this work and the application studies to be carried out. Regarding pre-processing, a new module was developed for the program *DamMesh*, originally created in LNEC for automatic generation of 3D finite element meshes of dam-reservoir-foundation systems, in order to enable the introduction of joint the finite element mesh of the dam. As for post-processing, several new graphical

representations were implemented in *DamDySSA*, and existing ones were improved, including a) graphics showing the evolution of natural frequencies according the water level, and 3D figures of mode shapes, to enable the comparison with experimental results, and b) 3D representations of deformed shapes with joint movements, fields of principal stresses, seismic stress envelopes, and damage distributions, in order to facilitate the evaluation of linear and non-linear seismic behaviour and the seismic safety assessment.

Additionally, during this work the first version of a new graphical user interface was also created for *DamDySSA*, which was adapted to accommodate the new modules, aiming to facilitate the performance of numerical simulations and the analysis and interpretation of the results.

The developed formulations were validated by using *DamDySSA* to perform several tests on the dynamic behaviour of dam-reservoir-foundation systems, involving the comparison of numerical results with experimental results or known analytical solutions. These tests included the analysis of modal parameters, the response in displacements and hydrodynamic pressures, and the influence of joint movements.

In this scope, it is worth highlighting the test conducted for analysing the hydrodynamic pressures on an arch dam, by comparing the pressure values calculated at the upstream face using a) *DamDySSA*, based on a coupled formulation, and b) Westergaard's formulation, commonly applied in added water mass models. Basically, the pressures calculated using Westergaard's formulation on a curved and flexible dam were clearly overestimated in comparison to those obtained using a coupled model. The presented results allowed to explain, for the first time, the need to apply an empirical added mass reduction factor (of around 50 to 70%) when using the classic added water mass models based on Westergaard's hypothesis, as has been recommended by some authors for dynamic analysis of arch dams.

Concerning computational efficiency, test calculations were carried out for linear seismic analysis of Cabril dam, using both the coarser mesh (one element in thickness) and the refined mesh (three elements in thickness), presented in chapter 5. Considering a seismic input with a duration of 10 s and a time step of 0.01 s, the time integration procedure was completed in around 10 minutes with the coarser mesh, and about 1hour with the refined mesh (using a laptop with a CPU processing speed of 2.2 GHz). However, in what concerns the non-linear seismic analysis, it took about a month to complete a 10 s calculation, considering that there are two iterative stress-transfer processes involved to simulate the non-linear behaviour of all joint elements and the concrete ruptures (tensile and compressive damage) in all dam elements.

6.1.2 SEISMIC AND STRUCTURAL HEALTH MONITORING SYSTEMS FOR DAMS

Regarding the contribution for the development of continuous dynamic monitoring systems installed in large concrete dams, in this thesis it was decided to develop computational tools for integrating the systems and for complementing their software component, with a view to optimise their operation and to obtain valuable experimental results for supporting structural health monitoring and seismic monitoring. Thus, two programs were implemented: *DamSSHM* and *DamModalID*.

The program *DamSSHM* was developed to carry out automatic analysis and management of continuous dynamic monitoring data from SSHM systems. In the scope of this work, *DamSSHM* was implemented for

testing in the central server of the SSHM system of Cabril dam, in 2018. Therefore, this first version of the program was specifically prepared and optimised to integrate the software component of the referred system. Essentially, *DamSSHM* is automatically executed every day, and it includes four modules in order to perform the following tasks: (i) read data files and use moving average filters to detrend the acceleration records; (ii) data analysis and management, including evaluation of the integrity of records and saving decimated files to external storage units and Google Drive folders; (iii) analysis of acceleration time histories to automatically detect vibrations induced by seismic events (and distinction from those induced by the operation of gates and by turbines of generator sets), and save backups when detection is successful; and (iv) perform the maintenance of the server storage and save backups of original files.

Once all these tasks are completed, *DamSSHM* automatically sends emails containing files with summaries of measured data and information regarding the available storage space of the server and external units. Furthermore, when seismic vibrations are detected, the program sends additional emails including files and figures of the recorded acceleration time histories.

The program *DamModalID* was developed for automatic modal identification of dams, aiming to estimate the main modal parameters based on continuous vibrations monitoring data. *DamModalID* is based on the frequency domain modal identification approach: the classic Frequency Domain Decomposition (FDD) method with Singular Value Decomposition (SVD) was implemented to calculate the spectral density matrix from measured vibrations and then to determine the corresponding singular values and singular vectors (natural frequencies are obtained as peaks of the singular value spectra and the corresponding singular vectors are used to estimate the mode shapes).

In order to improve the implemented FDD-SVD method and automate modal parameter identification, two original procedures were proposed in this thesis. The first procedure was developed for automatic selection of spectral peaks of the singular value spectrum using the Shifted Smoothed Threshold Curve (SSTC), which is computed as a smoothed version of the referred spectrum and considering the determination of the MAC index to distinguish closely spaced modes. The second procedure was developed to enhance the automatic identification of natural frequencies for dams over time based on Dam Frequency Influence Curves (DamFIC), which are defined for each vibration mode based on previous monitoring data and numerical results, considering the real reservoir water level variations, in order to group frequencies for each mode.

As a complement to this software, several graphical tools were also developed for analysis and interpretation of the observed dynamic behaviour, including representations of the evolution of natural frequencies over time and of modal configurations, and to simplify the comparison with results from numerical models, aiming to provide useful information for structural health control and informed management.

6.1.3 METHODOLOGIES

Besides the contributions and innovations described above, this work also made a relevant contribution at the level of the methodologies to analyse the performance of large concrete dams under dynamic actions, in particular for structural health control and seismic safety assessment.

The methodology proposed for structural health monitoring is based on the integrated use of SSHM systems and finite element numerical models, to enable the systematic comparison between vibration-based and numerical results, aiming at the detection of structural alterations due to evolutive deterioration processes that may occur on large concrete dams over time. Based on this methodology, the natural frequencies identified from recent monitoring data are compared with frequency values computed using a reference linear model, properly calibrated based on monitoring data from a reference period (e.g. the initial monitoring phase), and, if possible, using models that allow the simulation of evolutive damage.

As part of the process, simple and intuitive graphics, comparing identified and calculated frequencies, have been developed. These can be easily interpreted by owners or engineers responsible for dam safety in order to support informed management and enable an effective decision making in face of regular maintenance situations or of eventual emergencies.

In what regards the seismic safety assessment of large concrete dams, a new methodology was proposed in this work, based on the Endurance Time Method and using a non-linear model that enables the simulation of joint movements and concrete damage. Essentially, this is a seismic analysis procedure where the response is calculated under a pre-designed intensifying seismic action, and then the performance of the dam is evaluated based on the evolution of tensile and compressive damage. In this methodology, the adopted performance criteria states that the occurrence of significant volumes of the dam body in which concrete failure propagates across the entire thickness of the cantilevers is not considered acceptable, for both tensile and compressive damage. Therefore, the performance endurance limit is established as the maximum peak ground acceleration (or duration) of the seismic action that the dam can resist without unacceptable damage.

6.2 RESULTS

In addition to the contribution made with the proposed formulations and methods and with the developed programs, which can be used in future studies, this thesis also provided a tangible contribute by presenting results of great interest in Chapter 5, obtained in application studies performed for two large arch dams: Cabril dam (132 m high), in Portugal, and Cahora Bassa dam (170 m high), in Mozambique, two dams under continuous dynamic monitoring since 2008 and 2010, respectively.

6.2.1 CONTINUOUS DYNAMIC MONITORING: MODAL ANALYSIS AND SEISMIC BEHAVIOUR

First, this work presented, for the first time, the main results obtained from data of over 10 years of continuous dynamic monitoring for two large concrete dams, including the evaluation of dam behaviour in normal operating conditions and the analysis of measured response during low-intensity seismic events.

The analysis of the main modal parameters and their evolution over time was carried out based on the comparison between modal identification results, obtained with *DamModalID*, and finite element numerical results, computed using *DamDySSA*. In particular, the study of the evolution of the natural frequencies over time enabled, on the one hand, to demonstrate the influence of the reservoir level variations in the dynamic properties of the dam-reservoir-foundation system and consequently in the frequency values, and, on the other hand, to show the good agreement achieved between experimental and numerical results for both dams. The numerical models were also able to properly reproduce the mode shapes of the first three vibration modes for both dams. However, for the case of Cabril dam, the intake tower behaviour and the influence of dam-tower dynamic interaction still require further investigation.

In addition, based on the proposed methodology for damage detection, the comparison between the identified frequencies over the complete monitoring periods and the frequency curves computed using linear models (calibrated for reference periods) allowed to demonstrate that the performance of Cabril dam and Cahora Bassa dam has not changed over the past decade.

The seismic response of the dams was evaluated based on the comparison between the measured response during low-intensity seismic events and the response calculated using *DamDySSA*. The analysis of the recorded peak accelerations along the insertion and at the top of the dam allowed to determine the next seismic response amplification factors: (i) 2.8 times for Cabril dam, from the dam-rock interface (1.31 mg) at the right bank to the central section at the crest (3.62 mg); and (ii) 4 times for Cahora Bassam dam, between the downstream base (9.03 mg) to the top (37.76 mg), at the central section. Moreover, considering the specific real earthquakes applied on both dams, overall it was possible to reach a good agreement between measured and computed accelerations, taking into account the effect of the seismic input and the damping ratio: (i) for Cabril dam, using as input the seismic acelerogramas recorded near the right bank, a 10% damping ratio was required; and (ii) for Cahora Bassa dam, considering as input the acceleration time histories recorded at the downstream base (central section), a 1% damping ratio was enough.

Additionally, for the case of Cabril dam, the comparison was carried out using not only *DamDySSA* (coupled model in displacements and pressures, massless foundation approach) but also *Code_Aster* (coupled model in displacements and velocity potentials, foundation with energy dissipation). Similar results were obtained with both models, but a slightly better agreement was achieved with *DamDySSA*.

The performed application studies demonstrated: (i) the quality of the installed SSHM systems (and used devices) to automatically measure low amplitude vibrations induced by ambient/operational excitation sources or caused by low-intensity seismic events; (ii) the suitability of the methods proposed in this work for automating frequency identification, and thus the potential of the program *DamModalID* to carry out automatic modal identification of dams; and (iii) the potential and reliability of the program *DamDySSA*

for dynamic analysis of dam-reservoir-foundation systems, in particular of the proposed methods, including the state-space approach for complex modal analysis and the time-stepping method for linear seismic analysis.

Regarding the SSHM system installed in Cabril dam, it is worth mentioning that the testing period of *DamSSHM* has been very successful, allowing the daily reception of emails with relevant information, ensuring an adequate maintenance of the storage space of the server and of the external storage units, and, finally, the automatic detection of vibrations during seismic events.

Furthermore, the presented numerical results and the comparison with experimental data showed the suitability of the proposed coupled finite element formulations, namely the state-space formulation for modal analysis and the time-stepping procedure for numerical integration of seismic response in time domain, and therefore the potential of the program *DamDySSA* for linear dynamic analysis of concrete dams. Also, the advantage of the coupled models in relation to the classic added water mass models was shown once again here: the good agreement between identified and calculated frequencies and mode shapes was achieved by using as inputs only the real reservoir water levels and appropriate pressure wave propagation values, while the added water mass models usually require the use of empirical water mass reduction factors to roughly reproduce the modal parameters.

At last, the value of the proposed methodology for damage detection was demonstrated for both dams, by comparing natural frequencies identified from recent data and frequency curves computed using reference linear models and models that consider the effects of evolutive damage, showing that it can be used in the future for supporting structural health monitoring of large concrete dams.

6.2.2 NON-LINEAR SEISMIC BEHAVIOUR

This work also presented the main numerical results from prediction studies on the non-linear seismic behaviour of Cabril dam and Cahora Bassa dam, considering the effects of opening/closing and sliding joint movements and the behaviour of concrete up to failure under tension and compression. All finite element calculations were performed using the module of *DamDySSA* for non-linear dynamic analysis.

On a first phase, the non-linear studies focused on analysing the non-linear seismic response of both dams under a load combination including the dam self-weight, the full reservoir hydrostatic pressure, and a 10 s seismic load with a peak acceleration of 0.6g, applied in the upstream-downstream direction. The main goal was to evaluate the influence of joint movements on the structural response, by comparing results computed using linear models (without joints nor damage) and non-linear models (with joints and damage), and to examine the resulting tensile and compressive damage.

Overall, the achieved results showed that the opening movements of the vertical contraction joints resulted in considerable stress redistributions, namely in the release of arch stresses near the crest, where the larger joint openings occurred, and consequently in the increase of cantilever tensions and compressions along the downstream upper part of several cantilevers.

With respect to concrete dam, for the case of Cabril dam, tensile failure was mostly superficial and there was no compressive damage. Also, two hypotheses were tested for simulating the horizontal crack behaviour: assuming high stiffness (limited opening movements – high tensions and tensile damage around the crack) and lower stiffness (opening movements enabled – release of tensions and no damage around the crack). As for Cahora Bassa dam, being a thinner dam, stresses were higher and thus the areas with tensile failure were larger and propagated across the thickness. In summary, both dams showed a very good performance under a strong earthquake with a peak acceleration (0.6g) several times higher than the values assumed for the OBE and the MDE.

On a second phase, the seismic performance of both dams was analysed using the methodology proposed in this work for seismic safety assessment, based on the Endurance Time Method and on the evaluation of the evolution of tensile and compressive concrete damage, under an intensifying seismic action. The non-linear simulations were performed under the same load combination, now considering the application of a 15 s intensifying seismic action with peak accelerations gradually increasing from around 0.1g to about 1.5g. Also, more refined meshes of both dams were used, which enabled greater accuracy in the characterization of damage distributions.

With respect to Cabril dam, the endurance limit for tensile damage was set to 0.5g, a peak acceleration 5 times greater than the value assumed in this work for the OBE (0.1g), given that the accumulated tensile failure was mainly superficial. On the other hand, the endurance limit for compressive damage should be higher than 1.4g, 7 times higher than the assumed MDE (0.2g), as the first compressive failure occured only around t = 14 s. This seismic performance evaluation demonstrated that Cabril dam had an impressive resistance capacity under strong seismic excitations, and that its seismic safety would most likely be verified under seismic actions obtained in specific seismic hazard analysis for the dam site.

In what concerns Cahora Bassa dam, the endurance limit in terms of tensile damage was of 0.5g, about 6.5 times the peak acceleration defined for the OBE (0.076g), considering that tensile damage remained at an acceptable level. Moreover, the endurance limit in terms of compressive damage was established at a peak acceleration of 0.8g, corresponding to a value about 8 times greater than the acceleration prescribed for the MDE (0.102g), because under superior seismic excitation levels compressive failure ends up propagating across the whole thickness of the blocks below the surface spillway, resulting in concrete crushing and ultimately to local collapse with uncontrolled release of water. The seismic safety assessment of Cahora Bassa dam, a thin 170 m high arch dam, showed that it had a very good performance under increasing seismic excitation, as both endurance limits were considerably greater than the values defined in specific seismic hazard analyses for the dam site.

The performed application studies on the non-linear seismic behaviour of two large arch dams enabled to show: (i) the suitability of the proposed finite element formulation for simulating the non-linear dynamic behaviour of dam-reservoir-foundation systems, including the implemented constitutive models to account for joint movements and concrete damage in the dam, and consequently the potential of *DamDySSA* to carry out non-linear seismic analysis of arch dams; (ii) the value of the developed graphical representations to facilitate the analysis and interpretation of the final results; and (iii) the usefulness the proposed

methodology for seismic safety assessment of concrete dams, based on the Endurance Time Method and using advanced non-linear models, which can be applied to support seismic design of new dams or the safety re-evaluation of older dams.

6.3 FUTURE DEVELOPMENTS

The present thesis contains important contributions to dam engineering, namely with the development of finite element formulations for modal analysis and for linear and non-linear seismic analysis of dam-reservoir-foundation systems, implemented in the program *DamDySSA*, and for the evolution of SSHM systems installed in large concrete dams, with the implementation of software for monitoring data analysis and management (*DamSSHM*) and for automatic modal identification of dams (*DamModalID*). Furthermore, a relevant contribution was also made by presenting results of great interest on the dynamic behaviour of two large concrete dams located in low seismicity zones: Cabril dam, Portugal, and Cahora Bassa dam, in Mozambique.

Following the developed work, additional research needs and opportunities for future developments are identified, not only with regard to particular aspects of the current work but also to dam engineering in general, a field where important questions and challenges continue to arise.

First of all, it is considered of the utmost interest to make use of the computational tools developed in the scope of this thesis for analysing the dynamic behaviour of large concrete dams that have been subject to high-intensity earthquake ground motion, something that was not possible in the performed application studies (the return period for strong earthquakes is relatively high in Portugal and in the northern part of Mozambique). With that specific goal, and to contribute to the evolution of knowledge in dam engineering, it is therefore recommended the development of a web site to serve as an international platform to involve the scientific community interested in the study of the dynamic behaviour of dams, as well as the dam owners from several countries located in seismic zones (e.g., China, Japan, United States, Iran, etc.) and particularly those currently investing in large concrete dams. So, this platform should be developed in order to: (i) disseminate the latest scientific studies on the dynamic response of dam-reservoir-systems, aiming to encourage the investment in SSHM systems in large concrete dams worldwide; (ii) promote the sharing of data regarding the seismic response of dams located in high seismicity zones, in particular of seismic acceleration records measured on large arch dams under strong earthquakes; and consequently (iii) present the modelling and modal identification software developed in this work and present the main results obtained in studies for Cabril dam and Cahora Bassa dam.

Furthermore, the results presented in the application studies on the dynamic behaviour of two large arch dams in normal operating conditions and during seismic events, based on the comparison between experimental data and numerical models, clearly showed the value of the integrated use of complete finite element models and of SSHM systems and respective software for supporting structural health monitoring and seismic behaviour monitoring. Therefore, it is expected that this work will encourage the investment in the permanent instrumentation of dams for continuous dynamic monitoring over time, by installing

complete SSHM systems that include the largest possible number of accelerometers in the dam body, along the dam base, and if possible, in the free field (the use of optical fibre is recommended to ensure the connection of accelerometers located further away from the data acquisition units), and by implementing software to manage and analyse data and to perform other maintenance tasks (such as those developed in this work) in order to complement the systems, enhance their operation, and obtain better experimental data. This should be considered for new dams, to control their behaviour since the early operation years, and for old dams, to monitor their structural health and evaluate the effects of possible deterioration problems, and particularly for large concrete dams located in important seismic zones. As shown in this work, the operation of these type of systems can be of great value to analyse the dynamic behaviour of dam-reservoir-foundation systems, to enable a continuous evaluation of dam performance and perform damage detection, and to characterize the seismic actions and analyse the seismic response of dams. In addition, the collection of more data on a larger number of dams can provide useful insight to help calibrate and validate existing numerical models and support the development of new models and formulations. On the other hand, more dams with complete SSHM systems will mean more available data and more useful information that can be shared with the scientific community through platforms such as the one referred above (one of the main issues in this field continues to be the lack of available and easily accessible data to engineers and researchers).

Regarding the two large concrete dams chosen as case studies for this work, there are some elements in which there is room for improvement, both in terms of the finite element models and of the installed SSHM systems, with a view to achieve a deeper knowledge on the dynamic behaviour of the dam-reservoir-foundation systems in future studies.

Although the current finite element models enabled to achieve very good results, some improvements can be made in order to get a more accurate representation of some specific geometry details. In the case of Cabril dam, a new mesh that incorporates the intake tower can be valuable for providing further insight on the intake tower behaviour and for investigation the influence of the dam-tower dynamic interaction in the dynamic properties of the dam-reservoir-foundation system. For Cahora Bassa dam, a model with perfected geometry details in the dam (including the half-hollow crest, the spillways, and the upstream face concrete dams) may be useful to improve the agreement between identified and computed modal parameters, particularly the mode shapes. Additionally, it could be interesting to develop several meshes of the dam-reservoir-foundation with different reservoir discretisation, to test the influence of the geometry and length of the reservoir block in the dynamic properties.

Improvements on the SSHM systems installed in both Cabril dam and Cahora Bassa dam are also proposed. For Cabril dam it is recommended the installation of an additional triaxial accelerometer at the downstream base, aiming to a) improve the characterization of the seismic action and its spatial variation along the insertion, and b) enable the performance of further studies concerning the measured seismic response, using more appropriate seismic inputs in the numerical models. In what concerns the program *DamSSHM*, the implemented method for the detection of seismic vibrations can be improved based on more sophisticated techniques for pattern recognition, perhaps using machine learning methods. As for Cahora Bassa dam, the

installation of more accelerometers in other galleries of the dam can be considered, with a view to improve the estimation of vibration mode shapes and the evaluation of the measured response during seismic events.

With respect to the formulations and methods developed in this work and implemented in *DamDySSA* and *DamModalID*, some improvements can be made in the future. In *DamDySSA*, possible improvements include a) the further increase in computational efficiency, e.g., using parallel computing methods, b) the upgrade of the current post-processing tools, namely the 3D graphical representations, or the development of new ones in accordance with the studies to be carried out, and c) the update of the developed graphical user interface, e.g. to improve the transition mechanisms between menus or to include new options. In *DamModalID*, some ideas are a) to optimize the existing algorithm for automatic modal identification from monitoring data gathered over time, b) to improve the definition of the DamFIC for the various vibration modes of the dam, based on new experimental and numerical data, possibly using clustering techniques and machine learning.

Furthermore, these programs can continue to be used by researchers and PhD or MSc students in the scope of research projects, aiming to conduct studies on the dynamic behaviour of dam-reservoir-foundation systems. These studies should focus on topics that require further investigation or that may provide valuable data on the dynamic performance of dams, namely to evaluate important aspects in the numerical models as dam-water and dam-foundation dynamic interaction, to investigate the influence of the reservoir water level on the seismic response, to study the influence of the reservoir block length and geometry, to examine the effects of the type of seismic input, using accelerograms with varying frequency content (close and distant earthquakes), and to analyse the damping required as input in the models to reproduce the measured response under low, medium or high intensity seismic events.

In what regards the proposed methodology for damage detection, based on the comparison between identified frequencies and computed frequency curves (using reference models without damage and models that simulate evolutive deterioration), it can be interesting to explore new techniques for modelling the damage evolution over time, e.g., considering different parts of the dam body with varying damage occurrence. Moreover, since this is such a simple and intuitive methodology, its application can be considered for structural health monitoring of large concrete dams instrumented with SSHM systems.

Concerning the methodology proposed for seismic safety verification, a possible suggestion of improvement can be the consideration of additional factors to define the endurance limits, e.g., including the influence of different reservoir water levels or using accelerograms with different frequency content - in that case, a set of various endurance limits could be defined for a specific dam.

Finally, it is worth emphasizing that the referred methodology and the program *DamDySSA* can be used in the future to support the design of new dams or in studies for seismic safety reassessment of older dams (whose seismic design was carried out based on outdated methods and performance criteria). For example, as done in Switzerland (recall subchapter 2.4), a program for seismic safety reassessment of older large concrete dams of high potential risk could be undertaken in Portugal using the tools provided in this work.

REFERENCES

REFERENCES

ADINA R & D Inc. (2020). *ADINA*. ADINA R & D Inc., Watertown, Massachusetts, United States.

Alegre, A. (2015). *Análise do comportamento sísmico da barragem de Luzzone. Desenvolvimento de um programa de EF3D utilizando uma formulação em deslocamentos e pressões [Seismic behaviour analysis of Luzzone dam. Development of a 3DFE program using a formulation in displace*. Master Thesis, Instituto Superior de Engenharia de Lisboa (ISEL), Portugal.

Alegre, A., Carvalho, E., Matsinhe, B., Mendes, P., Oliveira, S., & Proença, J. (2019). Monitoring vibrations in large dams. *HYDRO 2019 - Concept to Closure: Practical Steps*, Porto, Portugal.

Alegre, A., Mendes, P., Carvalho, E., Matsinhe, B., Oliveira, S., & Proença, J. (2021). Use of SSHM data for dynamic behavior analysis and damage detection on large dams. The cases of Cabril dam and Cahora Bassa dam. *10th International Conference on Structural Health Monitoring of Intelligent Infrastructure (SHMII-10)*, Porto, Portugal.

Alegre, A., & Oliveira, S. (2019). *Development of DamDamage3D1.0. A MATLAB program for non-linear analysis of arch dams using a damage model*. LNEC Report.

Alegre, A., & Oliveira, S. (2020). Non-linear seismic analysis of arch dams considering joint movements and a concrete damage model. *4th Dam World Conference*, LNEC.

Alegre, A., Oliveira, S., Carvalho, E., Matsinhe, B., Mendes, P., & Proença, J. (2020). Seismic and Structural Health Monitoring of Cahora Bassa dam and Non-Linear Seismic Analysis. *HYDRO 2020 - Strategies for Future Progress*, Online event.

Alegre, A., Oliveira, S., Espada, M., & Câmara, R. (2019). Seismic analysis of an ultra-high arch dam using the 3DFE program DamDySSA3.0. Study on the influence of the reservoir water level. *Revista Portuguesa de Engenharia de Estruturas., Série III*(11), 115–126, ISSN 2183-8488.

Alegre, A., Oliveira, S., Espada, M., Câmara, R., & Lemos, J. V. (2017). Pressões hidrodinâmicas em barragens abóbada: resultados numéricos e experimentais [Hydrodynamic pressures on arch dams: numerical and experimental results]. *Mecânica Experimental APAET*, *28*, 55–62.

Alegre, A., Robbe, E., & Oliveira, S. (2020). Seismic analysis of Cabril dam. Measured response and comparison with numerical results from Code_Aster and DamDySSA. *4th Dam World Conference*, LNEC.

Allemang, R. J., & Brown, D. L. (1982). A correlation coefficient for Modal Vector Analysis. *IMAC1: International Modal Analysis Conference*, Orlando, Florida, USA.

Alves, S. W. (2004). *Nonlinear analysis of Pacoima dam with spatially non-uniform ground motion*. Report No. EERL 2004-11, California Institute of Technology, Pasadena, California.

Alves, S. W., & Hall, J. F. (2006). Generation of spatially nonuniform ground motion for nonlinear analysis of a concrete arch dam. *Earthquake Engineering and Structural Dynamics*, *35*(11), 1139–1357.

Anclair, J. (1936). *Les études experimentales de l'Office National des Recherches Scientifiques et Industrielles des Constructions [The experimental studies of the National Office for Scientific and Industrial Research on Construction]*. Recherches et Inventions, No. 265, Paris.

Andersen, P. (1997). *Identification of Civil Engineering Structures using Vector ARMA Models*. PhD Thesis, Aalborg University, Denmark.

ANSYS Inc. (2020). *Ansys*. ANSYS Inc., Canonsburg, Pennsylvania, United States.

Arabshahi, H., & Lotfi, V. (2008). Earthquake response of concrete gravity dams including dam–foundation interface nonlinearities. *Engineering Structures*, *30*(11), 3065–3073. https://doi.org/10.1016/j.engstruct.2008.04.018

Batista, A. L. (1998). *Análise do comportamento ao longo do tempo de barragens abóbada [Arch dams behaviour analysis over time]*. PhD Thesis, Instituto Superior Técnico (University of Lisbon), Portugal.

Batista, A. L., & Piteira Gomes, J. (2014). Diagnóstico e reabilitação de barragens afectadas por reações expansivas do betão [Assessment and rehabilitation of dams affected by concrete swelling reactions]. *Seminar - Dams in the Community of Portuguese Langue Countries: Experience, Solutions, and Challenges*, Maputo, Mozambique.

Bažant, Z. P., & Cedolin, L. (1979). Blunt crack band propagation in finite element analysis. *ASCE Journal of Engineering Mechanics*, *105*(EM2), 297–315.

Bažant, Z. P., & Oh, B. H. (1983). Crack band theory for fracture of concrete. *Materials and Structures*, *16*(3), 155–177. https://doi.org/10.1007/BF02486267

Bažant, Z. P., & Planas, J. (1998). *Fracture and Size Effect in Concrete and Other Quasibrittle Materials* (1st ed.). Routledge. https://doi.org/10.1201/9780203756799

Belytschko, T. (1977). Methods and programs for analysis of fluid-structure systems. *Nuclear Engineering and Design*, *42*(1), 41–52. https://doi.org/10.1016/0029-5493(77)90060-7

Belytschko, T. (1980). Fluid-structure interaction. *Computers & Structures*, *12*(4), 459–469. https://doi.org/10.1016/0045-7949(80)90121-2

Bendat, J., & Piersol, A. (2010). *Random Data: Analysis and Measurement Procedures* (4th ed.). John Wiley & Sons.

Bendat, J. S., & Piersol, A. G. (1993). *Engineering Applications of Correlation and Spectral Analysis* (2nd ed.). John Wiley & Sons.

Bishop, C. M. (1995). *Neural networks for pattern recognition*. Oxford University Press.

Bommer, J., & Acevedo, A. B. (2004). The use of real earthquake accelerograms as input to dynamic analysis. *Journal of Earthquake Engineering*, *8*(sup001), 43–91. https://doi.org/10.1080/13632460409350521

Boore, D. M. (2003). Simulation of Ground Motion Using the Stochastic Method. *Pure and Applied Geophysics*, *160*, 636–676.

Borges, F., Pereira, J., Ravara, A., & Pedro, J. O. (1963). Seismic studies on concrete dam models. *Symposium on Concrete Dam Models, LNEC*, New Delhi, India.

Bouaanani, N., & Lu, F. Y. (2009). Assessment of potential-based fluid finite elements for seismic analysis of dam-reservoir systems. *Computers and Structures*, *87*, 206–224.

Bouaanani, N., & Renaud, S. (2014). Effects of fluid–structure interaction modeling assumptions on seismic floor acceleration demands within gravity dams. *Engineering Structures*, *67*, 1–18. https://doi.org/10.1016/j.engstruct.2014.02.004

Braga Farinha, L. (2010). *Hydromechanical behaviour of concrete dam foundations. In situ tests and numerical modelling*. PhD Thesis, Instituto Superior Técnico (University of Lisbon), Portugal.

Braga Farinha, L., Tavares de Castro, A., & Pina, C. (2004). *Definição e exploração de sistemas de recolha automática de dados da observação de barragens [Definition and operation of automatic data acquisition systems for dam observation]*. LNEC Report 175/04.

Brincker, R., Andersen, P., & Jacobsen, N. J. (2007). Automated Frequency Domain Decomposition for Operational Modal Analysis. *IMAC25: International Modal Analysis Conference*, Orlando, Florida, USA.

Brincker, R., & Ventura, C. (2015). *Introduction to Operational Modal Analysis*. John Wiley & Sons.

Brincker, R., Ventura, C., & Andersen, P. (2001). Damping estimation by Frequency Domain Decomposition. *IMAC19: International Modal Analysis Conference*, Kissimmee, Florida, USA.

Brincker, R., Zhang, L., & Andersen, P. (2000). Modal identification from ambient responses using Frequency Domain Decomposition. *IMAC18: International Modal Analysis Conference*, San Antonio, Texas, USA.

Brownjohn, J. M. W. (1990). *Dynamic investigation of Hermitage dam*. Report UBCE-EE-90-13,

Department of Civil Engineering, University of Bristol, UK.

Brownjohn, J. M. W., Magalhães, F., Caetano, E., & Cunha, A. (2010). Ambient vibration re-testing and operational modal analysis of the Humber Bridge. *Engineering Structures*, *32*(8), 2003–2018. https://doi.org/10.1016/j.engstruct.2010.02.034

Brownjohn, J. M. W., Severn, R. T., & Taylor, C. A. (1986). *Ambient vibration survey of Contra dam*.

Bukenya, P. (2020). *Structural performance evaluation of concrete arch dams using ambient vibration monitoring and GNNS systems*. PhD Thesis, University of Cape Town.

Bukenya, P., & Moyo, P. (2017). Monitoring the structural behaviour of concrete arch dams: the case of Roode Elsberg dam, South Africa. *SANCOLD Conference 2017: Management of Dams and Reservoirs in Southern Africa*, Centurion, Tshwane, South Africa.

Bukenya, P., Moyo, P., Beushausen, H., & Oosthuizen, C. (2012). Comparative study of operational modal analysis techniques using ambient vibration measurements of a concrete dam. *25th International Conference on Noise and Vibration Engineering*, Leuven, Belgium.

Bukenya, P., Moyo, P., & Oosthuizen, C. (2014). Towards long term dynamic monitoring of Roode Elsberg dam. *SANCOLD Conference 2014*.

Bukenya, P., Moyo, P., & Oosthuizen, C. (2012). Modal parameter estimation from ambient vibration measurements of a dam using stochastic subspace identification methods. *3rd International Conference on Concrete Repair, Rehabilitation and Retrofitting*, Cape Town, South Africa.

Cahghey, T. H., & O'Kelly, M. E. J. (1965). Classical normal modes in damped linear dynamic systems. *Journal of Applied Mechanics (ASME)*, *32*, 583–588.

Calcina, S. V., Eltrudis, L., Piroddi, L., & Ranieri, G. (2014). Ambient Vibration Tests of an Arch Dam with Different Reservoir Water Levels: Experimental Results and Comparison with Finite Element Modelling. *The Scientific World Journal*, 1–12. https://doi.org/10.1155/2014/692709

Câmara, R. (1989). *Modelos para estudo do comportamento dinâmico de barragens de betão pelo método dos elementos finitos [Models for studying the dynamic behaviour of concrete dams based on the finite element method]*. Specialist Thesis, LNEC.

Câmara, R., Oliveira, S., & Portugal, A. (1993). *Estudo do comportamento dinâmico da barragem do Alto Lindoso (Study of the dynamic behaviour of Alto Lindoso dam)*. LNEC Report.

Cantieni, R. (2001). Assessing a dam's structural properties using forced vibration testing. *IABSE International Conference on Safety, Risk and Reliability - Trends in Engineering*, Malta.

Cantieni, R. (2005). Experimental methods used in system identification of civil engineering structures. *IOMAC: International Operational Modal Analysis Conference*, Copenhagen, Denmark.

Cantieni, R., Deger, Y., & Pietrzko, S. (1994). Modal analysis of a concrete gravity dam: Experiment, finite element analysis and link. *12th International Modal Analysis Conference*, Honolulu, Hawaii.

Cantieni, R., Wiberg, U., Pietrzko, S., & Deger, Y. (1998). Modal investigation of a dam. *16th International Modal Analysis Conference*, Santa Barbara, California.

Carvalho, A. (2007). *Modelação estocástica da acção sísmica em Portugal Continental [Stochastic modelling of the seismic action in continental Portugal]*. PhD Thesis, Instituto Superior Técnico (University of Lisbon), Portugal.

Carvalho, E., & Matsinhe, B. (2014). First steps on automatic data acquisition and analysis system in Cahora Bassa dam. *HYDRO 2014*, Como, Italy.

Carvalho, E., & Tembe, I. (2012). On-Line Dynamic Monitoring of Cahora Bassa dam. *International Symposium on Dams for a Changing World*, Kyoto, Japan.

Carvalho, E., Valentim, N., & Oosthuizen, C. (2014). On-Line Dynamic Monitoring of Cahora Bassa dam ... the next level. *International Symposium on Dams for a Changing World*, Bali, Indonesia.

Ceravolo, R., de Lucia, G., Lenticchia, E., & Miraglia, G. (2019). Seismic Structural Health Monitoring of

Cultural Heritage Structures. In M. P. Limongelli & M. Çelebi (Eds.), *Seismic Structural Health Monitoring* (pp. 51–85). Springer International Publishing. https://doi.org/10.1007/978-3-030-13976-6_3

Cervera, M., Oliver, J., & Faria, R. (1995). Seismic evaluation of concrete dams via continuum damage models. *Earthquake Engineering & Structural Dynamics*, *24*(9), 1225–1245. https://doi.org/10.1002/eqe.4290240905

Chakrabarti, P., & Chopra, A. K. (1973). Earthquake analysis of gravity dams including hydrodynamic interaction. *Earthquake Engineering & Structural Dynamics*, *2*(2), 143–160. https://doi.org/10.1002/eqe.4290020205

Chen, D.-H., Du, C.-B., Yuan, J.-W., & Hong, Y.-W. (2012). An Investigation into the Influence of Damping on the Earthquake Response Analysis of a High Arch Dam. *Journal of Earthquake Engineering*, *16*(3), 329–349. https://doi.org/10.1080/13632469.2011.638697

Chen, H. (1994). *Model test and program verification on dynamic behaviour of arch dam with contraction joints*. Report No. SVL-94/2 IWHR.

Chen, H. (2014). Seismic safety of high concrete dams. *Earthquake Engineering & Engineering Vibration*, *13*(1), 1–16.

Chen, L., & Talwani, P. (1998). Reservoir-induced Seismicity in China. *Pure and Applied Geophysics*, *153*(1), 133–149. https://doi.org/10.1007/s000240050188

Chopra, A. K. (1967). Hydrodynamic pressures on dams during earthquakes. *ASCE Journal of Mechanical Engineering Division*, *93*(6), 205–224.

Chopra, A. K. (1976). Earthquake Resistant Design of Concrete Gravity Dams. *Journal of the Structural Division*, *104*(6), 953–971.

Chopra, A. K. (2012). Earthquake Analysis of Arch Dams: Factors to Be Considered. *Journal of Structural Engineering*, *138*(2), 205–214. https://doi.org/10.1061/(ASCE)ST.1943-541X.0000431

Chopra, A. K. (2017). *Dynamics of Structures: Theory and Applications to Earthquake Engineering* (5th ed.). Prentice Hall, Pearson.

Chopra, A. K., & Chakrabarti, P. (1972). The earthquake experience at Koyan dam and stresses in concrete gravity dams. *Earthquake Engineering & Structural Dynamics*, *1*, 151–164.

Chopra, A. K., & Chakrabarti, P. (1981). Earthquake analysis of concrete gravity dams including dam-water-foundation rock interaction. *Earthquake Engineering & Structural Dynamics*, *9*(4), 363–383. https://doi.org/10.1002/eqe.4290090406

Chopra, A. K., & Hall, J. F. (1982). Hydrodynamic effets in the dynamic response of concrete gravity dams. *Earthquake Engineering & Structural Dynamics*, 333–395.

Chopra, A. K., & Tan, H. (1992). Modelling dam-foundation interaction in analysis of arch dams. *10th World Conference on Earthquake Engineering*, Madrid, Spain.

Chopra, A. K., & Wang, J.-T. (2010). Earthquake response of arch dams to spatially varying ground motion. *Earthquake Engineering & Structural Dynamics*, *39*, 887–906. https://doi.org/10.1002/eqe.974

Chopra, A. K., & Wang, J.-T. (2012). Comparison of recorded and computed earthquake response of arch dams. *15th World Conference on Earthquake Engineering*, Lisbon, Portugal.

Chouinard, L., & Roy, V. (2006). Performance of statistical models for dam monitoring data. *Joint International Conference on Computing and Decision Making in Civil and Building Engineering*, Montreal, Canada.

Clough, R. W. (1962). *The Stress Distribution of Norfork Dam*. Institute of Engineering Research, Final Report to the Corps of Engineers,.

Clough, R. W. (1991). Original formulation of the Finite Element Method. *Finite Elements in Analysis and Design*, *7*, 89–101.

Clough, R. W. (1980). Non-linear mechanisms in the seismic response of arch dams. *International Research Conference on Earthquake Engineering*, Skopje, Yugoslavia.

Clough, R. W., Chang, K. T., Houqun, C., Stephen, R. M., Ghanaat, Y., & Qi, J. H. (1984). *Dynamic response behaviour of Quan Shui dam*. Report No. UCB/EERC-84/20, University of California, Berkeley, California.

Clough, R. W., Chang, K. T., Houqun, C., Stephen, R. M., Wang, G., & Ghanaat, Y. (1984). *Dynamic response behaviour of Xiang Hong Dian dam*. Report No. UCB/EERC-84/02, University of California, Berkeley, California.

Clough, R. W., & Ghanaat, Y. (1987). Experimental study of arch dam-reservoir interaction. *Proceedings of the Joint China-USA Workshop on Earthquake Behaviour of Arch Dams*, Beijing, China.

Clough, R. W., & Penzien, J. (2003). *Dynamics of Structures* (Third). Computers & Structures, Inc.

Clough, R. W., Stephen, R. M., & Kuo, J. S. H. (1982). *Dynamic response analysis of Techi dam*. Report No. UCB/EERC 82/11, University of California, Berkeley.

Clough, R. W., & Wilson, E. L. (1999). Early finite element research at Berkeley. *Fifth US National Conference on Computational Mechanics*.

Clough, R. W., & Wilson, E. L. (1962). Stress Analysis of a Gravity Dam by the Finite Element Method. *Symposium on the USe of Computers in Civil Engineering*, Lisbon, Portugal.

CNPGB. (2021). *CNPGB - Dams in Portugal*. https://cnpgb.apambiente.pt/gr_barragens/gbingles/INDEX.HTM

COADI. (1922). *Arch Dam Investigations*. Reporst by the Commitee on Arch Dam Investigations, Vols. I, II,II.Engineering Foundation.

Cole, H. A. (1968, April). On-the-line analysis of random vibrations. *AIAA/ASME 9th Structural Dynamics and Materials Conference*. https://doi.org/10.2514/6.1968-288

Cooley, J. W., & Tukey, J. W. (1965). An Algorithm for the Machine Calculation of Complex Fourier Series. *Mathematics of Computation*, *19*(90), 297–301.

Cundall, P. A. (1971). A computer model for simulating progressive large scale movements in blocky rock systems. *International Symposium on Rock Mechanics (ISRM)*.

Cunha, Á., & Caetano, E. (2006). Experimental Modal Analysis of Civil Engineering Structures. *Sound and Vibration*, *6*(40), 12–20.

Cunha, Á., Caetano, E., Magalhães, F., & Moutinho, C. (2018). Dynamic identification and continuous dynamic monitoring of bridges: different applications along bridges life cycle. *Structure and Infrastructure Engineering*, *14*(4), 445–467. https://doi.org/10.1080/15732479.2017.1406959

Daniel, W. J. . (1980). Modal methods in finite element fluid-structure problems with mixed variables. *International Journal of Numerical Methods in Engineering*, *15*, 1161–1175.

Daniell, W. E., & Taylor, C. A. (1999). Effective ambient vibration testing for validating numerical models of concrete dams. *Earthquake Engineering and Structural Dynamics*, *1344*(January 1998), 1327–1344.

Darbre, G. R. (1995). Strong-motion instrumentation of dams. *Earthquake Engineering & Structural Dynamics*, *24*(8), 1101–1111. https://doi.org/10.1002/eqe.4290240805

Darbre, G. R., de Smet, C. A. M., & Kraemer, C. (2000). Natural frequencies measured from ambient vibration response of the arch dam of Mauvoisin. *Earthquake Engineering & Structural Dynamics*, *29*(5), 577–586. https://doi.org/10.1002/(SICI)1096-9845(200005)29:5<577::AID-EQE924>3.0.CO;2-P

Darbre, G. R., & Proulx, J. (2002). Continuous ambient-vibration monitoring of the arch dam of Mauvoisin. *Earthquake Engineering & Structural Dynamics*, *31*(2), 475–480. https://doi.org/10.1002/eqe.118

Darbre, G. R., Schwager, M. V, & Panduri, R. (2019). Seismic safety evaluation of large dams in

Switzerland: lessons learned. *International Water Power and Dam Construction*.

Dassault Systèmes Simulia Corp. (2020). *Abaqus 2020x* (6.20). Dassault Systèmes Simulia Corp. ,Johnston, Rhode Island, United States.

de Borst, R., & Sluys, L. J. (1999). *Computational Methods in Non-Linear Solid Mechanics*. Faculty of Civil Engineering and Geosciences. Delft University of Technology, Delft.

de Smet, C. A. M., Kraemer, C., & Darbre, G. R. (1998). Ambient tests at the dam of Mauvoisin. *16th International Modal Analysis Conference*, Santa Barbara, California.

Deinum, P. J., Dungar, R., Ellis, B. R., Jeary, A. P., Reed, G. A. L., & Severn, R. T. (1982). Vibration tests on emosson arch dam, Switzerland. *Earthquake Engineering & Structural Dynamics*, *10*(3), 447–470. https://doi.org/10.1002/eqe.4290100308

Delgado, R. (1984). *O método dos elementos finitos na análise dinâmica de barragens incluindo a interacção sólido-líquido [The finite element method for dynamic analysis of dams including solid-fluid interaction]*. PhD Thesis, University of Porto (FEUP).

DIANA FEA BV. (2020). *DIANA FEA* (10.4). DIANA FEA BV, Delft The Netherlands.

Dominguez, J., & Maeso, O. (1992). Model for the seismic analysis of arch dams including interaction effects. *10th World Conference on Earthquake Engineering*, Madrid, Spain.

DSR. (2018). Dam Safety Regulation. *Decree-Law Nº 21/2018 of March 28, Portuguese Republic Diary No. 62, Series I*.

Duron, Z. H., & Hall, J. F. (1988). Experimental and finite element studies of the forced vibration response of morrow point dam. *Earthquake Engineering & Structural Dynamics*, *16*(7), 1021–1039. https://doi.org/10.1002/eqe.4290160706

El-Aidi, B., & Hall, J. F. (1989a). Non-linear earthquake response of concrete gravity dams part 1: Modelling. *Earthquake Engineering & Structural Dynamics*, *18*(6), 837–851. https://doi.org/10.1002/eqe.4290180607

El-Aidi, B., & Hall, J. F. (1989b). Non-linear earthquake response of concrete gravity dams part 2: Behaviour. *Earthquake Engineering & Structural Dynamics*, *18*(6), 853–865. https://doi.org/10.1002/eqe.4290180608

EN 1998. (2004). *Eurocode 8: Deisgn of structures for earthquake resistance* (p. European Standard 1992). European Committee for Standardization (CEN), Brussels, Belgium.

Espada, M. (2010). *Desenvolvimento de modelos para análise dinâmica de estruturas. Aplicação a barragens de betão e estruturas auxiliares [Models development for structural dynamic analysis. Concrete dams and auxiliary structures]*. Master Thesis, Instituto Superior de Engenharia de Lisboa (ISEL), Portugal.

Espandar, R., & Lotfi, V. (2003). Comparison of non-orthogonal smeared crack and plasticity models for dynamic analysis of concrete arch dams. *Computers & Structures*, *81*(14), 1461–1474. https://doi.org/10.1016/S0045-7949(03)00083-X

Estekanchi, H. E., Vafai, H., & Sadeghazar, M. (2004). Endurance Time Method for Seismic Analysis and Design of Structures. *Scientia Iranica*, *11*(4), 361–370.

Euler, L. (1768). *Institutionum Calculi Integralis. Volumen Primum.* Petropoli: Impensis Academiae Imperialis Scientiarum.

Fanelli, M. (1980). *Automatic observation and instantaneous control of dam safety. Part one: an approach to the problem* (p. ISMES, Bergamo, Italy).

Fanelli, M. (1999). Models and Methods of Analysis. In J. O. Pedro (Ed.), *Arch Dams. Designing and monitoring for safety. International Centre for Mechanical Sciences (Courses and Lectures), vol 367* (pp. 79–288). Springer Vienna. https://doi.org/10.1007/978-3-7091-2488-8_2

Faria, R. (1994). *Avaliação do comportamento sísmico de barragens de betão através de um modelo de dano contínuo [Evaluation of the seismic behaviour of concrete dams using a continuous damage*

model]. PhD Thesis,University of Porto (FEUP).

Faria, R., & Oliver, J. (1993). A rate-dependent plastic-damage constitutive model for large scale computations in concrete structures. *Monografia Centro Internacional de Metodos Numericos in Ingenieria (CIMNE)*, *17*, Barcelona, Spain.

Faria, R., Oliver, J., & Cervera, M. (1998). A strain-based plastic viscous-damage model for massive concrete structures. *International Journal of Solids and Structures*, *35*(14), 1533–1558. https://doi.org/10.1016/S0020-7683(97)00119-4

Felber, A. (1993). *Development of a Hybrid Bridge Evaluation System*. PhD Thesis, University of British Columbia, Vancouver, Canada.

Felippa, C. A. (1988). Symmetrization of coupled eigenproblems by eigenvector augmentation. *Communications in Applied Numerical Methods*, *4*, 561–563.

Fenves, G. L., & Chopra, A. K. (1983). Effects of reservoir bottom absorption on earthquake response of concrete gravity dams. *Earthquake Engineering & Structural Dynamics*, *11*(6), 809–829. https://doi.org/10.1002/eqe.4290110607

Fenves, G. L., & Chopra, A. K. (1986). *Simplified analysis for earthquake resistant design of concrete gravity dams*. Report No. UCB/EERC-85/10, University of California, Berkeley, California.

Fenves, G. L., Mojtahedi, S., & Reimer, R. B. (1989). *ADAP-88: a computer program for non-linear earthquake analysis of concrete arch dams*. Report No. UCB/EERC-89/12, University of California, Berkeley, California.

Fenves, G. L., Mojtahedi, S., & Reimer, R. B. (1992). Effect of contraction joints on earthquake response of an arch dam. *Journal of Structural Engineering (ASCE)*, *118*, 1039–1055.

Fialho, L. (1955). *Princípios orientadores do projecto de barragens abóbada.Um novo método de traçado e dimensionamento [Guidelines for the design of arch dams. A new method of layout and design]*. LNEC Memoirs.

Fok, K. L., & Chopra, A. K. (1986a). Earthquake analysis of arch dams including dam-water interaction, reservoir boundary absorption and foundation flexibility. *Earthquake Engineering and Structural Dynamics*, *14*, 155–184.

Fok, K. L., & Chopra, A. K. (1986b). Hydrodynamic and foundation flexibility effects in earthquake response of arch dams. *Journal of Structural Engineering (ASCE)*, *112*, 1810–1828.

Fok, K. L., & Chopra, A. K. (1987). Water Compressibility in Earthquake Response of Arch Dams. *Journal of Structural Engineering*, *113*(5), 958–975. https://doi.org/10.1061/(ASCE)0733-9445(1987)113:5(958)

Fok, K. L., Hall, J. F., & Chopra, A. K. (1986). *EACD-3D: a computer program for three-dimensional earthquake analysis of concrete dams*. Report No. UCB/EERC-86/09, University of California, Berkeley, California.

Furgani, L., Hariri-Ardebili, M. A., Meghella, M., & Seyed-Kolbadi, S. M. (2019). On the Dynamic Capacity of Concrete Dams. *Infrastructures*, *4*(3), 57. https://doi.org/10.3390/infrastructures4030057

García-Palacios, J. H., Soria, J. M., Díaz, I. M., & Tirado-Andrés, F. (2016). Ambient modal testing of a double-arch dam: the experimental campaign and model updating. *Journal of Physics: Conference Series*, *744*, 012037. https://doi.org/10.1088/1742-6596/744/1/012037

Garrett, A. (2007). A instrumentação no controlo da segurança de grandes obras. Perspetivas de desenvolvimento [Instrumentation in the safety control of large civil engineering works. Development perspectives]. *ICM2007*, Lisboa, Portugal.

Gasparini, D. A., & Vanmarcke, E. H. (1976a). *SIMQKE, A Program for Artificial Motion Generation: User's Manual and Documentation*. Dept. of Civil Engineering, Massachusetts Institute of Technology.

Gasparini, D. A., & Vanmarcke, E. H. (1976b). *Simulated Earthquake Motions Compatible with Prescribed*

Response Spectra. Research Report R76-4, Dept. of Civil Engineering, Massachusetts Institute of Technology.

Gauron, O., Boivin, Y., Ambroise, S., Paultre, P., Proulx, J., Roberge, M., & Roth, S.-N. (2017). Forced-Vibration Tests of the Daniel-Johnson Multiple-Arch Dam. *Experimental Vibration Analysis for Civil Engineering Structures*, San Diego, California, United States. https://doi.org/10.1007/978-3-319-67443-8_34

GeoSIG. (2009a). *Strong motion network of Enguri arch dam (272 m)*. https://www.geosig.com/

GeoSIG. (2009b). *Strong motion network of Enguri arch dam (272 m)*.

GeoSIG. (2021). *GeoSIG - Applications: Seismic Instrumentation and Monitoring of Dams*.

Ghanaat, Y. (1993). *Theoretical Manual for Analysis of Arch Dams*. Technical Report ITL-93-1, U.S Army Corps Of Engineers. Washington, DC.

Gogoi, I., & Maity, D. (2010). A novel procedure for determination of hydrodynamic pressure along upstream face of dams due to earthquakes. *Computers & Structures*, *88*(9–10), 539–548. https://doi.org/10.1016/j.compstruc.2010.01.007

Goldgruber, M. (2015). *Non-Linear Seismic Modelling of Concrete Dams*. PhD Thesis, Graz University of Technology, Austria.

Goldgruber, M., Shahriari, S., & Zenz, G. (2013). Influence of damping and different interaction modelling on a high arch dam. *Vienna Congress on Recent Advances in Earthquake Engineering and Structural Dynamics*, Vienna, Austria.

Gomes, J. (2006). *Análise experimental de cenários de rotura em fundações de barragens de betão. Ensaios estáticos e dinâmicos. [Experimental analysis of failure scenarios on concrete dam foundations. Static and dynamic tests]*. Specialist Thesis, LNEC, Portugal; PhD Thesis, Universidade Federal do Rio de Janeiro, Brazil.

Gomes, J. (2010). Ensaio na mesa sísmica de um modelo de uma barragem abóbada [Earthquake shaking table test of an arch dam model]. *Congresso Nacional de Mecânica Experimental*, Guimarães, Portugal.

Gomes, J., Azevedo, N., & Oliveira, S. (2016). Caracterização do comportamento dinâmico da barragem do Alto Ceira II através da realização de ensaios de vibração forçada e de ruído ambiente [Characterisation of the dynamic behaviour of the Alto Ceira II dam through forced vibration and ambient vibrati. *10º Congresso Nacional de Mecânica Experimental*, LNEC, Lisboa, Portugal.

Gomes, J., & Carvalho, E. (2014). Ensaios de vibração forçada para caracterização do comportamento dinâmico de barragens de betão. Aplicação à barragem de Cahora Bassa. *5as Jornadas Portuguesas de Engenharia de Estruturas*.

Gomes, J., & Lemos, J. V. (2016). Ensaio de vibração forçada para a caracterização do comportamento dinâmico de barragens de betão [Forced vibration tests for the charachterization of the dynamic behaviour of concrete dams]. *10º Congresso Nacional de Mecânica Experimental*, LNEC, Lisboa, Portugal.

Gomes, J., Magalhães, F., Monteiro, G. S., Palma, J., Pereira, S., & Silva Matos, D. (2018). Seismic monitoring system of Baixo Sabor scheme for structural dynamic behavior monitoring and risk management. *26th ICOLD Congress on Large Dams*, Vienna, Austria.

Gomes, J., & Oliveira, S. (1994). *Estudo do comportamento dinâmico da barragem do Alto Lindoso. 3º ensaio de vibração forçada [Study of the dynamic behaviour of Alto Lindoso dam. 3rd forced vibration test]*. LNEC Report.

Guillaume, P., Hermans, L., & Van der Auweraer, H. (1999). Maximum Likelihood Identification of modal parameters from operational data. *IMAC17: International Modal Analysis Conference*, Kissimmee, Florida, USA.

Hall, J. F. (1988). The dynamic and earthquake behaviour of concrete dams: review of experimental behaviour and observational evidence. *Soil Dynamics and Earthquake Engineering*, *7*(2), 58–121.

https://doi.org/10.1016/S0267-7261(88)80001-0

Hall, J. F. (1998). Efficient non-linear seismic analysis of arch dams. *Earthquake Engineering and Structural Dynamics*, *27*(12), 1425–1444.

Hall, J. F., & Chopra, A. K. (1980). *Dynamic response of embankment concrete-gravity and arch dams including hydrodynamic interaction*. Report No. UCB/EERC-80/39, University of California, Berkeley, California.

Hamdi, M. A., Ousset, Y., & Verchery, G. (1978). A displacement method for the analysis of vibrations of coupled fluid-structure systems. *International Journal on Numerical Methods in Engineering*, *13*, 139–150.

Hariri-Ardebili, M. A., & Mirzabozorg, H. (2011). Reservoir fluctuation effects on seismic response of high concrete arch dams considering material nonlinearity. *Journal of Civil Engineering Research*, *1*(1), 9–20.

Hariri-Ardebili, M. A., & Mirzabozorg, H. (2012a). Seismic performance evaluation and analysis of major arch dams considering material and joint nonlinearity effects. *ISRN Civil Engineering*, *2012*, 1–10. https://doi.org/10.5402/2012/681350

Hariri-Ardebili, M. A., & Mirzabozorg, H. (2012b). Seismic Performance Evaluation and Analysis of Major Arch Dams Considering Material and Joint Nonlinearity Effects. *ISRN Civil Engineering*, *2012*, 1–10. https://doi.org/10.5402/2012/681350

Hariri-Ardebili, M. A., & Mirzabozorg, H. (2013). A comparative study of seismic stability of coupled arch dam-foundation-reservoir systems using infinite elements and viscous boundary models. *International Journal of Structural Stability and Dynamics*, *13*(6), 1–24. https://doi.org/10.1142/S0219455413500326

Hariri-Ardebili, M. A., & Mirzabozorg, H. (2014). Estimation of probable damages in arch dams subjected to strong ground motions using endurance time acceleration functions. *KSCE Journal of Civil Engineering*, *18*(2), 574–586. https://doi.org/10.1007/s12205-013-0264-6

Hariri-Ardebili, M. A., Mirzabozorg, H., & Estekanchi, H. E. (2014). Nonlinear seismic assessment of arch dams and investigation of joint behavior using Endurance Time Analysis Method. *Arabian Journal for Science and Engineering*, *39*(5), 3599–3615. https://doi.org/10.1007/s13369-014-1027-5

Hillerborg, A. (1985). Numerical methods to simulate softening and fracture of concrete. In *Fracture mechanics of concrete: Structural application and numerical calculation* (pp. 141–170). Springer Netherlands. https://doi.org/10.1007/978-94-009-6152-4_3

Hillerborg, A., Modéer, M., & Petersson, P.-E. (1976). Analysis of crack formation and crack growth in concrete by means of fracture mechanics and finite elements. *Cement and Concrete Research*, *6*(6), 773–781. https://doi.org/10.1016/0008-8846(76)90007-7

Houqun, C. (2020). Seismic safety analysis of tall concrete dams, investigation and insights on critical challenges. *Earthquake Engineering and Engineering Vibration*, *19*(3), 533–539. https://doi.org/10.1007/s11803-020-0578-6

Ibrahim, S. R. (1977). Random decrement technique for modal identification of structures. *Journal of Spacecraft and Rockets*, *14*, 696–700.

Ibrahim, S. R., & Milkulcik, E. C. (1977). A method for direct identifictaion of vibration parameters from the free response. *The Shock and Vibration Bulletin*, *47*, 183–196.

ICOLD. (1986). *Bulletin 52: Earthquake analysis procedures for dams*. International Commission on Large Dams.

ICOLD. (1989). *Bulletin 72: Selecting seismic parameters for large dams*. International Commission on Large Dams.

ICOLD. (1997). *Position Paper on Dams and the Environment*. International Commission on Large Dams.

ICOLD. (1998). *Bulletin 112: Neotectonics and dams*. Committee on Seismic Aspects of Dam Design,

International Commission on Large Dams.

ICOLD. (1999). *Bulletin 118: Automated dam monitoring systems. Guidelines and case histories*. International Commission on Large Dams.

ICOLD. (2001). *Bulletin 120: Design features of dams to effectively resist seismic ground motion*. Committee on Seismic Aspects of Dam Design, International Commission on Large Dams.

ICOLD. (2002). *Bulletin 123: Earthquake design and evaluation of structures appurtenant to dams*. Committee on Seismic Aspects of Dam Design, International Commission on Large Dams.

ICOLD. (2007). *Dams & The World's Water*. International Commission on Large Dams.

ICOLD. (2011). *Bulletin 137: Reservoirs and seismicity - state of knowledge*. Committee on Seismic Aspects of Dam Design, International Commission on Large Dams.

ICOLD. (2014). *Bulletin 149. Role of dams on the development and management of rivers basins. A general review*. International Commission on Large Dams.

ICOLD. (2016a). *Bulletin 148: Selecting seismic parameters for large dams – Guidelines (revision of Bulletin 72)*. International Commission on Large Dams.

ICOLD. (2016b). *Bulletin 169: Global climate change, dams, reservoirs and related water sources*. International Commission on Large Dams.

ICOLD. (2017a). *Bulletin 154: Dam safety management. Operational phase of the dam life cycle*. International Commission on Large Dams.

ICOLD. (2017b). *Bulletin 168: Recommendations for operation, maintenance and rehabilitation*. International Commission on Large Dams.

ICOLD. (2018). *Bulletin 158: Dam surveillance guide*. International Commission on Large Dams.

ICOLD. (2019a). *Bulletin 185: Challenges and needs for dams in the 21st century*. International Commission on Large Dams.

ICOLD. (2019b). *World Declaration on Dam Safety*. International Commission on Large Dams.

ICOLD. (2020). *International Commission on Large Dams*. http://www.icold-cigb.net

ICOLD. (2021). *Bulletin 173: Integrated operation of hydropower stations and reservoirs*. International Commission on Large Dams.

IJHD. (2020). *World Atlas & Industry Guide*. International Journal of Hydropower and Dams, Aqua Media Int. Ltd.

IPCC. (2018). *Global Warming of 1.5°C. An IPCC Special Report on the impacts of global warming of 1.5°C above pre-industrial levels and related global greenhouse gas emission pathways, in the context of strengthening the global response to the threat of climate change*. Intergovernmental Panel on Climate Change, Special Report, [Masson-Delmotte, V., P. Zhai, H.-O. Pörtner, D. Roberts, J. Skea, P.R. Shukla, A. Pirani, W. Moufouma-Okia, C. Péan, R. Pidcock, S. Connors, J.B.R. Matthews, Y. Chen, X. Zhou, M.I. Gomis, E. Lonn.

Itasca Consulting Group Inc. (2019). *FLAC 3D - Fast Lagrangian Analysis of Continua in Three-Dimensions* (7.0). Minneapolis: Itasca.

Itasca Consulting Group Inc. (2020). *3DEC — Three-Dimensional Distinct Element Code* (7.0). Minneapolis: Itasca.

Jirásek, M. (2002). Objective modeling of strain localization. *Revue Française de Génie Civil*, *6*(6), 1119–1132. https://doi.org/10.1080/12795119.2002.9692735

Kachanov, L. M. (1958). Time of the Rupture Process under creep conditions. *Izvestiia Akademii Nauk SSSR, Otdelenie Teckhnicheskikh Nauk*, *8*, 26–31.

Kachanov, L. M. (1986). *Introduction to continuum damage mechanics* (Vol. 10). Springer Netherlands. https://doi.org/10.1007/978-94-017-1957-5

Kao, C.-Y., & Loh, C.-H. (2013). Monitoring of long-term static deformation data of Fei-Tsui arch dam using artificial neural network-based approaches. *Structural Control and Health Monitoring*, *20*(3), 282–303. https://doi.org/10.1002/stc.492

Kemp, B. G. (1996). *Ambient vibration assessment of Ruskin dam dynamic properties*. Master Thesis, The University of British Columbia.

Kemp, B. G., Ventura, C., Anderson, D. L., & Felber, A. (1995). Ambient Vibration Measurement of Ruskin Dam for Seismic Assessment. *The Canadian Conference on Earthquake Engineering*, Montreal, Canada.

Koufoudi, E., Chaljub, E., Dufour, F., Bard, P. Y., Humbert, N., & Robbe, E. (2018). Spatial variability of earthquake ground motions at the dam–foundation rock interface of Saint Guérin: experimental and numerical investigations. *Bulletin of Earthquake Engineering*, *16*(5), 1751–1777. https://doi.org/10.1007/s10518-017-0266-8

Küçükarslan, S. (2004). Time-domain dynamic analysis of dam–reservoir–foundation interaction including the reservoir bottom absorption. *International Journal for Numerical and Analytical Methods in Geomechanics*, *28*(9), 963–980. https://doi.org/10.1002/nag.369

Küçükarslan, S., Coşkun, S. B., & Taşkın, B. (2005). Transient analysis of dam–reservoir interaction including the reservoir bottom effects. *Journal of Fluids and Structures*, *20*(8), 1073–1084. https://doi.org/10.1016/j.jfluidstructs.2005.05.004

Lau, D. T., Boruziaan, B., & Razaqpur, A. G. (1998). Modelling of contraction joint and shear sliding effects on earthquake response of arch dams. *Earthquake Engineering and Structural Dynamics*, *27*, 1013–1029.

Lemaitre, J. (1984). How to use damage mechanics. *Nuclear Engineering and Design*, *80*(2), 233–245.

Lemaitre, J., & Chaboche, J. (1978). Aspects phénoménologiques de la rupture par endommagement [Phenomenological aspects of fracture by damage]. *Journal de Mécanique Appliqué*, *2*(3), 317–365.

Lemos, J. V. (1987). *A Distinct Element Model for Dynamic Analyis of Jointed Rock with Application to Dam Foundations and Fault Motion*. PhD Thesis, University of Minnesota, Minnesota, USA.

Lemos, J. V. (1998). *Development of an arch dam analysis module for the program 3DEC*. LNEC Report.

Lemos, J. V. (1999). Discrete Element Analysis of Dam Foundations. In *Distinct Element Modelling in Geomechanics* (pp. 89–115). Routledge. https://doi.org/10.1201/9781315141398-4

Lemos, J. V., Oliveira, S., & Mendes, P. (2008). Analysis of the dynamic behaviour of Cabril dam considering the influence of contraction joints. *7th European Conference on Structural Dynamics EURODYN 2008*, Southampton, United Kingdom.

Li-EDF-KP. (2001). *Seismic Hazard Assessment of Cahora Bassa extension and Mepanda Uncua hydroelectric projects on Zambezi river /Mozambique*.

Li, H.-N., Li, D.-S., Ren, L., Yi, T.-H., Jia, Z.-G., & LI, K.-P. (2016). Structural health monitoring of innovative civil engineering structures in Mainland China. *Structural Monitoring and Maintenance*, *3*(1), 1–32. https://doi.org/10.12989/smm.2016.3.1.001

Liao, Z. P., Wong, H. L., Yang, B. P., & Yuan, Y. F. (1984). A transmitting boundary for transient wave analyses. *Scientia Sinica (Series A)*, *27*(10), 1063–1076.

Limongelli, M. P. (2020). SHM for informed management of civil structures and infrastructure. *Journal of Civil Structural Health Monitoring*, *10*(5), 739–741. https://doi.org/10.1007/s13349-020-00439-8

Limongelli, M. P. (2019). Vibration-based structural health monitoring: Challenges and opportunities. In A. Zingoni (Ed.), *Advances in Engineering Materials, Structures and Systems: Innovations, Mechanics and Applications. Proceedings of the 7th International Conference on Structural Engineering, Mechanics and Computation (SEMC 2019)* (pp. 1999–2004). Taylor & Francis.

Limongelli, M. P., & Çelebi, M. (Eds.). (2019). *Seismic Structural Health Monitoring*. Springer International Publishing. https://doi.org/10.1007/978-3-030-13976-6

Liseikin, A. V., Seleznev, V. S., & Adilov, Z. A. (2020). Monitoring of the natural frequencies of Chirkey arch dam. *Magazine of Civil Engineering*, *96*(4), 15–26.

Ljung, L. (1999). *System Identification: Theory for the User* (2nd ed.). Prentice Hall.

LNEC. (2003). *Observation of Cabril dam (Operation phase period from 1982 to 2001). Behaviour analysis and evaluation of safety conditions [Observação da Barragem do Cabril (Período da fase de exploração de 1982 a 2001). Análise do comportamento e avaliação das condiçõ*. Third Report, LNEC report 397/2003, NMMF/NO.

LNEC. (2009). *Cahora Bassa Hydroelectric Scheme. Analysis of the seismic dam behaviour*. LNEC Report 247/2009, NMMF.

Loh, C.-H., & Wu, T.-S. (1996). Identification of Fei-Tsui arch dam from both ambient and seismic response data. *Soil Dynamics and Earthquake Engineering*, *15*(7), 465–483. https://doi.org/10.1016/0267-7261(96)00016-4

Lokke, A., & Chopra, A. K. (2018). Direct finite element method for nonlinear earthquake analysis of 3-dimensional semi-unbounded dam–water-foundation rock systems. *Earthquake Engineering & Structural Dynamics*, 1–20.

Lotfi, V. (2005). Frequency domain analysis of concrete arch dams by decoupled modal approach. *Structural Engineering and Mechanics*, *21*(4), 423–435.

Lubliner, J. (1972). On the thermodynamic foundations of non-linear solid mechanics. *International Journal of Non-Linear Mechanics*, *7*, 237–254.

Lynch, J. P. (2007). An overview of wireless structural health monitoring for civil structures. *Philosophical Transactions of the Royal Society A: Mathematical, Physical and Engineering Sciences*, *365*(1851), 345–372. https://doi.org/10.1098/rsta.2006.1932

Lysmer, J., & Kuhlemeyer, R. L. (1969). Finite dynamic model for infinite media. *Journal of the Engineering Mechanics Division (ASCE)*, *95*, 759–877.

Maeso, O., Aznárez, J., & Dominguez, J. (2002). Effects of Space Distribution of Excitation on Seismic Response of Arch Dams. *Journal of Engineering Mechanics*, *128*(7), 759–768. https://doi.org/10.1061/(ASCE)0733-9399(2002)128:7(759)

Maeso, O., Aznárez, J., & Domínguez, J. (2004). Three-dimensional models of reservoir sediment and effects on the seismic response of arch dams. *Earthquake Engineering & Structural Dynamics*, *33*(10), 1103–1123. https://doi.org/10.1002/eqe.392

Magalhães, F. (2010). *Operational Modal Analysis for Testing and Monitoring of Bridges and Special Structures*. PhD Thesis, University of Porto (FEUP).

Magalhães, F., Cunha, Á., & Caetano, E. (2012). Vibration based structural health monitoring of an arch bridge: From automated OMA to damage detection. *Mechanical Systems and Signal Processing*, *28*, 212–228. https://doi.org/10.1016/j.ymssp.2011.06.011

Maia, N., & Silva, J. (1997). *Theoretical and Experimental Modal Analysis*. Research Studies Press Ltd.

Makha, R., & Moyo, P. (2012). Observations from the calibration of an arch dam model using ambient modal properties. In *Concrete Repair, Rehabilitation and Retrofitting III* (1st ed.). CRC Press.

Malm, R., & Ansell, A. (2011). Cracking of concrete buttress dam due to seasonal temperature variation. *ACI Structural Journal*, *108*, 13–22.

Malm, R., Hellgren, R., Ekströsm, T., & Fu, C. (2014). Cracking of a concrete arch dam due to seasonal temperature variations - Theme A. *14th ICOLD International Benchmark Workshop on Numerical Analysis of Dams*, Stockholm, Sweden.

Mashayekhi, M., Estekanchi, H. E., & Vafai, H. (2019). Simulation of Endurance Time Excitations Using Increasing SineFunctions. *International Journal of Optimization in Civil Engineering*, *9*, 65–77.

Mashayekhi, M., Estekanchi, H. E., Vafai, H., & Ahmadi, G. (2019). An evolutionary optimization-based approach for simulation of endurance time load functions. *Engineering Optimization*, *51*(12), 2069–

2088. https://doi.org/10.1080/0305215X.2019.1567724

Mata, J., Schclar Leitão, N., Tavares de Castro, A., & Sá da Costa, J. (2014). Construction of decision rules for early detection of a developing concrete arch dam failure scenario. A discriminant approach. *Computers & Structures*, *142*, 45–53. https://doi.org/10.1016/j.compstruc.2014.07.002

Mata, J., Tavares de Castro, A., & Sá da Costa, J. (2013). Time–frequency analysis for concrete dam safety control: Correlation between the daily variation of structural response and air temperature. *Engineering Structures*, *48*, 658–665. https://doi.org/10.1016/j.engstruct.2012.12.013

Mazars, J., & Pijaudier-Cabot, G. (1989). Continuum damage theory. Application to concrete. *ASCE Journal of Engineering Mechanics*, *115*(2), 345–365.

Meghella, M., & Furgani, L. (2014). Application of Endurance Time Analysis Method to the NonLinear Seismic Analysis of dams: Potentialities and Limitations. *ICOLD 82nd Annual Meeting*, Banff, Alberta, Canada.

Mendes, P. (2010). *Observação e análise do comportamento dinâmico de barragens de betão [Observation and analysis of concrete dams dynamic behaviour]*. PhD Thesis, University of Porto (FEUP/LNEC).

Mendes, P., Oliveira Costa, C., Almeida Garret, J., & Oliveira, S. (2007). Development of monitoring system to Cabril dam with operational modal analysis. *2nd Experimental Vibration Analysis for Civil Engineering Structures (EVACES)*, Porto, Portugal.

Mendes, P., & Oliveira, S. (2009). Influence of the dynamic behaviour of the intake tower on modal identification of Cabril dam. *3rd International Operational Modal Analysis Conference (IOMAC'09)*, Ancona, Italy.

Mendes, P., & Oliveira, S. (2007). Study of dam-reservoir dynamic interaction using vibration tests on a physical model. *2nd International Operational Modal Analysis Conference*, Copenhagen, Denmark.

Mendes, P., Oliveira, S., Guerreiro, S., Baptista, M. A., & Campos Costa, A. (2004). Dynamic behaviour of concrete dams: monitoring and modelling. *13th World Conference on Earthquake Engineering*, Vancouver, Canada.

Millán, M. A., Young, Y. L., & Prévost, J. H. (2007). The effects of reservoir geometry on the seismic response of gravity dams. *Earthquake Engineering & Structural Dynamics*, *36*(11), 1441–1459. https://doi.org/10.1002/eqe.688

Miquel, B., & Bouaanani, N. (2010). Simplified evaluation of the vibration period and seismic response of gravity dam–water systems. *Engineering Structures*, *32*(8), 2488–2502. https://doi.org/10.1016/j.engstruct.2010.04.025

Mirzabozorg, H., Akbari, M., & Hariri-Ardebili, M. A. (2013). Nonlinear seismic response of a concrete arch dam to spatially varying earthquake ground motions. *Asian Journal of Civil Engineering (BHRC)*, *14*(6), 859–879.

Mirzabozorg, H., Kordzadeh, A., & Hariri-Ardebili, M. A. (2012). Seismic response of concrete arch dams including dam-reservoir-foundation interaction using infinite elements. *Electronic Journal of Structural Engineering*, *12*(1), 63–73.

Mitchell, T. M. (1997). *Machine Learning*. McGraw-Hill, Inc.

Mivehchi, M. R., & Ahmadi, M. T. (2004). Evaluation of discrepancies between the dynamic characteristics of mathematical and prototype models of concrete arch dam. *13th International Congress on Large Dams*, Vancouver, Canada.

Mivehchi, M. R., Ahmadi, M. T., & Hajmomeni, A. (2003). Effective Techniques for Arch Dam Ambient Vibration Test: Application on Two Iranian Dams. *Journal of Seismology and Earthquake Engineering*, *5*(2), 23–34.

Monti, G., Fumagalli, F., Quaranta, G., Sgroi, M., & Tommasi, M. (2018). A permanent wireless dynamic monitoring system for the Colosseum in Rome. *Journal of Structural Integrity and Maintenance*, *3*(2), 75–85. https://doi.org/10.1080/24705314.2018.1463020

Moyo, P., Hattingh, L., & Oosthuizen, C. (2013). Ambient vibration measurements at Kouga dam - getting much more information than expected. *ICOLD Symposium*, Seattle, USA.

Moyo, P., & Oosthuizen, C. (2010). Ambient vibration survey trials of two arch dams in South Africa. *9th ICOLD European Club Symposium*, Innsbruck, Austria.

Mridha, S., & Maity, D. (2014). Experimental investigation on nonlinear dynamic response of concrete gravity dam-reservoir system. *Engineering Structures*, *80*, 289–297.

Newmark, N. (1959). A method of computation for structural dynamics. *Journal of the Engineering Mechanics Division (ASCE)*, *85*, 67–94.

Ni, Y. Q., Xia, Y., Liao, W. Y., & Ko, J. M. (2009). Technology innovation in developing the structural health monitoring system for Guangzhou New TV Tower. *Structural Control and Health Monitoring*, *16*(1), 73–98. https://doi.org/10.1002/stc.303

Niwa, A., & Clough, R. W. (1980). *Shaking table research on concrete dam models*. Report No. CB/EERC 80-85. Earthquake Engineering Research Center, University of California, Berkeley, USA.

Niwa, A., & Clough, R. W. (1982). Non-linear seismic response of arch dams. *Earthquake Engineering and Structural Dynamics*, *10*, 267–281.

Nordström, E., Hassanzadeh, M., Malm, R., Ekströsm, T., & Janz, M. (2019). *Structural safety of cracked concrete dams*. Technical Report 2019:623, Energiforsk.

Novak, P., Moffat, A. I. B., Nalluri, C., & Narayanan, R. (2007). *Hydraulic Structures* (4th ed.). Taylor & Francis.

Nozari, A., & Estekanchi, H. E. (2011). Optimization of endurance time acceleration functions for seismic assessment of structures. *International Journal of Optimization in Civil Engineering*, *1*, 257–277.

NP EN1998-1. (2010). *Eurocódigo 8: Projecto de estruturas para resistência aos sismos [Eurocode 8: Design of structures for earthquake resistance]* (p. Norma Portuguesa, NP EN1998). Instituto Português da Qualidade (IPQ), Portugal.

NPB. (1993). *Normas de Projecto de Barragens [Portuguese Standards for Dam Design]*. Decree No. 846/93 of September 10, Portuguese Republic Diary No. 213/1993, Series I-B.

Oberti, G. (1946). Studio sperimentale delle dighe [Experimental study of dams]. *Nuove Ricerche Nelle Construzioni Civili, Edizioni della Bussola: Roma*.

Ohayon, R. (1979). Symmetric variational formulations for harmonic vibration problems coupling primal and dual variables - application to fluid-structure coupled systems. *La Rechereche Aerospatiale*, *3*, 69–77.

Ohayon, R., & Valid, R. (1984). True symmetric formulation of free vibrations for fluid-structure interaction in bounded media - finite element results. In R. W. Lewis, P. Bettess, & E. Hinton (Eds.), *Numerical Methods in Coupled Systems*. John Wiley & Sons.

Okuma, N., Etou, Y., Kanazawa, K., & Hirata, K. (2008). Dynamic properties of a large arch dam after forty-five years of completion. *14th World Conference on Earthquake Engineering*, Beijing, China.

Okuma, N., Ikeda, K., Mazda, T., Kanazawa, K., & Nagata, S. (2012). Structural monitoring test for an aged large arch dam based on ambient vibration measurement. *15th World Conference on Earthquake Engineering*, Lisboa, Portugal.

Oliveira, E. A., & Pedro, J. O. (1986). The rise and decline of structural analysis as a research topic in structural engineering. *International Conference on Recent Advances in Simulation of Complex Systems*, Tokyo, Japan.

Oliveira, S. (2000). *Modelos para análise do comportamento de barragens de betão considerando a fissuração e os efeitos do tempo. Formulações de dano [Models for the analysis of concrete dams behaviour considering cracking and time effects. Damage formulations]*. PhD Thesis, University of Porto (FEUP).

Oliveira, S. (2002). *"'Continuous monitoring systems for the dynamic performance assessment of arch*

dams''. Sub-program D, in Study of evolutive deterioration processes in concrete dams. Safety control over time. National Program for Scientific Re-equipment funded by FCT, REEQ/815/ECM/2005, LNEC-FEUP.

Oliveira, S. (2013). Análise de Fourier e Aplicações em Dinâmica de Estruturas [Fourier Analysis and Aplications to Dynamic of Structures]. In F. Pestana da Costa, J. Pinto, & J. Buescu (Eds.), *Matemática do Planeta Terra* (pp. 235–284).

Oliveira, S., & Alegre, A. (2019a). Seismic and Structural Health Monitoring of Dams in Portugal. In M. P. Limongelli & M. Çelebi (Eds.), *Seismic Structural Health Monitoring* (pp. 87–113). Springer International Publishing. https://doi.org/10.1007/978-3-030-13976-6_4

Oliveira, S., & Alegre, A. (2020). Seismic and structural health monitoring of Cabril dam. Software development for informed management. *Journal of Civil Structural Health Monitoring*, *10*(5), 913–925. https://doi.org/10.1007/s13349-020-00425-0

Oliveira, S., & Alegre, A. (2019b). Seismic and structural health monitoring of Cabril dam. *3rd Meeting of EWG Dams and Earthquakes, an International Symposium*, Lisbon, Portugal.

Oliveira, S., & Alegre, A. (2018). Vibrations in large dams. Monitoring and modelling. *26th ICOLD Congress on Large Dams*, Vienna, Austria.

Oliveira, S., Alegre, A., Silvestre, A., Espada, M., & Câmara, R. (2015). Seismic safety evaluation of Luzzone dam. Use of a 3DFEM state formulation in pressures and displacements. *13th ICOLD International Benchmark Workshop on Numerical Analysis of Dams*, EPFL, Lausanne.

Oliveira, S., Espada, M., & Câmara, R. (2012). Long-term dynamic monitoring of arch dams . The case of Cabril dam, Portugal. *15th World Conference on Earthquake Engineering*, Lisbon, Portugal.

Oliveira, S., & Faria, R. (2006). Numerical simulation of collapse scenarios in reduced scale tests of arch dams. *Engineering Structures*, *28*(10), 1430–1439.

Oliveira, S., Faria, R., & Gaspar, N. (2003). Models of isotropic damage for analysing cracking of concrete dams. Apparent fracture energy and objectivity of numerical solutions. *VII Congresso de Mecânica Aplicada e Computacional*, University of Évora.

Oliveira, S., Ferreira, I., Berberan, A., Mendes, P., Boavida, J., & Baptista, B. (2010). Monitoring the structural integrity of large concrete dams: the case of Cabril dam, Portugal. *HYDRO 2010*, Lisbon, Portugal.

Oliveira, S., & Lima, J. (2012). *"'Task 5 - Improvement of Cabril dam monitoring system using GNSS. Development of Software MoniDam for automatic monitoring data analysis'" in GNSS accelerometers data fusion in large structures monitoring*. Project funded by FCT, PTDC/ECM-EST/2131/2012), LNEC.

Oliveira, S., Mendes, P., Garrett, A., Oliveira Costa, C., & Reis, J. (2011). Long-term dynamic monitoring systems for the safety control of large concrete dams. The case of Cabril dam, Poirtugal. *6th International Conference on Dam Engineering*, Lisbon, Portugal.

Oliveira, S., Rodrigues, J., & Campos Costa, A. (2004). Damage charachterization in concrete dams using output-only modal analysis. *22nd International Modal Analysis Conference*, Dearborn, Michigan.

Oliveira, S., Rodrigues, J., Campos Costa, A., & Mendes, P. (2003). Damage detection in concrete dams using dynamic continuous monitoring and numerical models. *Computational Methods in Engineering and Science*, 435–442.

Oliveira, S., Rodrigues, J., Mendes, P., & Campos Costa, A. (2003). Monitorização do comportamento dinâmico de barragens de betão [Monitoring the dynamic behaviour of concrete dams]. *VII Congresso de Mecânica Aplicada e Computacional*, Évora, Portugal.

Oliveira, S., & Silvestre, A. (2017). *Barragem do Cabril. Sistema para Monitorização de Vibrações em Contínuo [Cabril dam. System for Continuous Vibrations Monitoring]*. LNEC Report.

Oliveira, S., Silvestre, A., & Câmara, R. (2014). *Barragem de Ribeiradio. Obra construída. Verificação da segurança estrutural para ações estáticas e dinâmicas. Cenários correntes e de rotura [Ribeiradio*

dam. Built structure. Structural safety verification under static and dynamic loads. Current and fail. LNEC Report.

Oliveira, S., Silvestre, A., Espada, M., & Câmara, R. (2014). Modeling the dynamic behavior of dam-reservoir-foundation systems considering generalized damping. Development of a 3DFEM state formulation. *International Conference on Structural Dynamic EURODYN*, Porto, Portugal.

Oliver, J. (1989). A consistent characteristic length for smeared cracking models. *International Journal for Numerical Methods in Engineering*, *28*(2), 461–474. https://doi.org/10.1002/nme.1620280214

Olson, L. G., & Bathe, K.-J. (1983). A study of displacement-based fluid finite elements for calculating frequencies of fluid and fluid-structure systems. *Nuclear Engineering and Design*, *76*(2), 137–151. https://doi.org/10.1016/0029-5493(83)90130-9

Pedro, J. O. (1967). *Dimensionamento de Barragens de Betão pelo Método dos Elementos Finitos [Concrete dam design using the Finite Element Method]*. Specialist Thesis, LNEC, Portugal.

Pedro, J. O. (1977). *Dimensionamento de barragens abóbada pelo método dos elementos finitos [Concrete dam design using the Finite Element Method]*. Specialist Thesis (LNEC memoir 479), LNEC, Portugal.

Pedro, J. O. (1999). Safety and Performance of Arch Dams. In J. O. Pedro (Ed.), *Arch Dams. Designing and monitoring for safety. International Centre for Mechanical Sciences (Courses and Lectures), vol 367* (pp. 1–78). Springer Vienna. https://doi.org/10.1007/978-3-7091-2488-8_1

Pedro, J. O., & Câmara, R. (1986). Coupled models for dynamic analysis of arch dams. *8th European Conference on Earthquake Engineering*, Lisbon, Portugal.

Pedro, J. O., Câmara, R., & Oliveira, S. (1996). Mathematical models for the safety and performance evaluation of arch dams under seismic actions. *2nd International Conference on Dam Safety Evaluation, ICOLD and CBIP*, Trivandrum, India.

Pedro, J. O., & Pereira, J. (1979). Models for seismic analysis of arch dams. *13th International Congress on Large Dams*, New Dehli, India.

Peeters, B. (2000). *System identification and damage detection in civil engineering*. PhD Thesis, Faculteit Toegepaste Wetenschapen, Katholieke Universiteir Leuven.

Peeters, B., & Van der Auweraer, H. (2005). PolyMax: a revolution in Operational Modal Analysis. *IOMAC: International Operational Modal Analysis Conference*, Copenhagen, Denmark.

Pereira, J., & Ravara, A. (1973). *Estudo sísmico da barragem de Cahora Bassa [Seismic study of Cahora Bassa dam]*. LNEC Report.

Pereira, S. (2019). *Structural condition assessment of dams based on continuous dynamic monitoring*. PhD Thesis, University of Porto (FEUP).

Pereira, S., Magalhães, F., Cunha, Á., Moutinho, C., & Pacheco, J. (2021). Modal identification of concrete dams under natural excitation. *Journal of Civil Structural Health Monitoring*.

Pereira, S., Magalhães, F., Gomes, J., Cunha, Á., & Lemos, J. V. (2018). Dynamic monitoring of a concrete arch dam during the first filling of the reservoir. *Engineering Structures*, *174*, 548–560. https://doi.org/10.1016/j.engstruct.2018.07.076

Pereira, S., Magalhães, F., Gomes, J., Cunha, Á., & Lemos, J. V. (2017). Installation and results from the first 6 months of operation of the dynamic monitoring system of Baixo Sabor arch dam. *10th International Conference on Structural Dynamics EURODYN 2017*, Rome, Italy.

Pereira, S., Magalhães, F., Gomes, J., Cunha, Á., Paixão, J., & Lemos, J. V. (2021). Continuous Dynamic Monitoring System of Foz Tua Arch Dam: Installation and First Results. *EWSHM 2020: European Workshop on Structural Health Monitoring*, 316–326. https://doi.org/10.1007/978-3-030-64594-6_32

Pietruszczak, S., & Mróz, Z. (1981). Finite element analysis of deformation of strain-softening materials. *International Journal for Numerical Methods in Engineering*, *17*(3), 327–334. https://doi.org/10.1002/nme.1620170303

Pietrzko, S., & Cantieni, R. (1994). Modal testing of a gravity dam - Influence of the exciter placement on the quality of the identified modal parameters. *12th International Modal Analysis Conference*, Honolulu, Hawaii.

Pina, C. (1988). *Modelos de elementos finitos para estudo de barragens de betão. Cenários correntes e de rotura [Finite element models to study concrete dams. Regular and failure scenarios]*. Specialist Thesis, LNEC, Portugal.

Pina, C. (1999). *A análise estrutural no controlo de segurança de barragens de betão [Structural analysis on the safety control of concrete dams]*. Research program, LNEC.

Pina, C., & Gomes, J. (1996). *Barragem do Cabril. Ensaio de vibração forçada [Cabril dam. Forced vibration test]*. LNEC Report.

Piteira Gomes, J. (2007). *Modelação do comportamento estrutural de barragens de betão sujeitas a reações expansivas [Modelling the structural behaviour of concrete dams under swelling reactions]*. PhD Thesis, NOVA School of Science and Technology, Portugal.

Portugal, A. (1990). *Caracterização do comportamento dinâmico de barragens de betão através de ensaios in situ [Characterization of the dynamic behaviour of concrete dams based on in situ tests]*. Master Thesis, Instituto Superior Técnico (University of Lisbon), Portugal.

Portugal, A., & Caetano, E. (1992). Experimental evaluation of the dynamic characteristics of portuguese dams. *10th World Conference on Earthquake Engineering*, Madrid, Espanha.

Proulx, J., & Darbre, G. R. (2008). Earthquake response of large arch dams. Observational evidence and numerical modelling. *14th World Conference on Earthquake Engineering*, Beijing, China.

Proulx, J., Darbre, G. R., & Kamileris, N. (2004). Analytical and experimental investigation of damping in arch dams based on recorded earthquakes. *13th World Conference on Earthquake Engineering*, Vancouver, Canada.

Proulx, J., & Paultre, P. (1997). Experimental and numerical investigation of dam-reservoir-foundation interaction for a large gravity dam. *Canadian Journal of Civil Engineering*, *24*, 90–105.

Proulx, J., Paultre, P., Reheault, J., & Robert, Y. (2001). An experimental investigation of water level effects on the dynamic behaviour of a large arch dam. *Eartquake Engineering and Structural Dynamics*, *30*(8), 1147–1166. https://doi.org/10.1002/eqe.055

Rea, D., Liaw, C. Y., & Chopra, A. K. (1972). *Dynamic properties of Pine Flat dam*. Report No. EERC 72-7. University of California, Berkeley.

Reimer, R. B. (1973). *Deconvolution of seismic response for linear systems*. Report No. EERC 73-10. University of California, Berkeley.

Reis, J., & Oliveira Costa, C. (2009). *Cabril_Aquis. Manual do utilizador [Cabril_Aquis. User manual]*. LNEC Report.

Robbe, E. (2017). Seismic back analysis of Monticello arch dam - blind prediction workshop and additional analyses. *USSD 2017 Annual Conference and Exhibition*, Anaheim, California.

Robbe, E., & Humbert, N. (2019). DamQuake: More than just a database, a powerful tool to analyze and compare earthquake records on dams. In *Sustainable and Safe Dams Around the World* (pp. 2864–2871). CRC Press. https://doi.org/10.1201/9780429319778-256

Robbe, E., Kashiwayanagi, M., & Yamane, Y. (2017). Seismic analyses of concrete dam, comparison between finite-element analyses and seismic records. *16th World Conference on Earthquake Engineering*, Santiago, Chile.

Rocha e Silva, F., Silva, H. S., & Guale, R. (2005). Monitoramento ambiental da albufeira de Cahora Bassa [Environmental monitoring of the Cahora Bassa dam reservoir]. *7º Simpósio de Hidráulica e Recursos Hídricos Dos Países de Língua Oficial Portuguesa*, Évora, Portugal.

Rocha, M., & Serafim, J. L. (1948). Model Tests of Santa Luzia Dam. *3rd ICOLD Congress on Large Dams*, Stockholm, Sweden.

Rocha, M., & Serafim, J. L. (1958). The problem of safety of arch dams. Rupture studies on models. *6th ICOLD Congress on Large Dams*, New York, United States of America.

Rocha, M., Serafim, J. L., & Silveira, A. (1958). A method of quantitative interpretation of the results obtained in the observation of dams. *6th ICOLD Congress on Large Dams*, New York, USA.

Rodrigues, J. (2004). *Identificação Modal Estocástica. Métodos de análise e aplicações em estruturas de engenharia civil [Stochastic Modal Identification. Methods of analysis and applications for civil engineering structures]*. PhD Thesis, University of Porto (FEUP).

Rodrigues, M., & Oliveira, S. (2019). *Structural analysis of gravity dams considering non-linear behaviour in the dam-foundation interface. Development of a 3DFE code using MATLAB: DamSlide3D*. LNEC Report.

Rodrigues, M., Oliveira, S., Lima, J., & Proença, J. (2020). Displacement monitoring in Cabril dam using GNSS. *4th Dam World Conference*, LNEC.

Rodrigues, M., Oliveira, S., Proença, J., & Alegre, A. (2019). Safety control of Aguieira dam using hybrid HSCT-FEM models. *HYDRO 2019 - Concept to Closure: Practical Steps*, Porto, Portugal.

Roehm, L. H. (1971). *Comparison of computed and measured dynamic response of Monticello dam*. Report REC-ECR-71-45, Bureau of Reclamation, Denver, Colorado.

Rosça, B. (2008). Physical model method for seismic study of concrete dams. *Bulletin of the Polytechnic Institute of Iași - Construction, Architecture. Gheorghe Asachi Technical University of Iași, Romania*, *3*.

RSB. (2018). *Regulamento de Segurança de Barragens [Dam Safety Regulation]*. Decree-law No. 21/2018 of March 28, Portuguese Republic Diary No. 62, Series I.

Salamon, J., Hariri-Ardebili, M. A., Malm, R., Wood, C., & Faggiani, G. (2021). Numerical Analysis of Dams. Theme A: Seismic Analysis of Pine Flat Concrete Dam. In G. Bolzon, D. Sterpi, G. Mazzà, & A. Frigerio (Eds.), *15th ICOLD International Benchmark Workshop* (Vol. 91, p. Milan, Italy). Springer International Publishing. https://doi.org/10.1007/978-3-030-51085-5

Salazar, F., Morán, R., Toledo, M. Á., & Oñate, E. (2017). Data-Based Models for the Prediction of Dam Behaviour: A Review and Some Methodological Considerations. *Archives of Computational Methods in Engineering*, *24*(1), 1–21. https://doi.org/10.1007/s11831-015-9157-9

Sani, A. A., & Lotfi, V. (2010). Dynamic analysis of concrete arch dams by ideal-coupled modal approach. *Engineering Structures*, *32*, 1377–1383.

Serafim, J. L. (1958). *Análise geral crítica dos métodos de cálculo mais importantes das barragens-abóbada [Overview of the most important calculation methods of arch dams]*. LNEC Memoir 126.

Serafim, J. L., & Costa, J. P. (1961). Methods and materials for the study of the weight stresses in dams by means of models. *Bulletin RILEM*, *10*.

Serafim, J. L., & Oliveira, C. S. (1987). Effects caused by earthquakes on dams. *ICOLD Symposium*, Beijing, China.

Severn, R. T. (2010). The development of experimental methods in structural dynamics. *Structure and Infrastructure Engineering*, *6*(5), 503–520. https://doi.org/10.1080/15732470903068532

Severn, R. T., Jeary, A. P., & Ellis, B. R. (1980). Forced vibration tests and theoretical studies on dams. *Proceedings of the Institution of Civil Engineers, Part 2*, *69*(3), 605–634.

Sevim, B., Altunışık, A. C., Bayraktar, A., Akköse, M., & Calayir, Y. (2011). Water length and height effects on the earthquake behavior of arch dam-reservoir-foundation systems. *KSCE Journal of Civil Engineering*, *15*(2), 295–303.

Sevim, B., Bayraktar, A., & Altunışık, A. C. (2011). Finite element model calibration of berke arch dam using operational modal testing. *Journal of Vibration and Control*, *17*(7), 1065–1079. https://doi.org/10.1177/1077546310377912

Sevim, B., Bayraktar, A., Altunışık, A. C., Adanur, S., & Akköse, M. (2012). Determination of Water Level

Effects on the Dynamic Characteristics of a Prototype Arch Dam Model using Ambient Vibration Testing. *Experimental Techniques*, *36*(1), 72–82. https://doi.org/10.1111/j.1747-1567.2010.00671.x

Silva, H. S. (1993). *Estudo do envelhecimento das barragens de betão e de alvenaria. Alteração físico-química dos materiais [Study on the ageing of concrete and masonry dams. Physicochemical material changes]*. Specialist Thesis, LNEC.

Silva Matos, D., Tavares de Castro, A., Gomes, A., & Figueiredo, J. N. (2019). The behaviour of Foz Tua dam during the first filling of the reservoir and its first years of operation. *HYDRO 2019*, Porto, Portugal.

Silva Matos, D., Tavares de Castro, A., Gomes, J., Faria, A., Pimentel, D., & Lima, J. (2019). Static and continuous dynamic monitoring of Foz Tua arch dam. *HYDRO 2019*, Porto, Portugal.

Simo, J. C., & Ju, J. W. (1987). Strain- and Stress-Based Continuum Damage Models - I. Formulation / II. Computational Aspects. *International Journal of Solids and Structures*, *23*(7), 821-840 / 841-869.

Simon, A., Royer, M., Mauris, F., & Fabre, J. (2013). Analysis and interpretation of dam measurements using artificial neural networks. *9th ICOLD European Club Symposium*, Venice, Italy.

Structural Vibration Solutions. (2020). *ARTeMIS Modal* (No. 7). Structural Vibration Solutions A/S, Denmark.

Su, J.-Z., Xia, Y., Chen, L., Zhao, X., Zhang, Q.-L., Xu, Y.-L., Ding, J.-M., Xiong, H.-B., Ma, R.-J., Lv, X.-L., & Chen, A.-R. (2013). Long-term structural performance monitoring system for the Shanghai Tower. *Journal of Civil Structural Health Monitoring*, *3*(1), 49–61. https://doi.org/10.1007/s13349-012-0034-z

Tan, H., & Chopra, A. K. (1995a). Dam-foundation rock interaction effects in frequency-response functions of arch dams. *Earthquake Engineering & Structural Dynamics*, *24*(11), 1475–1489. https://doi.org/10.1002/eqe.4290241105

Tan, H., & Chopra, A. K. (1995b). Earthquake analysis of arch dams including dam-water-foundation rock interaction. *Earthquake Engineering & Structural Dynamics*, *24*(11), 1453–1474. https://doi.org/10.1002/eqe.4290241104

Tan, H., & Chopra, A. K. (1996). Dam-foundation rock interaction effects in earthquake response of arch dams. *Journal of Structural Engineering*, *122*, 528–538.

Tarinejad, R., Falsafian, K., Aalami, M. T., & Ahmadi, M. T. (2016). Modal identification of Karun IV arch dam based on ambient vibration tests and seismic responses. *Journal of Vibroengineering*, *18*(6), 3869–3880. https://doi.org/10.21595/jve.2016.16989

Tiliouine, B., & Seghir, A. (1998). Fluid-structure models for dynamic studies of dam-water systems. *11th European Conference on Earthquake Engineering*.

Ueshima, T., Shiojiri, H., & Kanazawa, K. (2017). Structural health monitoring of an aged arch dam using long-term continuous observation of ambient vibration/seismic motion. *16th World Conference on Earthquake Engineering*, Santiago, Chile.

UN. (2019a). *World Population Prospects 2019: Highlights*. United Nations, Department of Economic and Social Affairs, Population Division (ST/ESA/SER.A/423).

UN. (2019b). *World Population Prospects 2019: Wall Chart*. United Nations, Department of Economic and Social Affairs, Population Division (ST/ESA/SER.A/434).

UNESCO UN-Water. (2020). *United Nations World Water Development Report 2020:Water and Climate Change*. Paris, UNESCO.

USBR. (1930). *Model tests of Boulder Dam*. Boulder Canyon Project: Final Reporst. Bulletin No.3.

USBR. (1998a). *Linear elastic analysis addressing structural issues for the modification decision analysis for Deadwood Dam*. Technical Memorandum DEA-D8110-MDA-TM-98-1, United States Bureau of Reclamation (USBR), Denver, CO.

USBR. (1998b). *Linear elastic dynamic structural analysis including mass in the foundation for Hoover*

Dam. Technical Memorandum HVD-MDA-D8110-97-2, United States Bureau of Reclamation (USBR), Denver, CO.

USBR. (1999). *Linear elastic static and dynamic structural analysis of Monticello Dam*. United States Bureau of Reclamation (USBR), Denver, CO.

USBR. (2002). *Static and dynamic linear elastic structural analysis (EACD3D96), Morrow Point Dam*. United States Bureau of Reclamation (USBR), Denver, CO.

USCOLD. (1977). *Earthquake recordings on or near dams*. United States Comittee on Large Dams.

USSD. (2014). *Observed Performance of Dams During Earthquakes: Volume III*. Commitee on Earthquakes, United States Society on Dams.

Valamanesh, V., Estekanchi, H. E., Vafai, A., & Ghaemian, M. (2011). Application of the endurance time method in seismic analysis of concrete gravity dams. *Scientia Iranica*, *18*(3), 326–337. https://doi.org/10.1016/j.scient.2011.05.039

Valliappan, S., Yazdchi, M., & Khalili, N. (1999). Seismic analysis of arch dams - a continuum damage mechanics approach. *International Journal of Numerical Methods in Engineering*, *45*(11), 1695–1724.

Vamvatsikos, D., & Cornell, C. A. (2002). Incremental dynamic analysis. *Earthquake Engineering & Structural Dynamics*, *31*(3), 491–514. https://doi.org/10.1002/eqe.141

Van Overschee, P., De Moor, B., Dehandschutter, W., & Swevers, J. (1997). A subspace algorithm for the identification of discrete time frequency domain power spectra. *Automatica*, *33*(12), 2147–2157.

Van Overschee, Peter, & De Moor, B. (1996). *Subspace Identification for Linear Systems*. Springer US. https://doi.org/10.1007/978-1-4613-0465-4

Vargas-Loli, L. M., & Fenves, G. L. (1989). Effects of concrete cracking on the earthquake response of gravity dams. *Earthquake Engineering & Structural Dynamics*, *18*(4), 575–592. https://doi.org/10.1002/eqe.4290180411

Veletsos, A., & Ventura, C. (1986). Modal analysis of non-classically damped linear systems. *Earthquake Engineering and Structural Dynamics*, *14*, 217–243.

Wang, H., & Li, D. (2006). Experimental study of seismic overloading of large arch dam. *Earthquake Engineering & Structural Dynamics*, *35*, 199–216.

Wang, H., & Li, D. (2007). Experimental study of dynamic damage of an arch dam. *Earthquake Engineering & Structural Dynamics*, *36*, 247–366.

Wang, J.-T., & Chopra, A. K. (2008). *A computer program for three-dimensional analysis of concrete dams subjected to spatially-varying ground motion*. Report No. UCB/EERC-2008/04, Earthquake Engineering Research Center, University of California, Berkeley, California.

Wang, J.-T., & Chopra, A. K. (2010). Linear analysis of concrete arch dams including dam-water-foundation rock interaction considering spatially varying ground motions. *Earthquake Engineering & Structural Dynamics*, *39*(7), 731–750. https://doi.org/10.1002/eqe.968

Wang, J.-T., Lv, D.-D., Jin, F., & Zhang, C. (2013). Earthquake damage analysis of arch dams considering dam–water–foundation interaction. *Soil Dynamics and Earthquake Engineering*, *49*, 64–74. https://doi.org/10.1016/j.soildyn.2013.02.006

Wang, J.-T., Zhang, C., & Jin, F. (2012). Nonlinear earthquake analysis of high arch dam-water-foundation rock systems. *Earthquake Engineering & Structural Dynamics*, *41*(7), 1157–1176. https://doi.org/10.1002/eqe.1178

Wang, R. (2016). Key technologies in the design and construction of 300 m ultra-high arch dams. *Engineering*, *2*, 350–359.

Wang, R., Chen, L., & Zhang, C. (2018). Seismic design of Xiluodu ultra-high arch dam. *Water Science and Engineering*, *11*(4), 288–301. https://doi.org/10.1016/j.wse.2019.01.002

Wang, S. S., Zhang, Y. F., Cao, M. S., & Xu, W. (2015). Effects of Contraction Joints on Vibrational Characteristics of Arch Dams: Experimental Study. *Shock and Vibration*, *2015*, 1–7. https://doi.org/10.1155/2015/327362

Welch, P. (1967). The use of fast Fourier transform for the estimation of power spectra: A method based on time averaging over short, modified periodograms. *IEEE Transactions on Audio and Electroacoustics*, *15*(2), 70–73. https://doi.org/10.1109/TAU.1967.1161901

Westergaard, H. M. (1928). Theorical analysis of the structural action of the Stevenson Creek arch dam. In *Arch Dam Investigation* (Vol. 1). Americal Society of Civil Engineers.

Westergaard, H. M. (1931). Arch dam analysis by trial loads simplified. *Engineering News Records*, 141.

Westergaard, H. M. (1933). Water pressures on dams during earthquakes. *Transactions (ASCE)*, *98*, 418–472.

Wieland, M. (2005). Tensile stresses in concrete dams. *Water Power and Dam Construction*.

Wieland, M. (2010). Features of seismic hazard in large dam projects and strong motion monitoring of large dams. *Frontiers of Architecture and Civil Engineering in China*, *4*(1), 56–64. https://doi.org/10.1007/s11709-010-0005-6

Wieland, M. (2014). Seismic Hazard and Seismic Design and Safety Aspects of Large Dam Projects. In A. Ansal (Ed.), *Perspectives on European Earthquake Engineering and Seismology. Geotechnical, Geological and Earthquake Engineering* (pp. 627–650). Springer, Cham. https://doi.org/10.1007/978-3-319-07118-3_20

Wieland, M. (2016). Safety Aspects of Sustainable Storage Dams and Earthquake Safety of Existing Dams. *Engineering*, *2*(3), 325–331. https://doi.org/10.1016/J.ENG.2016.03.011

Wieland, M. (2019a). Models of Earthquake Ground Shaking Used in Seismic Design and Safety Checks of Large Dams. *International Journal of Civil Engineering*, *17*(4), 515–522. https://doi.org/10.1007/s40999-018-0339-3

Wieland, M. (2003). Earthquake safety of concrete dams and seismic design criteria for major dam projects. *Conference on Hydropower Stations*, Tehran, Iran.

Wieland, M. (2008). Large dams the first structures designed systematcally agains earthquakes. *14th World Conference on Earthquake Engineering*, Beijing, China.

Wieland, M. (2019b). Seismic design and performance criteria for large dams and methods of dynamic analysis. *International Dam Safety Conference*, Odisha, India.

Wieland, M., & Chen, H. (2009). Leassons learnt from the Wenchuan earthquake. *International Water Power and Dam Construction*.

Willm, G., & Beaujoint, N. (1967). Les méthodes de surveillance des barrages au service de la productin hydraulique d'Electricité de France - Problémes ancients et solution nouvells [Monitoring methods of dams in service of the hydraulic production of Electricité de France - Old problems a. *9th ICOLD Congress on Large Dams*.

Wilson, E. L. (1968). *A computer program for the dynamic stress analysis of underground structures*. SEL Report 68-1, University of California, Berkeley.

Yang, J., Jin, F., Wang, J.-T., & Kou, L.-H. (2017). System identification and modal analysis of an arch dam based on earthquake response records. *Soil Dynamics and Earthquake Engineering*, *92*, 109–121. https://doi.org/10.1016/J.SOILDYN.2016.09.039

Yu, H., Wu, Z., Bao, T., & Zhang, L. (2010). Multivariate analysis in dam monitoring data with PCA. *Science China Technological Sciences*, *53*, 1088–1097.

Zangar, C. N. (1952). Hydrodynamic pressures on dams due to horizontal earthquake effects. In *Engineering Monographs* (Vol. 11). United States Department of the Interior, Bureau of Reclamation.

Zhang, C., Pan, J., & Wang, J.-T. (2009). Influence of seismic input mechanisms and radiation damping on arch dam response. *Soil Dynamics and Earthquake Engineering*, *29*(9), 1282–1293.

Zhang, C., Xu, Y., Jin, F., & Wang, G. (2004). Studies on seismic behaviour of Xiaowan Arch dam and earthquake resistance measures. *13th World Conference on Earthquake Engineering*, Vancouver, Canada.

Zhang, C., Xu, Y., Wang, G., & Jin, F. (2000). Non-linear seismic response of arch dams with contraction joint opening and joint reinforcements. *Earthquake Engineering & Structural Dynamics*, *29*, 1546–1566.

Zhang, Y., Kurata, M., & Lynch, J. P. (2017). Long-Term Modal Analysis of Wireless Structural Monitoring Data from a Suspension Bridge under Varying Environmental and Operational Conditions: System Design and Automated Modal Analysis. *Journal of Engineering Mechanics*, *143*(4), 04016124. https://doi.org/10.1061/(ASCE)EM.1943-7889.0001198

Zhou, J., Lin, G., Zhu, T., Jefferson, A. D., & Williams, F. W. (2000). Experimental Investigations into Seismic Failure of High Arch Dams. *Journal of Structural Engineering*, *126*(8), 926–935. https://doi.org/10.1061/(ASCE)0733-9445(2000)126:8(926)

Zienkiewicz, O. C. (1967). The finite element method in vibration analysis. *Symposium on Numerical Methods in Vibration Problems*, University of Southampton.

Zienkiewicz, O. C., & Bettess, P. (1978). Fluid-structure dynamic interaction and wave forces. An introduction to numerical treatment. *International Journal on Numerical Methods in Engineering*, *13*, 1–16.

Zienkiewicz, O. C., & Cheung, Y. K. (1967). *The Finite Element Method in Structural and Continuum Mechanics* (1st ed.). McGraw-Hill, Inc.

Zienkiewicz, O. C., Irons, B., & Nath, B. (1965). Natural frequencies of complex free or submerged structures by the finite element method. *Symposium on Vibration in Civil Engineering*, Butterworths, London.

Zienkiewicz, O. C., & Nath, B. (1963). Earthquake hydrodynamic pressures on arch dams - an electric analogue solution. *Proceedings of the Institution of Civil Engineers*, *25*(2), 165–176.

Zienkiewicz, O. C., & Taylor, R. L. (1985). Coupled problems - A simple time-stepping procedure. *Communications in Applied Numerical Methods*, *1*, 233–239.

Zienkiewicz, O. C., Taylor, R. L., & Fox, D. D. (2014). *The Finite Element Method for Solid and Structural Mechanics* (Butt (Ed.); 7th ed.). Elsevier. https://doi.org/10.1016/C2009-0-26332-X

Zienkiewicz, O. C., Taylor, R. L., & Zhu, J. Z. (2013). *The Finite Element Method: Its Basis and Fundamentals* (7th ed.). Elsevier Butterworth-Heinemann. https://doi.org/10.1016/b978-1-85617-633-0.00020-4

Zienkiewicz, O. C., Wood, W. L., Hine, N. W., & Taylor, R. L. (1984). A unified set of single-step algorithms. Part 1: General formulation and applications. *International Journal on Numerical Methods in Engineering*, *20*, 1345–1359.

Zou, L., Yu, J., Yang, H., & Mu, J. (2006). Design of Xiaowan high arch dam. *Hydropower International Conference*, Kunming, China.